



VOLCANOES

GLOBAL PERSPECTIVES

John P. Lockwood and Richard W. Hazlett

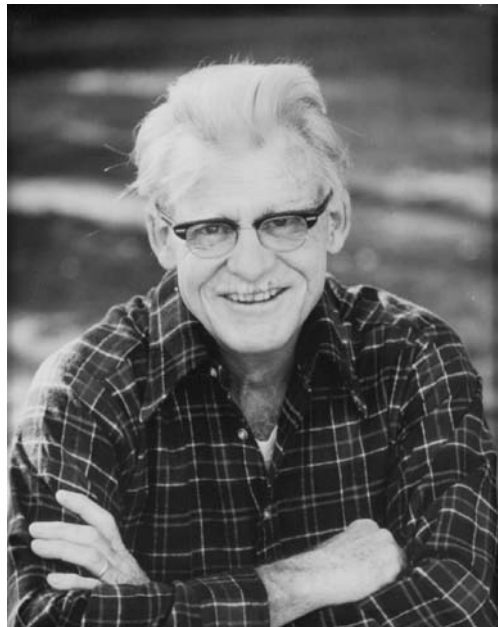


 WILEY-BLACKWELL

VOLCANOES

DEDICATION

We dedicate this book to Gordon A. Macdonald (1911–78), a great volcanologist, teacher, and dear friend, who wrote an excellent textbook (Volcanoes – 1972) that served as the progenitor of this work, and also to the memory of all volcanologists who, motivated by concerns for their fellow human beings and by their desires to understand volcanoes better, came “too close to the flames,” and paid the ultimate price.



Rob Cook, Elias Ravian

Karkar, 1979

David Johnston

Mount St. Helens, 1980

Salvador Soto Piñeda

El Chichón, 1982

Alevtina Bylinkina, Andrei Ivanov, Yurii Skuridin, Igor Loginov

Kluhevskoi, 1951–1986

Alexander Umnov

Karymsky, 1986

Maurice & Katia Krafft, Harry Glicken

Unzen, 1991

Victor Perez, Alvaro Sanchez

Guagua Pichincha, 1993

Geoff Brown, Fernando Cuenca, Nestor Garcia, Igor Menyailov, Jose Zapata

Galeras, 1993

VOLCANOES

Global Perspectives

John P. Lockwood and **Richard W. Hazlett**

 **WILEY-BLACKWELL**

A John Wiley & Sons, Ltd., Publication

This edition first published 2010, © 2010 by John P. Lockwood and Richard W. Hazlett

Blackwell Publishing was acquired by John Wiley & Sons in February 2007. Blackwell's publishing program has been merged with Wiley's global Scientific, Technical and Medical business to form Wiley-Blackwell.

Registered office: John Wiley & Sons Ltd, The Atrium, Southern Gate, Chichester, West Sussex, PO19 8SQ, UK

Editorial offices: 9600 Garsington Road, Oxford, OX4 2DQ, UK
The Atrium, Southern Gate, Chichester, West Sussex, PO19 8SQ, UK
111 River Street, Hoboken, NJ 07030–5774, USA

For details of our global editorial offices, for customer services and for information about how to apply for permission to reuse the copyright material in this book please see our website at www.wiley.com/wiley-blackwell

The right of the author to be identified as the author of this work has been asserted in accordance with the Copyright, Designs and Patents Act 1988.

All rights reserved. No part of this publication may be reproduced, stored in a retrieval system, or transmitted, in any form or by any means, electronic, mechanical, photocopying, recording or otherwise, except as permitted by the UK Copyright, Designs and Patents Act 1988, without the prior permission of the publisher.

Wiley also publishes its books in a variety of electronic formats. Some content that appears in print may not be available in electronic books.

Designations used by companies to distinguish their products are often claimed as trademarks. All brand names and product names used in this book are trade names, service marks, trademarks or registered trademarks of their respective owners. The publisher is not associated with any product or vendor mentioned in this book. This publication is designed to provide accurate and authoritative information in regard to the subject matter covered. It is sold on the understanding that the publisher is not engaged in rendering professional services. If professional advice or other expert assistance is required, the services of a competent professional should be sought.

Library of Congress Cataloging-in-Publication Data

Lockwood, John P.

Volcanoes : global perspectives / John P. Lockwood and Richard W. Hazlett.

p. cm.

Includes bibliographical references and index.

ISBN 978-1-4051-6249-4 (hardback) – ISBN 978-1-4051-6250-0 (pbk.)

1. Volcanism – Textbooks. 2. Volcanology – Textbooks. 3. Volcanoes – Textbooks.

I. Hazlett, Richard W. II. Title.

QE522.L63 2010

551.21–dc22

2009038742

A catalogue record for this book is available from the British Library.

Set in 11/14pt Adobe Garamond by Graphicraft Limited, Hong Kong

Printed in Malaysia

Contents

PREFACE	vii	Further Reading	109
		Questions for Thought, Study, and Discussion	110
PART I – INTRODUCTION	3	PART III – VOLCANIC ERUPTIONS AND THEIR PRODUCTS	113
1. Eruptions, Jargon, and History	5	5. Classifying Volcanic Eruptions	115
A “Grey Volcano” in Eruption – Galunggung – 1982	6	Lacroix Classification System	117
A “Red Volcano” in Eruption – Kilauea – 1974	16	Rittman Diagrams	118
Some Basic Terminology	22	Geze Classification Diagram	119
History of Volcanology	27	Walker Classification System	119
Further Reading	39	Volcanic Explosivity Index (VEI)	123
Questions for Thought, Study, and Discussion	40	Further Reading	125
		Questions for Thought, Study, and Discussion	126
PART II – THE BIG PICTURE	43	6. Effusive Volcanic Eruptions and Their Products	127
2. Global Perspectives – Plate Tectonics and Volcanism	45	Mafic and Intermediate Effusive Eruptions	128
Birth of a Theory	45	Pāhoehoe and `A`ā	135
Volcanoes along Divergent Plate Boundaries	51	Pyroducts	138
Volcanoes along Convergent Plate Boundaries	53	Pāhoehoe Surface Structures	147
Intraplate Volcanoes	60	Lava Flow Internal Structures	157
Further Reading	63	`A`ā Surface Structures	162
Questions for Thought, Study, and Discussion	64	Block Lavas	166
		Radiocarbon Dating of Prehistoric Lava Flows	170
3. The Nature of Magma – Where Volcanoes Come From	65	Further Reading	171
Origins of Magma	65	Questions for Thought, Study, and Discussion	172
The Physics and Chemistry of Melting	68	7. An Overview of Explosive Eruptions and Their Products	173
Classification of Magma and Igneous Rocks	72	Ejecta Classification	174
Principal Magma Types	73	Explosive Eruption Styles and Their Products	188
Magmatic and Volcanic Gases	78	Pyroclastic Density Currents (PDCs)	204
Further Reading	86	Further Reading	220
Questions for Thought, Study, and Discussion	87	Questions for Thought, Study, and Discussion	221
4. The Physical Properties of Magma and Why it Erupts	89	8. A Closer Look at Large-scale Explosive Eruptions	223
Magma Temperatures	89	Measuring the Sizes of Plinian Eruptions	224
Magma Rheology	91	Plinian Eruption Dynamics	224
Magma Ascent and Emplacement	94	Pyroclastic Density Currents (PDCs)	235
“Frozen Magma” – Subvolcanic Intrusives	100	Directed Blasts	255
Triggers for Volcanic Eruptions – Why Volcanoes Erupt	105	“Super-Eruptions”	258
Repose Intervals	108	Further Reading	261
		Questions for Thought, Study, and Discussion	262

PART IV – VOLCANIC LANDFORMS AND SETTINGS	265	PART V – HUMANISTIC VOLCANOLOGY	395
9. Constructional (“Positive”) Volcanic Landforms	267	13. Volcanoes: Life, Climate, and Human History	397
Large Igneous Provinces	267	Volcanoes and the Origin of Life	397
Shield Volcanoes	270	Volcanoes, Atmosphere, and Climate	398
Composite Volcanoes	283	Volcanic Influence on Soil Fertility and Agriculture	406
Minor Volcanic Landforms	290	Volcanoes and Human History	407
Volcano Old Age and Extinction	308	Social Impact of Volcanic Eruptions	408
Further Reading	314	Further Reading	411
Questions for Thought, Study, and Discussion	315	Questions for Thought, Study, and Discussion	412
10. “Negative” Volcanic Landforms – Craters and Calderas	317	14. Volcanic Hazards and Risk – Monitoring and Mitigation	413
Small Craters	318	Hazards and Risk	414
Calderas	321	Active, Dormant, and Extinct Volcanoes	414
Post-caldera Resurgence	331	Volcanic Hazards	416
Caldera Formation Mechanisms	335	Volcanic Risk	425
Caldera Roots – Relationships to Plutonic Rocks	336	Volcano Monitoring	443
Volcano-tectonic Depressions	336	Volcanic Crisis Management	455
Further Reading	338	Further Reading	462
Questions for Thought, Study, and Discussion	339	Questions for Thought, Study, and Discussion	463
11. Mass-wasting Processes and Products	341	15. Economic Volcanology	465
Landslides, Avalanches, and Sector Collapses	341	Earth Energy Relationships	465
Lahars	347	Volcano Energy	466
Causes of Lahars	350	Stored Energy: Geothermal Power	467
Lahar Dynamics	354	Volcanoes and Ore Deposits	470
Lahar Destructiveness	356	Other Useful Volcanic Materials	475
Further Reading	358	Further Reading	477
Questions for Thought, Study, and Discussion	359	Questions for Thought, Study, and Discussion	478
12. Volcanoes Unseen and Far Away	361	Epilogue: The Future of Volcanology	479
Submarine and Subglacial Volcanoes – The Meeting of Fire, Water, and Ice	362	References	481
Extraterrestrial Volcanoes	377	Index	521
Further Reading	392	Appendix: List of Prominent World Volcanoes	538
Questions for Thought, Study, and Discussion	393	Map: Prominent World Volcanoes	540

Preface

This book has a long history. It was originally conceived as a revision of Gordon Macdonald's classic book *Volcanoes* (Prentice-Hall, 1972), following his too-early passing in 1978. We had both worked with Macdonald, who friends called "Mac," and wanted to see his plans for a second edition of *Volcanoes* fulfilled. Originally John "Jack" Lockwood (JPL) planned a simple updating of Mac's text, and Richard "Rick" Hazlett (RWH) planned to contribute artwork to make a more attractive new edition. We quickly found that a simple updating of the original *Volcanoes* would not be sufficient, however, as much of Macdonald's writing reflected the uncertainties of his time, which meant a major revision would be needed. Over the years, under the guidance of several Prentice-Hall editors, the focus of our book changed; less and less of Mac's original writing remained, and a decision was eventually made by Prentice-Hall to abandon preparation of a second edition. Arrangements were then made for publication of this book by Wiley-Blackwell Publishing. Although Gordon Macdonald no longer is formally listed as a co-author of this book, his legacy of volcanic knowledge was heavily relied upon, and some of his original words remain in this text (with the permission of Prentice-Hall and Mac's family).

Rick joined the project as co-author in 1993. His long experience in teaching volcanology to students at universities in Hawai'i and California adds invaluable academic perspectives to this book.

When Gordon Macdonald wrote *Volcanoes* in 1970, the science of volcanology was poised at the threshold of a new era of discovery and understanding, but that threshold had not yet been crossed. In his influential 1972 book, Mac wrote that "Comparatively little progress has been made in understanding the fundamental processes of volcanic activity." How true those words were in 1970, but how untrue now! In the decades since the 1972 edition of *Volcanoes*, people have undoubtedly learned more about the causes and nature of volcanism than in all previous time: Inclusion of this new knowledge and placing it in a global framework has been the foremost challenge before us.

Revolutionary new tools and techniques have also been developed since Macdonald wrote the original *Volcanoes*. Our knowledge of volcanism at that time was almost entirely based on observations of subaerial volcanoes, since those were the only ones readily available for study. Manned deep submersible vehicles, originally used mostly for biological observations, have subsequently become available as "field tools," and have increasingly been deployed for direct observations of submarine volcanoes and volcanic terrain on the floors of the world's oceans. These observations, along with new side-scan sonar imaging techniques, Remotely Operated Vehicles (ROVs) and extensive research drilling of the oceanic crust, have at least quadrupled the numbers of known volcanoes around the world. Exploration of the Solar System over these years has now revealed that volcanoes are actually commonplace extraterrestrial features. Volcanic eruptions have taken place on the Moon, Mars and Venus, and active volcanoes (of a sort very different than those of Earth) have been observed on the moons of Saturn, Jupiter and Uranus.

The eruption of Mount St Helens in 1980 had a major impact on volcanology. Not only was this complex eruption one of the best documented in history, but it also served to change the perceptions of millions of North Americans, who learned that they too had active volcanoes in their backyard – just like the volcanologists had been saying all along! This eruption provided examples of numerous volcanic

processes that had been poorly understood and never observed in detail before; illustrations from Mount St Helens are used liberally throughout this new edition. Four other major volcanic eruptions followed (or began) over the next 15 years, and were also well studied by volcanologists before, during, and after their principal activity – the long-lived East Rift zone eruption of Kīlauea that began in 1983, the Mauna Loa eruption of 1984, the Mt Pinatubo eruption of 1991, and the ongoing eruption of Soufrière Hills volcano, Montserrat – which began in 1995. Each of these five eruptions was very different from one another, and each provided important new information about “how volcanoes work” – information that we have relied on extensively.

While writing this book, we have carried on Macdonald’s emphasis on descriptive rather than “interpretive” aspects of volcanology, although the processes that form volcanic features are also described where understood. In some sections we touch upon more theoretical aspects of contemporary volcanology, but only to provide an idea of some approaches that can be taken rather than to provide comprehensive treatments. Our bibliography points the way forward for those who are more deeply interested in theory. We have also unashamedly tried to emphasize “applied” aspects of volcanology where appropriate. The applied interfaces between volcanic activity, global ecology, and human society are summarized in Part V: “Humanistic Volcanology.” That term was coined by Thomas Jaggar, founder of the Hawaiian Volcano Observatory, and was used by Gordon Macdonald in his writings. We have strived to continue this “humanistic” focus in our book, and are carrying on the chain of human contacts that lead from Jaggar to Macdonald, and now to us and to this book.

We are grateful to many colleagues who shared important insights and knowledge of subjects they know far more about than we do. Many of our colleagues have reviewed parts of the manuscript at various times and shared their ideas and constructive criticisms over the years, including Steve Anderson, Oliver Bachmann, Charley Bacon, Steve Bergman, Greg Beroza, Kathy Cashman, Ashley Davies, Pierre Delmelle, Dan Dzurisin, John Eichelberger, Bill Evans, Tim Flood, Patricia Fryer, Darren Gravley, Michael Hamburger, Ken Hon, Tony Irving, Caryl Johnson, Steve Kuehn, Ian Macmillan, Mike Manga, Doug McKeever, Calvin Miller, John Mahoney, Chris Newhall, Harry Pinkerton, Karl Roa, Mike Ryan, Hazel Rymer, Tim Scheffler, Steve Self, Phil Shane, Ian Smith, Jeff Sutton, Carl Thornbur, Bob Tilling, Frank Trusdell, and Colin Wilson. Having had so many well-qualified geologists comment on parts of this book has caused a minor problem: we’ve found that there is no universal agreement as to what should be included, and it is clear that no single book will “make everyone happy.” We have learned from each of these reviewers, and have humbly tried to accommodate their oft-conflicting suggestions as best we could. Many other colleagues have contributed photographs for this book, or provided insights from their own expertise. These include Mike Abrahms, Shigeo Aramaki, Tom Casadevall, Bill Chadwick, Yurii Demyanchuk, Bill Evans, Dan Fornari, Brent Garry, Magnus Gudmundsson, Cathy Hickson, Rick Hobblit, Caryl Johnson, Stefan Kempe, Hugh Kieffer, Minoru Kasakabe, Takehiko Kobayashi, Yurii Kuzman, Paul-Edouard de Lajarte, John Latter, Brad Lewis, Andy Lonero, Jose Rodríguez Losada, Sue Loughlin, Yasuo Miyabuchi, Setsuya Nakada, Tina Neal, Vince Neall, Hiromu Okada, Paul Okubo, Tim Orr, Yurii Ozerov, Tom Pierson, Jeff Plescia, Mike Poland, Ken Rubin, Mike Ryan, Etushi Sawada, Lee Siebert, Tom Sisson, Don Thomas, Dorian Weisel, Chuck Wood, and Ryoichi Yamada. The late Tom Simkin of the Smithsonian Institution and five USGS colleagues (Pete Lipman, Jim Moore, Chris Newhall, Bob Tilling, and the late Bob Decker) deserve special acknowledgement for their wisdom shared with us over the years, and for the ideas we have purloined from their many seminal publications. We are indebted to support personnel at the University of Hawai‘i, Pomona College, and the US Geological Survey, for encouragement and expert advice over the years, including Jim Griggs of the USGS and Dianne Henderson of the University of Hawai‘i, who gave extensive help with preparation of photographs and line illustrations. Paul Kimberly of the Smithsonian Institution and Wil Stetner of the USGS provided the Dynamic Map files we used in the *Volcanoes of the World* map. (In the text numbers within square brackets following a volcanic site’s name refer to that site’s position on this map.) Ari Berland and Todd Greeley, both Pomona College undergraduates, and Jacob Smith of the University of Hawai‘i at Hilo compiled extensive data bases, reviewed writing from a student standpoint, and prepared maps. Andrika Kuhle spent long hours

compiling and organizing book figures. Julie Gabell's careful editing greatly improved parts of the manuscript. Our friends Maurice and Katia Krafft, who were tragically killed at Unzen Volcano in 1991, provided invaluable background information from their wealth of volcano knowledge, and loaned historical photographs, several of which are used in this book. Bob McConnin and Patrick Lynch of Prentice-Hall, and Ian Francis, Rosie Hayden, and Janey Fisher of Wiley-Blackwell provided critical editorial guidance, as did many other staff at Wiley-Blackwell. A sabbatical semester Lockwood spent at the University of Hawai'i at Manoa in 1988 gave important logistical support and stimulation, as did a research period at Pomona College in 2003. The US Geological Survey's Volcanic Hazards Program supported Lockwood for many years – enabling him to investigate volcanic eruptions and disasters in many lands, and to learn “under fire” from colleagues and foreign volcanologists. A 2002 sabbatical stay at the Alaska Geophysical Institute, and a 2006 sabbatical semester at the University of Auckland provided Hazlett with wonderful facilities and colleagues to aid in final writing.

I (JPL) wish to express gratitude to my wife Martha, who has been my able but unpaid field companion and assistant in the falling ash, mud, and sulphurous fumes of active volcanoes around the Pacific, and who has always kept on, even when paid assistants have faltered because of fatigue, boredom, or fear. She has also been a constant source of editorial and technical counsel as this edition has come to completion over the past several years, and has endured extensive “loss of companionship” over the final months as “The Book” took priority over normal marital responsibilities.

Part of the royalties from this edition will be used to establish a *G. A. Macdonald Student Volcanological Field Research Fund* at the University of Hawai'i, so that young men and women at the University will be better able to seek volcanological knowledge from the ultimate source – the volcanoes themselves.

John P. (“Jack”) Lockwood, Ph.D.

Jack Lockwood worked for the US Geological Survey for over 30 years, including 20 years in Hawai'i, based at the Hawaiian Volcano Observatory. In Hawai'i he monitored dozens of eruptions of Kilauea volcano, and the last two of Mauna Loa. During non-eruptive times he deciphered the prehistoric eruptive history of Mauna Loa by geologic mapping, and became a leader of USGS international responses to volcanic crises and disasters worldwide. He has monitored eruptive activity of volcanoes as diverse as Gamalama, Nevado del Ruiz, Nyiragongo, and Pinatubo. Increasingly he has become focused on “humanitarian volcanology” – the application of volcanology to the needs of society. He left the USGS in 1995 to form a consulting business, Geohazards Consultants International, to continue international service. He is a commercial pilot, and with his wife Martha operates a ranch near the summit of Kilauea.



Photo by G. Brad Lewis.

Richard W. (“Rick”) Hazlett, Ph.D.

Richard Hazlett is Coordinator of the Environmental Analysis Program and a member of the Geology Department at Pomona College in Claremont, California, where he teaches an upper-level course in physical volcanology. He has undertaken and supervised geologic mapping, geochemical studies, and stratigraphic analyses on many volcanoes worldwide, including a hazards assessment at San Cristobal volcano in Nicaragua, seismogenic landslide analysis at Vesuvius in Italy, study of blue-glassy pāhoehoe and phreatomagmatic ejecta at Kilauea, Hawai'i, and most recently, research on the late prehistoric history of Makushin, one of the most active volcanoes in the Aleutian Islands. His work has involved detailed examination of ancient volcanic terrains as well, focusing upon the Mojave Desert region in the US Southwest. Further interests include environmental science and *agroecology* – the development of sustainable agriculture by applying the principles of ecology to food production.







PART I

INTRODUCTION

Volcanology is a specialized field of geology – the science of volcano study. *Volcanologists* are not only the scientists who study volcanoes (mostly geologists, geophysicists, geochemists, and geodesists), but also the devoted technicians who spend their lives monitoring volcanoes at observatories.

To become a volcanologist, one must certainly study a great deal of geology and other physical science, but the title cannot be meaningfully earned by reading books or bestowed by any university. Volcanoes themselves are the best teachers of volcanology, and the most respected volcanologists are those who have studied volcanoes in the field for many years. Volcanologists strive for a better understanding of volcanoes, and are concerned about how their work will contribute to human social needs. Protecting life and property, utilizing the tremendous stores of volcanic energy for society, and perhaps learning to lessen the dangers of certain volcanic phenomena – these are noble goals to strive for!

This Part contains only one chapter, an important one that begins with introductory narratives for a clearer understanding of what volcanic eruptions are like to experience first-hand, discusses some basic terminology, and includes a section on the history of our young science.

Chapter 1

Eruptions, Jargon, and History

*Volcanoes assail the senses. They are beautiful in repose and awesome in eruption;
they hiss and roar; they smell of brimstone.
Their heat warms, their fires consume; they are the homes of gods and goddesses.*
(Robert Decker 1991)

Volcanic eruptions are the most exciting, awe-inspiring phenomena of all the Earth's dynamic processes, and have always aroused human curiosity and/or fear. Volcanoes, volcanic rocks, and volcanic eruptions come in many varieties, however, and to begin to understand them one must absorb a great amount of terminology and information. We'll get to that material soon enough, but first let's explore what volcanoes are *really* like! The facts and figures in subsequent chapters could prove boring if you lose sight of the fact that each volcano and every piece of volcanic rock that you will ever study was born of fire and fury, and that all volcanic rocks are ultimately derived from underground bodies of incandescent liquid called **magma** – molten rock. Every volcanic mountain or rock that you will ever see or touch once knew terrible smells and sounds that you must close your eyes to imagine.

French volcanologists loosely divide the world's volcanoes into two general types: *Les volcans rouges* (red volcanoes) and *Les volcans gris* (grey volcanoes). “Red volcanoes” are those volcanoes that are mostly found on mid-oceanic islands and are characterized by **effusive** activity (flowing red lava). The “grey volcanoes,” generally found near continental margins or in island chains close to the edges of continents, are characterized by explosive eruptions that cover vast surrounding areas with grey ash. This is a pretty good rough classification for most volcanoes, although there are many that have had both effusive and explosive eruptions throughout their

Volcanoes: Global Perspectives, 1st edition. By John P. Lockwood and Richard W. Hazlett. Published by Blackwell Publishing Ltd.

histories (or during individual eruptions). The volcanic hazards and risks posed by each of these types of eruptions differ greatly, and will be described in detail in later chapters.

We hope that in this chapter you will gain some understanding of the look, smell, and *feel* of erupting volcanoes, and that this will put the material of the subsequent chapters in a more relevant light. To provide this we will describe our personal experiences during eruptions of two volcanoes – one “grey” and one “red.” The first narrative will describe events during the large 1982 explosive eruption of Galunggung volcano [99] (Indonesia), and the second will describe some small 1974 effusive eruptions of Kilauea volcano [15] (Hawai‘i). Each eruption was different, and each exemplifies opposites of volcanic behavior. The first eruption had serious economic impact on millions of people, whereas the second ones were primarily of scientific interest to the observers and caused no economic loss.

In this and a few other places, the first person “I” will be used in reference to personal accounts of the authors and identified by our initials, JPL (Lockwood) or RWH (Hazlett).

A “Grey Volcano” in Eruption – Galunggung – 1982

Fine ash was falling in a dim light that afternoon in July 1982, limiting visibility to about a hundred meters outside the Volcanological Survey of Indonesia (VSI) Cikasah Emergency Observation Post. Light grey ash covered everything in sight and could have been mistaken for snow, were it not for the broken coconut palms and the sweltering tropical heat. The narrow road in front of the VSI Observation Post was clogged with fleeing refugees who, with heads covered with newspapers or plastic bags and faces covered with cloth breathing filters, carried their bundles and baskets quickly down the road (Fig. 1.1). Children carried babies and led water buffalo. An occasional small flatbed truck, almost obscured by its overflowing human cargo, crawled along with the refugees.

The fresh-fallen ash muffled the sounds of footsteps, and the people were silent as they hurried down the road away from danger. The only constant sounds were Muslim prayers, wailed in Arabic over a loudspeaker at a refugee camp on a high, relatively safe ridge 1 km away. Thunder and the dull booming of explosions from the direction of Galunggung’s crater 7 km away became louder and more frequent while ash fell more heavily, so I (JPL) turned to go back inside the observation post.

Inside the post, a beehive atmosphere prevailed as technicians busily checked seismographs and shouted out readings to communications specialists in an adjoining room. Their reports were being radioed to Civil Defense Headquarters in the city of Tasikmalaya, 17 km away (Fig. 1.2) and to the VSI Headquarters in Bandung, 75 km to the west: *Tremor vulkanik mulai naik – amplitud duabelas millimeter sekarang – kami mendengar letusan-letusan dari kawah!* (“Volcanic tremor is beginning to increase – the amplitude is now 12 mm – we hear explosions from the crater!”) The observation post was set up in a well-built house in the evacuated zone, but extremely fine volcanic dust nonetheless managed to infiltrate cracks and was everywhere. Note-taking was difficult since fine ash continuously settled on the paper and clogged our pens. The dust formed golden halos around the naked light bulbs dangling from the ceiling, and observers all wore cloth masks over their faces to facilitate breathing. We were in the dangerous Red Zone, as close to Galunggung’s central crater as possible, where no one but emergency personnel were allowed to stay at night, and the thought nibbled at the edge of my



Fig. 1.1 Refugees from falling ash at midday, outside the Galunggung Volcano Observatory, Cikasasah, Indonesia, August, 1982. USGS photo by J. P. Lockwood.



Fig. 1.2 Location of Galunggung and other major active volcanoes (starred circles) of central Java, Indonesia. Major metropolitan centers (bars) are also indicated.

consciousness – “Do I really want to be here?” That thought never progressed very far, however, since I knew that at that moment I was one of the most fortunate volcanologists anywhere. *Reading* about volcanoes is fine, but *being* at a volcano, especially during an eruption, is the best means to discover new knowledge. I suspected that the next three months at Galunggung were going to include some of the most concentrated learning experiences of my life.

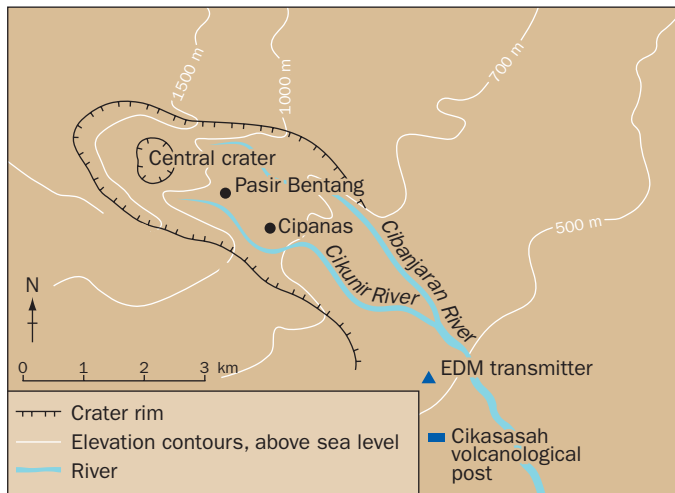


Fig. 1.3 Galunggung volcano, Indonesia. Terrain features and locations of geodetic survey stations during the 1982–3 eruption.

central crater in 1918. The VSI monitors the volcano on an annual basis, but the previous “check-up” in 1981 had shown nothing anomalous. Galunggung’s potential danger was well-known to local authorities, however, as about 4000 people had been killed downstream of the volcano by hot *lahars* (mudflows) in 1822. Legends of devastating prior eruptions abound in the records of the local Tasikmalaya Sultanate.

Residents did not need to be told what to do when a sharp earthquake was felt by Galunggung farmers on the evening of April 4 and snakes reportedly began to emerge from the ground. Those living within and near the central crater around the volcanic dome that had grown there in 1918 quickly began to evacuate. Earthquakes continued that night, and a violent eruption tore apart the center of the crater the next morning. Because the people had fled during the night, no one was killed, though many homes were destroyed. The VSI was alerted, and the first team of volcanologists arrived on April 6. Their portable seismometers showed high levels of earthquake activity, and they recommended an immediate evacuation of all people within the Galunggung “horseshoe.” Their warning came none too soon, as a powerful explosion on the evening of April 8 devastated a wider area up to 4 km from the crater and generated highly fluid, incandescent pyroclastic flows which poured about 5 km down the Cibanjuran River, incinerating several small villages. Again, because the people had been warned, there were no casualties. Eventually more than 100,000 residents left their homes for “temporary” refugee camps which had been hurriedly constructed just outside the danger area.

The Galunggung activity continued to increase in violence over the next several months. Explosive eruptions repeatedly sent churning clouds of ash and steam more than 16 km into the sky. Galunggung’s activity was noted on international news wires on June 24 when a British Airways 747 with 250 people aboard entered an ash cloud over central Java during an explosive night eruption of the volcano. The jet was flying between Singapore and Perth at 11,300 m when it entered the ash cloud and abruptly lost power in all four engines. After gliding free of the ash, the pilot was able to restart three engines and barely make it back to Jakarta airport for a “blind” emergency landing (the windshields had been frosted by ash abrasion).

These ash clouds deposited their loads over a wide area, and ash fell as far as Jakarta, 190 km away. About 25 million people were affected by “nuisance” ash, which required repeated cleanup. More than 500 million cubic meters of ash eventually blanketed much

Galunggung is at the center of the most fertile, heavily populated agricultural land in central Java. It is a horseshoe-shaped volcano, whose central portions had been blown out by a catastrophic prehistoric eruption (Fig. 1.3). For many kilometers to the east, the plain is littered with thousands of small hills, each representing a shattered fragment of the volcano’s heart. Hard-working farmers had established a productive complex of rice terraces and fish ponds inside Galunggung’s amphitheater, an area that was renowned in all Java for its beauty and agricultural efficiency. All was quiet during the early months of 1982, and there had been no activity at the volcano since the formation of a large dome during a small non-explosive eruption within the

of west Java. An area of about 10,000 km² was covered by ash at least one centimeter deep which clogged irrigation systems, damaged crops, and seriously lowered food production in the heart of central Java's rich farmland. At one point, a half-million people faced serious food shortages that required expensive relief efforts by the Indonesian government.

I (JPL) first learned about the Galunggung eruption in early April, when John Dvorak called the US Geological Survey's (USGS) Hawaiian Volcano Observatory (HVO), after having seen the first explosion from the summit of Merapi volcano, 290 km to the east. John was in Indonesia as a participant in a cooperative program between the USGS and the VSI, supported by the US Agency for International Development (USAID). This program was designed to introduce the VSI to modern volcano monitoring techniques in use at HVO. I was slated for a four-month assignment to Indonesia that summer, and spent the remainder of the spring at HVO preparing equipment for the trip.

My family and I left for Indonesia in July, burdened by an incredible load of tripods and other survey gear. While enroute, we read that yet another jet had been forced down after an encounter with a Galunggung ash cloud. We knew nothing of the seriousness of that episode, however, but were amazed on our flight between Singapore and Jakarta when I looked outside and counted *three* engines on the starboard wing! The pilot was walking down the aisle at the time and I asked him what sort of strange airplane this must be with six engines. "No, there are only *five*," he said, "the extra one on the starboard wing is being carried to Jakarta to replace one of the damaged engines on the plane downed by Galunggung."

At the Jakarta airport, we could see the Singapore Airlines 747 parked off to one side with its badly sandblasted windshield and paint. The circumstances were similar to those of the earlier British Airways incident: The plane had flown into an ash cloud at 10,000 m and had lost power in three of its four engines. The disabled jetliner with its 230 terrified passengers had descended to 4000 m before the pilot was able to restore partial power to two engines and limp to Jakarta airport. Examination of the engines later revealed that the Galunggung ash had melted within each and had been deposited as glass on the turbine blades. After this second near-disaster, commercial aircraft re-routed their flights far from Galunggung for the duration of the eruption, and the aviation industry, in close cooperation with volcanologists, began major efforts to educate pilots about volcanic ash hazards (Chapter 14).

Upon our arrival at the VSI headquarters in Bandung, I was told by Dr Adjat Sudradjat, the VSI Director, that because of the mounting economic and social impact of the continuing Galunggung eruption, he would prefer that I not work primarily at Merapi as previously planned, but instead prepare to spend most of my time at Galunggung. I was delighted, and traveled to Galunggung that night.

Two critical questions urgently required answers from the volcanologists at Galunggung: i) When would the eruption stop? (critical information, which would dictate how long Government relief efforts would be required); and ii) Was there any chance that a much larger eruption might occur, and if so, was the evacuated zone large enough – was the city of Tasikmalaya safe? The 1883 eruptions of Krakatau [98] had killed more than 30,000 people in Java, and memories of that tragedy had not been forgotten.

Electronic Distance Measurement (EDM) instruments were some of the most important tools available to us for answering these questions. John Dvorak and his Indonesian colleagues had established a small EDM network in mid-May, and had set up laser reflectors close to the



Fig. 1.4 Night view of Galunggung volcano in eruption, September, 1982. This two second exposure indicates the continuous lightning activity associated with the eruption of electrostatically charged ash. USGS photo by J. P. Lockwood.

crater. However, those were destroyed by a violent eruption a few hours after the field party had left the area. Because of continuing eruptive activity, no one was able to visit the crater area for the next few months. The major eruptions occurred every few days, and were incredibly spectacular at night (Fig. 1.4). The continuing eruption was causing major economic impact on Indonesia, however, and there was no way to enjoy the fireworks. The eruption had already devastated a large area of fertile farmland near the volcano, more than 50,000 residents had been evacuated to refugee camps, and the lives of millions of people were being disrupted by widespread ash across central Java. By late July, it was apparent that a larger EDM network, including stations

closer to the central crater, was critically needed. This would allow us to estimate the size of the magma reservoir beneath the volcano and thus assess the danger of larger eruptions, as well as to better predict individual eruptive phases. We somehow *had* to establish new stations closer to the crater.

Our EDM equipment consisted of a laser transmitter and special reflectors. The transmitter (or “gun”) was set up at one survey point (Fig. 1.5) and the reflectors at another; the



Fig. 1.5 Monitoring inflation of Galunggung volcano between eruptions by EDM from Cikasah station, 6 km from the rim of crater, where volcanologists have set up a temporary laser reflector. USGS photo by J. P. Lockwood.

precise distance between gun and reflector can then be measured to the accuracy of a few millimeters by computerized comparison of the light signals leaving the gun and the returned light from the reflectors. To establish reflector stations closer to the crater, we had to figure a “safe” time to approach closer. Small explosions were nearly continuous at the crater but the violently explosive, more dangerous eruptions were occurring at intervals of one to seven days. We soon noticed that these larger eruptions were all preceded by a brief period of eruptive quiet, followed by 2–3 hours of gradually increasing activity building up to the most violent explosions. Thus, it looked as if a volcanological team would have time to make a quick visit to the outer rim of the central crater and install EDM reflectors during the pre-eruptive “quiet” period with sufficient time to flee when the eruptive intensity began to increase. Furthermore, a sophisticated seismic monitoring network had just been installed around Galunggung by my HVO colleague Bob Koyanagi and a joint USGS-VSI team so that we would have good information on earthquake activity during our trip to the crater.

Galunggung’s crater was clear on the morning of August 7 (Fig. 1.6), and the seismographs showed no activity, so volcanologists Dedy Mulyadi (Indonesia), Maryanne Malingreaux (Belgium) and I decided to set out before the violent eruption we now expected could begin. We loaded our EDM reflector gear into a jeep and were able to drive about halfway to the crater into a world increasingly barren and devoid of life. At the point where the road ended about 4 km from the crater, the only sign of life was an Indonesian entrepreneur who had set up a “store” in the ruins of an ash-crushed building. His only wares were a dozen bottles of soda which he carried to his store each day in the hope of a sale to a rare passerby. We bought three sodas for our packs and hurried on by foot. We soon had to cross the Cikunir River (see Map, Fig. 1.3), a normally small stream that was now a deep gorge cut into fresh volcanic mudflow (lahar) deposits that blanketed the land and villages surrounding the river bed to a depth of



Fig. 1.6 View into Galunggung’s prehistoric horseshoe-shaped crater during a lull between major explosive eruptions in August, 1982. The pyroclastic deposits from these eruptions have built up the rim of the inner crater. Note the drooping, broken palm fronds which are a universal trademark of “grey volcano” eruptions anywhere in the tropics, and result from even minor accumulations of volcanic ash. USGS photo by J. P. Lockwood.

Fig. 1.7 Ruins of Cipanas village, three kilometers from the central crater of Galunggung. Volcanic ash (tephra) can accumulate thick enough to collapse roofs in only a few hours, especially when damp and heavy from rainfall. Although typically light grey in color, it can look like fresh-fallen snow when blanketing the countryside. USGS photo by J. P. Lockwood.



more than 10 m. Crossing the river was easy at the time because only a few centimeters of muddy water were present. We knew we had to return before the next lahars were generated, however, or else we could be helplessly stranded on the other side of the Cikunir with no possibility of re-crossing to the safety of our jeep.

We hurried on through areas where only shells of broken homes (Fig. 1.7) gave evidence of the lives of the people who had fled the area. In one of the ruined villages we met a barefoot man, illegally in the Red Zone, who had come on this day to see his rice paddies and the wreckage of his home. He explained that he was being asked by the government to leave Galunggung forever and move to faraway Sumatra to begin a new life with government help. However, he told us that he could never leave his ancestral home and the graves of his forefathers. He had planted the next season's rice crop in a safe area and would transplant the seedlings to his own land whenever the eruption ended. "*Kepan selesai?*" (When will it end?) he asked. We didn't know, and couldn't answer, so we moved on even faster, knowing that the reflectors we carried could help to provide an answer for this man and the hundreds of thousands of others whose lives were being ravaged by Galunggung.

We installed a reflector station above the ruins of Cipanas village, tested it with a measurement from the "gun" 5 km away, and raced on towards the crater, now less than 2 km away. The area we were crossing had once been heavily forested, but all the trees had been incinerated or swept away, and nothing but the desolation of grey ash, pock-marked by volcanic bomb craters, could be seen on all horizons. It was a scene of devastation more complete than in any war zone, except perhaps for the ground zero of Hiroshima. In fact, the cumulative explosive power of Galunggung had already far exceeded the "small" nuclear bombs exploded in 1945.

Suddenly, our radios crackled to life with the message that earthquake flurries had begun anew beneath the crater, indicating the onset of the next eruptive phase. "*Kembali – kembali*

sekarang!” (“Return – return immediately!”) We could see that the visual forewarnings had not yet begun, however, and knew from our previous experience that it was probably still safe, so we ignored the radios and hurried on. Just as we reached a ridge directly below the crater rim at 09:45, we heard small explosions in the crater above us and saw small puffs of steam and ash rising from beyond the crater rim.

We set up our laser reflectors in record time, then called the survey crew back at Cikasah by radio and asked them to begin the EDM readings – quickly! We were asked to forget the readings and hurry back, but after coming this far we were hardly ready to quit. So, we took the critical temperature readings as the red laser light began to flicker at the gun 6 km away. As the readings seemed to drag on, explosions within the crater became quite loud and angry black “cauliflower” clouds began to boil from the crater. Large blocks of lava up to 0.5 m in diameter were being thrown from the crater, making muffled sounds as they landed in the soft ash a few hundred meters away. The readings were finally finished at 10:10. As we began to pack up our gear, small pyroclastic flows began to pour over the crater rim in our general direction (Fig. 1.8). Our new station was located on a narrow ridge radial to the crater, however, and we felt quite safe – for the moment – as the small ash clouds parted around the ridge and were deflected into the Cikunir River far below. To allay the concerns of our worried colleagues at Cikasah, we radioed them to say we were on our way back. But we secretly decided to stay just a little while longer, because I knew from the scores of similar phases we had observed previously that we probably had several more minutes of relative safety. In hindsight, it was foolish to tempt fate (many volcanologists have died doing so); but the extra few minutes we remained there were some of the most incredible moments of my life. Times like this are far



Fig. 1.8 EDM reflector at Pasir Bentang station below the erupting crater of Galunggung, August 1982. A small pyroclastic flow is beginning to cascade down the crater wall, and the thin deposits left by similar small Haws are seen behind the reflector tripod. Note the permanent reflector mounted on stake to left. Photo by Dedy Mulyadi.

too busy for written notes. Furthermore, to remove one's eyes from the scene before us would have been a terrible waste of observation time, as well as rather hazardous. Instead, as we did our work, I spoke into a tape recorder, an invaluable tool for times like this. My recorded words, spoken with a rather serene calmness (belied by the background roar of the volcano), follow:

09:53 – Steam and ash clouds have increased in intensity, and at this moment a black cauliflower cloud boils out of the northeast side of the crater looking like the puffing from a giant steam locomotive.

10:00 – The entire crater is now the source of nearly continuous explosions. The roar is deafening and the ash clouds have reached 2 to 3 km above our heads. Blocks begin to fall at the crater's rim and unseen lightning is thundering above.

10:08 – Large angular blocks are falling on the outside of the crater wall above us with loud “whoomp-whoomp-whoomp” sounds. They're really not falling – they are ballistically propelled – shot out laterally by the violent explosions – not “falling” from the clouds. They land as groups in distinct impact areas about 100 × 200 meters in area following particularly loud explosions, and bounce and roll down the slope toward us, but deflect around our ridge and down into the Cikunir gorge.

10:10 – Readings finished. We begin packing up.

10:18 – The eruption continues to increase in violence, and gray-black ash flows are boiling over the crater rim and glide almost silently down slope in our general direction, never coming closer than about 150 m. The lightning becomes very intense in the clouds overhead and the explosions are very loud, almost deafening. The lightning begins to strike the crater rim above us and the black ash clouds have mushroomed above our heads, leaving only the horizon to the east clear. We realize that things could get out of control pretty quickly, and decided to retreat – I don't need to breathe more ash! [The truth is, I had seen the autopsy reports of the Mount St Helens [27] 1980 victims and was thinking about their ash-clogged throats. Would our simple particle masks be adequate for breathing if those ash clouds above collapsed? I have no notes for the next ten minutes as we scrambled down slope toward safety. We passed Cipanas at a run and didn't stop to look back – the roaring behind us was louder and we all must have been thinking that maybe we cut this one a bit too close].

10:28 – (out of breath) [We reach the destroyed village of Lingajadi, 1.4 km from Pasir Bentang – and stop to look back]. Ash is now falling on the hills directly behind us and Pasir Bentang is completely obscured. We're going to keep on moving.

10:52 – Reached jeep after crossing Cikunir with no difficulty. We've been in a fine ash fall for the past 10 minutes. The light is fading fast and there is no horizon – visibility about 300 m. The soda salesman had left long ago, and his table and our jeep were already covered by several millimeters of gray ash.

Survival Tips for Field Volcanologists

Whenever feasible, approach eruptive areas from the upwind side. “The smell of sulphur may not be entirely unpleasant to volcanologists (or sinners!)”, but we prefer fresh air whenever we have the choice. Small ash eruptions won't hurt you – but the fine ash can wreak havoc on camera gear and visibility, and remember – upwind beats downwind every time!

11:15 – *As we drive closer to Cikasah we move through crowds of refugees leading their water buffaloes and carrying baskets of baby fish from the few fish ponds they had kept open.* These people had come from the nearby refugee camps in the morning to clean ash from the roofs of their abandoned homes which would collapse from the weight of ash unless it was removed daily (Chapter 14).

11:30 – *Reached the Cikasah Observatory!* Our VSI colleagues treat us a bit like ghosts, and as I look at Maryanne I see part of the reason – she smiles and her white teeth make a striking contrast to her otherwise light gray, ash-covered face. The falling ash has stuck to all of our faces and turned us gray too, just like everything around us.

But we had reason to smile. The Pasir Bentang and Cipanas EDM stations were ready, and if they survived this eruption, we'd be able to measure those critical distances in the morning. By 13:35 the ash cloud overhead had totally blocked out the sun's light, and it was *black* at Cikasah – the blackest black I have ever seen. It really is “impossible to see your hand in front of your face” during heavy ashfall, and my hand bumped into my nose as I gave the old saying a test.

The reflectors we installed *did* survive the eruption, and EDM observations during the ensuing eruptions proved critical to our analysis of Galunggung's underlying magma chamber. We learned that ground deformation did not extend far from the central crater, which showed the magma chamber to be small and not likely to cause larger eruptions. We also learned that inflation of the crater area preceded most eruptions and that deflation accompanied eruptive activity – i.e. survey lines between Cikasah and the near-crater stations were normally longer *after* eruptions, showing that deflation had occurred. We were thus able to determine when the volcano was inflated and thus more likely to erupt. This gave us a means to predict individual eruptions and enabled the VSI to quantitatively demonstrate the quieting of Galunggung as the underlying magma chamber became less and less active.

The reflectors we established lasted for the next six months of activity and almost miraculously were never destroyed, although large bombs formed impact craters as much as two meters in diameter a few meters from the Pasir Bentang station. Almost two meters of ash was deposited at Pasir Bentang over this period, and the reflectors which were originally established more than a meter *above* ground level were soon *below* that level and had to be dug out after each major eruption (Fig. 1.9). Eventually narrow trenches had to be dug in front of the reflectors to allow “lines of sight” to the EDM gun stations.

The numerous eruptions were especially awe-inspiring at night, and my family and I spent many sublime hours admiring the thunderous eruptive grandeur of Galunggung along with silent groups of emergency workers and refugees.

The Galunggung eruption ended on January 8, 1983, and the refugees, except for the 10,500 who had been permanently moved to Sumatra, returned to the areas where their villages, rice paddies, and fish ponds had once been. The intricately terraced water systems, which had taken hundreds of years to build, were cleaned out and reconstructed within two years. By 1986 everything appeared normal once again. Homes had been rebuilt and the rice paddies were healthy with no sign of the deep ash which had deeply buried them in early 1983. Where had all that ash gone? I found that the incredibly hard-working farmers had simply



Fig. 1.9 R. I. Tilling excavating line-of-sight path for EDM measurements at Pasir Bentang station, Galunggung, October, 1982. The reflectors had to be re-excavated after every tephra fall event – this is the same reflector that had been above ground two months earlier (Fig. 1.8). USGS photo by J. P. Lockwood.

proved to be! 1974 unfolded as one of the most volcanically active years in Kīlauea’s recorded history. I was about to learn firsthand that volcanoes are living, breathing entities, and that **magma** (molten rock stored underground) and **lava** (magma that has reached the Earth’s surface – whether still molten or long-cooled) are more than geological abstractions! I would soon learn from HVO’s talented technical staff how to monitor that magma movement with innovative tools, and would have many opportunities to witness the awe-inspiring moments when magma breached Earth’s surface and finally became “lava.” I was also to learn about and to gain respect for the tradition of *Pele*, the Hawaiian goddess of fire and volcanoes. Pele was about to produce a set of spectacular eruptions to welcome me to my career in volcanology.

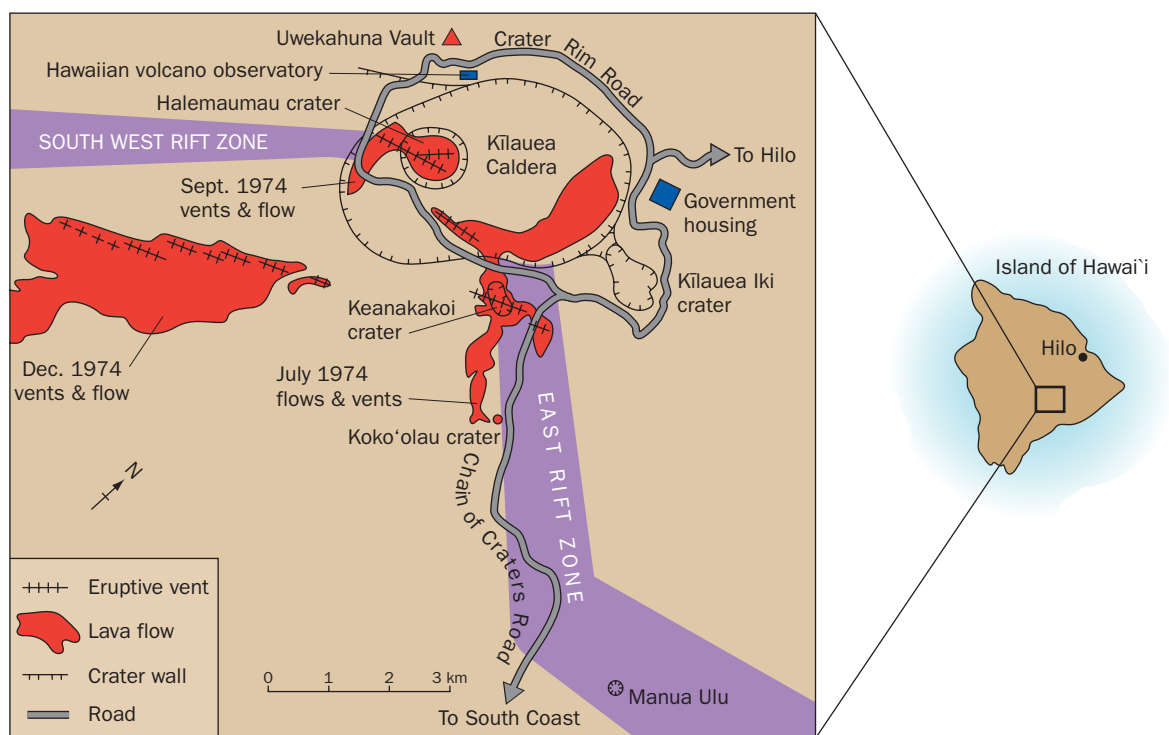
Richard “Rick” Hazlett (RWH), then an undergraduate researcher from Occidental College, also arrived on the HVO staff during that time, and was learning how to track the underground migrations of molten rock and how to forecast volcanic eruptions. His arrival led to an academic career in volcanology that has ever since remained an element of our friendship. We here recount some of our experiences during that exciting time when we were “baptized by fire.” First, some background.

“buried” the ash in their fields. They dug under the ash, removed the fertile and impervious topsoil, and placed it back above ash as much as a meter thick! Mineral nutrients from the underlying ash would now slowly seep upward, making the paddies more fertile than before.

A “Red Volcano” in Eruption – Kīlauea – 1974

BACKGROUND

I (JPL) first saw flowing lava during a brief vacation visit to Hawai‘i in 1971, and subsequently began to hope and scheme for an opportunity to work at the USGS’s Hawaiian Volcano Observatory (HVO) – located near the summit of Kīlauea, the world’s most active volcano. My chance came in January 1974 when my family and I moved to Hawai‘i for a HVO tour. There had been a lull in Kīlauea’s volcanic activity, however, and I feared that perhaps there would be no eruptions at all during my scheduled two-year HVO assignment. How ungrounded my fears



MAUNA ULU ACTIVITY

In late 1969, molten rock from Kilauea's magma reservoir system worked its way to the surface about 10 km from the summit of the mountain in a zone of weakness called the East Rift Zone. What had been a gently sloping forested highland suddenly became the stage for an eruption of gushing lava that ultimately constructed a satellitic volcanic edifice nearly 1 km across at the base and some one hundred meters high. Local Hawaiians named it Mauna Ulu "Growing Mountain" (Fig. 1.10).

Mauna Ulu's vent-filling lava lake demonstrated episodic lava fountaining activity that alternated with periods of lava drainage in late January of 1974. The high fountaining episodes involved gas-charged geysers of lava up to 100 m in height that would sometimes play for hours on end. This activity was followed by copious lava overflows, noisy de-gassing, and then rapid lava lake drainage and lake surface lowering. The periods of fountaining were especially awesome because of their noise. Frequently, while asleep in our government housing on the summit of Kilauea, we would be awakened by a rhythmic rattling of window panes caused by the intense roaring from the Mauna Ulu lava fountains 10 km away. Outside, the night sky in the direction of Mauna Ulu would turn bright orange-red, reflecting off overhead clouds when they were present. Such events made it necessary to drive to HVO to check instruments and make certain that no dangerous change in eruptive style was occurring (one of the most important missions of the Observatory is to advise the Hawai'i Volcanoes National Park of any eruptions that could endanger park visitors and campers).

Don Peterson, the HVO scientist-in-charge, and I (JPL) had driven to the Observatory late one night in the winter of 1974 to check a new surge of activity indicated by a glow on

Fig. 1.10 Principal features of Kilauea volcano summit area. Modified from Lockwood et al. (1999).

the skyline from Mauna Ulu. After noting an increase in seismic activity in that area on HVO seismographs, we decided to hike out to the eruptive area to inspect the action at closer range. Together with our wives, the four of us drove as close as possible and began to hike over fresh lava flows to inspect the erupting vent. The surfaces of pāhoehoe (smooth surfaced lava) solidified quickly, and within a half hour or so the solid crusts were thick enough to support one's weight (a 5 cm thick crust is strong enough so long as the crust is underlain by molten lava and not by a gas bubble!). We had to keep moving across the hot flows so that the soles of our boots didn't get too hot, as this can cause painful steam burns. We learned quickly what sorts of boot soles hold up under these conditions; the soft rubbery kinds catch fire too quickly and melt easily. The first warning you may have of this is when your footing becomes slippery!

As the four of us reached the rim of Mauna Ulu's crater, we found that the lava surface had lowered about 15 m below the vertical rim of the 40 m wide lava lake. The radiant heat from the pooled lava below was reminiscent of that from a giant blast furnace, but the hot air rose vertically rather than spreading out horizontally to drive us away. When the winds did shift and the sulphur fumes were stronger, I thought of Mark Twain's words, written after his exposure to volcanic fumes from Halema'uma'u in 1873: "The stench of sulphur is not entirely unpleasant to the sinner!" If I may, I would like to amend Twain's wording to add "nor to the volcanologist!"

Mauna Ulu's lava lake was directly connected by subterranean conduits to the principal magma chamber underlying Kīlauea's summit, 10 km away, and as I watched the pulsating surface of the lake surface below me, I realized that I was looking at an exposed top of this sprawling magma system. Up until then the term "magma chamber" seemed to be little more than a mysteriously abstract way of explaining instrumental measurements at the Observatory. Now here it was – *for real!* The roiling lava lake I was privileged to be watching was directly connected via subterranean dikes to the principal magma chamber beneath Kīlauea caldera. That chamber was itself connected by a nexus of passageways downwards to the area some 60–80 km below the surface where fresh basalt magma was being "sweated" out of the earth's upper mantle far below the Earth's crust. This sweating process, called "partial melting,"

(Chapter 3) had created the magma that was now reaching the Earth's surface for the first time after its formation – perhaps only months or maybe years before. As this magma reached the Earth's surface in the crater below me, it could at last be called lava.

There was little sound from the lake, other than "blurping" noises as large gas bubbles frequently broke the lava surface. The lava surface was gently convecting, and plates of descending crusts would trigger fountaining at the crater's edge (Fig. 1.11). Don, Betty, and Marti were on the south rim, and I had walked about 75 m to the west for a better look into the roiling lava below.

As I was enjoying the view of the lava lake that night, I heard a persistent "popping"

Fig. 1.11 Mauna Ulu lava lake. Thin lake crust is descending into "drain-back" at the margin of the lake, accompanied by 5 m-high fountains. USGS photo by J. P. Lockwood.



sound behind me and noted that a crack was slowly opening about 5 m back from the rim. I stood over the slowly widening fissure and saw that the crack was spreading eastward toward my companions. It began to open faster, exposing glowing rock below and opening up like a zipper towards Don and our wives, who were mesmerized by the lava lake circulating below. I shouted an alarm. They saw the advancing crack and began running south – away from the lake. I ran fast behind them, but they were about 25 m ahead of me when I heard a loud splashing sound and the clouds above me turned bright red as a large fragment of crater rim plunged into the lake below.

Don slowed down to look back as I ran toward him, and I saw him gaze upwards at the column of lava spatter that rose above us. “Keep running!” he screamed. I needed no encouragement, and almost *flew* down slope over the rough lava to rejoin the others in a safe area. No worse for the experience, we went back to the Observatory to inspect the seismic records and found that the collapse of this large crater rim had indeed been recorded on a nearby seismometer. It was comforting to see that our technology worked on such a fine scale!

A few days later, as I probed with my geologist hammer into small toes of fluid lava that emerged from flows descending down the flanks of Mauna Ulu, I realized that my hand was directly connected to a non-broken conduit of primordial fire, fire that led down to the birthing place of magma itself within the so-called “hotspot” beneath Hawai‘i. I humbly thanked Pele for this incredible privilege; I would never again be able to view volcanoes without thinking of their magmatic roots and about the crucibles of fire that lead to their creation.

THE SUMMIT ERUPTION OF JULY 19–21, 1974

My last view of molten lava at Mauna Ulu was on July 10th. Nine days later, Don Peterson and I were at sea off the west coast of Hawai‘i exploring undersea volcanic features from a US Navy deep sea submersible. Rick Hazlett was lucky enough to be on duty at HVO on July 19, as a new chapter in Kīlauea’s eruptive pattern was about to open. Here is his narrative of what happened:

*Around 03:30 on the morning of July 19 the tremor alarms sounded in park housing, and a few bleary-eyed HVO staffers drove quickly over to the Observatory to see what was going on. **Tremor**, a continuous shuddering of the Earth related to the shallow movement of magma, commonly precedes eruptions. Perhaps Mauna Ulu was about to experience another major overflow! Preliminary indications showed that the source of this shallow earthquake activity lay much closer to the Observatory, however, and was only 2 to 5 km distant along the southern rim of Kīlauea’s caldera. For this reason the HVO response team quickly called upon park rangers to evacuate the southern part of Crater Rim Drive and all of Chain of Craters Road (Fig. 1.10), areas that would ordinarily be swarming with visitors and tour buses soon after sunrise.*

I arrived at HVO at 08:00 to find Bob Tilling in charge of the crisis response. No eruption had yet started, but he sent two crews of observers into the now-closed area to report on any visible changes in the ground surface possibly related to the strong earth tremor, which by now had shifted close to a small pit crater called Keanakako‘i, where ancient Hawaiians once mined fine-grained basalt for stone tools. I rode with one crew down the Chain of

Survival Tips for Field Volcanologists:

Pay attention to sounds when on eruptively active volcanoes – especially along the margins of craters. Rocks commonly begin to fracture slowly at first as they begin to fail – making audible cracking sounds before sudden failure. Major phreatic explosions have been preceded by audible sound changes. Pay attention to the “normal” sounds a volcano makes, and be concerned if those sounds begin to change!

Craters Road, while the other field team parked along Crater Rim Drive right at the northern rim of Keanakako`i, within sight of the Observatory. After driving only a few miles our vehicle came to a sudden stop, as up ahead we saw fist-sized holes opening in the asphalt. It took only a few minutes for each new hole, deep and black, to open, and every few tens of seconds we felt sharp earthquakes. Making a hasty radio report to the Keanakako`i team, our crew drove further upslope along the evacuated highway, closer to seismic “ground zero” where Kīlauea was likeliest to begin erupting. We parked in woods next to Koko`olau Crater, another prehistoric vent. Stepping out to an overlook, the strengthening volcanic tremor was now physically apparent. The ground seemed to sway gently, but erratically, as if standing on a giant bowl of vibrating gelatin. Every few tens of seconds a sharp jolt interrupted the continuous rocking. Some of the surrounding trees nearby creaked and moaned though little wind blew.

No more than a couple of minutes of this unusual experience elapsed when a park ranger’s patrol car arrived and our radio burst to life with Tilling’s words: “The eruption has started by Keanakako`i! The vent is opening in your direction – get out fast!” We were now in a race with time to avoid being trapped. As we raced back up the road, we soon saw roiling light blue, brown, and white eruption clouds rising above the tree line to the west, getting closer by the second. The instruments had indeed been accurate in forecasting an outburst in this area, and our closely-timed ground observations had been useful for corroborating this pre-eruption seismic monitoring. The opening fissure intersected the road no more than a minute or two after we drove past.

Reunited at the edge of Keanakako`i, the two field crews watched as a sheet of fountaining lava ripped the ground open across the southern end of the 35 m deep crater about 400 m away, safely propagating at a right angle to our lines of sight. I was impressed that the escaping magma seemed to ignore the presence of the crater; the opening vent followed its linear path irrespective of any surface landform. Cascades of blood-red lava soon poured over Keanakako`i’s rim and erupted through the tear in its southern wall and base – volcanic chaos taking place simultaneously over just a few square kilometers of landscape. From 1 km away the eruption sounded like surf crashing on a distant shore. Up close, however, it sounded like thousands of fire hoses blasting away all at once.

The unsteady rolling of the ground continued off and on where we stood, when suddenly one of our team, exploring about 30 meters away cried out, “Hey, look at this. Another crack is opening!” We made haste to join him, and sure enough watched a fresh linear trench widen and deepen where flat earth had existed moments before. Knowing what was coming next, we stepped back, upslope and upwind, and within a few minutes a billowing mass of dense white steam poured out, quickly fading to the telltale blue of nose-pinching volcanic fumes and soon followed by the ejection of plate-sized globules of lava. The ends of this new fissure lengthened at the rate of a slow, steady walk, and within a half hour mounds of quenched lava ejecta, called spatter ramparts, had grown several meters high all along its upslope rim. As we were studying these developments, a colleague obtained a memorable photo from his vantage point at HVO 3 km away (Fig. 1.12).

The eruption climaxed only about 45 minutes after the outbreak began and the development of new vents ended. For the next three days, activity gradually simmered down. This is typical of many eruptions at red volcanoes; they wax rapidly and wane slowly. Little did we appreciate at the time, however, that this small but spectacular eruption heralded the end



of the long-lived activity at Mauna Ulu – which has not been active since. Kīlauea had once again changed her eruptive style – the next two eruptions, in September and December, would also be in the summit area (Lockwood et al. 1999).

CONCLUSIONS

Some useful generalities emerge from these eruption narratives:

- 1 Volcanic eruptions evoke feelings of awe, excitement, and to a greater or lesser extent, concern and fear for those nearby.
- 2 Effusive red volcanoes such as Kīlauea tend to have frequent, gentle eruptions that can be studied close up, whereas eruptions of the explosive grey volcanoes are less frequent but have far-reaching impacts.
- 3 Eruptions of grey volcanoes are more dangerous than those of red ones, and much more caution is needed during close observation.
- 4 People's lives can best be protected in areas where eruptive activity is frequent (e.g. Java, Hawai'i). This is because in areas of relatively frequent eruptive activity, residents are better informed and are more likely to recognize early warning signs of impending activity, and volcanologists will be able to prepare more accurate predictions of future activity. Most

Fig. 1.12 July, 1974 eruption of Kīlauea volcano as viewed from the Hawaiian Volcano Observatory a few minutes after outbreak of typical “curtains of fire” from multiple en echelon vents near Keanakako'i crater. A USGS monitoring crew is observing the middle vents. USGS photo by John Forbes.

important, local residents are more likely to accept the advice of public officials and comply with mitigation efforts such as evacuation.

- 5 The magma reservoirs beneath effusive volcanoes are typically complex and dynamic, and can send dikes great distances at shallow depths underground, even tens of kilometers from the volcano's top. Flank eruptions are common, and can be the norm. In contrast, the magma systems beneath typical explosive volcanoes are usually more localized beneath volcano summits.
- 6 Erupting lava and gases are the major concerns of effusive eruptions on red volcanoes, but simple field precautions can usually prevent disaster. In contrast, explosive eruptions of grey volcanoes typically involve serious hazards such as falling ash and pyroclastic ash flows (Chapter 7), and mudflows (Chapter 11). Eruptions may threaten extensive areas, and evacuations of large numbers of people are often necessary. This makes a major volcanic eruption as much a sociological and economic event as a geological one.

These eruption accounts illustrate some of the reasons that volcanoes are being studied and illustrate the sort of practical use volcanologists are trying to make of their knowledge. The modern science of volcanology combines well-documented field observations and instrumental surveillance of active volcanoes, as well as careful field mapping of older volcanoes to learn their histories. Laboratory studies that reveal how magma is formed, stored, and evolves beneath active volcanoes are also vitally important. The long-term goal of all volcanologists is to have a better understanding of “how volcanoes work”. Only such understanding of volcanoes can lead to the knowledge and development of tools needed to fulfill our ultimate goal – the protection of human lives and property. Volcanologists seek to recognize hazardous areas and evaluate risk, warn of danger, and thus save lives. In addition to these benefits, volcano studies have revealed many other equally important connections between volcanic activity and the human experience. The final section of this book, entitled “Humanistic Volcanology,” explains the relationship of volcanoes to our history, our climate, and to the metals and energy that we use and to the soils whose productivity provide our food. It is no exaggeration to state that without volcanic activity life might never have developed on Earth. Without the ore-concentrating roles of magmatic systems and volcanoes technical civilization would be impossible. Volcanoes are infamous for their destructiveness, but they are also beautiful, have created much of the land we live on, and help sustain the world in ways which few of us fully grasp.

Generalizations being what they are, there are exceptions and elaborations needed for each of the statements made above, and we shall touch on them again throughout this book. For the time being, however, we've shared some of our personal experiences, and hopefully hinted at reasons why this science is an exciting humanistic as well as a scientific journey.

Some Basic Terminology

As humans develop specialized knowledge, whether it be about the baking of bread, ballroom dancing, brain surgery or whatever, new words are coined to describe common features or processes. These words become “shorthand” to express thoughts in a few words rather



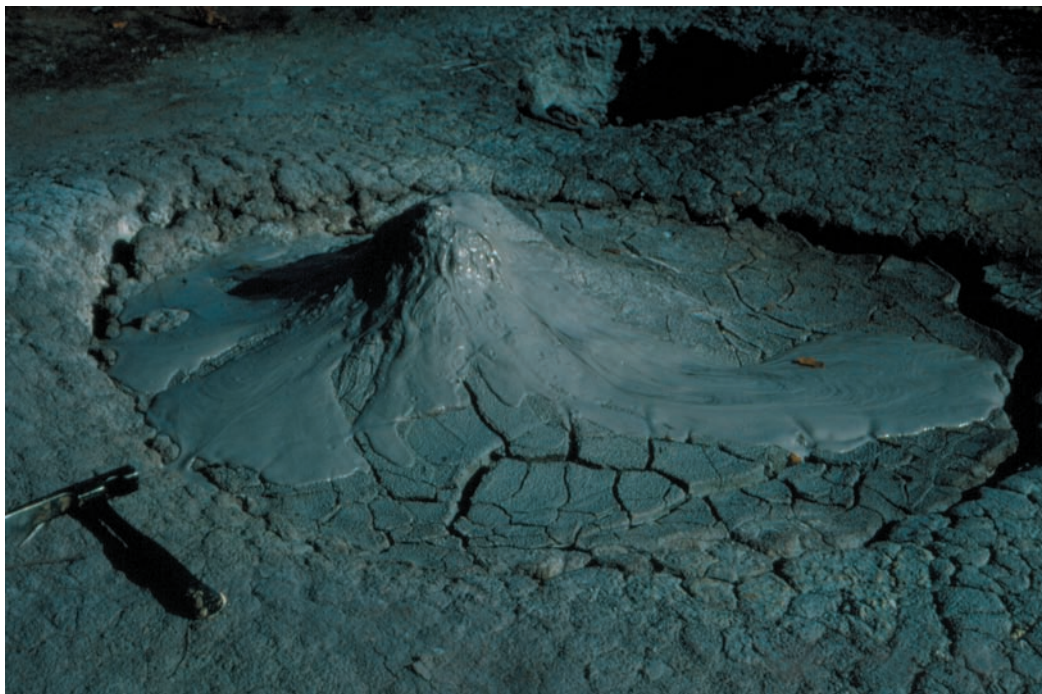
than many. Volcanologists have their own shorthand jargon, though we strive to avoid complex terminology as this can be a barrier to effective communication with the general public. We here define some of terms we will be using in this book – in narrative form rather than presented in a glossary. The Index (p. 526) will also direct you to further definitions when needed.

First, just what is a **volcano**? Most people first think of volcanoes as those beautiful, steep-sided, symmetrical, pointed cones like Mount Fuji [113] in Japan, Mount Shasta [26] in California, or Mount St Helens in Washington State (at least as it was before the catastrophic eruption of 1980!). But in fact most volcanoes have shapes and forms that differ greatly from the postcard views and cartoon sketches we all learn to draw in school. Volcanoes come in many shapes and sizes, from small hills to the largest mountains on earth, and to even larger mountains on other planets. Their shapes vary from majestic cones (Fig. 1.13) to inconspicuous hills, huge, lake-filled craters with volcanic rims, and vast lava-covered plains.

In this book we accept the common understanding of what a volcano is – a mountain or hill (an edifice) that develops when molten rock reaches (or closely approaches) Earth's surface and erupts. But while this serves as a practical definition, it has limitations. For example, the floors of the world's oceans are dominantly underlain by lava flows, but those volcanic rocks are mostly derived from elongated fissure vents within deep sea rift valleys in ways that commonly did not allow for construction of conspicuous near-vent edifices. Vast areas of the

Fig. 1.13 Kronotsky volcano, on the eastern shore of Lake Kronotsky, Kamchatka. The 3500 m high summit of this perfectly symmetrical composite volcano was the site of minor phreatic explosions in 1923. When the lake surface is smooth, the reflection of this volcano on the water is one of the most beautiful sites in the world. USGS photo by J. P. Lockwood.

Fig. 1.14 A small “mud volcano” in the Uzon geothermal basin, Kamchatka. This one was formed by rising steam above a “mudpot”; other mud volcanoes, rising from sedimentary basins because of density contrasts, can spread out to cover vast areas. USGS photo by J. P. Lockwood.



continents are also blanketed by incredibly voluminous outpourings of lava or hardened volcanic ash that buried pre-existing topography, but resulted in no conspicuous “volcanoes” that grew above the land. In an instance like this, the “edifice” built is not a mountain or hill with a crater on top, but rather are sprawling gently sloping volcanic plains that can be related to a common source vent or cluster of vents. It might seem a stretch to call features like this volcanoes, but they are.

Some non-volcanic landforms such as the “mud volcanoes” of sedimentary basins and geothermal areas (Fig. 1.14) and the “asphalt volcanoes” found on the seafloor above salt domes are also sometimes referred to as volcanoes, and can form very large submarine edifices (e.g. Fryer et al. 2000). Although they can also impact large subaerial areas (e.g. the devastating Indonesian mud volcano “Lusi;” Davies et al. 2008), they are not true volcanoes in our sense, because they do not serve as vents for molten rock, and will not be considered here. Terrestrial volcanic eruptions mostly involve the escape of siliceous magma and gas, but other sorts of very different volcanic activity can also occur on the outer planets of the solar system, where the make-up of “rock” is quite unlike what we find on Earth (Chapter 12).

Igneous rocks result from the cooling of molten material originating inside the Earth. They are divided into two related clans: **volcanic** (or **extrusive**) and **plutonic** (or **intrusive**) rocks. Volcanic rocks are products of erupted magma, whereas the plutonic rocks are formed from magma that crystallizes underground. In general, volcanic rocks have sparse visible mineral crystals (**phenocrysts**) owing to rapid cooling of magma after eruption; whereas plutonic rocks are usually coarsely crystalline owing to slow cooling. Compositionally, most igneous rocks range from those like **basalt** typically containing low relative proportions of silica molecules (SiO_2), to those like **rhyolite** and **granite** that are silica rich. Rocks like **andesite** and **dacite** that have

moderate amounts of silica are said to be **intermediate** in composition. As you will learn, silica content plays an important role in eruptive processes (Chapter 3).

Large bodies of magma underlie most volcanoes, and the terms **magma reservoirs** and **magma chambers** have been used interchangeably by many writers to describe them. Bachman and Bergantz (2008) would distinguish between the two terms on the basis of magma eruptibility. We prefer to define magma “chambers” as single bodies of fluid melt and magma “reservoirs” as the overall magmatic system underlying a volcano or volcanic center – a system that may well consist of several separate magma chambers and feeder conduits. Magma chambers may cool to form masses of coarsely crystalline intrusive rocks called **plutons**, and especially large plutons or closely spaced plutons may form extensive **batholiths** beneath volcanic belts. When exposed by later erosion, such batholiths may form majestic mountain ranges like the Sierra Nevada of California, their volcanic covers completely eroded away. Coarse-grained igneous rocks can also form at shallow depths directly beneath volcanoes. If directly related to overlying volcanoes, such rocks, whether coarse or fine-grained, are referred to as **subvolcanic** or **hypabyssal** rocks.

The passageways that supply magma from subterranean chambers to the volcanoes above are called volcanic **conduits**, and come in many shapes. When magma freezes in elongate fractures, the thin, sub-vertical tabular structures called **dikes** are formed (Chapter 4). Magma may also intrude laterally from magma chambers (or from dikes) to form the sub-horizontal structures called **sills**.

Eruptions may take place from single pipe like vents or from long fissures. The eruptions may be **explosive**, blowing out large amounts of fragmented (**pyroclastic**) debris (or “ejecta”) consisting mostly of quenched magmatic lava fragments, commonly mixed with older rock material; or they may be **effusive**, erupting mainly fluid lava. Pyroclastic material is classified according to the sizes and shapes of fragments with the finest material, dust to fine sand-sized particles termed volcanic **ash**. Solidified ash beds are called **tuffs**, and **welded tuff** results where settling ash particles are so hot that they melt together. Coarser pyroclastic fragments include **lapilli**, **bombs**, and **blocks** (Chapter 7). Volcanic **breccias** are accumulations of large, blocky fragments embedded in finer, generally pyroclastic material. If the blocks are separated from one another so that they are not in mutual contact, then they are said to be “matrix supported.” Otherwise they are “clast supported.”

In contrast to pyroclastic debris and breccias, lava flows are classified according to their surface features. Smooth flows, as mentioned above, are called **pāhoehoe**, and rubbly ones **ʻaʻā**. There are also **blocky lava flows** (Chapter 6).

Eruptions resulting from the direct action of magma or magmatic gas are **magmatic** eruptions. There are various kinds of magmatic eruptions, classified according to their relative explosiveness and volcanic products, including Hawaiian, Strombolian, Vulcanian and Plinian-type activity. Eruptions generated by the heating of water external to the magma (**hydrovolcanic eruptions**) may take place either in shallow water (Surtseyan-type eruptions), or on land, where magma interacts with shallow groundwater (Chapter 7). **Phreatic** eruptions, from the Greek word for “well,” are dry-land steam-blast explosions which throw out only the solid fragments of surrounding older rocks. Similar eruptions in which the material ejected is partly or wholly magmatic are termed **phreatomagmatic** eruptions. Phreatomagmatic eruptions produce **maars** – wide, low-rimmed craters commonly occupied by lakes.

Fig. 1.15 The shield form of Mauna Loa volcano, Hawai‘i – as viewed across Kīlauea caldera. Mauna Loa (4170 m) is the Earth’s most voluminous volcano (> 50,000 km³), with a base more than 5 km below sea level. The shield profile of Kīlauea volcano’s summit is also evident, beyond the fuming Halema‘uma‘u crater. USGS photo by J. P. Lockwood.

Eruptions are invariably driven by the expansion of dissolved gases (**volatiles**) within the magma as it nears the surface. Some eruptions show mixed explosive and effusive characteristics, in some instances taking place simultaneously on different parts of the same volcano. The pyroclastic material accumulating from explosive eruptions may be deposited by powerful, extremely dangerous ground-hugging ash clouds called **pyroclastic density currents** (PDCs), or by material falling from above – **airfall**, or simply **fall** deposits.

Geologists recognize several distinctive types of volcanic edifices (Chapters 9–12). Those long-lived, large ones that grow from repeated eruptions through the same conduit system are referred to as **polygenetic**, while those that result from a single eruption are called **monogenetic**. Polygenetic volcanoes include **shield** volcanoes and **composite** (or “**strato**”) volcanoes. Monogenetic volcanic edifices can be separate, individual volcanoes or distributed as structures at satellitic vents on the flanks of larger polygenetic volcanoes, and include **pyroclastic cones** (spatter, cinder, pumice, or ash), volcanic **domes**, and **lava shields**.

Shield volcanoes, such as those characteristic of Hawai‘i and most other mid-oceanic islands, include the largest volcanoes on Earth, have very long lives, and are mostly made up of long, thin lava flows that form broad, gently sloping (generally 5–10°) shield-shaped mountains (Fig. 1.15). Many eruptions occur on the flanks of these volcanoes tens of kilometers from their summits, in some instances localized along radial fracture zones termed **rift zones**.

Composite volcanoes (Chapter 9) are the massive, steep sided (30–35°), “pointy” mountains of classical shape like Mt Fuji or Kronotsky [127] (Fig. 1.13). These volcanoes are built up over long periods of time from hundreds or thousands of eruptions. They are composed of layers of pyroclastic material, primarily volcanic ash, interbedded with lava flows.



Of the monogenetic volcano types, **cinder cones** (sometimes also called **scoria** cones) are the most common subaerial volcanoes on Earth. They are made up of a bubbly type of lapilli called cinder, and have cup-shaped craters at or near their summits. Some are horseshoe shaped and may be associated with lava flows. Cinder cones have short lives and may build up in a few days or a few decades at most. A volcanic **dome** is a jagged mound of lava that was very stiff and partly or even completely solidified as it escaped the vent. Domes may form gradually over a period of years, swelling from within and occasionally exploding or oozing out sluggish lava tongues.

In some areas, clusters of volcanoes and minor volcanic landforms exist around a central volcano called a **volcanic center**. The central volcano and surrounding edifices may share the same magma reservoir or may maintain separate conduits to their sources of melt, which in turn derive from a common source of heat. Especially large clusters of volcanoes, with or without volcanic centers, comprise **volcanic fields**.

Many volcanic centers are centered around **calderas**, large collapse craters generally many kilometers in diameter formed from the sudden withdrawal of magma and gases from a shallow underlying magma chamber (Chapter 10). The largest and structurally most complex calderas occur in continental settings. Much simpler and generally smaller ones occur on mid-oceanic islands.

There you have it – a starter potpourri of terms. Now let's learn about the history of volcanology.

History of Volcanology

THE AGES OF SUPERSTITION

Among all creatures subject to volcanic eruptions, human beings are unique in that they feel compelled to understand the reason why “fire” should come from the Earth.

The earliest explanations of these fearsome “fire mountains” were given in religious terms based on superstition, and usually invoked the actions of subsurface gods who were either displeased with the terrestrial world or were fighting among themselves. Many of these legends are well described in books by Sigurdsson (1999) and Vitaliano (1973), but conversations with long-time residents of any volcanic area will reveal other unrecorded legends that are still being passed down by story-telling.

The knowledge of traditional peoples living near volcanoes should not be underestimated. Their stories are worth listening to, for no matter how embellished they may be by “poetic license” of generations of story-tellers, “grains of truth” from which the legends have sprung are found in most of these stories. Although traditional peoples did not have modern tools or knowledge, their stories of past eruptions are mostly based on actual observations, and attempts to reconcile these human accounts with modern volcanic knowledge can be a most fruitful source of information for volcanologists interested in understanding “prehistoric eruptions.” As examples, I (JPL) was fascinated to find that native peoples in the Virunga volcanic belt (eastern Congo and Rwanda) knew very well which volcanoes had been active in pre-written



[Japanese kanji: “Fire Mountain”]

history because they distinguished between “female” and “male” volcanoes. The lady volcanoes were those that had “emitted blood” (i.e. lava) in times past, whereas the male volcanoes were the ancient ones that had not erupted for a very long time. Their accounts matched scientific observations very well.

A Navajo woman in Grants, New Mexico once told me a story to explain a long, narrow pāhoehoe flow (the McCartys flow) that extends more than 50 km between Gallup and Albuquerque. The woman apologized before sharing the legend saying, “Of course you won’t believe this – this is just old superstition,” and then recited a detailed tale about a battle between an evil giant and young brave: “When the giant (Ye’litsoh) was felled by a stone from the young man’s sling, he fell to the earth and made the ground shake all over. The giant’s blood poured forth as a red torrent that flowed like a river across the land. When the red blood dried it turned black – you can see this dried-blood river today.” This eruption (the youngest in New Mexico) took place over 3,000 years ago – yet the events (earthquakes and eruption) that people witnessed are still vividly documented through story-telling – a testimony to the power of oral tradition.

Seismic activity almost always precedes volcanic eruptions, and is commonly described in legendary accounts. Another example comes from Hawai‘i, where “prehistoric” time conventionally refers to the period before European written accounts. Although there are many credible legends about pre-European eruptions of Kīlauea volcano, none had been known about prehistoric Mauna Loa [13] eruptions, until I came across a previously overlooked story dealing with the origin of some littoral cones (“Na Pu‘u O Pele”) along the southwest coast of Hawai‘i Island. Westervelt (1963) recounted a tale he had been told by an old Hawaiian man about the origin of these cones, a story of Pele’s ire after she had been jilted by two chiefs who had spurned her romantic advances. In the story, Pele was so mad at the chiefs that she had “caused the earth to shake by stomping her feet on the ground in anger” before sending two lava flows to the sea, trapping the chiefs between them and turning them into the cones. Later mapping showed that two separate flows had indeed been erupted at this time and that the “legend” was an accurate description of the sequence of events that formed the two cones. This eruption was radiocarbon dated at 300 BP, showing that Mauna Loa’s humanly recorded history began long before Hawai‘i was “discovered” by Captain Cook! Hawaiians understood basic volcano processes very well – long before Westerners came for formal study. They knew that their chain of island-volcanoes is younger to the southeast, and interpreted this as evidence for the migration of Pele from west to east over time. They also knew that magma was stored beneath the summit of Kīlauea Volcano, and that this magma (i.e. Pele in their oral traditions) could travel along subterranean pathways to erupt on Kīlauea’s lower flanks.

The Bible is also a source of possible volcano legends. The Old Testament (Genesis 19: 24–26) speaks of a possible volcanic eruption in the Israel–Jordan region (Chapter 13), and a “pillar of fire” is mentioned in Exodus 13:21–22 – could this also be an eruption reference? Geologic studies indicate that the volcanoes of these areas near the Dead Sea erupted long before the time of biblical stories, but perhaps the writers of these words had known about volcanic activity that did occur nearby in Old Testament times – on the Arabian Peninsula and in the Red Sea? Another volcano figures in the account of Genesis 8:5: “On the seventeenth day of the seventh month after The Flood, Noah’s arc landed on Mount Ararat . . . [a dormant



Fig. 1.16 Mount Ararat, a dormant volcano in northeastern Turkey, viewed from the north in Armenia. This is the volcano where Noah's arc is reported to have landed after The Flood (photographer unknown).

5165 m volcano (Fig. 1.16)].” On the first day of the tenth month after The Flood the top of a nearby, younger volcano appeared above the receding waters (see Fig. 1.16), but probably Noah did not appreciate the volcanological significance of his historic expedition! Some eruptions may be the source of legends that have lost their volcanic affinities, such as the possible volcanic destruction of the “Lost Continent of Atlantis” (Chapter 13).

As classical Greek civilization spread across the Mediterranean 2500 years ago, a panopoly of gods were devised to explain the natural world. **Hephaestus** (εφέαττος) was the son of the all-powerful god Zeus, but had been thrown down from heaven by his father after an argument and was condemned to spend his days on (and within) the Earth. He was badly injured on landing, and although lame and ugly (Fig. 1.17), he was a gentle god and became responsible for all artisans, including weavers, sculptors, and blacksmiths. To forge metal, he sought fire in the Earth and was henceforth associated with active volcanoes of the Mediterranean. When the Roman Empire vanquished Greek civilization 2200 years ago, they accepted many of the Greek gods as their own, but gave them different assignments to suit their imperial needs. They renamed

Fig. 1.17 Hephaestus, Greek god of blacksmiths and other artisans, later named Vulcan by the Romans. Sculpture by R. Spada. Photo J. P. Lockwood.





Fig. 1.18 Vulcan, the Roman god of volcanoes and blacksmiths, as depicted by a 17 m-high statue in Montgomery, Alabama, where it looms above Vulcan Park, in honor of Birmingham's steel industry. This is the world's largest cast iron statue, and is much larger than any Vulcan statues found in Italy. Photo by M. L. Kennedy, courtesy of Vulcan Park Foundation.

enters were courageous to look beyond the supernatural in seeking explanations for natural phenomena, and they paved the way for the Age of Science that was about to unfold. By the mid eighteenth century, academic discussion began to focus on an explanation that volcanoes are the products of erupted molten material formed deep inside the Earth. At that time, French geologists, notably Jean-Etienne Guettard (1715–86) and Barthelemy Faujas de Saint-Fond (1741–1819) recognized the volcanic origin of various cones and craters in the Clermont-Ferrand region of south-central France. They recognized the existence of former volcanoes in a landscape, and came to epitomize the *School of Volcanists* – those who believed that volcanic activity had been more common in the world than people imagined.

Abraham Gottlob Werner (1749–1817), a German professor of mineralogy from the School of Mines in Freiburg, developed a competing **geognosic theory** of geology, based on biblical interpretation that was widely embraced by the religiously conservative “establishment” of the day. He posited that the earth had cooled solid long ago (forming granites and metamorphic rocks), but had later been covered by a primitive, global, ocean from which all stratified rocks and minerals making up the crust (including lava flows) precipitated. Fossils in

Hephaestus *Vulcan* (Fig. 1.18) and his duties were focused only on the forging of metal; he became responsible for manufacturing swords and armor. His principal forge was beneath the active island-volcano north of Sicily named Vulcano which has lent its name as a descriptive term to all other volcanoes of the Earth and to the science of volcanology. Roman philosophers made many important speculations about the origins of volcanoes (Macdonald 1972), but the decay and fall of the Roman Empire marked the end of an interest in natural explanations for natural phenomena. The Western world then plunged into a dark millennium where only religious dogmas were allowed to flourish. Active volcanoes were considered to be gateways to Hell and were thus to be avoided!

THE AGE OF ENLIGHTENMENT

Around 600 years ago, as the Renaissance dawned, men began to seek more logical natural phenomena to explain volcanic activity, but encountered stiff opposition from conservative authorities who preferred religious interpretations. Non-believers in prevailing dogma could be condemned to death for heresy. Early alchemists (who spent most of their efforts attempting to transform materials into gold) attributed volcanoes to pent-up gases ignited by burning coal, sulfur, or oil, to electricity, or to frictional heating of air blowing through confined passages. Because of their inability to travel or to explore, they never made field observations. While their ideas might seem strange to us today, these experim-

some strata, though absent in lava flows, were good evidence of marine origin. Volcanoes were merely anomalies, associated with burning coal deposits. There were, Werner pointed out, extinct volcanoes in the Bohemian coal fields – evidence that burning coal had produced them. A powerful public speaker who held his post for 40 years, Professor Werner did not travel more than a few tens of kilometers from his home town and so, like most of his predecessors, was hampered by lacking solid physical evidence for his hypotheses. But his logic, though misplaced, was internally consistent, and he was very persuasive. His theory fit in well with religious belief in a Great Flood, and Werner's perspectives became known as the **Neptunist** School. Meanwhile, resulting from these observations, an epic controversy arose between Werner's Neptunists and many of the leading scientists of the day. Even the great German poet Goethe (an accomplished naturalist in his own right, who had climbed Vesuvius [79] and observed erupting lava during a spectacular eruption in 1787) questioned the popular conclusions of Werner (see the epigraph for Chapter 3).

The leading opponent of Werner's theories was James Hutton (1726–97), an influential Scottish geologist with great field experience, who had seen undeniable proof that many igneous rocks had been intruded into sedimentary rocks from below – an impossibility if the layered rocks were younger. Hutton and his fellow disbelievers were called **Plutonists**, and were much disparaged by their opponents. Hutton was honest about the limits of his knowledge, and respected the limits of what is knowable, unlike some of his scientific predecessors. In 1788 he wrote: “Our knowledge is extremely limited with regard to the effects of heat in bodies, while acting under different conditions, and in various degrees.” He knew that molten rock is active in earth's crust but did not pretend to know why. It would take nearly two centuries and much additional scientific controversy before answers emerged, thanks to the development of new geophysical techniques for examining the earth's interior and to the discovery of plate tectonics in the 1960s (Chapter 2).

One of Werner's influential students was Leopold von Buch (1774–1853). Although originally a staunch Neptunist, he traveled extensively and made observations of volcanoes and lava flows in Italy and France that seemed to have no relation to the presence of coal beds required by Werner as a causative agent for volcanism. His further observations of lava flows in the Canary Islands in 1815 showed that they were too obviously related to volcanoes and not to sedimentary processes, and he finally broke with his professor and became an avid supporter of the Plutonist school. Unfortunately, he went too far and began to posit that the intrusion of molten material from below caused the *uplift* of many volcanoes and even mountain ranges like the Alps! He developed a widely accepted “Craters of Elevation” theory which sought to explain the inclined lava flows around volcanoes as evidence that volcanic landforms were caused by internal magmatic intrusions that uplifted and deformed originally flat-lying lava flows.

THE EMERGENCE OF MODERN VOLCANOLOGY

Volcanic action exhibits itself chiefly in the eruption or exhalation of heated matter in a solid, semi-liquid, or gaseous state, from openings in the superficial rocks that compose the crust of the globe. (Scrope 1862)



Fig. 1.19 George Poulett Scrope.
Photo © Natural History Museum, London.



Fig. 1.20 James D. Dana, “America’s first volcanologist.” Dana devoted his life to the study of volcanoes and mineralogy, and was editor of the *American Journal of Science*. Lithograph by Rudolph Hoffmann – after photo by Matthew Brady, Courtesy of Yale University Library.

The modern science of volcanology began to develop in the early nineteenth century, after the fundamentals of geology had been established by geologists of the preceding century. The first scientist to devote most of his life to the study of volcanic activity was George Poulett Scrope (1797–1876) (Fig. 1.19). Scrope was a cosmopolitan, well-educated gentleman who made contributions to many fields in addition to volcanology; he is also known for his writings in economics and for his pioneering social work. He studied at both Oxford and Cambridge, there under the pioneer geologist Adam Sedgwick. He was a friend of Charles Lyell, and like Lyell realized the critical importance of fieldwork. He was fascinated by active volcanism and spent his early years observing the active volcanoes of Italy, carefully observing eruptive activity at Stromboli [83] and Etna [82] and studying the eruptive products of Vesuvius and the Phlegraen fields. In later years he went on to study older volcanoes near Rome and the extinct volcanic fields of France and Germany. Although born George Julius Thomson, he married the wealthy heiress Emma Phipps Scrope in 1821, changed his last name, and was elected to Parliament where he worked tirelessly to improve the welfare of England’s poor. While still a young man in 1826 he published the first-ever modern textbook in volcanology, entitled *VOLCANOES – The Character of their Phenomena, their Share in the Structure and Composition of the Surface of the Globe, and their Relation to its Internal Forces: with a Descriptive Catalogue of all known Volcanoes and Volcanic Formations* (Scrope 1862). Scrope made many important observations, including a recognition of the role of water (steam) as the driving force of explosive eruptions. He also became a partisan in the raging debate over von Buch’s “craters of elevation” theory, using his wealth of field studies to refute von Buch’s ideas. Scrope and his contemporary Charles Lyell together proved the essential role of careful field studies, and paved the way for the major advances in volcanology that were about to occur as a new generation of geologists began systematic exploration of active volcanoes around the world.

James D. Dana (1813–95) (Fig. 1.20) studied under Benjamin Silliman at Yale, traveled to the Mediterranean after graduation, witnessed an eruption of Vesuvius, and had already authored his classic *System of Mineralogy* when he was selected (at age 25) to join the US Exploring Expedition, the “Wilkes Expedition,” for a four-year scientific exploration of the Pacific Ocean. This four-year voyage gave Dana a global perspective of volcanology, and enabled him to recognize the evolution of young volcanic islands through old age and eventual submergence beneath atolls. During Dana’s month-long stay in the Hawaiian Islands in 1840–1, he saw Kīlauea in eruption and met the “missionary volcanologist” Titus Coan (Chapter 5). This friendship was to prove seminal in fostering his life-long interest in volcanology. Returning to Yale University to teach, he married Benjamin Silliman’s daughter Henrietta, later became Chairman of the Department of Geology and Editor of the influential *American Journal of Science*, where he ensured that many classic volcano studies were published. After publication of his classic *Characteristics of Volcanoes* in 1890, Dana became generally regarded as America’s first volcanologist.



An important development was about to revolutionize volcanology – the development of a worldwide telegraph system in the last half of the nineteenth century. The telegraph made it possible for news of volcanic eruptions in far-away places to reach scientists in near real time and for expeditions to be mounted to investigate major eruptions. The cataclysmic 1883 eruption of Krakatau volcano was reported around the world almost before the tsunami waves had receded, and major international expeditions were soon mounted to begin investigations of the tragedy. The report of the Dutch expedition to their colony (Verbeek 1895) was the most comprehensive documentation of a major volcanic eruption that had ever been prepared. The contrast between the reporting of the Krakatau eruption with the lack of documentation of previous major devastating eruptions (e.g. Asama – 1783 or Tambora – 1815) is revealing. Before the Age of Communications began less than 200 years ago, news of major eruptions never reached the scientific community.

Mt Pelée [63] rose with apparent innocence above the island of Martinique in the southeastern Caribbean in 1902. Although the mountain had been “smoking” for a long time, and earthquakes had been shaking the island for months, residents of the important city of St Pierre did not realize that Mt Pelée was a dangerous volcano about to erupt. When the volcano did erupt violently on May 8, 1902, almost 30,000 people lost their lives (Fig. 1.21). The entire world was shocked by the tragic loss of life, and scientific commissions flocked to Martinique to investigate the tragedy. The Mt Pelée eruption was one of three large eruptions around the margins of the Caribbean in 1902 (devastating eruptions also occurred that year at La Soufrière-St Vincent¹ [62] and Santa Maria [46] volcanoes), and was soon followed by another devastating eruption of Vesuvius volcano in 1906. These eruptions at the dawn of the twentieth century focused the world’s attention on volcanic activity, had a major impact on the development of volcanology, and would change the careers of three people who were not volcanologists at the time. These three men, Lacroix, Jaggar, and Perret, had never considered the study of volcanoes particularly important before 1902, but would go on to make major contributions to volcanology as they bridged the gap between two centuries.

François Alfred Lacroix, (1863–1948) (Fig. 1.22) was a well-known French mineralogist who had never studied volcanoes before he was sent to Martinique after the 1902 disaster.

Fig. 1.21 Ruins of St Pierre, Martinique, after the devastating eruption of Mount Pelée in 1902. Photo by C. D. Arnold, courtesy of US Library of Congress.

¹ There are two volcanoes named “La Soufrière” in the Lesser Antilles – this one, more specifically referred to as “La Soufrière-St Vincent,” and another 300 km to the north on the island of Guadeloupe.

Fig. 1.22 Alfred Lacroix (second from left) inspecting pyroclastic flow deposits above St Pierre, Martinique after the 1902 Mt Pelée disaster. It was here that Lacroix coined the term “nues ardentes” to describe the PDCs that form such deposits. Photo from the Krafft Archives.



He spent a year on the island, conducted critical interviews of eye-witnesses, and published the most detailed reconstruction of the events that preceded and accompanied the eruption. He was the first to recognize the nature of the deadly flowing clouds of hot gas and rock that he named “*nues ardentes*,” an internationally used term equivalent to “pyroclastic flows”. He founded the Observatoire Volcanologique de la Montagne Pelée and went on to study the major eruption of Vesuvius in 1906. Although mainly known for his contributions to mineralogy, he continued to advise the French Government about volcanic crises for the rest of his life. His meeting with Thomas Jaggar in the ruins of St Pierre was doubtless a factor in the evolution of Jaggar’s career.

Thomas A. Jaggar (1871–1953) (Fig. 1.23) was a young Harvard geology professor in 1902 and had made important studies of many geologic processes – but had never seen a volcano. Following the tragic eruption of Mt Pelée in 1902 he was dispatched on an emergency mission to Martinique by the US Government. Although he only spent a few weeks there, the experience of walking among the ruins of St Pierre and viewing the corpses of thousands of victims still lying in the ruins completely changed his life. As he wrote in his biography (1956):

As I look back on the Martinique expedition, I know what a crucial point in my life it was and that it was the human contacts, not field adventures, which inspired me. Gradually I realized that the killing of thousands of persons by subterranean machinery totally unknown to geologists and then unexplainable was worthy of a life work.

His career did indeed change and the rest of his life was devoted to the study of volcanoes. He made several volcano expeditions in the next few years: to Vesuvius (1906), to the

Aleutian volcanoes (1907), to Hawai'i and Japan (1909), and to Costa Rica (1910) in order to gain understanding of volcanic activity and hazards. His 1906 trip to Italy was especially important as he there met Frank Perret (see below) and Tempest Anderson (who had described the 1902 La Soufrière eruption), and again worked with Lacroix. He also learned about the important work of the historic Osservatorio Vesuviano, founded in 1841 (see Chapter 16). These expeditions convinced Jaggar that *expeditionary* volcanology (mostly after disasters) could never be successful for understanding the *processes* of volcanism. Without an understanding of volcanic processes, there was no possibility of ever *predicting* eruptions, and prediction had to be the primary goal of what he termed "*Humanistic Geology*." He made fervent public appeals for the establishment of permanent observatories to continuously monitor volcanoes and seismic regions.

After the 1906 San Francisco earthquake disaster he succeeded in urging the Geological Society of America to pass a resolution calling on "Governments and private enterprise to establish volcano and earthquake observatories"; and, in a widely-read article in *The Nation* (1909), he decried the preoccupation of geologists with studies only of the past ("the bones of Jurassic reptiles, and in finding out all about iron and coal") and urged young men to devote their lives to "humane rather than historical" science. After his visit to Kīlauea volcano in 1909, he resolved to found a permanent volcano observatory there, and spent the next three years raising funds to accomplish his goal. He took "leave of absence" from MIT in 1912, left his family behind, and moved to Kīlauea to found the Hawaiian Volcano Observatory (HVO). He never returned to MIT (nor to his first family), and the rest of his life was devoted to assuring that the HVO record of volcano observation would be unbroken. He was a prolific writer on many subjects besides volcanology, an avid inventor of new devices for volcano monitoring, and an eloquent spokesman for his "humanistic" beliefs. He was *not* a very good observer, however, and his descriptions of Hawaiian volcanic eruptions are so entwined with his interpretations that they are of limited value today. As Gordon Macdonald told me (JPL) in frustration one day, "Jaggar always thought like a promoter, not like a geologist – he never made a map to let us know what happened!"



Fig. 1.23 Thomas A. Jaggar, founder of the Hawaiian Volcano Observatory, in 1928 alongside a prototype of the amphibious landing craft he invented. USGS photo from Hawaiian Volcano Observatory Archives.

Frank A. Perret (1867–1940) also was touched (more indirectly) by the Mt Pelée disaster and subsequently became one of the most fascinating of the early twentieth-century volcanologists. Perret never finished college, nor had formal training in geology, yet his contributions to volcanology in the form of his lucid descriptions of explosive volcanic activity are timeless. Perret was self-educated as an electrical engineer, worked directly with Thomas Edison, and later founded his own company in New York to manufacture electric motors and batteries. When word of the 1902 Mt Pelée disaster arrived in New York, his only previous awareness of volcanism was associated with his viewing the “amazing sunsets” associated with the 1883 eruption of Krakatau as a young man. His health began to fail in 1902, however, and while on a recuperation visit to the Caribbean, he stopped by Martinique to visit the ruins of St Pierre. Like Jaggat and Lacroix before him, Perret’s life was forever changed by the destruction wrought by Mont Pelée, and he devoted the rest of his life to the study of volcanoes.

To learn about active volcanism, he abandoned his business, traveled to Italy in 1904, and apprenticed himself to R. V. Matteucci, Director of the Vesuvius Volcano Observatory. He lived in Naples for 20 years, witnessed the devastating 1906 eruption of Vesuvius, and wrote

a classic description of the eruption and its effects (Perret 1924). He later became affiliated with the Carnegie Institution in Washington, DC, where all of his volcano studies were published. Although plagued by ill health, he traveled widely to active volcanoes of the world, and his frail, dapper figure, well-dressed with Van Dyke beard and straw hat (Fig. 1.24) became a well-known sight during volcanic eruptions. He traveled to Hawai`i with R. A. Daly and Thomas Jaggat in 1909, made some of the first ever quantitative measurements of molten lava temperatures, and was one of the first people to recognize the importance of explosive activity in Kilauea’s past. When Mt Pelée returned to activity in 1929, Perret returned to Martinique the following year to observe the activity and advise local residents about future activity. He lived in a shack high on the flanks of the volcano to better observe the activity, and was nearly killed by a nuee ardente in 1930. His nonchalant eye-witness accounts of this activity (see Chapter 7) make for some of the most exciting reading in the annals of volcanology.

Active volcanoes are found throughout the world, and it is no surprise that the major volcanologists of the twentieth century have come from countries facing the greatest eruptive perils.

Fig. 1.24 F. A. Perret with an improvised “seismometer,” listening to subterranean noises at the Campi Flegrei, Italy. Photo from the US Library of Congress.



Alfred Rittman (1893–1980) (Fig. 1.25) was born in Basel, Switzerland, and there met the wealthy Swiss banker Immanuel Friedlander, a widely traveled amateur volcanologist who published the influential journal *Zeitschrift für Vulkanologie* (1914–36), and privately founded the Institute of Volcanology based in Naples. Rittman was named the Director of Friedlander’s institute, and there pioneered the use of petrographic, geochemical, and geophysical methods to better understand volcanic processes; his studies of the magmatic evolution of Vesuvius and Etna were major contributions to the foundations of volcanology. When Friedlander’s institute closed on the eve of World War II, Rittman was offered a university position in Germany, but refused the appointment as he did not wish to associate with the Nazi Party. He taught for a while in Egypt, and later became Director of the Institute of Volcanology in Catania. His influential textbook *Volcanoes and their Activity* (1962) remains in use today. The English language reference cited here is a translation of the original *Vulkane und ihre Tätigkeit* (1936), which was also translated into French and Italian. His system for “Eruption diagrams” (see Chapter 5) is an excellent, but largely overlooked, graphical means to portray the nature of individual eruptions. He was one of the longest serving Presidents of the International Association of Volcanology and Chemistry of the Earth’s Interior (IAVCEI) from 1954 to 1963.

There are more than 30 active volcanoes in Russia, all part of the Pacific “Rim of Fire” extending from Kamchatka down the Kuril Islands. The Soviet Union produced many great volcanologists in the twentieth century to study these volcanoes, but because most of their publications are in Russian, and because Cold War complexities made travel for Soviet scientists and international exchanges difficult, not much has been known about their work. Georgii S. Gorshkov (1921–75) (Fig. 1.26) was able to travel widely and became well known in the west. He began his volcanological studies with extensive field work along the length of the Kuril Islands, and then began to study the numerous active volcanoes of Kamchatka. Gorshkov was primarily a volcano seismologist, and pioneered the study of *teleseisms* (earthquake waves generated by distant earthquakes) to define the geometries of magma chambers underlying closer volcanoes. He documented the 1956 eruption of Bezymyannii volcano [128] (Gorshkov 1959), a volcano whose pre-eruptive behavior closely mimicked the pre-eruptive behavior of Mount St Helens as that volcano approached its 1980 eruption. Unfortunately, volcanologists in Washington did not appreciate the similarity in eruptive style, and did not realize that the catastrophic eruption that was about to occur on May 18 was almost an exact duplicate of the catastrophic eruption precursors that Gorshkov described at Bezymyannii.



Fig. 1.25 Alfred Rittmann (1893–1980), pioneering Swiss volcano-petrologist who spent most of his life studying the magmatic evolution of Vesuvius and Etna. Photo by G. A. Macdonald.

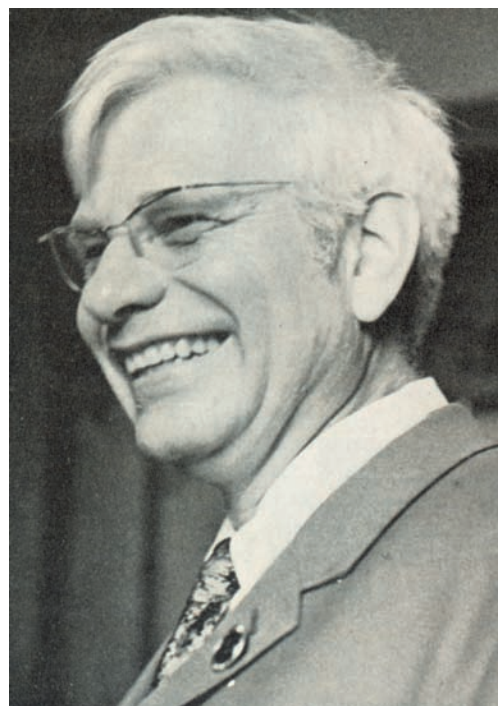


Fig. 1.26 Georgii S. Gorshkov, pioneering Soviet volcanologist. Photographer unknown.



Fig. 1.27 Professor Takeshi Minakami, the founder of modern Japanese volcanology and leading volcano seismologist. Photo courtesy of Shigeo Aramaki.

Japan is one of the most volcanically active areas on Earth, and has more than 40 on-land volcanoes that have erupted in historical time – almost 70 if one counts minor islands and submarine volcanoes in its territory. From a public safety standpoint, however, earthquakes have been a more serious threat to human life and property, and Japanese earth science was traditionally focused on the field of seismology. When Thomas Jaggard founded the HVO, he turned to Japan for expertise, and HVO’s original seismometers were designed by Fusakichi Omori (1868–1923), the pioneering Japanese seismologist whom Jaggard had met in 1909. Omori gave Jaggard one of his seismographs and plans for a seismic vault, and HVO’s Whitney Seismological Laboratory was constructed in accordance with these plans. Volcanology itself was not an important focus of Japanese science, however, until Takeshi Minakami (1910–83) (Fig. 1.27) was assigned to the Asayama Physics Research Laboratory on the slopes of Asama volcano [112] northwest of Tokyo in 1934. Minakami had trained as a seismologist at Omori’s Imperial University, but at Asama his interests in volcanology blossomed, and he can rightfully be called the “Father of Japanese Volcanology.” Asama was extremely active while Minakami was there, and with great effort (he needed to carry heavy batteries upslope to his laboratory for several years as there was no electrical service) he pioneered the field of volcano seismology. He recognized two different classes of volcanic earthquakes, and analyzing them allowed him to successfully forecast several eruptions. His “Minakami Classification” of type “A” (deep, sharp) and type “B” (shallow, long-period) volcanic earthquakes is now used worldwide to recognize the ascent of magma within volcanoes. Minakami’s visit to Indonesia before World War II was critical to enabling Indonesian volcano observatories to function during the war years under military occupation. His many students and junior associates have gone on to make Japan one of the world’s leading centers for volcano research. A historic visit of Minakami and his associates to HVO in 1963 for cooperative research studies set the stage for the close cooperation between Japanese and American volcanologists that continues today.

There are many recently deceased “pioneers” in volcanology whose contributions we should perhaps honor, but that list is long, and we must be getting on with the rest of this book. Suffice it to say that most of today’s volcanologists owe their careers to the influence of great teachers who have passed away in recent years. These teachers include giants like Robert Decker, Peter Francis, Dick Stoiber, and George Walker – dear friends and incredibly productive volcanologists whose contributions to our science and to hundreds of their students are immense and long-lasting.

FURTHER READING

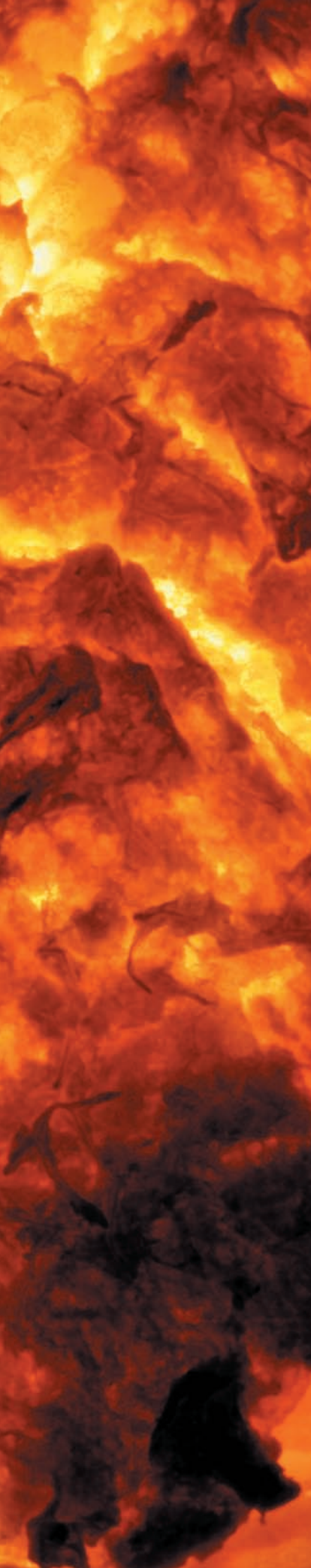
- Gourgaud, A. et al. (1989) The 1982–83 eruption of Galunggung (Indonesia) – A case study of volcanic hazards with particular relevance to air navigation. *Volcanic Hazards – Assessment and Monitoring*, 151–62.
- Lockwood, J. P. et al. (1999) *Magma Migration and Resupply During the 1974 Summit Eruptions of Kilauea Volcano*. Hawai'i. US Geological Survey, US Government Printing Office.
- Parfitt, E. A. and Wilson, L. (2008) *Fundamentals of Physical Volcanology*. Oxford, Blackwell.
- Sigurdsson, H. (1999) *Melting the Earth: The History of Ideas on Volcanic Eruptions*. Oxford, Oxford University Press.
- Sigurdsson, H. (2000) *Encyclopedia of Volcanoes*. San Diego, Academic Press.
- Simkin, T. and Siebert, L. (1994) *Volcanoes of the World*. Tucson, Geoscience Press in association with the Smithsonian Institution Global Volcanism Program.
- Tilling, R. I. et al. (1987) The 1972–1974 Mauna Ulu eruption, Kilauea Volcano: An example of quasi-steady-state magma transfer. In R. W. Decker, T. L. Wright, and P. H. Stauffer, (eds.), *Volcanism in Hawai'i*: US Geological Survey Professional Paper 1350, vol. 1, pp. 405–69.
- Tootell, B. (1985) *All Four Engines Have Failed: The True and Triumphant Story of Flight BA009 and the Jakarta Incident*. London, Andre Deutsch Press.

Chapter 1

Questions for Thought, Study, and Discussion

- 1 Outline the major differences between the eruptions of “red” and “grey” volcanoes. Why are these volcanoes designated with these colors?
- 2 Contrast the hazards of doing volcanological field work at Kīlauea and Galunggung volcanoes. Do you think it would be any easier to have a serious accident studying one volcano or the other? Explain your answer.
- 3 Why is the definition of a volcano simply as a “mountain or large hill that erupts” inadequate?
- 4 Would you define “volcano” any differently than we have? Why, or why not?
- 5 What are the two largest kinds of volcanoes, and how would you recognize each? What are three smaller kinds of volcanoes, and how are they distinguished?
- 6 A steep-sided volcano consisting of many layers of hardened lava alternating with beds of cinder suddenly rips open with a sluggish flow of molten rock pouring out of a crack extending down its flank. No ejecta are disgorged and volatile release is minor. (a) What kind of volcano is this? (b) What kind of vent opened up? (c) What kind of eruption is this?
- 7 Eruptions of highly fluid lava with very little associated pyroclastic material create what kinds of volcanic features?
- 8 Contrast the Neptunist and Plutonist schools of thought. What evidence finally allowed the Plutonists to overcome the Neptunists?
- 9 There are admirable goals and benefits to both “pure” volcanological research focused on the expansion of human knowledge, and to “applied” volcanology focused on the immediate social and economic needs of society. What is the proper balance between these two end uses of volcanology? What balance would *you* hope to strike if you pursue a career in volcanology?





PART II

THE BIG PICTURE

This Part consists of three chapters that describe the global environment in which volcanism operates on the surface of the Earth, including the revolutionary impact of on the Earth Sciences, and the nature of “magma” (molten rock below the Earth’s surface) – how magma is generated, and how it ascends to the surface. **Chapter 2** discusses the realization that our Earth has a dynamic, ever-changing surface upon which volcanoes play vital roles, describes the various tectonic environments in which volcanoes occur and how they differ depending on these environments. **Chapter 3** discusses how magmas form, how they cool to form volcanic rocks, and the all-important role of volcanic gases – important but often overlooked magmatic constituents. **Chapter 4** describes the physical properties of magmas, how they reach the surface of the Earth, and the mechanisms that trigger volcanic eruptions – “why volcanoes erupt.”

Chapter 2

Global Perspectives – Plate Tectonics and Volcanism

A map of the Earth on which the position of volcanic vents is marked shows at a glance that their distribution can hardly be a matter of chance.
(Bonney 1899)

Birth of a Theory

In the decades following the triumph of the Plutonists over the Neptunists (Chapter 1), geologists established a broad consensus that there are three fundamental kinds of rocks making up Earth's crust and surface. James Hutton proved that **igneous** rocks form from the cooling of magma. (The term “igneous” ultimately stems from a Sanskrit root, *agni*, meaning “fire.”) **Sedimentary** rocks are formed by the deposition and compaction of loose sediment resulting from weathering, erosion, and transport of rock fragments, or by the evaporation and chemical precipitation of saline waters. Either sedimentary or igneous rocks may further be transformed through compaction, heating, and mineralogical changes into **metamorphic** (“changed”) **rocks** by deep burial and deformation. By the middle of the nineteenth century, geologists also sensed that rock materials could in time be recycled through all three states – igneous, sedimentary, and metamorphic – in a process that eventually came to be called the **rock cycle**. The modus operandi of the rock cycle remained a mystery, however, as did the strange distribution of one great subclass of igneous rocks – the volcanic rocks.

For nearly two centuries after the birth of modern geology, no one could explain why volcanoes occur where we find them. In 1945, for example, Thomas Jaggar wrote the following about the chains of volcanoes fringing the Pacific Rim (Jaggar 1945, p. 1):

Volcanoes: Global Perspectives, 1st edition. By John P. Lockwood and Richard W. Hazlett. Published by Blackwell Publishing Ltd.

The Pacific girdle of fire is the most systematic series of partitions on the globe, dividing its surface by means of downgoing, upright, lava-filled fractures. Such a partition goes down perhaps 1800 miles to the core of the globe between Alaska and Patagonia, between Kamchatka and Java, divided into curved cracks in plan; no one knows “why” . . .

Then, with stunning rapidity and from sources wholly unexpected, the great “why” posed by Jaggard was answered. Like so many seminal leaps forward in science and technology, it took modern techno-industrial warfare to develop the new research tools and funding that allowed people to explore new fields and investigate areas that they might otherwise have ignored. In a mid-twentieth-century effort to improve ways of locating and tracking enemy submarines, researchers used sonar to map the bathymetry of the deep sea, and ship-towed magnetometers to plot ocean floor magnetic properties – important for navigational purposes. Several astonishing results emerged. Most spectacularly, investigators confirmed that the major ocean basins are crossed by a system of gigantic, undersea mountain belts called the Mid-Ocean Ridge (MOR). Parts of this enormous feature had been discovered a hundred years earlier by soundings in the central Atlantic, but the interconnectedness of it all had not been appreciated at the time. It wound around the whole planet, like the seam on a giant baseball, sending out branches here and there that could be related in a simple glance of the map to noteworthy features such as the Gulf of California and the East African Rift Valley.

Scientific breakthroughs are often nurtured by coincidental factors, and such events combined to focus the life’s work of one of the twentieth century’s most influential geologists – Harry Hess (Fig. 2.1). Hess was a graduate student at Princeton University in 1931, when he was asked to accompany the Dutch oceanographer F. A. Vening Meinesz on a submarine expedition to measure gravity fields in the Lesser Antilles. This was Hess’s introduction to a lifelong interest in the origin of ocean basins, and initiated his wonderment about why oceanic trenches were marked by major gravity lows. His PhD dissertation on serpentinite belts of the Appalachians raised further questions about the role of ultramafic rocks in certain mountain

ranges. Then, as a US Navy Captain during World War II, he discovered strange, flat-topped seamounts on the Pacific floor that he named **guyots** (pronounced “GEE-ohs”), whose summits all seemed to systematically deepen with distance from the MOR. The summits of these guyots were later found to be composed of coral reefs and associated lagoonal deposits, which develop in shallow water. Because of this, Hess reasoned, some unknown process active in the ocean floor must be submerging them deeper the farther one travels away from the ridge crest. Indeed, the *whole ocean floor*, not simply the guyots, deepened.

Likewise, new undersea mapping refined the understanding that some ocean basins are bordered by deep **marine trenches**. These were parallel to long, gracefully curving archipelagos characterized by active volcanoes, called **island arcs**, though in some places the trenches are close to continental shorelines, as along the coast of South America.

Finally, researchers found that ocean floor lavas preserved a record of past reversals in Earth’s magnetic field. **Magnetic reversals** happen when the Earth’s magnetic polarity (referring to the positions of the north and south magnetic poles) suddenly flip. The North Magnetic Pole suddenly becomes the South

Fig. 2.1 Harry H. Hess, originator of the “seafloor-spreading” hypothesis. Photo courtesy of Princeton University Library.

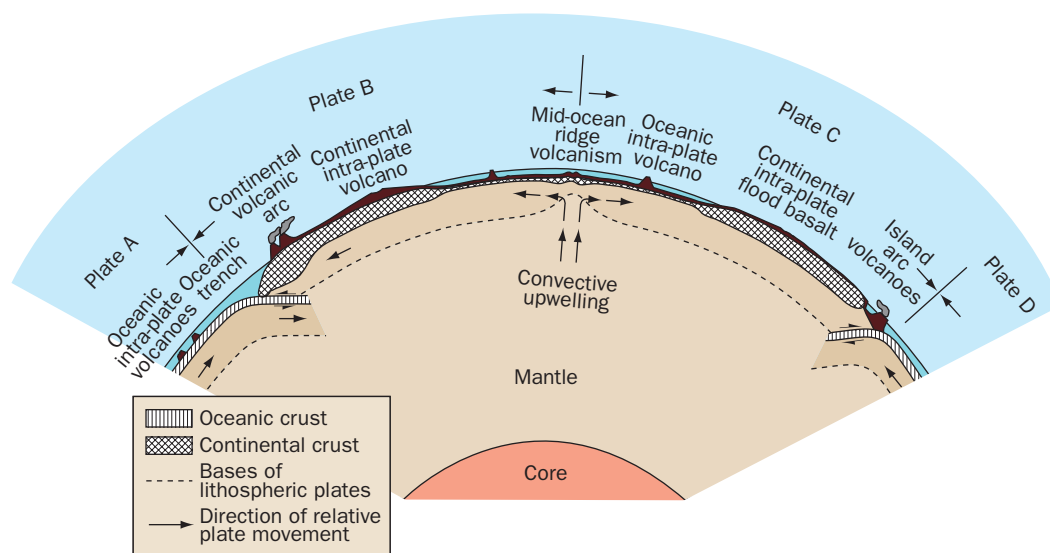


Magnetic Pole, and visa versa. Lava flows contain magnetic minerals such as magnetite, and when these flows cool, these internal magnets record ambient magnetic field directions and intensities, Lava flows thus record the history of the Earth's magnetic field, and show the most recent field reversal about 700,000 years ago, with prior reversals occurring thousands of times in Earth's distant past. By the late 1950s, enough data had accumulated to begin showing a remarkable pattern of reverse-normal magnetic stripping parallel to and symmetrical about the MOR, recording a history of pole reversals going back nearly a hundred million years.

Sir Arthur Holmes, one of the greatest geology teachers and thinkers of the past century, provided a speculative explanation for all these later observations around the time that Vening Meinesz was doing his early gravity work in the late 1920s. He postulated that great cells of convecting hot rock welled up from the deep earth to stretch and tug at Earth's crust beneath continents. The crust fractured to reveal underlying basaltic crust and to form new oceans, which then drifted away riding piggy-back on outward-sweeping convection currents. As the shifting sea floor descended at continental margins it converted to dense eclogite, which helped to maintain convective circulation. Holmes failed to realize the young age of the oceans, but his ideas did presage later models for global plate tectonics. Unfortunately, Holmes was too far ahead of his time with these revolutionary ideas. The related observations of a well-known contemporary, Alfred Wegener, were being severely attacked by many influential professional geologists. Wegener had postulated in 1911–12 that Earth's continents had drifted apart from one another over time. What else could explain the trans-oceanic coincidences in the distributions of many fossils, mineral deposits, and geographical features such as the "fit" of western Africa's coast with that of eastern South America? His **continental drift** theory suffered from lack of a testable, even "reasonable" explanation, and was generally ridiculed. Wegener – a meteorologist by training – suggested that inertial forces caused by Earth's rotation were responsible for the separation of continental fragments and the opening of oceans such as the Atlantic. But geophysicists quickly demonstrated this couldn't possibly be happening, given the well-tested strength and mechanical properties of rocks. Continents didn't "plow through the ocean bed," like ships moving through the sea, as Wegener suggested. No matter the stronger merits of Holmes' insights, the rebuke of Wegener rung in his appropriately cautious ears.

Harry Hess enters the story again, however, by taking the newly discovered information of the 1940s and 1950s, brushing off the older model of Holmes, combining with his own oceanographic observations, and giving it a respectable update. Holmes was on the right track, Hess concluded. The paleomagnetic, bathymetric, radiometric, and gravity data all showed it. In 1960 he informally printed and distributed to colleagues a new, well-integrated view of how the world works, arguing that the creation of new crust through magmatic intrusion and volcanic activity at the MOR provided a suitable explanation for Wegener's continental drift (Hess 1960). Moreover, he proposed that the ocean floor was destroyed wherever it entered the trenches, its atoms to be recycled slowly in Earth's perpetually overturning interior (Hess 1960). The high-standing continents were simply passive passengers in the process, embedded *within* rather than plowing *through* the surrounding oceanic crust. He called his explanation, which was not formally published until 1962, "an essay in geopoetry." In a companion paper Fisher and Hess (Fisher and Hess 1963) also correctly proposed that volcanoes of arcuate island chains were evidence of melting above the zones where oceanic crust sank back into the deep Earth.

Fig. 2.2 Schematic Earth cross-section, showing locations of volcanoes relative to major plate tectonic features. Vertical scales are distorted.

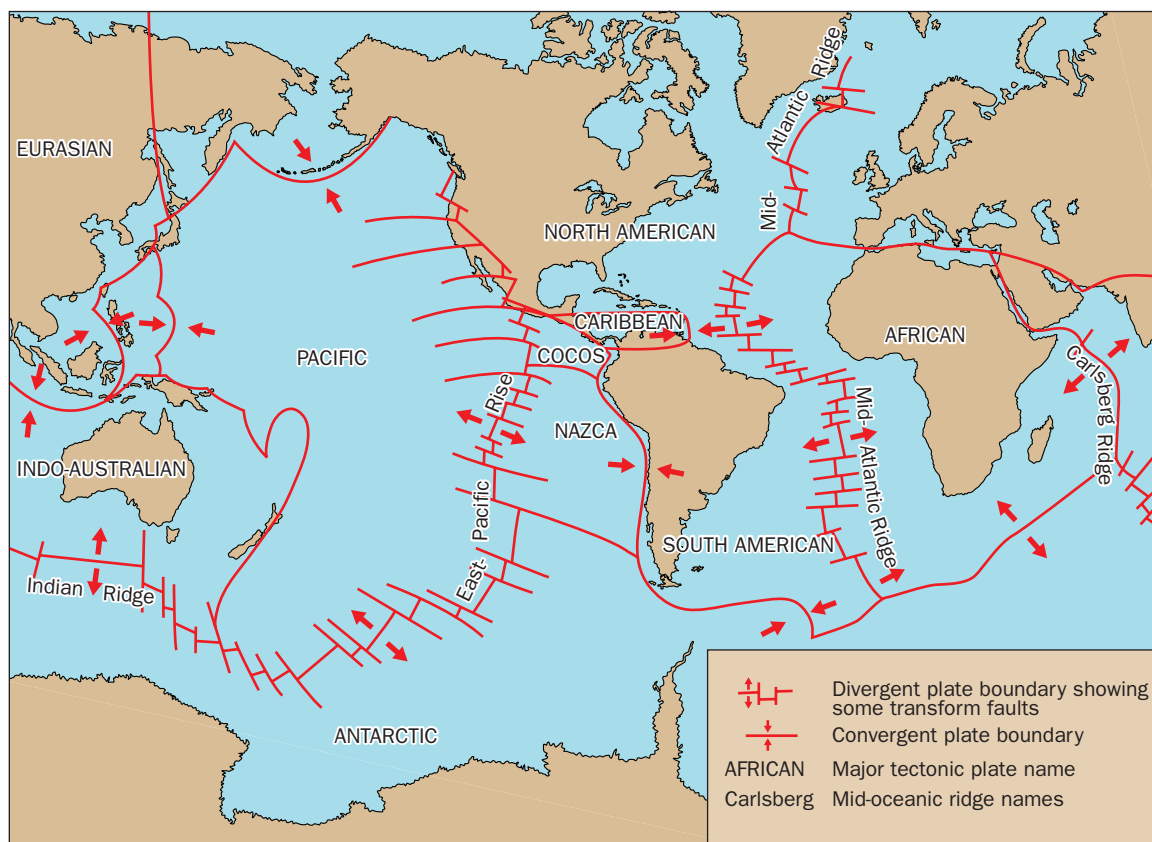


Hess's theory was testable, and in succeeding years verifications of his basic model have come from diverse fields, including paleomagnetism, seismology, paleontology, geochronology, and geodesy. His model, referred to as *sea-floor spreading* by others, provided the fundamental conceptual framework for an integrated approach to global analysis of tectonics and volcanism (Fig. 2.2). The Earth's crustal structure is much different from, and more complex than, that imagined by Hess, but his "geopoetry" remains as the basis for the "plate tectonics" revolution of earth sciences, which at last has explained the order in volcano distribution puzzled at by Bonney.

By 1968, the revolution in new understanding was complete, and the world's first holistic theory of how our planet works became popularly known as **plate tectonics**. "Tectonics" derives from the Greek work for "builder," *tekton*, and the term "plate" originated with Vening Meinesz to describe areas of ocean floor that are enclosed by prominent features such as the MOR, trenches, and the edges of continental shelves. The "type plate" identified by Meinesz was the Caribbean Basin. "Plate" now refers to any coherent area of the Earth's shallow layering, whether continental or oceanic, that is capable of independent movement relative to other plates.

It is now generally accepted that the Earth's outer surface is segmented into about a dozen major plates (and numerous minor ones) which are continuously being slowly moved about by mantle convection at speeds ranging from a few millimeters to several centimeters per year (Fig. 2.3). These plates vary from less than 50 to perhaps 200 km in thickness and have their bases in a zone of low seismic wave transmission velocities, termed the **Low Velocity Zone** (LVZ), in the upper mantle (Condie 1982). The plates consist of Earth's crust plus a layer of rigid upper mantle. Geophysicists call this combination of crust and upper mantle slice the **lithosphere** (from the Greek *lithos* "rocky" plus *sphaira* "sphere"). The plastic, partially molten layer beneath the lithosphere is the **asthenosphere** (from the Greek *asthenēs* "weak" plus *sphaira* "sphere") (Fig. 2.4).

Three fundamental kinds of plate interactions take place in response to underlying mantle convection: **divergent**, **convergent**, and **transform** plate boundaries. Because little, if



any, volcanic activity takes place along transform plate boundaries (**strike-slip faults**), we will not discuss them further.

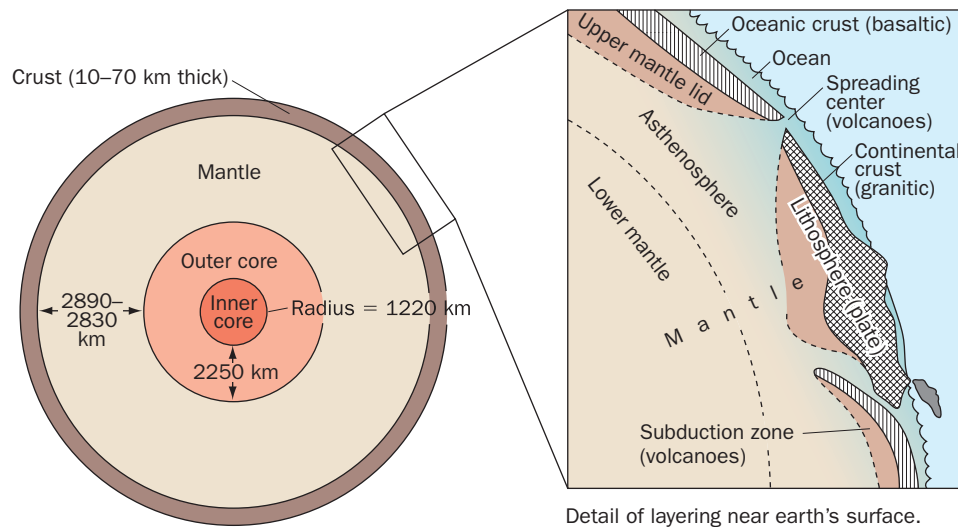
Divergent plate boundaries exist where plates separate, as through sea-floor spreading. “Spreading center” is a synonym for divergent plate boundary, but this term is a bit misleading, since the formation of new crust through volcanic activity occurs along a boundary *line* and not a *center*. Most divergent plate boundaries occur on the ocean floor, because oceanic crust covers a larger percentage of Earth’s surface than continental crust, and because the lithosphere beneath oceans is thinner and weaker than it is in continental areas. Most of the world’s volcanic activity occurs along divergent plate boundaries, though it takes place largely unseen beneath the world’s oceans.

Convergent plate boundaries exist where plates collide (Fig. 2.5). Most of these boundaries lie near the edges of ocean basins, because the contact between continental masses and the sea floor tends to be structurally weak. Lithosphere weighted with dense, heavy oceanic rocks will generally plunge beneath continental lithosphere as continental and oceanic plates collide, since continents are constructed of lower density rocks.

In some regions convergent plate boundaries trend across oceanic basins. The over-riding oceanic plate is generally smaller than the plate sinking beneath it, and in most cases is rigidly attached to a nearby continental land mass. The body of water atop the over-riding plate is termed a **marginal sea**. Numerous marginal seas, such as the Sea of Japan, for example, fringe the western Pacific Ocean.

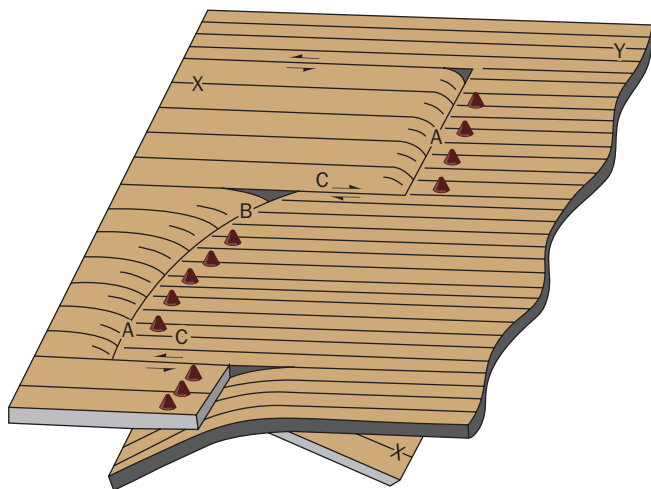
Fig. 2.3 The Earth’s major tectonic plates and mid-ocean rises, showing divergent, convergent, and major transform fault boundaries. Effusive volcanoes tend to occur at divergent plate boundaries and explosive volcanoes tend to occur at convergent plate boundaries. Compiled from various sources, including Heirtzler (1968, p. 59) and McClelland et al. (1989). See the map at the end of this book for more details.

Fig. 2.4 Layering inside the earth.



Detail of layering near earth's surface. Note that the boundary between the asthenosphere and lithosphere do not correspond to the boundary between the mantle and crust. The lithosphere (making up the "plates") includes all of the crust plus a slice of the uppermost mantle). See text for discussion.

Fig. 2.5 Various geometric configurations for boundaries between convergent plates ("X" and "Y"), showing most common volcano loci. A = subduction normal to plate convergence, B = Subduction oblique to plate convergence, C = Transform (strike-slip) fault boundary. Modified from Gill (1981, p. 391).



Subduction (meaning "under-moving") is the term used to describe the processes whereby one plate dives under another. Deep marine trenches stretching from hundreds to thousands of kilometers typically mark the sites of subduction on the Earth's surface. Individual trenches may be several tens of kilometers wide and as much as 7 km deep relative to the surrounding ocean floor. Some trenches lying close to large river mouths, such as the Columbia River in the northwestern United States, fill with sediment, and cease to be expressed as depressions in the Earth's surface. They nevertheless remain "trenches" purely from the standpoint of tectonic behavior, since the underlying bedrock continues to bend and sink along these loci, carrying considerable amounts of sediment mixed with seawater down into the mantle. Trenches appear arcuate on maps, simply owing to the fact that the intersections of curving surfaces on a sphere will form arcs.

The relationship of subduction to volcanic activity, as noted by Hess, will be explored further later. For the present, it is important to note that most oceanic trenches have parallel belts of volcanoes rising along the fringes of the over-riding plates (Fig. 2.6). The distance between the trench and the volcanic belt, termed the **arc-trench gap**, is a function of the steepness of the subduction zone, with smaller arc-trench gaps associated with more steeply subducting lithospheric slabs. This implies that processes responsible for creating subduction zone magmas must occur at nearly the same depth inside the earth. Plates that subduct at very shallow angles (less than about 15°) have

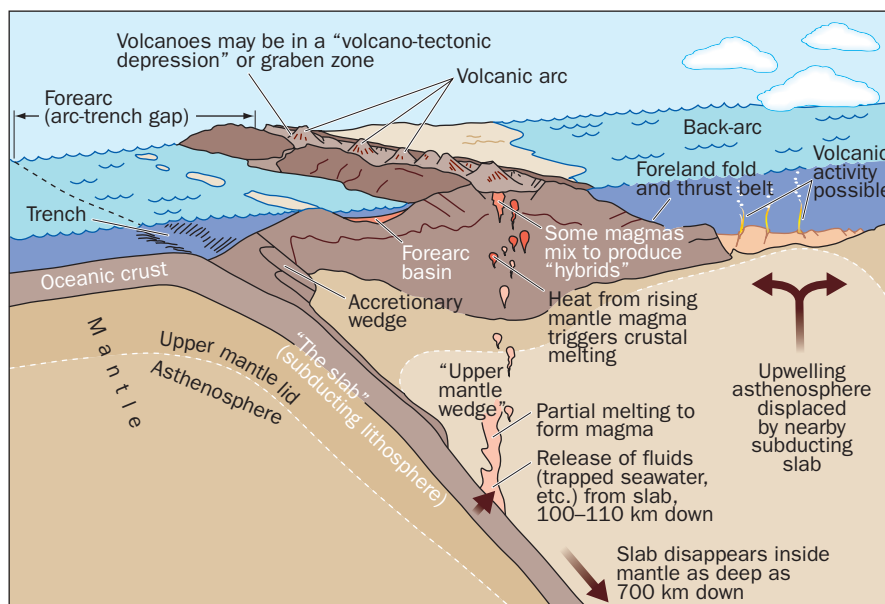


Fig. 2.6 Oblique cutaway showing major geographical features and dynamic processes of a convergent plate boundary. There are, of course, many variations on this pattern. For example, back-arc regions are not everywhere submerged. Nor do coastal islands in many places mark the presence of an offshore accretionary wedge. In ocean areas, only the tops of the arc volcanoes may stick above sea level, forming “island arcs.”

no associated volcanoes, which is another important clue to the origin of melts in this setting. Arc–trench gaps range from a few tens to several hundred kilometers in width. If the volcanoes grow upon a continental foundation, they form what are called **continental arcs**. If they form volcanic islands fringing a marginal sea, such as the Northern Mariana or Antilles archipelagos, they constitute **island arcs**. Volcanic arcs are typically no more than a few tens of kilometers wide. The volcanoes of continental and island arcs are similar, being mostly “grey volcanoes” characterized by steep slopes and explosive activity, but there are distinctive and important differences as well. In some regions, volcanic activity also occurs behind the arc on the floors of marginal seas and within continental interiors. This **back-arc volcanism** is also plainly related to subduction, and tends to be widespread relative to the narrowly confined volcanism within arcs. In general, back-arc volcanism is less vigorous as well as more widely dispersed than arc volcanism. But, in fact, some of the largest eruptions known to have ever occurred have taken place in back-arc continental environments.

The geometry and names of the major plates and their boundary zones, along with locations of the Earth’s most important volcanoes are shown on the map at the end of this book. From this map it is indeed apparent that most volcanoes are located at or very near plate boundaries. The exceptions (Intraplate or “**hot spot**” volcanoes) will be discussed separately following the sections on plate boundary volcanoes.

Volcanoes along Divergent Plate Boundaries

Divergent plate boundaries are, for the most part, marked by the approximately 65,000 km-long discontinuous Mid-Oceanic Ridge (MOR) system along which new oceanic crust is being generated (Fig 2.3). The magma erupted here is the most “primitive” (least evolved) to reach

the surface from the mantle – a highly fluid type of lava termed **tholeiitic basalt**. Most other melts are contaminated to one degree or another by older rocks, or compositionally modified before eruption. Submarine volcanism is further discussed in Chapter 12.

The crest of the slower-spreading parts of the MOR, such as the Mid-Atlantic Ridge (25 mm/yr) is marked by an axial rift valley the floor of which is distinguished by networks of subparallel fractures (“rifts”) – conduits for the escape of volatiles, hot mineralized water, and lava. The valley is a **graben**, a down-dropped block of crust bounded by faults resulting from tectonic extension. Because of the ongoing dilation, the basaltic accumulations are being continuously, slowly torn apart and spread out in this setting, so that few distinct volcanoes form. Those that do are primarily elongate broad structures less than a few hundred meters high and complexly deformed (Fornari et al. 1987), and even these are mostly ephemeral features destined to be destroyed as seafloor spreading continues. Where spreading is much faster (e.g., the East Pacific Rise, at 80–120 mm/yr), axial valley development is subdued or non-existent, and there is even less chance for a substantial volcanic edifice to grow.

The MOR system emerges above sea level in just a couple of places – Iceland and the Afar region of Ethiopia. There, broadly elongate shield volcanoes cut by fissure systems parallel to the plate boundary are active, exemplified by Krafla [72] and Askja [73] in Iceland, and Erta Ale [91] in the Afar – which although 50 km across at the base rises only 600 m at its summit. Erta Ale is one of the most active basaltic volcanoes on Earth, in fact, having been in almost continuous eruption since 1967.

CONTINENTAL RIFT ZONE VOLCANOES

Mechanically, these zones of active volcanism are related to extension of continental plates by mantle upwelling, and they bear dynamic similarities to the divergent-plate volcanism of the mid-ocean ridges. The associated volcanoes are of very different geochemical composition, however, apparently due to differing depths of melting, to different mantle source materials, or to contamination during ascent. Because continental rift zones are characterized by high heat flow, they are of considerable importance because of possible geothermal resources. Three examples of rift zone volcanism in continental settings will be described: one directly related to divergent-plate volcanism, and two from more stable continental environments.

The East African rift valleys are southwest-trending extensions of the Carlsberg Ridge-Red Sea spreading system (Afar Triangle) and result from the pulling apart of the crust with the sinking of a long, narrow blocks (grabens) between fault scarps. The grabens have been filled with thick sediments of largely volcanoclastic origin, and it is here that the oldest traces of early humans and their predecessors have been found. Adjoining the Red Sea (Afar Triangle) the rocks are tholeiite basalts similar to those of the mid-ocean ridges (Tazieff 1970), but further south the lavas are moderately to very deficient in silica and rich in sodium or potassium, or both. Some of them are among the poorest in silicon and richest in alkalis of any volcanic rocks on earth.

Another example is the Rhine Graben of southwestern Germany – a Y-shaped split in the crust associated with a gentle broad up-arching above an area of continental extension, related to intrusion of magma from below. Several volcanic fields are associated with it. The Vogelsberg field lies directly astride the eastern arm of the Y, and the Kaiserstuhl lies within its leg. To the

east of the arms lie the volcanoes of the Hesse and Rhone districts, between the arms lie those of the Westerwald, and to the west lie those of the famous Eifel district, where over 200 monogenic volcanoes have developed, many associated with diatremes (Chapter 4) and maars (Chapter 10). Some of these volcanoes are of Holocene age, as are young volcanoes in central France (Chaîne des Puys) and northeastern Spain (Garrotxa Volcanic Field). Because of their long Quaternary eruptive histories, none of these volcanic areas should be considered extinct, and the odds are good that future eruptions will occur in these areas. As is true of most volcanoes associated with continental crustal extension, the volcanic rocks of these fields are alkalic and deficient in silica.

The Rio Grande Rift is a downfaulted depression and series of deep sedimentary basins that extends over 1000 km from southern Colorado in the US to northern Mexico. It is characterized throughout its length by normal faulting related to crustal extension, recently active volcanism, and high heat flow. Rifting began in this zone about 30 million years ago, and produced volcanoes varying in composition from basalt to rhyolite. Basaltic volcanism increased in intensity four to seven million years ago, and has continued into Quaternary time (Eaton 1979). Although the Rift is believed to be underlain by a sill-like body of basaltic magma at depth (see Chapter 3), seismic activity and geodetic measurements suggest that no extensional rifting is occurring at the present time (Sanford et al. 1979).

Volcanoes along Convergent Plate Boundaries

Whereas divergent plate boundaries mark the places where new lithospheric crust is created, convergent boundaries are the zones where lithosphere is destroyed (or at least largely hidden from view) through the process of subduction. Over two-thirds of the world's known subaerial volcanoes occur in this environment, most of them in the circum-Pacific "Ring of Fire," both in continental, and in island-arc settings. On a gross, global scale, the Pacific Basin is shrinking as the Atlantic grows wider. This slow consumption of Earth's largest oceanic region at the expense of a younger, growing ocean on another side of the world has been going on since Mesozoic time and the breakup of the ancient supercontinent of Pangaea, creating the interlinked system of arcs called the Ring of Fire. The Ring, in fact, is not a complete loop – it more resembles a "Horseshoe of Fire." To the southwest, it begins on the North Island of New Zealand, extending northward through Melanesia into eastern Indonesia, the Philippines, Japan, and Kamchatka, eastward through the Aleutian Islands and southern Alaska, and southward along the western coast of the Americas to southern Chile (see the map at the end of this book) and the South Sandwich Islands, beyond which it terminates in a few lonely volcanoes close to Antarctica's Palmer Peninsula. To be sure, there are gaps in the line, such as that from Alaska to southern British Columbia, and northern California to Mexico, where transform faulting rather than plate convergence dominate. But even there some volcanic activity takes place, evidence of melting in the restless mantle below.

The great Alpine–Tethys collision zone between the African and Eurasian plates is another major location for convergent-plate volcanoes. In the Mediterranean, a dying sea where Africa is about (in geological time frames) to collide with Europe, the plate boundary consists of a complex zone of microplates along which are located the active volcanoes of Etna [82],

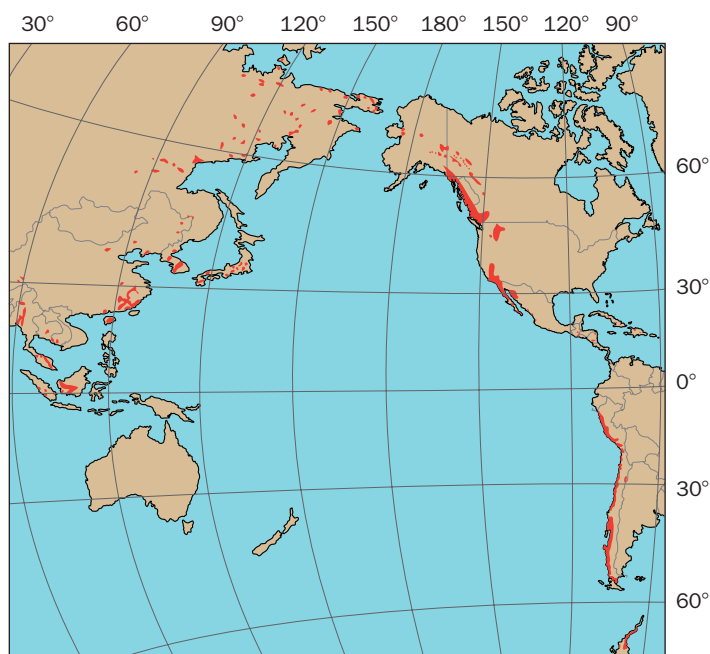


Fig. 2.7 Distribution of Mesozoic plutons in the circum-Pacific region. (Bateman and Eaton 1967, p. 602). Tens of thousands of now eroded-away volcanoes must have once been active above these plutons.

subaerial volcanoes are rapidly cut away by erosion. Their original characteristics must be inferred by studies of their deep roots or of their partially-preserved products. The oldest subaerial volcanoes that retain their original constructional forms are of Pliocene age – probably none of them more than 10 million years old. Although this book focuses on the young, mostly active volcanoes we can presently see, no volcanologist should be so mesmerized by the present that the hundreds of thousands of volcanoes which have lived their moments of fire and glory in past times are forgotten.

A map showing the distribution of Mesozoic plutonic rocks in the Circum-Pacific region (Fig. 2.7) hints at the extensive volcanic activity of that age. Although erosion has removed most of the proof of direct connection between these batholiths and surface volcanoes, most if not all of these deep-seated plutons must have vented to the surface in many places and over the long, complex history of batholith emplacement, which can exceed 50 million years.

No two volcanic arcs are quite alike. To appreciate the variation in volcanism that may take place within and between them, it is instructive to discuss two well-studied examples, one from the northwestern United States and one from northeastern Russia.

“CASCADIA” – THE CASCADE ARC

The Cascade volcanic arc stretches 1250 km from northern California into southern British Columbia (Fig. 2.8). It results from the relatively slow (4 cm/yr) convergence at a highly oblique angle (N50°E) of two plates, the oceanic Juan de Fuca to the west and continental North American plate to the east. The southern terminus of the arc presently lies in the area of Lassen Volcanic National Park, California. The northern boundary is less easy to define, in large part because of past glaciations. Isolated groups of young volcanoes continue from southern British Columbia all the way into the Yukon Territory. These northern volcanoes are not related to

Stromboli [83], Vesuvius [79], and Vulcano [81] – the namesake of volcanology. These volcanoes were known to ancient Mediterranean civilizations (Chapter 1), and it is here that much of our volcano knowledge has been, and continues to be, gained. Older volcanoes are found further east in this collision zone, and include Elbrus [92], the highest mountain in Europe (5642 m), Ararat [94], landing place for Noah’s ark, and the numerous and varied volcanoes of Turkey (Yürür and Chorowicz 1998).

The above discussion has been restricted to the active Holocene volcanoes of convergent plate boundaries, as these are the ones which can be seen and most easily studied. In contrast to most submarine volcanoes, however, which can retain their general shapes for over 100 million years in their protected locations beneath the sea (until their inevitable destruction at colliding plate boundaries),

the low-angle ($10\text{--}18^\circ$) subduction of young ocean floor responsible for volcanism in the main Cascade Range, however. If we use this subduction as a criterion for defining the Cascade arc, the northernmost possible extent of Cascadian volcanic activity appears to be the Garibaldi volcanic belt, directly inland from central Vancouver Island (Souther 1990).

The volcanoes of the Cascade arc include 30 large polygenetic composite volcanoes and volcanic centers, three young, topographically well-defined calderas, three 50-km wide back-arc mostly basaltic polygenetic shield volcanoes, and approximately 2300 small, monogenetic shield volcanoes and cinder cones of basaltic and andesitic composition, principally located in Oregon and northern California (Fig. 2.9) (Luedtke and Smith 1981; Guffanti and Weaver 1988; Hildreth 2007). The big polygenetic volcanoes range from knobby piles of explosive, intermediate to high-silica domes (e.g., Mount Garibaldi [24]) to near symmetrical edifices constructed mostly of low-silica lava flows (e.g., Mount McLoughlin [25]). Some of these polygenetic centers have erupted a wide compositional range of lavas and pyroclastic deposits (e.g., Mount St Helens [27]). Others are compositionally homogeneous (e.g., North Sister [30]). Although the small monogenetic volcanoes greatly outnumber the polygenetic ones, by far most of the volcanic material erupted in the arc has come from the latter (Hildreth 2007). Volcanism has taken place atop a foundation of older sedimentary and metamorphic rocks uplifted as much as 1500–2000 m above sea level. Crustal extension has faulted and down-dropped much of this terrain in the southern part of the arc.

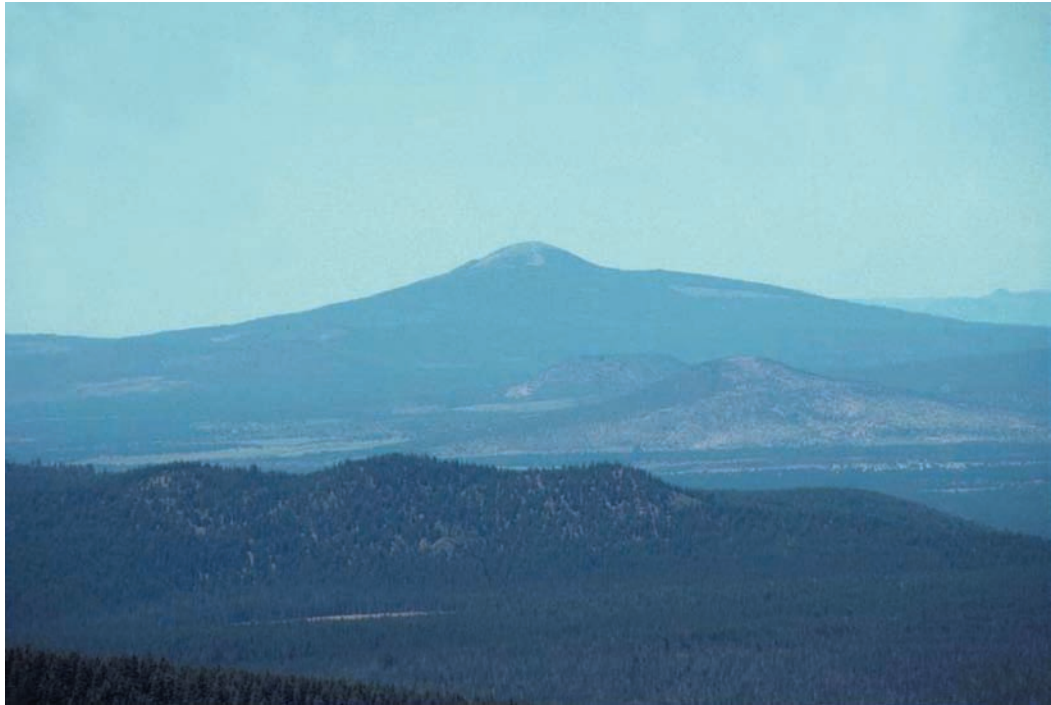
At least 50 eruptions have occurred in the Cascade arc since the start of historical observations, around 1750. These have taken place at eight volcanoes, all but two of which are composite edifices. Interestingly, only three of these eruptions have occurred since 1900 (if we count the on-and-off again Mount St Helens activity since 1980 as one eruption), underscoring how irregular volcanism can be within individual arcs. A large subduction-related earthquake centered beneath the northwest coast of Washington State late in the eighteenth century may have stimulated, or be related to the burst of ensuing nineteenth-century volcanism, but there is no way of proving this at present (Harris 2005).

One can calculate the mean spacing between the large composite cones of the Cascade arc easily enough with a ruler and a map. It comes out to be 87 km. But this is a misleading figure, for that spacing is by no means regular. It ranges from 35 to 170 km – a standard deviation of 45 km. The distribution and types of Cascade volcanoes are closely tied to tectonic processes and to the make up and thickness of the lithosphere within the volcanic arc. Rather than forming a continuous trend, the alignment of prominent composite cones takes sharp jogs in places, possibly reflecting the presence of deep bedrock faults that have permitted melts to penetrate areas off the arc. In addition, there are prominent gaps in the distribution of volcanoes – the largest over 130 km long – notably north and south of the Mt Shasta [26] and between the volcanoes of the Mt Garibaldi group and Mt Baker [29] in northern Washington. Presuming



Fig. 2.8 Large polygenetic volcanoes of the Cascade Range. Black triangles are composite volcanoes. Open triangles are shield volcanoes (Chapter 9).

Fig. 2.9 Goosenest, near Mt Shasta, California; one of thousands of small and medium-sized monogenetic volcanoes in the southern Cascades. Goosenest is a shield volcano composed of andesitic blocky lava flows enclosing a central core of pyroclastic material, mostly cinder, bombs, and blocks, which protrude to form the summit cone. This type of volcano is uncommon or non-existent in other arcs. Photo: R. W. Hazlett.



that the generation of magma is occurring *throughout* the underlying slab–mantle wedge it is difficult to explain the presence of such gaps. Hildreth (2007) argues that they probably represent the presence of lithosphere that compositionally and structurally inhibits the ascent of melt all the way to the surface.

The predominance of monogenetic low-silica largely basaltic volcanism in the southern Cascade arc implies that subduction is generating a different kind of magma to the south than in the north. But this is not necessarily so. The difference probably is due to the fact that tectonic extension in the south permits the direct ascent and eruption of numerous small batches of mantle-derived basaltic melt that stall out in the thicker, more compressed lithosphere to the north (Hildreth 2007). Other arcs, such as the Indonesian and Central American, lack noteworthy monogenetic volcanic fields because they do not experience significant extensional tectonism. The volcanism that builds the big composite cones of the Cascades and these other arcs represents a more complex evolution of magma that will be discussed further in the next two chapters.

Volcanism in the Cascade arc appears to have been episodic during its 32 million year history, but, by a rough estimate, eruption rates have declined six-fold during this time as plate convergence has slowed down (by a factor of five) and the obliquity of convergence has increased (Verplank and Duncan 1987; Hildreth 2007). Let's contrast this situation with an arc that has arisen from more direct and rapid plate collision.

KAMCHATKA

The Kamchatka Peninsula extends from the eastern tip of Siberia southwestward toward Japan, enclosing the Sea of Okhotsk to the west. As in the case of the Cascades, the Pacific plate is

colliding with this region of continental crust, but at double the rate (8–9 cm/yr), and nearly head on, perpendicular to the trench. The subducting plate is less hot than it is beneath the Cascades, being located much further from the mid-ocean ridge where it originated, and this may contribute to its very steep angle of subduction – about 50° – owing to somewhat greater density. Because most subduction-related melts tend to be generated above slabs that have sunken to depths of roughly 100–110 km, this also means that the arc–trench gap is substantially less in Kamchatka than it is in the Cascades (175–200 km versus 320–450 km).

The average spacing between composite volcanoes or related calderas on the Kamchatka Peninsula in eastern Russia is a mere 29 km, though spacing here too is irregular, and includes some offsets and gaps. The arc extends about 750 km as a landward continuation of the much longer (1400 km) Kuril–Hokkaido island arc. Some 30 active volcanoes exist in Kamchatka alone, along with nearly 200 extinct or dormant ones. About 70 of these are large polygenetic volcanoes and calderas less than a million years old, and there are over a thousand monogenetic cones, domes, rings, and maars. Included in this group is Klyuchevskoi [129], one of the largest composite volcanoes in the world.

While only three geologically young calderas exist in the Cascade Range, the Kamchatka arc is noteworthy for its concentration of young calderas, most of which, unlike Crater Lake [19], Oregon, did not form from collapse of a pre-existing composite volcano, but rather developed from wholesale collapse of the crust above large, shallow magma bodies. Eight large calderas occur, with one 150 km segment of the arc consisting of nothing but adjacent and overlapping calderas and their attendant edifices. This cluster includes Uzon Caldera in Kronotsky National Park, an area active with hot springs and geysers and as scenically wonderful as Yellowstone National Park in Wyoming, and the Klyuchevskoi volcanic center, that includes the active volcanoes Klyuchevskoi, Bezymianny [128] and Ploskii Tolbatchik [126] (Fig. 2.10).



Fig. 2.10 View of the Klyuchevskoi volcanic complex from the International Space Station, including Sheveluch Volcano further north (toward the upper margin of the image). Photo courtesy of the NASA Image Science and Analysis Laboratory, Johnson Space Center (ISS-001-E-6505).



Fig. 2.11 Major features of the Kamchatka volcanic arc. Dark triangles are large, geologically young polygenetic edifices. Hachured circles are young calderas. Map modified from Fedotov and Masurenkov (1991).

Some vigorously active volcanic arcs on thin or youthful continental lithosphere develop large grabens, tens of kilometers wide, hundreds of kilometers long, and hundreds of meters deep, striking along their axes. Arc volcanoes align along the lengths of these grabens, which as a result are often called **volcano-tectonic depressions**. Examples include the Nicaraguan and Sumatran depressions. Arching of the overriding plate during convergence must account for formation of volcano-tectonic depressions, causing the broad crest of the uplifted arc to collapse like a gigantic keystone block. The Central Kamchatka Depression might appear to have formed in the same way – and indeed is bounded along its eastern side by a normal fault system, typical of volcano tectonic depressions. But given that the current arc lies largely to the east of this feature, it is more likely that it is just an artifact of two parallel volcanic ranges growing adjacent to one another, augmented by mild back-arc extension.

Despite the differences in the concentration and explosiveness of volcanoes in Kamchatka and the Cascades, there is not necessarily a substantial difference in the total volume of volcanic products produced in these two arcs within the past few million years. The difference lies more in the styles of volcanism than in the amount of fresh new volcanic material produced. Hildreth (2007) making first-order comparisons of volcanic output between the Cascades, Alaska Peninsula, Andean and other continental volcanic arcs found rough parity and even

The Kamchatka arc consists of two parallel chains of volcanoes (Fig. 2.11). The most vigorous and recent volcanism takes place in the Eastern belt, which closely fringes the Pacific coast of the Peninsula. Roughly 200 km inland from this alignment is the 450 km long Sredinny (Central) belt, which has a record of intensive effusive, shield-building activity within the past 2–3 million years, but is now apparently dead. The Sredinny Range could mark the existence of an older subduction zone that ceased to be active when an ancient island arc (the Kronotski terrane) collided with and accreted to Kamchatka. Subduction beneath the peninsula continued, however, in the ocean basin to the east of the newly added landmass. That gave birth to the presently active volcanic belt. (e.g., Avdeiko et al. 2006). The anomalously vigorous volcanic activity in the Klyuchevskoi-Shiveluch [130] group apparently marks the edge of the downgoing slab, where intensive mantle upwelling might be expected owing to stirring of the mantle around the sinking margin of the plate. The slab subduction angle in this region is only around 35°, accounting for the westward offset of the Klyuchevskoi-Shiveluch volcanoes relative to the remainder of the active arc.

TABLE 2.1 COMPARISONS OF VOLCANIC ARC PRODUCTIVITY DURING QUATERNARY TIMES (THE PAST 1.8 MILLION YEARS).

Arc (and research source)	Length of arc (km)	Number of major polygenetic volcanoes	Volume of material erupted (km ³)
Cascades (Hildreth 2007)	1250	30	6400
Andean Southern Volcanic Zone (Hildreth 2007)	1400	80	5300
Alaska Peninsula (Hildreth 2007)	1150	55	2000–3000
Central America (Carr et al. 2003)	1100	39	3464
Northeast Japan (Aramaki and Ui 1982)	1000	45	1480*

* Most of these volcanoes are less than 500,000 years old. If the rate of productivity in this time scale is expanded to include all of the Quaternary, then the productivity of this arc increases to almost 6000 km³.
From data presented by Hildreth (2007).

greater Cascades volcanic output during Quaternary times than in other arcs with greater concentrations of large polygenetic cones and volcanic centers (Table 2.1). The comparison to island arcs is more tenuous, given the submergence of so much of their eruptive material, but it may be that because the lithosphere is thinner and less evolved in those settings that a larger proportion of intruding magma can erupt. For instance, recent studies of magmatism in the Aleutian arc suggest that it has been enormously productive; between 89 and 120 km³ of igneous material – including plutonics – per kilometer of arc length every million years (Jicha et al. 2006).

EPISODICITY AND “VIGOR” OF ARC MAGMATISM – REAL OR IMAGINED?

From time to time people believe that the amount of volcanic activity around the world is increasing, and some popular media popularize these notions. Those who believe in apocalyptic endings for the Earth pay keen attention to such “trends.” But are they real? Does volcanic activity occur in pulses world wide? Is the world heating up to a fiery self-immolation? (Newhall and Self 1982) note:

careful study of the record of the past 100 years shows [an] apparent drop in global volcanism during periods in which [news]editors and scientists were preoccupied with other things, such as world wars, and apparent increases during periods of universally strong interest in volcanism, such as the years immediately following . . . [the eruptions of] Krakatau and Mont Pelée.

Coats (1951) noted that major pulses in the numbers of reported eruptions in the remote Aleutian arc correspond to the times of exploratory expeditions. People documented volcanic activity whenever they were close at hand and paying attention, in other words.

Taking into consideration these very human factors, the *historical* pattern of global volcanic activity shows no evidence of increasing, decreasing, or even pulsating worldwide.

However, bursts of volcanic activity do appear to occur in certain regions from time to time, which might be correlated to episodic plate motions or releases of pent-up energy along volcanic arcs. Especially noteworthy are very explosive eruptions at three widely-spaced volcanoes in the Caribbean region in 1902 and a spasm of volcanic outbursts in the Bismarck archipelago in 1972–5 (Cooke et al. 1976). In another example, Prueher and Rea (2001) studied sea-floor volcanic ash layers in the northwestern Pacific and found evidence for simultaneous, pulsating volcanism in the Aleutian and Kuril–Kamchatka arcs. Each episode of increased volcanic vigor lasted from about 10,000 to a few hundred thousand years, and was separated by somewhat more sluggish intervals lasting as long as a half-million years. A similar period of intensive volcanism appears to have effected island arcs throughout the western and northern Pacific in late Eocene and early Oligocene times (Jicha et al. 2006).

Newhall and Self (1982) compared the volcanic activity in different arcs, and set up a standard of comparison between the various arcs which they call **volcanic vigor**. Volcanic vigor may be defined in several ways, whichever is most convenient for a particular researcher. Vigor may be:

- 1 the number of volcanoes active within the past 10,000 years in a volcanic arc, divided by the length of the arc; or . . .
- 2 the total duration (say, during a century) in which documented eruptions have taken place in an arc, divided by the length of the arc; or . . .
- 3 the total number of documented eruptions (say, during a century) above a certain level of explosiveness (VEI>3; see Chapter 5) divided by the length of the arc.

Newhall and Self (1982) suggest that there is a definite, albeit weak correlation between the dip of the subducting slab beneath an arc, and volcanic vigor. “Sluggish” arcs tend to be associated with shallow-dipping slabs. In contrast, the steep plunge of the Pacific Plate along the east coast of Kamchatka correlates with one of the world’s most “vigorous” volcanic arcs.

The thickness of the overriding plate also influences the vigor of a volcanic arc. Where upper plate thicknesses are less than 20 km (e.g., the Tonga–Kermadec and Izu–Mariana islands in the western Pacific), arc volcanism tends to be less vigorous – or at least less powerfully explosive – than along arcs with thick upper plates (25–35 km) and similar subduction angles. Newhall and Self (1982) further suggest that weak volcanism ensues where young, relatively warm oceanic lithosphere subducts beneath an arc. An example of this is the Cascade Range.

Intraplate Volcanoes

Not all volcanoes can be ascribed to the interactions of plate boundaries. Perhaps only three-quarters of them are so associated worldwide. The rest lie in locations often thousands of kilometers from the nearest plate edge, and must somehow have other explanations. Fortunately, the insights learned in studying plate tectonics, and a better grasp of Earth’s interior properties, enables us to develop some reasonable hunches about what is going on.

By far the largest group of “intraplate” (off-plate margin) volcanoes can be related to so-called **hot spots**. The term “hot spot” is misleading, however, in that we do not really know

if heat, or heat alone is responsible for the production of molten rock in these areas, since other phenomena, such as reduced pressure or increased volatile content, can also cause rocks at high temperature and pressure to melt (Chapter 3). Because there is no direct evidence that hot spots are really all that “hot,” we prefer to call them **melting sources**, but since “hot spot” is in general use, we shall accept it (warily) to describe these areas of intraplate volcanic activity. Such hot spots underlie areas of concentrated volcanic activity, generally accompanying uplift and seismic activity over broad areas, and are typically associated with the genesis of linear volcanic chains thousands of kilometers long. Several dozen linear volcanic chains are present on the Earth’s surface, most of them on oceanic crust – especially trending across the Pacific (Fig. 2.12). The most famous of these volcanic island chains is associated with the Hawaiian hot spot, a melting source presently centered beneath the southern half of the Island of Hawai‘i near the center of the Pacific Plate. Extending north-west of the Hawaiian hot spot, a chain of over 70 volcanoes in progressively increasing states of erosion and submergence continues all the way to the Aleutian Trench, more than 5000 km away (Fig. 2.12). The increasing age of volcanoes with distance from the “hot spot”, led Canadian geologist J. Tuzo Wilson (1963) to propose that the volcanic chain developed as the Pacific Plate shifted over a fixed melting source rooted in the sublithospheric mantle beneath present day Hawai‘i. Subsequent radiometric dating of the volcanoes along the Hawaiian-Emperor chain has shown the rate of plate motion is about 8–9 m per century, and validates Wilson’s model. Jason Morgan (1971) suggested that a source for this melting might be analogous to the hot air mixed with smoke that rises from a chimney or smoke stack. The stream of polluted hot air does not spread out at once as it exits the mouth of the chimney, but continues to ascend tens to hundreds of meters into a still sky, well-defined and narrow, owing to its great buoyancy relative to the surrounding, cooler air. Fluid mechanicians refer to this as **thermal plume** behavior. Similarly, according to Morgan, hot spots represent localities on Earth’s surface where thermal plumes welling up from great depth are impinging upon the underside of the crust. He referred to them as **mantle plumes**, and suggested that they might originate from positions on the core–mantle boundary, 2900 km below the Earth’s surface.

The Hawaiian–Emperor volcanic chain consists of more than 100 individual volcanoes (Clague and Dalrymple 1987), and is the best studied example of such hot spot tracks. This feature extends west-northwestward 2700 km as a series of islands and atolls from Hawai‘i Island to Yuryaku seamount – just beyond Midway Atoll, and then bends sharply to continue north another 2500 km in the form of the Emperor Seamounts (Fig. 2.13). But there are other spectacular examples too. For instance, the Snake River Plain is the track of the Yellowstone hot spot, with a chain of volcanic centers aging southwestward all the way to the long-extinct McDermott Caldera in Oregon. Along the axis of the Great Dividing Range of eastern Australia, a conspicuous hot spot track links the 40,000 year old Newer Volcanics of Victoria

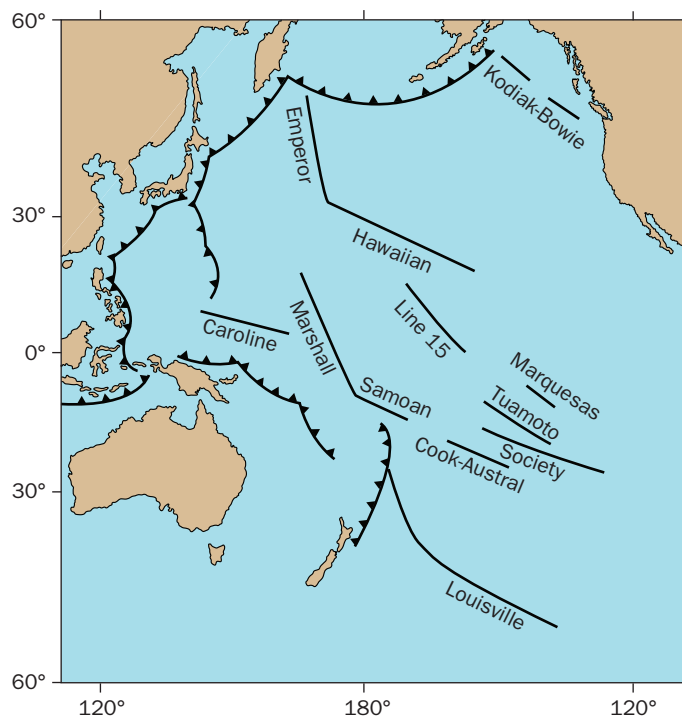


Fig. 2.12 Linear hot spot volcanic island chains and seamounts in the Pacific Ocean. Most of the volcanoes along these chains are represented by atolls or submerged seamounts. Compiled from Epp (1979) and Duncan and Clague (1985).

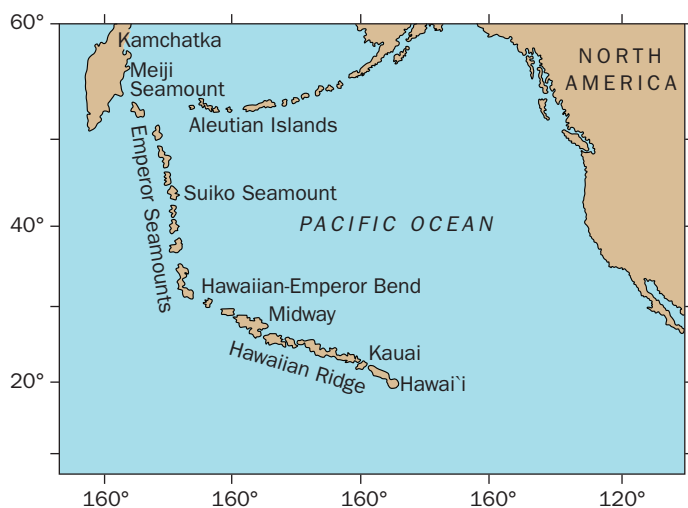


Fig. 2.13 Location of the Hawaiian–Emperor volcanic island and seamount “hotspot” chain. After Clague and Dalrymple (1987).

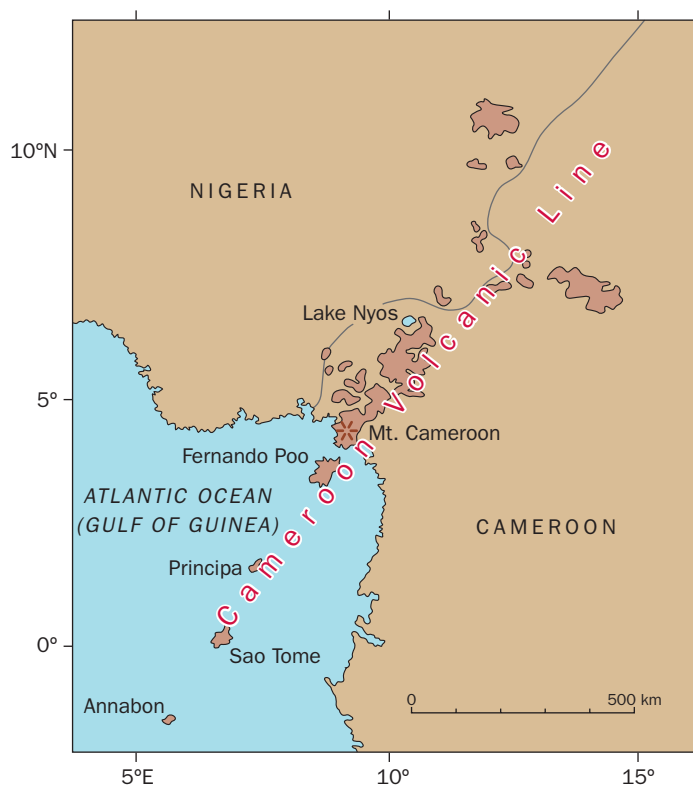


Fig. 2.14 Distribution of Quaternary volcanic rocks along the “Cameroon Line,” a 1500 km-long belt of intraplate volcanoes which cut across both oceanic and continental crust on the African plate. Modified after Fitton (1980).

with the 25 million year old Glasshouse Mountains volcanic center in Queensland (Cohen, Vascancelos et al. 2004).

For the past quarter century, geophysical and geochemical studies have attempted to find evidence confirming the existence of Morgan-style mantle plumes. Only indirect evidence at best can be mustered. Some geochemists examining gases released by volcanoes such as Kilauea [15], for example, find unusually large traces of osmium, an element thought to be concentrated in large quantities in the lower mantle and core. But this interpretation remains controversial (Lassiter 2006). Optimally, seismologists would like to detect loss of seismic wave speeds passing beneath hot spots to discern vertical columns of rising, unusually hot rock. Recent seismic studies provide more detailed information confirming reduction in seismic wave speeds beneath at least 32 sub-volcanic localities, including a spectacular plume-like “root” extending 500 km beneath Wyoming’s restless Yellowstone caldera [40], and a low-velocity plume extending to the core-mantle boundary beneath Hawai’i (Montelli et al. 2003).

OTHER LONG AND SHORT-LIVED “HOT-SPOT” MELTING SOURCES

The Cameroon Line (Fitton 1980) is a 1500 km-long chain of Tertiary to Recent volcanoes which extends across oceanic and continental portions of the African plate from the Gulf of Guinea into Cameroon and Nigeria (Fig. 2.14). Most of the volcanoes along this chain produce alkalic basalt lavas, many of which contain xenoliths of sub-crustal peridotite. Perpetually shrouded in clouds, Mt Cameroon [76] is the largest volcano in the chain, and rises to 4100 m above the West African coast. Presently, this is the only active volcano along the Cameroon Line, and has had nearly a dozen historic eruptions. The Cameroon Line is marked by over 30 maar lakes of various ages in western Cameroon, including Lake Nyos, infamous for its release of deadly CO₂ gas in 1986 (Chapter 14). In contrast to “hot-spot” volcanic chains like the Hawaiian–Emperor system, there is no clear age progression

along this volcanic chain, nor is there any indication of crustal extension as in the continental rift zone volcanic belts (Fitton 1980). Fitton considers the chain to mark a zone of weakness related to an inactive arm of a triple-junction spreading center related to the Mid-Atlantic Ridge.

In a few cases, “hot spot” mantle plumes may develop along the MOR and other divergent plate boundaries. Iceland is a spectacular example of one such hot spot. The reason that this island in the North Atlantic exists, in fact, is largely owing to anomalous heat-induced (“thermotectonic”) uplift coupled with high output of volcanic material. Likewise, the Afar hot spot in Eritrea and Ethiopia lies at the junction of three divergent plate boundaries, forming the Gulf of Aden, Red Sea, and East African Rift Valley. Volcanism at this *triple point* is much more vigorous than along adjacent plate boundary segments.

The Hawaiian hot spot has been active for a long time – at least 70 million years. The Yellowstone hot spot is not nearly as venerable, dating back about 16.5 million years. But this is nonetheless impressively persistent, given how dramatically geologic change has occurred in this same span of time elsewhere in the American West. Other hot spots, such as the ones underlying the cities of Flagstaff, Arizona, and Auckland, New Zealand, are only a few tens or hundreds of thousands of years old. Will these thermal anomalies persist, or die out in short order? The geologic evidence suggests that many relatively short-lived “transient” hot-spots have occurred elsewhere in the geologic past. Alternatively, these sites might simply represent areas of localized crustal extension that stimulate magma to form in the immediately underlying shallow mantle because of lowered confining pressure (Chapter 3; Koopers et al. 2003).

In some cases, volcanic activity can be ascribed to plate boundary interactions taking place many hundreds or thousands of kilometers away. Over the past 45 million years, India, once a large island like Greenland, has been in collision with Asia, owing to subduction of the intervening prehistoric Tethyan sea floor. The elevated Himalayan Mountains, Tibetan Plateau, and Gangetic Plain are consequences of this collision. In central Mongolia’s Hangay region, 2000 km from the leading edge of the Himalayan collision zone, a basaltic cinder cone field has grown over the past few hundred thousand years in response to collisional strain transferred far north into the Eurasian plate.

FURTHER READING

- Condie, K. C. and Pease, V. (2008) *When Did Plate Tectonics Begin on Earth?* Boulder, Geological Society of America.
- Foulger, G. R. and Jurdy, D. M. (2007) *Plates, Plumes and Planetary Processes*. Boulder, Geological Society of America.
- Hill, R. L. (2004) *Volcanoes of the Cascades: Their Rise and Their Risks*. Guilford, Falcon.
- Oreskes, N. (2001) *Plate Tectonics: An Insider’s History of the Modern Theory of the Earth: Seventeen Original Essays by the Scientists Who Made Earth History*. Boulder, Westview.
- Sutherland, L. (1996) *The Volcanic Earth: Volcanoes and Plate Tectonics: Past, Present and Future*. Sydney, University of New South Wales Press.

Chapter 2

Questions for Thought, Study, and Discussion

- 1 If mantle convection slows down over great spans of future geologic time, how will this change what is seen at Earth's surface, both tectonically and volcanically?
- 2 Why do you think there are so few subduction zones fringing the Atlantic Ocean, while the Pacific Ocean is ringed with them? Why does the MOR divide the Atlantic Ocean floor symmetrically, while it lies well off to one side of the Pacific Ocean floor (mostly to the southeast).
- 3 Why don't we see substantial volcanoes grow along the MOR? It is, after all, one of the most volcanically active zones on Earth.
- 4 Why are there substantial differences in the volcanic activity seen in the Cascades and Kamchatkan volcanic arcs?
- 5 What might explain why arc volcanoes are spaced above subduction zones? (Why doesn't a single, through-going volcanic ridge develop along the crest of an arc rather than the distinctively separated volcanoes that we see?)
- 6 How do hot spot volcanoes differ from those of volcanic arcs?
- 7 Why should the Cameroon Line not be regarded as a hot spot track in the same sense as the Hawaiian chain?

Chapter 3

The Nature of Magma – Where Volcanoes Come From

*Basalt, der schwarze Teufelsmohr,
Aus tiefster Hölle bricht hervor,
Zerspaltet Fels, Gestein und Erden,
Omega muß zum Alpha werden.
Und so wäre denn die liebe Welt
Geognostisch auf den Kopf gestellt.
(Goethe 1827)*

*Basalt, dark devil's blackman,
Breaks out of deepest hell,
Splits rocks, stones and earth,
And omega must become alpha
And thus the dear old world
is geologically turned upside-down*

Origins of Magma

Throughout human history people living near active volcanoes, including Goethe, have strived to explain the source of the terrifying fires volcanoes bring forth (Chapter 1). We readily observe that erupting lava is “hot” and thus the origin of that heat is

Volcanoes: Global Perspectives, 1st edition. By John P. Lockwood and Richard W. Hazlett. Published by Blackwell Publishing Ltd.

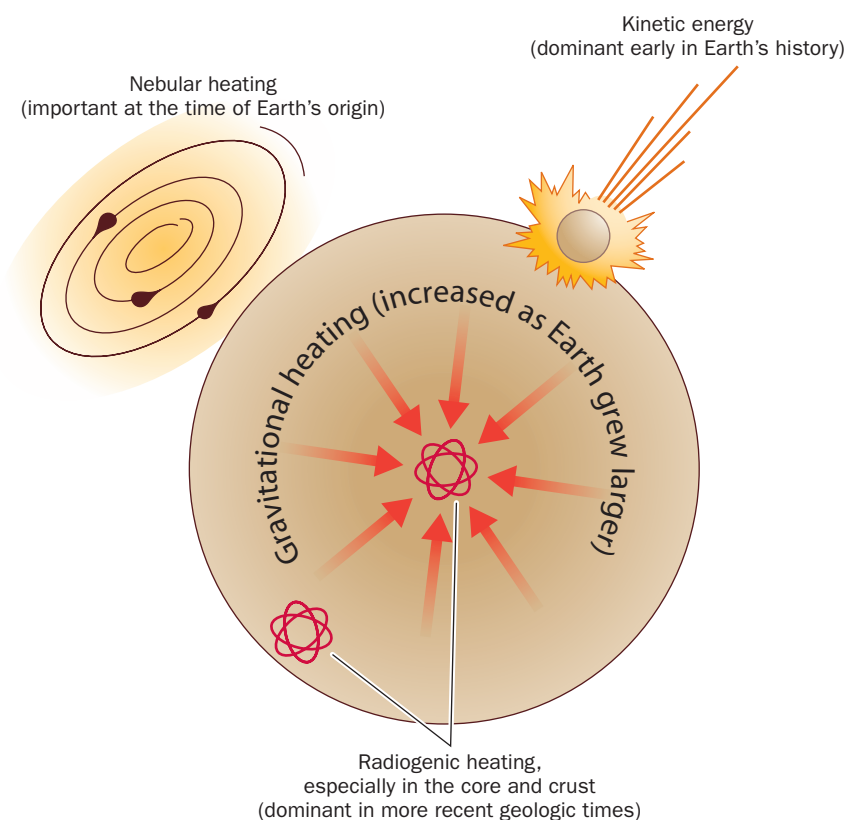


Fig. 3.1 Sources of Earth's heat.

critical to understanding the origin of magma – even though factors other than heat alone (pressure, composition, and volatile content) can cause hot rocks to actually melt. A lot of heat needs to be present for these other factors to be relevant, however, so the source of that heat is important to understand.

Four primary sources of heat have been active inside the Earth since its formation: nebular, kinetic, gravitational, and radiogenic (Fig. 3.1). Solid particles ranging in size from dust to bodies many kilometers across (*planetoids* and *planetisimals*), still warm from the solar nebula out of which they condensed, accreted to form our planet during just a few million years time some four-and-a-half billion years ago. Earth greatly warmed above original nebular temperature, however, thanks to the great amount of heat released as various large bodies collided to add their masses to the growing planet. Geologists presently believe that this **kinetic heat** was great enough to melt much of the young Earth. Thin crust floated on a magma ocean many hundreds of kilometers deep, during which time, some believe, the planet may have arranged itself into an early version of the compositional layers we see today; crust, mantle, and core (Chapter 2). The oldest lavas covering the primordial Earth's surface included one type, **komatiite**, not produced by volcanoes in modern times that suggests the early existence of a hotter planetary interior. Geochemical studies indicate that komatiite flows erupted at temperatures in excess of 1600°C, some 400°C greater than the hottest lavas erupted today (Zimbelman and Gregg 2000). Effusive flood volcanism was probably extensive as the planet continually repaved its surface with every new major impact of extraterrestrial debris.

As the debris in the Solar System thinned out with the growth of planets, Earth began to cool by radiation and release of entrapped gasses. Inside the growing solid mass, gravitational compaction and redistribution of mass released heat, but not enough to keep the globe entirely molten. The molten fraction of Earth’s interior greatly diminished in volume by four billion years ago.

Research by the Comte de Buffon in France in the eighteenth century and by the famous British mathematician William Thomson (Lord Kelvin) in the nineteenth attempted to constrain the age of the Earth assuming that the planet could not be older than the time it would take for it to cool solid *from an entirely molten state*. They presumed that Earth’s interior cooled by simple heat conduction – the same phenomenon that makes the metal handle of a pan hot to touch on a stove top. Their calculations ranged from 75,000 (Buffon) to 40 million years (Kelvin). Because of the existence of active volcanoes, by this reasoning, Earth *must* be less than 40 million years old. Geologists, though, having documented many ponderously slow rates of natural change, had good reason to doubt this calculation. They argued that the Earth must be much older, and that there must be an additional, unknown source of heat keeping the planet hot inside. That heat source – radioactive decay – was finally discovered by Henri Becquerel, the French physicist, in 1895.

Many elements decay radioactively to less heavy particles. A byproduct of this decay, which occurs continuously inside the Earth, is heat (Table 3.1). Since it takes billions of years for some elements in rocks to decay, this means that heat can build up and remain within a stony planet like ours essentially throughout its existence. At some point after four to four-and-a-half billion years ago, **radiogenic heating** superseded kinetic heat as the major source of Earth’s thermal energy. That heat could not escape Earth’s interior by simple conduction, however,

TABLE 3.1 RELATIVE CONTRIBUTIONS OF HEAT ESCAPING FROM THE PRESENT-DAY EARTH FROM RADIOGENIC DECAY, BASED UPON GEONEUTRINO STUDIES (ARAKI ET AL. 2005). NOTE THE DISCREPANCY BETWEEN THE ESTIMATED SUM TOTAL OF RADIOGENIC HEAT RELEASED AND THE TOTAL DIRECTLY OBSERVED FROM MEASUREMENTS AT EARTH’S SURFACE. THIS DISCREPANCY REMAINS UNEXPLAINED, BUT GEOSCIENTISTS ARE NOW CONFIDENT THAT RADIOGENIC DECAY IS THE PRIMARY HEAT SOURCE FOR DRIVING PLATE TECTONICS AND, ULTIMATELY, VOLCANISM.

Decay series	Primary location inside Earth of decay	Heat energy released (in terawatts, TW)
Thorium-232	Core	8.3
Uranium-238	Core	8.0
Potassium-40	Continental crust	3.0
Total estimated radiogenic heat release (from geoneutrino research)		19.0
Total directly observed heat release through Earth’s surface		31.0

as Buffon and Kelvin presumed. Something else must be facilitating its release because heat conduction is too slow a process, otherwise the planet would simply have remelted.

Scotsman Sir Arthur Holmes, whom we introduced in Chapter 2, provided a solution to this paradox in 1928, proposing that convection rather than conduction, is the primary vehicle for releasing Earth's pent-up heat energy – as well as driving its tectonic plates. A good table-top model of convection is a pot of boiling water. Hot water is more buoyant than cold, so cells of ascending hot water well from the bottom of a pot to the surface, radiate heat, cool, and descend again to gather more heat from the bottom. Holmes proposed that cells of hot rock ascend from Earth's core-mantle boundary, spread out just beneath the surface, lose heat in part by conduction as well as radiation, and descend again. A complete cycle of overturning boiling water may take only a few seconds in the pot. For heated rock in Earth's mantle, the turnover may take as long as a couple of hundred million years. Several layers of "stacked" convecting cells may exist between surface and core as well.

It is difficult to imagine that solid rocks can move like a fluid, but indeed, over great periods of time at high temperatures this is possible. Holmes was quick to point out that the mobility and plasticity of solid rock can be seen in the graceful folds of sedimentary strata and gneisses. Glaciers, too, are good examples of solid material moving in response to gravitational forces over long periods of time.

Holmes' insights helped to explain the discrepancies between geology and mathematics, although seismic investigations of mantle plumes indicate that the realities are not simply a matter of geometrically elegant "boiling pot"-shaped convection cells (Montelli et al. 2003). We still have much to learn about our planet's internal structure and internal dynamics.

The Physics and Chemistry of Melting

We now know that several factors are important in determining whether or not rock will melt to form magma: temperature, composition, pressure, and "water" (volatile) content are each vital. Various combinations of these factors, all related to early Earth history, convection and plate tectonics, are responsible for magma production at a few distinctive levels and places inside Earth.

Most rocks are made up entirely of minerals, which are defined as unique arrangements of non-living matter having crystalline structures. A crystalline structure is an orderly, symmetrical arrangement of atoms. Most of these atoms tend to bond with one another ionically, meaning that they come together because some atoms are deficient in electrons whereas others, to which they are drawn, have some electrons to spare. Atoms having an unequal number of protons and electrons are electrically charged, and we call them **ions**. Nature tends to neutralize electrical charge wherever it arises, so ionically bound minerals are the norm.

Ions that have the same charge (possess the same number of electrons out of balance with protons) repel one another, with higher charges leading to greater repulsive forces. Silicon, which is the most common **cation** – or ion lacking electrons – on Earth, also has an especially high charge. Silicon ions are highly repulsive of one another, but being very common, they also are found in the vast majority of rocks and minerals. Silicon bonds with oxygen, the most common **anion** (ion having excess electrons) on Earth, and so minerals and rocks tend to be

made up largely of silicon ions fixed into position by intervening oxygens. Since oxygen atoms are much larger than silicons, four oxygen ions snuggle around each silicon ion in crystals, never more, never less. The result is a molecular arrangement shaped like a tetrahedron, the **silica tetrahedron** (Fig. 3.2). Silica tetrahedra are not charge-balanced arrangements, despite the efficient use of space. Each oxygen ion, having two extra electrons, has a charge of -2 , whereas each silicon, lacking four electrons, has a charge of $+4$. There is an excess negative charge of -4 in other words. To deal with this, nature employs a couple of strategies. One is to tuck additional cations in between the tetrahedra in crystal structures, so that the oxygens split their charges between the silicons and surrounding cations. This happens, for example, in the common volcanic mineral olivine. The other is to actually combine the tetrahedra so that each oxygen shares its charge with two adjoining silicons. Oxygen atoms that so partition their charges are termed **bridging oxygens**. In the common mineral quartz, all tetrahedra are interlinked and all oxygens are bridging, and the two-to-one proportion of silicons and oxygens – the only elements found in quartz – gives the mineral its chemical formula, SiO_2 .

Silicon ions tend to be spaced more closely together in arrangements where tetrahedral oxygens are non-bridging than where they are bridging. This has important implications, because it means that minerals such as quartz tend to be less stable when heat energy is present than minerals such as forsterite (magnesian olivine). If minerals are mixed together, their melting temperatures are suppressed even further – a phenomenon called **fluxing**. The heat energizes the ions, allowing them to break their bonds, and high-charge ions in close proximity to one another can do this with relative ease. The result is that the mineral melts. Since no two mineral species are quite alike, this means that a rock made up of different kinds of minerals *will not melt all at once, but rather mineral type by mineral type*. For instance, the melting point of pure quartz is $1650 \pm 75^\circ\text{C}$, while the melting point of forsterite, with its more widely spaced silicon ions, is around 1900°C . If fluxed in a rock also containing abundant H_2O -bearing minerals, however, quartz can start melting at temperatures as low as 700°C .

Norman L. Bowen, using laboratory furnaces at the Carnegie Institute in Washington DC, began studying this phenomenon by examining the feldspar mineral group around 1910 (Bowen 1913). He modeled and experimentally documented the melting and crystallization of granitic rocks and discerned the sequence, now known as Bowen's Reaction Series, in which the crystallization of cooling granite magma is essentially just the reverse process of melting

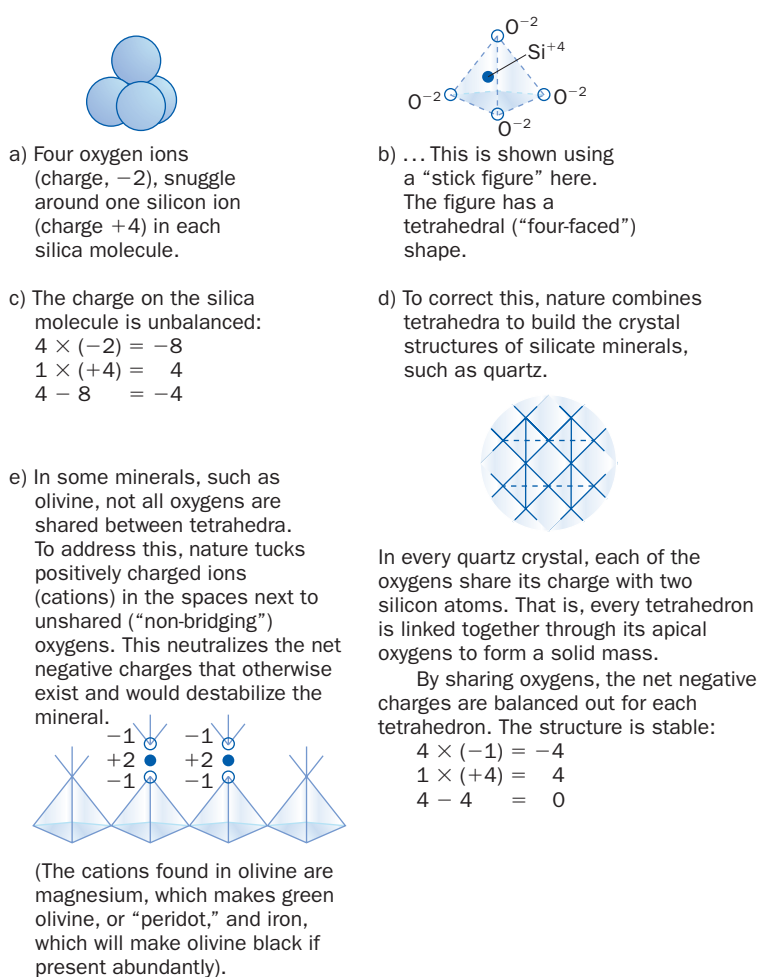


Fig. 3.2 The silica tetrahedron.

if considered as a closed system. He found that three kinds of mineral melting reactions take place. In the **discontinuous reaction series**, consisting of biotite (magnesium-rich mica), clino-amphibole, calcium pyroxene, and olivine, a mineral will partially melt at a specific critical temperature, reacting to form another structurally and chemically similar, but more stable mineral in the process. Hence, calcium pyroxene will break down to form olivine when temperature rises to a certain level in a melting rock, called a **peritectic point** by chemists. In the **continuous reaction series**, made up of the plagioclase mineral series, melt is *continuously released* and mineral compositions *continuously change* as temperatures rise. Sodium-rich plagioclase (albite) is stable at low temperatures in granite. At higher temperatures, calcium-rich plagioclase (anorthite) persists until melting is complete. At temperatures in between, plagioclase contains both calcium and sodium in temperature-sensitive proportions. If one can establish the pressure and H₂O content of a melt, the ratio of these two cations can be measured to determine the temperature at which a particular plagioclase existed at the time it acquired that composition (Kudo and Weill 1970). Minerals whose make-ups provide such information are called **geothermometers**. (There are also mineral **geobarometers** developed for pressure determination.) Using geothermometers, it is possible to calculate the maximum temperature a rock reached as it was partially melted, or conversely, to calculate the approximate eruptive magma temperature of volcanic rocks even millions of years old. The chemical variations seen in plagioclases, in particular, provide important clues to the cooling histories of magmas and the causes of volcanic eruptions (e.g., Tepley et al. 2000). One type of geothermometer, involving volcanic glass, can even be used to determine thermal histories of past eruptions (e.g., Helz and Thornber 1987).

Finally, Bowen noted that some minerals do not change their compositions or react out as they heat up and melt. When melting occurs, the liquid they release matches the chemistry of the original minerals. In the jargon of chemistry, they melt **congruently**. Potassium feldspar and quartz are examples of such minerals.

Bowen used his discovery about how molten rocks melt and crystallize to formulate a general theory that states how a range of igneous rock types can differentiate (form step-wise) from a single parent magma. Magmatic differentiation can most easily be explained by imagining that the crystals that develop early in a melt sink and accumulate in a layer of distinctive composition at the bottom of a magma chamber. The remaining melt crystallizes a newer suite of minerals as it cools, which in turn may settle out to build a bottom layer of another composition—and so on, the end product being a layer-cake of rock types which might have been mixed together to form a single blend had gravity not influenced the crystallization process. There are other ways that differentiation can take place, too, but this particular method, called **gravitational fractional crystallization**, seemed the most obvious to Bowen, and has stimulated thinking about magmas ever since.

So certain was Bowen about his theory that he wrote (Bowen 1928):

The only rival hypothesis [to differentiation is] the doctrine of the mixing of two fundamental magmas (basaltic and rhyolitic) but this has been found to fail so completely that the concept of differentiation has come to be regarded as a fact as well established as the observed rock associations themselves.

However, current research shows that fractional crystallization is less important and magma mixing more important for explaining the wide variety of igneous rocks than Bowen ever believed (Reid 1993; Thornber 2003). It is not always wise to be absolutely certain about your beliefs!

In a laboratory Bowen could remove and quench samples of melted rock whenever he chose. But under natural conditions, the molten fraction tends to separate before enough heat accumulates to melt rock *completely* at any given point inside the Earth – at least outside of the core. The separating liquid migrates along crystal grain boundaries and through fractures that may open in the surrounding crust in response to stress, heating, and the buoyancy of the new magma. It also tends to be more silica (SiO_2) enriched than the unmelted residue it leaves behind.

Pressure tends to keep ions together in crystalline structures. Hence, with increase in pressure, there is an increase in the temperature at which a rock of any given composition and H_2O content will melt. Rocks having high silica content tend to melt at lower temperatures than rocks with low silica contents, given the same level of pressure.

Many rocks contain H_2O and other volatiles in pores, fractures, and even along grain boundaries between crystals. Each H_2O molecule has a slight charge imbalance from one side of the molecule to the other. Given this property, H_2O molecules are slightly attracted to the ionically charged surfaces of adjoining crystals. Given heat, the H_2O makes it easier for ions to diffuse and melting to occur than under dry conditions, hence H_2O -bearing rocks tend to melt at lower temperatures than dry rocks.

Most melting takes place at three general localities inside the earth: the outer core, the asthenosphere, and in the upper mantle-lid (or “wedge”) above subducting plates. The Earth’s outer core, from 2900 to 5155 km deep, mostly consists of molten iron and nickel. It represents the largest known magma body in the Solar System. Yet being so deep it feeds no volcanoes. Melting in the crust is largely due to heating from intruded mantle derived magmas (Bergantz and Dawes 1994).

Earth’s mantle, lying between 70 and 2900 km deep, is mostly solid, but hot enough to convect, as mentioned above. It is made up of silicate rocks, in contrast to the core. At the core–mantle boundary, the rock has a higher melting temperature than the iron and nickel. Yet, its solidness is only sustained by very high pressures. Were a typical specimen of hot mantle rock suddenly taken to the low pressure of sea level, the rock would melt at once into extremely fluid lava. However, at one level in the mantle, between 100 and 640 km down, the pressure is just low enough and the temperature just high enough, for partial melting to take place. This is the level of the asthenosphere, the soft bed upon which the rigidly overlying plates slide. Mantle convection cells reach their highest level in this layer. The partial melt fraction rises as basaltic magma, the main form of molten rock erupting from sea floor spreading centers, continental rift valleys and other regions of tectonic extension (crustal stretching). At these loci, plate separation enables asthenospheric mantle to well up within a few kilometers of Earth’s surface, inducing intensive partial melting. Most of the world’s volcanic activity results from this **decompression melting**. Where mantle plumes ascend, a similar form of melting occurs: the plume rock, bringing with it great heat from deeper inside the planet, enters shallow, lower-pressure regions, and begins to melt.

Somewhat different processes operate beneath volcanic arcs. Large volumes of trapped seawater and moist sediment ride downward into the earth where masses of heavy oceanic plate are subducted into the mantle. At a depth of around 100–110 km the great heat of the surrounding mantle drives off the seawater – or various components of it within the sinking plate, making rocks in the overlying wedge of mantle less dense and more buoyant. The escaping fluids may induce partial melting, owing to the effect of H₂O on melting temperatures described above. Whether this happens or not, however, the upwelling, volatile-bearing mantle rock decompresses, which most certainly triggers partial melting. The resulting basaltic magma ascends into the overlying crust, assimilating parts of it while heating other parts enough to induce further partial melting, especially in silica-rich rocks. Granitic magma bodies result, accompanied by metamorphism in neighboring rocks that are sufficiently refractory to remain solid (Blatt et al. 2006).

Classification of Magma and Igneous Rocks

Geologists distinguish two subclasses of igneous rocks; **plutonic** and **volcanic**. Plutonic rocks form by cooling and crystallization of molten rock deep beneath the Earth's surface, whereas most volcanic rocks form by solidification of magma erupted onto the surface or emplaced at shallow depths beneath volcanoes. Some volcanic rocks form from fragmental material erupted during explosive eruptions (Chapter 7), but, as for the ones that cool directly from erupted magma, they may usually be distinguished from plutonic rocks in hand specimen by their grain size and the common occurrence of gas bubbles or **vesicles**. The various chemical elements present in magma typically have the time to organize themselves into discrete, visible crystals, and dissolved gases have time to escape when melts cool slowly underground, producing crystalline rocks. Volcanic rocks, which cool more rapidly typically show only a small percentage of readily visible mineral grains, termed **phenocrysts**, which represent the crystals that were able to develop for the most part before the melt erupted. The matrix for these phenocrysts in typical volcanic rocks is very fine-grained or glassy, and in most cases consists of a featureless stony matter called **groundmass**. Glass-rich volcanic rocks generally indicate rapid cooling of the magma, although some glassy lavas indicate formation by other processes (Chapter 6).

Apart from the “volcanic” versus “plutonic” distinction described above, geoscientists have also developed more refined approaches to classifying magmas and igneous rocks, according to specific need. Historically, the first efforts at classification were based upon direct observations – the practical description of the colors and textures of rocks seen with the unaided eye. For purely practical reasons, special attention was given to those rocks of interest in mining and construction. The word “basalt,” for instance, can be traced back to the ancient Egyptian quarryman's “basanos.” The growth of mineralogy as a scientific field, especially beginning in the eighteenth century enabled more precise rock classification, because observers recognized that certain kinds of minerals are characteristically restricted to certain kinds of rocks. But it was the development and proliferation of modern analytical instrumentation that really allowed detailed understanding of the *elemental* make-up of materials and permitted their systematic classifications based on chemical compositions. Combined with experimental studies, such as

those of N. L. Bowen, this has also enabled geoscientists to decipher with great precision the origins and ages of many igneous rocks.

One generally used classification scheme for volcanic rocks is based on the ratios of the alkalic elements sodium and potassium vs silica (Fig. 3.3). Note that the alkali elements are presented as oxides, just as silica is. The terms **ultramafic** and **mafic** (or sometimes **ultrabasic** and **basic**) refer to low-silica igneous rocks containing lots of iron and magnesium. **Felsic** rocks (sometimes referred to as **acid** rocks) are highly siliceous, and contain lower quantities of iron and magnesium but more potassium and aluminum than their mafic counterparts.

Note that this figure does not distinguish between lavas and pyroclastic rocks of similar composition. That distinction is made by using the volcanic composition as a term-modifier; for example, **basaltic ash** and **basaltic lava**. So, ultimately, the textures, structures *and* chemical compositions of particular volcanic deposits must be considered to render a complete rock identification. We shall explore some of these textural and structural aspects further in subsequent chapters.

For further information on the classification of igneous rocks, we recommend that you explore the International Union of Geological Sciences (IUGS) Subcommittee on the Systematics of Igneous Rocks, available on-line and in most igneous petrology textbooks (e.g., Blatt et al. 2006). The treatment above simply illustrates the great variation in volcanic rock and magma compositions, and provides context for the names of rocks and minerals that we'll present later in this text.

Principal Magma Types

BASALTIC MAGMAS

Basaltic melt is the most common type of magma on Earth, as it appears to be elsewhere on the inner planets and moons of our Solar System (Chapter 12). It is the product of decompression melting in the upper mantle, erupting at all spreading centers worldwide. It also erupts within and behind some volcanic arcs, and in areas of extending continental crust – places far from the closest plate boundary. The residue of the partial melting that creates basalt is **harzburgite**, a chemically depleted, olivine and pyroxene-rich form of peridotite that occasionally appears as xenoliths (fragments) within basalt flows. Harzburgite is inferred by seismic studies to form a high-density layer or zone underlying some active basaltic volcanoes (e.g., Okubo et al. 1997). The most widespread basalts on Earth are those erupted on the seafloor, on oceanic islands and in areas of shallow mantle upwelling, called **tholeiitic basalts**, after Tholey, in the Saarland (Germany). Tholeiites are notably richer in iron and lower in alumina than those along convergent plate margins.

Minerals typical of basalt include olivine, pyroxene, and calcic plagioclase, which are all stable at higher temperatures than most silicate minerals. This indicates that basalt magma must

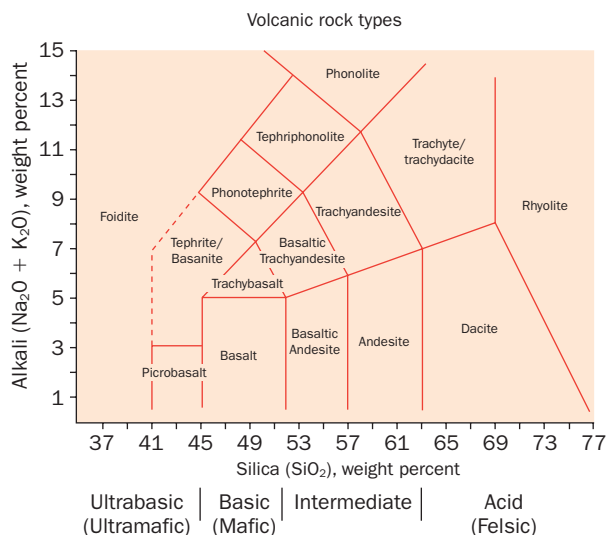


Fig. 3.3 The International Union of Geological Sciences (IUGS) Total Alkali versus Silica (TAS) diagram for volcanic rocks. Note that chemical composition alone is the basis for this classification. From Le Bas et al. (1986).

form at higher temperatures than other magma types. Some basaltic flows lack phenocrysts altogether. Such **aphanitic** (fine-grained) flows may have lost their phenocrysts due to crystal settling in the source magma reservoir prior to eruption, but some may represent melts that erupted at temperatures so high that crystallization had no chance to begin before they cooled. High temperature melts have low viscosity – that is, greater fluidity. They also are less dense than surrounding source rock, are buoyant (Chapter 4) and can rise rapidly – in some instances traversing kilometers of crust in a matter of just a few days or weeks (Klein et al. 1987; Rutherford 2008).

As magma cools to crystallization (or **liquidus**) temperatures, viscosity increases because silica (SiO_2) tetrahedra begin linking together within the melt. Even before crystal nuclei develop, long silica-based polymer chains will form in the cooling magma. The more silica present within the melt, more viscous it tends to be at any given temperature. Of all magma types, basaltic magma contains the least amount of silica, which contributes to its high fluidity during ascent.

Relative to other magma compositions, basaltic magma generally contains only small amounts of volatiles, ranging from about 0.5 to a little more than 1 percent of the total weight of the magma that reaches the surface. On the basis of vesicle volumes as related to experimentally determined magmatic solubility of water, Moore (Moore 1970) concluded that basaltic magmas erupted on the deep ocean floors contain from 0.25 to 0.9 per cent H_2O . These low values are typical. In contrast, some subduction-related erupting basalts may contain as much as 6 per cent H_2O (Roggensack et al. 1997). Lack of volatiles, especially dissolved water, plainly plays a role in explaining the eruption behavior of most basaltic magmas. Low volatile content explains why explosive basaltic volcanic eruptions are not frequent, nor typically large. While there are some exceptions, and basaltic ash and pumice does exist, basalt erupts primarily as highly fluid lava. An entire class of less-common basalts, **alkalic basalts**, characterized by higher amounts of NaO and K_2O , form under different melting conditions than do tholeiitic basalts, and are frequently associated with the earliest and late stages of Hawaiian volcanism, and are characteristic of basalts erupted in continental areas. Alkalic basalts are more fluid and rise to the surface faster than do normal basalts, and commonly are hosts for **xenoliths** (embedded fragments) of ultramafic, mantle-derived rocks.

ANDESITIC AND MORE SILICA-RICH MAGMAS

Andesitic magma occurs primarily along convergent plate boundaries, where subduction has generated melting in the upper mantle wedge separating the down-going plate from the lithosphere above. The origin of andesite is still somewhat unclear. Geochemical evidence of both crustal and mantle contributions exists in typical andesite. Volcanic rocks that are chemically classed as andesites can vary considerably in physical appearance. Some are dark, resembling basalts, others are lighter gray in color, and contain numerous long phenocrysts of plagioclase and hornblende. A general consensus is that andesites must be derived from the upper mantle above dewatering, subducting slabs, initially perhaps as basaltic magmas that later become modified by assimilating material from the lower crust. Andesites can also form by the mixing of basalt with more silica-rich magma in magma reservoirs (Blatt et al. 2006). Andesites and basalts often erupt in close proximity to one another, further suggesting a genetic

connection. In younger oceanic island arcs, basalt tends to be more prevalent (Devine 1995), while in older island arcs (e.g., Phillipines and Indonesia) and continental areas, andesites usually predominate over basalts, suggesting that partial melting of silica and alumina-rich continental rocks are important to andesite production (Eichelberger 1978). This appears to be confirmed by the enrichment of elements such as lanthanum, barium, and potassium in many andesites – elements concentrated in continental crust and derived sediments (Rogers and Hawkesworth 2000).

Like andesites, dacites and their intrusive equivalents (granodiorites) primarily occur along convergent plate boundaries. Many early petrologists like Bowen thought that dacites, andesites, and granite itself formed primarily through gravitational fractional crystallization in basaltic magma. While it is clear that this process is important in some long-sustained mafic magma reservoirs (Gunnarsson et al. 1998; White and Urbanczyk 2001; Haase et al. 2006), the regional volumes of other igneous rock types relative to mafic rocks seem to rule this out as the only mechanism to describe their origin (Blatt et al. 2006). Impossibly large bodies of basalt magma would be required to generate the great volumes of more siliceous – igneous rocks found in continental mountain ranges, although some dacites and granodiorites may well derive from fractionated mafic melts. Some might also develop from partial melting of lower crustal rocks, such as gabbro (e.g., Smith and Leeman 1987). Most, however, result from crustal partial melting and the mixing of silica-rich granitic magma with silica-poor basaltic or andesitic magmas, as shown by field relationships (e.g., Wiebe 2001; Harper et al. 2004; (Fig. 3.4).

H₂O and other volatiles lower magma liquidus temperatures. This is because these volatiles are generally ionized in solution at a high temperature and are apt to form temporary bonds with other elements, hence inhibiting the development of stable crystal nuclei. As molten rock approaches the surface the escape of volatiles causes the melt to suddenly become more viscous and to start crystallizing new minerals. Evidence of this occurs in many lava flows and domes,

Fig. 3.4 Block from the Williams Crater area, near the western rim of Crater Lake caldera, Oregon. Shows the mingling of two distinctive magma types of greatly different viscosity – highly silicic material (light-colored) and darker, glassy mafic material. Photo by R. W. Hazlett.



which contain two distinctive populations of crystals – coarse phenocrysts formed by slow cooling deep underground, and numerous fine, generally needle or lath-shaped crystals, termed **microphenocrysts** and **microlites**, which represent sudden crystallization from water loss during ascent to the surface. In many cases, suddenly stiffening magma will stop rising altogether and solidify at shallow depth, such as beneath the growing dacite dome of Mount St Helens [27] in 2004 to 2006 (Cashman et al. 2008). Some of these very shallow magma bodies have the textural appearance of surface lava, even including minor vesicles, although if water is entrapped rapid growth of large phenocrysts is possible. Geologists call them **hypabyssal** (meaning “very shallow”).

In contrast to basalt that originates in the mantle, siliceous magmas form in the silica-rich crust at lower melting and liquidus temperature conditions (Clemens 1998; Chappell and White 2001). Because of lower temperatures and higher silica contents, molten granite and its volcanic equivalents are much more viscous than basaltic magma. Moreover, since continental crust contains more bonded H₂O than the mantle, granitic melts have a considerably higher volatile content than basaltic melts. The viscosity of ascending granitic melt may increase due to volatile losses as it rises closer to the surface. Consequently, proportionately much less granitic magma can erupt (to form rhyolite) than to form basaltic melt. And if it does erupt, it is apt to do so accompanied by significant explosive activity. Rhyolitic pyroclastic rocks are thus much more abundant than rhyolitic lava flows. In fact, the most powerful known volcanic eruptions are associated with high-silica magmas.

Granites, dacites, andesites, and continental basalts (those that occur along continental convergent plate boundaries) are relatively rich in aluminum and calcium. Petrologists call them **calc-alkaline** or **high-alumina** rocks. **Alkaline rocks**, as mentioned earlier, contain higher amounts of alkali elements, notably potassium in continental areas, and sodium in oceanic settings. Laboratory experiments indicate that alkaline compositions arise from small amounts of mantle partial melting at great depths – as much as 100 to 150 km, sometimes associated with subduction, as shown by Italian volcanoes, which are notably alkalic in composition. More typically, alkalic volcanic rocks are associated with areas of extending continental crust far from any plate boundaries, and with the initial and final stages of mantle plume (hot spot) volcanism, as mentioned above for alkalic basalts in the Hawaiian Islands. Geologists have introduced a plethora of exotic names to describe alkalic volcanic rocks, reflecting differences in relative silica and alkali ion compositions – for example: hawaiiite, phonolite, tephrite, ankaramite, benmoreite, and leucitite.

CARBONATE-BASED MAGMAS

The rarest type of terrestrial magma is not based on silica chemistry, but upon carbonate. This magma, essentially molten baking soda, has erupted at about 50 highly localized sites, primarily in a few young or immature continental spreading centers, notably including the Rhine Graben of western Germany and the East African Rift Valley (Wooley and Church 2005). The principal product of such eruptions is a light-colored rock called **carbonatite**, occurring both as lava flows and in pyroclastic deposits. Carbonatites also are found as veins within some volcanic diatremes (Chapter 4), all located in areas of thick, otherwise stable continental crust.

The only historically active carbonatite volcano is in East Africa. The 2000 m high basaltic composite cone of Oldoinyo Lengai [90] (“The Mountain of God”), in the Gregory Rift Valley of Tanzania, has intermittently erupted sodium-rich carbonatite ash and lava during its roughly 300–400,000 years of cone growth. In the later half of the twentieth century carbonatite eruptions filled its northern summit crater to the brim with mottled brown, white, gray and black lava flows studded with spike-like spatter cones (Church and Jones 1995). The explosive summit eruption of 2007–8, destroyed this fantastic landscape however, leaving a gaping collapse pit in its place.

Although pure calcite (CaCO_3) has a high melting temperature (1339°C), alkali-rich carbonate minerals such as those found in carbonatites, in some instances mixed with minor amounts of nepheline and pyroxene, require much less heat to melt. Hence, most carbonatite lavas are at the cold end of the magma temperature range, typically around 550°C , only about half the temperature of erupting basalts. This means that molten carbonatite flows lack the incandescence of active silicate lava, resembling dark mud or porridge as they spill out (Fig. 3.5). Carbonatite lava also is much less viscous, with a consistency resembling that of motor oil at the moment of eruption. Active flows may be only a few centimeters thick, and run in channels across which one can easily step. The flows can spread more rapidly than conventional lavas, but eruptive volumes tend to be small, so the lava rarely travels very far.

Chemists and carbonated beverage drinkers alike well know that the solubility of carbon dioxide increases with pressure on a liquid. Experimental studies indicate that for mantle-derived basalts originating at depths of greater than 80 km, as much as 40 percent of the bulk weight of the source magma may

Fig. 3.5 Fresh carbonatite lava flow, Oldoinyo Lengai volcano, Tanzania. Flow in lava channel about 2 m across, and indicates high emplacement fluidity by smooth surface textures. Photo by Donald McFarlane.





Fig. 3.6 Volcanic degassing plume from Halema'uma'u crater, Kīlauea volcano, Hawai'i in May, 2008. This plume, consisting dominantly of water vapor, also contains around 10–15 percent SO_2 . Halema'uma'u has been producing 500–1,000 tonnes of SO_2 per day, which has caused extensive agricultural damage downwind. Note that the rising plume rotates according to northern hemisphere coriolis forces, and that it flattens and is deflected downwind when reaching its “neutral buoyancy level” (Chapter 4) about 1500 m above Kīlauea's summit. Photo by J. P. Lockwood.

be dissolved CO_2 (e.g., Wyllie and Huang 1976), suggesting a connection between the upper mantle and carbonatites. Indeed, observations of gaseous emissions (CO_2 , He, N_2 , Ar) from the northern crater of Oldoinyo Lengai show patterns essentially identical to emissions from divergent plate boundaries on the ocean floor, where mantle upwelling clearly facilitates volcanic activity (Teague et al. 2008; Fisher et al. 2009)

In many of its occurrences, carbonatite is closely associated with a few distinctive types of sodium-rich silicate rocks, including nepheline basalt, fenite, phonolite, and ijolite, which originate from small amounts of partial melting beneath the relatively thick lithosphere of continents. Neodymium and strontium isotope measurements and other mineralogical data suggest that as the carbon-dioxide rich silicate magma rises and the solubility of the CO_2 drops, a carbonatite melt fraction is capable of separating to erupt independently (Dawson 1998; Ulrich and Sindern 1998). Evidence for this includes rounded nodules of silicate rock within some carbonatite bodies (Bell and Simmonetti 1996). The phase separation likely takes place in the shallow crust (Lee and Wyllie 1997), explaining how Oldoinyo Lengai and other similar, now extinct volcanoes have been able to produce these two very different kinds of volcanic material from single conduits.

Magmatic and Volcanic Gases

Although volatile compounds (dissolved gases in magma) are not normally considered as eruption products (all the attention is usually focused on lava and ash), they are an important magmatic constituent, and constitute the greatest *volume* of material erupted by volcanoes (Fig. 3.6). The critical role of gases in explosive volcanic activity can easily be underestimated if only their mass is considered; their volume is much more important. Dissolved gases typically account for no more than about 1 percent of the weight of basaltic magmas, and 7 percent of highly silicic melts. The exsolution and expansion of gases as magma approaches the surface exert astounding forces. Bardintzeff and McBirney (2000) cite the example of one cubic meter of typical rhyolitic magma with dissolved gases stored deep underground, which

can expand to 670 m³ of fragmental material and gas upon reaching atmospheric pressure. It is no wonder that volcanic explosions take place!

Gases are the most important volcanic product in terms of influence on eruptive style and on world climate and atmosphere. Were volatiles not present within magmas there would be far fewer volcanic eruptions on Earth, and those that did occur would simply involve the passive extrusion of lava, perhaps in response to the rare impacts of giant meteorites as has happened on the Moon (Chapter 12).

The amount of volatiles that can be dissolved in magma depends on the non-volatile magma components and on the magma's temperature and confining (**lithostatic**) pressure. Gas solubility increases with increasing pressure and decreases with increasing temperature. The standard unit of pressure in volcanology is the megapascal (MPa), where one MPa is equivalent to ten bars, or approximately ten times the pressure of the atmosphere at sea level. For example, Hamilton et al. (1964) showed that andesitic magma can contain 4.5 percent dissolved H₂O (by weight) at 100 MPa and 10.1 percent at 530 MPa. The solubility of water in basaltic magma in this range is slightly less. **Henry's Law** is the relationship describing how solubility of volatiles changes with pressure – which in the case of volcanoes, can be taken to mean depth in a magma column beneath a vent as well:

$$C_v = kP^\beta \quad (3.1)$$

where C_v is the concentration (mole fraction) of H₂O or gas dissolved in the melt, P is the pressure of the melt (MPa), k is a constant, which differs according to the kind of volatile being studied and the composition and temperature of the melt (Table 3.2b). “ k ” typically ranges from about $4.1 \cdot 10^{-6} \text{Pa}^{-0.5}$ at the low end for siliceous magmas, to $6.8 \cdot 10 \text{Pa}^{-0.7}$ for mafic magmas. β is another constant dependent on magma composition, with values from 0.5 in rhyolitic melts to 0.7 for basaltic liquids (Woods 1995). Note the exponential relationship of β in equation (3.1). This signifies that even small changes in pressure can induce great changes in the solubility of volatiles. As volatiles come out of solution, they expand – about 1600-fold in the case of an ordinary mole of water at atmospheric pressure. Henry's

TABLE 3.2(A) SOLUBILITY OF WATER IN ANHYDROUS GRANITIC MELT AT 800°C, AVERAGED FROM FOUR DATA SETS REPORTED IN BEHRENS AND JANTOS (2001)

Pressure (MPa)	Water content (weight %)
50	2.8
100	4.3
150	5.0
200	6.0
250	6.8
300	7.4
400	8.6
500	9.5

TABLE 3.2(B) CHANGE OF WATER SOLUBILITY IN RHYOLITE MELT AT 100 MPA, EXPERIMENTALLY DETERMINED BY YAMASHITA (1999). NOTE THAT RISING TEMPERATURE (AS THROUGH INJECTION OF A HOTTER MELT FROM BELOW) DRIVES THE WATER OUT OF THE MAGMA AS A VAPOR, WHICH COULD PRESS AGAINST THE ROOF OF A MAGMA RESERVOIR AND INCREASE POTENTIAL FOR ERUPTION.

Temperature (°C)	Water content (weight %)
800	4.0
900	3.8
1000	3.6
1100	3.4
1200	3.3

TABLE 3.3 SAMPLE COMPOSITIONS OF VOLCANIC GASES IN VOLUME PERCENT OF GASES RELEASED.

	Sample					
	1	2	3	4	5	6
H ₂ O	49.14	97.1	95.0	88.87	77.20	37.00
CO ₂	23.41	1.44	4.53	6.64	11.30	48.90
CO	0.49	0.01	–	0.16	0.44	1.51
SO ₂	25.94	0.54	0.02	1.15	8.34	11.84
H ₂ S	–	0.23	–	1.12	0.68	0.04
S ₂	–	–	–	0.08	–	0.02
HCl	0.42	2.89	0.02	0.04	0.42	0.08
HF	–	0.26	–	–	–	–
H ₂	0.49	0.70	–	1.54	1.39	0.49

1 Sample from basaltic eruption fume, Etna [89], 1970, convergent plate margin (Huntingdon 1973).

2 Sample from fumarole atop Momotombo volcano [53], Nicaragua, at 820°C, convergent plate margin (Symonds et al. 1994).

3 Average of four “low-temperature” fumarolic gas analyses, Shiveluch volcano [141], Kamchatka, convergent plate margin (Fedotov & Masurenkov 1991).

4 Gases emitted by an andesite flow at 915°C, Merapi volcano [110], Java, convergent plate margin (Symonds et al. 1994).

5 Gases from the lava lake of Erta Ale [99], Ethiopia, at 1130°C, divergent plate margin (Symonds et al. 1994).

6 Kīlauea summit basalt flow, 1170°C, hot spot/mantle plume volcano (Symonds et al. 1994).

Law quantitatively shows that the rapid exsolution of volatiles associated with reductions in magma pressure – the causes of volcanic explosions – must occur within the bodies of large volcanoes themselves rather than beneath them. Volcanic gases consist mostly of H₂O, CO₂, and SO₂ (Table 3.3).

WATER

Most of the “smoke” seen issuing from volcanic craters and fumaroles consists of water vapor. Effusive eruptions usually begin with the billowing of white steam from opening fissures before lava reaches the surface. Water vapor (steam) is invisible when its temperature exceeds its boiling point and only shimmering heat waves may be seen rising directly from high-temperature vents, but visible steam will reappear higher above, due to cooling and condensation. Most of the water emitted from volcanic vents is **meteoric** – that is derived from heated groundwater. Studies of stable hydrogen isotopes in volcanic steam indicate, however, that re-heated groundwater alone cannot account for all of the water that issues from volcanoes. There is also a primary “magmatic” (or **juvenile**) component, at some volcanoes exceeding 50 percent of total steam emissions (Giggenbach 1987; Hedenquist and Aoki 1991).

CARBON DIOXIDE

The various constituents of volcanic fumes have differing solubilities in magma which independently change as a function of pressure as well as temperature. That means that the volatile make-up of magma and the compositions of its gas bubbles change as the melt rises from its point of origin to the vent. Carbon dioxide is thought to be the dominant gas dissolved within mantle-derived melts rising through the lower to middle crust, and has been estimated to comprise as much as 0.7 weight per cent of juvenile basaltic magma (Gerlach et al. 2002). The solubility of carbon dioxide drops drastically with reduction of pressure, however. A typical batch of molten basalt becomes over-saturated with respect to CO₂ even before it reaches the shallow crust, causing the exsolution of CO₂. Increases in CO₂ emissions thus commonly precede eruptive activity.

Carbon dioxide emissions from volcanic arc and mantle-plume related “hot-spot” volcanoes tend to be notably higher than they are from volcanoes along mid-ocean ridges and in mature continental rift zones. In volcanic arcs, carbon dioxide enrichment could derive from several sources: Subduction and partial melting or the metamorphism of siliceous carbonate rocks and sediments can provide substantial CO₂ to arc magmas (Marty et al. 2001). Arc volcanic gases can also incorporate carbonate-rich fluids from crustal metamorphic and metasomatic reactions, many of them triggered by magmatic heating. A third source is simply the volatilization of entrapped seawater itself, which contains about 40 mg/kg dissolved carbon dioxide at mean pressure and temperature – a huge storehouse of potential carbon dioxide gas.

Where magma reservoirs and intrusions cool slowly in the shallow crust, carbon dioxide continues to leak out steadily even after substantial crystallization. In fact, a key indicator of shallow ascending magma is a slow but measurable diffusion of CO₂ and helium from the ground, a phenomenon called **soil efflux**, which excludes other kinds of volcanic gas because of their higher solubilities in magma or groundwater. A particularly worrisome case of soil efflux began at Mammoth Mountain, a popular ski resort in east-central California in 1989, as molten rock ascended to within a couple of kilometers of the surface. Carbon dioxide above the intrusion infiltrated forest soils next to Horseshoe Lake, at the southern foot of the volcano. Ordinarily, the amount of CO₂ in the soil pores of healthy forests is no greater than about 1.5 volume percent; but at Horseshoe Lake soil pore concentrations quickly rose to 30–90 percent,

poisoning tree roots and turning the forest into a wasteland. Over a period of 15 years some 40 hectares of forest died, and by the late 1990s Mammoth Mountain was still releasing nearly 50–150 tonnes of CO₂ a day through passive soil emissions – comparable to the level of many frequently active volcanoes (McGee and Gerlach 1998). The last eruption at Mammoth Mountain was a minor phreatic event about 600 years ago, but gas emissions tell us that the volcano is still magmatically active at depth.

Fumaroles that primarily emit carbon dioxide are called **mofettes**. Mofette gases typically have temperatures much below the boiling point of water and sometimes are nearly as cool as the surrounding air. CO₂ is a heavier-than-air gas, and may accumulate in closed basins and can drain down small valleys, causing an uncommon, but lethal volcanic hazard (Chapter 14).

Carbon monoxide is a minor constituent of some high-temperature fumaroles. The abundance of carbon monoxide relative to carbon dioxide is a function of the temperature of the erupting magma and the issuing fume. CO₂ gradually decreases and CO concentration rises by some two orders of magnitude with a change in eruption temperature from 800 to 1200°C. The oxygen bonds in carbon dioxide break down, forming carbon monoxide with increasing heat (Heald et al. 1963).

SULFUR

After water and carbon dioxide, sulfur is the next most abundant volatile present in typical magmas (Table 3.3). Owing to multiple valences (sulfur may carry charges of 0, –2, or +6) sulfur produces many kinds of volcanic gas, reflecting various degrees of oxidation and reaction with CO₂ and water. S₂, SO, SO₂, SO₃, H₂S, H₂SO₄, COS, and CS₂ are all present in volcanic fume (Heald et al. 1963), although the most common species by far are SO₂ and H₂S. The apparent color of SO₂-rich fume clouds changes with the nature of incident light. When viewed through transmitted light (as when looking into the sun) clouds will appear brownish in color; when viewed by reflected light (as when the sun is behind you) the same clouds will appear bluish.

Volcanic SO₂ emissions potentially have great environmental impact (Chapter 13). Pinatubo volcano [104] in the Philippines released an estimated 20 million tons of sulfur dioxide during its paroxysmal eruption on June 15, 1991, most of which entered the stratosphere as a persistent aerosol haze. The amount of SO₂ released by continuously active volcanoes of the world is very large, and has been estimated at 4.6×10^5 t/yr from Kīlauea volcano [16] alone – although this is only about 4 percent of the typical yearly global volcanic output (Sutton et al. 2001).

HALOGENS

The halogens, chlorine, fluorine, and bromine are minor volcanic gas constituents. While H₂O, CO₂, and SO₂ are measurable as weight percents, halogens are measurable only in parts per million (ppm), with chlorine and fluorine rarely exceeding 5000 ppm in a silicate melt, and bromine typically less than 250 ppm (Carroll and Holloway, 1994; Aiuppa et al. 2009).

Water vapor reacts with fluorine and chlorine to create HF and HCl, both of which are extremely acidic aerosols in volcanic fume. Where molten lava enters the sea, boiling of the salt water creates steam clouds rich in hydrochloric and sulfuric acid droplets. Hawaiians refer to

this irritating, corrosive steam as **laze** (“lava” plus “haze”). With a pH of 1.5–2.5, rain drops condensing from laze steam will sting the eyes, and eat holes in clothing of observers in a short time. If the laze contains HF, camera lenses and eyeglasses may also be damaged. It is definitely good practice to observe the interactions of molten lava and seawater from the *upwind* side!

Chlorine is less soluble in silicate magmas than CO₂. And CO₂ is less soluble than sulfur. This means the early releases of fume from ascending magma will be more enriched in chlorine relative to sulfur and carbon dioxide than at a later stage, and gases of sulfur will become dominant in fumarolic emissions after an eruption has ended. Some long-lasting post-eruptive vents issuing only steam and sulfur with minor carbon dioxide are called **solfataras**, and can be easily spotted from a distance owing to the yellow coloration of the sulfur crystals lining the vents. Halogen-dominated fumaroles, similar to mofettes and solfataras do not develop, since the concentrations of chlorine and fluorine tend to be so low in magmatic gases.

Some geochemists have attempted to use the ratios of sulfur (primarily SO₂) to chlorine in volcanic fume as an index of the readiness of particular volcanoes to erupt. But the difficulty of accurately measuring chlorine, in particular, makes this approach daunting. Another volcano monitoring approach involves measuring the total emissions of SO₂ alone, independent of chlorine (e.g. Edmonds et al. 2003). The quantity of SO₂ released from fumaroles around a volcano will tend to increase as magma approaches the surface then slowly taper off following eruption to be replaced by H₂S, steam and other gases. If no fresh batches of magma rise to revive fumarolic activity, the remaining magmatic gases gradually disappear as well leaving only steam vents behind which in turn slowly die as underground heat dissipates.

New volcanic gas species in very minor amounts continue to be discovered in volcanic emissions, recently including HNO₃ and NO_x (an active irritant in urban smog) both of which result from the thermal breakdown of atmospheric air near the surface of molten lava pools. Halogen oxides and halocarbons (including natural chlorofluorocarbons, or CFCs), can form through chemical reactions between volcanic fluids and enclosing rocks (Mather et al. 2004). One of the more interesting of these exotic gases is bromium monoxide (BrO), which has been detected in the eruptive clouds of several volcanoes, including Soufrière Hills [60] following the renewal of volcanic activity in 1995.

Like volcanic chlorine and commercial CFCs, BrO plays a role in depleting life-protecting stratospheric ozone (O₃) by causing dissociation of ozone molecules into ordinary diatomic oxygens (O₂). In fact, though far less abundant than chlorine in volcanic emissions, BrO may annually contribute to as much as a third of all **volcanogenic** ozone depletion globally. So corrosive is BrO to ozone that local ozone holes can appear temporarily above volcanoes which have expelled a large amount of this gas (Bobrowski et al. 2003). Bromium and chlorine oxides injected into the upper atmosphere by a large Plinian eruption will attack ozone by the

Brx-Clx-Ox Reaction:



[N.B. – The term M^* refers to the energy and momentum provided by collision with a third particle]

Perhaps 20–40 percent of all atmospheric ozone depletion is triggered by bromine compounds, from both natural and artificial sources. Natural biological processes and human manufacture, however, create by far the largest concentrations of bromine in the stratosphere. Volcanic sources of chlorine and bromine amount to no more than a few percent of the total (Russell et al. 1996).

HELIUM

Inert gases such as nitrogen, helium, and argon are among the least concentrated of volcanic emissions, although almost always present in trace amounts. Nevertheless, helium has been of special interest because it provides a useful tracer for the mantle contribution to volcanic exhalations. There are two isotopes of helium, ^3He and ^4He . Helium-4 is widely produced in Earth's crust by the radiogenic decay of thorium and uranium. Helium-3 however is only concentrated in the mantle as a residual element left from the planet's early formation. Only a minor amount has managed to escape from the deep interior, and that has done so by processes related to volcanism. At present the ratio of ^3He to ^4He is about 1 : 100,000,000 in the air we breathe. Measuring fumarole or soil efflux samples with higher ratios therefore is a good sign that molten rock is welling up from the mantle. Around fumaroles and high-temperature springs in arc settings, vapors commonly record $^3\text{He} : ^4\text{He}$ levels 5 to 10 times that of ordinary air, while at hot spot volcanoes such as those of Hawai'i and Iceland the difference can be as great as a factor of 15. Mid-Ocean Ridge basaltic glasses commonly record an intermediate 10-fold enrichment of ^3He relative to ^4He at spreading centers (Craig and Lupton 1981).

At Mammoth Mountain [36] prior to 1989, $^3\text{He} : ^4\text{He}$ levels were 3.5–4 times atmospheric levels, as measured in fumarolic emissions. But in 1989 the onset of the seismic activity stimulated by the Horseshoe Lake intrusion accompanied a rise in this value to 5–6, where it has hovered ever since. Mammoth Mountain has erupted primarily rhyolitic material throughout its fitful history, but the high ^3He emissions indicate that it must have some sort of “chemical communication” with the mantle. Molten basalt working its way into the lower crust is not only causing partial melting of more silicic magma at shallower depths, but must be transferring mantle volatiles to it as well. A similar observation has been made at Yellowstone caldera, Wyoming, [40] where gas emissions from the Mud Volcano steam field yield $^3\text{He} : ^4\text{He}$ ratios comparable to those of mid-oceanic hot spots. The presence of a thick continental crust is no impediment to the escape of helium-3 from the mantle (Sorey et al. 1998; Christiansen et al. 2002).

MINERAL SUBLIMATES AND FUMAROLE ALTERATION PRODUCTS

Persistent fumaroles, active sometimes for centuries, form atop the conduits of shallow, still partially-molten magma bodies, and are marked by the presence of sublimate minerals, deposited by escaping gases. They are important features for our atmospheric gas composition,

because most of the gas released by volcanoes, perhaps by an order of magnitude, comes from slow, steady fumarolic emissions *between* eruptions, rather than during the eruptions themselves (Stevenson and Blake 1998). One of the best-known examples of a long-lasting fumarole field is the one on the floor of Solfatara Crater, in the suburbs of Naples, Italy. Known as the Forum Vulcani in Roman times, the solfataras here have remained continuously active for over two-thousand years, and have been a constant draw for tourists and campers. Only one small volcanic eruption, toward the end of the twelfth century, has occurred at Solfatara throughout this long interlude.

Temporary fumaroles, lasting only a few weeks to months, may form at the mouths of cracks in the surfaces of cooling lava and ash flows. As gases escape from the fumaroles they typically sublime and condense brightly-colored minerals. Stoiber and Rose (1970), in a survey of fumarole minerals forming around several Central American volcanoes, discovered that the chemistry of these sublimates varies according to the location of a fumarole relative to the eruptive vent as well as the time elapsed from the last eruption. Where halogen gases are present we often find deposition of chlorides. The commonest are ammonium, aluminum, and ferric chloride, the first two forming bright white, and the last brilliant orange incrustations. Sulfates and hydrous sulfates are also common and include white anhydrite (CaSO_4), gypsum [$\text{CaSO}_4(2\text{H}_2\text{O})$], alunite [$\text{K}_2\text{SO}_4\text{-Al}_2(\text{SO}_4)_3$], alum [$\text{KAl}(\text{SO}_4)_2\cdot 12\text{H}_2\text{O}$], thenardite (used as a rat poison; Na_2SO_4) and epsom salt ($\text{MgSO}_4\cdot 7\text{H}_2\text{O}$). Hydrogen sulfide (H_2S) rising from depth is oxidized at the surface to sulfur dioxide or to pure yellow sulfur that often forms masses of beautiful delicate needle-like crystals (**flowers of sulfur**) around the mouths of solfataras. Minor amounts of metallic minerals may also be deposited, including metallic chlorides and sulfates, and oxides of iron, copper, lead, zinc, arsenic, antimony, and mercury. Many of these metals are transported as chloride complexes in the vapor state. Water combines with ferric chloride to give soluble hydrochloric acid and insoluble ferric oxide (Fe_2O_3) that is deposited on the walls of fumaroles as a lining of tiny brilliant steel-gray to black plates of specular hematite. The fumarolic acids eat away the older rock lining the mouth of the fumarole, and may leave behind residues of ochre-colored limonite (hydrated iron oxide) and, if solutions are highly acidic ($\text{pH} \leq 3$), milky opal. Other residues include lustrous black magnesioferrite (MgFe_2O_4) and yellow-brown goethite [$\text{FeO}(\text{OH})$ named in honor of the poet whose quote opens this chapter]. For those who marvel at minerals, fumaroles can produce a feast for the eyes!

Many anti-environmentalist arguments point out that people “aren’t the only polluters; volcanoes also pollute the environment” – and even more so. But such arguments are spurious because the total pollutant loads, as in the case of bromine and chlorine mentioned earlier, are far less than supposed. For example, while volcanoes do release an estimated 130–230 million tonnes of CO_2 into the atmosphere annually human consumption of fossil fuels, production of cement, and natural gas flaring release over 22 billion tonnes per annum (Gerlach 1991, Marland et al. 1998). Similar studies comparing sulfur output of volcanoes to anthropogenic sources, primarily coal-fired power plants and heavy industries, indicates an order of magnitude difference with humans being the clear heavy-weights. We know that under natural conditions the atmosphere can easily reprocess the volcanogenic input, or life would have become impossible long ago. But coupled with the enormous human production of SO_2 and CO_2 , the Earth System can simply be overwhelmed.

FURTHER READING

- Ebinger, C. J., Baker, J., Menzie, M. A. et al. (2002) *Volcanic Rifted Margins*. Geological Society of America Special paper 362, 236 p.
- Hibbard, M. J. and Hibbard, M. (2002) *Mineralogy: A Geologist's Point of View*. McGraw Hill, 576 p.
- Scholl, D. W., Kirby, S. H. and Platt, J. P. (1996) *Subduction: Top to Bottom*. American Geophysical Union Monograph Series, vol. 96, 384 p.
- Sigurdsson, H. (1999) *Melting the Earth: The History of Ideas on Volcanic Eruptions*. Oxford, Oxford University Press, 272 p.
- Young, D. (2003) *Mind over Magma: The Story of Igneous Petrology*. Princeton University Press, 704 p.

Chapter 3

Questions for Thought, Study, and Discussion

- 1 *How* and *why* have sources of heating inside the Earth changed since the time of the planet's formation?
- 2 What is the silica tetrahedron, and why might it be regarded as the basic building block of minerals?
- 3 Describe the roles of pressure and H₂O in melting.
- 4 What enables basaltic magma to erupt so easily, and why is it more difficult for granitic magma to do so?
- 5 What are the factors considered in the classification of igneous rocks and magmas?
- 6 What was N. L. Bowen's great contribution to our understanding of magma?
- 7 Why were the nineteenth-century scholars Buffon and Kelvin wrong in their calculations for the age of the Earth?
- 8 What was Sir Arthur Holmes' great contribution to our understanding about the cooling of the Earth?
- 9 How might measurements of SO₂ from a volcano be a useful indicator of its potential eruptive state?
- 10 Why is the environmental significance of BrO? Do you think that we should be concerned about the impact of volcanic gases and the global environment? Why/why not?

Chapter 4

The Physical Properties of Magma and Why it Erupts

Magma is not accessible to direct observation; its very existence is inferred, and its properties have to be deduced by circumstantial observations in nature and by laboratory experiments.

(T. F. W. Barth 1952)

We discussed how magma is formed and how different magma types are classified in the previous chapter, but here we need to add that of all the molten rock generated below and within the Earth's crust only a small fraction – probably less than 10 to 15 percent – ever makes its way to the surface to form volcanic rocks. Most magma solidifies far below the surface to form *plutonic* rocks – never to see the light of day until cooled and exposed by erosion. This chapter explores the factors that enable magma to reach the surface and thus form the volcanoes, lava flows, and tephra deposits that are the principal focus of this book. But first, some more background about magma temperatures and viscosity – critical factors affecting magma mobility.

Magma Temperatures

In the last chapter we introduced the application of **geothermobarometry** – the study of mineral compositions to estimate original temperature–pressure conditions of igneous minerals at the time they cool and crystallize. Geothermobarometry can provide important insights about conditions that govern magma emplacement and related volcanic activity (Table 4.1). For example, Wark et al. (2007) employed the Ti-in-quartz geothermometer to document temperatures in the

Volcanoes: Global Perspectives, 1st edition. By John P. Lockwood and Richard W. Hazlett. Published by Blackwell Publishing Ltd.

TABLE 4.1 SOME IMPORTANT GEOTHERMOBAROMETERS.*

Type	Notes	Developers and important reference papers
Plagioclase geothermometer	Uses anorthite-albite ratios to determine temperature of plagioclase crystallization in magma	Kudo & Weill (1970); Stormer & Carmichael (1970)
Fe-Ti “two oxide” geothermometer	Estimates magma temperature based upon iron and titanium oxide mineral chemistry	Buddington & Lindsley (1964); Anderson & Lindsley (1988); Ghiorso & Sack (1991)
Al-in-hornblende geobarometer	Estimates depth of magma body emplacement based upon aluminum content in hornblende	Hammarstrom & Zen (1986); Anderson & Smith (1995)
Mg-volcanic glass geothermometry	Uses MgO content of volcanic glasses to estimate temperature at time of eruption and quenching	Helz & Thornber (1987)
Ti-in-quartz geothermometer	Magma temperature based on Ti-content of quartz. Useful for granitic rocks formed at 10kb pressure or less	Wark & Watson (2006)
Ti-in-zircon, Zr-in-rutile geothermometers	Magma temperatures based on zircon and rutile mineral chemistries in intermediate and silicic rocks. May be sensitive to pressure, even at less than 10 kb	Watson et al. (2006); Ferry & Watson (2007)

* For more information on geothermometers, barometers, and silicic plutonic rocks, see Anderson et al. (2008).

magma body that erupted to form the Bishop Tuff in central California, as recorded in the rims of quartz phenocrysts preserved within the tuff. The temperatures measured closely match those of earlier Fe-Ti two oxide geothermometry – in the range of 720–790°C (Hildreth, 1981). Evidence was found that a small thermal pulse (ca. 60°) from injection of fresh mafic melt into the lower part of the magma chamber may have triggered the eruption of the Bishop Tuff – one of the largest explosive North American eruptions of the past million years.

Optical pyrometers, developed for use in foundries over a century ago, were long used to estimate lava flow temperatures based upon radiated colors, which are also useful for visual estimates (Table 4.2). Volcanologists now use hand-held radiometers and thermocouples for more precise measurements. **Radiometers** measure temperatures based upon infrared radiation emissions from heat sources. **Thermocouples** (a voltmeter connected to high melting point wires – typically chromel–alumel) serve for direct measurements of lava temperatures, and involve insertion of bimetallic probes directly into or against the heat source – a difficult undertaking on active lava flows.

Lava begins cooling the moment it erupts, meaning that a single flow will exhibit a wide range of temperatures as it is emplaced. Using radiometry, Pinkerton et al. (2002) classified four “thermal components” of a typical active lava flow on Kīlauea volcano [15], including a flow core (greater than 1050°C), thin stretching crust (750–900°C), rigid solid crust (less than 750°C), and the flow margins (less than 175°C). Some greatly localized portions of the flow, such as active tumuli and pyroduct openings (Chapter 6) can be as much as 150°C hotter than the surrounding surface.

TABLE 4.2 CORRELATION BETWEEN THE TEMPERATURE OF LAVA AND ITS COLOR.

Color	Temperature (°C)
White	≥1150
Golden yellow	1100
Orange	900–1000
Bright cherry red	700–800
Dull red	550–625
Lowest visible red	475
Pizza oven temperature	260–315

Lava begins flowing at temperatures above about 700°C.

Source: US Geological Survey, Cascade Volcano Observatory.

Magma Rheology

Rheology is the study of how solids and liquids respond to **stress** – the application of *force per unit area*. In a broad sense, we can classify magmas (and lava flows) as being “elastic,” “viscous,” or “viscoelastic” in their rheological behaviors under differing conditions. An **elastic** substance is one like a rubber band; you can stretch it, but once you let it go (release the stress imparted by your fingers), it will return to its original size and general shape. It may seem counterintuitive, but solid rocks can also be regarded as being elastic bodies. If subjected to sudden blows a rock will simply transmit the shock energy through its body and return to the same state of rest as it had before being struck. This is how earthquake shock waves are transmitted through the Earth; the “rubber band” stretching of rock takes place with arrival of each seismic wave, but the energy then is transferred to the adjacent mass of rock as a compressive pulse or shearing movement along the line of travel, and the original rock mass returns to its rest position, unperturbed. There are limits, of course, to how hard and how fast you can strike a rock without it breaking. This limit defines the **strength** of a rock. **Faults**, the sources of earthquake shock waves, represent planes of rupture where rock strength was exceeded by powerful tectonic forces.

Viscous materials respond to stress by flowing rather than transmitting energy. The degree to which they do so defines their viscosity. Liquids of low viscosity flow readily; those of high viscosity flow only very slowly and with difficulty. As pointed out in the previous chapter solids like glaciers and hot mantle rock can also flow, and might in fact be regarded as high viscosity fluids. A liquid of low viscosity, such as water, quickly spreads into a broad thin sheet when poured out onto a table top. A liquid of higher viscosity, such as cold molasses, poured out in a similar manner spreads slowly and never attains as thin and widespread a sheet as does the water. Still more viscous substances, like cold tar or shoemaker’s wax, remain standing for a time as a steep-sided lump on the table, but over a period of a few days or weeks gradually flatten and spread out. Even window panes and the hard slabs of stone benches in very old cemeteries deform and flow under the pull of gravity.

Two classes of viscous materials of particular interest to us: the Newtonian and non-Newtonian fluids. **Newtonian fluids** are those like water in which the value of the viscosity does not change, irrespective of how fast the fluid moves across a slope:

$$\tau = \mu (du/dx) \quad (4.1)$$

where τ represents the “shear stress” – the stress imparted by a fluid in the direction of its flow going from the base of the current to its top (assuming that this surface is in full contact with the air); and du/dx is the changing speed of the flow also going from its base to top. Viscosity (μ) is the constant of proportionality in this equation. Newtonian fluids will maintain their fluid properties irrespective of how fast they are stirred or mixed. At constant temperature and pressure, most magma and molten lava are Newtonian in behavior.

A **non-Newtonian fluid** is one in which viscosity changes according to the rate at which shear stress is applied. An example is pudding in a cup. You can stir it, but a hole will open in the wake of the stirring implement that only gradually re-fills. Non-Newtonian behavior can be induced by mixing certain substances together. Take corn starch and stir it into a glass of water. At a certain critical point when the corn starch and water have developed a more or less uniform consistency, the solution undergoes **shear thickening** and it becomes non-Newtonian. “Shear thickening” means that as the mixture is stirred, its viscosity jumps. The mixture stiffens. Put a finger slowly into the cup and turn it slowly, and it behaves like a liquid. But poke it rapidly, and it responds like a rubbery solid. Likewise, turn the cup over all at once and the mixture will stay stuck in the cup, only slowly slurping out as a single mass.

A **viscoelastic** substance is one in which, as the name implies, there is both viscous and elastic behavior. A viscoelastic substance will respond to stress by deforming, but after the stress is relieved, it will only partly recover its original shape and size. A significant type of viscoelastic behavior in volcanology is that of **Maxwell bodies**. You can make a Maxwell body by attaching a spring to a **dampner**, which is essentially just an empty syringe in which you compress trapped air. The spring represents the elastic response of the system, while the dampner represents the viscous response. Of course, Maxwell bodies don’t all come with syringes and springs, but within their homogeneous masses they combine behavioral aspects of both. If a Maxwell material is suddenly subjected to stress it will respond instantly just like any elastic body, but then it will continue deforming beyond its **elastic limit**, at a constant, unrecoverable rate, meaning that when the stress is relieved, the Maxwell body will only *partly* recover its original shape and size. The elastic response (ϵ_{rev}) is defined by:

$$\epsilon_{rev} = \sigma/E \quad (4.2)$$

and the viscous by

$$\epsilon_{irrev} = t_1(\sigma/\mu) \quad (4.3)$$

with σ equal to the stress, t_1 the total time that the stress is applied to the body, and E a constant called the **Elastic modulus**; more or less the “springiness” of the system.

The walls of some deep-seated magma conduits and of large, long-lived magma chambers consist of heated rock that softens and responds to pressures exerted by the magma viscoelastically.

This is shown by the folded and sheared country rock associated with the margins of some deeply eroded granitic plutons, such as in the Sierra Nevada Range of California. The degree of deformation intensifies with proximity to the borders of these plutons. Such viscoelastic behavior may have an important bearing on the ability of the certain magma chambers to erupt, because it is more difficult for critical fracturing to initiate in their walls (Jellinek & DePaolo 2003).

Just as Newtonian bodies can change into non-Newtonian bodies, so too can elastic substances become viscoelastic and even viscous. The partial melting that generates magmas begins when solid elastic rock heats to the point where it becomes a viscoelastic mass until finally it melts and becomes fully viscous. The process works in reverse too. Consider the cooling skins of molten lava flows, or of fluid volcanic bombs tossed out of some volcanic vents. These bombs cool to the point of becoming viscoelastic as they sail through the air. They continue to cool and are deformed into aerodynamic shapes as they travel toward their points of impact, where sudden collision with the ground causes them to deform even further or to fracture.

Lava flowing out from vents is much more viscous than most liquids with which we are familiar. Sometimes lava appears to be very fluid, and one often hears it said that such lava “flowed like water.” Actually, the most fluid silica-based lava known (at 1100°C) has a viscosity about 100,000 times that of room-temperature water, with rare carbonate-based lavas having lower viscosities than this, but still much greater than water. The false appearance of great fluidity results from the high density of lava, as much as three times that of water, which because of momentum on slopes causes it to assume the flow characteristics of a liquid of much lower density and volume. From this “low” viscosity, lava ranges to very high viscosity and, in fact, grades into a solid condition. Viscosity is the principal factor that determines the ultimate shape of lava flows, from thin pāhoehoe (Chapter 6) to extremely thick lava domes (Chapter 9). Field studies of lava flow morphologies is one of the best ways to evaluate the rheology of lava (Moore 1987).

The viscosity of magma depends on several factors, including its chemical composition (especially silica content), the amount and condition of included gas, the amount of solid load being carried, and its temperature. The presence of solid fragments (either phenocrysts, micro-lites, or fragments of foreign origin) in magma also increases its bulk viscosity simply by increasing the frictional resistance to flow. Likewise, a rough bed beneath flowing lava flowing on a slope will impart friction that raises flow viscosity. The effects of gas are more complex. Vesicles may increase, or decrease viscosity dependent upon their shapes as well as the steadiness of flow. Spherical gas bubbles tend to make steadily moving flows more viscous, in a manner analogous to suds in a solution of soap in water; one can set a mass of soapsuds on a table top and have it remain there without flowing appreciably until the bubbles have burst. Vesicles elongated in the direction of flow, however will reduce viscosity by facilitating shear. If the flow is unsteady, viscosity effects depend upon the ability of vesicles to change their shapes according to changing flow conditions. If vesicles cannot adjust their shapes fast enough to keep pace with changing flow conditions, flow viscosity tends to drop (Llewellyn & Mangan 2004).

The basic unit of measurement of viscosity in the cgs system is the **poise**, which is measured in units of grams per centimeter per second (g/cm/s). In the SI system viscosity is measured in **pascal-seconds**, in which 1 pascal-second (Pa s) is equivalent to 10 poises. The viscosity of water is equivalent to 1×10^{-2} poises. By comparison, air has a viscosity of 17.4×10^{-6} ; olive oil of 81×10^{-3} , tree pitch of 2.3×10^8 , and glass of more than 10^{20} poises.

TABLE 4.3 SOME SAMPLE IGNEOUS MELT VISCOSITIES.

Type	Viscosity (poises)
Basaltic melt at 1200°C	10^2 – 10^3
Andesitic melt at 1200°C	10^4 – 10^5
Rhyolitic melt at 1200°C	10^6 – 10^7
Erupting basalt	10^3 – 10^4
Erupting andesite	10^5 – 10^7
Erupting rhyodacite	10^{11}

Temperature is the most important influence on viscosity. Given constant pressure, the higher the temperature of magma, the lower its viscosity. This is particularly evident in the behavior of lava flows. As they travel away from vents, they lose heat by radiation and conduction into the air above and the ground beneath, and the viscosity steadily increases. Macdonald (1972) reported that a flow on Mauna Loa [13] was found to be more than twice as viscous 19 kilometers down the mountainside as it was when it issued from the vent. On Etna [82], Walker (1967) found that the viscosity of a small flow increased about 375-fold (from 0.4×10^5 to 1.5×10^7 poises) in a distance of only about 450 meters. He also found that the viscosity at which lava stops moving is between 10^9 and 10^{11} poises, depending on slope angle. Freshly erupted basalt on this same volcano has viscosities at low as 9.4×10^4 (Pinkerton & Sparks 1978).

Neuville et al. (1993) examined the viscosities of andesite and rhyolite at a range of temperatures. At 764°C, they measured a viscosity of 1×10^{10} poises in the laboratory for a sample of andesite, which dropped to 1×10^3 poises at a temperature of almost 1400°C. For a sample of much more siliceous rhyolite, the range of viscosity values was from 1×10^{16} poises at 647°C to 1×10^4 poises at 1643°C. The influence of dissolved water on the viscosity of magma is also important, as shown by the laboratory research of Shaw (1972) in which he demonstrated that a 4–5 weight percentage increase in magmatic H₂O can decrease the viscosity of a basaltic melt from 10^9 to 10^5 poises, depending on temperature. Table 4.3 gives viscosities of different melts as reported by Blatt et al. (2006).

Every house has a plumbing system, and so does every volcano . . .
(Professor G. P. L. Walker addressing a classroom at
the University of Hawai`i, October, 1988)

Magma Ascent and Emplacement

It is now known that the level to which magma rises beneath (or within) volcanoes is largely controlled by local equilibrium between the density of the magma and the density of enclosing rocks. Ryan (1987a) noted that:

Magmatic fluids, generated at depth in the Earth's mantle often come to rest at surprisingly shallow levels within the crust. It is, of course, remarkable that so long an odyssey should be interrupted just short of subaerial or submarine eruption.

TABLE 4.4 SOME ESTIMATED MAGMA ASCENT RATES BENEATH VOLCANIC AREAS.

Volcano	Type of volcano and tectonic setting	Rate of ascent (m/sec)
Mount St Helens, Washington State	Composite cone, volcanic arc	0.007–0.15
Soufrière Hills, Monserrat	Composite volcano, island arc	0.001–0.015
Mt Unzen, Japan	Composite volcano, volcanic arc	0.002
Kīlauea, Hawai`i	Hot spot volcano, Hawaiian mantle plume	0.03–1.7*
Kimberlite diatreme	Explosive volcanic pipes (see text below)	1.1–30

* See Klein et al. (1987).

Source: Modified from Rutherford (2008).

Ryan then went on to introduce the concept of **neutral buoyancy** to describe the critical role of density in governing the rise of magma beneath volcanoes. The level of neutral buoyancy is the level where the density of magma equals the density of the surrounding country rocks, and is the depth at which magma may accumulate to form magma chambers. This concept is based on the realization that magma is a fluid (albeit normally a very viscous one), and will respond to the laws of gravity like any other fluid or plastic medium and will seek local mechanical equilibrium. If the density of magma is less than that of the surrounding rocks (positive buoyancy), it will attempt to rise; if its density is greater (negative buoyancy) it will tend to sink. The same principle was earlier observed by Francis (1982), who noted that “hydrostatic equilibrium” governed the injection of basaltic lava sills into layered Paleozoic sedimentary rocks of northern England. Walker (1989) applied the neutral buoyancy concept to a wide variety of volcanic settings, demonstrating its importance to understanding all volcanic processes that involve the storage and migration of molten rock.

More is known about the generation, ascent, and emplacement of magma beneath oceanic volcanoes than about magmatic processes that take place below and within continental volcanoes, mainly because the processes involved are less complex, and the travel times from origin to eruption are usually much shorter (Table 4.4). In some parts of the world tectonic activity has also exposed the deep roots of oceanic volcanoes and their magma plumbing systems in places where oceanic crust has thrust up (**obducted**) onto the edges of continents at convergent plate boundaries (e.g., Dilek & Robinson 2003).

Many of the concepts about magma ascent and emplacement have been developed in Hawai`i, based on petrologic and geophysical studies. Some late-stage alkali basalts ascend to the surface at high velocity (several m/sec) and this allow these fluid lavas to carry fragments of the upper mantle (**mantle xenoliths**) with them to the surface. Some of these peridotite xenoliths are cut by pyroxenite veins that are structurally similar to the veining in granitic migmatites (Wilshire & Kirby 1989). It may seem odd that brittle fractures and veins could form in the very hot, plastically deforming mantle, but perhaps rapid decompression may be involved, causing mantle rocks to snap apart like rapidly-stretched putty. It may also be that these veins form by fracturing of larger mantle fragments after transport to cooler crustal levels. Magma quickly exploits any pathways for escape and fills them. The rate at which it can rise from the mantle can be ascertained at Kīlauea volcano in Hawai`i, where volcanic tremor originating in the region of partial melting 40–60 km down may be tracked migrating upward into the volcanic edifice over a period of just a few months. These earthquakes most likely

represent cracking of wall rock along the path of ascent by batches of melt (Aki & Koyanagi 1981). Sometimes, the magma entering the volcano apparently does so continuously and relatively passively, with little or no apparent seismic activity. Continuous recharge has largely been the case since onset of eruption in the east rift zone of Kīlauea in 1983 (Thornber 2003). At other times, magma ascent is episodic. Mike Ryan (pers. comm. 2007) writes that when such events occur “there are several lines of evidence, including studies of microseismicity, rock mechanics, and eruption dynamics, that indicate [the] magma does not ascend along continuously open pathways, but instead rises as disconnected batches.” The ascent rates of magma have been determined by seismic observations at several volcanoes.

Although, xenolith-bearing alkali basalts found at many continental monogenic volcanoes and on some oceanic volcanoes like Hualālai [12] (Hawai`i) must rise rapidly from their source areas and may erupt without significant pausing, this is more the exception than the rule (Clague 1987); most rising magma stalls and accumulates at certain neutral buoyancy levels in the crust. These magma storage sites may prove temporary, if magma density decreases during storage and allows migration of residual melts to higher levels (see “Eruption Triggers” section below). Two such magma storage levels are thought to exist under active Hawaiian volcanoes. One level lies at the mantle-crust boundary, the so-called **Mohorovicic (M) discontinuity**, where seismic waves passing through the mantle slow down upon entering the lower-density crust. The M-discontinuity lies about 25 kilometers beneath the largest of the active Hawaiian volcanoes, Mauna Loa, and is somewhat shallower beneath Kīlauea. Magma accumulates here temporarily because of decrease in density contrast and loss of buoyancy upon entering the crust.

At a shallower level, the rising magma stalls and accumulates at the level where its density matches that of the surrounding crust, or volcanic shield. Volcanoes with long histories or repeated eruptions almost invariably are fed from shallow magma chambers stabilized by neutral buoyancy. The magma reservoir immediately underlying Kīlauea’s summit lies 1.5–5 km down and is several km wide (Fig. 4.1). Seismological evidence suggests that it is not actually a spherical, liquid-filled void as depicted in some simplistic cartoons of volcanoes, but rather a spongy mass of plastic or viscous very hot rock permeated with channels of more fluid, eruptible magma (Ryan 1988; Dawson & Chouet 1999). Because the level of neutral buoyancy in large volcanoes like Kīlauea rises as the volcanoes grow and are compacted (become more dense) at depth, it is likely that their shallow-level magma chambers gradually shift upward over time as well, while maintaining their neutral buoyancy (Fig. 4.2) (Decker et al. 1987; Ryan 1988).

Crustal extension and related faulting also greatly influence the pattern of magmatic intrusions within Kīlauea. While the north flank of the volcano is buttressed by the adjoining mass of Mauna Loa, the south flank is unsupported and slopes to the 5 km-deep ocean floor. As Kīlauea swells with magma, stress imparted to its southern flank has caused large-scale slumping and faulting across most of the mountainside – an area measuring roughly 60 by 80 km. An interplay of forces has developed that involves periods of (sometimes violent) movement in the south flank, opening spaces within the volcano for more magma to migrate horizontally along neutral buoyancy horizons. The infilling of magma, and compaction of the underlying regions of the volcano, adds additional weight and pressure to the weak flank, which eventually responds by slipping further to accommodate yet another round of intrusions.

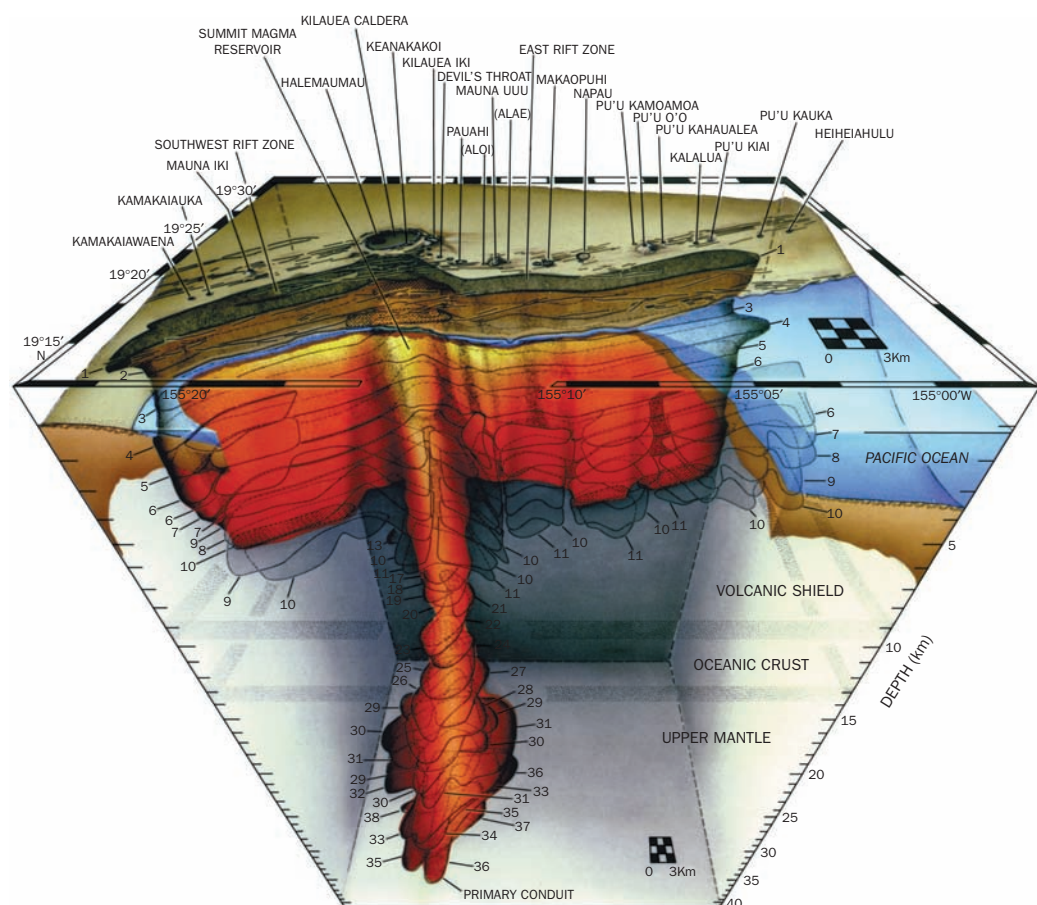


Fig. 4.1 The structure of Kīlauea volcano's magma system, as viewed from the south. This model is based on an analysis of over 25,000 earthquakes measured in this area between 1969 and 1985. Magma is seen to rise through complex channelways from its place of origin in the upper mantle, through the oceanic crust, and to its level of neutral buoyancy, where it accumulates in a shallow magma chamber beneath Kīlauea caldera and migrates along rift zones. From Ryan (1988).

It is impossible to discern cause and effect in this geological interplay; one form of behavior leads to the other in a feedback process. As a result, two narrow bands of extensional dilation, magmatic intrusion, and fissure eruptions, termed **rift zones**, extend as far as 120 km from the summit of Kīlauea. Each marks the crest of the volcano's southern flank, and both are artifacts of gravity guiding the upwelling of melt as it approaches the surface. Similar rift zones are present on most of the world's oceanic shield volcanoes.

Although the summit magma chamber of Kīlauea actually lies within the body of the volcano, this is not the case for comparable magma chambers underlying most "grey" volcanoes. Perhaps this is because these volcanoes typically have smaller volumes than the Hawaiian shields, and their density structures require lower levels of neutral buoyancy at which magma can reside. The magma feeding the catastrophic eruption of Mount St Helens [28] on 18 May, 1980, for example, originated at depths of 7–14 km beneath the base of the mountain. All subsequent dome-building eruptions from 1981 to 1986 tapped magma stored at a shallower depth – less than 4 km, suggesting a close relationship with the channel feeding molten rock from a deeper-seated reservoir (Blundy & Cashman 2006). At Vesuvius [86], mineral chemistry and seismological data indicate that the magma reservoir also is "deep seated" – or was originally. Recent data suggest that it has shifted upward over the past 20,000 years some 9–11 km, with an ascent of 3–5 km between 79 and 472 CE – the dates of two very explosive eruptions. Scaillet et al. (2008), who provide these data, suggest that

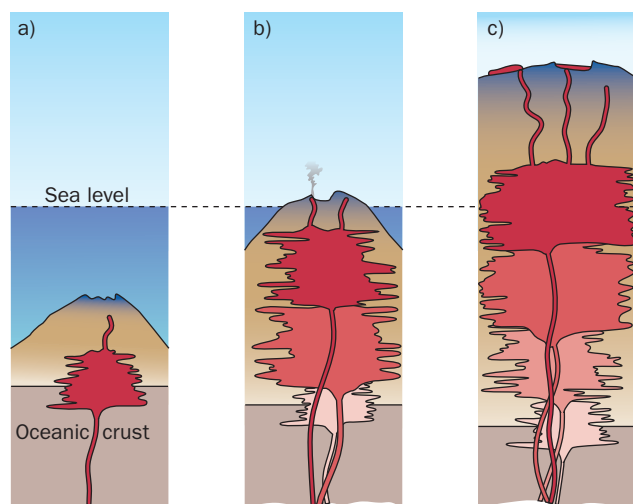


Fig. 4.2 Magmatic evolution of an oceanic volcano. As surface eruptions build volcanic edifices higher, the density of lower parts of the volcano increase, owing to compaction, mineralization, and accumulation of dense minerals. Active magma chambers (red) must thus ascend upwards through growing volcanoes with time, always seeking their “Level of Neutral Buoyancy.”
 a) Submarine volcano; b) Immature subaerial volcano; c) Mature oceanic shield volcano, with summit lava lake and flank eruptive activity. Note that submarine slopes are steeper than subaerial ones, and that the base of the growing volcano subsides owing to isostatic adjustments. Modified after Ryan (1987b).

changing stress field conditions, including caldera collapse and gravitational spreading of the mass of Vesuvius, plus differences in volatile content of the magma could account for this remarkable change.

To think that all volcanoes must have single long-lived magma storage systems is probably erroneous. Koyaguchi and Kaneko (1999) provide evidence for short-lived magma reservoirs beneath some volcanoes that experience repeated solidification and remelting events. That multiple ephemeral magma storage chambers (a complex magma reservoir system) may feed a single volcano is also possible. This appears to be the case with Ruapehu, New Zealand [134] – the most active volcano in Australasia (Gamble et al. 2003). Anna Myers (2007, p. 36) comments:

The picture is emerging, rather than having one big magma storage chamber, Ruapehu has a complex plumbing and reservoir system of relatively small-scale magma stores distributed throughout the crust beneath the volcano. Each magma batch evolves on its own timescale, assimilates surrounding crust, and then mixes with other batches. . . . Ruapehu [has] . . . an “open” plumbing system, with the magma exchanging both heat and material with the surrounding crust.

Similarly, Newberry [34] and Medicine Lake [32] volcanoes in the Cascade arc appear to be fed by multiple small magma storage sources spanning a wide range of compositions (Donnelly-Nolan 1988; MacLeod & Sherrod 1988; Fig. 4.3).

At the other end of the spectrum from the numerous small magma sources of Ruapehu and the Cascade volcanoes with are the large, discrete magma chambers underlying silicic calderas such as Yellowstone [40] and Long Valley [37] (from which the earlier mentioned Bishop Tuff erupted). These single magma bodies may have volumes greater than 5000 km³, the size of the most voluminous known volcanic eruptions (Chapter 10). The Yellowstone magma chamber underlies an area measuring 40 by 80 km – comparable to the city of Los Angeles, with a roof only about 8 km thick. Seismic data indicate that only about 10–30 percent of the chamber is presently liquid – the rest is a mushy bed of uneruptible phenocrysts (**mush**) and solid but very hot rock fully crystallized from the melt (Bachman & Bergantz 2008). Nonetheless, this vast pocket of magma is still quite active. Between 2004 and 2006, fresh mafic melt apparently flooded into the bottom of the chamber, causing the surface above to rise as fast as 7 cm/year, three times the historical rate of caldera uplift (Chang et al. 2007). Analogs of similar magma bodies – granitic plutons long crystallized and exposed by erosion – occur throughout the rugged western United States, revealing varying degrees of interaction with mantle-derived melts (Miller & Miller 2002). The largest silicic magma bodies are elongated lenses typically only a couple of kilometers thick, but from 10 to 20 kilometers wide. Those associated with vigorous high-silica volcanism appear to lie mostly in the depth range of 4–10 km (Lindsay et al. 2001).

The development of **seismic tomography** (slice picture) techniques, based on the observed variation of seismic wave velocities as teleseisms (from distant earthquakes) pass through and below volcanoes, has allowed great refinement in our understanding of volcanic structures and magma reservoir geometries. Higher velocity zones indicate the presence of dense, crystalline rocks, whereas low velocity areas indicate the presence of high-temperature or partially molten rocks. Results show that some vigorously active volcanic centers such as Krafla (Iceland) [72] and Rabaul caldera (Papua New Guinea) [122] show low velocity anomalies, whereas others such as Taupo caldera (New Zealand) [135] and Hekla (Iceland) [67] show no clear anomaly structures at all, suggesting either extremely shallow or very deep magma reservoirs, or the lateral feeding of magma from distant sources (Finlayson et al. 2003; Lee 2007).

One of the many questions in volcanology concerns where magma reservoirs and their overlying volcanoes establish themselves where they do. In the United States Pacific Northwest, many large volcanic cones are positioned within grabens, which apparently formed as down-dropped blocks of crust pulled open in gaps between the ends of parallel strike-slip faults. The extension developed within these blocks would make it easy for rising magma to form full scale reservoirs, simply by leaking into fractures incrementally opened by fault motion. It is not certain that this has happened in the Pacific Northwest, although in southern Greenland, plutons crop out throughout a deeply eroded region between the ends of large strike-slip faults whose motion appears to have permitted passive, simultaneous ascent of magma by pulling apart the crust (Harrison et al. 1990). In the Ivrea-Verbano zone in the Italo-Swiss Alps, mantle-derived melts accumulated at the base of rapidly extending metamorphic terrane in late Paleozoic times (Quick et al. 1992). Similar situations may have governed Miocene volcanism in the Los Angeles Basin, where tear faults along the San Andreas Fault System created tensional openings that resulted in extensive basaltic eruptions (McCulloh et al. 2005).

Further evidence to support faulting as a mechanism for accommodating upwelling magma comes from the Mopah Range of southeastern California (Hazlett 1990). There, detachment faulting occurred simultaneously with volcanism 16–23 million years ago. In this area of extreme crustal extension, volcanic vents and their feeder systems became aligned along the most intensively active normal faults in the upper plate of the regional detachment structure (Fig. 4.4). The numerous alkalic basalt volcanoes of Europe (The Eifel volcanic field in western Germany, the Chaîne des Puys volcanoes of central France, the scoria cones of the Czech Republic and the La Garroxta volcanic field in northeastern Spain) were very active in Pleistocene time, producing cinder cones, lava flows and explosive maars whose locations appear to have been controlled by extensional tectonics. Although there have been no eruptions for the past ten thousand years or so in these countries, there are probably still pockets of magma beneath them, and no one should ignore the possibility of future fireworks in these areas.

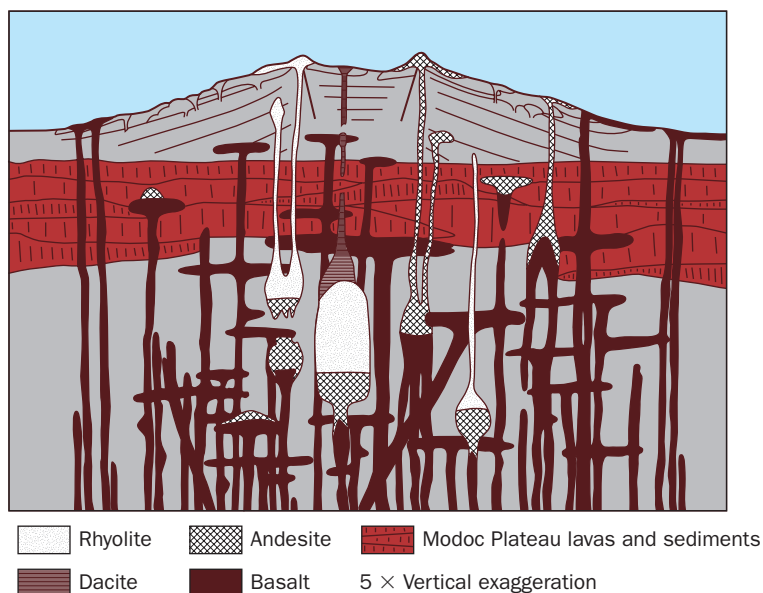


Fig. 4.3 Cartoon sketch showing the inferred complexity of the magma reservoir system beneath Medicine Lake Volcano, California. Seismic studies indicate that no single large magma chamber is present. The width of feeder dikes is greatly exaggerated. From Donnelly-Nolan (1988).

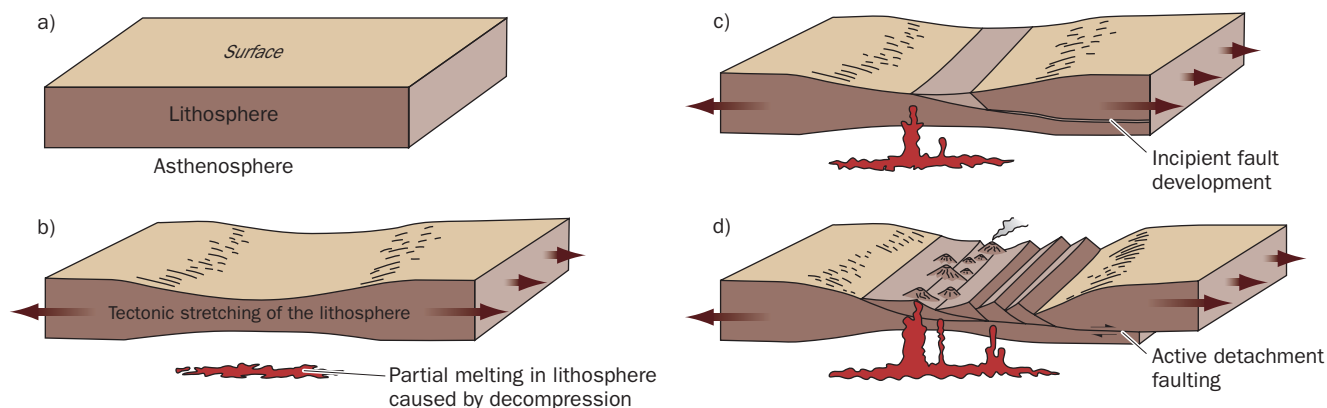


Fig. 4.4 Schematic relationship between faulting and volcanic activity seen in the Mopah Range, California and in other areas of rapidly extending continental crust.

“Frozen Magma” – Subvolcanic Intrusives

The relationships between plutonic rocks and their overlying volcanic rocks can be exceedingly complex. The great Sierra Nevada Batholith of California was apparently roofed in places by its own volcanic cover, yet this cover was itself intruded by later plutonic rocks and partly melted to form new igneous rocks, some of which solidified as plutons, and some of which probably reached the surface to form volcanoes anew. Steeply inclined or vertical pipe-like volcanic conduits and dikes commonly link magma reservoirs to overlying volcanoes (e.g., Takada 1988; Furman et al. 1992; Day 1993; Okubo & Martel 1998; Gudmundsson 2006). The dikes commonly radiate around conduits extending all the way up into volcanic edifices, or may form parallel to one another in long linear rift zones on volcano flanks.

Where large magma chambers only a few kilometers deep inflate and lift their roofs, a pattern of inward-dipping concentric dikes, referred to as **cone sheets**, commonly develop. Magma drainage and subsidence can generate another, almost vertically inclined set of concentric dikes enclosing the sinking roof block of the chamber, termed **ring dikes** (Johnson & Schmidt 2002). These special sorts of dikes are discussed further in Chapter 10. Volcanic eruptions may be fed through central conduits or wherever dikes intersect the surface (Fig. 4.5).

Plugs are the solidified igneous rocks frozen within former volcanic conduits. They commonly resist erosion more effectively than the surrounding altered and fractured crust, causing the former conduits to rise as **volcanic necks**. Formation of plugs at the tops of conduits that are still partially active may have led to quiet periods that preceded many explosive eruptions as at Mount St Helens (1980) and Galunggung [99] (1982). Eventually, plugs become so thick as magma supply wanes that volcanic activity is no longer possible.

Plugs and necks range in size from a few tens of meters to over a kilometer in diameter. Some necks rise as high as 500 m, and are usually steep-sided, often serving as pedestals for shrines, fortifications, and castles in Europe. Devil’s Tower is a famous volcanic neck in north-eastern Wyoming, USA (Fig. 4.6). This pinnacle of phonolite (a silica-poor fine-grained alkaline rock) may represent an intrusion of hypabyssal rock that never reached the surface to form a volcano (River & Harris 1999). Shiprock, New Mexico, is another spectacular volcanic neck that probably once did feed an explosive volcano and maar crater at a long-ago eroded-away surface (Fig. 4.7). Dikes radiate in three principle directions from the base of this neck (Delaney

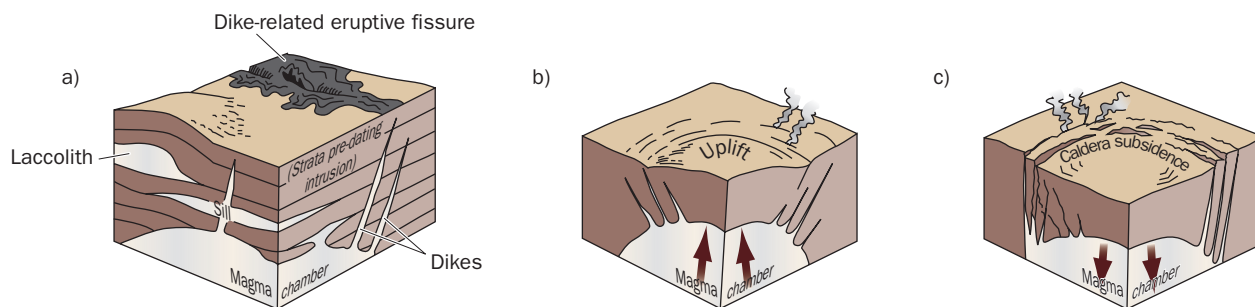


Fig. 4.5 a) Dikes, sills, and laccoliths are common intrusive structures associated with magma reservoirs; b) Cone sheets can develop in the roofs of magma chambers accumulating in the shallow crust; c) Ring dikes can develop in response to the withdrawal of magma from underlying chambers.

& Pollard 1981). The dikes consist of hypabyssal lamprophyre (a dark, porphyritic volcanic rock), whereas the neck is mostly made up of tuff and breccia (Chapter 7). A volatile-rich magma quickly ascended from great depths to form this neck, fracturing bedrock around the conduit and filling those fractures with melt to produce the massive dikes. When the conduit-filling magma breached the surface, explosions ensued that apparently filled the pipe with a mixture of ash and rubble from both above and below. Fine veins of calcite criss-cross the neck, evidence of late-stage carbon dioxide percolating through the breccia.

Explosive volcanic conduits such as Shiprock are called **diatremes**. They are distinguished from the conduits feeding shield volcanoes and probably most composite volcanoes, because of the predominance of explosive (generally alkaline) fill material. They are restricted to regions underlain at depth by Precambrian continental crust, and are of economic interest because

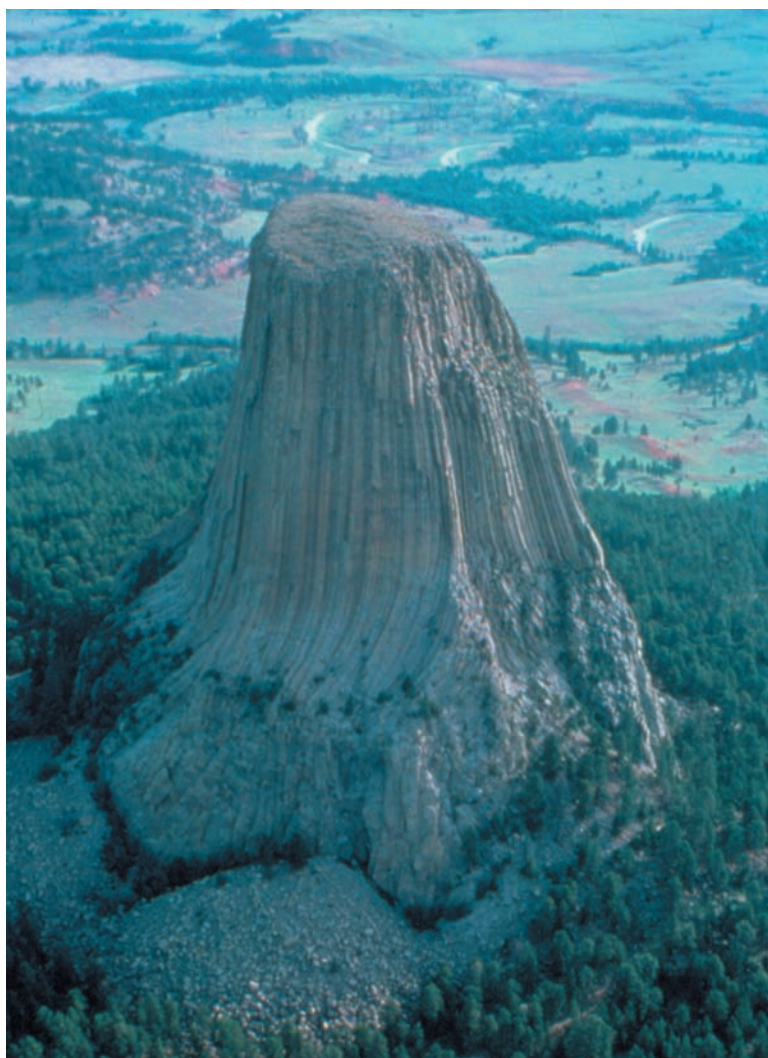


Fig. 4.6 (right) Aerial view of Devil's Tower, Wyoming, showing spectacular development of columnar jointing, which suggests a period of slow hypabyssal cooling. This 254 m-high volcanic plug is composed of phonolite lava, and may or may not have fed a volcano at the surface. Photo courtesy of Devil's Postpile National Monument.

Fig. 4.7 View to west of a 500 m-high volcanic pipe and associated dikes near Shiprock, New Mexico. The pipe is a diatreme filled with welded tuff breccia that is more resistant than the surrounding soft sedimentary rocks, which have been eroded away over the 25–30 million years since the diatreme was emplaced. Note the radially oriented, resistant dikes of minette lava that were emplaced during this eruption. Photo by D. L. Baars.



some contain diamonds – an indication of their great source depths. Some, if not all, represent the exposed conduits of maars (Chapters 1 and 7, Martin et al. 2007).

Hans Cloos (1941) published the pioneering work on diatremes, describing a group of 300 plugs and necks in Swabia, not far south of Stuttgart, Germany. These 15–18 million-year-old conduits, each a product of a single short-lived volcanic eruption, cut plateau-forming carbonaceous sedimentary rocks of Jurassic age, and are filled with a mixture of tuff, lapilli, finely ground sediment, and sedimentary blocks (Fig. 4.8). The tuff consists of consolidated glassy ash. The blocks are of the same sedimentary rocks that make up the walls of the necks. These blocks are not arranged randomly, as they would be if they had fallen back into the conduit after being thrown into the air. Instead, many of them, particularly larger ones, are derived from the immediately adjacent wall rocks, which may be different from those a short distance above or below, and have simply moved outward and a little downward into the conduit. Flow structure is typically well developed in the tuff, with wedge-shaped fissures penetrating the conduit walls and the sedimentary blocks.

Many volcanic plugs show connections with underlying dikes. While some plugs are nearly circular in ground plan, others are oval, and in extreme cases they are gradational into fissure fillings; they become dikes at depth. Alignments of plugs are common, and strongly suggest their localization above deep-seated magmatic fissures. As magma in dikes approaches the surface, the unequal reduction of pressure along the crest of the dike encourages magma to focus its ascent at sites of least resistance, forming one or several narrow, cylindrical conduits (e.g., Mastin & Pollard 1988).

DIKE FEATURES

Most dikes exposed by erosion extend as linear features for long distances, but some are broadly curved in plan, depending on the crustal stress field controlling their injection. In detail they commonly consist of numerous short fairly straight segments. The detailed courses of many are obviously governed by pre-existing fractures. Dikes cutting pyroclastic debris tend to be regular and sharply bounded at deep levels within tephra cones, but may become very irregular or even feather out into the tephra at high levels, where confining stresses are low, and the material surrounding the intrusion is poorly consolidated. A spectacular example of a dike-fed fissure intersecting a small spatter cone may be seen high in the northeast rift zone of Mauna Loa on the Island of Hawai'i. Where the dike intruded solid flows to either side of the cone, a distinct eruptive fissure opened at the surface. But where this same dike penetrated the loose spatter, a coherent fissure was unable to form, and a shallow graben developed instead.

Dikes are commonly bounded by selvages of glass, generally only a few mm or cm thick, resulting from quenching of magma against the cooler wall rocks. Some dikes are highly vesicular, but most are more dense than the lava flows they may penetrate. Their density is partly due to escape of the gas bubbles before consolidation of slowly cooled intrusive magma, but more commonly dike density probably results from pressure of the overlying column of magma, in the same way that bubbles are prevented from forming in lava flows in deep water. Under lesser pressure at the tops of dikes the escaping gas expands to form bubbles in the liquid, forming fragmented dikes and feeding lava fountains.

Cooling of dikes by radiation and conduction of heat from their two approximately parallel boundary surfaces commonly results in well-developed **columnar jointing** approximately at right angles to the dike walls, and in the case of nearly vertical dikes, the exposed masses of columns may look surprisingly like great stacks of cordwood.

Although there can be no question that many dikes are the fillings of conduits that once fed surface eruptions, it is not often that one is exposed to reveal the connection with the lava flow it produced such as the outcrop shown in Fig. 4.9. This is because lava usually drains



Fig. 4.8 Detailed view of the tuffaceous breccia (right) comprising a diatreme intruded into solid limestone (left center) in Swabia, southwestern Germany. The height of the visible exposure here is about 3 meters. Photo by R. W. Hazlett.

Fig. 4.9 Cross-section of a Quaternary dike that supplied a fountain-fed `a`ālava flow near Salto di Cani, north flank of Mt Etna, Sicily. The dike intruded upper Tertiary sediments along a fault that is downropped to the east, and built a low spatter rampart on the upslope side of the erupting vent. Photo by J. P. Lockwood.



down, or explodes out of a fissure during the final phase of eruptions, severing any connection with surface flows.

I (JPL) am probably one of the only people who has ever seen a dike forming – during a December, 1974 summit eruption of Kīlauea volcano, Hawai`i. Subsurface magma was radiating outward down the volcano's Southwest Rift Zone (SWRZ) (Fig. 1.10) and surface fissures were spreading up and down the SWRZ. I was in line with the zone of propagating fissures that night, when a crack started to slowly open in the ash a few meters away, and a line of steam marked the new fissure. The steam would have been white in daylight, but was now colored a brilliant pink from the light of active fountains downrift. Within about 30 seconds, the red fumes turned darker, and a foolishly sampled whiff showed that the steam had turned to SO_2 . The fissure rapidly opened to 10 cm or so, and the sulfur gases began to burn with blue flames. The roots of a small bush growing next to the crevice were being stretched taut across the widening crack. Suddenly, with a snap like a banjo string breaking, the root broke. At this time I could hear a crackling, hissing, rumbling sound, and out of curiosity I straddled the rapidly opening crevice. I was amazed and fascinated to see red lava slowly rising in the fissure about 10 m below me! I stood over the rapidly widening crack for only a few seconds – but what a thrill – watching the top of a lava dike ascending to the surface beneath my legs! The top of the dike began to spatter and eject blobs of lava, and I quickly moved away. Within a few minutes, lava fountains were shooting up from the dike to more than 25 m height!

PSEUDODIQUES

Just to add a complexity, not all volcanic dikes form from magma intruding from below – some dikes in Hawai`i can be shown to have been fed from surface lavas that poured into open

(or opening) fractures on the sides of volcanoes (Easton & Lockwood 1983). Vast quantities of lava have been observed to pour into open fractures during Hawaiian eruptions, and such “surface-fed” dikes may be much more common in volcanic terrains, at least those associated with fluid basaltic eruptions, than is generally recognized. We call these features **pseudodikes**. Elsewhere in the world, notably at the well-known Big Pumice Cut near Long Valley in eastern California, clastic sediment fills older fissures, creating sheet-like bodies resembling dikes from a distance, but packed full of material resembling ordinary stream gravel and sand.

SILLS AND LACCOLITHS

Less common than dikes, **sills** are also tabular intrusive bodies. They tend to be nearly horizontal in orientation, and instead of cutting across stratification as dikes typically do, they form parallel to, or intrude directly along the boundaries separating layered rocks of contrasting rigidity (Kavanagh et al. 2006). Such conditions prevail in layered roof rocks above shallow magma chambers or zones of intensive intrusion. A **laccolith** is a sill-like structure that is lens shaped with the overlying layering arched upwards. It forms through repeated injections of melt along the same horizon (Menand 2007). Some researchers argue that sills and laccoliths can evolve into full-fledged magma chambers as they incorporate melt from sustained dike intrusions (e.g., Gudmundson 1986; Miller et al. 2005; Hawkins & Wiebe 2007).

Like dikes, shallow sills may develop columnar joints, vertical in orientation in contrast to the horizontal columns of dikes. This can cause difficulty for geologists, for sills may be mistaken in cross-section for buried lava flows. Fortunately, a few useful criteria exist for telling them apart. For example, lava flows will not contain any inclusions of an overlying (younger) stratum. A sill, however, may dislodge fragments of an overlying stratum as it intrudes, incorporating them as xenoliths. Also, shallow sills may heat and thermally alter or mineralize wallrock, both above and below. This, however, can only happen at the base of lava flows. In addition, many of the finer-scale structural features of lava flows, such as flow joints, breccia at the tops and bottoms of `a`ā, pyroclasts, zones of intensive vesicle formation, etc., are lacking in sills.

Triggers for Volcanic Eruptions – Why Volcanoes Erupt

It is becoming increasingly clear that the magma reservoirs underlying the world’s active volcanoes are, for the most part, in a delicate state of gravitational equilibrium with enclosing rocks, and that many factors can contribute to their destabilization and to subsequent eruptive activity. Eruption “triggers” are mostly related to processes that increase the buoyancy and mobility of a magma body, and can be separated into three categories: processes taking place *below* magma chambers, processes *within* them, and processes taking place *above* them. The processes operating below and within a magma chamber unfold over long time periods, and typically set the stage for eruptive activity by transforming conditions, including melt temperature, volatile content, pressure, shape, and size. Such processes may control the eruption timing for volcanic systems that are already “primed.”

Potential eruption triggering processes occurring *below* a magma reservoir are related to the rise of new material migrating from storage areas or magma generation sites in the mantle below, in most cases involving the injection of mafic melts into more silicic magma above. Summarizing the thinking of many researchers, Martin et al. (2007, pp. 89–90) comment:

Replenishment of a cool silicic reservoir with hot mafic magma may have a number of possible effects. The simple addition of a new volume of magma to a magma chamber has the potential to create an overpressure large enough to cause failure of the chamber walls and result in an eruption. Cooling of the mafic magma and heating of the resident magma [more silicic melt above] may result in volatile exsolution which will also contribute to chamber overpressurization. Heating may also cause convective uprising and remobilisation of the resident magma, possibly resulting in eruption.

As a case in point, Martin et al. (2007) suspect that intrusion of basaltic andesite melt into the bottom of the dacitic magma chamber of Santorini volcano, Greece, [91] triggered the onset of a three-year long eruption cycle one month later (1925–8). Intrusion of basaltic magma beneath Mt Pinatubo [104] also set the stage for the 1991 eruption (Palister et al. 1996).

Magma chamber overpressurization is an important process within magma chambers. It is the development of fluid and gas pressure within a magma chamber sufficient to fracture its walls allowing for a runaway feedback process culminating in eruption. The feedback works like this: Upon initial fracturing of the chamber walls, loss of pressure causes additional volatiles to come out of solution (exsolve) which, because of the expansion of gases into the fractures, forces further fracture development and propagation, reduces pressure in the remaining melt, and causes volatile exsolution in a sustained, possibly even accelerating process. Fracture propagation is generally easiest in upward directions through the ceilings of magma chambers, because it is here that the crust tends to be weakest. An eruption occurs when – and if – these fractures reach the surface permitting the melt to escape.

The chemical and mineralogical differentiation of magma (Chapter 3) over time can serve as a significant “internally generated” trigger for volcanic eruption. As magmas cool, heavy minerals will form and sink towards the lower parts of magma chambers and lighter minerals together with exsolving volatiles will rise. In the uppermost part of the chamber a lower density, more buoyant and silica-rich melt fraction will develop, potentially overpressurizing ceilings and seeking higher levels of neutral buoyancy. Other processes that may occur in magma chambers are related to the fragmentation of chamber walls and the sinking of dense blocks downwards (**stopping**) – which abet the processes of magma rise.

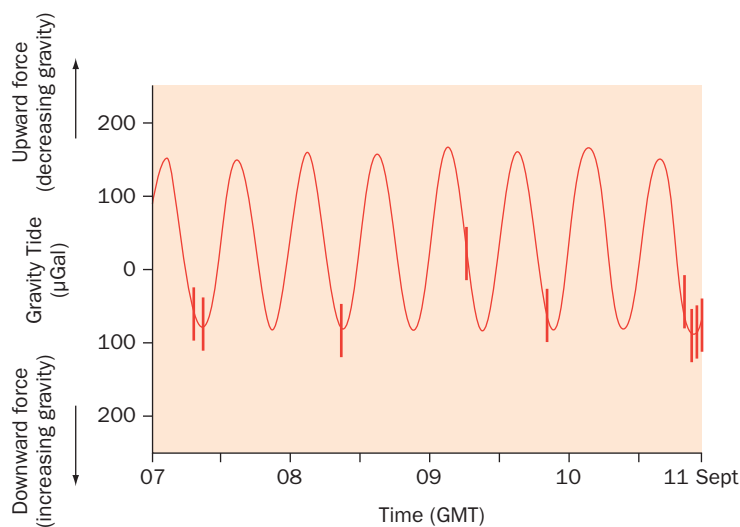
Potential triggers operating *above* magma chambers include a general weakening of roof crust because of hydrothermal and fumarolic activity, and short-term non-volcanic phenomena that can ever-so-slightly reduce confining pressure on the chambers or induce fracturing in their roofs. These “superficial” factors are diverse, and include the effects of earth and ocean tides, glacial melting, precipitation, and perhaps even variations in atmospheric pressure. Excessive precipitation has been shown to correlate with subsequent explosive activity of volcanic domes at Mount St Helens (Mastin 1994), Piton de la Fournaise [95] (Violette et al. 2001), and at Soufrière Hills volcano [60] (Mathews et al. 2009).

Earth tides – elastic rise and fall of Earth’s surface up to 40 cm caused by the gravitational attraction of the Moon and Sun – play a well-established role in triggering many short-term eruptions (Hamilton 1973; Mauk & Johnston 1973). Volcanic eruptions correlated with earth tides have been observed at volcanoes as diverse as Augustine [19], Fuego [96], Kīlauea, Mayon [106], and Stromboli [83]. Ocean tides have also been shown to affect the activity of submarine volcanic activity (Kasahara 2002). Earth tides are complex and have periodicities ranging from 12 hours to 19 years. The most important tides that have been shown to trigger volcanic eruptions are the **semidiurnal** tides that occur about every 12 hours, and the **fortnightly tides** that occur about every two weeks (when the Moon is either full or in “new moon” status – times when the Sun and Moon are aligned with the Earth). Some volcanoes show heightened eruptive activity at both tidal minima and tidal maxima (e.g., Fuego [96]; Martin & Rose 1981), some will respond to minima only, others are more sensitive during tidal maxima, while many others show no tidal responsiveness at all. No universal pattern exists, though correlations with fortnightly tides – when tidal stresses are greatest – are more common than semidiurnal ones.

Let’s consider a few examples: Dzurisin (1980) demonstrated that Kīlauea preferentially erupts at times of fortnightly tidal maxima. As a result, Hawaiian Volcano Observatory (HVO) staff tend to be more alert when the level of summit inflation is high (Chapter 14) and the moon is full. In contrast, eruptions at Kīlauea’s close neighbor, Mauna Loa show no tidal correlation. Several thousand kilometers to the southwest, the three week eruption of Gamalama volcano [107] (Mollucas island arc, Indonesia) in 1980 consisted of 34 individual Vulcanian eruptive explosions that devastated the central portions of Ternate Island and caused most of the island’s population to evacuate for safety. A subsequent investigation (unpublished) showed that these well-timed eruptions corresponded well with semidiurnal tidal minima (Fig. 4.10). The effect of tidal stresses on sub-volcanic magma chambers probably depends in great part on the shapes of those chambers (vertically extensive chambers will react differently compared with horizontally extensive ones) and to preexisting regional stress fields. Given all the possibilities, and the fact that we can’t be quite certain how magma chambers are configured beneath most volcanoes, it would certainly be useful for volcanologists to bring along earth tidal plots or software to generate them when responding to eruptive episodes – just to see if patterns emerge that could be useful for predicting future activity at those particular volcanoes.

How small a pressure change can provide the critical “trigger” to initiate explosive decompression of a magma chamber – how small a straw can “break the camel’s back?” A hint comes from the timing of the climactic eruption of Mt Pinatubo on June 15, 1991. It was perhaps no coincidence that a major cyclone – Typhoon Yunya – passed within 75 km of Mt Pinatubo that morning, and that at 11:00 a.m. the greatest pressure drop associated with passage of the cyclone (6.3 mbar) was recorded at Clark Air Force Base (Oswalt et al.

Fig. 4.10 Semidiurnal earth tides for the period September 7–11, 1980 and associated explosive eruptions at Gamalama volcano, Ternate Island, Indonesia. Eight of the nine eruptions during this time period occurred at or near tidal minima, which were the times of greatest compressive stress affecting the underlying magma chamber.



1996). The nine hour-long paroxysmal eruption of the volcano began less than three hours later, at 1:42 pm (Wolfe & Hobblitt 1996). Indications that slight changes in barometric pressure can affect the timing of eruptions has also been observed at Oldoinyo Lengai [90] (Fred Belton, pers. comm. 2007).

Of course the passage of Typhoon Yunya did not “cause” the Mt Pinatubo eruption, but this may have provided the critical trigger that initiated an eruption that would have occurred anyway. Pallister et al. (1996) have used petrologic research to demonstrate that the primary factor that set the stage for this eruption was the apparent intrusion of basaltic magma into the base of a silicic magma chamber beneath the volcano, which began almost three months before the June eruption.

Rest intervals

The **rest interval** of a volcano is the time elapsed between eruptions. No two volcanoes are alike in this regard. Most have irregular rest intervals, but some have repetitive behavior on roughly regular schedules. Rest intervals may range from days to centuries. Jellenik and DePaolo (2003) postulate that the minimum time interval (T_{\min}) between successive eruptions of a volcano is proportional to the volume of the magma chamber:

$$T_{\min} = \Delta V_{\min} / Q_{\min} \quad (4.4)$$

with ΔV_{\min} the minimum increase in magma chamber volume required to pressurize it to the point of erupting, and Q_{mean} the chamber’s average magma replenishment rate. This equation suggests that a volcano having a constant magma recharge rate will erupt at a regular interval, like Old Faithful Geyser; or if not regularly, then with the sizes of its volcanic eruptions increasing in direct proportion to the rest intervals between them. Smith (1979) pointed out that there is indeed a correlation between the energy released by eruptions and the rest times between the eruptions of many explosive volcanoes. The hiatus since the volcano’s last eruption is a measure of the size of the next eruption to follow. Smith developed the following correlation law to show this trend:

$$\log \text{rest interval (years)} = \log \text{magma volume (km}^3\text{)} + 3 \quad (4.5)$$

This relation is empirical, and was modified by Trial and Spera (1990) using a more recent data set for eruptions involving release of 1–100 km³ of magma:

$$\log \text{rest interval (years)} = \log \text{magma volume (km}^3\text{)} + 2.5 (\pm 0.5) \quad (4.6)$$

The rest intervals between extremely violent eruptions may be so long that persons living around a potentially active volcano may forget past eruptions, or lack a historical record of them. Newhall and Self (1982) note that the mean rest interval prior to 25 of the world’s most violent, documented eruptions is 865 years. Looking at 21 of these most powerful blasts, they warn that 17 of the eruptions were the *first reported volcanic activity* at the volcanoes where they took place.

The repose-interval equations are quantitative expressions of the critical role played by consistent magma chamber supply in triggering volcanic eruptions. But they only really pertain to volcanoes that are in what Wadge (1982) calls a **steady state of activity**; that is producing lava and pyroclastic material at an approximately continuous rate through time, be it through many short, small eruptions, a few large ones, or a mix of both. In fact, however, there are also many volcanoes that do not show steady-state behaviors (Lipman 1980), implying that their magma supply rates vary over time. Some, such as Kīlauea and arguably Vesuvius, show mixed steady-state and non-steady state behavior in their histories. No one yet knows how typical steady-state behavior is for volcanoes.

FURTHER READING


- Annen, C. and Zellmer, G. F. (2008) *Dynamics of Crustal Magma Transfer, Storage, and Differentiation*. Geological Society of London Special Publication 304, 288 p.
- Breitkreuz, C. and Petford, N. (2004) *Physical Geology of High-Level Magmatic Systems*. Geological Society of London Special Publication 234, 253 p.
- Duba, A. G., Durham, W. B., Handin, J. W., et al. (1990) *The Brittle-Ductile Transition in Rocks: The Heard Volume*. American Geophysical Union Geophysical Monograph Series vol. 56, 243 p.
- Faybishenko, B., Witherspoon, P. A. and Benson, S. M. (2000) *Dynamics of Fluids in Fractured Rocks*. American Geophysical Union Monograph Series vol. 112, 400 p.
- Sparks, R. S. J. and Hawkesworth, C. J. (eds.) (2004) *The State of the Planet: Frontiers and Challenges in Geophysics*. American Geophysical Union Monograph Series vol. 150, 418 p.

Chapter 4

Questions for Thought, Study, and Discussion

- 1 The intrusion of a high temperature, volatile-poor mafic melt into the base of a low-temperature, volatile-rich silicic magma reservoir can trigger a highly explosive eruption, as in the case of the Bishop Tuff. Consider however what would happen if the reverse situation took place, with a more silica-rich melt introduced into the base of hotter mafic reservoir. (Evidence for this indeed exists in some historical cases.) Construct and explain a scenario.
- 2 Explain how the rheological behavior and viscosity of a lava change as it cools and hardens.
- 3 Why do suppose that slowly rising dikes begin to develop pipe-like conduits only when they get close to Earth's surface and not deeper down?
- 4 Dikes (and sills too for that matter) are planar bodies that tend to form perpendicular to directions of extension. How can this be demonstrated using a stick of chalk?
- 5 Why should a sill or laccolith not easily form where stronger, more rigid layers *underlie* a weaker, less rigid layer?
- 6 What are some non-volcanic analogs to magma overpressurization?
- 7 How do explain the fact that many volcanoes erupt repeatedly through the same conduit rather than form new ones with each new eruption?
- 8 How would you interpret the historical record of a volcano that shows non-steady state behavior for part of its existence, and steady-state behavior for the rest?
- 9 Why is the repose interval concept important for assessing volcanic hazards?
- 10 If you were going to try to forecast the readiness of a volcano to erupt, what factors and conditions related to the volcano would you like to know about and why?





PART III

VOLCANIC

ERUPTIONS AND

THEIR PRODUCTS

This is the largest of all the book's Parts, comprising five chapters that are important for understanding volcanic eruptions and the many varieties of rocks and ash deposits that volcanoes produce. **Chapter 5** describes some of the classification systems that are used to describe and categorize different kinds of eruptions. **Chapter 6** discusses eruptive processes and volcanic products of the red volcanoes – those characterized mostly by lava flow activity. **Chapter 7** discusses the eruptive processes and volcanic products of grey volcanoes – those characterized by explosive activity that commonly blankets large areas of surrounding land with thick (and sometimes deadly) deposits of grey volcanic ash. **Chapter 8** discusses the eruptive mechanics of the largest explosive eruptions – including the very infrequent “Super Eruptions” that have the power to alter the Earth's climate and human history.

Chapter 5

Classifying Volcanic Eruptions

To be useful, a classification must be as simple as possible; above all, it must be useable in the field.
(C. F. Park, Jr 1964)

One of the great achievements of The Age of Enlightenment has been the effort to categorize what we see in the natural world as a basis for better understanding. Many terms and concepts have been proposed that have not survived the test of time, and some older terms that *did* survive ought not to have done so because of the confusion and complexity they add to the present. This is especially true in a still-developing field such as volcanology. It is important to recognize that the most pressing need of the first volcanologists was to invent a language for communicating observations about volcanic behavior, both between themselves and to the authorities and public at large. Ultimately, it was a question of public safety as well as scientific understanding (Chapter 14).

To complicate matters, the very term **eruption** is fraught with semantic ambiguity. For example, many volcanoes burst to life by generating a series of explosions, each separated by a few minutes of quiescence. But what if the time breaks are, say, several weeks, or several years in length? Are we still talking about the same eruption, or a series of separate ones? There is no agreed-on protocol for categorizing volcanic events with longer time breaks such as these. For the sake of discussion, we propose that a lull of a year or more between outbursts on a very active volcano should take place for them to be considered as separate eruptions, and suggest that eruptive activity which occurs after shorter periods of quiescence be termed **phases** of the same eruption. The year “cut-off” interval is not entirely arbitrary: There is much greater

Volcanoes: Global Perspectives, 1st edition. By John P. Lockwood and Richard W. Hazlett. Published by Blackwell Publishing Ltd.

likelihood that independent disturbances in the magma supply involve at least a year of time – and a single eruption should, we think, be related to a unique event (e.g., the upwelling of fresh melt) within the plumbing system of the volcano.

The term **phase** also refers to a *distinctive period of eruptive behavior* within a continuous eruption. Every volcanic eruption demonstrates varying behavior over its duration. Some eruptions may change from dominantly explosive phases to dominantly effusive activity as they progress, and all eruptions vary in phases of eruptive output – usually from initially high rates to zero as activity ends.

The effusive eruptions of red volcanoes commonly have three phases, beginning with low **lava fountaining** along long linear fissures, later followed by higher **point-source fountaining** at restricted vent areas, then in turn by the sustained production of lava flows with or without low fountains. Explosive eruptions of grey volcanoes often begin with violent vent-clearing discharges of older rock, followed by sometimes cataclysmic eruptions of pumice and ash, commonly culminating with the rather sluggish growth of lava domes – again, three phases of activity. The transitions from phase to phase relate to critical thresholds in magma overpressure and release of volatiles to which we will allude in the chapters to follow.

In some cases, the phases of a single eruption may consist of cycles of changing, repeated behavior. An example is the East Rift Zone outbreak of Kilauea [15], which began in January, 1983. During the first few years of this activity each phase of the seemingly endless eruption began with sudden high fountaining and degassing of lava at the Pu`u O`o vent, which lasted just for few days then simmered down into quiet sloshing of molten rock in a crater vent that continued for several weeks.

On much longer time scales, eruptive patterns, often separated by years or even centuries, may be repeated, even with startling regularity. Such **eruption cycles**, for example, are one of the distinguishing features of Vesuvius [79], with extremely violent eruptions of similar character occurring 25,000, 22,000, 17,000, 15,000, 11,000, 8000, 3800, and 2000 years ago; the latest outbreak infamous for destroying Pompeii and Herculaneum in 79 CE. That is a frequency of one very violent eruption every 2000–5000 years. With this record, it seems inevitable that Vesuvius will erupt in the same way sometime in the next few millennia. More recently at Vesuvius, a cycle of eruptions – each consisting of a persistently mild, decades-long effusive phase culminating in a violently explosive phase – took place between 1631 and 1944. Individual eruptions in this sequence were separated by quiescent intervals lasting no more than 7 years. The regularity and rough predictability of this pattern inspired the establishment of the world's first volcano observatory (Chapter 14). The 1944 outburst apparently ended the three-century long period of rhythmic activity, and the mountain has remained ominously quiescent ever since.

How do we measure a volcanic eruption? What would *you* consider to be the most obvious things to record and report about an active volcano – apart from the obvious personal threats (Chapter 1)? Aspects of eruptive behavior that might be considered important in comparing one eruption with another might include:

- *Whether or not lava is flowing out*, and if so, how fluid (“viscous”) the lava is.
- *The kind of vent that has opened up*. Is it a fissure, or is it from a point-source on the side or top of an older volcanic cone? Or, is a new cone growing in a previously non-eruptive area?

- *The height and width of an explosion cloud*, if any.
- *The color of the eruption cloud*.
- *The amount of older rock and debris that is being thrown out*, versus fresh eruption products.
- *The kinds of fresh ejecta being discharged*.
- *The presence of any rhythmic variations or patterns in the eruption*. Is the eruption continuous, pulsational, or occasional? If so, how long are the time intervals between different phases of the eruption?

Perhaps you can think of some additional observational parameters?

Many eruption characterization systems have been proposed over the past century, based on eruptive style, volume and composition of erupted products, and energetics. We here mention only some of those we consider most important.

Lacroix Classification System

Although Vesuvius has the longest record of direct volcano observation, there are hundreds of other potentially threatening volcanoes in the world – and so the challenge before long became to develop a common language to describe volcanic eruptions that was international in scope. Finally, a French mineralogist, François-Antoine Alfred Lacroix (1863–1948), discussed matters with Italian colleagues and proposed the first comprehensive classification of volcanic behavior. He designated four kinds of eruptions, giving them the names of the volcanoes at which they often occur: Hawaiian, Strombolian, Pelean, and Vulcanian – taking into consideration their relative effusiveness or explosiveness, and their characteristic types of ejecta, vents, and patterns of eruption. This was a start, and fortunately a good one, reflected by the fact that much of our contemporary approach to classifying types of volcanic activity derives directly from Lacroix’s original work. But objections have sometimes been raised to these names on the basis that no volcano always exhibits the same sort of activity. In fact, two or more different types of eruptive behavior may develop simultaneously at different vents on the same volcano. It is quite possible to find three different vents, for instance in the crater of Stromboli, producing Strombolian, Hawaiian, and Vulcanian eruptions *all at once*. But it is also a fact that most volcanoes have a characteristic habit of eruption; and although they may depart from that habit in varying degree from time to time, so long as we remember that the names for an eruption type designate only a particular kind of volcanic behavior, why not continue to using Lacroix’s general terminology?

In fact, other eruption patterns were observed in other parts of the world that Lacroix had never witnessed. These include “Plinian” and “Surtseyan” eruptions. Also, because it is difficult to distinguish Pelean from some Plinian and Vulcanian deposits in ancient strata, the term “Pelean” began suffering a loss of popularity, especially after the 1980 Mount St Helens [27] eruption, and has since disappeared from most discussions of volcanic behavior. To make matters worse, the authors of many different textbooks and scientific articles have each proposed their own spin on the Lacroix classification scheme, because its qualitiveness allows some wiggle-room for interpretation and embellishment. This is especially true in distinguishing Vulcanian from Plinian-style eruptions. We’ll no doubt be guilty of committing the same

TABLE 5.1 MODIFIED LACROIX SYSTEM OF CLASSIFYING ERUPTIVE BEHAVIOR.

Class	Description
Hawaiian	Effusive eruptions of lava with little or no explosive activity apart from lava fountaining. Primarily basaltic. Originate at fissure vents. Associated with building of shield volcanoes and flood-basalt plains. VEI* = 0–2 (and higher for flood-basalt eruptions).
Strombolian	Moderately explosive eruptions producing cinder, bombs, and ash which are initially incandescent as they leave the vent. Blasts often periodic, associated with bursting of very large gas bubbles in the vent. Typically basaltic and andesitic, with steam-rich light-colored ash clouds. VEI = 1–3.
Vulcanian	Moderate to violent ejection of solid fragments of cold rock (Ultravulcanian eruption), or of solid, recently hardened lava (ordinary Vulcanian eruption). Associated with the clearing of conduits, often plugged with domes. Blast clouds tend to be notably darker (more ash and less steam rich) than in the case of Strombolian eruptions. In addition to numerous blocks, large amounts of ash are produced. Eruption columns feature much lightning, and accretionary lapilli may be abundant with ordinary ash fall. Dense, ground-hugging pyroclastic clouds (PDCs) possible. Any composition, but not often basaltic. VEI = 2–5 [†]
Plinian	Highly violent eruption of large amounts of pumice and ash, generally associated with PDCs. Airfall pumice beds and ash-flows, sometimes including ignimbrites, are characteristic. Caldera collapse is often associated with Plinian eruptions. Eruption columns 20–55 km high penetrate the stratosphere, injecting large quantities of water and sulfur aerosols into the upper atmosphere. Temporary global cooling may ensue. VEI = 4–8

Ranking is from least explosive to most explosive.

* Volcanic Explosivity Index, described later in the text.

[†] The older term “Pelean eruption” refers to a form of Vulcanian eruption specifically involving the clearing of a dome or cryptodome above a volcanic conduit. Many Pelean eruptions have been directed blasts (not necessarily accompanied by debris avalanches) that are followed almost at once by Plinian eruptions.

sin to a certain extent in this book, try as we might to avoid doing so. Table 5.1 is our best effort for the four “classic kinds” of eruptions Lacroix defined. We’ll soon add a few others to this list.

Rittmann Diagrams

Following Lacroix, pioneering volcanologist Alfred Rittmann (1962) proposed a useful means of diagrammatically portraying the variations of behavior during individual eruptions through use of schematic figures he called “Eruption Diagrams” (Fig. 5.1). He intended such diagrams to be used semiquantitatively, plotting readily observable eruptive parameters on vertical axes (such as eruption column height for explosive eruptions, or lava production rates for effusive eruptions) versus time on the horizontal axis. Such figures have proven especially useful for characterizing long-lived, multi-phase eruptions.

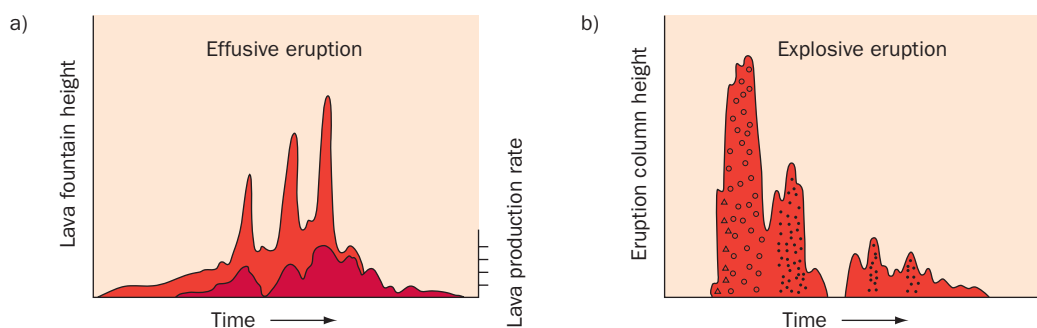


Fig. 5.1 Schematic Rittmann “eruption diagrams” can be very useful for depicting variability of eruption styles during the course of eruptive activity, as shown in these hypothetical examples. (a) For an effusive eruption the variations in height of lava fountains (light red) and lava effusion rates (dark red) are plotted against time. (b) For an explosive eruption eruption column height variations are plotted against time. Episodes of vent clearing are indicated by triangles, pumice-rich pyroclastic flows are indicated by circles, ash eruption is shown by dots, and clear areas depict periods of fuming without ash emission.

Geze Classification Diagram

Geze (1964), provided a simplified version of the Lacroix scheme that remains broadly useful, classifying eruptions using a ternary diagram (Fig. 5.2) in which the major magmatic products involved in eruptions, be they liquid, solid, or gas, are indicated. It is sometimes best to introduce students to volcanoes using the Geze perspective first, because it lends itself well to more in-depth development as the subject matter unfolds.

Walker Classification System

The LaCroix, Rittmann, and Geze schemes are most useful for characterizing eruptions in progress, but the mapping and interpretation of ancient eruptions requires different criteria. Field geologists over a period of decades began to realize that kinds of volcanic activity not recognized by Lacroix must have left the deposits that they were finding and describing.

To address these problems of nomenclature, and to add quantitative rigor to the system of classifying eruptions, Walker (1973) proposed a new classification scheme based upon factors that could be measured directly in the field. His work was in part derived from an earlier attempt by Tsuya and Morimoto (1963) to create an explosive magnitude index for volcanic eruptions, rather along the lines of the highly successful Richter magnitude already in place to study earthquakes. Walker’s proposal was distinctly advantageous in that it could be applied to pre-historic or unobserved eruptions. Walker (1973) noted “Fewer than 10% of the explosive eruptions of the present century have been reasonably documented scientifically, and few volcanologists have the opportunity to observe more than 3 or 4 large explosive eruptions in their lifetime.” He reasoned that the dispersal area (D) and degree of fragmentation (F) of air fall ejecta from any given eruption could be measured and correlated with at least some of LaCroix’s traditional eruption types (Fig. 5.3).

To measure air fall dispersal, Walker proposed isopach mapping. **Isopach maps** resemble ordinary elevation contour maps, but instead of representing equal-elevation positions, the isopachs represent positions of *equal deposit thickness*. For simplification, he proposed that only a single isopach be mapped for any given eruption, having $1/100$ the thickness of the *maximum* air fall deposit thickness for that eruption – the “ $0.01 T_{\max}$ isopach,” as he put it. In other words, if an eruption has dumped a layer of ash that *at most* is 4 m thick, the T_{\max}

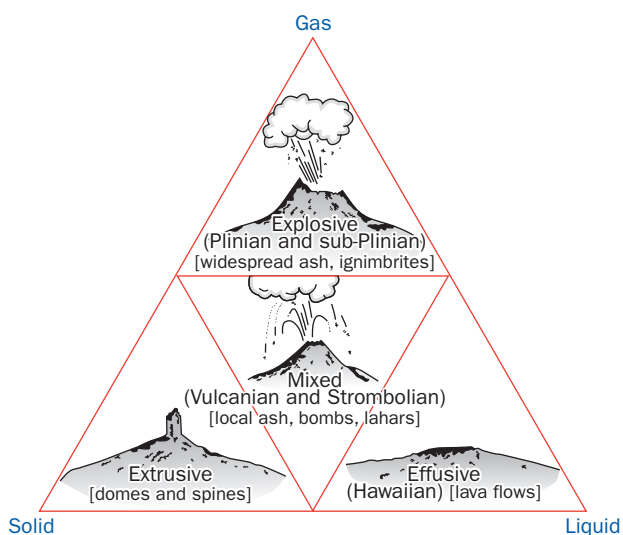


Fig. 5.2 A simple classification of major eruption types, based on the proportion of gases, solids, and liquids erupted. Modified from Geze (1964).

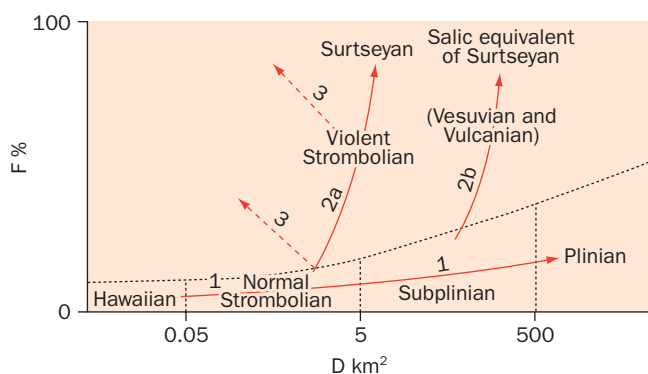


Fig. 5.3 The Walker eruption classification diagram. The F axis is percentage of ejecta in an air fall deposit with a grain size of less than 1 mm, as measured at the $0.01 T_{\max}$ isopach (see text). The D axis is the area enclosed within the $0.01 T_{\max}$ isopach for a given eruption air fall. Trend line 2a represents increasing explosive power in basaltic eruptions, and 2b the same for eruptions involving highly viscous, silica-rich magmas. Trend line 3 indicates weak eruptions that can only throw fine ejecta beyond their crater rims. From Walker (1973).

isopach will be designated on a map where ash deposits thin to 4 cm thickness (Fig. 5.4). Outside this area the deposit thickness would be less than 4 cm, thinning out to nothing. After delineating this isopach, the area enclosed by it (D) would then have to be measured. Extrapolation (surveying by “eye-balling”) between eroded outcrops could be necessary, and for deposits older than a few tens of thousands of years, accurately determining fall dispersals could well be impossible. Walker was also careful not to count fall deposits associated directly with the construction of the cones and rims around volcanic vents.

To measure tephra clast sizes, Walker proposed that materials be sampled from a position along the $0.01 T_{\max}$ isopach farthest from the vent (Figure 5.4), then sieved to determine the weight percentage of fragments having a diameter of less than 1 mm. This would constitute the **fragmentation index** (F) of the sample. Walker (1973) also proposed that F could be used to indicate the degree to which volatiles were involved in the eruption that produced the deposit. The greater the value of F; the more explosive and powerful the eruption, owing to the tremendous force of expansion as water transforms into steam. (Bear in mind that *power* is a concentration of energy – energy released as a function of time.) Lines 2a and 2b in Fig. 5.3 represent different eruptive styles reflecting this variable.

By comparing the F and D parameters, Walker proposed several new eruption types to add to the Lacroix scheme (Table 5.2). There were certainly good reasons for doing so, based upon field observations. For example, Strombolian eruptions predominantly produce cinder, with F values less than 10 weight percent of total ejecta. Macdonald (1972) and Walker referred to these as “normal” Strombolian eruptions. But in some instances the emissions of ash and other fine particles less than 1 mm in diameter are considerably greater, despite the fact that eruptive characteristics remain broadly similar. For example, at Parícutín [43], a 400 m high cinder cone which grew in Mexico in 1943–52 (Chapter 14), 70 percent of samples contain greater than 50 percent material finer

than 1 mm *within* the $0.01 T_{\max}$ isopach, where, if anything, one would expect to find generally coarser materials, because of proximity to the vent. Because of this, Macdonald (1972) referred to Parícutín as a “violent” Strombolian eruption, and Walker adopted this term. Observers report that there was indeed a larger amount of groundwater involved in the Parícutín activity than in shorter-lived “normal” Strombolian eruptions (e.g., Segerstrom

1950), seemingly vindicating Walker’s assertion about the role of volatiles in fragmentation trends.

Surtseyan (phreatomagmatic) eruptions develop when magma breaches the bottoms of shallow bodies of water, and may transition into violent Strombolian eruptions as water is excluded from magma contact. The difference is not simply one of fragment size, but also of the shapes of fragments, especially ash particles. Walker (1973, p. 437) notes: “[Ash] particles have shapes related to their origins. In Strombolian / Hawaiian deposits they are often ragged and in part bound by smooth or rounded surfaces molded by surface tension. In Surtseyan they are bounded by fracture surfaces and the inner walls of broken vesicles.” They are steam-shattered, in other words.

Walker and Croasdale (1972) further proposed that an intermediate type of eruption be designated between normal Strombolian and Plinian activity. Walker cited as an example of this “new,” intermediate eruption type the Hekla [67] basaltic explosions of 1970 in Iceland, in which ash fell over 200 km from the vent fissure. As far as 18 km from the volcano, fall beds as much as 6 cm thick contained no more than 4 percent by weight fragments less than 1 mm

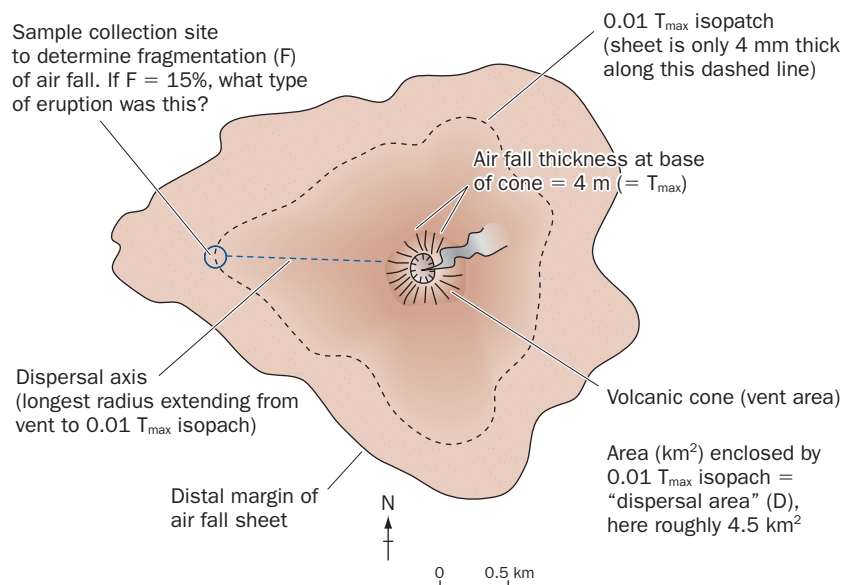


Fig. 5.4 Schematic map of an imaginary volcano showing tephra information to be noted in order to apply the Walker (1973) classification system.

TABLE 5.2 ADDITIONAL ERUPTION TYPES DESIGNATED AFTER LACROIX

Class	Description
Violent Strombolian	Eruptions resembling those of “normal” Strombolian activity, but producing notably larger quantities of fine ash, perhaps due to greater involvement of groundwater. Many of the largest Strombolian eruptions are “violent.”
Surtseyan	Basaltic phreatomagmatic eruptions taking place in shallow water. Often rhythmic, like Strombolian eruptions, with largely white eruption clouds of dense steam. In some eruptions, cypressoid behavior is exhibited, in which short, sharp blasts create jagged black “roostertail” ash-rich clouds shooting from the main steam-rich eruption cloud.
Sub-Plinian	A rather ambiguous category of eruptions; either very energetic Surtseyan-style eruptions, or very weak Plinian eruptions can produce deposits that may be termed as sub-Plinian.
Phreatoplinian	Plinian eruptions taking place through shallow bodies of water. Abundance of ash, accretionary lapilli, pyroclastic surge beds, etc., is much greater in Phreatoplinian deposits than in Plinian deposits. PDCs in such eruptions are extremely powerful and highly mobile.

Ranking is from least explosive to most explosive.
 Source: After Walker and Croasdale (1972), Walker (1973), and Self and Sparks (1978).

in diameter. The deposit showed the distinctive scoriaceous (highly vesicular) appearance of a mammoth cinder cone eruption. This was a “super” Strombolian event in other words, or as Walker and Croasdale preferred to call it, given the unusually wide dispersal area of its ash fall, a **Sub-Plinian eruption** (Fig. 5.5, Table 5.2). Many, though certainly not all Vulcanian eruptions, have dispersal patterns in the range of sub-Plinian desposits. They differ in terms of the degree of fragmentation, with Vulcanian ejecta consisting mostly of broken, highly angular rock fragments, and sub-Plinian ejecta consisting mostly of broken bits of vesicular glass. Walker proposed that the involvement of steam, as in the case of violent Strombolian eruptions, also was important in explaining this difference in particle shape. With even greater amounts of water, he postulated a “salic [silicic] equivalent of surtseyan” style of eruption – an extremely powerful phreatomagmatic type eruption for which he could not provide a specific example at the time. Self and Sparks (1978), however, provided just such a description a few years later, based upon careful study of several deposits including the 26,000 year old Oruanui Tuff [136] in New Zealand and the 1870 eruption of Askja [73] in Iceland. Self and Sparks proposed replacing “salic equivalent of surtseyan” with the term **Phreatoplinian**. We shall consider Phreatoplinian eruptions in much greater detail later (Chapter 8). They include the most fearsomely powerful eruptions known.

The Walker classification scheme is limited by the fact that not all volcanic deposits, especially older ones, are amenable to the stratigraphic analysis he proposed. In addition, Walker recognized that events develop which can modify the ordinary patterns of pyroclastic fall deposition. Accretionary lapilli (Chapter 7) can be deposited from ash clouds, forming much larger clast sizes than associated ashfall. Rain can also flush ash out of an eruption cloud to produce a bed of fine-grained material anomalously close to a vent. Some blasts throw out large quantities of fine material formed in earlier pyroclastic eruptions, mixing deposits in a confusing way. Walker’s scheme also ignores some “trademark” aspects of certain eruption styles that may be the only evidence one has to interpret past volcanic activity. Working in the remote Mopah Range of California’s Mojave Desert, for instance, RWH mapped several lenses of ash-poor, oxidized orange-red cinder up to 10 m thick and 100 m long sandwiched between early Miocene-aged basaltic flows. The cinder was a tell-tale sign of Strombolian activity, quite apart from pyroclast dispersal information, which after 18 million years of erosion was impossible to recover. Despite these shortcomings, Walker’s 1973 classification scheme, as modified by Self and Sparks (1978) remains a good basis for approaching the classification of volcanic eruptions, especially younger, more explosive ones. D. M. Pyle (1989) recognized that fall depositional characteristics change exponentially with distance, and developed further improvements over the Walker methods for plotting field measurements. Pyle’s methods are especially useful for the calculation of total fall deposit volumes.

Walker (1980) later defined five quantitatively measurable eruption parameters useful in categorizing an eruption, and these terms are now used universally:

- 1 **Intensity:** the rate at which magma leaves a vent (i.e., its discharge rate), measured in kilograms per second (kg/s). Eruptive intensity commonly varies with time during most eruptions, and eventually falls to zero as the eruption ends.
- 2 **Magnitude:** the total mass (or volume) of material erupted, measured in kilograms (kg), cubic meters (m³), or cubic kilometers (km³).

- 3 **Dispersive power:** the area over which the eruption products are spread by spending some time being transported high in the atmosphere before falling to Earth, measured in square kilometers (km^2)
- 4 **Violence:** For explosive eruptions, the distribution of products directly thrown away from a vent and scattered by **ballistic momentum**. (Think of “ballistics” as being like the trajectory of a baseball thrown through the air from one player to another.)
- 5 **Destructive potential:** the damage caused by an eruption to urban and agricultural lands, to vegetation, and other objects that can be used to measure impacts. In cold-hearted economic terms, this is measured in dollars or euros, numbers of injuries, fatalities, etc.

Volcanic Explosivity Index (VEI)

The **Volcanic Explosivity Index**, or **VEI** (Table 5.3), now universally accepted as a means to categorize the relative sizes of explosive eruptions, was developed by Newhall and Self (1982) at the suggestion of Robert Decker, then a Dartmouth College professor. The higher the VEI number, the more powerful the eruption. The VEI correlates the volume of volcanic ejecta and various other observed physical criteria, such as eruption column height and eruption duration. As we will see later, it is possible to infer some of these physical criteria based on careful field study of past eruptive deposits. A somewhat parallel approach was proposed by Fedotov (1985), who devised a scale for explosive eruptions based logarithmically on magma discharge rate during eruptions.

Decker (1990) undertook a statistical study of the VEIs of eruptions to calculate the frequencies of eruptions having particular levels of explosivity. His research reinforced the observation that the smaller and less explosive the volcanic eruptions, the more frequently they occur. On a log-log plot of eruption frequency versus VEI, eruptions ranging from VEI 2 to 6 plot in a line with a slope of 0.5, meaning that each increase in eruption magnitude correlates with a 5-fold decrease in frequency. For eruptions having VEI's of 6 to 7, the slope of the line increases to 1 (a 10-fold decrease in frequency for every unit increase in VEI), and from 7 to 8, the slope increases to 10. From this analysis, he estimated that the average number of worldwide eruptions as a function of VEI magnitude is as follows (Fig. 5.5):

- VEI \geq 2, 15 eruptions/year;
- VEI \geq 3, 3 eruptions/year;
- VEI \geq 4, 1 eruption every 2 years;
- VEI \geq 5, 1 every 10 years;
- VEI \geq 6, 1 every 50 years;
- VEI \geq 7, 1 every 450 years;
- VEI \geq 8, 1 every 300,000 years or more (Self 2006)

The upper limit of volcanic explosivity lies somewhere between 8 and 9 on the VEI scale, exemplified by the Toba super-eruption (Chapter 8).

TABLE 5.3 THE VOLCANIC EXPLOSIVITY INDEX (VEI): CRITERIA FOR DETERMINATION.

	VEI → 0	1	2	3	4	5	6	7	8
Criteria									
Size description	Non-explosive	Small	Moderate	Moderate-Large	Large	Very large			
Volume of ejecta (m ³)	< 10 ⁴	10 ⁴ –10 ⁶	10 ⁶ –10 ⁷	10 ⁷ –10 ⁸	10 ⁸ –10 ⁹	10 ⁹ –10 ¹⁰	10 ¹⁰ –10 ¹¹	10 ¹¹ –10 ¹²	> 10 ¹²
Eruption column height (km)*	< 0.1	0.1–1	1–5	3–15	10–25	> 25			
Description of explosivity	gentle, effusive	gentle, effusive	explosive	explosive	explosive	explosive	explosive	explosive	explosive
Classification		Hawaiian	Strombolian		Vulcanian		Plinian	Plinian	Ultraplinian
Duration of continuous blasts (hr)		< 1							> 12
Injection of lower atmosphere (troposphere)	Negligible	Minor	Moderate	Substantial					
Injection of upper atmosphere (stratosphere)		None		Possible	Definite	Significant			
<i>VEIs of the nine most powerful volcanic eruptions since 1400[†] CE</i>									
Year									
1991	Volcano					Other well-known eruptions			
1912	Pinatubo, Philippines	6	1982	El Chichón, Mexico	5				
1907	Novarupta, Alaska	6	1980	Mount St Helens, USA	5				
1883	Santa María, Guatemala	6							
1815	Krakatau, Indonesia	6							
1660(?)	Tambora, Indonesia	7							
1641	Long Island, New Guinea	6							
1580(?)	Parker, Philippines	6							
1452	Billy Mitchell, Solomon Islands	6							
	Kuwaae, Vanuatu	6							

* For VEIs from 0 to 2, the column height is km above the vent; for VEIs greater than 2, column height is km above sea level.

† Data from Briffa et al. (1998).

Source: Newhall & Self (1982).

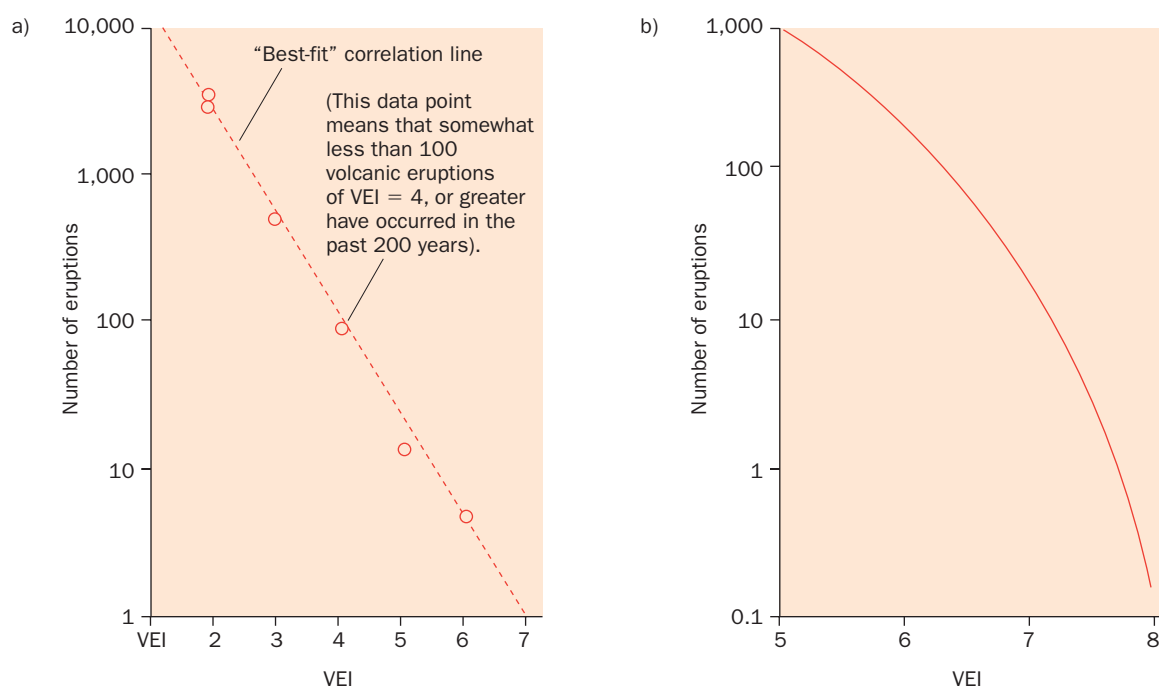


Fig. 5.5 a) Plot of frequency of eruptions of specific VEI and greater during the past 200 years, based upon statistical analysis of the eruption data base of Simkin et al. (1981) by Decker (1990); b) Number of large eruptions over the past 10,000 years.

In practice, it is often best to describe different phases of an on-going eruption using the revised Lacroix nomenclature (with its amendments from Walker, and Self and Sparks), while classifying the overall eruption in terms of its VEI or Walker pyroclast dispersal characteristics. Because the Walker and VEI systems are quantitative, they are more valuable for comparing different volcanic eruptions than the simple Lacroix classification, but the VEI system depends heavily on observations of on-going eruption parameters. For prehistoric eruptions whose only records are left by their deposits, VEI estimations are impractical and imprecise. Hence, we think it is critical to be able to recognize the *kinds of deposits* left by eruptions. As in the case of the Mojave Desert cinder lenses, it may be that the appearance of a few outcrops is the only evidence available for evaluating past volcanic activity. Field recognition and correct interpretation of style-dependent depositional characteristics (Cas and Wright 1987) are critical for analyses.

FURTHER READING

- Scarth, A. (2009) *Vesuvius: A Biography*. Princeton University Press, 352 p.
- Thordarson, T., Self, S., Larsen, G., et al. (2009) *Studies in Volcanology: The Legacy of George Walker*. IAVCEI Publications, International Union of Geodesy and Geophysics, 416 p.
- Wood, C. (2009) *World Heritage Volcanoes: Global Review of Volcanic World Heritage Prospects: Present Situation, Future Prospects, and Management Requirements*. International Union for the Conservation of Nature World Heritage Studies No 8, 62 p.

Chapter 5

Questions for Thought, Study, and Discussion

- 1 Discuss the merits and limitations in application of the classification schemes of Rittmann, Geze, LaCroix, and Walker. When would it be most appropriate to use any one of these schemes in preference to all of the others? Could several schemes be usefully applied to describing and studying a *single* eruption? Explain how and why.
- 2 A series of explosions rock the summit of a composite volcano, throwing out numerous blocks of older lava amidst roiling clouds of ash and steam. An estimated $5 \times 10^{5.5} \text{ m}^3$ of ejecta are thrown out. Classify this eruption in as many ways and as precisely as you can.
- 3 Steam explosions throwing out occasional tails of dark, wet ash accompany the emergence of a new volcanic island out of the sea. Once the vent is sealed off, a series of rhythmic explosions throwing out clots of lava and dark clouds of ash begin to build up a young cone. Later, this explosive activity dies down as a fissure opens on one flank of the cone releasing a torrent of lava, with low lava fountaining occurring all along its length of the fissure. Where the fissure meets the sea, though, periodic steam blasts rip the shoreline, temporarily setting back the construction of new land. Classify this eruption.
- 4 Can an eruption have both high intensity and low magnitude? Explain.
- 5 Can an eruption have both high intensity and show low violence? Explain.
- 6 According to Self (2006), The great Oruanui–Taupo caldera eruption of 26,000 years ago had a VEI of over 8. Occurring today, this eruption would have impacted most of the North Island of New Zealand, home to hundreds of thousands of people. How concerned should residents and authorities really be about the threat of eruptions like this?

Chapter 6

Effusive Volcanic Eruptions and Their Products

*E Pele e
Ke akua o na pōhaku`ena`ena
`Eli`eli kau mai
[Oh Pele, Goddess of the burning stones,
let a profound awe possess me]
[Traditional Hawaiian oli (chant)]*

The first thing that people picture or children draw when thinking about volcanoes is **lava**, the outpouring of fluid magma onto the earth's surface (Fig. 6.1). Lava flows are common wherever molten rock reaches the surface without fragmenting explosively. Such flows come in many shapes and sizes, and feature many kinds of distinctive surface with differences mostly controlled by variations in magma viscosity and supply rates at the time of eruption. Lava flow types may be classified either according to their compositions (rock types, Fig. 3.3) or by their distinctive appearances (Table 6.1).

Most of our emphasis in this chapter will be on basaltic eruptions and their lavas rather than on silicic lava flows, primarily because basaltic lavas are much more voluminous on Earth (and on the other rocky planets (Chapter 12)) and are much more likely to be seen in action in places like Hawai`i or at frequently active volcanoes like Etna [82]. Siliceous eruptions also tend to be quite explosive, with thick flows rarely erupting and traveling beyond the immediate vicinity of a vent. (We'll discuss siliceous eruptions and their products much more extensively in the following two chapters.)

Volcanoes: Global Perspectives, 1st edition. By John P. Lockwood and Richard W. Hazlett. Published by Blackwell Publishing Ltd.



Fig. 6.1 A “typical volcano,” as envisioned by a 6-year-old child.

TABLE 6.1 RELATIONSHIP OF THE SURFACE TYPES OF LAVA FLOWS TO THEIR COMPOSITIONS AND SOURCE VENTS.

Roughness classification	Common composition	Source vent structures
Pāhoehoe (smooth, hummocky surface)	Basalt	Shield volcanoes, cinder cones, composite cones
`A`ā (covered with loose, spiny rubble)	Basalt, andesite	Shield volcanoes, cinder cones, composite cones
Blocky (lithic)	Basaltic andesite, dacite	Cinder cones, block-lava shields
Blocky (glassy)	Dacite, rhyolite	Domes

Mafic and Intermediate Effusive Eruptions

HAWAIIAN-TYPE ERUPTIONS

François-Antoine LaCroix proposed using the term **Hawaiian eruptions** to identify all forms of effusive volcanic activity that involve the eruption of fluid lavas, typically basaltic in composition, and usually involving both lava fountains and flows. A Hawaiian-style eruption begins where a dike breaches the surface. Swarms of sharp, shallow earthquakes precede the opening of a fissure in advance of the dike. Dilation of the ground above the ascending dike may form a narrow, linear graben. A fissure opens on the floor of the graben, parallel to its margins. The magma at first shoots into the air all along the length of the fissure, forming a curtain of incandescent, fountaining lava which may reach a few tens, or even hundreds of meters into the air. Such sheets of erupting lava present spectacular panoramas typically stretching from a few hundred meters to 10 or 20 km in length, the celebrated Hawaiian “Curtain of Fire” (Fig. 1.12).

When one watches a curtain of fire in action, the heat and massive amounts of dancing liquid spatter being thrown upwards give the impression that lots of lava is erupting, but this is not necessarily so. When fluid lava is fountaining up into the air during effusive eruptions, this is much less a display of erupting lava than it is a display of erupting gas. For typical lava fountains, more than 90 percent of the new material being erupted (by volume) is actually gaseous. The blobs of red lava are mostly gas bubbles too – highly inflated masses of spongy molten rock much like popcorn or styroform in texture (Fig. 6.2). Even more significant to the gas–lava balance is the fact that the volatile mass being erupted represents entirely fresh output, whereas a lot of the molten spatter is simply being recycled – much of it has already been ejected, fallen back into the pools of lava at the bases of fountains and shot up again several times. Some of the gushing lava falls back around fissures, quickly building steep-sided ridges of spatter, termed **spatter ramparts**, which rarely exceed 5–10 m high. The spatter clots are highly fluid and these fragments spread out after impact, collecting to form loosely welded aggregates (Fig. 6.3). If the fissure is on a slope, spatter ramparts will develop only on the upslope side of the vent, since **fountain fed lava** will incorporate and transport spatter as it flows away on the downhill side. Newly formed ramparts are inherently weak edifices, and may slump and collapse where constituent hot agglutinate oozes from their bases. Tongues of

oozing agglutinate may develop into pāhoehoe, or more typically `a`ā flows (Table 6.1) ranging up to 5–15 m thick and hundreds of meters long. Such secondary flows typically contain pieces of agglutinate, some of them meters in diameter, which did not coalesce into homogeneous liquid during flow. The resulting rock has been termed **clastogenic lava** (Cas & Wright 1987; Sumner 1998).

Many Hawaiian eruptions cease within a few hours or days, but some may continue for much longer, even persisting through various phases of activity for decades. After the first few hours, lava fountaining will become concentrated at certain points along the initial fissure where flow rates and fountain heights rapidly increase, while lava production ceases everywhere else. The concentration of lava production at one point establishes a feedback mechanism that increases conduit flow rates further. Greater discharge at a single point erodes and streamlines underlying dike walls, facilitating stronger flow. As fountaining increases in vigor and height, larger amounts of **reticulite** (porous, pumice-like scoria consisting of intricate glass filaments) and **Pele's hair** (long threads of volcanic glass) will form in addition to frothy spatter. Instead of an elongate spatter rampart, a single much taller volcanic edifice (**spatter cone**) begins to grow (Fig. 6.4), reaching over a hundred meters in height given a long enough eruption.

The construction of a prominent edifice and concentration of fountaining at one (or a few) points along a fissure may be regarded as the second phase of a Hawaiian eruption. The third phase may develop with gradually widening of the vent, owing to erosion of the conduit walls and collapse into the underlying dike. The surrounding cone may be partially consumed when this happens, and lava may pool up over the vent to form an **active lava lake**, overflows of which construct a gently-sloping lava shield on the remains of the earlier, steeper-sided agglutinate cone. High lava fountaining is no longer possible because of decreased discharge of lava and associated longer time for degassing, which becomes much gentler (Fig. 6.5).



Fig. 6.2 Spatter rampart in formation. Kīlauea east rift zone eruption – 2003. Photo © Brad Lewis.



Fig. 6.3 Welded basalt spatter deposited on the inner wall of an eruptive vent during the 1969 eruption of Kīlauea volcano, Hawai'i. Photo by J. P. Lockwood.

Fig. 6.4 Spatter cone forming on Kīlauea volcano's East Rift Zone, April, 1983. Lava fountains about 40 m high. The cone is kept open by a flowing river of lava that carries away spatter falling on its surface. USGS photo by J. P. Lockwood.



LAVA LAKES

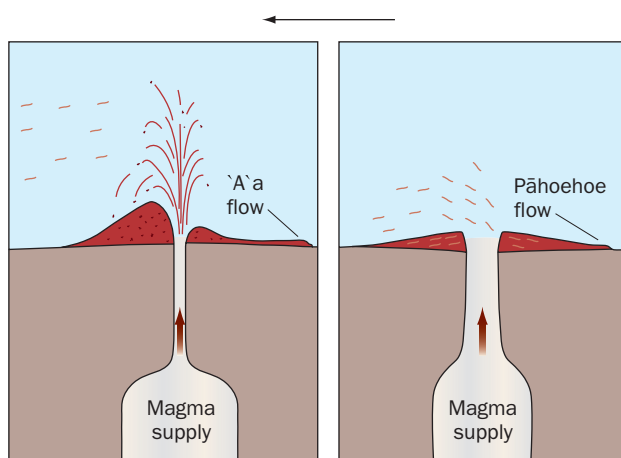


Fig. 6.5 Effect of vent conduit diameter on eruption style for Hawaiian-style fluid lavas. For constant magma supply rates narrow conduits will result in higher ascent velocities, which allow less time for bubble migration and degassing. Narrow conduits (a), typical of early eruption phases, favor high fountaining, formation of spatter cones, and production of “shelly” pāhoehoe and `a`ā flows (Table 6.1). Wide conduits (b), that develop by vent erosion with time, favor formation of lava shields, lava lakes, and production of “tube-fed” pāhoehoe flows.

Active lakes directly above vents constantly churn as new lava wells up from below and cooler surface lava becomes denser than surrounding molten rock and founders. The thin semi-plastic silvery crusts on these lakes are in continuous slow movement across the lake surface, owing to convection of underlying lava. Duffield (1972) observed that the movements of lava crust plates across the Mauna Ulu lava lake (Chapter 1), mimicked the movement of tectonic plates across the Earth's surface. Indeed, there are striking parallels to be seen, including examples of “sea-floor spreading” as new crust forms, “transform faulting,” and “subduction,” as older crust founders beneath younger (Fig. 6.6).

The supply of new lava to these lakes is constantly changing, and the balance between incoming new lava and consumption of old lava by the process called **drainback** is complex. The balance may be static, at which times lava lake levels will remain constant for long periods, or excess drainback may cause sudden, rapid lowering of the lake's level. An excess of supply will cause the lava lake to overflow as sheet-like surface flows, or to feed long-sustained pāhoehoe flows through subterranean conduits in the submerged walls of the vent lake, which may transport lava many tens of kilometers downslope.

In some areas, lava may fill neighboring craters or low areas to create **passive lava lakes**, which though not positioned directly over vents, may behave just like an active-vent lava lake as long as they continue to be fed fresh lava. But while small lava fountains often play across the surface of such active lava lakes, the gas pressure isn't sufficient to cause substantial fountaining.

In November and December, 1959 a spectacular eruption of Kīlauea [15], Hawai'i filled the Kīlauea Iki pit crater to a depth of 135 m with olivine-rich tholeiite basalt (Fig. 6.7) and provided an excellent natural laboratory to study the cooling behavior of a very thick lava body. For a few days after cessation of the eruption on December 20 the new crust was thin and unstable, but by late January geologists were walking on the very hot crust to measure changes in its level. By April, 1960 the crust was strong enough to support heavy equipment, and a program of scientific drilling began to measure the rate of crustal growth and the physical and geochemical properties of the growing crust and diminishing melt. Drills penetrated the lake's crust 26 times during the next three decades (R. Helz, 2012, pers. comm.). Kīlauea Iki is now the best studied natural example of basalt solidification processes in the world, and has yielded a treasure trove of over 200 scientific papers in petrology, geophysics, and geochemistry. These studies have enabled petrologists to study the ways in which basaltic magma changes in composition and mineralogy over time as temperatures drop and heavy minerals (principally olivine) grow and sink gravitationally within it (Helz 1980; Helz & Thornber 1987; Jellenik & Ross 2001).

The crust of the lava lake at Kīlauea Iki initially thickened very rapidly (over a meter a month), during which time radiation was the principal means of cooling. As the crust insulated the underlying basalt melt from radiative cooling, however, conductive cooling became predominant, with the rate of crustal thickening proportional to the square root of time:

$$\text{Thickness} = n \cdot \sqrt{t} \quad (6.1)$$

where n is a constant dependent on environmental factors, principally rainfall, and t is time, in months.



Fig. 6.6 Kupaianaha lava lake, Kīlauea volcano, Hawai'i in 1987. Note the numerous plates of surface lava, which are in constant slow motion across convecting lake surfaces. USGS photo by J. P. Lockwood.



Fig. 6.7 Aerial view of Kīlauea Iki lava lake from the east. The source vent for the 1959–60 eruption that fed this lava lake is at the far western margin of the lake, and is marked by a tall spatter cone and devastated forest zone downwind (southwest) of the high lava fountains from the actual vent. This passive lava lake is 1.5 km long, over 100 m deep, and provided a natural laboratory for studying how basalt lavas cool and differentiate over a long period of time. Photo by J. P. Lockwood.

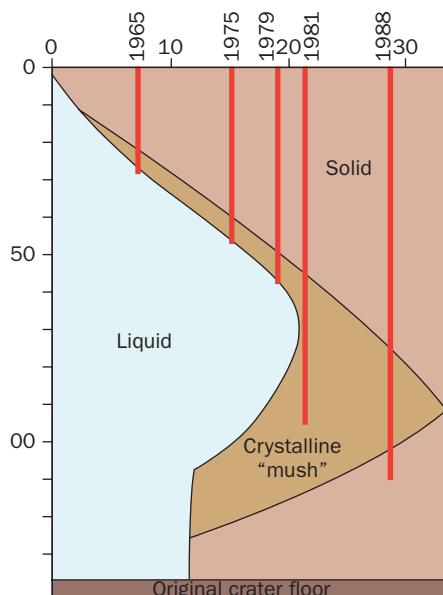


Fig. 6.8 The cooling of Kīlauea lava lake – 1959 to 1988. Data from various USGS studies.

This relationship held for the first three years at Kīlauea Iki, but in the years following the lava lake crust thickened at a somewhat faster rate. The boundary between solid and melt at the base of the crust became increasingly complex, both because of the formation of plastic, largely crystalline “mushes” (which were neither solids nor mobile fluids) and because of compositional inhomogeneities within the zone of crystallization. No “melt” (in the sense of material too fluid to drill through) existed in Kīlauea Iki after 1981, although a large, partially molten, incandescent plastic core still existed within the center of the lake (Fig. 6.8). Crystallization of this plastic core proceeded from both above and below, and researcher Rosalind Helz (2000, pers comm.) calculated that the Kīlauea Iki lava lake completely solidified sometime around 1994 or 1995, about 35 years after the eruption.

Lava lakes can be formed in ways other than through vent erosion during Hawaiian eruptions and the passive entrapment of lava within pre-existing craters. In some cases, largely degassed magma chambers stope all the way to Earth’s surface with little eruptive fanfare. The top of the active magma chamber feeding Nyiragongo [88] has appeared many times in the deep central crater of that volcano (Fig. 6.9), and an active lava lake marked the exposed top of Kīlauea’s magma chamber almost continuously for about a century between 1823 and 1924 (Fig. 6.10).

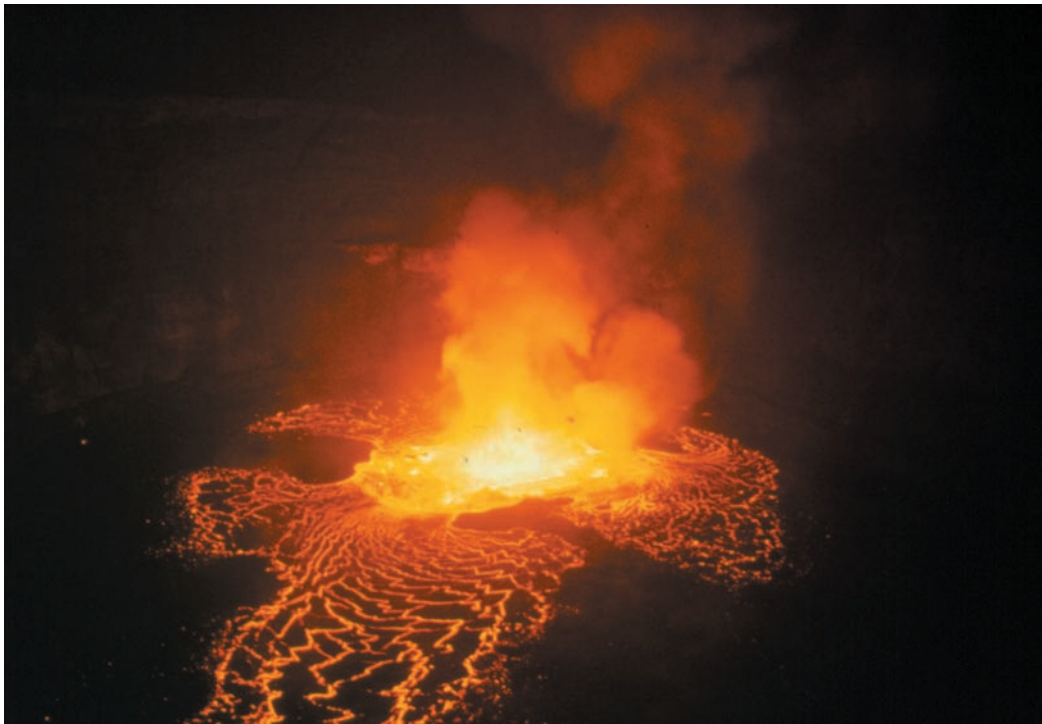


Fig. 6.9 View of Nyiragongo summit crater, 1994. This lava lake is nearly 1 km in diameter. The active fountains are about 50 m across, although the undulating crust showed the molten lake extended beneath the entire crater. USGS photo by J. P. Lockwood.



Fig. 6.10 Halema'uma'u lava lake, Kilauea volcano, Hawai'i – 1917. This lake was almost continuously active for nearly a century. Note the circular form and bounding lava levees – which are formed by short overflows from a rising lake surface. Photographer unknown.

STROMBOLIAN-TYPE ERUPTIONS

Strombolian eruptions, like Hawaiian, are common forms of basaltic volcanic activity. The mechanical difference is that gas exsolution in Hawaiian eruptions takes the form of numerous, small, escaping vapor bubbles that cause the magma to fountain continuously or passively flow out, whereas in Strombolian eruptions, very large bubbles develop in the conduit, leading to rhythmic moderately explosive discharges as they escape (James et al. 2008). The explanation for the contrasting styles of vesiculation generally relates to variable magma ascent rates; slow rising magma has a chance to develop larger bubbles, fast rising magma does not (Parfitt 2004; Gonnerman & Mangan 2007). Why some volcanic areas favor more rapid

ascent of basaltic melts relates to tectonic setting, composition, magma supply rate, and gas content. Slightly more viscous mafic melts contribute to reduced ascent rates and favor Strombolian eruptions.

Seismic and Doppler radar studies have been made of the bubble formation which causes the bursting behavior so characteristic of Strombolian eruptions. Evidence suggests that individual bursts may originate as deep as several hundred meters within the magma conduit. Long-period seismic frequencies record the initiation of explosions up to a second or two prior to anything becoming visible at the surface (Rowe et al. 2000). At Etna's SE crater, bubble formation at conduit depths of 500 m has been inferred, with eruptive blasts following approximately 2–3 minutes later (Dubosclard et al. 2004).

Strombolian activity generally takes place at open vents where moderately fluid lava stands at a high level in the conduit, often just a few tens of meters below the rim. Some of the clots thrown up by blasts strike the walls of the conduit near the rim while they are still molten and form spatter agglutinate; others cool during their flights through air, and strike the surrounding ground in an essentially solid condition. Commonly, they are still glowing red when they leave the vent, but have become black by the time they impact. If the magma level rises, more of the ejecta will exit the vent in a partly fluid condition, piling up around the vent as spatter. The eruption then seemingly grades into one of Hawaiian type, but rhythmic jetting of incandescent material at the vent continues every few seconds or minutes, much in contrast to ordinary Hawaiian lava fountaining.

The type-locality for Strombolian eruptions, Stromboli volcano [83], is located off the southwest coast of Italy. Its eruptions have been nearly constant, and consistent in character, since before the first Greek colonists settled the region over 2500 years ago. The most typical activity consists of explosive ejections of incandescent cinder and spheroidal or fusiform bombs thrown to heights of a few tens to several hundred meters above source vents. This activity may or may not be accompanied by discharge of a lava flow. If lava does emerge, it is generally somewhat more viscous than that of Hawaiian eruptions and forms somewhat shorter and thicker flows. Most ejecta are nearly solid when they strike the ground but larger materials are semi-molten and flatten appreciably, at times forming "cow-dung bombs" as much as a meter in diameter (Chapter 7).

Stromboli's ordinarily mild activity is punctuated at intervals of a few months to a few years by episodes of more violent eruption (VEI greater than 2) lasting no more than a few days each, in which showers of incandescent cinder and bombs are thrown to heights of as much as a thousand meters and great black ash clouds rise above the volcano. Bombs may fall at a distance of several kilometers from the vent. The general nature of the ejecta is the same as in the milder eruptions, except that glassy ash becomes much more abundant and occasional blocks of old rock are found in the ejected debris. The violent activity usually lasts for only a few hours or days and is commonly followed by a short interval of quiet during which only fumarolic activity occurs.

Cinder cones also develop from Strombolian eruptions that generally persist for only a few weeks or years – an outstanding example being Parícutín volcano [43] in central Mexico, which grew between 1943 and 1952 (Chapter 9). Cinder cones often cluster together in volcanic fields. Parícutín, for example, is merely the youngest in a group of several dozen similar cones, while the San Francisco volcanic field in central Arizona consists of over 600 scattered edifices.

FLOOD BASALT ERUPTIONS

Many volcanologists classify flood basalt eruptions as a distinct type of effusive volcanic activity, although in fact they share the same general features as ordinary, lower-volume Hawaiian eruptions. The difference is largely one of scale; a lot more comes out of the ground when flood basalts erupt. But they also never build large, discrete polygenetic volcanoes, which may seem ironic considering the vast amount of magma that feeds them. Instead, they create wide lava plains and tablelands.

It is fortunate that no major flood-basalt eruption has occurred in human history, because discharge rates are so great, and flood-basalt flows move so fast, that it might be difficult to evacuate a threatened region in time. Whereas the volumes of typical large Hawaiian or Icelandic basalt flows range from less than one to a few km³, individual flood basalt flows, termed **great flows** by Tolan et al. (1989), range in volume up to 2000–3000 km³. A 55 km long lava flow erupted in Hawai'i in 1855–6 is impressive in comparison with other historically-observed flows, but prehistoric flood-basalt flows as long as 750 km are known. The most detailed studies of flood basalt volcanism have focused on the Columbia River Basalt province (CRB) in the northwestern United States. There, between 17.5 and 15.5 million years ago, lava poured out across an area exceeding 150,000 km² – almost equivalent in size to the whole of Washington State (Fig. 6.11). The sources of most of these flows are preserved in the Chief Joseph Dike Swarm of northeastern Oregon. Dikes in the Monument Dike Swarm several hundred kilometers farther west also fed numerous flows. Remnants of large spatter ramparts and pumice cones have been found where many of these dikes served as eruption feeders. Wright et al. (1989) estimate that the initial eruptive fissures of individual flows typically stretched 70–200 km! Given their huge volumes, the late-stage inflation of such flows (about which more soon) probably took much longer than in the case of their ordinary Hawaiian counterparts – perhaps as long as several years as opposed to days or months (Swanson et al. 1975; Thordarson & Self 1998). Large as the CRB lava fields are, they are dwarfed by the much more voluminous late-Cretaceous Deccan Volcanic Province basalts of southern India. The products of these very largest flood basalt eruptions are called **Large Igneous Provinces** (LIPs), and are discussed further in Chapter 9.

Only two flood basalt eruptions have occurred in recorded history, both of them in southern Iceland. The poorly documented Eldgjá eruption took place in 934 CE when a fissure about 30 km long opened in a sinking graben that quickly filled to overflowing with lava. It was larger than the 1783 Laki [71] fissure eruption, which broke out in the same area, but being an earlier time was poorly documented. These eruptions did not produce great flows, and the rate of lava extrusion was less than that inferred for the Columbia River Plain. The rate of lava production was nonetheless far in excess of that ordinarily observed in Hawaiian-type eruptions. We may regard the Laki-Eldgjá eruptions as “intermediate” in scale between those of typical Hawaiian eruptions and the vast prehistoric flood basalt provinces. They are of particular interest today because of their documented impacts on global climate (Chapter 13).

Pāhoehoe and `A`ā

People living in basaltic volcanic terrains noted long ago that some lava flows were easy to cross on foot and some were not, and names were soon devised to describe the two types.

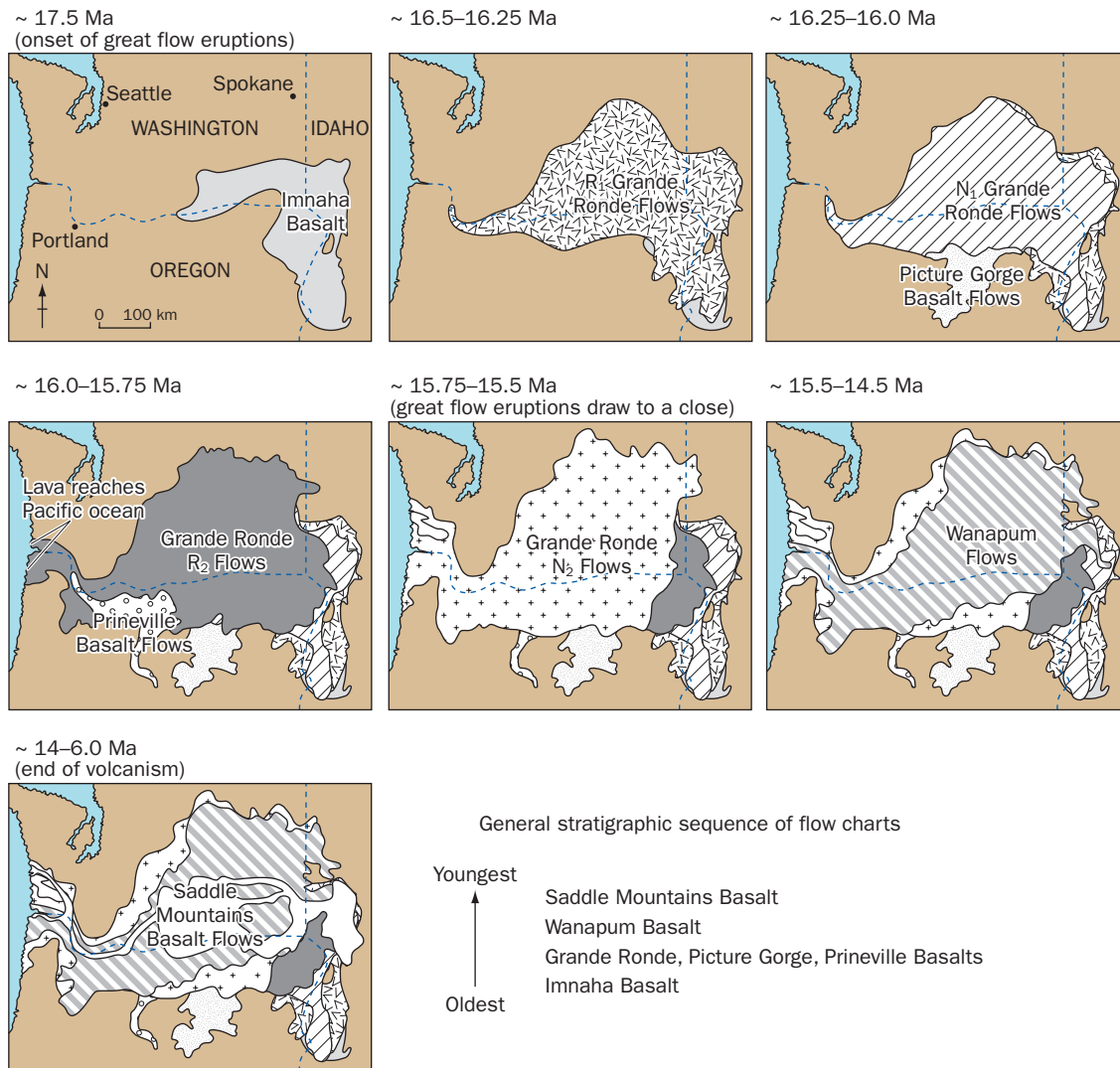


Fig. 6.11 Rise and decline of Columbia River basalt volcanism. Modified from Tolan et al. (1989). Ma = millions of years ago.

Hawaiians (to whom the distinction was critical, as they usually went barefoot!) called the smooth-surfaced flow type **pāhoehoe** and the rough-surfaced type **`a`ā** (Table 6.1). Icelanders called the two types **helluhraun** and **apalhraun**, respectively (Thorarinson & Sigvaldason 1962). The rough-surfaced type was called **marubi** in Japan, and **malpais** (“bad country”) in Mexico. When C. E. Dutton introduced the Hawaiian terms into the scientific literature in 1884, they met with strong opposition from British geologists. Bonney (1899, p. 79) scoffed that the terms are “the barbarous [expressions] of an insignificant and uncivilized race in a small archipelago in the North Pacific,” and preferred the (more civilized?) terms **slaggy** and **clinkery**. T. A. Jaggar went to Greek civilization for his now-forgotten terms **dermolith** and **aphrolith** (1917, p. 280). In the end, the Hawaiian words won out, and pāhoehoe (properly pronounced PAH-hoy-hoy) and `a`ā (ah-AH) are universally used (Fig. 6.12). These terms are presently used not only to describe the surface appearances of cold flows, but also the active lava that forms them.



Fig. 6.12 Pāhoehoe and `ā`ā flows formed during different phases of the 1972 Kīlauea eruption. Where both lava types are produced during the same eruption, it is most common for the pāhoehoe to be younger. Photo by J. P. Lockwood.

THE PĀHOEHOE–`Ā`Ā TRANSITION

Although compositionally identical when formed during the same eruption and originally intended only to describe contrasting surface features, pāhoehoe and `ā`ā flows develop by distinctly different processes. While there are some “transitional” flows featuring aspects of both `ā`ā and pāhoehoe, most flows are either of one type or another. Both are commonly produced during the same eruption.¹

In general, `ā`ā flows represent a slightly more viscous lava than pāhoehoe, and this is illustrated by a common observation made during Hawaiian eruptions: Early in an eruption, high vigorous lava fountaining will create fountain-fed flows, as described earlier, in which the falling spatter loses temperature before coalescing into flowing lava at the base of the fountains. That heat loss is critical, and the result is that fountain fed flows often move as `ā`ā. Later, as eruptive vigor wanes, spatter falls from lesser elevations, or lava may emerge directly from a vent. Little air cooling occurs before the flowage begins, and hotter, less viscous pāhoehoe results. One result of this change in lava production is that where one sees pāhoehoe and `ā`ā of the same eruption in mutual contact, the pāhoehoe more often than not occurs as the younger, overlying lava.

High-versus-low lava fountaining is not the sole explanation for the relative proportions of `ā`ā and pāhoehoe seen in a basaltic flow field however. Much `ā`ā can form by transition from pāhoehoe later during an eruption. The transition is a function both of the viscosity of the active pāhoehoe and the amount of stirring or **shear stress** to which it is

¹ There is a bit of a semantic problem involved, since fluid lava emerging from a vent is really neither Pāhoehoe nor `ā`ā, and has the ability to solidify into either form. The terms are best applied to the solidified lavas after flows cool, but are also used to describe moving flows.

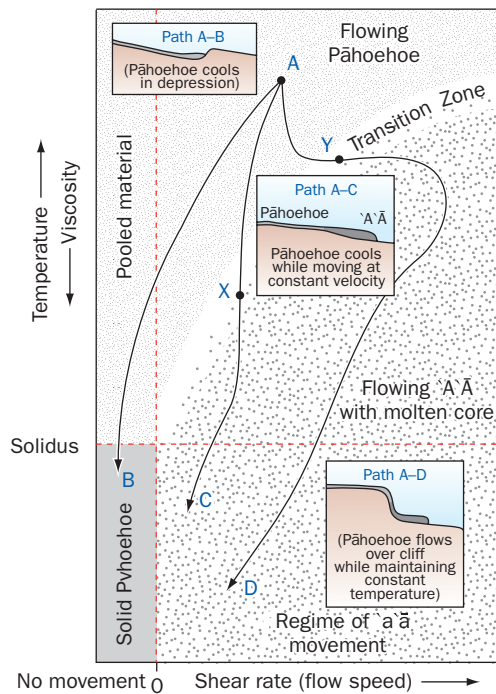


Fig. 6.13 The rheological basis for the pāhoehoe–ʻaʻā transition. For path A–B, flowing pāhoehoe comes to rest while in a fluid state and continues to cool until solidification. For path A–C, flowing pāhoehoe continues to move as its temperature drops below a critical point (determined largely by composition); at point X, it can no longer flow as a fluid and by rupture cooler parts of the flow will convert to the ʻaʻā form. For path A–D, the pāhoehoe maintains a constant temperature, but converts to ʻaʻā at point Y where the flow’s velocity suddenly increases (as by flow over a cliff). Theoretical aspects of the pāhoehoe–ʻaʻā transition are clearly discussed by Hulme (1974); field aspects by Peterson and Tilling (1980).

subjected (Fig. 6.13) (Peterson & Tilling 1980). Shear stress is the concentration of force in a material causing it to stretch out like a deck of cards being spread across a table. When pāhoehoe pours down a steep slope the highly fluid molten interior will accelerate as the crust lags, generating considerable shear throughout the flow and decreasing its ability to move as a coherent stream. Instead of chilling into ordinary pāhoehoe crust, the solidifying portion may abruptly tear into detached fragments of ʻaʻā.

On gentler slopes at uniform grade and constant and slower flow speeds, the commonly observed change of pāhoehoe to ʻaʻā results largely from an increase in viscosity due to cooling, loss of gas, and increasing degree of microlitic crystallization. Many flows show transitional textures across part or even all of their surfaces, including fragmented plates of spiny pāhoehoe crust interspersed with patches of true ʻaʻā clinker.

Once flowing lava has transitioned to fragmental ʻaʻā, it can never revert back to pāhoehoe, although the liquid cores of ʻaʻā flows occasionally break out from flow interiors with build up of pressure or change in slope to spread and cool as pāhoehoe (Jurado-Chichay & Rowland 1995; Kauahikaua et al. 2003). Good examples of this were seen during the 2002 eruption of Nyiragongo volcano, Democratic Republic of Congo, where many homes were destroyed in the city of Goma up to two days after the ʻaʻā flows had come to rest. The fluid cores of the immobile ʻaʻā flows, gradually building up pressure from continued internal flowage of lava from upslope, emerged unexpectedly to feed destructive lobes of pāhoehoe (Fig. 6.14).

Pyroducts

Although flowing molten lava is spectacular to behold, this is not how most pāhoehoe lava is emplaced. During long-lived eruptions, most of the “action” takes place in conduits beneath solidified crust, and flowing lava is mostly unseen. Such subterranean conduits allow lava to flow long distances with little heat loss, and are one of the factors responsible for the gentle slopes of typical “red volcanoes.” As flows solidify, most of this subterranean lava will solidify in place, and little evidence for these conduits may persist. If lava drains downslope from these conduits in the waning stages of eruptive activity, however, elongate caves may be formed. Such caves, found in pāhoehoe lava flows worldwide, are commonly called “lava tubes,” “lava tunnels,” “lava pipes,” and so on, but the preferred term is **pyroduct** – a term coined by an eye-witness describing active subterranean “rivers of fire” during the 1843 eruption of Mauna Loa. Pyroducts come in many shapes and sizes (few of them “tubular”) and form in many different ways, which we shall discuss later. First, the story of Titus Coan and his 1843 eye-witness account:



Fig. 6.14 Source of pāhoehoe flow that “leaked” out of `a`ā flow after the 2002 Nyiragongo eruption. This pāhoehoe flow appeared one day after the `a`ā flow had come to rest. Photo by J. P. Lockwood.

Reverend Coan was a pioneering Congregational missionary in Hawai`i, and a well-educated naturalist who provided excellent descriptions of all the Hawaiian eruptions that took place between 1832 and 1880. His interest in the scientific aspects of volcanic activity was piqued by his meeting with a young J. D. Dana (Chapter 1) when the Wilkes Expedition visited Hawai`i in 1840–1. Coan described subsequent eruptive activity of both Kīlauea and Mauna Loa volcanoes for the next four decades in letters to Dana, who published them in the *American Journal of Science*. These letters give us some of the earliest detailed observations of many volcanic phenomena that had never been directly witnessed before. His reports on the 1843 eruption of Mauna Loa volcano (Coan 1844) were the first direct observations of any eruption on this giant Hawaiian shield volcano, and are particularly important because they accurately describe the sustained transport of molten pāhoehoe beneath solid crust. After being awakened in his Hilo home on January 10 by a ruddy glow from far-away Mauna Loa, he decided to explore this major eruption firsthand, and made an arduous three day climb through the rainforest to the open flat saddle between Mauna Loa and Mauna Kea [14]. Accompanied by a fellow cleric, but soon abandoned by his porters, he ascended the north flank of Mauna Loa’s Northeast Rift Zone the next day, traversing the length of an active pāhoehoe flow and describing in great detail what he saw:

The lava on which we were treading gave indubitable evidence of powerful igneous action below, as it was hot and full of seams, from which smoke and gas were escaping. But we soon had ocular demonstration of what was the state beneath us; for in passing along we came to

an opening in the superincumbent stratum, of twenty yards long and ten wide, through which we looked, and at the depth of fifty feet, we saw a vast tunnel or subterranean canal, lined with smooth vitrified matter, and forming the channel of a river of fire, which swept down the steep side of the mountain with amazing velocity. The sight of this covered aqueduct or, if I may be allowed to coin a word, this pyroduct – filled with mineral fusion, and flowing under our feet at the rate of twenty miles an hour, was truly startling. One glance at the fearful spectacle was worth a journey of a thousand miles. We gazed upon the scene with a kind of ecstasy, knowing that we had been traveling for hours over this river of fire, and crossing and recrossing it at numerous points. As we passed up the mountain, we found several similar openings into this canal, through which we cast large stones; these, instead of sinking into the viscid mass, were borne instantly out of our sight upon its burning bosom. (Coan, 1844)

In describing the 1880–1 Mauna Loa lava flow in his autobiography Coan (1882, pp. 332–4) again defined pyroducts, and specifically mentioned their role in insulating lava from heat loss. Coan's observations were not widely believed at the time, mainly because no formally trained scientist had ever had the opportunity to study an active lava flow firsthand. In fact, J. D. Dana, the influential Yale professor and Editor of the *American Journal of Science*, challenged Coan's observations and wrote that what Coan had seen were actually deep volcanic fissures in the flanks of Mauna Loa – propagating down slope to feed the terminus of the 1843 flow (Dana 1852). But, the missionary was correct, and the professor was wrong. Good field observations usually trump academic theories!

We have several reasons for wishing to revive Coan's 170-year old term, finding it both appropriate and practical (Table 6.2). Although the word “tube” is currently in vogue, it has pejorative connotations for some, and gives no indication of how these features were formed. Furthermore, while tubes are defined in the dictionary as cylindrical structures, the molten feeder channels within lava flows are rarely tubular in geometry. Some are shaped like vertical slots with keyhole-shaped cross-sections, and others are nearly horizontal flat-roofed chambers, with their shapes continuously changing inside an active lava flow. In many cases, primary feeder conduits evolve into slots or sheet-like lenses at distal parts of flows and partially solidify to form bands of lava laced with numerous small lens-shaped channels.

We define the term **pyroduct**, then, as *any internal lava conduit in a flow, irrespective of shape and size, regardless of whether it contains molten lava during eruptive activity or is preserved as an elongate cave after eruptive activity ends and molten rock drains away*. Etymologically, the word pyroduct (“fire conduit”) could also describe surface lava channels, but we shall restrict the term only to describe subsurface features – Coan's original usage. For convenience sake, we will employ his term accordingly throughout this book, referring on occasion to lava caves as “drained pyroducts,” knowing full well that this may raise some hackles among those who prefer to use currently more popular, but potentially misleading terms.

PYRODUCT FORMATION

On steeper slopes (near source vents) pāhoehoe flows are typically fed by well-defined channels, and if lava production rates are relatively constant and the eruption is long-lived, these

TABLE 6.2 HIGHLIGHTS IN THE DEVELOPMENT OF THE TERM “LAVA TUBE” IN THE GEOLOGICAL LITERATURE.

Publication year	Reference	Description
1799	Rosenmüller & Tillesius	They refer to caves (hölen) that “served for channels of the earthfire molten rivers.”
1803	Kant	Kant states that lava caves (die hölen) “dried from the outside while still being fluid inside” and that when “fluid finally dries up and retracts, then caves are created.”
1825	Scrope	Scrope (First Edition) refers to “caverns formed beneath the surface of a lava-stream,” with “pseudo-stalactitic projections made by the subsistence of the liquid.”
1844	Coan	Coan observed subterranean lava rivers during the 1843 eruption of Mauna Loa, correctly determined their genesis, and coined the term pyroduct to describe them.
1852	Dana	Dana used the term tunnel as he discredits Coan’s observations.
1857	Coan	Coan again correctly described the genesis of lava conduits in the 1855–6 Mauna Loa flow, but referred to them as subterranean pipes .
1872	Scrope	Scrope referred to these features as hollow gutters and caverns .
1882	Coan	In his biography, Coan called these features both subterranean ducts and pyroducts in his recollections of the many Hawaiian eruptions he witnessed from 1840 to 1881. He wrote that “under this crust the torrent runs highly fluid, and retains nearly all its heat.”
1884	Dutton	Dutton described then cold pyroducts of the 1880–1 Mauna Loa lava flow, and called them lava tunnels .
1896	Powell	Powell refers to these caves as volcanic pipes .
1909	Brigham	Brigham described these structures as subterranean pipes , and dismissed Dana’s incorrect criticism of Coan’s views with the words: “Those who have never seen a lava-flow cannot well understand its action. I believe Mr. Coan’s briefest account conveys a better idea [of these features] than the most elaborate theorizing of those who have never seen one.”
1919	Jaggard	Jaggard used the terms tunnel and tube interchangeably to describe pyroducts of the 1919 Mauna Loa eruption. This may be the first use of the term tube to describe these features.
1941	Anderson	Anderson popularized the term lava tube in his classic study of the Modoc Plateau lava caves
1950	Perret	Perret favored the term lava tunnel in his important memoir.
2008	Numerous	“Lava tube” has become the most commonly used term for drained pyroducts, although they are still also referred to as “tunnels” in many publications.

channels will commonly crust over to form pyroducts (Fig. 6.15). The formation of pyroduct roofs involves two processes: a) narrowing of the channel rims by freezing of lava levees along channel walls, and b) the accretion of plates of crust that are skimmed off channel surfaces where flow obstructions are encountered. Once a pyroduct roof segment is established, that roof forms a blockage for crustal fragments moving downstream and the roofed-over area will rapidly propagate upstream as more crustal fragments plate onto the pyroduct entrance. Pyroduct roofs are also thickened by new lava that may flow onto them from overflowing channels or fresh extrusions of lava upslope. Where pāhoehoe flows reach more gentle terrain, channel development mostly ceases and is much less important a mode of pyroduct development. Most lava instead is supplied by high pressure inputs beneath inflating crusts (Hon et al. 1994). Such flowage tends to be concentrated along the most efficient pathways, which

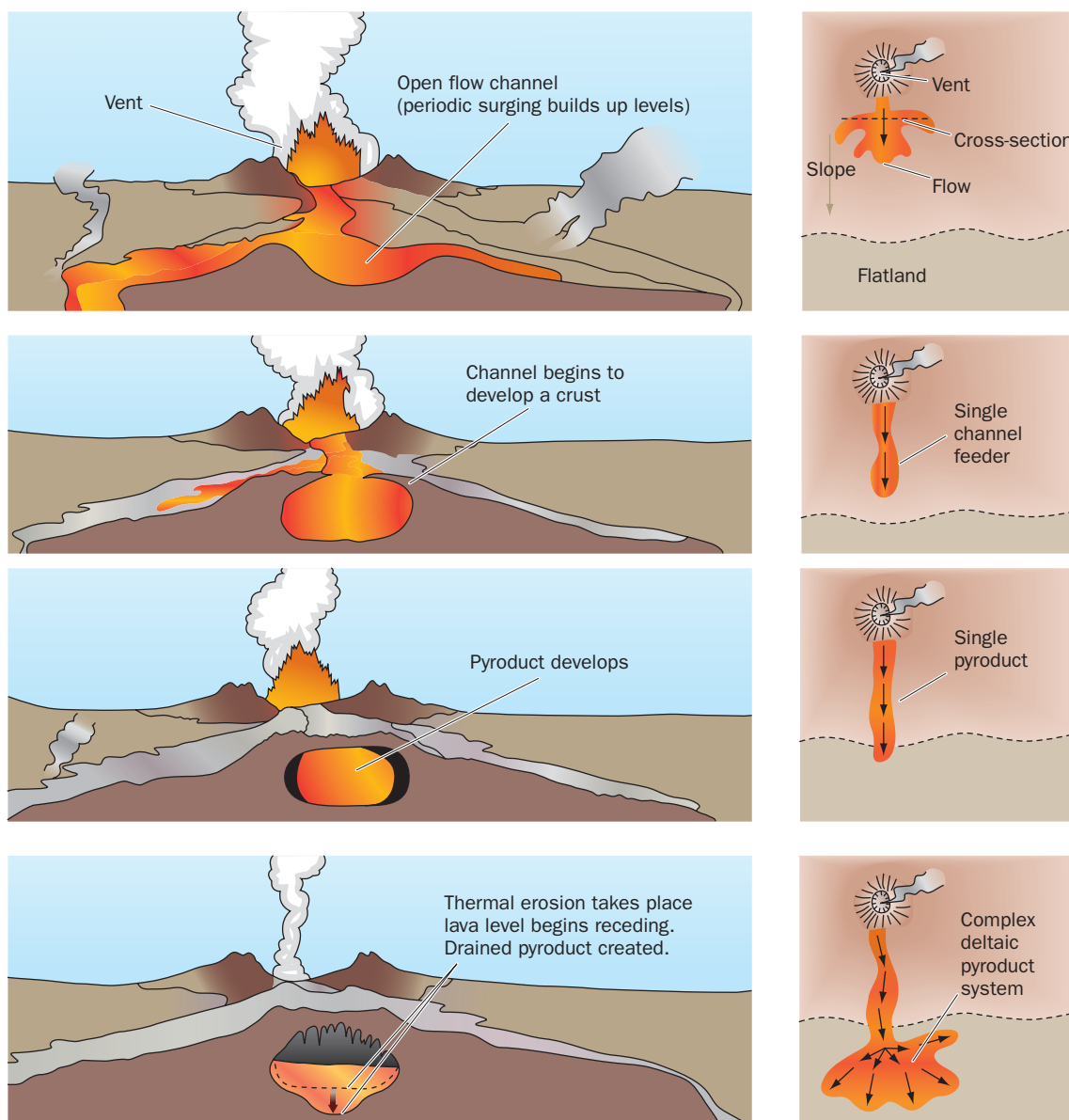


Fig. 6.15 Mechanism for pyroduct formation, as an open lava channel crusts over during flow (view upstream towards source vent) and lava supply conduits are subsurface. Complex pyroduct systems may also form beneath inflating lava crusts on more gentle slopes, unrelated to surface channels. On plan views (side bars) dashed arrows indicate subcrustal flow.

evolve into persistently active pyroducts as eruption continues. Sudden extrusions of fresh molten lava may occur practically anywhere through the chilled crust overlying highly-pressurized pyroducts in the lower reaches of an active flow, and in places the repeated raising and lowering of pressurized pyroduct roofs can lead to formation of the circular accumulations of broken rock known as **shatter rings** (Fig. 6.16) (Kauahikaua et al. 2003). Sluggish movement may continue at a flow front even after an eruption has ended as channel-formed pyroducts upslope continue draining into the “flow-inflation” pyroducts at lower elevation.

Most likely all large pāhoehoe flows develop pyroducts to transport lava beneath their crusts as they advance. Their presence can only be inferred in most cases unless open skylights (Figs. 6.17, 6.18) are present, as geophysical detection methods have proven to be ambiguous. Even in cross-section, filled pyroducts may be indiscernible from the surrounding lava,

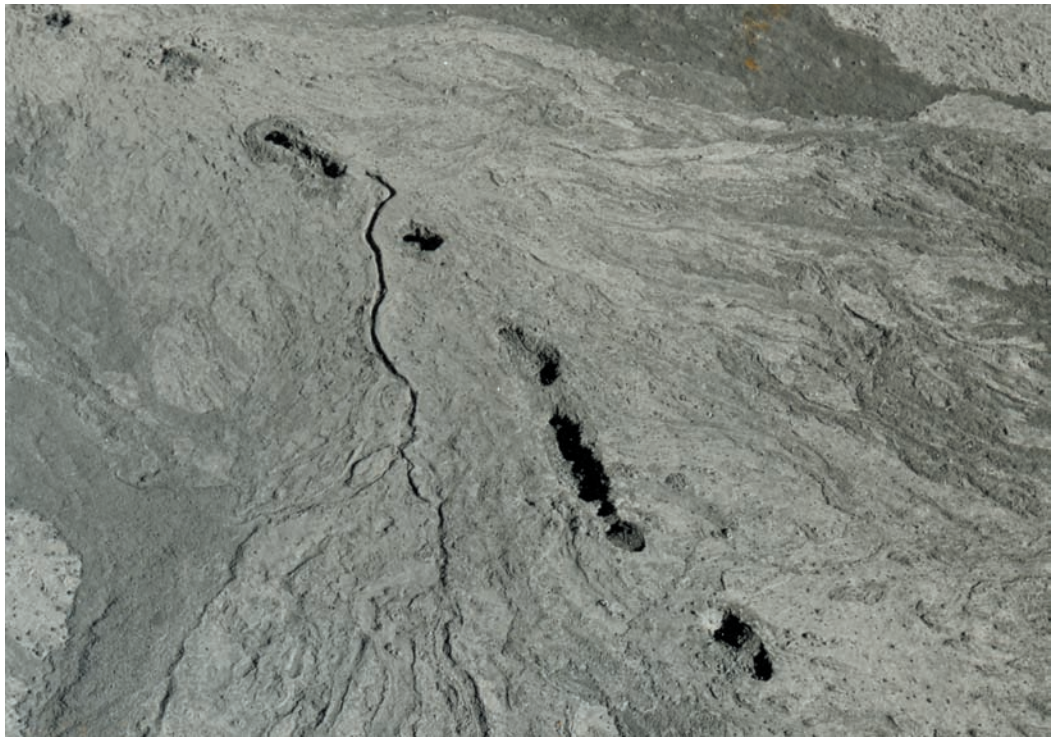


Fig. 6.16 A shatter ring formed in 1991 by the repeated flexing of a roof above a major active pyroduct 5 km below the Kupaianaha lava lake, East Rift Zone, Kīlauea volcano, Hawai'i. The ring is 58 m × 46 m in plan view, and its rim ranges from 3 to 5 m high. USGS photo by Tim Orr, looking to the southeast.



Fig. 6.17 The “Waha Mano” (Shark Mouth) window into a pyroduct of the 1859 lava flow, Mauna Loa, Hawai'i. The red color was caused by high-temperature oxidation as atmosphere-contaminated gases poured out of this window, melting rock to form the stalactites visible on the pyroduct ceiling. Photo by J. P. Lockwood.

Fig. 6.18 Series of “windows” or “skylights” above a prehistoric pyroduct on the southeast slope of Mauna Loa. The skylights are 4–5 m in diameter. Photo by J. P. Lockwood.



although many are obvious (Fig. 6.19). Skylights along active pyroducts provide useful opportunities for quantitative flow measurements and lava sampling. Throwing markers such as branches into an opening, the speed of flow can be measured by clocking the time required to travel to the next skylight downstream, and show that lava travels much faster when it is internally confined than it does when spreading directly across the surface. Temperature measurements reveal that heat loss during pyroduct, is very slight, as little as a half degree centigrade per kilometer.

Exploration and detailed mapping of drained pyroducts (Kempe 2002) has revealed the complex dynamic history of these long-lived conduits as they evolve. They commonly deepen by thermal and mechanical erosion of their floors with time, and may develop complex intertwining passageways at multiple levels. Atkinson et al. (1975) describe the longest pyroduct system in the world, in pāhoehoe flows from 19 my old Undara volcano, western Queensland, Australia. It has an inferred length of over 100 km, entirely formed during a single eruption, but is for the most part not accessible for exploration. Much more impressive and open for exploration are the 65 km-long contorted pathways of prehistoric Kazamura Cave, a nexus of accessible, archaeologically important passages underlying the shallow eastern flank of Kīlauea, with skylights providing entry at multiple locations. Notable features of the Kazamura system are **lava falls** (Kempe 2002). These are abrupt drops in the floor of the cave passage, like the waterfalls along a stream. Some are as much as 20 m high and require rappelling gear to descend. Lava falls commonly open down slope into large chambers with skylights in their ceilings. The chamber floors consist of lava plunge-pools as much as several meters deep, many of which contain accumulations of rubble. Many have sharply incised lips, suggesting minor up-channel erosion from rubble scour.



Fig. 6.19 Cross-section of a filled pyroduct at Makapu'u Point, on the eastern end of Oahu Island, Hawai'i. Note the concentric banding, that records the narrowing of the pyroduct as the lava supply waned and lava began to freeze inwards. Photo by J. P. Lockwood.

The ceilings of pyroducts are typically marked by **lava stalactites** (Fig. 6.20a, b). These may resemble icicles, or they may be long pencil-like rods often covered with rounded protrusions resembling bunches of grapes. They are formed by the freezing of molten lava dripping from the ceiling of the pyroduct. Sometimes this is liquid left by a rapid lowering of the lava level, but most commonly they are formed by melting of the solid roof rock by the heat of burning gases, or by drips from pockets of molten lava above. If liquid continues to drip from the stalactites onto the floor of the cave after lava has stopped flowing, it will solidify to build up features called **lava stalagmites** (Fig. 6.20c).

Elsewhere, prominent horizontal ledges of lava or horizontal "high lava marks" line the walls of drained pyroduct passageways, in some instances as high as several meters above the floor. These represent incipient development of crusts atop flowing lava temporarily maintained at constant levels or reflect deepening of pyroducts by erosion of their floors (Fig. 6.21). In some cases pyroducts bring magma to the surface to discharge as lava (Fig. 6.21).

Fig. 6.20 Pyroduct features. a) Conical stalactites (to 10 cm length) that are typically formed by multiple inundations of pyroduct ceilings. The dark brown color indicates oxidation of iron – many are unoxidized and black. The cream color of the latest inundation shows advanced oxidation by air flooding the pyroduct in its final stage. b) Less-common cylindrical stalactites (to 25 cm length), formed by secretion of molten lava from fluid pockets within the pyroduct ceiling. The contorted ones are called lava helectites. c) Lava stalagmites, formed by the dripping of fluid lava from stalactites above. These are uncommon, as they are usually carried away by flowing lava on pyroduct floors. d) Large pyroduct passage in the Manjang Kul, Jeju Island, South Korea. The high-lava marks on the pyroduct walls probably record a history of lowering lava levels as flowing lava eroded the floor during enlargement. Photos a), b), c) Hawaiian pyroducts, by J. P. Lockwood. Photo d) © Ed Waters.

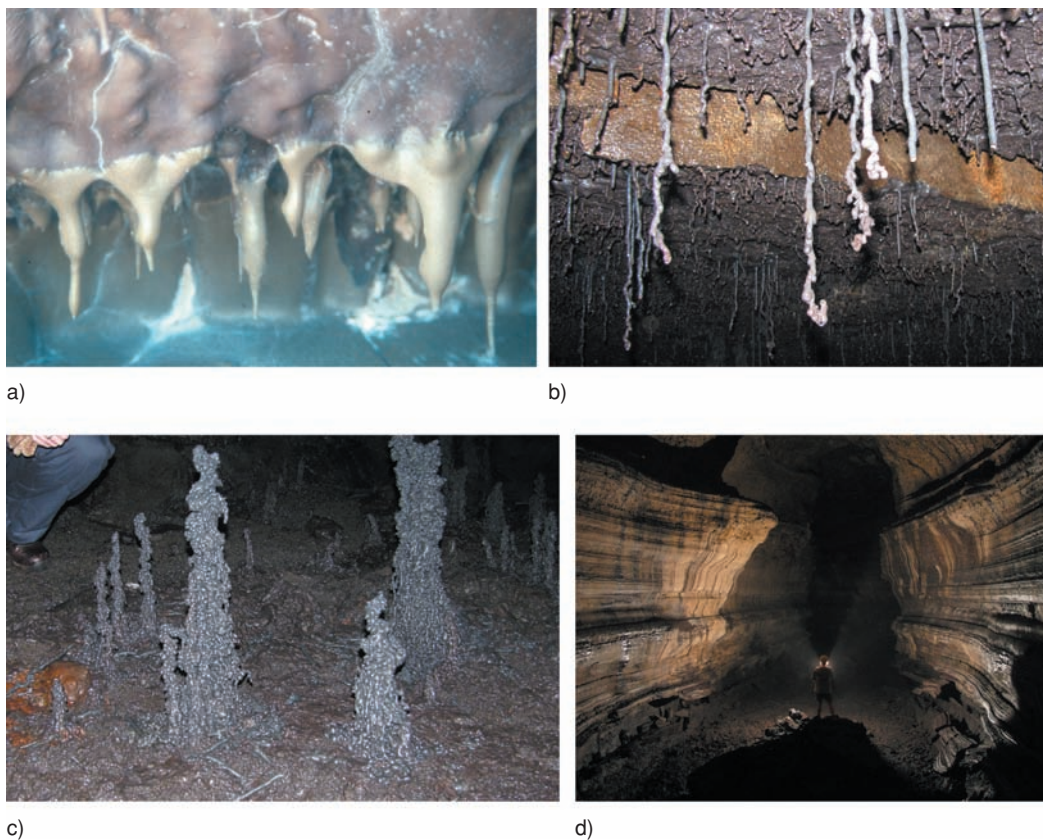


Fig. 6.21 The end of a long trip! The pyroduct in the background has transported magma upward from far beneath Kīlauea volcano's summit, down the East Rift Zone, through a 10 km-long pyroduct, and is here disgorging what can finally be termed "lava" as magma sees its first sunlight! The pyroduct opens into a lava channel that carries lava the final 50 m to its 2009 rendezvous with the boiling sea. The channel has begun to roof over by accretion of frozen lava at its edges, and became a covered pyroduct shortly after this photo was taken. Photo © G. Brad Lewis.



The role of pyroducts in the development of pāhoehoe flows can hardly be overstated. Thanks to the insulation from heat loss, lava moving through pyroducts will travel farther and spread wider than if it were continuously exposed to cool air and radiation heat loss after leaving the vent. For island shield volcanoes like those of Hawai'i or the Galapagos, which are largely built up of pāhoehoe flows, this means that their land areas are larger, and their slopes much gentler than they would be if pyroducts did not form. Indeed, volcanic “shield” shapes owe their existence to pyroduct activity and to the great fluidity of basalt lava.

Pāhoehoe Surface Structures

Many pāhoehoe flows have relatively flat upper surfaces – extending horizontally for kilometers – “flat enough to ride a bicycle on” (although it would be a bumpy, slow ride!). More typically, the upper surfaces of pāhoehoe flows are marked by a characteristic “mini-topography;” with relief on a scale of a few meters or more, including discrete hillocks called tumuli, uplifted blocks called lava rise terraces, broad depressions, and steep-walled holes – termed inflation pits. Lava channels are commonly present in the upper reaches of a flow, and as described in the previous section may be roofed over in places to form pyroducts. (Fig. 6.22).

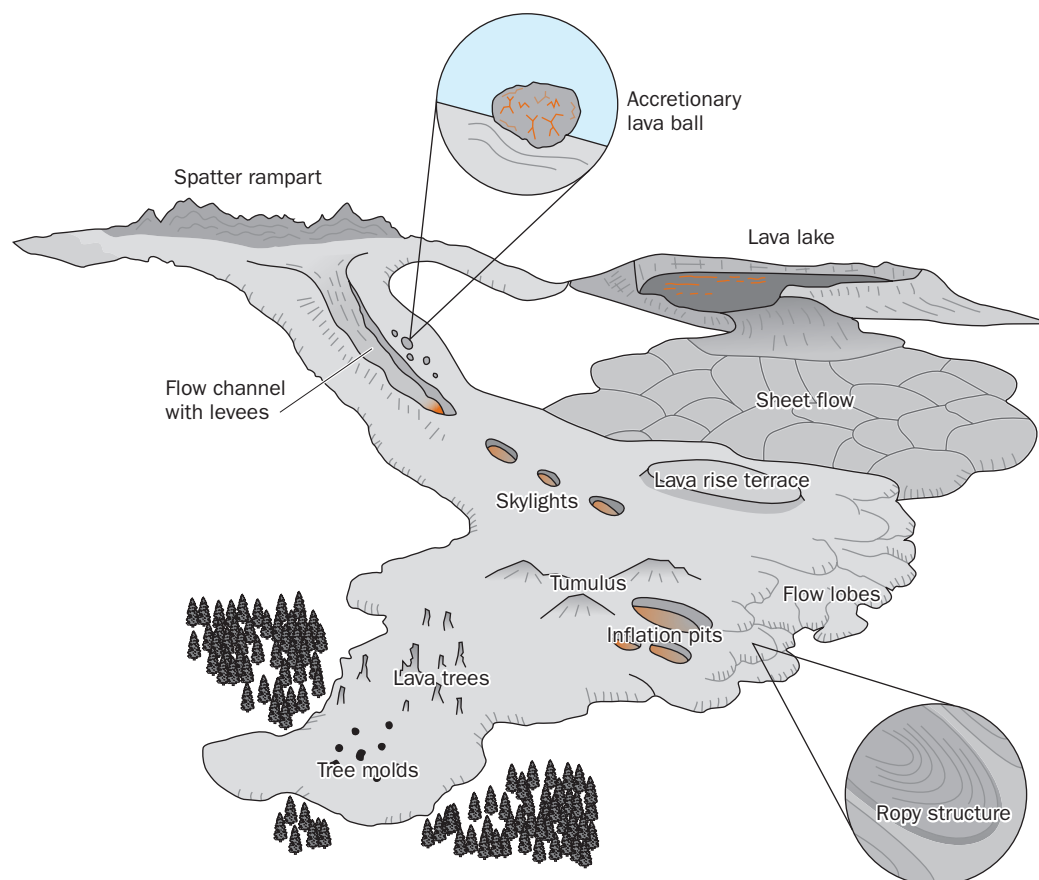


Fig. 6.22 Distinctive surface features of pāhoehoe flows.

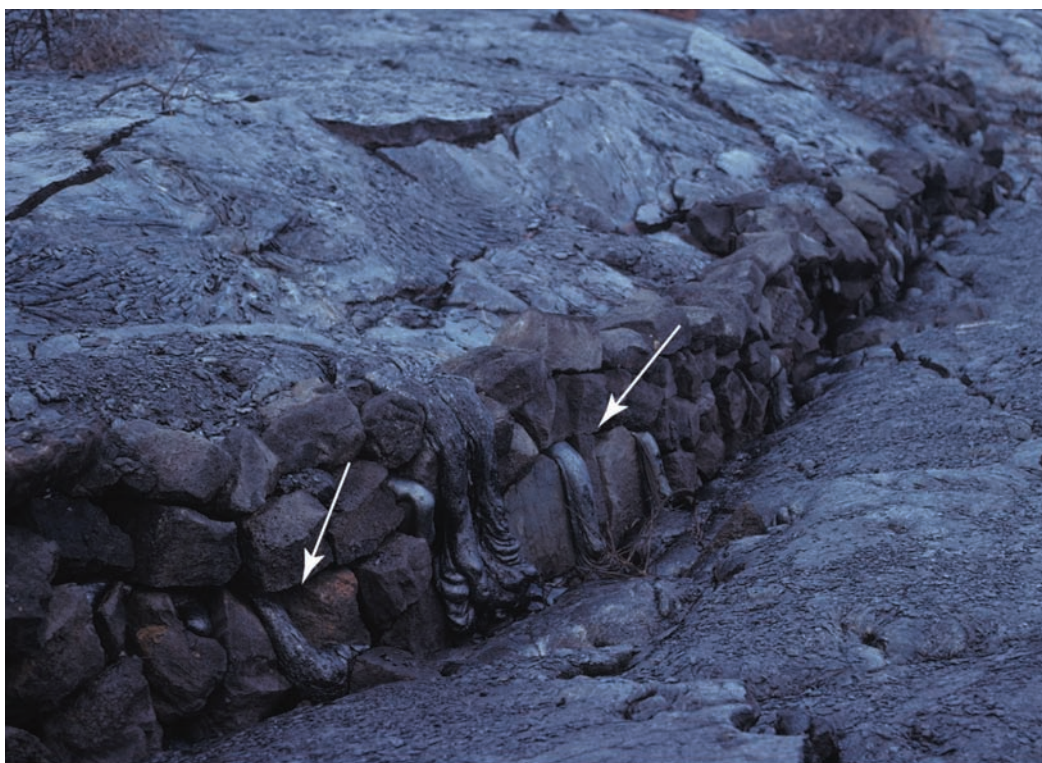
Survival Tips for Field Volcanologists:

When crossing a major pāhoehoe flow, make the effort to climb to the tops of major tumuli rather than walk around them. The air will be much cooler, refreshing breezes will be stronger up there, and the high ground makes a good vantage point to plan the easiest traverse path ahead.

Such irregular features are characteristic of most pāhoehoe flows, especially those resulting from basaltic eruptions characterized by the relatively steady production of lava over long time periods. In some high-discharge effusive eruptions, however, extremely rapid extrusion onto nearly level ground causes the lava to spread out as laterally extensive, interfingering **sheet lobes**. Cracks separating low convex plates meters in diameter may be the only features marking the surfaces of these “hummocky parking-lot” flows.

The initial emplacement of pāhoehoe flows may only be the beginning of their development, since molten lava from source vents often continues to inject the interior of flows sometimes for weeks or months after they develop rigid upper crusts and stop spreading across the landscape. As a result, like bread rising in an oven, the lava flow **inflates** (Hon et al. 1994; Walker 2009). This, in fact, is when much of the mini-topography described above may develop. Gradual inflation can thicken a flow by as much as several times (Fig. 6.23). Features originally at the surface – including minor details like “ropy texture” (see below) and objects engulfed by the original flow, such as burnt off trees, old cars and bathtubs – will remain on that original surface as the flow’s thickness increases dramatically beneath them. But inflation is not the only means by which a pāhoehoe flow acquires its final thickness. The build up of pressure from fresh lava injected beneath the crust can cause it to split open (a **breakout** in volcanological parlance), releasing a tongue or lobe of fresh molten lava which quickly develops its own crust and “repaves” the flow surface to greater depth (Fig. 6.24). Multiple breakouts and lobe extrusions from a flow front can also advance the flow for days after the vent upslope has ceased activity. The smaller lobes, termed **pāhoehoe toes** (Fig 6.25), may measure only a few centimeters across. Larger ones may span tens of meters in width. This process repeats

Fig. 6.23 Infiltration of a wall of unmortared stones by an inflating pāhoehoe flow enclosing and partially inundating the compound of the thirteenth-century Wahaula Heiau, a prehistoric Hawaiian sacrificial site on the southern coast of Kīlauea volcano. Note the fingers of pāhoehoe that have oozed between the stones (arrows). Photo by R. W. Hazlett.



countless times, so that a cross section of a typical pāhoehoe flow will appear as a great stack of flattened sand-bag like masses, many of them hollow from later drainage of the conduits which fed them (Fig. 6.26) (Gregg & Keszthelyi 2004).

While some surfaces of stationary pāhoehoe flows **inflate**, other portions will **deflate**. Flow deflation can be easily imagined if one thinks of a thick, porridge like fluid spilling down a slope. The initial outpouring of porridge may be quite thick, but as the liquid mass spreads away, it will grow thin near the source unless the rate of supply (discharge) is maintained or even increased. Most flows show evidence of simultaneous flow deflation near their vents with corresponding flow inflation at their lowland termini. Even at the scale of a single outcrop only a few meters across one can see examples of inflation in one area and deflation in another, reflecting local redistribution of subsurface pāhoehoe in the final stages of solidification.

Everywhere one looks across the surface of a fresh pāhoehoe flow, rinds of glass provide a medium gray to black surface that may be highly reflective and take on a silvery, almost polished metallic appearance in sunlight. The rinds may only be a few millimeters thick, and are rarely thicker than a centimeter except where flows have been quenched by water. Surface glass grades inward into the microcrystalline interiors of flows through zones of mixed glass and microlites. Exposed to the elements and subject to devitrification the glass breaks down readily, and a pāhoehoe flow develops a dull flow surface that transitions to tan and then red-brown colors over hundreds or thousands of years.

TUMULI

Nineteenth-century geologist Reginald Daly introduced the term **tumulus** (plural **tumuli**) to refer to the steep sided mounds found on surfaces of many pāhoehoe flows. The word had earlier been used to describe burial mounds in Europe and the eastern United States, and before that was applied by early Romans to identify the rounded, convex shields of their legionnaires.

Tumuli may be gentle domes or rugged obstacles with steep to overturned sides difficult to climb over and easier to walk around. They range in size to 15 m or more in diameter and commonly 1.5–3 m in height (Fig. 6.27), but in places are much larger (Fig. 6.28); most are oval in ground plan, but some are nearly circular. Many are rent by deep

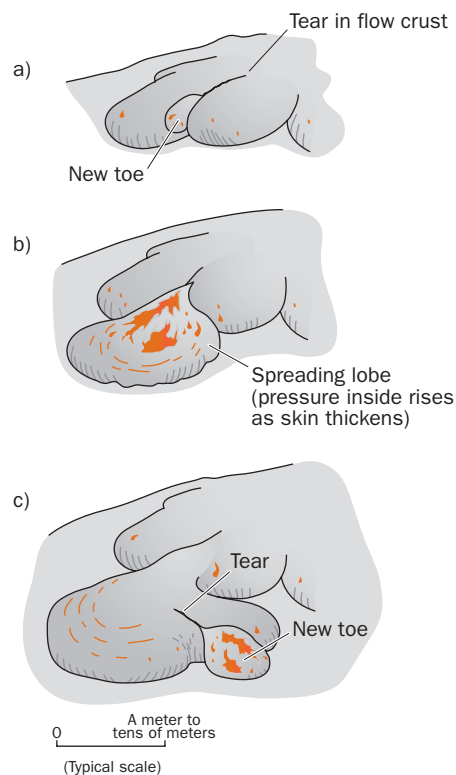


Fig. 6.24 The fronts of pāhoehoe flows commonly move by spreading in lobes that freeze, then split as molten lava pressure rises inside, to feed new lobes.



Fig. 6.25 Flowing pāhoehoe toes on the flanks of Mauna Ulu, Kilauea volcano, Hawai'i in April, 1974. The incandescent, fast-moving toe on the left is about 20 cm in width. The toe on the right is about 3 minutes old, and has developed a flexible, black glassy crust about 1 mm thick over a molten interior. This toe is still moving sluggishly, bounded by "strike-slip faults" in the crust along margins. USGS photo by D. W. Peterson.



Fig. 6.26 Multiple pāhoehoe flow lobes formed during a single eruption of Kīlauea volcano in 1972. Three separate lobes are shown here, each separated by a zone of red oxidation. Note the typical hollow voids in the overlying flow – caused by the coalescence and expansion of exolved gases during flow. Photo by J. P. Lockwood.

open fissures at their tops – openings that formed as their once-flat surfaces were broken apart by intruding lava below. The tumulus crust commonly splits apart during uplift, and molten lava may squeeze up through the fractures to feed small flows that dribble down the sides. The molten lava beneath large tumuli may drain away laterally, leaving grottos large enough to admit people (Halliday 1998). Not all tumuli form by uplifting of the original surface, however. Some may form as lava is withdrawn from surrounding areas and the overlying crust subsides. In fact, it may be impossible to judge which surfaces went up in absolute terms and which went down – even if one is standing nearby as the surface slowly deforms!



Fig. 6.27 3 m. high tumulus on a 2003 pāhoehoe flow, Kīlauea volcano, Hawai‘i. This structure was formed by upwelling lava that broke open a once-horizontal flow surface, and oozed out at the top. Note well-developed “ropy pāhoehoe” on the uplifted surface. Photo by J. P. Lockwood.



Fig. 6.28 Giant tumulus formed on the 1843 pāhoehoe flow, Mauna Loa, Hawai‘i. This feature rises about 15 m above the surrounding pāhoehoe terrain. Note the 1843 ‘a‘ā flow in the foreground. Photo by J. P. Lockwood.

INFLATION PITS

Inflation pits are common on some pāhoehoe surfaces, and have been erroneously referred to as “collapse pits.” These features may be less than a meter across or tens of meters in diameter (Fig. 6.29). Most have near-vertical or overhanging rims, and they may be several meters deep. They certainly *look* as though they formed by collapse processes, but most form by differential uplift of the surrounding crust. I (JPL) have stood on inflating pāhoehoe flows as these pits slowly develop over a period of hours, and while visually persuaded they were subsiding, instrumental measurement showed in fact that the (hot) crust on which I was standing was going up – while the floors of the pits remained stationary.

ACCRETIONARY LAVA BALLS

Accretionary lava balls (bombes en enroulement), are distinctive features found alongside pāhoehoe lava channels and on the surfaces of many basaltic ‘a‘ā flows. They are typically egg-shaped, smooth-sided boulders 1–3 m in diameter that consist of low density internal cores enclosed by glassy rims. Most originate within spatter cones formed by lava fountains during the early phases of long-lived eruptions. As described at the beginning of this chapter, spatter cones are incredibly unstable and fragile during growth, with large masses frequently dislodging and tumbling into the roiling lava lakes they enclose. The agglutinated fragments are substantially cooler than the molten vent lava in which they suddenly become immersed,

Fig. 6.29 Inflation pit on the 1843 pāhoehoe flow, Mauna Loa volcano, Hawai‘i. Although these features indeed look like they formed by collapse, they actually form as the surrounding pāhoehoe flow is inflated by the injection of molten lava, leaving the original, uninflated crust behind. Photo by J. P. Lockwood.



and they immediately acquire selvages of quenched glass. Because the bulk density of these porous, lava-coated spatter masses is much less than surrounding melt, they immediately bound back up to the surface, where they are rafted or tumbled end-over-end downstream in flow channels. The lava balls may float with as much as half their volumes above a conveying current. Some are destined to drift into large diameter pyroducts, and may be expelled from windows downstream. Others are swept by surges up out of channels onto the surrounding flow surfaces; and indeed one of the most common places to find them is on the banks of pāhoehoe lava channels, where they may be recoated and made even smoother by later surges of lava (Fig. 6.30a). When a pāhoehoe flow transforms into `a`ā, the lava balls will continue to ride along buoyantly, sometimes carried as far as 20 km from their points of origin (Fig. 6.30b). Accretionary lava balls can also form as fragments of channel walls fall into lava rivers and are coated by glassy rims.

SURFACE APPEARANCES

Geologists have termed the surface appearances of pāhoehoe “ropy,” “corded,” “elephant-hide,” “shark-skin,” “entail,” “festooned,” “filamented,” “shelly,” and “slabby” (transitional pāhoehoe). Some surfaces combine aspects of different types, e.g., “shark-skin ropy pāhoehoe.” Each term usefully conveys an image of physical appearance. It is beyond the scope of this book to discuss them all in detail. But consider the three following, distinctive examples.

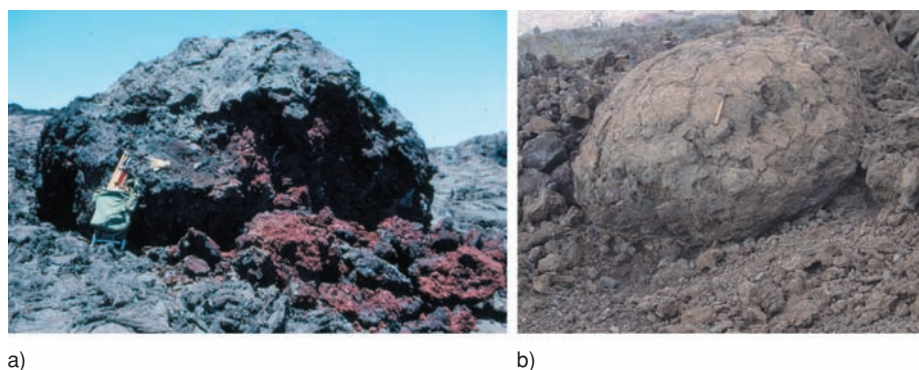


Fig. 6.30 Accretionary lava balls on prehistoric Mauna Loa lava flows, Hawai'i. a) Accretionary lava ball on the edge of a lava channel in a 250 year-old pahoehoe flow. Note the welded spatter interior of this lava ball after the thin lava "shell" was broken. b) Accretionary lava ball on a 200 yr-old 'a'ā flow, about 25 km from spatter cone source (note hammer for scale). Photos by J. P. Lockwood.

Ropy pāhoehoe

A characteristic feature of pāhoehoe surfaces is the occurrence in some areas of crust that is wrinkled and twisted into forms resembling the folds in heavy cloth, or parts of coils in rope (Fig. 6.27). These forms result from the dragging and twisting of the thin, hot, plastic crust of the flow by movement of the liquid lava underneath. Friction results in the edges of narrow lava streams moving less rapidly than the middle. Where **ropy structure** forms on the crust of such a stream, the "ropes" are bent into curves that are convex in the direction of the stream movement. Such a directional indicator does not provide a good sense of the overall motion of a lava flow, however, since many displays of curved ropy structure result from small eddies and other chaotic local movements. Statistically significant measurement of many rope structures must be made to gain an idea of the overall flow direction of an old lava flow in terrain where the original lay of the land is no longer evident.

Entrail pāhoehoe

Ropy pāhoehoe tends to form on gentle to moderate slopes, while on steep slopes, cascading pāhoehoe may form **entail pāhoehoe** instead. The name "entail pāhoehoe" describes the startling appearance of this lava type, like a great heap of intestines, which consist of a great mass of overlapping pāhoehoe toes, each of which grew quite elongate owing to the pull of gravity on the slope (Fig. 6.31).

Shelly pāhoehoe

Near overflowing vents, rapid outpouring of gas-rich, low-viscosity pāhoehoe leaves a surface of fragile, glass-rich plates, in many places twisted into large folds. This crust overlies numerous void spaces, some as deep as several



Fig. 6.31 "Entail pāhoehoe," formed where fluid pāhoehoe lava tongues flowed down a cliff face in 1972, Kīlauea volcano, Hawai'i.

Survival Tips for Field Volcanologists:

Channel levees are normally elevated above the surrounding terrain and the flowing lava below, and make excellent vantage points for viewing, but care must be taken to approach them from the upwind side, and to be alert for signs of instability. The sides of active lava channels, whether in pāhoehoe or `a`ā flows, are potentially hazardous as they are often unstable and subject to sudden collapse. Also, because lava in these channels is generally agitated and not covered by lava crusts, they are extremely hot environments with copious sulfur fumes close to erupting vents.

decimeters. To walk across such lavas without sturdy boots, long sleeves, tough trousers, and gloves, is to risk deep cuts, as one inevitably will break through surface plates. It feels and sounds like “walking on egg-shells.” **Shelly pāhoehoe** is so fragile that it does not survive for more than a few thousand years before breaking down. Shelly pāhoehoe exemplifies a type of lava Swanson (1973) terms “fountain-fed pāhoehoe,” since it is typical of pāhoehoe close to lava fountain sources. As pāhoehoe flows further away from vents, sufficient gas will be released that flow surfaces generally become stronger and more stable. Where molten pāhoehoe travels for any distance underground in subsurface conduits, it generally is extensively de-gassed and forms the smooth-surface flows Swanson termed “tube-fed pāhoehoe.” (We would, of course, prefer that such lavas be called “pyroduct-fed pāhoehoe” in the future – since most of these conduits are anything but tubular!)

ENVIRONMENTAL CONDITIONS ON AN ACTIVE PĀHOEHOE FLOWS

Active pāhoehoe flows moving across relatively flat terrain may be a bit disappointing to first-time visitors by day, as most of the active parts of the flow are covered by apparently stationary, silver-gray crust, with molten lava only visible in a few places, mostly near flow margins where lobes of blood-red to orange fluid ooze from cracks in plates of upraised crust here and there. There is almost no conspicuous noise, except for the occasional creaking or rasping sound as one section of crust moves relative to another. Barely audible may be a continual “clicking” noise, caused by tiny chips of glass spalling off cooling, contracting surfaces. The splendors of an active pāhoehoe flow are greatest after twilight. Whereas “red rock” is hard to see during the day, “fire” will be visible everywhere at night, and myriad cracks in the lava show incandescent yellow orange lava below. Molten rock reflects off vapors at night, creating a dull red color in the sky. Every active outbreak of molten lava, apart perhaps from the rare low-temperature carbonatites (Chapter 3), may be seen from afar at night.

Pāhoehoe crusts are relatively strong when underlain by molten lava (but not where overlying gas cavities!). It is actually possible (but not advisable) to walk across an active pāhoehoe flow only a half hour or so old, as it takes only a few centimeters of crust to support a person’s weight. The crust may sag and bend like “rubber” ice on a partly frozen pond, but it probably won’t break. Crust in this state is still very hot, of course, which will cause boot soles to melt or even burst into flame if one stands for more than a few moments in any given place, and the chance of heat stroke is a great danger. Flows will retain dangerous levels of heat for days, or even several weeks after they form. In 1987, RWH led a field party across a wide pāhoehoe flow several days old to visit the Kupaianaha vent on Kīlauea. The excursion began under a sunny, tropical sky. But by noon it was raining, and after examining the vent, the team became immersed in the midst of a lava-heated steam cloud too dense for even reading a field compass because of condensation inside of the compass glass. By “dead-reckoning” several kilometers through this natural sauna, the group safely found its way back, warm, and thoroughly soaked. But this was certainly good luck. In places where heavy rain or wave splash falls on openly flowing lava, steam may be scalding, even deadly.

Active pāhoehoe flows are continually releasing hot gases, especially near source vents. The flows lose their volatiles from exposed melt and from cracks that penetrate the hot crust opened

during movement and cooling. An especially active portion of a spreading flow surface can easily be spotted from a distance by a combination of heat-shimmer and emerging brown to bluish-gray fume. Geologists quickly learn to approach active pāhoehoe flows from the upwind direction, since the heat and choking fumes blowing downwind from such flows are often unbearable. I (JPL) came close to death when standing near the margin of a large expanse of ponded pāhoehoe a few hundred meters below the Mauna Ulu vent of Kīlauea in 1974. The wind suddenly shifted direction and caught me in a plume of hot, sulfur-rich gas. I tried to run, but soon found that my throat had closed shut – an automatic physiological reaction to limit lung damage from breathing SO₂.

THE WORLD'S MOST FLUID PĀHOEHOE

Very fluid pāhoehoe can move several tens of kilometers per hour down steep slopes, and may leave residual flows only a few centimeters thick. During the 1977 eruption of Nyiragongo volcano in central Africa, exceptionally low viscosity nephelinite lava left residual flows less than 2 cm thick on the steep upper slopes of the volcano (Tazieff 1977). During the 2002 eruption, the margins of residual lava flows surrounding small kipuka were less than 1 mm thick in places near source vents (Fig. 6.32), although the “high lava marks” on adjacent burned trees showed the flow had been about two meters thick as it rushed downslope. The thin flow margins consisted of glass quenched on the cold soil. The fact that voluminous lava had traveled down the mountainside without leaving more material behind shows the lava had no yield strength, and was in fact an exemplary Newtonian fluid (Chapter 4). During the same eruption, fast moving, fluid flows 2–3 m thick rushed past banana plants, burning off leaves, but not toppling the fragile plants. Many fluid pāhoehoe flows in Hawai`i and at Piton de la Fournaise volcano [95] in the Indian Ocean are initially less than a few decimeters thick on their leading edges, although they generally thicken within a few hours through flow inflation.

PĀHOEHOE, FORESTS, AND FOSSILS

When pāhoehoe first erupts, flows may be quite thick near vents, because the initial pāhoehoe output is typically high, and the lava is typically inflated with gas bubbles and may be frothy. But as the flow spreads out, drains down slope and loses gas, deflation sets in. Where especially fluid lava sweeps through forests, it can freeze around living trees, sometimes forming casts around them. These will remain standing as the surrounding, more liquid lava drains away, forming ghostly hollow pillars of basalt called **lava trees** (Fig. 6.33) (Lockwood & Williams 1978). During the 1962 eruption at Aloi Crater on Kīlauea, lava trees as tall as 8 m formed – the highest yet reported. Lava trees are fragile, geologically ephemeral features, and are never preserved on older flows.

Elsewhere, where deflation does not occur, the trunks of trees that burn away completely in the hot lava may remain preserved as cylindrical holes in the flow surface, called **tree molds**, some still showing the detailed impressions of burned wood in their sides, even to the scale of paper-thin partitions of lava showing the traces of fine cracks that formed in heat-shrunken



Fig. 6.32 Small kipuka surrounded by 1 mm thick pāhoehoe flow, Nyiragongo volcano eruption, 2002. Photo by J. P. Lockwood.

might readily be perceived as safe by unwary flow watchers. This phenomenon is most typical and more violent alongside advancing ʻaʻā flows, perhaps because of their greater thicknesses and slower travel rates. The explosions never occur where a lava-invaded forest grows atop an older, weathered ʻaʻā flow, as such substrates have few cavities large enough to develop explosive concentrations of gases. A lava-invaded forest growing atop an older, weathered pāhoehoe flow, however, is a dangerous place to be. Numerous void spaces occur, largely related to partial drainage of pyroducts preserved within the overgrown flow. Methane, distilled from buried vegetation, will build up in these cavities, and can easily form explosive cocktails when mixed with the proper amount of air. Sometimes the detonations are small and merely cause muffled rumbling noises underfoot, but at times violent explosions can blast craters up to 5 m in diameter, scattering shattered tree trunks through the air like javelins, and throwing blocks and dust over 100 m high. These explosions can commonly be heard several kilometers away, and may sound like cannon fire in the distance. We call these

wood. Unlike lava trees, tree molds are much more durable, and are commonly preserved in once-fluid lavas thousands of years old. Some tree molds project vertically through the upper surfaces of flows (Fig. 6.34); more commonly they are found sub-horizontally, representing trees that were knocked down by the flow, encased in frozen selvages, and carried along as their contained wood carbonized and burned away, or was destroyed by later biological activity. Tree molds as much as a meter wide and 4 m deep occur in some Mauna Loa lava flows, and where obscured by vegetation can pose a hazard to travelers.

Lava trees and tree molds commonly preserve features that enable one to determine the direction of lava movement (Fig. 6.35). As lava encounters a tree, it will flow around the trunk and converge on the opposite side, in many cases forming a seam line (Fig. 6.34). Such seam lines indicate the direction that the flow was moving, and may be useful for indicating original slope directions (Lockwood & Williams 1978).

Lava of any kind moving through a forest will distill organic matter from underlying buried forest litter and plants. Organic gases (mostly methane) commonly form in this environment, and may migrate out from underneath the flow along subsurface passages to accumulate in subsoil pockets tens of meters away from the flow margin – places which

violent (and very hazardous) events **methane bursts**, although other gases besides methane are likely involved.

I (JPL) have seen trees 50 cm in diameter and large blocks hurled tens of meters into the air by methane bursts near advancing flows. I was watching an advancing pāhoehoe flow one night on Kīlauea, when a large, ancient tumulus behind me exploded violently. Unfortunately, my colleague (Chris Gregg) was standing on this tumulus taking pictures. I heard him scream, and as I turned around I saw in the eerie red light that Chris had been thrown several feet in the air, and was now coming down, along with a massive amount of pāhoehoe blocks from the shattered tumulus. Chris and the rocks landed in an intertwined mass behind me, and he was moaning horribly. I feared the worst, but after he extricated himself from rocks and a crumpled camera tripod, he quickly regained his cheery composure. After a few minutes of rest and thanks to Pele, we continued with our observation duties, with renewed appreciation for this unpredictable hazard.



Fig. 6.33 “Lava Tree” formed during the July, 1974 eruption of Kīlauea volcano, Hawai‘i. These lava trees are about 3 m high, and indicate the thickness of the lava flow that surrounded these trees, before the molten flow interior drained away downslope and the crust subsided to the present level. Photo by J. P. Lockwood.

FOSSIL PRESERVATION

Not only tree trunks, but leaf pattern impressions and even the forms of animals may be preserved where entrapped by fast-flowing pāhoehoe. The lava forms thin selvages of glass, in part from quenching by water boiled out of the organic matter. The selvages prevent molten lava from filling in the holes left as the enclosed substances burn away, and perfect delicate molds can result (Fig. 6.36).

Animal fossils are rare in lava, but a possible mold of an entrapped prehistoric mini-rhinoceros was found within Columbia River basalt flows in Washington State (Chappell et al. 1961), and elephants killed by extremely fast moving lavas on the slopes of Nyiragongo volcano, Zaire in 1977 left perfect molds, down to the details of their trunks (Fig. 6.37). I (JPL) tried to locate these “elephant molds” in 1989, but found out that farmers had discovered they could be excavated to reach underlying soil at shallow depths, and all had been planted with banana trees. The numerous clumps of bananas scattered about the field of pāhoehoe indicated where a herd of elephants had perished in 1977.

Lava Flow Internal Structures

VESICLES

Vesicles are “frozen gas bubbles” preserved in solid lava (Fig. 6.38). They mostly form because of reduced pressure on the melt as magma ascends, but also in part due to the crystallization of minerals, which increases the percentage of volatiles in the remaining liquid to above saturation levels. Most gas bubbles begin forming in the magma prior to eruption, but many others form during eruptions, especially when molten lava ingests steam and gases from

Survival Tips for Field Volcanologists:

Sometimes it’s safer to walk directly on the surface of the advancing flow (assuming the crust is sufficiently thick and not too hot!) than to walk in the forest at the edge of an active flow. Methane blasts can occur many hours after the advancing flow has come to rest.

Fig. 6.34 “Lava tree” formed during the July, 1974 eruption of Kīlauea volcano, Hawai‘i. These lava trees are about 3 m high, and indicate the thickness of the lava flow that surrounded the trees, before the molten flow interior drained away downslope and the crust subsided to the present level. Photo by J. P. Lockwood.

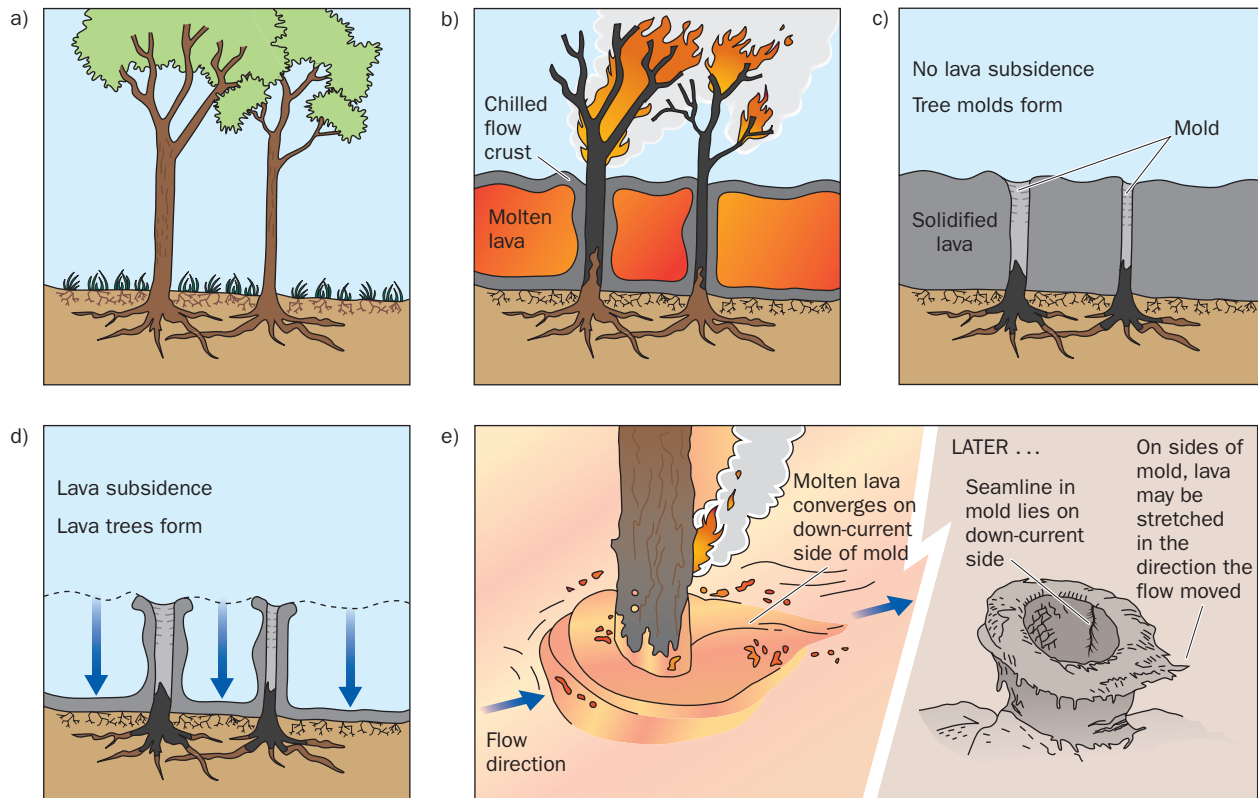


Fig. 6.35 A pristine forest (a) is entered by lava (b), The lava subsequently chills around tree trunks, leaving deep molds (c); or, if after chilling, the lava recedes (d), it creates standing hollow pillars called lava trees. Lava trees and tree molds both can preserve seamlines (e) that serve as indicators of original flow direction.

overridden water bodies or vegetation. In thicker, lower viscosity flows the bubbles rise buoyantly, resulting in the concentration of vesicles in upper parts of flows. This may be useful for distinguishing flow top directions in deformed older terrains (Sahagian 1985). Thin flows cool too quickly to allow much movement of the bubbles, and are commonly quite uniformly vesicular throughout.

Vesicles vary widely in shape, size, and distribution within flows (Figs. 6.38, 6.39). Spherical to spheroidal vesicles are most typical of pāhoehoe, whereas sub-angular to angular vesicles are more typical of `a`ā flows, where high viscosity during the final stages of flow motion twists and distorts them. The sizes of vesicles range from sub millimeter to large voids tens of centimeters across. Rarely, nearly spherical vesicles up to 30-cm across are found with walls that are botryoidal (smoothly lumpy in a manner resembling a bunch of grapes), sometimes with small, sharp seams of lava projecting into cavities.

Ingestion of steam from moist earth or water below pāhoehoe flows commonly results in linear or roughly cylindrical groups of vesicles extending up into the lava from flow bases. Small tubular voids, known as **pipe vesicles**, can also form, usually less than a centimeter in diameter and projecting upward several centimeters to a couple of meters into the flow. The upper ends of pipe vesicles commonly are bent downslope in the direction of flow movement (Fig. 6.38). Where the lower skin of the flow is glassy and impermeable, the steam may burst upward into the overlying fluid lava explosively, creating an irregular cylindrical opening called a **spiracle**. These range in size from a few mm up to 10 cm in diameter. Generally, they terminate within the body of the flow, but in the Pedragal lava flow on the outskirts of Mexico City some of them pass entirely through the flow and are more than 30 m in vertical length. Mud from the underlying ground surface is in places carried up into the spiracle by the rising steam.

Gases and aerosols trapped in vesicles during cooling eventually diffuse through microcracks in the solid rock. Before dissipating, however, some sublimate minerals may



Fig. 6.36 Imprint of palm frond and other plant remains at the base of a 4000-year-old pāhoehoe flow, Hilina Pali, Kīlauea volcano, Hawai'i. Photo by J. P. Lockwood.



Fig. 6.37 (right) Bone-filled elephant cast in 1977 pāhoehoe near the base of Nyiragongo volcano, Democratic Republic of Congo. This pygmy elephant was about 2 m long. Note the mold of the elephant's trunk at the top of the photo. Photo by Katia Krafft.

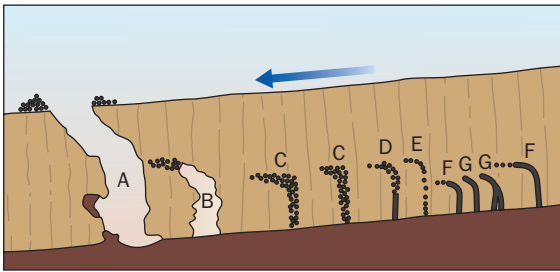


Fig. 6.38 Cross section showing the various kinds of vesicles that may be found within a lava flow: (A) A large spiracle, or “mega-vesicle” blasted completely through the flow to its surface, with some underlying sedimentary material scooped up and included; (B) a spiracle passing into a vesicle cylinder; (C) vesicle cylinders; (D) a pipe vesicle terminating upward in a vesicle cylinder; (E) a vesicle train; (F) pipe vesicles passing into vesicle trains; and (G) pipe vesicles. (C) to (G) are proportionally exaggerated in comparison to the spiracles. Figure and caption modified from Macdonald (1972).

be deposited on vesicle walls, commonly light-colored needle-like zeolites. Zeolite precipitation often commences even before an eruption ends, and may continue for days or weeks following. On a somewhat longer timeline, hydrothermal solutions percolating through the rock readily accumulate within vesicles, where they slowly precipitate their cargo of dissolved mineral matter derived from the breakdown of minerals along their paths of ascent. Many vesicles fill up completely with hydrothermally precipitated mineral matter forming masses known as **amygdules** (from the resemblance in shape of many of them to almonds).

JOINTS

Almost all lava flows are cut by cracks known as **joints**. Joints have several different origins. In older flows most represent tectonic deformation of the earth’s crust, mass wasting, or weathering long after their eruption. But those in younger flows originate almost entirely during flow emplacement. Joints parallel to the tops and bottoms of flows due to shearing during movement may be readily visible in outcrops (Fig. 6.40). They generally develop

as lava continues to deform for a short time after the viscosity becomes too high to sustain liquid or plastic flow.

Columnar joints are the most spectacular examples of emplacement related flow jointing (Figs. 6.41, 6.42). As lava flows cool, they shrink, setting up tremendous internal stresses. The most prominent joints form at approximately right angles to cooling surfaces, which are usually the tops or bottoms of flows but may be on sides as well, as for example where a flow cools against the wall of a former river canyon or gorge. The joints tend to develop in three directions at roughly 60° to each other and form multi-sided columns. The columns commonly are hexagonal in cross section, but range from four- to eight-sided.

Cooling surfaces commonly generate their own sets of columnar joints, which work their way stepwise into slowly solidifying flow interiors of all but the thinnest of lava flows. Over a period

Fig. 6.39 Shapes of vesicles in *ʻaʻā* and pāhoehoe. a) Typical subrounded to spherical vesicles in pāhoehoe lava. b) Typical angular and subangular vesicles in *ʻaʻā* lava. Note cognate xenolith near knife – such “ghost xenoliths” represent fragments of associated, earlier-cooled lavas that have been incorporated in younger molten material during flowage. Photos by J. P. Lockwood.



a)



b)

of days, weeks, or months (depending upon the thickness of flows), joint sets propagating from opposite cooling surfaces may meet to form single, through-going columns. Extension begins as stress builds up at the tip end of a partly developed joint, followed by sudden fracturing of the rock a few centimeters farther inside. The rock is momentarily relaxed after each spasm of propagation, but tension readily begins to accumulate with ongoing cooling until the breaking point once again is reached. The cyclical nature of this process results in paneled joint surfaces (Ryan & Sammis 1978). Where exposed by later erosion, the face of each panel typically features a feathery structure, termed a **plumose pattern**, the fine lines of which spread apart in the direction the panel opened over a period of microseconds and terminate in sharp, wedge-shaped edges termed **hackles** – the line of inception of fresh cracking (Pollard & Aydin 1988).

The episodic growth of columnar joints in cooling flows generates shock waves that may be heard as muffled “cracking” sounds at flow surfaces. That the downward growth of one column ultimately perfectly matches the upward growth of another growing from below testifies remarkably to the fact that both sets of columns are responding to a common field of tensional stress. During the 1970s, seismometers operated on the surface of Kīlauea Iki lava lake recorded the development of cooling joints and other cooling-related microearthquakes.

Flood basalt lava flows a few tens of meters or more thick commonly develop multiple tiers of cooling columns (Fig. 6.43). Above a thin basal zone with poorly developed inconspicuous jointing comes a zone with well-developed vertical columns from less than a meter to as much

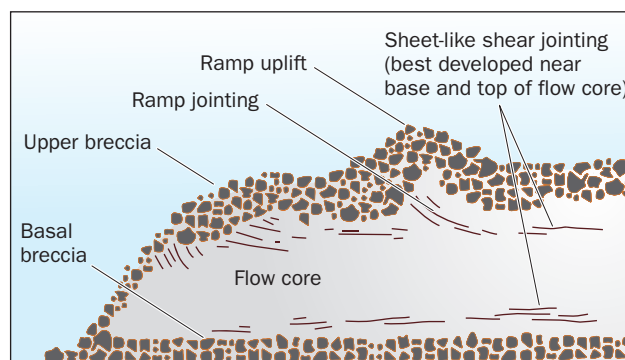


Fig. 6.40 Shear-related jointing in cooling `a`ā flows.

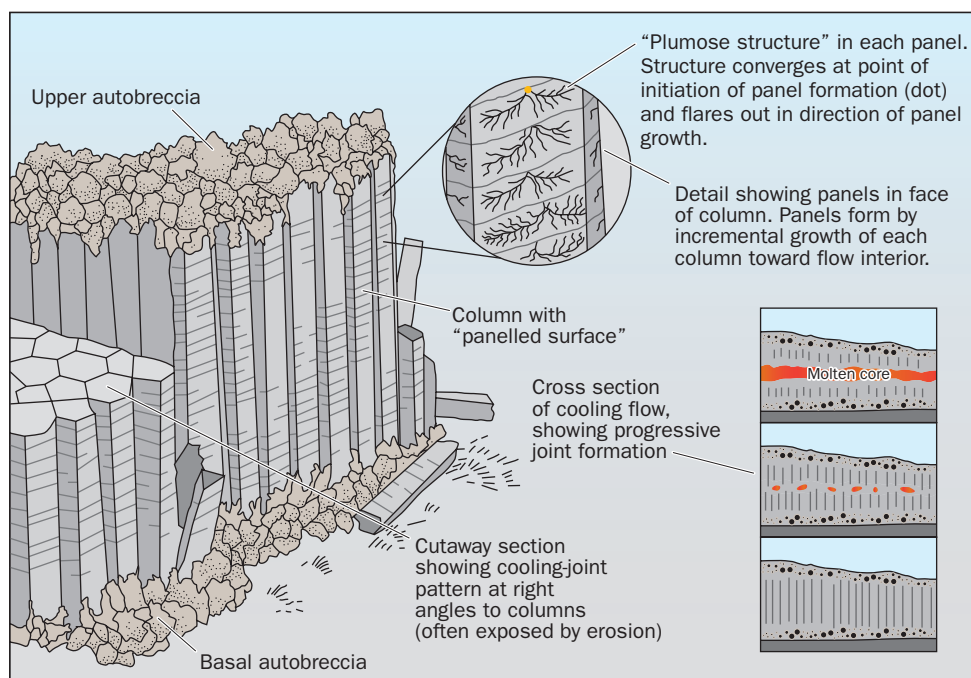


Fig. 6.41 Columnar jointing in an `a`ā flow. (Similar jointing forms as thick pāhoehoe flows and lava lakes cool.)

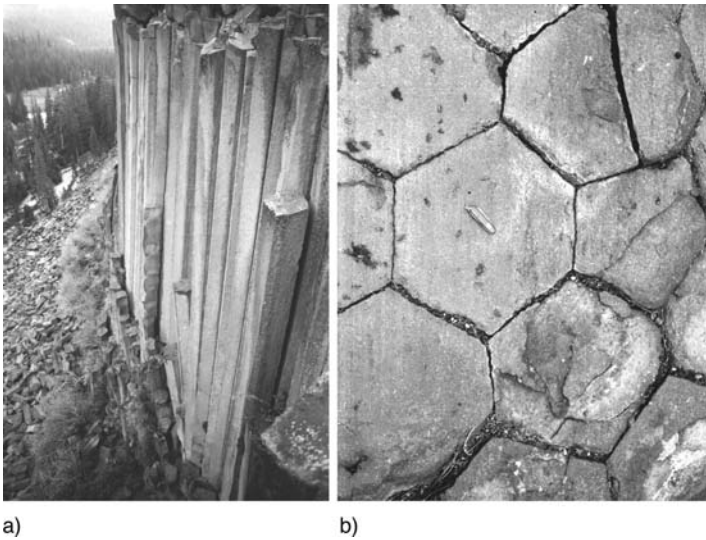


Fig. 6.42 Devil's Postpile National Monument, California. A late Quaternary lava flow was impounded along the Middle Fork of the San Joaquin River and cooled very slowly, forming well-preserved columnar jointing along its base. Subsequent glacial erosion removed overlying parts of this flow, providing excellent exposures of the columns. a) 15 m-high columns. b) Glacially polished cross-section of typical columns. Most columns are 6-sided, but 4-, 5-, and 7-sided columns are also present. Photos by J. P. Lockwood.

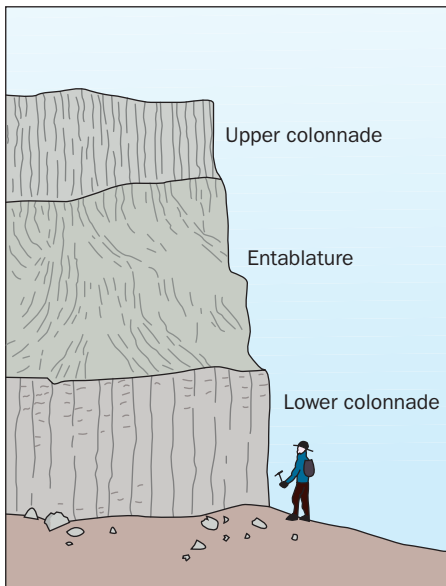


Fig. 6.43 Idealized flood basalt cooling joint pattern.

accumulates as a **basal breccia** pad, matching in general appearance the surface breccia layer above, with the flow core sandwiched in between. Though not a perfect analog, the moving tracks of a caterpillar tractor provide a useful image of the overall process

as 20 m long known as the **lower colonnade**. Lower colonnades commonly encompass the basal 10–30 percent of an especially thick flow. Next upward comes a zone in which the columns are much narrower and commonly have a variety of orientations, in some places forming fan-like rosettes or chevron-like structures. This zone is known, using another architectural term, as the **entablature** (Tomkeieff 1940). Entablatures in many flows make up as much as 60 percent of the flow mass. At the top of the flow comes a thinner zone, the **upper colonnade**, in which the columns are again wide but much less perfectly developed (Fig. 6.44). In some flows, entablature is lacking, and in others there may be multiple sets of entablature and colonnade jointing present.

ʻAʻā Surface Structures

ʻAʻā flows are characterized by exceedingly rough, rubbly surfaces, in contrast to the relatively smooth surfaces of pāhoehoe flows. These surfaces consist of loose, angular, jagged fragments, many of which may be covered with tiny sharp spines. Vicious-looking angular spires of ʻaʻā may project above flow surfaces (Fig. 6.45). ʻAʻā is commonly extremely difficult to cross without losing balance; leather gloves are well-advised, as falling can lead to some serious scrapes and cuts. It is difficult to convey with words an adequate idea of the roughness of a typical ʻaʻā flow. It must be seen and walked on to be appreciated fully. Gordon Macdonald (1972) described the perils of ʻaʻā well, when he wrote:

While mapping the active Hawaiian volcanoes, we had to cross and recross many kilometers of ʻaʻā. The loose fragments rolled under our feet and we fell frequently. Repeated lacerations of our hands soon taught us to wear gloves, and heavy work boots were often cut to ribbons in a week of hiking.

An ʻaʻā flow advances as the draining molten **flow core** in its interior overrides clinkery rubble shed from an oversteepening flow front. The rubble, which is termed **autobreccia**, originates as the lava surface chills and tears itself to shreds as it cools. Where overridden, the rubble



Fig. 6.44 Wanapum Basalt flows in the Columbia River Series at Palouse Falls State Park, Washington. The base of the 50 m thick upper cliff face (Frenchman Springs Member) shows a lower colonnade with a middle zone of entablature and a crudely developed upper colonnade. Photo by R. W. Hazlett.

(Fig. 6.46). Because of their higher relative viscosities, active flows may seem unimpressive as they advance very slowly across flat terrain. There may be little obvious movement of the flow, other than episodic cascades of lava fragments down the frontal face of a large, thick flow. Their molten interiors are mostly masked during the daytime by their overlying carapace of dark fragmentary material. At night, however, their appearance changes dramatically, as illustrated by another quote from Gordon Macdonald (1972) describing the movement of a large flow from Mauna Loa's Southwest Rift Zone in 1950:

The rate of advance was only about 30–40 feet an hour. The flow front, 50 feet high and half a mile broad, was a steep bank of reddish-brown to black clinkery rock buried by a heap of clinkery fragments that was accumulating at its base. For short periods it was quite motionless and appeared dead, except for small amounts of sulfurous fume and the peculiar odor of hot iron, resembling that of a foundry, that characterizes active basaltic lava flows. An incessant grating and cracking noise resulted from the shrinking and shifting of blocks on the flow surface and an occasional boulder tumbling down the flow front. At night, myriad red “eyes” glared out through holes in the dark cooler cover. During such quiet times, the amount of heat radiating from the flow was so small that it was possible to go right up to the flow front, and even climb part way up it. The upper molten mass of the flow interior moved more rapidly than the lower part, which was cooling and growing rigid against the ground. As a result, the flow front grew gradually steeper until eventually it became unstable at some point and a chunk of the dark clinkery rock began to separate from the mass of the flow behind it. Sometimes blocks leaned slowly forward as the crack behind it grew wider, until finally it tore free and tumbled down the slope. At other times they started to slowly slide forward and downward along the forward edge of the flow – buoyed by unseen molten lava beneath. From



Fig. 6.45 Spiny `a`ā surface of 1999 Mt Cameroon lava flow, Cameroon. Photo by J.-B. Katarawa.

the brightly glowing edge of the separation plane little streams of red-hot sand trickled down, formed apparently by the crushing and granulation of the incandescent lava. Eventually, the separation of the block became complete, and it also tumbled down the steep flow front. The surface left on the lava mass by the blocks separating from it glowed a bright orange-red with a temperature estimated to be about 900°C. The blocks also, where they broke open as they tumbled down, were brightly incandescent on the inside, but when the growing surface was exposed to the air, it cooled quickly and became darker, and within less than a minute most of them had become completely black. Yet, when a corner of such a block was knocked off with a hammer, the inside often was still cherry red a few millimeters below the surface. This illustrates well the low heat conductivity of the lava. The process of collapse was repeated over and over again all along the flow front, fragments rolling down to add to the bank of loose material at its foot. At the same time the middle and upper parts of the flow crept almost imperceptibly forward. The main mass of the flow was a very viscous paste-like material, so viscous that it was impossible to push anything into it, but still sufficiently fluid to flow. As it oozed forward it carried along on its back a cover of clinkery blocks, and at the same time it buried the fragments that had been accumulating at the foot of the flow front. A pall of reddish-brown dust hovered over the advancing flow.

Another excellent description of a faster-moving `a`ā flow was made by Sir William Hamilton, British ambassador to the Kingdom of Naples, in his account of the March-April 1766 Vesuvius eruption (quoted in Phillip, 1869, pp 70–1):

The lava had the appearance of a river of red-hot and liquid metal, such as we see in the glass-houses, on which were large floating cinders, half-lighted, and rolling one over another with great precipitation down the side of the mountain, forming a most beautiful and uncommon cascade. [...] It flowed like a torrent, with violent explosions and earth-shakings; the heat was such as to forbid a nearer approach than 10 feet. It ran with amazing velocity in the first mile, with a rapidity equal to that of the river Severn at the passage near Bristol. [...] The lava began to collect cinders, stones, &c, and a scum was formed on its surface, so that the whole appearance was like that of the river Thames, after a hard frost and great fall of snow, when beginning to thaw, carrying down vast amounts of snow and ice. The lower end of the current was covered with red-hot stones, a kind of wall 10 or 12 feet high, which rolled on irregularly and slowly about 30 feet in an hour.

As in pāhoehoe flows, central feeder channels and even rare pyroclasts may form in `a`ā. But `a`ā flows lack the complex distributary pyroclasts characteristic of pāhoehoe (Fig. 6.47),

and the central channels seen on the surfaces of some, if not all `a`a flows are only the exposed crests of broader molten flow cores (Fig. 6.48). Lipman and Banks (1987) provided evidence of this relationship while studying an `a`a flow during the 1984 Mauna Loa eruption. They observed that as surges of lava traveled down the channel, the margins of the flow to either side swelled up as much as a meter or more. When the surge passed and the level of the molten lava in the channel dropped, the flow margins settled back down as well.

In contrast to slow-moving `a`a, the front of a fast moving `a`a flow, is almost continuously on the move, with an on-going shower of tumbling fragments which are noisily buried as the flow advances. The faster advance of such flows may be caused by a steeper underlying slope, by a higher temperature (and thus lower viscosity) of the molten core, or by higher supply rates of new lava. `A`a flows have been observed moving as fast as 2 km/hr down steep slopes, even faster than ordinary pāhoehoe flows (Figure 6.49). Even by daylight, incandescence is conspicuous at the restless snouts of these flows.

The radiant heat output of fast moving `a`a flows is much higher than it is for pāhoehoe, because flowing pāhoehoe will be largely covered with plates of non-incandescent crust, whereas such heat-shielding crusts may not form on the `a`a.

I (JPL) learned this dramatically on a pre-dawn morning flight with Donald Peterson (then Scientist-in-Charge at HVO) over Mauna Loa during the brief but spectacular 5 July, 1975 eruption:

We were flying over a very active `a`a flow that was cascading down Mauna Loa's north flank. The entire flow was incandescent and radiating heat energy. We were over a kilometer above and to the upwind side of the fast moving (500 m/hr) `a`a flow, and I sensed no danger. The night air was cool (2°C on my Outside Air Temperature gauge), when suddenly I noticed "water" dripping off our wings. The "water" turned out to be paint, and we left that area very quickly! On landing we found that dark paint on the plane had blistered and we had burned several small holes in the fabric-covered wings. At the time we were unaware of Stefan's Law, which states that radiant heat transfer is proportional to temperature to the fourth power.

$$Q = nT^4 \quad (5.2)$$

where Q is the rate of radiant heat release. T is the temperature of the surface releasing the heat, and n is a constant.

Stefan's Law means that even a small increase in the temperature of a radiative surface will lead to a very great increase in the amount of heat released. A highly incandescent lava flow can heat objects above them far more than one which is even slightly less incandescent. Dark paint is a better "black-body" than light paint – so absorbed more radiant energy and blistered.

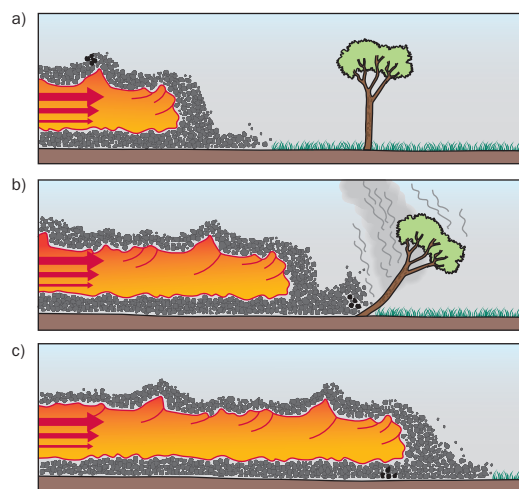


Fig. 6.46 An `a`a flow buries its own surface rubble as it advances. Note the changing position of some "reference blocks" (black) as they tumble over the flow front and are buried as the flow advances – propelled by the fluid lava within.

Survival Tips for Field Volcanologists:

The ends of young `a`a flows are commonly hazardous places to climb, because the clinkery rubble here is generally loose and unconnected to interior solid portions of the flow. The middle and near-vent sides of these flows are generally much safer places to climb to flow tops, because the flows are thinner, and the fragments are commonly welded to one another or to the interior portions of the flows.



Fig. 6.47 `A`ā flows descending down the east flank of Piton de la Fournaise volcano, Reunion Island in 2005. Note the well defined central feeding channels – typical for `a`ā flowing on steep slopes. Photo © Paul Edouard Bernard De Lajartre.

shorter, and move much more slowly than the basalt flows erupted from oceanic volcanoes. Whereas a typical pāhoehoe flow may be hundreds or thousands of times longer than it is thick, a rhyolite or dacite flow may be only ten or a hundred times so. Many volcanologists in English-speaking countries term such fattened, high-silica flows **coulees**. But this word, which simply means “flow” in French, is applied to *all* compositions of lava in French-speaking parts of the world, so its use internationally has potential for confusion. The high viscosity of siliceous flows gives them steep flow fronts commonly over a hundred meters high – an order of magnitude greater than typical basaltic `a`ā flows. Dacite block lava flows in Crater Lake National Park, Oregon, approach 400 m in thickness! High-silica flows rarely extend more than a few kilometers from their vents, though there are some spectacular exceptions.

Block Lavas

`A`ā fragments come in many shapes, ranging from rounded to angular to platy. Some are spiny and rough, and some are bounded by smooth fractures and are called **block lavas** (Fig. 6.50). Macdonald (1972) and other authors consider block lavas to be an entirely separate category of flow distinct from pāhoehoe and `a`ā. Spiny fragments can be found in some block lava flows, however, and some smooth blocks can be found in many spiny `a`ā flows. Many flows consisting of conventional spiny `a`ā throughout most of their length become blocky near their distal ends. Because of the gradations between all `a`ā types we will here consider block lava flows to be an `a`ā textural variant, reflecting somewhat higher viscosity during fragmentation than typical spiny `a`ā. Block lavas are characteristic of basaltic andesites and silicic lava flows, and are commonly associated with flows emanating from domes (Table 6.1). They generally contain a larger amount of autobreccia relative to their solid cores than do spiny `a`ā flows and blocks tend to be notably less vesicular.

SILICEOUS LAVA FLOWS

Because of their higher viscosities (Fig. 6.51), siliceous lavas typical of flows erupted from many continental volcanoes are thicker,



Fig. 6.48 Prehistoric aa flow cross section, Mauna Kea volcano, Hawai'i. Note the fragmental aa above and below the central core. Because atmospheric oxygen is present beneath cooling aa flows, underlying soils are commonly oxidized to a brick-red color (arrow). Photo by J. P. Lockwood.



Fig. 6.49 Rapidly advancing aa flow in Royal Gardens, Hawai'i – 1983. The flow, about 4 m thick is advancing at about 200 m/hr down the road surface. An accretionary lava ball is being pushed along in front of the flow. Photo by Ben Talai.

Fig. 6.50 Basaltic andesite block lava flow on the flank of Pleistocene Brown Mountain volcano, near Fish Lake, southern Oregon. The thickness of the flow ranges up to approximately 75 m. Photo by Stanley Mertzman.



The Elephant Back rhyolite flow in Yellowstone National Park, for instance, is 16 km in length (Christiansen 2001), and some rhyolite flows in neighboring Idaho comprise as much as 200 km³ of lava (Bonnichsen & Kaufmann 1987).

The surface of a typical high-silica flow commonly wrinkles into ridges and troughs, termed **ogives** (similar to the ogives on glaciers), with amplitudes of 10–20 m or more (Fig. 6.52). The ogives result from the freezing of the flow front while melt continues to drain from the vent. Compression forces the surface of the flow near its terminus to buckle and warp as the additional flow mass accumulates behind the stagnated, dam-like flow terminus. In this sense, then, ogive formation is analogous to the late-stage inflation of pāhoehoe flows. Near the vent, movement of the center of the flow often continues after consolidation of the flow margins, forming **levees** as the level of the flow upslope subsides with spreading of the lava downslope. Spines may puncture the flow surface in many places, especially near the vent, which may be marked by a towering lava dome. Blast pits, too, commonly pock mark the flow top, as the flow explosively releases pent-up gases.

SILICEOUS GLASS

Siliceous lava flows tend to be quite glassy, and many rhyolite flows consist almost entirely of glass. This is because the high viscosity of siliceous melts suppresses the diffusion of ions

and growth of microlites as degassing occurs prior to eruption. The most common type of high-silica volcanic glass is **obsidian**, a typically black, commonly bubble-free glass that readily fractures to develop conchoidally-ribbed surfaces. **Vitrophyre** is a phenocryst-rich variety of obsidian. Knapped obsidian was a favorite source of arrowheads and spear points in early cultures worldwide. Many late prehistoric trade systems, notably in western North America and the Middle East, grew around the use of this material. The glass is brittle enough to flake and shape using horn, bone or shell fragments. Although most obsidian is black, it occurs in many colored as well as transparent forms. Iron oxidation during late-stage flow and cooling may lead to red-brown colored glass (**mahagoni obsidian**) that occurs in stand-alone masses or as streaks and patches embedded in ordinary black obsidian. The compositions of obsidian range from high-silica dacite to rhyolite. The darkness of obsidian arises primarily from the iron, and to a lesser extent the magnesium content of the magma.

Many obsidian bodies contain **spherulites**, which are spheres of radiating fibrous or needle-like, microscopically fine crystals (Fig. 6.53) from only a few millimeters to over a centimeter in diameter. They result from the nucleation and incipient growth of crystals in solid obsidian developing at close to the minimal cooling rate for glass formation (Lofgren 1971). Melts quenched more rapidly will not become spherulitic. The minerals making up spherulites are commonly forms of high-temperature, low-pressure silica such as tridymite and cristobalite, plus more ordinary quartz and alkali feldspar (especially adularia) – the last minerals to crystallize in Bowen's Reaction Series. Feldspar may be the only mineral present in some spherulites.

In some samples of obsidian, large, spheroidal bubbles up to several centimeters across, perhaps coalesced vesicles unable to escape the magma, are retained and lined with microscopic crystals through gas sublimation to form light-grey **lithophysae** (Fig. 6.53). Some of these bubbles may remain mineral free. Small vesicles are typically not present in obsidian, because the quenching process inhibits exsolution.



Fig. 6.51 Edge of the thousand-year-old Glass Mountain rhyolite flow, Medicine Lake volcano, northern California. The steepness of the flow margin is indicative of the great viscosity of the lava as it erupted. Photo by R. W. Hazlett.

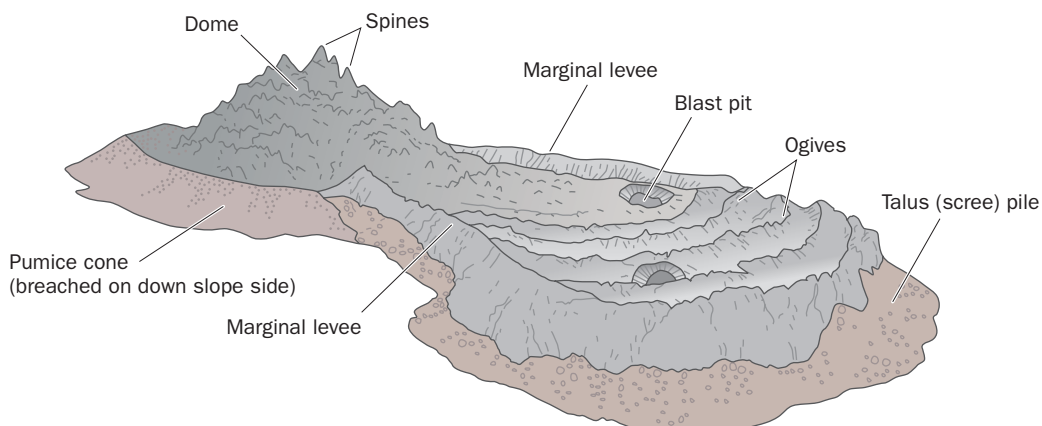


Fig. 6.52 Typical features of a high-silica (rhyolite or dacite) lava flow.

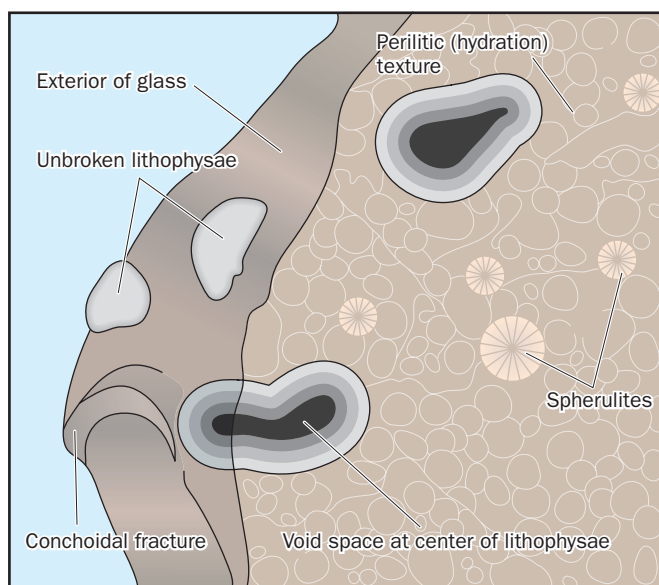


Fig. 6.53 A sketch of spherulites, lithophysae and perilitic texture in obsidian. Features are shown at natural scale, though perilitic fractures and spherulites may be microscopically fine.

Radiocarbon Dating of Prehistoric Lava Flows

Understanding a volcano's past history is critical for an evaluation of future volcanic hazards and risk. Prior to the 1940s, however, no accurate method existed for dating prehistoric eruptions less than a few hundred thousand years. Then, Willard Libby at the University of Chicago developed a technique for age determinations that involved the natural radioactive decay of ^{14}C , an isotope of carbon. Libby received the Nobel Prize for his revolutionary research.

Radiogenic isotope ^{14}C continuously forms as solar radiation interacts with nitrogen gas high in earth's atmosphere. Incident solar neutrons break nitrogen atoms, the most common substance in air, into ^{14}C and hydrogen

atoms. Although the ^{14}C atoms are constantly decaying, their replenishment results in a semi-constant atmospheric ratio of ^{14}C to other, more common carbon isotopes (^{13}C and ^{12}C). When an organism is alive, the carbon in its tissues reflects this ratio, but upon death radioactive decay lowers that ratio at a constant rate. Libby identified the decay rate for ^{14}C (half-life: 5730 \pm 40 years), which allowed the calculation of time elapsed since death based upon the proportions of carbon isotopes. Radiocarbon dating of carbonaceous material preserved beneath lava flows or within pyroclastic flows is the principal means of dating eruptions less than 40,000 years old.

When organic material is buried by molten lava, the heat rapidly distills off volatile components and all vegetable matter is usually burned quickly to ash – no carbonaceous material remains. In reducing environments, however, where access to atmospheric oxygen is restricted, elemental carbon (charcoal) may be formed and preserved. Charcoal can also form slowly at lower temperatures, and cannot be “burned” to ash at temperatures lower than about 500°C. Because of complete burning, above-ground vegetation is rarely preserved beneath lava flows,

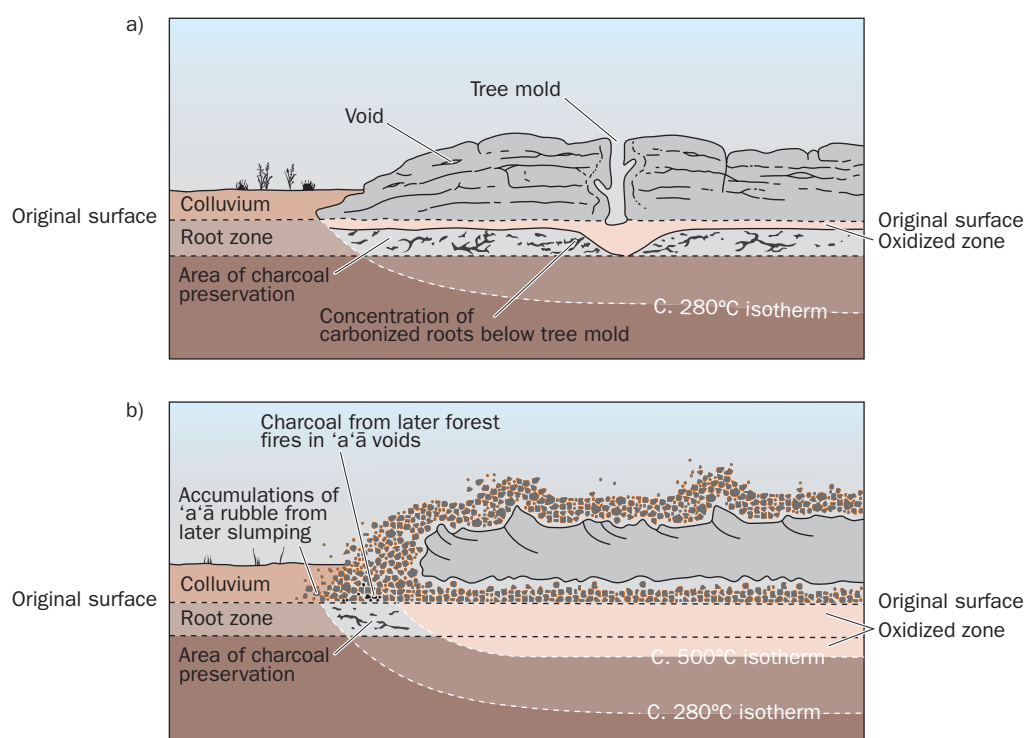


Fig. 6.54 Sketch showing preservation environment for charcoal beneath a) pāhoehoe and b) `a`ā flows. Note that charcoal may be preserved anywhere beneath pāhoehoe flows where oxygen circulation is limited, but only beneath the margins of `a`ā flows – in areas where temperatures did not reach the combustion temperatures for charcoal. From Lockwood and Lipman (1980).

but carbonized plant rootlets may be present in soils beneath these flows. Such carbonized rootlets can be found beneath any parts of pāhoehoe flows, as the impermeable pāhoehoe cover commonly prevents the atmospheric oxygen circulation required for complete combustion of buried organic matter. In contrast, the high permeability at the bases of `a`ā flows usually permits the circulation of atmospheric oxygen, and results in the complete combustion of charcoal to ash residue. Carbonaceous material can best be collected beneath the margins of `a`ā flows (Fig. 6.54), where heat from the cooling lava was high enough to form charcoal, but not high enough to burn it completely away (Lockwood & Lipman 1980). Charcoal may also be preserved in pyroclastic density current deposits (Chapter 7; Fig. 8.20b), where trees are swept up and carbonized in the hot ash.

FURTHER READING

- Hon, K., Gansecki, C. and Johnson, J. (2000) *Lava Flows and Lava Tubes: What They Are, How They Form*, DVD, Volcano Video Productions, Volcano Hawai`i, 75 minutes.
- Lewis, G. B. and Bernard de Lajartre, P. E. (2007) *Red Volcanoes: Face to Face with Mountains of Fire*. New York, Thames and Hudson, 144 p.
- Manga, M. and Ventura, G. (2005) "Kinematics and dynamics of lava flows." Geological Society of America Special Paper 396, 218 p.
- Shackley, M. S. (2005) *Obsidian: Geology and Archaeology in the North American Southwest*. Tucson, University of Arizona Press, 264 p.

Chapter 6

Questions for Thought, Study, and Discussion

- 1 What aspects of eruptive behavior distinguish Hawaiian from Strombolian eruptions, and why do these two eruptive styles differ, even when erupting compositionally identical material?
- 2 What generally determines where a pāhoehoe flow will deflate or inflate?
- 3 What is the role of pyroclasts in the spreading of pāhoehoe and the building of volcanic landforms?
- 4 Why should the ground around the margins of active lava flows be avoided in forests?
- 5 How are tree molds and hollow lava trees useful flow direction indicators?
- 6 What textures would allow you to distinguish in cross-section a typical pāhoehoe flow, an a`ā flow, a high-silica rhyolite flow, and a flood basalt flow?
- 7 What primary physico-chemical factor accounts for the difference in the various kinds of siliceous volcanic glass?
- 8 Why is the presence of datable charcoal so much more widespread beneath pāhoehoe flows than it is beneath a`ā and blocky flows?

Chapter 7

An Overview of Explosive Eruptions and Their Products

He looketh on the earth, and it trembleth: he toucheth the hills, and they smoke.
(Psalm 104:32)

Volcanic explosions differ greatly from chemical or nuclear ones – which involve complex changes in molecular or atomic structure. Volcanic explosions are much simpler – they are all due to the expansion of volatiles, as liquids convert to gaseous state. The most important volatile to consider is H₂O – which expands some 1600 times in volume as water converts to steam (at atmospheric pressure), and is the driving force for most types of volcanic explosions. Carbon dioxide is another important driver for some volcanic explosions – but only increases in volume about half as much as water when converting from fluid to gas. This chapter will focus primarily on the *products* of explosive eruptions; the focus of the next chapter will be on the *processes* that form these products.

Whereas the red volcanoes described in the preceding chapter dominantly produce lava flows during typical eruptions, the grey volcanoes are characterized by the production of immense volumes of pyroclastic material that can blanket thousands of square kilometers surrounding and downwind from these volcanoes. The dominant eruptive products (by volume) during explosive eruptions are the gases that drive explosions (Chapter 3), but only the ejected ash and rocks remain behind to record such activity. Accordingly, we will begin this chapter with a discussion of **ejecta** – the various kinds of materials that can be blasted out of volcanoes by gases – especially during early phases of long-lived eruptions, then will focus on the various

Volcanoes: Global Perspectives, 1st edition. By John P. Lockwood and Richard W. Hazlett. Published by Blackwell Publishing Ltd.

sorts of explosive eruptions that produce these materials. Potentially deadly pyroclastic flows and surges (pyroclastic density currents – PDCs) can be produced by different types of explosive eruptions, and will be briefly reviewed at the end of the chapter.

Ejecta Classification

Volcanic explosions produce fragmentary debris; everything from large, house-size boulders to finely crushed rock material, and to magma explosively sprayed into a mist of molten droplets and fragmentary glass and crystals. **Ejecta** is a catch all term for anything blasted out of the craters of an exploding volcano. The word is used in both a singular and a plural sense, probably improperly. (The singular is **ejectum**, but it rarely appears in volcanological literature). Synonyms include **pyroclasts** and **pyroclastic material**. The term “pyroclast” derives from Greek and Latin roots meaning “fire-broken” rock. The term **tephra** describes airfall ejecta.

Volcanic ejecta may be classified in different ways – by their sources, modes of emplacement, general compositions, sizes, shapes, or by the degree of post-depositional consolidation. The different classification systems are useful for different purposes. Considering them first from the standpoint of source, H. J. Johnston-Lavis in 1885 proposed the following classification, still in use today: **Juvenile (essential) ejecta** are derived directly from molten magma, although the magma may have solidified first before fragmenting – for example by forming a crust across a pool of periodically bursting lava in the crater of a volcano. Since magma-derived bombs are thrown out in a molten condition and cooled rapidly in the air or on the surface of the ground, they are partly or entirely glassy (**vitric**). **Accessory (cognate) ejecta** are older volcanic rock fragments that were formed within the same volcano. Some accessory ejecta are coarsely crystalline, formed from parts of magma bodies that crystallize at depth, in part as minor intrusions within the volcano, and perhaps in part on the outer edges of magma chambers. Accessory ejecta may be torn from the walls of the conduit by gases during explosive discharge, or may be floated upward in the rising magma and explosively blown free at the surface. Fragments of non-volcanic rocks or of non-related volcanic rocks are called **accidental ejecta**. Such fragments typically show some evidence of thermal metamorphism owing to the great heat imparted to surrounding rocks through the walls of the volcanic conduit. Limestone fragments, for example, may be recrystallized to marble, a common metamorphic rock, and silicate rocks converted to a dense, dark material called **hornfels**. Hydrothermal solutions also commonly alter older wall rocks, and hydrothermally altered lithic fragments are very common around some vents.

Because the various kinds of ejecta may be difficult to classify without detailed microscopic and chemical studies (especially when it comes to comparing accidental with accessory fragments), volcanologists often simply refer to glassy ejecta as **vitric**, and all nonglassy ejecta as **lithic** – regardless of genesis.

The most widely used and useful classification of ejecta is that based on fragment size, which is easily measured in the field for larger particles, or by laboratory sieving for finer material. The sizes of clasts in volcanic deposits of all types are measured directly in millimeters (mm), but are commonly plotted according to their ‘**phi (ϕ) numbers**’ – a shorthand for grain size ranges used by sedimentologists. In addition to grain size, volcanic ash can be further

TABLE 7.1 PARTICLE SIZE SCALE FOR VOLCANIC TEPHRA.

Volcanic Clast Name	<i>Blocks</i> (angular) <i>Bombs</i> (rounded)		<i>Lapilli</i>			<i>Coarse ash</i>				<i>Fine ash</i>				<i>Dust</i>			
ϕ No.	-8	-7	-6	-5	-4	-3	-2	-1	0	1	2	3	4	5	6	7	8
Maximum Diameter (mm)	256	128	64	32	16	8	4	2	1	0.5	0.25	0.125	0.062	0.031	0.016	0.008	0.004

Source: After Schmidt (1981).

classified through microscope study of ash composition (Table 7.1). Larger ejecta fragments can also be subdivided on the basis of their shapes, which reflects their physical condition at the time they were ejected (Fig. 7.1).

MODES OF EJECTA EMPLACEMENT

Ejecta may be emplaced *ballistically* (where horizontal forces are involved and fragments impact the ground at angles from vertical) or by vertical *fall* from overhead clouds (trajectories only influenced by gravity and prevailing winds). Finer-grained, lower density ejecta tends to be emplaced as fallout, while larger, higher density fragments are commonly emplaced ballistically. A ballistic particle is one that is thrown in an arc-like trajectory, like a ball tossed through the air, from a point of release to a point of impact (Fig. 7.2). Ballistic fragments are especially abundant (and dangerous) products of smaller explosive eruptions.

We use the terms **airfall**, **fallout**, or simply **fall** ejecta to describe pyroclastic material that spends time drifting in the air, generally windborne, before falling back to the surface. Ash and larger pyroclastic fragments that fall vertically to the ground from eruption clouds (without ballistic trajectories) is called **airfall**, **fallout** or simply **fall ejecta**. Resultant deposits are referred to as **tephra** (derived from the Greek word for ash), but that word can also include pyroclastic material emplaced by other means. The time spent adrift can range from minutes to days. More powerful volcanic explosions generate vast amounts of fall pyroclasts, but will throw out ballistic ejecta in the proximal areas of vents too. In general, finer, lower density ejecta, including ash, tends to be emplaced as fallout, while larger, higher density fragments are emplaced ballistically (Table 7.2).

Finally, substantial amounts of all types of ejecta may be deposited through the activity of PDCs, with most pyroclastic fragments spending little if any time passing through the open air at all.

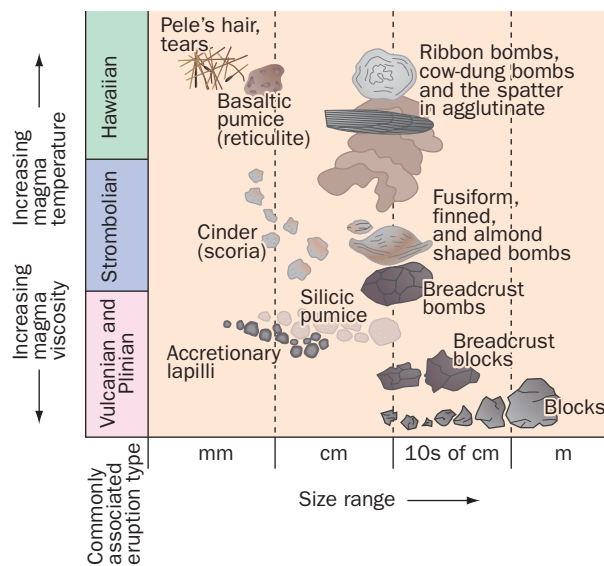


Fig. 7.1 Shapes and sizes of the different kinds of volcanic ejecta, as a function of eruptive conditions.

TABLE 7.2 RELATIONSHIP OF COMMON KINDS OF EJECTA (FIG. 7.1) TO MODES OF EMPLACEMENT.

Type of ejecta	Primary modes of emplacement
Ash	Fallout & PDC
Lapilli	(Depends on type of lapilli)
a) Accretionary lapilli	a) Fallout
b) Cinder (scoria)	b) Ballistic
c) Silicic pumice	c) Fallout and PDC
d) Reticulite, Pele's hair, Pele's tears	d) Fallout
Blocks	Ballistic and PDC
Bombs	Ballistic
Spatter agglutinate	Ballistic

A CLOSER LOOK AT BALLISTIC EJECTA

Recall from Chapter 6 that Hawaiian eruptions can be mildly explosive and generate prodigious amounts of glassy spatter that accumulates around vents to form agglutinated spatter cones and ramparts. In an episode of high fountaining, spatter may be thrown a couple of hundred meters from a vent, rarely further, with most of the ejecta falling much closer to vents.

Spatter can also erupt during some Strombolian eruptions, but ejecta mostly consists of cinder and larger **volcanic bombs**, which are viscous masses of lava ejected in fluid or plastic states. Bombs are commonly rounded sub-rounded or streamlined owing to travel through the air. Particular varieties, including **spindle** or **fusiform** bombs, are identified according to

Fig. 7.2 Night view of lava fountains showing ballistic trajectories of spatter bomb fragments, as a "littoral cone" formed at the south coast of Kīlauea volcano, Hawai'i – January, 1996. Fountains are about 20 m high – 10 sec. exposure. USGS photo by Carl Thornber.



their particular shapes (Fig. 7.3). Bombs range from less than a centimeter to over a meter in length. The fluidity of volcanic bombs varies greatly and is responsible for their shapes (Fig 7.4). Some land while still quite molten and will flatten out or shatter on impact. Others solidify before they reach the ground, and can burrow deeply into soft volcanic ash.

The fluid cores of bombs commonly contain high concentrations of gases that continue to exsolve after eruption, stretching and cracking their chilled crusts to create a characteristic **breadcrust texture** (Fig. 7.4). Some breadcrust bombs are deeply fractured, and some may completely disintegrate as they continue to expand after impact leaving a pile of rubble instead of a coherent bomb. Some will even accumulate enough gas pressure to explode in mid flight – and have been known to burst even hours after impact! Following the 1980 Vulcanian eruption



Fig. 7.3 Spindle bombs from prehistoric Strombolian eruptions on Mauna Kea volcano, Hawai'i, showing aerodynamically modified shapes as liquid lava traveled through the air before solidification and impact. The scale is 30 cm long. Photo by J. P. Lockwood.



(a)



(b)



(c)

Fig. 7.4 Ballistically emplaced lava bombs, showing effect of fluidity.

a) “Cow-pie” bomb formed as fluid spatter impacted the ground during a 1969 eruption of Kīlauea volcano, Hawai'i. b) Classic breadcrust bomb from the rim of Bolshoye Tol'batchik volcano, Kamchatka. This bomb, erupted in 1975, shows the crustal surface fracturing that occurred after impact as the bomb's fluid interior expanded. c) A more viscous breadcrust bomb that shattered from internal fracturing after impact on the rim of Gamalama volcano, Ternate Island, Indonesia. USGS photos by J. P. Lockwood.



Fig. 7.5 Large block ejected from Galunggung volcano [108] crater during a 1982 sub-Plinian eruptive phase. The block was thrown clear of the rising ash column and landed almost a kilometer from the crater rim – behind the observers! USGS photo by J. P. Lockwood.

of Gamalama volcano [107] in Indonesia, I (JPL) found craters caused by bomb impact blasts as far as two kilometers from the source vents. The rainforest had been shredded around these craters, leaving angular lava fragments driven into the trunks of surrounding trees.

Volcanic blocks are another form of ballistic ejecta, thrown out as solid, angular fragments of older rock. They are also usually of volcanic origin, plucked from the walls of the conduit or rim around a vent during an eruption, but may be fragments of non-volcanic rock from deeper sources. Some blocks are impressively large, as much as meters in diameter, and may be thrown hundreds of meters from violently exploding craters (Fig. 7.5).

Blocks are a “trademark” product of Vulcanian eruptions, although Strombolian and Plinian eruptions can produce them too. **Bomb sags** form where ejected blocks land and depress soft, underlying muddy ash layers (Fig. 7.6). Such structures (which despite their names are usually caused by falling **blocks**, not bombs) are especially common in muddy tephra deposits within a few hundred meters of vents, and may be expressed to depths of decimeters beneath points of impact.



Fig. 7.6 “Bomb sag” caused by impact of large block in wet tephra during formation of the prehistoric Laguna maar, Gamalama volcano, Ternate Island, Indonesia. USGS photo by J. P. Lockwood.

Concentrations of blocky rubble embedded in ash or other matrix material are termed **breccias**. Not all volcanic breccia clasts are necessarily ballistically ejected blocks, but may simply be rubble swept out of a vent by a PDC, or even result from collapse of a conduit or caldera wall during simultaneous deposition of pyroclastic material (see, e.g., Lipman 1976; Chapter 10).

A CLOSER LOOK AT FALL EJECTA

Pyroclastic fallout from an eruption cloud is a lot like falling snow – it will drape (**mantle**) a landscape to uniform depths over broad areas as it settles out, irrespective of the topography (Fig. 7.7). Such uniform blanketing contrasts with the variable thickness of PDC deposits, which accumulate on valley floors and in depressions, and are thinner on high-standing terrain. A bed of fallout ash may be as thick on a ridgeline as it is in an adjacent valley, though post-depositional slumping may thin layers on steep slopes, and wind can blow away the loose material from ridge crests and hilltops for months or years following an eruption. During tephra fall, strong winds may also affect the thickness of deposits around obstructions. Fallout beds gradually thin towards the distal areas of deposition, and isopach maps showing thicknesses of specific layers can be a valuable tool for identifying their sources (Chapter 5).



Survival Tips for Field Volcanologists

Approaching an active grey volcano (or any volcano with the potential for explosive behavior) requires special fieldgear. A strong hardhat is *essential*. Human skulls are quite fragile, and even small blocks falling from above can be lethal. Hardhats will also keep fine tephra out of your hair! Particle masks and eye protection are important to carry in one's field pack – when ash begins to fall you'll need them!

Fig. 7.7 Fallout scoria and ash deposits downwind from a prehistoric eruptive vent on Mauna Kea volcano, Hawai'i. Note the uniform thickness of individual layers, which mantle pre-existing topography – hallmarks of tephra deposits. Photo by J. P. Lockwood.

ASH

Volcanic ash is in no sense a product of burning, as are other “ashes.” It is simply pulverized or finely fragmented magmatic material, with individual grains less than 2 mm in diameter. The forces that cause this explosive fragmentation are poorly understood (Zimanowski et al. 2003). Like other forms of ejecta, ash particles may be essential, accessory, or accidental, and either solid or liquid when they are thrown out, though because of their small size the liquid ones cool and solidify very quickly. Sometimes, when the magma contains numerous crystals, the solid bits may be blown free of the melt to chill as **crystal ash**, each particle consisting of a single crystal or fragments of crystals with traces of adhering magmatic glass. Ash consisting of more than one type of material is customarily given a compound name: **vitric-crystal ash**, vitric-crystal-lithic ash, etc.

By far the most common variety of ash is vitric ash formed by the explosive disruption of liquid lava as gas expands in an open volcanic conduit. The gas exsolves to form a froth as the magma wells up from deep in the conduit, and as the bubbles continue to grow, the froth is literally torn apart as the molten rock approaches the surface. Some of the larger clots of froth remain as lumps of pumice, but most of it disintegrates to the point that all that remains are the septa separating individual bubbles, chilled to glass, and carried upward by the out-rushing column of gas. The shapes of the individual ash fragments clearly reveal their origin in the concave surfaces that once were the walls of bubbles. The curved and forked fragments of vitric ash are often referred to as **shards**. Some shards may be lightly coated with glass, suggesting that they were immersed again in molten material before being ejected for a final time.

Ash and **tuff** (solidified ash) beds often contain some fragments of larger size, quite apart from crystals. Those in which moderately to very abundant lapilli-sized ejecta (Table 7.1) of lithic material or pumice are scattered through the finer matrix are called **lapilli-ash** or **lapilli tuff**. Those containing blocks are known as **tuff-breccia**, and those containing bombs may be called **tuff-agglomerate**.

Near the vents each individual explosion during an eruption results in a shower of fragments that fall as a layer over the adjacent countryside. Each layer is the result of a separate explosion. Such beds are commonly well sorted according to size of the fragments (see pages 187–8), and show a size gradation both vertically and laterally. Particles are usually larger near the base of the layer, because the larger fragments ejected by any one explosion have faster settling speeds than the small ones, and so strike the ground first. For the same reason, the largest fragments tend to fall closer to the vent, while smaller ones are swept farther by the wind. Occasionally, ash beds are found in which the grain size increases upward. This can signify two diametrically opposed things: The gradation may result from increasing intensity of explosive activity, with larger fragments being thrown higher and drifting farther from the vent so that at any one place the fragments falling to the ground are larger than those preceding them; or it could result from **decreasing** strength of explosion, the magma being less completely blown apart so that the fragments formed are somewhat larger in later stages than they were earlier. Some ashfall beds also show fine internal laminations made up of slightly different particle sizes that can be related to abrupt fluctuations in the heights of eruption clouds (Walker 1980). Typically, these laminations are traceable laterally a variable distance away from the vent, representing the differing strengths of the eruption that produced them.

Fallout ash deposited by phreatomagmatic eruptions tends to be more conspicuously laminated than dry ashfalls, with groups of thin, subparallel layers separated by pyroclastic surge bedding (described later). Wet ash fall beds may also be slightly vesicular, owing to the steaming of moisture trapped by the hot ash, or from underlying heat emitted by previously accumulating material. The presence of a modest amount of moisture can actually strengthen a bed through the collective effect of the surface tension of water films around particles. Such wet cohesion improves the ability of some layers to resist wind and gas-blast erosion, and to cling more effectively to slopes. But if too much moisture is present, wet ash on slopes, particularly on slopes $>10^\circ$, will remobilize and slide. Internal laminations fold and rumple as they slump downslope, much like a carpet being slid into a wall. This phenomenon is called **soft sediment deformation**. Soft sediment deformation rarely occurs in dry ash fall layers, which will slump and mix under the influence of gravity on steep slopes, but lack the internal cohesiveness to retain any semblance of original stratification.

The areal extent of ashfall from extremely powerful eruptions can be literally world wide. Extremely fine ash (“dust”) from the 1883 eruption of Krakatau volcano [98] may have circled the earth three times. Long range ash distribution can also have important economic impacts. For example, the valuable bauxite ore deposits on the non-volcanic Island of Jamaica may derive from the fallout and weathering of ash, generated over millions of years by Antillean arc volcanoes lying approximately 1500 km upwind (Corner 1974).

The lateral movement of ash in the atmosphere depends on high level wind speeds. Some of the 1.1 km^3 of ash from the 1980 Mount St Helens [27] eruption in Washington State drifted 1000 km to the east in a little less than 10 hours, indicating a high-altitude wind speed of nearly 100 km/hr. Far larger than the Mount St Helen’s blast, the 1912 Novarupta [17] eruption in Alaska released some 25 km^3 of ash and pumice, which darkened skies over an area of $260,000 \text{ km}^2$. The ashfall reached a thickness of about 30 cm at the village of Kodiak, 160 km from the site of the eruption. The even stronger explosion of Tambora [103] in the eastern part of Indonesia in 1815 ejected over 100 km^3 of ash, enough to bury the whole Island of Manhattan a kilometer deep!

Ash layers interbedded with ancient rocks of other types often are of great importance geologically, because they provide a widespread time datum of unrivaled precision. A single ash bed traceable over tens of thousands of square kilometers represents an event that took place within a period of only a few days – a mere instant in the eons of the earth’s history. It furnishes a means of correlating the associated rocks in time – rocks that may have formed under very different conditions and consequently be of very different character and contain very different types of fossils in different parts of the ash-covered region. As an example, a distinctive ash bed of Ordovician age widespread over eastern North America and Northern Europe is a critical marker horizon for dating a gigantic eruption that occurred some 450 million years ago – before formation of the Atlantic Ocean (Huff et al. 1992).

The correlation of rock units by dating of interbedded ash layers is called **tephrachronology**, and was pioneered by Thorarinsson (1967), who was able to correlate late prehistoric and early historic volcanic and other historical events over large parts of Iceland. In the United States fallout ash from the great eruption of Mt Mazama (Chapter 10) has been traced as far east as central Montana and northward into British Columbia and Alberta, establishing the synchronism of associated rocks in the Cascade Range, Columbia Plains, Rocky Mountains,

and western Great Plains (Wilcox 1965; Sarna-Wojcicki et al. 1983; Foit et al. 2004). Ashfall erupted at the time of the formation of the Bishop Tuff in the northern end of the Owens Valley, California about 740,000 years ago has been identified as far east as central Nebraska (Izett et al. 1970). Ash from the eruption of Glacier Peak, Washington, about 12,000 years ago (Mastin & Waitt 2000), has also been traced eastward as far as Montana; and the Pearlette ash, erupted during the late Kansan Ice Age, is found from western Texas to southeastern South Dakota, and possibly westward into Nevada. Tephrochronology has assisted in the dating of prehistoric fault movements (e.g., Anderson & Hawkins 1984) and in archaeology, paleontology, and climate change studies (Rapp & Hill 2006; Dorn 2009).

Ash layers, commonly altered to clay minerals, may appear very similar in hand specimen, and microscopic or geochemical methods may be required for correlation, although other features such as thickness, color, and stratigraphic position may be helpful (Westgate & Gorton 1981). The compositions and refractive index of any preserved glass fragments and relative abundances of the phenocrysts may also be important. For instance, the Mazama ash can be distinguished from the otherwise very similar Glacier Peak ash by the presence of crystals of augite, which are lacking in that from Glacier Peak (Powers & Wilcox 1964). An ash layer erupted from Mt Rainier [31] about 2000 years ago can be told from the Mazama ash by the higher refractive index of its glass (Wilcox 1965).

Another challenge for geologists studying ash distribution is the possible change in ash composition with varying distances from the point of eruption. Most volcanic ash, consists of a mixture of phenocrysts and glass fragments. The phenocrysts generally contain considerably less silica, and more iron, magnesium and calcium, than does the glass, are more dense, and fall faster from the eruption cloud. As a result, ash that falls at greater distances from vents typically contain less phenocrysts and may be richer in silica. This change of bulk ash composition by aerial sorting has been called **aeolian differentiation**.

LAPILLI

Lapilli are pyroclasts in the range 2–64 mm (Table 7.1). The singular form of lapilli is **lapillus**, derived from a Latin word meaning “little stone.” Like ash, lapilli may be essential, accessory, or accidental, ejected either in a liquid or a solid condition. Very fluid lapilli may weld together to form spatter, or agglutinate. There is no consistency in the terminology applied to accumulations of lapilli. Fisher (1961) and Schmid (1981) have suggested that consolidated masses of lapilli be called “lapillistone.” To be more specific, perhaps it is best to call masses of rounded lapilli, **lapilli agglomerate**, and those of angular lapilli, **lapilli breccia**.

The rough clots of highly vesicular basaltic lava produced by Strombolian eruptions, called **cinder**, are typically lapilli-sized. The terms **scoria** and **slag** are synonyms for cinder, though “slag” is falling into less use over time, and “scoria” tends to be more loosely applied to any coarse, highly vesicular pyroclast (including some pumice deposits). Cinder is ballistic in its deposition, tending to leave a vent in a liquid state while solidifying during flight. Volcanic cones consisting largely of cinder are described further in Chapter 9.

Explosive eruptions produce vast amounts of finely divided ash particles that form the principal solid components of eruption clouds. All of this ash will eventually fall to Earth as discrete particles, but in many cases, ash particles will coalesce to form layered ash balls

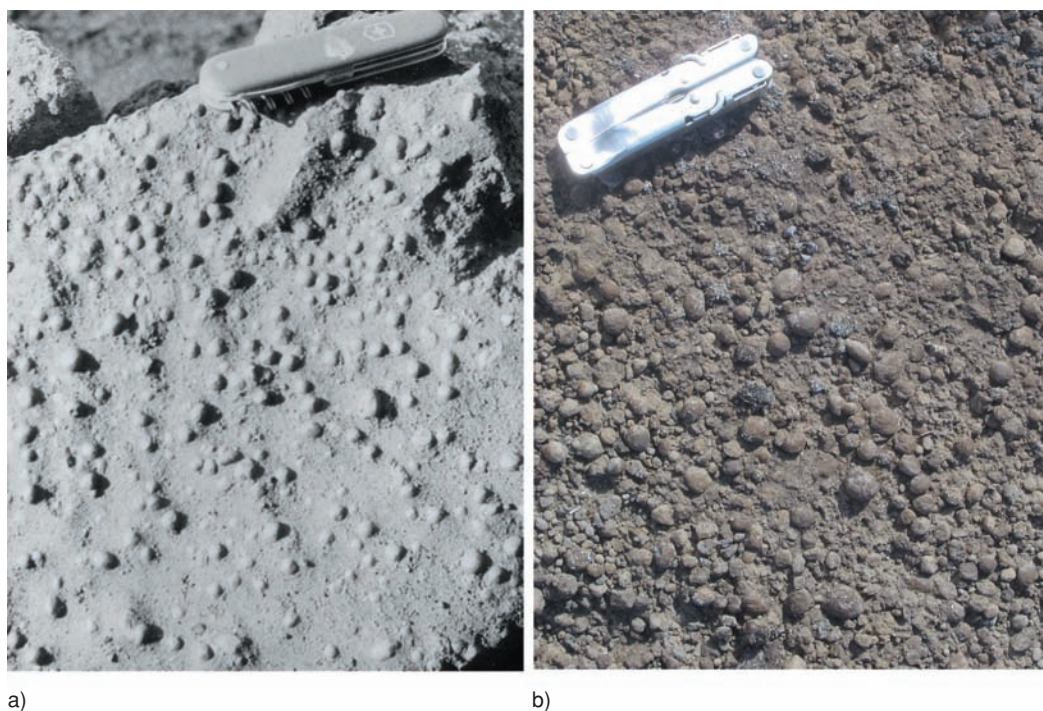


Fig. 7.8 Accretionary lapilli deposits. a) Most common type, where accretionary lapilli were deposited simultaneously with ashfall (Laguna maar explosion debris, Gamalama volcano, Ternate Island, Indonesia). b) Concentrated deposits, where accretionary lapilli fell out of eruption cloud before ashfall (1790 Keanakakoi Ash, Kīlauea volcano, Hawai'i). Knives 8 cm long. Photos by J. P. Lockwood.

called **accretionary lapilli**, or ash **pisolites** in older literature. These distinctive lapilli are commonly thought to form around water droplets, or by the adherence of moist ash particles in ash clouds to form muddy raindrops, which develop in much the same way that hailstones form around ice or particulate nuclei in thunderstorms (e.g., Gilbert & Lane 1994), but form in other ways (Heiken 2006). “Hailstone” accretionary lapilli commonly are well-indurated and marked by nearly concentric fine layering. When observed to fall from ash clouds they may appear damp, and often accumulate as aggregates of semi-spherical lapilli enclosed in fine ash matrices (Fig. 7.8). They typically are 3–10 mm in size, but can reach more than 2 cm in diameter. Some muddy accretionary lapilli continued to grow after landing on loose ash during the 1924 phreatic eruption of Kīlauea volcano [15], when they were observed to roll along on loose ash after impact and enlarge like rolling snowballs (Stearns 1925).

Accretionary lapilli can also form by electrostatic attraction, falling as loose aggregates of fine ash that have no muddy matrix, and apparently maintain their cohesion by electrostatic means (Gilbert et al. 1991; Schumacher & Schmincke 1995). Such “electrical” accretionary lapilli were observed to fall during an eruption of Galunggung volcano [99] in 1982, and disintegrated into unconsolidated ash piles when they impacted hard surfaces – like volcanologists’ hardhats or outstretched hands. They were preserved only where they dropped onto extremely loose, “fluffy,” uncompacted fine tephra that was falling near-simultaneously. The tephra entombed the lapilli *within it* by backfilling of penetration holes with loose ash (Fig. 7.9).

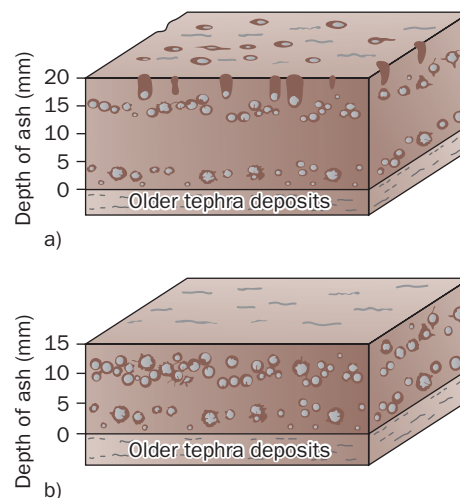


Fig. 7.9 Formation of accretionary lapilli during the August 13, 1982 eruption of Galunggung volcano, Indonesia. a) Accretionary lapilli have fallen in two periods, one contemporaneously with fine ash and one following the last ashfall. These last lapilli have drilled down up to 5 mm deep in the loose ash. b) After rainfall compaction, the younger lapilli are now overlain by the older ash. Sketch by M. Summers from field notes by J. P. Lockwood.

PUMICE – HIGHLY VESICULAR LAPILLI

The fourth-century BCE Greek philosopher Theophrastos of Eremos called pumice “worm-eaten wood.” He conjectured that it was the product of sea-foam interacting with fire, a reasonable hypothesis at the time (Heiken & Wohletz 1985). Pumice occurs widely as interlayers and patches with obsidian in lava domes and flows (Chapter 6), but here we discuss only as ejecta. Individual pumice pyroclasts range from less than a centimeter to as much as several meters in size – exceeding the size range of lapilli as strictly defined (Table 7.1), though more as an exception than the rule. Specimens occur in airfall deposits as well as clasts in pyroclastic flows. Some low-density basaltic scoria, **reticulite**, is even less dense than ordinary siliceous pumice, but the bubbles in reticulite are mostly unsealed and interconnected.

The existence of pumice is the strongest evidence we have that magma can froth much like the foam on a fresh stein of beer, as melt exsolves gases in the upper portion of a magma conduit. Pumice fragments may be regarded as bits of quenched, glassy magmatic foam. Most have high-silica content, reflecting the fact that high-silica magmas are more viscous than basaltic magmas, do not release their entrapped volatiles as efficiently, and tend to produce very explosive and gaseous eruptions.

Because pumice has low density and sealed vesicles, pumice clasts can float on water – the only stone known to do so (Fig. 12.7). During large pumice-producing submarine or littoral eruptions, such as the 1883 Krakatau eruption, fields of thick floating pumice typically accumulate over large areas. Some floating pumice fields are so thick that they can support the weights of people, wildlife, and downed trees. It is even likely that floating pumice has played a role in distributing flora and fauna to new lands, especially in explosively volcanic archipelagos like Indonesia (Symonds 1888; Simkin & Fiske 1983; Bryan et al. 2004). Pumice clasts gradually become water-logged, however, and over a period of months most fragments will sink, although individual rounded clasts commonly wash ashore thousands of kilometers from their sources.

The solid portions of pumice clasts consist of volcanic glass blown into thin cellular walls and strands, typically silver-grey in color. This color might be due as much to the thinness of the glass and the internal reflection of light within its numerous vesicles as to its composition (Klug & Cashman 1994). In fact, were the glass in an ordinary clot of pumice re-melted to form a bubble-free solid, most would become ordinary black obsidian, as shown gradationally in mixed pumice-glass domes and the *fiamme* found in many ignimbrites. Nonetheless, pumices of variegated color also exist. Watanabe (1986) describes prehistoric orange pumice beds at Aso caldera [110], Japan. Imai et al. (1993) examined highly oxidized, sulfur-rich yellow pumice erupted in 1991 from Mt Pinatubo [104] in the Philippines. Paulick and Franz (1997) analyzed multi-colored pumices from the 5000-year old Meidob volcanic [93] field in Sudan, where brown, buff, black, and ordinary grey pumices originated during the same eruptive sequence. They discovered that the color differences relate to differing concentrations of tiny magnetite and hematite (iron oxide) crystals dispersed in the volcanic glass, which in turn may be related to the mixing of two separate magmas with distinctive ferric iron abundances.

Some pumice clasts show compositional banding – remarkable evidence for magma mingling (Smith 1979). Three to five percent of the June 1912 Novarupta pumice at Katmai, Alaska, for example, is made up of streaks of dark andesite within tan-colored rhyolite, with

some mixed andesite and dacite samples from the upper part of the associated PDC deposits (Fierstein & Wilson 2005). Such pumice clasts indicate that during the process of eruption, melts of different viscosities occupied the same vent. The tabular or streaky structure of components in many mingled composition pumices suggests that the uprush of gas from the top of a magma column stretched and sheared inhomogeneous melt into fragments of varied composition. Continued expansion of gases within the molten glass expands the pumice and with aerodynamic drag during descent, may explain why so many pumice fragments are rounded.

Measured pumice porosities range from 64–85 volume percent, with considerable variation seen even in the products of single eruptions (Houghton & Wilson 1989; Gardner et al. 1996). This range relates in some critical but as yet poorly understood way to magma viscosity – or more particularly, the viscosity of the molten films which separate gas bubbles at the moment the pumice forms (Klug & Cashman 1994). Molten pumice with bubble wall viscosities of less than about 10^9 Pa s can continue expanding after ejection from the vent (Thomas & Sparks 1992), increasing the porosity of the final samples and causing the chilled crusts of pumice clasts to inflate and crack, forming breadcrust structure. At even lower viscosities (less than 10^5 Pa s), the expanding gases may break their enclosing films, merge, and escape altogether, causing the fragile structure of the pumice to collapse as it exits the vent. The low end of the pumice porosity range – 64 percent – therefore represents the lowest possible pore volume of specimens that ordinarily do not collapse during eruption. “64 percent” may also be regarded as the approximate *minimal volume percentage* of gas bubbles needed for pumice-forming explosions to commence at the top of magma columns (Gardner et al. 1996).

Pumice vesicularity also circumstantially relates to eruption intensity, as suggested by the work of Allen (2001) who studied the Kos [94] ignimbrite, a Plinian eruption deposit in the Greek Aegean. During the early phreatomagmatic periods of low to moderate discharge from the vent, pumice clasts were small, the size of fine lapilli, and moderately vesicular. All were rhyolitic in composition. As discharge (mass flux) increased and the eruption gained a Plinian character, rhyolitic pumices up to the size of blocks erupted with notably higher vesicularity. At the climax of the eruption, as the Kos caldera collapsed, banded pumices (rhyolite plus andesite) appeared, showing deep evacuation and mingling of melts within the magma chamber.

The initial sizes of pumice fragments can also be correlated with gas bubble volume and the relative permeability of the magma to escaping gases. Klug and Cashman (1996) concluded that pumices as small as 1 cm across develop if the magma is mostly gas-bubble impermeable and the volume of bubbles in the melt less than 70 percent. Given an increase in bubble volume to 90 percent in a highly permeable magma, pumice clots exceeding 10 cm in size can easily blast out of the vent. Gas permeability is generally boosted by rapid eruption rate.

Both ash and pumice are commonly erupted *together* during large eruptions, and usually have the same composition. The proportions of each may relate to variable ability of gas bubbles to coalesce within the magma in the moments leading up to an eruption, indicating that vesiculation of shallow magma often does not occur homogeneously. The melt in an erupting conduit may be visualized as having some areas in **volumetric equilibrium**, in which the volume of gas bubble formation is matched by the total volume of gas escaping from the magma (Fig. 7.10). In this situation, typical for basaltic magmas, molten rock is erupted as spatter or lava flows. **Volumetric disequilibrium** prevails for erupting siliceous magmas,

Fig. 7.10 The volumetric equilibrium concept of escaping magmatic gases.

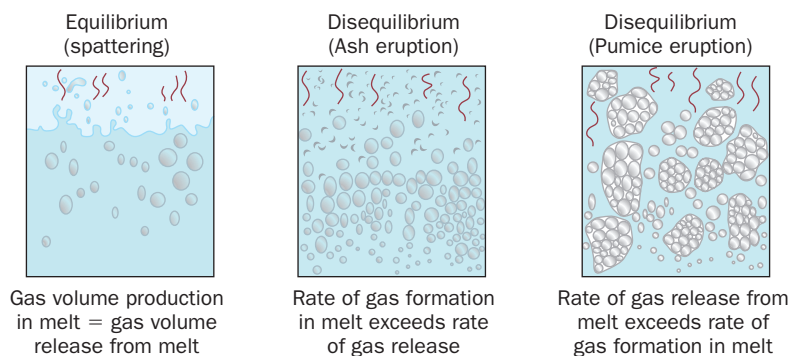
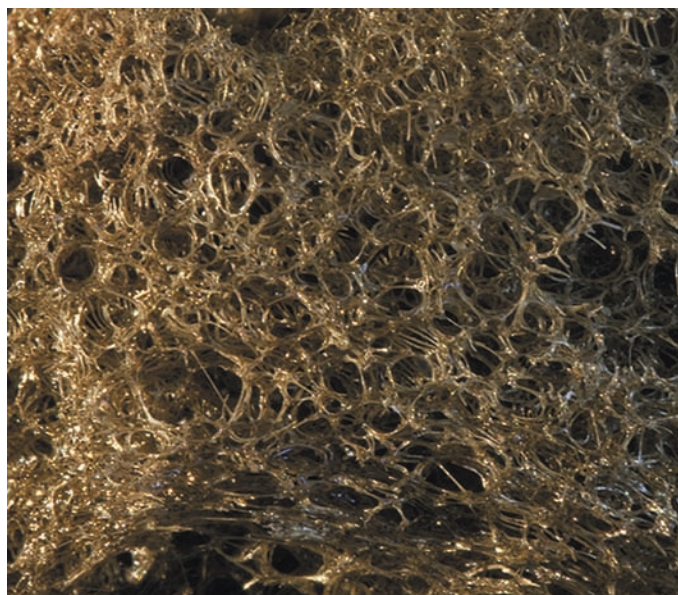


Fig. 7.11 Internal structure of basalt reticulite from a 1969 eruption of Kīlauea volcano, Hawai'i, showing delicate network of glass filaments. Note that there are no closed bubbles, in contrast to pumice. J. D. Dana called such material "thread-lace scoria". View about 4 mm across. Photomicrograph by Ben Gaddis.



leading to explosive discharge of pumice and ash. If the formation and expansion of gas bubbles exceeds the rate of gas release, then bubble walls burst into small, curved ash shards. On the other hand, if the rate of gas release exceeds that of bubble expansion, then the melt becomes foamy and is blown into pumice fragments. The capacity of the magma to release its pent up gases depends upon many factors, foremost the temperature, viscosity and total volatile content (Klug & Cashman 1996, Blower, 2001; Mueller et al. 2008).

Basaltic pumice, termed *reticulite* (Fig. 7.11), is the most vesicular of all pumices, with porosities as high as 98 percent, characterized by close-packing of polyhedral bubbles with open walls (Mangan & Cashman 1996). In intermediate to high-viscosity siliceous melts, surface tension in the walls of vesicles maintains spherical shapes. But in low-viscosity magma, bubbles expand to impinge against one another so that polyhedral walls are ruptured, giving reticulite a permeability that makes it *sink* in water almost at once. Individual bubble sizes are much smaller than those which may be found in siliceous pumices, typically only a fraction of a millimeter in diameter. In contrast, vesicles in rhyolitic pumice may be as much as several centimeters in size.

Reticulite has the typical color of basaltic glass (**sideromelane**), representing the internal play of light on material that is significantly more iron and magnesium-rich than that of siliceous pumices. Most reticulite forms during Hawaiian-style lava fountaining, from the frothing of clots of spatter. The addition of a mere 0.05 wt percent H_2O to melt may be all that is required for a Hawaiian-type eruption to shift from one of quiescent lava effusion to lava fountaining and reticulite production, with an increase in bubble nucleation rate of three orders of magnitude (Mangan & Cashman 1993). Observations of reticulite falls near lava fountains reveal that a range of fragment sizes develops, and that many larger fragments shatter and break into finer pieces as they strike the ground. Other forms of pumice are not quite as delicate as reticulite, but shattering must still play a role in modifying fragment sizes, especially during the transport of pumice in pyroclastic flows.

SORTING AND LAYERING IN PYROCLASTIC DEPOSITS

The study of layering and layering order in natural rock deposits is called **stratigraphy**. Thicker layers (greater than 1 cm) are termed **beds**, and thinner ones (less than 1 cm) are called **laminations**. It is possible for a single bed to contain internal laminations, or to thin out laterally with distance into a sequence of laminations. There is also a rough correlation between grain size and layer type in ejecta deposits, with finer particle sizes commonly making up the thinner layers.

The way in which different particle sizes in fallout deposits are distributed is termed **sorting**. Perfectly sorted layers consist of particles of the same size, composition, and density. Moderately and poorly-sorted layers show progressively wider ranges of fragment sizes mixed together (Fig. 7.12); The sorting of ejecta deposits directly reflects the way in which it was deposited. Fall layers, for example, show excellent sorting, while those of PDCs tend to be poorly sorted. Different sorting patterns reflect very different emplacement mechanisms for pyroclastic falls, flows, and surges. The excellent sorting of fall deposits reflects gravitational transport in air with very little turbulence. Particles of different weight and density fall according to their terminal velocities, with the heaviest particles dropping closest to the vent and falling faster from eruption clouds than lower density ejecta.

Many well-sorted layers show gradations of grain sizes (Fig. 7.13). If grain sizes are smaller upwards, then the bed is said to show **normal grading**. If grain sizes coarsen (are larger) upwards,

Fig. 7.12 Qualitative sorting grades in pyroclastic deposits.

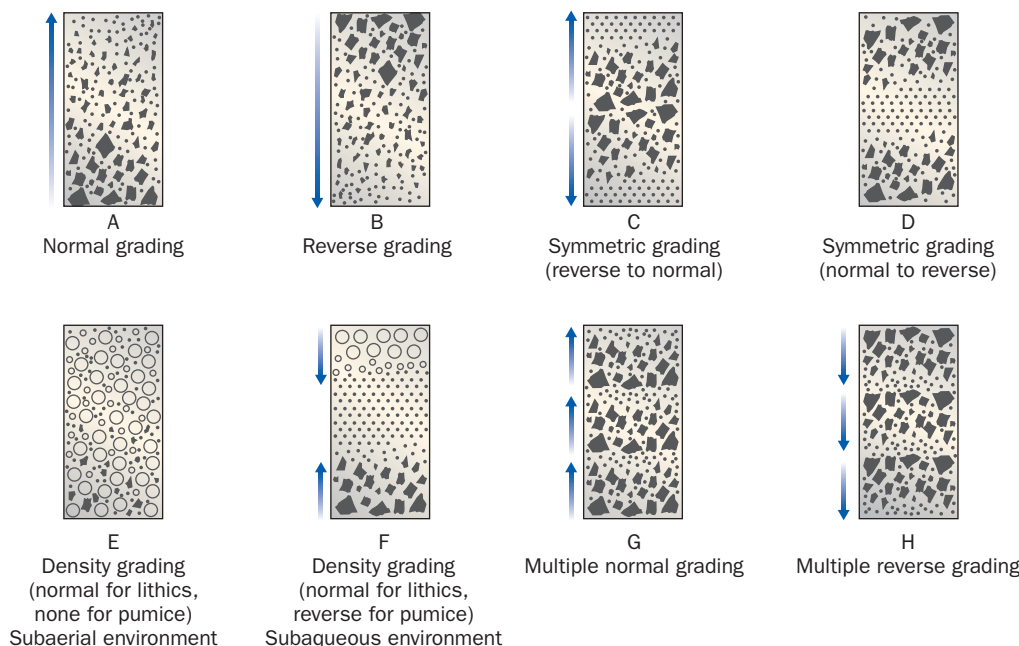
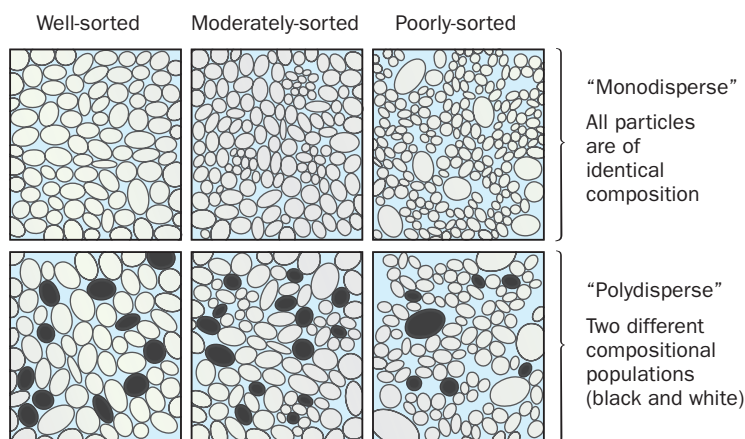


Fig. 7.13 Types of grading commonly observed in pyroclastic deposits. Black particles are relatively high density lithic fragments. Open circles are relatively light weight pumice clumps. Dots represent ash particles. From Fisher and Schmincke (1984).

then the bed displays **reverse grading**. A deposit that neither shows grading, nor any internal layering, is called **massive**. The presence of grading in a layer may indicate that the conditions of deposition or the nature of source materials were changing as the layer accumulated. For example, normal grading often indicates a decrease in the intensity of the eruption, while reverse grading illustrates just the opposite (p. 280). However other factors, too, can explain these same grading features, including shapes and densities of clasts. Dense clasts will fall to earth more quickly than low-density ones regardless of size and will end up at the bottom of beds. This is the process Professor George Walker called *the lady's handbag effect*!

Explosive Eruption Styles and Their Products

Following the above discussions of what is erupted during explosive eruptions, we turn to brief descriptions of the several principle types of explosive activity, roughly in order from least to most violent eruptions, along with descriptions of the rock deposits associated with each type. In doing so, we'll use three terms to describe the way in which gases and/or ejecta emerge from active vents: "volcanic clouds," "plumes," and "columns." A **volcanic cloud** is any visible emission of gas and particles from a volcano (including aerosols and vapors as well as solids). **Plumes** are volcanic clouds that are easily scattered and spread by ordinary winds. An eruption **column**, in contrast, is a volcanic cloud with great thermal and kinetic energy that ascends convectively from explosive vents and is not easily disrupted by winds until it reaches high altitudes. Eruption columns characterize the most powerful volcanic explosions, and if sustained for long enough generally feed wide-ranging plumes from their crests.

Volcanic explosions vary in intensity from the weak spattering that commonly accompanies the eruption of very fluid basaltic lava (Chapter 6) to cataclysmic blasts that throw debris many kilometers into the atmosphere. Our usual conception of an explosion is a sudden violent outburst of very short duration – essentially a single brief impulse, like that of a booming cannon. Some volcanic explosions are like that, but most are of longer duration, including continuous ejections of gas, rock fragments, and molten lava that persist episodically for several weeks or months. The culminating phase of the great eruption of Vesuvius [86] in April, 1906 was a tremendous, 12-hour long discharge of gas from a 300–400 m wide vent that roared 13 km above the mountaintop. Macdonald (1972, p. 122) comments that "it was less like the explosion of a gun, or even a relatively slow quarry blast, than it was like the blowing off of steam from a boiler (Perret 1924), or the continuous blast from a rocket."

VULCANIAN ERUPTIONS

Vulcanian eruptions are commonly driven by shallow explosions involving the expansion of water or carbon dioxide (Fig. 7.14). They range from **Ultravulcanian** blasts, which only eject solid, older rock material, not directly related to the magma or heat-source triggering the eruption, to blasts of freshly-solidified lava commonly derived from recently emplaced domes or plugs and mixed with some incandescent ejecta from the molten rock underneath. This latter debris is the trademark product of "ordinary" Vulcanian eruptions. Ultravulcanian eruptions



are primarily steam-generated, whereas more typical Vulcanian outbursts derive their power from much larger proportions of purely magmatic gas.

Vulcanian deposits are characterized by large amounts of poorly sorted blocks and lapillized angular lithic fragments mixed together with ash. Sorting improves with distance from a vent, and even farther out the ash fall deposits of Vulcanian eruptions may be indistinguishable in appearance from those of non-Vulcanian blasts unless examined microscopically. When viewed under a microscope, Vulcanian ash grains commonly appear as highly angular bits of pulverized, pitted rock matter mixed with lesser amounts of vitric ash shards (Fig. 7.15). Very large Vulcanian blasts may also include lumps of pumice, which are more common in

Fig. 7.14 Small Vulcanian explosion from Tavuvur volcano, Rabaul caldera [133] – 1998. Note small blocks falling from eruption cloud. Such blocks are a significant hazard to observers, as they may be blasted far from normal ash fall deposits. Photo by J. P. Lockwood.

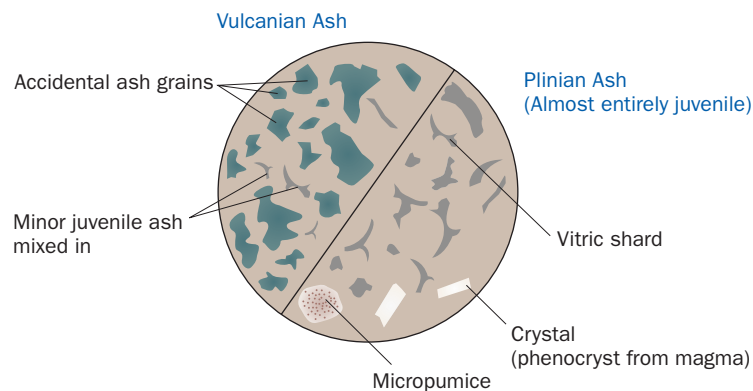


Fig. 7.15 Contrasting compositions and textures of volcanic ash from typical Vulcanian (left) and Plinian (right) eruptions.

Plinian eruption deposits. In fact many, if not most Plinian explosions, commence with a Vulcanian phase, typically associated with “vent-clearing” activity that ejects older country rock and may precede later magmatic eruptions.

Likewise, many, if not most ordinary Vulcanian eruptions begin with an Ultravulcanian phase. Ultravulcanian outbursts commonly last no more than a few hours, starting with opening of a new, typically short fissure across the summit or flank of a volcano, or less commonly in an older hydrothermal area away from any young volcanic cone. A blast pit forms at a point along the fissure, often near its midpoint. Dark showers of accidental debris accumulate around the new vent to form a low block or block-and-ash cone. These deposits lack any vitric ash, spatter, or bombs whatsoever.

A good example of an especially destructive Ultravulcanian eruption is provided by Bandai volcano [117], on northern Honshu, Japan. Bandai is an 1800 m high volcanic complex of overlapping andesitic composite cones. The dominant central one, 50,000 year old Ko-Bandai, last erupted large amounts of juvenile material 25,000 years ago. Twenty-five thousand years seems like a long time, but Ko-Bandai is still a living volcano. It produced three major phreatic blasts between 3000 BCE and 806 CE. Then, shortly after dawn on July 15, 1888, came the fourth in this series. Like the previous disturbances, the 1888 eruption derived its power from magmatically heated steam building up pressure at shallow depth, within a hydrothermal field that had been quietly developing on the upper northern flank of the volcano for many years. The only warning of impending disaster for local villagers was an ominous rumbling coming from the mountain, which preceded by only a half hour a moderately strong explosion centered in the north slope hydrothermal field. Continuous and strong earth tremors commenced with this first explosion, probably generated by the sudden release of subterranean gas pressure and the consequent high-pressure flow of a large amount of escaping vapor. While the ground was still trembling fifteen minutes later another moderately strong explosion shook the landscape, followed over the next few hours by 15 to 20 more, all focused in the same general locality. The blasts tossed blocks and finer stony debris to a height of 1300 m above the mountain's disintegrating northern flank, and a black, dust-laden pall of steam drifted up an additional 5 km. Condensing steam mixed with ash produced a shower of scalding hot mud, which cascaded all the way to the foot of the mountain. As the blasts continued, a large debris avalanche tore away the north flank of Ko-Bandai, quickly burying several villages. Farther downslope, it changed into a large lahar, wreaking more havoc and killing almost 500 people as it entered adjacent stream valleys. Later in the day, when the dust cleared, a new, steep-walled, dust-filled amphitheater could be seen, extending 2300 m into the volcano. The old hydrothermal field had vanished, quite literally, into thin air. Approximately a cubic kilometer of debris had been blown out, consisting entirely of old rock, some of which had partly decomposed to white clay before the eruption owing to intensive corrosion by strong hydrothermal acids.

Vulcano [81], the island-volcano providing the name for Vulcanian eruptions, is located in the Lipari islands north of Sicily, and its 1888 eruption typifies activity that begins with an Ultravulcanian phase and becomes Vulcanian as time progresses. The first records of activity at Vulcano date from about the fifth century BCE soon after Greek fishermen settled the adjacent island coastlines. Between then and 1800 CE at least 10 explosive eruptions occurred. During the nineteenth century activity began with a small eruption in 1831, followed by nearly



Fig. 7.16 Flank of Fossa di Vulcano, the active cone of Vulcano, Lipari Islands, that looms over the nearby harbor of Levante. It is easy to see, given this perspective, why this volcano is regarded as a threat! Photo by David Buesch.

40 years of complete repose. Vulcano reawakened in 1873, with weak explosions that were repeated with increasing vigor in the years 1876–9 and 1886. In each instance, the explosions threw out an abundance of fine ash mixed with angular fragments of rock. Some blocks were hot enough to glow dully at night but showed no signs of having been molten when ejected. Then, on August 3, 1888, phreatic explosions became especially violent, tossing out rocks weighing up to several tons. Some heated debris flew a kilometer and a half and destroyed wooden boats anchored in the harbor at Porto di Levante (Fig. 7.16). The fragments were of preexisting, magmatically heated rocks; none were of fresh lava. After a two week long hiatus explosions began again on August 18 and continued at brief intervals over the next 19 months. Up to this point, the activity would still be called Ultravulcanian.

The resumption of the eruptive episode on August 18 brought a change in the sorts of material ejected. Fragments of freshly-cooled, glassy lava were also now apparent, mixed in with the numerous blocks of older rock. The magma had risen significantly closer to the surface. Among the juvenile ejecta were breadcrust bombs having pumice cores enclosed in thin, cracked crusts of dense obsidian glass. Some bombs were still sufficiently plastic to flatten out very slightly without breaking when they plopped to the ground. The Italian volcanologist G. Mercalli, who suggested the term “Vulcanian” to Lacroix, described the general appearance of the eruption clouds rising during the 1888 explosions at Vulcano. His observations (1907, pp. 132–3) typify Vulcanian eruption clouds seen worldwide:

In the less violent explosions large ejecta were lacking and the jet consisted of a dense gray mass of lapilli, sand, and ash that rose slowly, taking the form of a great cauliflower or giant mushroom . . . The strongest [explosions] commenced with a pine-tree [shaped] cloud that was

absolutely black in daylight, culminating in arrow-like projections which rose very rapidly, within a few seconds reaching heights of many hundreds of meters, while from the flanks and summit of the cloud separated black streaks of stones and fine detritus. Large black rocks shot higher than the cloud, and within the cloud darted lightning flashes, followed by short sharp claps of thunder, quite different from the rumbling that accompanied the beginning of the explosion. Then the cloud expanded in dense globes and volutes, finally building up to a height of 3 or 4 km, and becoming gray and then whitish as it gradually freed itself of heavier solid materials.

Mercalli's vivid descriptions are excellent, but he assumed incorrectly that when the eruption clouds turned color from black to white it meant that the clouds were losing "heavier solid material." In fact, when black Vulcanian clouds turn to grey and white it usually indicates that superheated (invisible) water has cooled enough to condense into visible white steam.

The bright lightning flashes within the ash clouds or between the clouds and the ground are characteristic features of Vulcanian eruptions. Volcanic lightning in an ash cloud results from differences in electrical potential due to the initial explosive fragmentation, and later to collisions between turbulently suspended ejecta particles. Lightning will strike when the potential reaches a certain critical magnitude, starting as a nearly instantaneous, visible current of electrons rushes all at once toward an area that is highly positively charged.

Seismic detection of volcanic lightning during the 1992 eruptive episode at Mt Spurr [22], Alaska, showed a strong correlation between the strength of lightning bolts and the amounts of eruption tremor and gas released (McNutt & Davis 2000). Lightning commenced 21–26 minutes after the start of each eruption, indicating that the explosive levels of static charge difference developed well within the rising eruption clouds rather than at the vent. Each lightning bolt was launched in the upper parts of the eruption clouds toward the positively-charged matter which had fallen, or was in the process of falling to the surface (McNutt & Davis 2000). During eruptions of Redoubt volcano [21], not far from Mt Spurr, Hoblitt (1994) was able to correlate the numbers of lightning bolts directly with the magnitude (VEI) of explosions.

Some Vulcanian eruptions produce small to moderate-sized PDCs. In May 1902, one such cloud of hot ash, rubble and gases, originating from Mt Pelée [63], overwhelmed the port city of St Pierre 6 km away. Despite abundant warning signs of an impending eruption, citizens were encouraged to stay in town by local political authorities awaiting an election, and 29,000 people died there near-instantaneously (Chapter 1). Only two people, both badly injured, are known to have survived.

PLINIAN ERUPTIONS

The prototypical Plinian eruption was that of Vesuvius in 79 CE, the eruption that buried the Roman city of Pompeii. This eruption type is named after Pliny, a Roman naturalist who witnessed, but did not survive the eruption. Plinian eruptions occupy the upper end of the VEI scale, and are the most energetic and potentially devastating of all volcanic activity, especially when PDCs are generated. **Phreatoplinian eruptions**, which are closely related, are

essentially just Plinian eruptions that break out in shallow bodies of water. They tend to be even more powerful than ordinary Plinian eruptions because of the added explosive energy provided by larger volumes of incorporated steam.

Individual Plinian eruptions produce prodigious amounts of juvenile ash and pumice, with subsidiary lithic fragments. A typical eruption culminates in a towering eruption column of hot gas and steam mixed with millions of tons of ejecta blasted above the vent at speeds of up to hundreds of meters per second. Sheer inertial momentum sustains this column initially, but expanding steam and entrained, heated air sucked into the base of the column give it the convective boost it needs to climb kilometers higher into the atmosphere (Bursik et al. 1992). Eruptive columns with higher water and steam contents (greater than 5 weight percent H₂O) are more likely to start convecting than those that are drier, or have much higher proportions of CO₂ and other magmatic gases than of water (Sparks & Wilson 1976). Pliny's nephew (Pliny the Younger) witnessed a rising convection column above the summit of Vesuvius from 35 km away on August 24, 79 CE, and thought the column resembled a rapidly growing pine tree of a local species (*Pinus pinea*) with a tall narrow trunk supporting a densely spreading crown or "umbrella" of roiling ash clouds (Fig. 7.17). The umbrella developed where the column flattened out as it finally lost positive buoyancy in the stratosphere. Calculations based on fall deposits allowed Carey and Sigurdsson (1987) to calculate that the 79 CE column reached 32 km in height above Vesuvius! The term **Plinian column** is used to describe these boiling clouds of ash and steam that rise more than about 15–20 km above volcano tops, and **sub-Plinian** for clouds that rise to lesser heights. **Ultraplinian** describes those rare columns that rise above 40 km or so into the stratosphere (Fig. 7.18). Eruptions of Krakatau (1883) and Tambora (1815) may be the only historic examples of this latter category. Most of what is known about Plinian eruptions come from studies of their distinctive fallout deposits, and this will be the focus of the remainder of this section.

Plinian eruption deposits (Fig. 7.19) found throughout the world typically consist of four primary sub-units, here listed from bottom to top:

- 1 well-sorted basal pumice fall beds up to several meters thick; overlain by
- 2 cross-laminated pyroclastic surge beds; capped by
- 3 pyroclastic flow deposits that can be as much as several tens of meters thick. These latter deposits are typically a poorly-sorted mixture of ash, pumice, and minor lithic fragments, with concentrations of angular lithic rubble at their bases and larger pumice fragments toward the top; and
- 4 a capping layer of well-sorted, unstratified ash up to several tens of centimeters thick (termed "co-ignimbrite ash").

Jurado-Chichay and Walker (2001) related this "standard" Plinian depositional sequence to eruption dynamics, beginning with the basal pumice fall layer which represents the initial, heavier-particle fallout from the plume as it begins to spread from the top of the eruption column across the surrounding landscape (Fig. 7.20). A typical pumice fall bed is distinguished by an inversely-graded lower part, reflecting a waxing in column strength; a uniformly sorted middle section showing steady state column activity; a horizon of coarsest pumice clasts showing greatest intensity of eruption; and finally a normally graded upper part that represents



Fig. 7.17 Sub-Plinian eruption of Galunggung volcano, Indonesia – August, 1982, photographed from the city of Tasikmalaya, 17 km to the southwest. This convective, ash-laden column has risen to about 12 km above the erupting crater. USGS photo by J. P. Lockwood.

post-climax weakening of the column. The column then collapses or “boil-over” processes ensue (Chapter 8), forming PDCs that bury the pumice fall bed. Finally, as the eruption shuts down, the fine ash lingering in the air above the freshly veneered volcanic terrain settles out to develop the co-ignimbrite layer.

Would that the world were so simple, but in many places – even where exposure is complete – the stratigraphic layering described above is not fully expressed in outcrops. One basic explanation is simply geographical – *unique factors control distribution of air-fall and PDC deposits*. Prevailing winds at the time of eruptions guide plumes and their resulting airfall patterns, while directional eruption foci and topography greatly affect pyroclastic current distribution. Fallout deposits may accumulate on one side of a volcano while pyroclastic flows and surges charge down the other, leading to local stratigraphic sections that are unrepresentative of the full eruption sequence (Carey & Sparks 1986). Such, for example, is recorded in the 79 CE Vesuvius deposits, in which air fall took place primarily to the south-southeast, while pyroclastic currents poured down both the southern and western flanks.

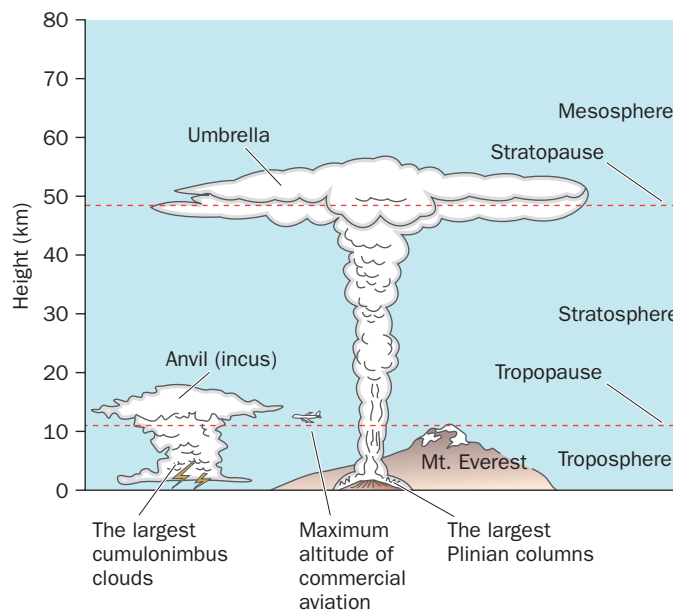


Fig. 7.18 Comparative heights of Plinian columns and atmospheric clouds.

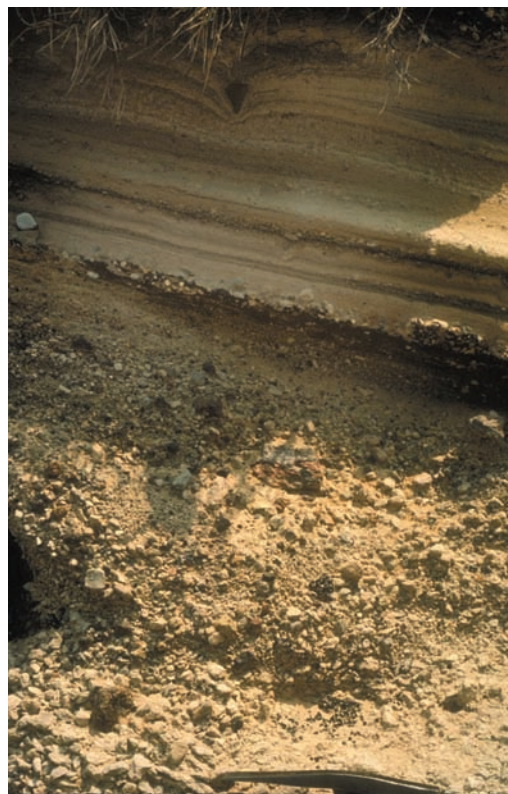


Fig. 7.19 Plinian deposits from the 22,000 year-old eruption of Monte Guardia, Lipari island, Italy. Pyroclastic surge and fall deposits overlie pumice-rich, fine-depleted air fall. Note bomb sag in the uppermost layers of this meter-thick section. Photo by R. W. Hazlett.

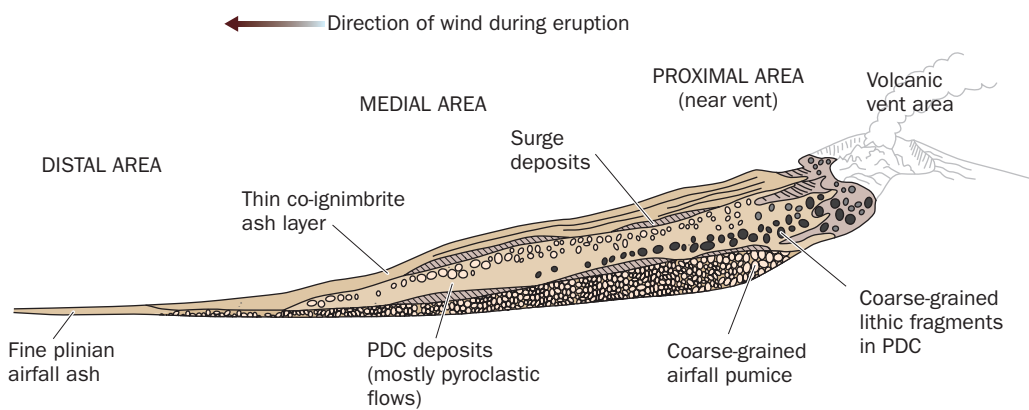


Fig. 7.20 Proximal to distal anatomy of a typical Plinian eruption deposit.

Note: scales greatly exaggerated and variable

Another geography-related depositional factor has to do with proximity to eruption site. In general, the complexity and thickness of Plinian eruption deposits increases as one approaches source vents (Fig. 7.20). For a typical deposit, the most distal material simply consists of a thin bed of fine, well-sorted tephra, which may distinguished from Vulcanian ash only through microscopic examination. Within a few tens of kilometers of vents ash particles noticeably coarsen, and the basal layer of air fall pumice first appears. Pumice lapilli may be no larger than bird seed when first spotted, but they too coarsen ventward, with mean diameters exceeding the size of grapefruit within a few kilometers of sources. PDC deposits appear between the basal and air fall layer closer to the vent, documenting the reach of pyroclastic currents during the eruption. Within a few kilometers – the so-called **proximal area** – the stratigraphic layering more completely reflects the complex history of vent clearing, eruptive column development and collapse. Sorting deteriorates significantly, and blocks of ballistically-ejected lithic material may stand out in the deposit. Local concentrations of poorly-sorted lithic fragments might actually exceed those of all other pyroclastic materials in total volume and weight. The proportion of fine ash typically decreases, in no small part due to reincorporation of finer ejecta into the active convective column during eruption (Valentine 1998). Interlayering of the two types of PDCs (pyroclastic flows and pyroclastic surges) may also be present in alternating or random sequence, indicating rapid and localized transitions in particle concentrations as air was entrained into a collapsing eruption column. Rowley et al. (1981), described the unconsolidated, 20 m thick near-vent layer left by the 1980 Mount St Helens eruption as a **proximal bedded pyroclastic-flow** (PBPF) deposit. There is considerable lateral variation in proximal deposits, variations that provide important clues about the complex dynamics of eruption at Plinian eruptive vents.

Finally, not all Plinian eruptions unfold in a “standard” pattern. For example, in some eruptions gas thrust waxing in the eruption column is so rapid that mean air fall pumice sizes change abruptly, rather than gradationally upward. The 1947 eruption column from Hekla volcano [67] in Iceland, for example, ascended nearly 30 km in 20 minutes (Thorarinsson 1954). Discharge rates might also oscillate erratically. Carey and Sigurdsson (1987) estimate that

during the 79 CE Vesuvius eruption, pumice discharge ranged from 7.7×10^7 to 1.5×10^8 kg/sec and column height from 26 to 30.5 km. Waning, too, can be abrupt, recorded by the absence of graded bedding and the presence of sharp contacts between pyroclast sizes. Rapid shifts in eruptive column behavior can develop as vents increase in diameter during eruption and as exit speeds of ejecta and gas change. The topography of the surrounding landscape can also greatly influence PDC dynamics. Valentine et al. (1992) noted that if a large amount of tephra hits the ground within the rim of an enclosing caldera, considerable amounts of pyroclastic material will pour back toward the vent where it is swept up and recycled in further discharge. The added mass may be sufficient to hasten column collapse, and will certainly make eruption dynamics more complicated and erratic. On the other hand, if tephra is shed exclusively outside a caldera rim little material can be recycled, and a convection column may continue to play without significant change as long as other factors, including vent diameter, mass discharge, and exit speed are steady (Woods 1988).

The classic Plinian eruption of 79 CE was mostly over in less than a day. The initial pumice fall put down a layer as much as 1.4 meters thick across the small city of Pompeii over a period of about 18 hours, enabling most of the population (about 90 percent of some 20,000 residents) to escape by foot and cart, though how many eventually reached safety is unknown. Many evacuees carried mattresses, pillows, or other protection on their heads to escape injury from pelting, though from archaeological remains it is clear that some were felled horribly in their tracks. Some 12 hours after the development of the eruptive column, PDCs were already underway, initially directed toward the port of Herculaneum a few kilometers west of Pompeii (De Carolis & Patricelli 2003). When the first pyroclastic current finally reached Pompeii itself, the city's defensive wall managed to restrain it, but the accumulating ash and pumice provided a ramp on the upslope side of the wall for subsequent currents to overtop with ease. Magnetic studies of the PDC deposits indicate that the grid of city streets locally controlled the movement and subsequent depositional fabric of the basal parts of the incoming torrents of ash, pumice, and gas (Fig. 7.21) (Gurioli et al. 2005).

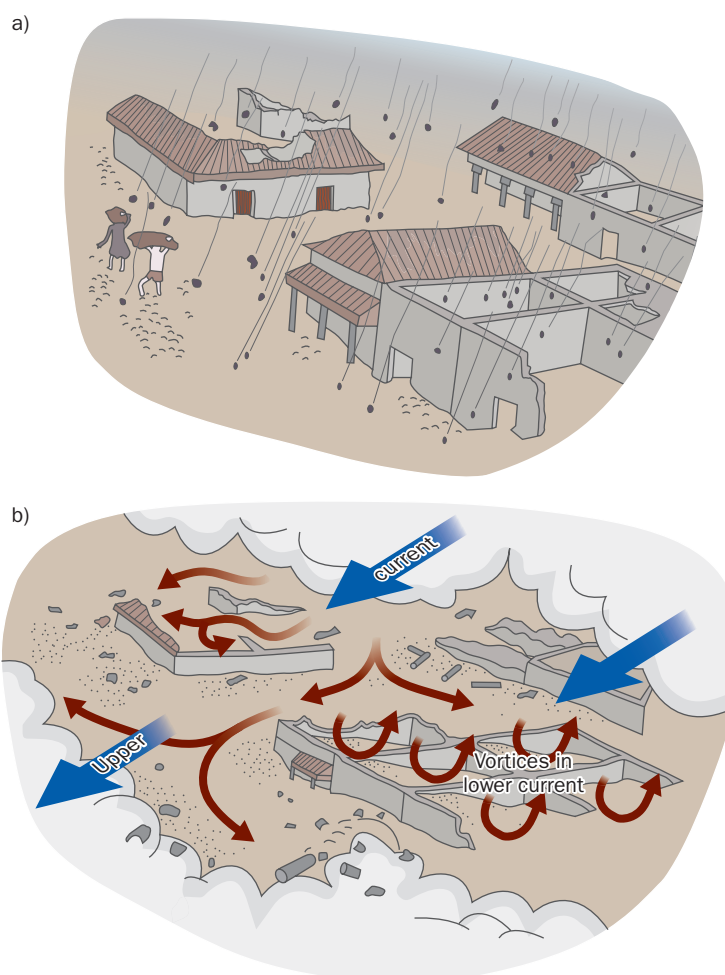


Fig. 7.21 The 79 CE eruption of Vesuvius impacted Pompeii in several ways: a) An early air fall pumice phase began collapsing roofs within the first 6 hours of eruption. According to forensic work by Luongo et al. (2003), 38 percent of all fatalities in the town were caused by roof and building collapse. About half of the victims (mostly women and children) were indoors, the other half in the streets. b) Subsequent pyroclastic currents raced over the town. The upper parts of the currents were not deflected by buildings, but work by Gurioli et al. (2005) indicates that movement in the lower parts of the currents was significantly modified by city structures.

The few people remaining in Pompeii at the time that had not already been buried or escaped certainly perished at this stage.

Pliny the Younger described the final phase of the 79 CE eruption in his Second Letter to the historian Tacitus, witnessed as he fled his uncle's estate near Vesuvius with his mother:

A dense dark mist seemed to be following us, spreading itself over the country like a cloud. "Let us get off the highway," I said, "while we can still see, for fear that, should we fall in the road, we will be crushed by the crowds that are following us." We had scarcely sat down when night came upon us, not such as we have when the sky is cloudy, or when there is no moon, but that of a room that is shut up, and all the lights put out. You might hear the shrieks of women, the screams of children, and the shouts of men; some calling for their children, others for their parents, others for their husbands, and seeking to recognize each other by the voices that replied . . . It now grew rather lighter, which we imagined to be the forerunner of an approaching burst of flames rather than the return of day; however, the fire fell at a distance from us; then we were immersed again in thick darkness, and a heavy shower of ashes rained upon us, which we were obliged every now and then to stand up to shake off, otherwise we would have been crushed and buried in a heap . . . At last this dreadful darkness was dissipated by degrees, like a cloud or smoke; the real day returned, and even the sun shone out, though with a lurid light, like when an eclipse is coming on. Every object that presented itself to our eyes (which were extremely weakened) seemed changed, being covered with deep ashes as if with snow.

A BASALTIC PLINIAN ERUPTION – TARAWERA 1886

Although most Plinian eruptions involve silicic or intermediate magmas (andesites, dacites, and rhyolites) more basic magmas can also generate Plinian activity. In the central part of the Taupo volcanic zone [135] on the North Island of New Zealand, the small, rugged volcanic complex of Tarawera [140] rises from forest and pastureland and the shores of several beautiful lakes, formed where past volcanic eruptions have blocked rivers and streams. In 1886, numerous Maori villagers lived close to the volcano, and, together with the European colonial observers in nearby Rotorua, provided excellent eye-witness accounts of the great eruption that took place that year. Tarawera is a quartet of steep-sided, coalescing rhyolitic domes stretching 9 km southeast–northwest, along a zone of weakness that includes the Waimangu geothermal area, one of the most active hot spring and thermal pool fields in the world. The 700 year old Tarawera domes showed no sign of having involved basaltic activity during their growth. But on June 10, 1886, an intense earthquake swarm began, centered at the spiny crest of Tarawera. An hour later, ash eruption commenced, with incandescent ejecta columns observed rising from two of the domes. Activity spread as a series of 11 additional blast craters formed in an 8 km-long-chain along the topographic axis of Tarawera. The mountain was splitting open lengthwise as a huge basaltic dike intruded its interior, taking advantage of previously weakened crust beneath. Clouds of basaltic ejecta shot up from the entire length of the breach, with the largest plume rising as high as 10 km. The dike continued to extend to the southwest, eventually intruding the Rotomahana geothermal field and triggering the series of powerful

phreatomagmatic blasts that destroyed the world famous Pink and White Terraces. Ultimately, 17 km of fresh fissure developed – not actually a continuous crack in the ground, but a chain of closely spaced and in some cases overlapping craters, at least 50 of which formed along the original 8 km segment (Nairn & Cole 1981). By dawn the eruption ended even more abruptly than it started. In the meantime, rapid accumulation of ash on the rooftops of terrified and sheltering local residents caused most of the 108 fatalities of the eruption as those roofs collapsed. Four Maori villages were totally destroyed.

Most of the Tarawera vents erupted showers of cinder in ordinary Strombolian-style, pulsating explosions. Four vents, however, produced high-standing eruption columns, depositing a large volume of scoriaceous basaltic pyroclasts close to the vents, many cored with rhyolitic lithic fragments, and casting air fall debris over 10,000 km². Much of this debris contributed to construction of high rims within 400 m of the vents, mostly via fallout from the margins of the plumes. Rates of proximal accumulation ranged from 1.5 to 13 m/h, with substantial amounts of material welding to form agglutinate that fed short-range clastogenic flows sluggishly moving back toward vents.

The Tarawera ejecta dispersal pattern is, however, somewhat unique for Plinian air falls. In typical Hawaiian and Strombolian eruptions, air fall deposits thin to one-half their proximal, or maximum isopach thicknesses within 20 m or so of a vent, while for silicic Plinian eruptions, this half-distance is 4–100 km, depending upon the magnitude of the eruption. The Tarawera fall half-distances lie *between* these values, possibly because of mixing of column-related fall material with much more localized Strombolian fall out to produce multi-sourced fall beds (Sable et al. 2006). Cinder and ash are the sole products of the Tarawera eruption, like at Hekla. No pyroclastic flows or surges developed.

DIRECTED BLASTS

One of the most powerful explosive phenomena associated with volcanic activity are **directed blasts**, incredibly destructive currents of hot gases and entrained material that can move at near supersonic speeds across large areas on the flanks of “exploding” volcanoes, when magma chambers explode almost instantaneously, rather than releasing their energy gradually through constrictive summit vents. These highly destructive blasts cause widespread mayhem, but leave relatively sparse deposits, so are only recognized around young volcanoes where eye-witness accounts or devastated forests are left to record their effects. The May 18, 1980 Mount St Helens directed blast devastated an area of about 600 km², but its varied deposits were much less than 1 m thick in most places (Hoblitt et al., 1981). Directed blast mechanisms will be discussed in detail in the next chapter.

HYDROVOLCANIC ERUPTIONS

Hydroexplosions result from the sudden generation of steam where water comes in contact with hot rock or melt, as when molten lava rises through water-saturated rocks or is extruded into a lake or the ocean. **Phreatic** and **phreatomagmatic eruptions** are both end-member types of hydroexplosions, the former involving steam only, and the latter steam + magma.

Phreatoplinian eruptions are especially large and powerful phreatomagmatic eruptions whose dispersal areas ($0.01 T_{\max}$ of Walker, 1973) exceed 50 km^2 .

Explosive eruptions triggered by the heating and expansion of external, non-magmatic water into steam span the scale from those originating at shallow depths underwater to sub-aerial explosions triggered by geothermal steam explosions. Lava flows pouring over lakes or marshes can also produce violent eruptions and explosion craters, such as the “pseudo-craters” of Myvatn [77], Iceland. Ultravulcanian phreatic blasts merely discharge older rock material, while phreatomagmatic eruptions also eject vitric debris. For instance, some of the maars in the Rhine region of Germany are surrounded by low block-and-ash rims constructed from fragments of the surrounding sedimentary rocks. The explosions that formed them may have been wholly phreatic; but the presence of magmatic ejecta in some otherwise similar cones nearby suggests that magmatic gases played a part in the explosions that formed most of the cones, even though at some no molten material reached the surface. The low, wide rims surrounding Ubehebe craters [38], a popular tourist destination at the northern end of Death Valley, California, consist largely of accidental ejecta, but also contain a few volcanic bombs, showing that although the explosions that formed them may have been very largely phreatic, magma and magmatic gases were also involved. Such craters may be underlain by diatremes at depth (Chapter 4).

The explosiveness of all types of eruptions increases where rising magma comes in contact with groundwater at shallow depths. The effect is most conspicuous in the case of Hawaiian or Strombolian-type eruptions that otherwise would be only mildly violent. The nature of the Laki [76], Iceland flood-basalt eruption, described briefly in Chapter 6, strongly suggests that its explosiveness was at least partly due to the boiling of shallow groundwater. Another example is the 1960 flank eruption of Kilauea, which began with the opening of fissures and the sinking of a shallow graben in an area where groundwater lay only about 25 m below the surface. During the first few days of the eruption violent, black ash-laden steam was ejected, with much more explosive activity than that of typical Hawaiian eruptions.

Submarine eruptions in shallow water or near the margins of oceanic islands usually involve explosive hydrovolcanic activity (Fig. 7.22), and commonly precede the formation of new volcanic islands. Explosive submarine eruptions involving hydrovolcanic activity will also be discussed in Chapter 12, but since many of these eruptions transition the ocean-land boundary, we shall provide one good example here, that of Capelinhos [65] at the western end of Fayal Island in the Azores in 1957–8 (Cole et al. 2001). The Capelinhos eruption began in September, 1957 when small earthquakes were felt and brownish-yellow, discolored water appeared a kilometer offshore. Within two weeks incandescent fragments were being ejected from the sea explosively, and a new island quickly formed. By late October the new island stood 80 m above sea level, but eruptive activity was episodic, and island growth was irregular as explosive hydromagmatic activity, characterized by jagged, **rooster-tail** or **cypressoid** ejections of black, ash-laden steam jets (Figs. 7.22, 7.23) continued from several independent vents. Convecting “cauliflower” clouds of white steam rose kilometers over the entire eruptive zone as vents migrated eastward, toward Fayal. As vents became better sealed from seawater, activity became less explosive, and generated Strombolian fountaining and minor lava flows. By 1958 the emerging tuff cones had joined the island to form a new peninsula. Tephra blanketed most of Fayal, destroyed hundreds of homes, ruined agricultural fields, and led to a major population



Fig. 7.22 Hydrovolcanic eruption that is burying the (fortunately uninhabited) island of Hunga Ha'apai, northwest of Nuku'alofa, Tonga, with tephra and blocks on March 18, 2009. The island represents the subaerial rim of a large submarine caldera in the very active Tonga volcanic belt, on the western margin of the Tonga trench. Large blocks falling from the 500 m-high cloud can be seen impacting on the sea. Photo by Lothar Slabo/AFP/Getty Images.

exodus. Over 2 km² of new land was added to Fayal, but the pyroclastic rocks are poorly consolidated and weak, and over half this land has been eroded away in the past 50 years.

Less than a decade after the Capelinhos eruption, a very similar outburst took place in the shallow sea off the southwest coast of Iceland, leading to growth of the new island of Surtsey between 1963 and 1967. This well-studied event gave rise to the name for the characteristic style of phreatomagmatic activity associated with eruptions through shallow water bodies – **Surtseyan eruptions** (Thordarson 2000).

Phenomena associated with Surtseyan eruptions are not restricted to oceanic volcanoes, and good examples are also found wherever volcanic activity occurs beneath fresh-water lakes (Godchaux et al. 1992) or water-filled volcanic craters. Renewed eruptive activity beneath these crater lakes can violently eject their waters in a Surtseyan manner, as New Zealand geologist Peter Otway and a colleague discovered on snow-covered Ruapehu volcano [145] in 1971. Ruapehu is a dangerous volcano, with a summit crater lake known for a history of hydrovolcanic explosions accompanied by destructive lahars. Their team had been dropped off by helicopter near the summit to monitor activity, and were routinely surveying when part way through their work they noticed puffs of steam rising from the middle of the grayish-green, sulfurous lake. The steaming patch suddenly exploded, and jets of black ash steam and large angular blocks shot upwards. Peter, who was on the snow-covered rim of the crater, pulled out his camera to take a snapshot, when suddenly the explosions increased in violence; Ruapehu's crater lake had begun a series of violent hydrovolcanic explosions, and the New Zealanders were directly in the path of ejecta. Each had only a few seconds to grab ice axes and dig in, lying flat to the ground and holding on for dear life. A torrent of muddy water cascaded down, mixed with angular blocks that made sharp thuds as they impacted nearby. The water

was fortunately not scalding, and neither man was swept away during their three minutes of terror. John Latter and an assistant were surveying on the other side of the crater outside the impact apron, and were able to photograph the explosions from 300 m away (Fig. 7.23). Analysis of his movie film showed that the cypressoid ejecta jets blasted out at speeds up to 150 m/sec. towards Otway. Latter was convinced that his colleagues had been killed. Down below, observers knew that an eruption had started as the seismographs were going wild. A helicopter pilot was called, and maneuvered above clouds to see a column of convecting ash and steam obscuring the summit. He feared he had just “lost four geologists,” but approaching closer, he found the mud-covered survey team and courageously rescued them from further danger. As Surtseyan eruptions go this one was relatively small – had pyroclastic surges been generated, the field party would have been wiped out. The summit glacier was left mantled with a black, thin bed of muddy ash, and the ejected water poured down the mountainside generating a lahar (Chapter 11). No one was injured, though the mudflow split a restaurant in half.

Nuclear engineers concerned with reactor safety have long been interested in the potential for explosions as coolant water mixed with molten material, finding that the degree of explosivity depends critically upon the volumetric ratio of melt (the fuel) to water: the **fuel-coolant interaction ratio** (FCI) (Sandia Laboratories 1975). Extending this research to magma-water interactions, experimental work further suggested that hydrovolcanic eruptions appear to be most explosive when with one part magma can mix well three parts water (FCI = 1 : 3; Wohletz & McQueen 1984). Magma rarely interacts with “pure” water, and factors such as vent geometry, fuel-coolant interaction and suspended aqueous sediment load can play critical roles too (White 1996). In any case, Strombolian eruptions appear to grade into Violent Strombolian and finally Surtseyan eruptions with increasing FCI.

The range in magma-water fuel-coolant ratios is reflected in the vesicularities of individual pyroclastic fragments. Explosions triggered purely by anhydrous magmatic degassing tend to produce pyroclasts such as pumice whose vesicularities are clustered narrowly toward higher percentages (70–80 percent of sample volumes). The steam-rich magmatic blasts of the 1800 year old Rotongaio Ash, New Zealand, in contrast, show vesicularities across a broad spectrum, from 20 to 60 percent. This seems to be typical of eruptions in which expanding steam, rather than magmatic degassing, initiates an explosion (Houghton 1993). The lower level of vesicularity in hydrovolcanic juvenile ejecta is a function of the power involved in gas expansion. Because the coefficients of expansion of magmatic gases such as CO_2 , H_2SO_4 , and H_2S are much lower than those of water flashing to steam, it is possible for numerous non-hydrous bubbles to form in the magma before it explodes. Expanding steam, on the other hand, shreds much of the melt before such initial fine-scale vesiculation can take place (Fig. 7.24).

The shapes and mixtures of ash and fine lapilli fragments ejected by Surtseyan blasts can provide important clues about the phreatomagmatic eruption process. For example, fragments showing mixed angular and subrounded edges with mud coatings are likely to have been recycled by falling back into a vent for later re-ejection a second or even a third time. Subrounded grains indicate ejection from melt that has not yet developed a crust, whereas angular grains result from solidification followed by explosive fragmentation of a crust (Houghton 1993). Because collapse of conduit and crater walls is much more common in wet eruptions than dry ones, perhaps due to the enormous lateral pressure pulses associated with shallow steam blasts, there tends to be an increase in the accidental lithic contents of hydrovolcanic deposits



a)



b)

Fig. 7.23 Hydrovolcanic explosion in the summit crater of Ruapehu volcano New Zealand – May 8, 1971. a) Initial blast from lake surface about 3 secs after initiation – “rooster tail” ejecta trails radial to explosion source rise about 300 m. above crater lake surface. b) Photograph taken 14 seconds after (a). This is a new, larger blast that has ripped through the first explosion column, and later sent a steam column to 8 km height. This is the blast that nearly killed observers on the south rim of the crater. Photos by J. H. Latter.

Fig. 7.24 Contrasting vesicularity and fragmentation of volcanic material according to explosion source. Houghton (1993).

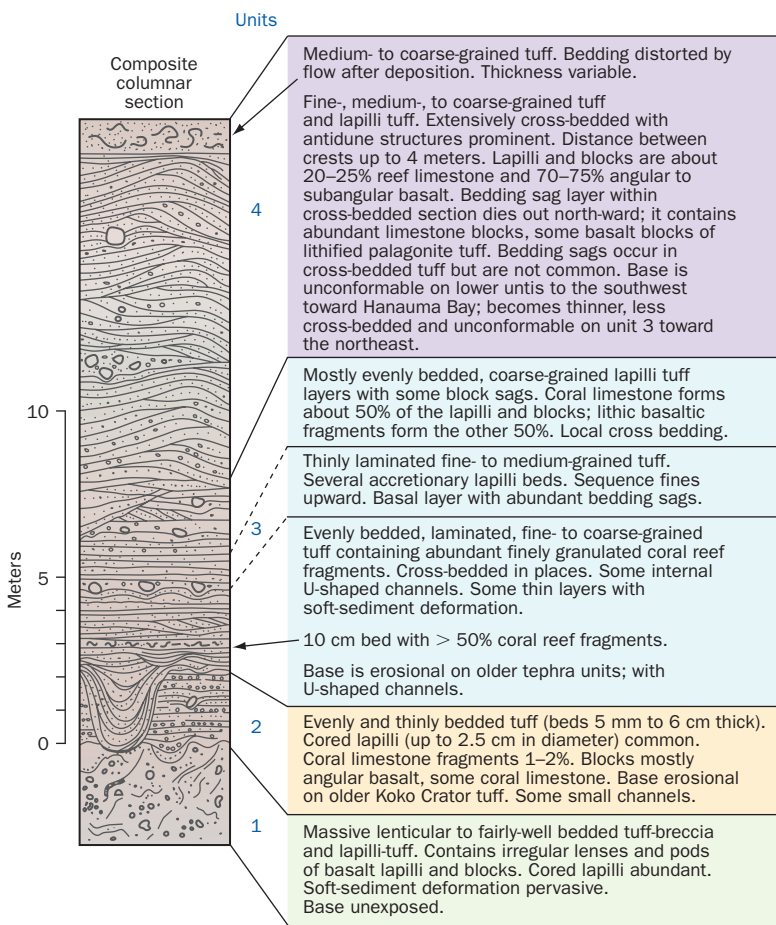
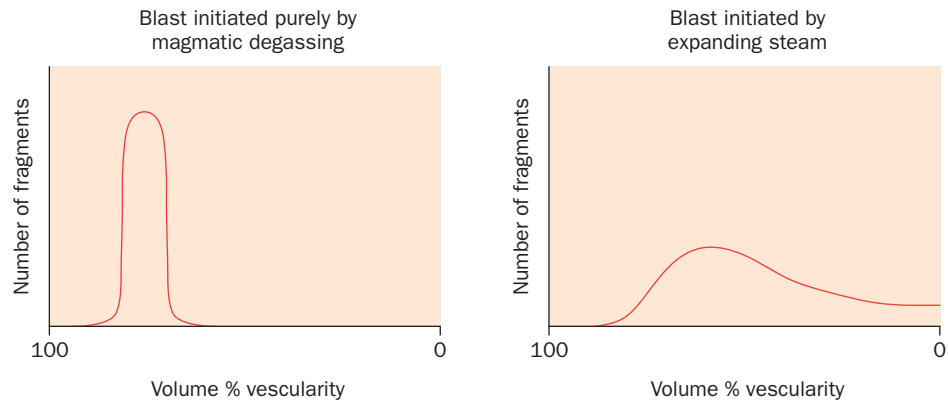


Fig. 7.25 Stratigraphy of the Koko Head tuff cone deposits (Oahu Island, Hawai'i) – products of explosive hydrovolcanism and surge processes accompanying the formation of a littoral tuff cone. From Fisher (1977).

with increasing magma-water interaction (Romagnoli et al. 1993). In fact, variation in the lithic concentration of layers often provides better evidence of slight changes in magma-water interaction than simple fragmentation.

On land near shorelines, where groundwater levels are quite shallow, hydromagmatic blasts are common where magma approaches the surface, and distinctive vent structures called **ash** and **tuff cones** result (Figure 7.25). In addition to the aspects of wet tephra deposition already mentioned, internal stratification of these edifices can show great structural complexity.

PYROCLASTIC DENSITY CURRENTS (PDCs)

As has been discussed, pyroclastic density currents are potentially deadly, ground-hugging torrents of volcanic ejecta mixed with gases that can pour down volcano flanks on many different scales, from the minor ones described at Galunggung (Chapter 1) to devastating outpourings that can blanket thousands of km² in deposits hundreds of meters thick – they are potentially the most devastating phenomena

generated by large explosive eruptions. Because of their violence, geologists cannot directly observe the internal processes involved, but can only infer them from external field observation of active currents, through modeling, and by careful study of their deposits.

As a simple illustration of the phenomena involved, pouring a handful of flour onto the ground might impress (and perhaps distress!) you by how far and how easily the powdery white mass travels. The fine, light-weight particles trap air as they approach the surface, mixing with it to produce a highly mobile, air-plus-solid mixture that rushes across the floor very much like a moderately viscous fluid. This experiment is a quick and easy demonstration of how PDCs work (Colin Wilson, pers. comm. 2006). Instead of flour, of course, a typical PDC consists of various kinds of ejecta, including, blocks, ash, and in many cases pumiceous lapilli. Many PDCs are extremely hot; hot enough to glow incandescently (hence the French name: **nueés ardentes**). The heat, in fact, helps buoy and mobilize the whole mass through the expansion of trapped gases. The mixture of gas, air, and solid matter varies in these ground-hugging eruption clouds, from rarefied masses having the consistency of dusty sandstorms, to denser media that spread out like fast-spreading sand or flour avalanches choked with abundant lithic blocks.

PDC deposits are commonly classified as either of **pyroclastic flow** or **pyroclastic surge** origin, although the processes that form them are complexly interrelated, and gradational interfaces between these end members are common and difficult to classify rigorously (Branney & Kokelaar 2002). The internal complexities of pyroclastic surge deposits (cross-bedding and internal erosion features) suggest that deposition of these PDCs involve turbulent flow, whereas pyroclastic flow deposits are more homogeneous and likely reflect more laminar, sheet-like flowage.

In more powerful volcanic eruptions, PDCs transport ejecta of all sizes. Topography exerts a strong influence on the course of these surface-bound currents, which generally follow major valleys and dissipate against opposing mountain slopes, although extremely powerful currents can surmount high ridgelines. The deposits left by PDCs are distinctively different from airfall and ballistic accumulation, and different kinds of PDCs leave different kinds of deposits, as illustrated in Fig. 7.26. It is worth spending a few minutes studying this figure before we move into exploring pyroclastic flows and surges in greater detail. But perhaps throughout it is wise to bear in mind the words of Carey (1991, p. 39) who concluded “It is . . . unrealistic to hope that all flowage deposits can be conveniently classed into either category and that a single set of transport and depositional processes would apply to each case.” Nature throws us many instructive ambiguities!

PYROCLASTIC FLOW DEPOSITS

Two general categories of pyroclastic flows exist; **block and ash flows**, which are especially characteristic of Vulcanian eruptions, and the much larger and energetic **ash flows**, which more commonly occur during Plinian eruptions. Block and ash flow deposits tend to be highly localized around volcanoes, while ash flows lay down much thicker, more widespread sheets

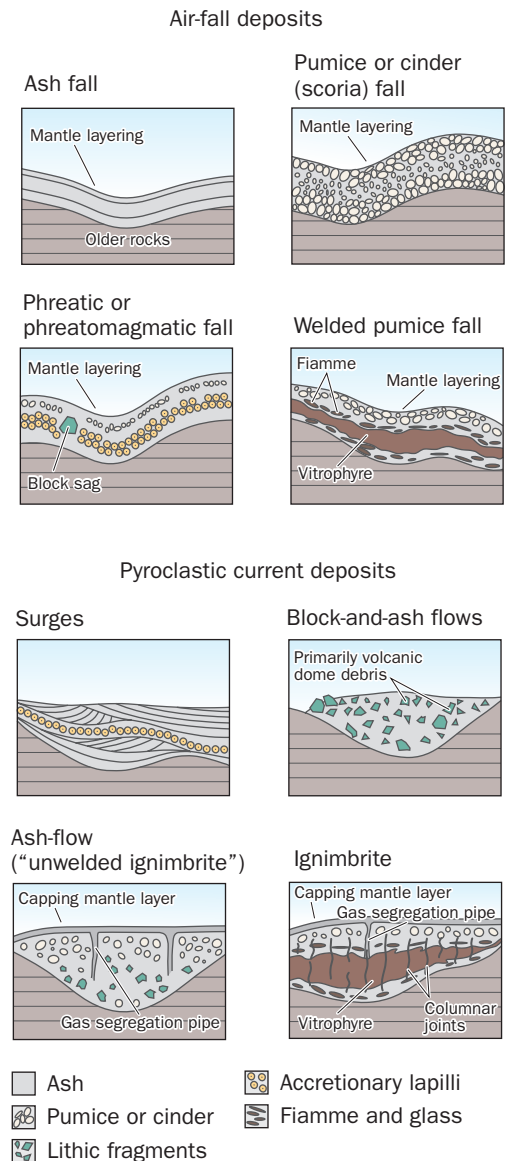


Fig. 7.26 Some diagnostic features of pyroclastic deposits. After McPhie (1993).

of ejecta, most commonly around highly explosive silicic volcanic centers. In fact, volumes of individual flow deposits range over six orders of magnitude (Smith 1979) from the low-range block and ash flows (mostly less than 1 km^3), to single massive ash flows sheets exceeding 1000 km^3 in volume.

Block and ash flows

Block and ash flows are a category of pyroclastic flows that are derived from the explosive disintegration of growing domes (Chapter 9) or from the margins of steep sided active silicic lava flows. Their deposits differ from most other PDCs in that they typically include little or no pumice and contain abundant angular blocks derived from source domes, embedded in glassy volcanic ash (Fig. 7.27). Unlike many ash flows, they also show little or no welding. Lithic clast sizes grow finer and less abundant toward the distal ends of deposits, similar to ordinary rock avalanches. Flow margins are very steep, but the tops are typically gently sloping and broad with hummocky surfaces of poorly sorted to extremely poorly sorted material. When a typical block and ash flow is emplaced, its sides commonly come to rest before its medial mass does, creating **lateral levees** as much as several meters high as the flow continues draining downslope. On gentler ground, the front of the flow also tends to slow before the central mass, resulting in a bow-like terminal mound rippled from compression by the time everything comes to rest. In map view block-and-ash deposits have a smooth, lobate or spatulate shape, with the “spoon handle” extending upslope. Block-and-ash flow deposits formed from the explosive collapse of actively growing domes tend to have a larger proportion of fine ash relative to blocks than in deposits left by gravitational collapse of older domes (Freundt & Bursik 1998).



Fig. 7.27 Block and ash flow along the Gendol River, Merapi volcano, Indonesia. Note the matrix-supported angular blocks from the summit dome and the concentration of large blocks at the base of the flow. Similar pyroclastic flows and lahars have killed thousands of people on Merapi's lower flanks in recent times. USGS photo by J. P. Lockwood.

These deposits rarely exceed 2 km³ in volume or spread more than a few km from their sources. We'll tell you more about their origin in the next chapter.

Ash flows

Ash flows are extremely powerful PDCs consisting largely of ash and pumice mixed with variable amounts of lithic material. Their deposits are distinguished from block and ash flows primarily because they tend to be more pumiceous. The term **ignimbrite**, derived from Latin, ("fire-rain") was introduced by Marshall (1935) who originally applied it to describe only those ash-flow tuffs in New Zealand that showed **welding**: the fusing together of very hot ash particles and other ejecta shortly after emplacement to create a hard, brick-like or glassy mass. Since then, the word has acquired broader connotations and now generally refers to all ash flow deposits irrespective of their degree of welding. Ignimbrites from individual eruptions can form great sheets across hundreds or even thousands of square kilometers (Fig. 7.28). The largest ash flow sheets form gently sloping uplands around source calderas tens of kilometers wide. Some are so thick – up to hundreds of meters – that they cover all the older highs and lows in the topography across which they erupted, and are said to be **landscape burying**. Marshall (1935) and Macdonald (1972) referred to these enormous accumulations as

Fig. 7.28 Flat landscape typical of areas buried by ash flows – the Valley of Ten Thousand Smokes, formed by the June 1912 Novarupta eruption on the Alaska Peninsula, in what is now Katmai National Park. This ignimbrite bed covers approximately 100 km², and is as much as 210 m thick. USGS photo by Robert McGimsey.



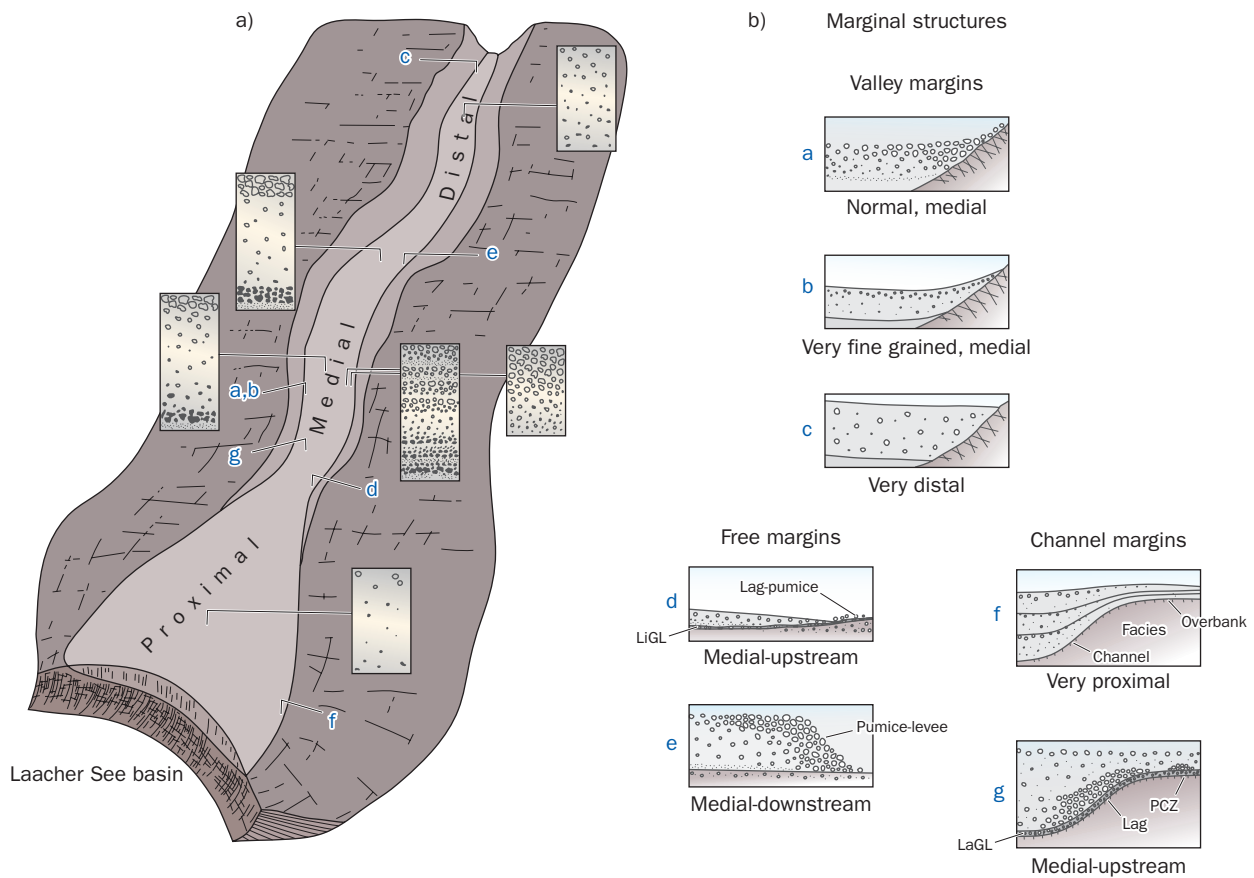
Fig. 7.29 Pyroclastic deposits from the 13,000 year-old Laacher See eruption, as exposed in the Wingertsbergwand quarry, Eifel District, Germany. The deposits reflect the great complexity of the Laacher See eruption, and consist dominantly of surge deposits (when water entered the eruptive vent) and lesser pyroclastic flow and Plinian fall deposits when purely magmatic activity was involved. Photo by Björn Osterloh.



rhyolite plateaus. Good examples are the Yellowstone Plateau in Wyoming, and the tableland around Lake Taupo in New Zealand. Ross and Smith (1961) wrote a classic resource for the field identification and petrographic interpretation of ignimbrites – a paper still useful today.

The main unit of many, if not most, ignimbrites is characterized by a massive, poorly-sorted mixture of pumice lapilli, lithic fragments and juvenile ash, though owing to density contrast, pumice fragments may be concentrated toward the tops of individual sheets with lithic fragments towards the bottom. Variations in component clasts and textures can be quite informative about the emplacement history of an ignimbrite. Some deposits show faint traces of bedding, either from sudden change in the supply of material to a gradually accumulating bed from laminar (sheet-like) flow during deposition, or from brief intervals in deposition during which fall ejecta accumulates atop flow surfaces (Wilson & Hildreth 2003). Changes in sparse lithic fragment composition may be all there is to show of a break in eruption between two pulses of ash flow deposition. From a distance of even a few meters, this compositional difference may not be obvious. One has to back away further, or observe the outcrop at a certain angle of lighting, or under dry conditions to observe the subtle layering that may be present. What in fact are two stacked ash flow units may appear to be a single massive sheet in some outcrops (Wilson & Hildreth 2003).

A good example of the sorting and grain size variations possible in ignimbrites may be seen in the deposits of the Laacher See [82] eruption (Fig. 7.29). Laacher See was a very large, VEI = 6–7 eruption about 13,000 years ago that formed a caldera 3 km in diameter in the Eifel District of Western Germany. We do not often think of Central Europe as being volcanically active – but quaternary volcanism has occurred here. The Laacher See eruption produced Plinian-phreatomagmatic deposits that spread tephra over much of northern Europe from Spain to Germany. Both pyroclastic flows and surges formed near the vent. The Plinian flows were generally warmer (300–500°C) than the “water-cooled” phreatomagmatic ones (less than 200°C) but are unwelded. Many of these flows were confined to steep-sided valleys, which they filled to overflowing within a few kilometers of the vent. Freundt and Schmincke (1986) identified three zones in these valley-confined flows – “proximal,” “medial,” and “distal” – each displaying a unique set of depositional features. They also identified eight characteristic marginal deposit types, each showing the variable influence of changing flow parameters and topographic confinement on the sorting of loads at the edges of the PDCs (Fig. 7.30).



In many ignimbrites the abundance of lithic clasts makes portions of them resemble ordinary block-and-ash flows. Extreme examples have been recorded in which lithic fragments make up nearly half of an ignimbrite, reflecting widening of the vent by blast-erosion, collapse of conduit wall rock during eruption, or most catastrophic of all, caldera collapse. Three km³ of the 60 km³ 160,000-year old Kos [86] ignimbrite in the Greek Aegean, for instance, consists of lithic fragments (Allen 2001). Such lithic clasts make up 6 km³ of the Mazama Tuff in Oregon (Bacon 1983), and 7 km³ of the Bishop Tuff (Hildreth & Mahood 1986). In each case, there is a dominant concentration of lithic breccia in single layers near the base of the ignimbrite, with most rubble in fines-depleted facies concentrated near the vent. Proximal breccia layers such as these, ranging from 1 to 20 m thick, are termed **co-ignimbrite lag breccias**. Both lithic and poorly vesicular juvenile blocks may be present in the breccias, which may feature narrow, laterally localized accumulations of larger fragments called **breccia trains**. Individual lithic blocks often exceed 50 cm in diameter, and may approach several meters in size. Although some larger breccia-rich deposits stretch distally as far as 20 km from their source, most are restricted to within just a few kilometers (Wright & Walker 1977).

In addition to the sorting characteristics described above, ignimbrites typically show evidence of the escape of gases trapped within them at the time of emplacement. **Gas segregation pipes** are narrow, vertical “trails” left by the concentration and ascent of hot air and

Fig. 7.30 a) Proximal to distal variation in valley-fill pyroclastic flows at Laacher See, Germany; b) marginal deposits, with blue letters keyed to schematic localities shown in figure (a). After Freundt and Schmincke (1986).

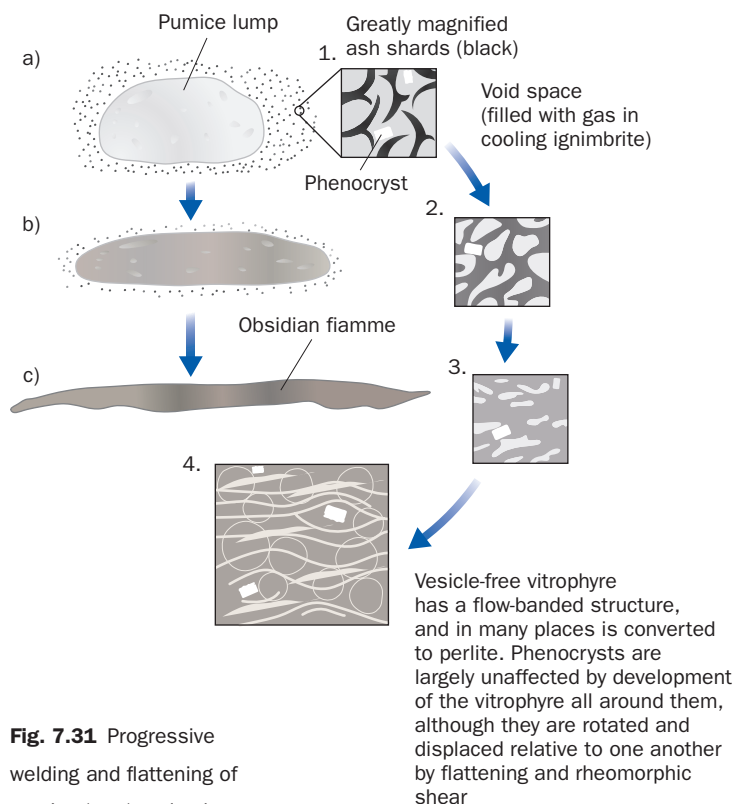


Fig. 7.31 Progressive welding and flattening of pumice (a–c) and ash (1–4) fragments in ignimbrite.

other volatiles through loose, settling ejecta (Fig. 8.20). They are commonly marked by distinctively coarser sorting and discoloration, and in places are cemented by siliceous sinter. Escaping gases and steam help cool an ignimbrite, though to what degree is not well known. Interaction of released high-temperature volatiles with the atmosphere contributes to oxidation reactions, which commonly redden the surface and uppermost parts of ash flow sheets (see p. 214).

Ignimbrite welding is shown in thin sections by the fusing-together of the molten edges of ejecta fragments. As vesicles close up, the gases within are expelled and may stream up into overlying gas segregation pipes or disperse more generally. Flattened, compressed pumices fuse under mounting pressure and temperature into irregular lenses of jet-black obsidian, a feature named **fiamme** (“flames”) by Italian volcanologists. In cross section, fiamme appear as conspicuous black lenses, often with fuzzy ends, in a gray or brown matrix. Fiamme are usually elongated in directions parallel to deposit surfaces. Geologists call this distinctive streaked structure **eutaxitic** (Figs. 7.31 and 7.32).

Fig. 7.32 Fiamme in the Bishop Tuff, California. These elongate glassy clasts were once sub-angular to subrounded pumice fragments that were compressed and stretched during internal flow and compaction of the ash-flow matrix. Photo by J. P. Lockwood.



McBirney (1965) described an unusual occurrence in several Central American ash flow tuffs in which fiamme are restricted to areas where the ash flows came to rest on river-laid sand and gravel that may have been saturated with water at the moment of burial. McBirney suggests that water vapor filtering upward through the hot ash and pumice beds was absorbed by glassy fragments, locally lowering their melting temperatures sufficiently to allow the glass to remelt and aggregate into fiamme.

The zone of most intense welding is usually somewhat below the middle of pyroclastic flow deposits, where heat was retained for the longest time following eruption. There, a layer of vitrophyre (phenocryst-bearing volcanic glass) up to several meters thick commonly develops in the days and months following an eruption, and may develop columnar jointing on cooling. The boundaries of the original ash particles welded together are often still clearly discernible under the microscope, as intricately curving and convoluted lines marked by stains or granules of iron oxide. A vitrophyre layer may be very extensive and retain rather uniform thickness over broad areas; but in other instances vitrophyres are markedly lenticular and may pinch out, for example from 10 m to 30 cm or even to zero, within horizontal distances of less than a hundred meters.

The degree of welding in ignimbrites varies with several factors, the principal of which are the thickness of the flow, its temperature when it came to rest, and the amount of gas it contained. Laboratory experiments show that the minimum temperature of welding of “dry” glass shards is probably about 750°C, but slight welding may take place in the presence of gases at temperatures as low as 535°C (Smith et al. 1958; Sheridan & Wang 2005). A landscape-burying ash flow tuff may be unwelded where it is thin over hills and densely welded where it is thick over valleys. That thickness is not the only factor is shown by the fact that thin flows may be thoroughly welded, whereas some thick flows show little or no welding at all. The Walcott Tuff in Idaho is only 7 m thick but is densely welded, whereas the Battleship Rock ignimbrite in New Mexico shows no dense welding in a cooling unit 80 m thick (Smith 1960). In some deposits the degree of welding decreases with distance from sources, reflecting a cooling of the ash during emplacement. But in the Owens Gorge area of the Bishop Tuff, welding actually increases 20–40 km away from the vent, mostly because the Tuff accumulated to greater thickness in these areas. The tuff erupted as multiple ash-flows in quick succession. While the earliest ash flow encountered rugged terrain, which slowed it down, it smoothed out the landscape to make it easier for later flows to travel farther (Wilson & Hildreth 2003). Calculations show that in 100 m thick sheets with emplacement temperatures of 850°C, dense welding may be completed within a week; in caldera-fill deposits 1 km thick with initial temperatures of 650°C, welding may continue for about a year (Bierwirth 1982).

When ash flows erupt in rapid succession, the stack of flows may at first have about the same temperature throughout the entire mass and cool as a single body, constituting what Smith (1960) coined a **cooling unit**. Freundt and Schmincke (1986) coined a parallel term, **eruptive unit**, to designate a sequence of closely related pyroclastic flows not hot enough to weld. In the San Juan Mountains of Colorado, the Bachelor Mountain Rhyolite is a series of ignimbrites that issued from vents associated with a caldera near the town of Creede. At a distance from the vents, the formation consists of three separate members, but close to the caldera it consists of a single cooling unit almost 1 km thick (Steven & Lipman 1976). The accumulation of ignimbrite layers near the vents was so nearly continuous that one did not have time to cool appreciably before the next one piled atop it, but only occasionally did exceptionally

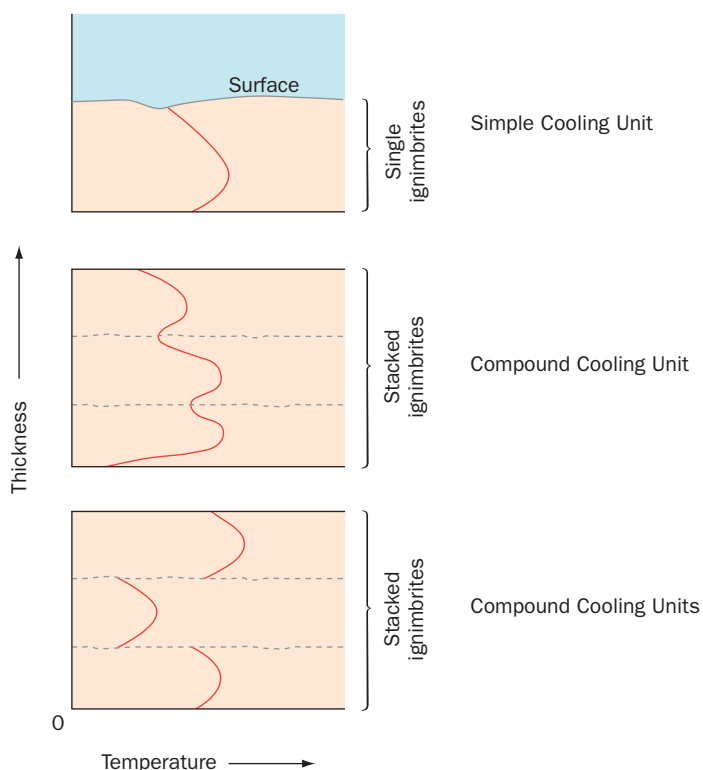


Fig. 7.33 Cooling curves show the temperatures inside an ignimbrite just as it has settled and begun to cool. The curves can be reconstructed to varying degrees of precision based upon degrees of welding observed in the field and paleomagnetic studies. The three end-member cooling unit types are shown above.

separate cooling profiles. The contacts between each ignimbrite in a composite stack may be highlighted by the development of soil horizons, or even deposition of sedimentary layers.

This identification of cooling units can be challenging, and it is wise to be cautious. Wilson and Hildreth (2003) mapped Bishop Tuff welding in the Owens Gorge area, where, as mentioned above, multiple ash flows accumulated in quick order. Welding does not correspond neatly to the contacts between the separate ash-flow sheets in this deposit, but cuts across them in places. In some exposures two welding bands appear in the same vertical section, while in others welding merges into a single broad zone. There is no clear correspondence between welding and the total thickness of the depositional package, and the densest welding, somewhat inexplicably, appears to correspond to steeper slopes. Wilson and Hildreth ascribe this pattern to irregularly increasing overall thickness of the ash flow stack during the eruption, after cooling had already commenced in the lowermost deposit. They also note that emplacement temperatures changed during the eruption, due not only to flux in primary magma temperatures, but also to variable cooling during eruption and transport of ejecta. For example, ash-flows generated by convective column collapse are likely to be cooler than ash flows from the same host magma generated by boil-over (Chapter 8). Paleothermometry studies showed that the lowermost ignimbrite of the Bishop Tuff cooled from magma at a temperature of 723–737°C, while the magma of the uppermost sheet was emplaced at 749–790°C (Wilson & Hildreth 1997). Intensive volatile streaming moistened the ejecta near the surface of the Tuff as the uppermost ash flow settled into place, further reduced melting temperature, softening the glassy ash particles and causing welding to take place at very shallow levels, largely unrelated to thickness of overburden.

voluminous flows reach the distal areas (Ratte & Steven 1967). Other groups of ignimbrites that accumulated within some of the calderas of the San Juan region formed single cooling units as much as 1.5 km thick that are almost entirely densely welded (Lipman, 2006).

Smith (1960) and later researchers (e.g., Christiansen 1979; Reihle et al. 1995) have distinguished several kinds of cooling units. A solitary ash flow with a normal cooling profile, as shown in Fig. 7.33, constitutes a **simple cooling unit**. Heat loss is somewhat more rapid through the top of the ash-flow than through the base, given the relative thermal conductivities of convective air versus ground at ambient temperature. A **compound cooling unit** is shown when ash-flows stack together rapidly, as in the case of the San Juan, Colorado ignimbrites mentioned previously, with **welding maxima** and **minima** marking the cores and contacts of the separate ash sheets. Wright (1981) provides an excellent study of a compound cooling unit, the Rio Caliente ignimbrite in Mexico. **Composite cooling units** are separate but related ignimbrites that accumulate more slowly, each showing

The colors of ignimbrites vary according to composition and degree of welding. Poorly welded silicic deposits are light gray or even white in color. Ignimbrites emplaced at high temperatures will develop characteristic pink tops – products of oxidation in contact with air (Fig. 7.34). With progressive degrees of welding, they acquire first a pink or pale brown coloration, then orange-brown, red, and with complete fusion to glass, a black tone. In general, hotter ash flows will tend to form darker, more strongly-colored tuffs. Highly welded ignimbrites also develop columnar jointing as they cool. The joint planes tend to be less planar than those of columnar basalt, and they are commonly more widely spaced. For instance, cooling columns in the Los Chocoyos Ash, Guatemala, and the Bandelier Tuff, New Mexico are spaced as much as a meter apart. The more strongly welded the deposit – the better developed the jointing.

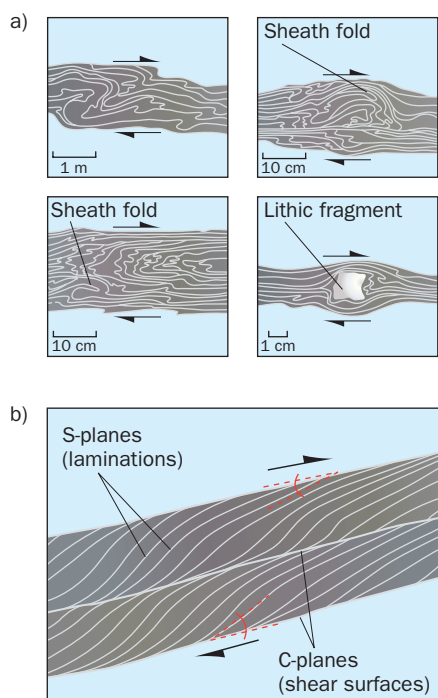
Welding is not a phenomenon unique to ash flows. Fallout deposits may rarely be welded from compaction of very hot material near vents. The dacitic 3600-year old Thera and Therasia tuffs of Santorini, Greece are outstanding examples (Sparks & Wright 1979). In other places, lava flows or other very hot deposits may weld underlying fall material. For example, in south-central Washington, where the Pomona Basalt (an extensive lava flow of the Columbia River flood basalts) overlies a mantle bed of vitric tuff, the tuff is welded at the contact with the basalt in many places, to thicknesses of as much as a meter. The texture and minerals found in the tuff are identical to those of welded ignimbrite (Schmincke 1967). Similar welded air-fall tuffs are recorded beneath ignimbrites in Arizona (Enlows 1955), in Yellowstone National Park (Boyd 1961), on Tenerife in the Canary Islands (Soriano et al. 2002) and adjacent to a flow of rhyolite lava in Nevada (Christiansen and Lipman 1966).

RHEOMORPHIC IGNIMBRITES

As a very hot ash flow settles, it is held in place by the microscopic interlocking of countless tiny, highly angular pyroclasts – a sort of tenuous strength found in all deposits of loose material called **pseudocohesion**. But as welding takes place this interlocking weakens, and the whole ash and pumice bed begins sliding even on very gentle slopes, lubricated by internal films of molten fluid. The most densely welded vitrophyre-forming portions flow like sluggish lava, shifting and shearing over days or even weeks following an eruption in a manner akin to the gravitational creep of soils on slopes or to the flow of glacial ice. Ritmann (1958, 1962) coined the term **rheomorphism** (“deformation-shaping”) to describe this late-stage movement, which can develop a very distinctive set of structures (Branney & Kokelaar 1994), but which also may create a structure closely resembling an ordinary high silica lava flow (Henry & Wolff 1992). Rheomorphic adjustments may extend the original length of an ignimbrite by several hundred meters, while reducing its initial bed thickness as much as several meters.



Fig. 7.34 Pyroclastic flow from the “Super-eruption” of Lake Atitlan caldera, Guatemala, about 84,000 years ago. The pink top of this unit is characteristic of high temperature pyroclastic flow deposits, and is formed by oxidation during cooling. Photo by J. P. Lockwood.



"S-C tectonite" fabric formed by flow laminations and shear zones in rheomorphic deformation. Dark headed arrows show sense of shear responsible for rotating and shear laminations (irregularities are smoothed out in this representation in order to illustrate concept)

Fig. 7.35 a) Contorted laminations within rheomorphic glassy ignimbrite in Nevada. Arrows indicate sense of shear responsible for creating contortions. From Christiansen and Lipman (1966); b) "S-C" fabric formed by flow laminations and shear zones in rheomorphic deformation. Dark headed arrows show sense of shear responsible for rotating and shearing laminations. Irregularities are smoothed out in this representation in order to illustrate concept.

Rheomorphic welded zones and vitrophyres are characteristically laminated, with planes of lamination highlighted by concentrations of flow-oriented crystal fragments, contrasting vesicularities, and even different colors resulting from hydrothermal alteration and weathering that was guided by lamination structure. The laminations record viscous flow in the form of very tight, irregular folding, including **sheath folds**, which are curving folded structures stretched in the direction of flow (Branney et al. 2004). In some deposits intricate sets of laminations also merge into shear zones resembling those found in obsidian domes and `a` flows that have slowly cooled inward from their margins while still moving. In some instances, the presence of large stretched vesicles may play a role in the development of shearing (Pioli & Rosi 2005). Sets of laminations and related shears can form fabrics resembling the **S-C tectonites** of structural geology, in which the angle of intersection of laminations and shears reveals the sense of movement responsible for developing the structure (Fig. 7.35) (Soriano et al. 2002).

Continual flow of the rheomorphic core of a deposit will disrupt the overlying lesser welded portions of the flow that are riding piggy-back on its top. Pumice fragments may be stretched and pulled apart by late-stage deformation, with some grains undergoing rotation to open up void spaces within the deposit (Schmincke & Swanson 1967). The shearing, flowing mass beneath may intrude the loose materials atop to create laminated, dike like masses which can extend all the way to the surface of the ignimbrite. These **autointrusions** may appear as ridges or curving parapets of glassy rock as much as several meters high. Autobreccias may also develop in the border between the densely welded center of the ignimbrite and the looser superficial material, or even at the contact with the unwelded base of the deposit.

The rare welded air fall layers that show rheomorphic behavior tend to be especially potassium rich, including peralkaline rhyolites and phonolites. Such compositions have lower glass melting temperatures and viscosities than more common calc-alkaline silicic materials. Soriano et al. (2002) describe welded rheomorphic pumice fall beds as much as 50 m thick around the rim of Las Canadas caldera in the Canary Islands. They introduced the term **welding sequence** to describe the well-preserved transition, generally over intervals less than 8 m, between unwelded air fall and "lava-like" material.

LATE STAGE MINERALIZATION OF IGNIMBRITES

In addition to the post-depositional changes discussed above, other subtle changes may occur in ash flows long after the sky clears following eruptions, taking place unseen beneath the surface of fresh volcanic tephra. A pyroclastic flow, especially an ash flow, will discharge

large amounts of gas and steam as it settles and cools. The build up of vapor pressure in pockets within the cooling ejecta, notably after heavy rainfalls, can trigger small phreatic blasts creating craters as wide and deep as tens of meters, weeks or even months after the deposit settles. Thick ash flows can remain hot and be re-mobilized to generate secondary PDCs as much as four years after primary emplacement, as was learned after the Mt Pinatubo eruption (Torres et al. 1992). This long cooling history and associated slow degassing of pyroclastic flows involves the transport and precipitation of a large amount of ions dissolved in hot vapors. Cooling and condensation leads to the growth of new minerals as both sublimates and precipitates, a process called **vapor-phase crystallization**, which acts to cement the flow. This is an important first step toward hardening it into tuff. The new crystals most commonly form in the open spaces between shards or fines-depleted coarser fragments, or in pores of incompletely collapsed pumices. In the densely welded portions deeper down, where gases are completely trapped as the ash-flow welds all around them, pockets form that become lined with crystals upon cooling, including the lithophysae described in Chapter 6.

Cristobalite and tridymite, two low-pressure, high-temperature forms of SiO_2 are among the most abundant minerals formed by vapor-phase crystallization. The silica often hardens (“**sinters**”) the ash around gas segregation pipes making them resistant to erosion. The surfaces of some ignimbrites are pock-marked with fumarolic mounds up to 3 or 4 m high and 10 or 20 m across. Notable examples include the Sherwin Grade area of the Bishop Tuff and the hummocky tableland of the Mamaku Tuff west of Rotorua, New Zealand. The mounds are the egress points of gas pipes that have resisted wind and water erosion since the first years following eruption, when the airfall layers atop each ignimbrite were especially susceptible to removal. In more spectacular cases, silica-hardened gas pipes stand out as sharp, narrow pinnacles tens of meters high in deeply eroded tuff beds. Examples include the Mazama Tuff in Crater Lake National Park, Oregon, and the Bandalier Tuff within Jemez Caldera in New Mexico.

Other important vapor-phase minerals include alkali feldspar, celadonite (which can turn an ash-flow dark green as it hardens into tuff), and zeolites such as clinoptilolite. Zeolites are especially important minerals, because they can easily absorb dissolved ions by bonding with H_2O . This has made zeolite-bearing ignimbrites an attractive medium for the proposed storing of high-grade nuclear waste in the Yucca Mountain area of southern Nevada. The assumption is that any radioactive leakage from storage containers will be impeded by zeolites in the tuff. Laboratory experiments verify that zeolites readily absorb toxic radionuclides, but they can also disintegrate into colloids easily transportable by groundwater, tempering optimism about these “wonder-minerals” as potential sealants for radioactive waste (Wilshire et al. 2008).

Devitrification, or the natural crystallization of glass, is a second type of mineralization associated with cooling ash-flows. While vapor-phase crystallization takes place during the slow cooling of an ash-flow, devitrification persists long after the flow has cooled to ambient temperatures. Indeed, glass alteration may continue for tens of millions of years following an eruption, and original glass becomes increasingly uncommon in older pyroclastic rocks.

PYROCLASTIC SURGE DEPOSITS

Pyroclastic surge deposits reflect extremely turbulent flow during emplacement, and are characterized by evidence of mechanical erosion at the bases of depositional units. Internal erosion channels, unconformities, and cross-bedding are also characteristic features. Surge deposits associated with hydrovolcanic activity are characterized by abundant shards of quenched glass. Surge deposits associated with Vulcanian activity commonly contain abundant lithic blocks and breadcrust bombs.

Crowe and Fisher (1973) and Wohletz and Sheridan (1979) studied the make up of pyroclastic surge beds around Ubehebe Crater [38] at the northern end of Death Valley, California. They found that deposits near the vent consist of thin layers of coarse ash showing very gentle cross-stratification. They proposed that this structure developed wherever fast moving, turbulent gases blew ash grains into low, regularly-spaced piles, or dunes, much as Moore (1967) had observed at Lake Taal [105] in the Phillipines. They designated this type of surge deposit a **waveform facies**, with the pyroclastic dunes called **sand waves** (Allen 1982; Cas & Wright 1987). The geological term **facies** refers to an “environment or conditions of deposition.” The depositional “environment” of the waveform facies is one of high energy particle blasting. Farther from the vent, Crowe and Fisher also mapped lower energy “massive” and “planar” surge facies (Fig. 7.36).

Like normal wind-blown dunes, a typical pyroclastic sand wave has a gradual **stoss side** facing the direction from which the wind, or current traveled, and steeper **lee side** facing the direction the current moved (Fig. 7.36). The sharp, ridge-like dune **crests** are oriented at right angles to wind direction. Thin beds and laminations, representing pulsations in deposition form parallel to the lee slope and readily help define each sand wave in cross-sectional exposures. Contrasting particle sizes highlight layer boundaries, which are commonly truncated by **erosional surfaces** defining the stoss side of the sand wave (Fig. 7.37). The erosion results from the plucking or rolling of fragmental debris, often set into motion by impacting fine particles swept along in the surge cloud. The material eroded from one side of the growing dune quickly re-accumulates in the calmer pocket of air on the other, lee side, adding a fresh layer and causing the crest of the wave to advance in the down-current direction. **Unconformities**, which are simply buried erosional surfaces, may be found truncating layering in many parts of surge deposits. Scouring and deposition frequently shifts from place to place as dunes try to adjust to changing conditions. Abrasive, particle-laden winds can erode earlier-formed beds and pre-existing land surfaces to depths of as much as several meters, only to refill erosional depressions with fresh ejecta a moment later, especially vigorous on steep slopes where speeds and turbulence may be greater (see Fig. 7.25).

To describe the shape of sand waves or dunes, we customarily refer to two measurements; **amplitude**, or wave height taken from the base of a dune to its crest, and **wavelength**, as measured from one wave trough to the next. Amplitudes and wavelengths range widely within surge deposits. They vary not only in response to changing surge conditions, but in response to the surfaces on which they form. For instance, at Ubehebe Crater it can clearly be seen that the dune wavelength/wave height ratio in any given area relates directly to the angle of the depositional slope. The ratio increases on steeper slopes (Crowe & Fisher 1973).

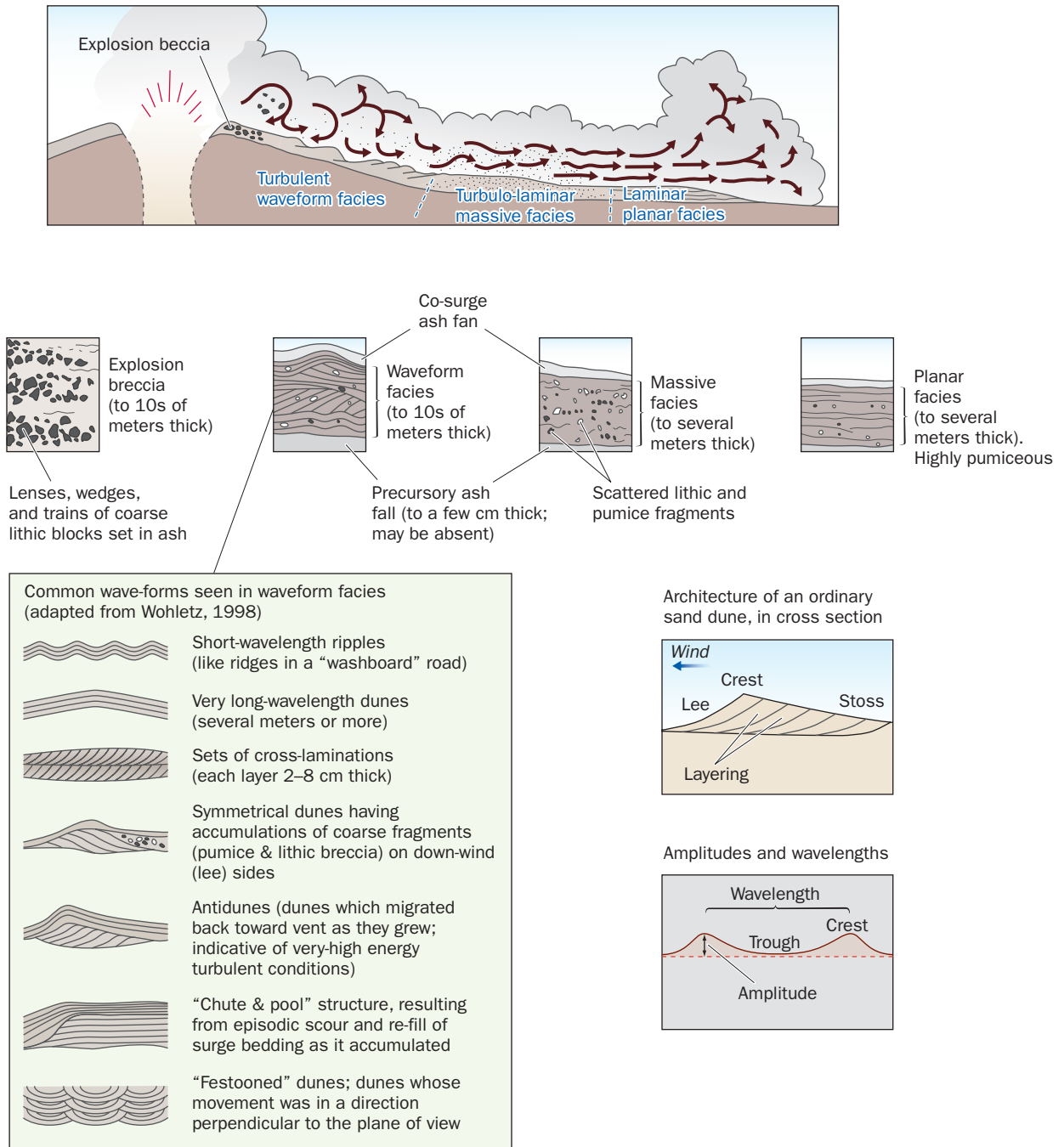


Fig. 7.36 Dunes and the development of surge facies in a blast surge deposit.

Fig. 7.37 Pyroclastic surge bedding in a late prehistoric PDC deposit in the Pollena-Trochia area, western flank of Vesuvius volcano, Italy. Note the cross-bedding and erosional truncating of earlier beds, which testifies to the violence of surge emplacement processes. Photo by R. W. Hazlett.



MORE ABOUT PDC SORTING

In general, **most** pyroclastic surge and flow deposits can be distinguished from each other by their sorting and particle size ranges. Murai (1961), Fisher (1964), Passega (1964), Sheridan (1971), Walker (1971) and Buller and McManus (1973) were the first researchers to attempt to characterize the sorting of pyroclastic deposits in terms of origin. They concluded that: *pyroclastic falls are better sorted than pyroclastic surges, which in turn are better sorted than pyroclastic flows*. Lirer and Vinci (1991) examined 414 different pyroclastic deposits and concluded that although there is some overlap in sorting, effective discrimination on the basis of sorting alone can be done based on mean phi values. For example, deposits with -3ϕ sizes are most likely to be fall-related; 1ϕ to be pyroclastic flow-related, and 7ϕ pyroclastic surge related (Fig. 7.38).

Fig. 7.38 Histogram presented by Lirer and Vinci (1991) showing mean grain size ϕ -values for pyroclastic falls, flows, and surges, from a population of 414 eruption deposits.

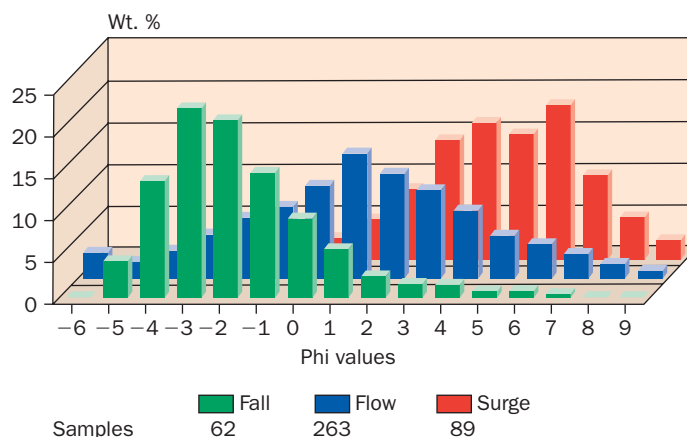


TABLE 7.3 CHARACTERISTICS OF PRINCIPAL PYROCLASTIC DEPOSITS.

Pyroclastic deposit Type	Origin	Deposition mechanism	Deposit characteristics
Fall ejecta	Gravity settling from overhead ash clouds	Accumulation by gravity settling through air or water, potentially affected by prevailing winds or water currents.	Typically poorly consolidated layers of uniform thickness that drape pre-existing topography. Size sorting is moderate to good.
Pyroclastic surge	Ash column collapse, phreatic or phreatomagmatic eruption	Deposition from low concentration, relatively low-temperature mixtures of ash, broken rock fragments and gases. Surges are characterized by turbulent flow.	Usually poorly sorted and poorly consolidated. Dune and internal erosion structures are typical and result in irregular thicknesses over short distances. Commonly contain ballistically emplaced blocks – bomb sags are common in proximal areas. Accretionary lapilli common.
Pyroclastic flow	Boiling of magma chambers, ash column or dome collapse. Most commonly associated with caldera-forming eruptions	Deposition from high-concentration, high-temperature clouds of mixed ash, gas, and juvenile magma fragments. Characterized by laminar flow.	Poorly stratified, with thicker deposits filling valleys and thinner or absent deposits on highlands. Commonly shows poor grading, with denser fragments near bases. Evidence of high-temperature origin include welding, deformation of glassy pumice fragments, pink-oxidized tops and gas pipes.
Directed blast	Violent explosions of suddenly depressurized magma chambers, typically triggered by massive landslides or sector-collapse	Extremely complex, and may involve deposition by pyroclastic surges, pyroclastic flows and airfall. May be preceded by initial erosive of high-velocity hot gases activity.	Recognized by extreme violence of deposition mechanisms. Massive accumulations of uncharred logs may attest to devastated forest in young deposits. Deposits widespread and may accumulate in separate basins. Incorporation of eroded material from underlying substrates common in basal deposits.

SUMMARY

Pyroclastic deposits and their differing origins may be grouped into five principal classes: 1) ballistic ejecta; 2) fall ejecta; 3) pyroclastic surges; 4) pyroclastic flows; and 5) directed blast deposits (Table 7.3). Recognition of these deposits is critical to understanding the volcanic history of many areas dominated by grey volcanoes.

FURTHER READING

- Branney, M. J. and Kokelaar, B. P. (2002) *Pyroclastic Density Currents and the Sedimentation of Ignimbrites*. London, Geological Society of London.
- Fisher, R. V. and Schmincke, H. U. (1984) *Pyroclastic Rocks*. New York, Springer-Verlag.
- Heiken, G. and Wohletz, K. (1992) *Volcanic Ash*, Oakland, University of California Press.
- Kokelaar, B. P. (1983) "The mechanism of Surtseyan volcanism." *Journal of the Geological Society of London*, 140, 939–44.

Chapter 7

Questions for Thought, Study, and Discussion

- 1 Describe the criteria we use to classify volcanic ejecta. Why are these criteria practical?
- 2 What are the main types of ballistic ejecta?
- 3 What criteria are used to distinguish the various kinds of volcanic ash?
- 4 How can we distinguish in ancient deposits the layers left by “wet” versus “dry” ash falls?
- 5 How might tephrochronology be useful in determining the age of latest faulting in a geological cross section exposed by erosion or road cut?
- 6 What distinguishes Vulcanian from Plinian eruption deposits? Describe the characteristic features of each.
- 7 How do volcanic plumes differ dynamically from eruption columns.
- 8 Why does the full sequence of typical Plinian eruption deposits not always appear, even in well-exposed cross-sectional outcrops?
- 9 What are directed blast eruptions, and why are their deposits so hard to discern in the geologic record?
- 10 In what fundamental ways do pyroclastic surge deposits differ from pyroclastic flow deposits?
- 11 What are “cooling units,” and what knowledge do we gain by distinguishing them?
- 12 How do the dynamics and deposits of hydrovolcanic eruptions differ from those of Strombolian eruptions?

Chapter 8

A Closer Look at Large-scale Explosive Eruptions

The stupendous and terrific character of these catastrophes, the rarity of their display, and the dreadful extent of injury often resulting from them to the lives and property of the inhabitants of the surrounding country, make them the subject of general remark during and long after the period of their development.

(George Poulett Scrope, 1862)

Given the extreme eruptive power of great explosive eruptions, their pertinence to global climate and atmospheric chemistry, and their implications for volcanic hazards analyses, we consider it important to explore the dynamics of these exceptional volcanic phenomena and other large explosive eruption types further in this chapter. We begin with a discussion of how to measure the sizes of these eruptions by study of their deposits, then describe Plinian eruption and pyroclastic density current (PDC) dynamics. We will also here describe the special class of explosive eruptions widely termed “Super-eruptions” by scientists and the media. These extremely violent eruptions, with VEI greater than 8 (Chapter 5), have never occurred within human-recorded history, and none are likely to occur within the lifetimes of those who will read this book, as they are exceedingly rare events in the Earth’s history. They involve the same physical processes described here for more typical Plinian eruptions, and we will refer to them again in Chapter 10 in our discussion of giant calderas, as these are the “Super-volcanoes” that produce “Super-eruptions.”

Volcanoes: Global Perspectives, 1st edition. By John P. Lockwood and Richard W. Hazlett. Published by Blackwell Publishing Ltd.

Measuring the Sizes of Past Plinian Eruptions

Recall from Chapter 5 the important terms **magnitude** (the total mass (kg) erupted throughout the duration of the activity), and **peak intensity** (the maximum rate of magma discharge (kg/s)). Carey and Sigurdsson (1987) attempted to constrain the factors responsible for the peak intensity and magnitude of Plinian eruptions. They investigated 45 mostly prehistoric Plinian eruption deposits and discovered that individual deposits range in magnitude from 2.0×10^{11} to 6.8×10^{14} kg, showing three orders of magnitude range. Intensity values also ranged over three orders of magnitude, from 1.6×10^6 to 1.1×10^9 kg/s. The authors concluded that intensity is directly related to magnitude of explosive eruptions and suggested that the rate of magma discharge is directly related to the size of the magma chamber being tapped.

Eruption magnitude determination is a relatively straightforward mapping exercise. The area and range of thickness of a deposit can be ascertained for younger eruptions by constructing an isopach map of fall deposits (Chapter 5; Sottili et al. 2004). Area (m^2) and thickness (m) are simply multiplied by the mean density of the fragments composing the deposit (kg/m^3) to arrive at the total mass (kg). There are, of course, enormous challenges in practice and volume calculations are complex (Pyle 1989). Many deposits are highly irregular in distribution. Erosion removes lots of material soon after eruptions, especially thin distal fall materials. Furthermore, the underlying bedrock topography, necessary for precisely determining thicknesses, may not be known. But under most circumstances for Plinian eruptions less than a few tens of thousands of years old, reasonably accurate estimates of mass can be made. The estimation of eruption intensities involves an entirely different field approach, however, called **isopleth mapping** (Urbanski et al. 2003). Isopleths show contours of the *maximum diameters* of particular kinds of ejecta, primarily lithic fragments that don't break into smaller pieces upon impact, which pumices have the habit of doing. Sieving is required to sort out the largest fragments, which can be done in conjunction with determining overall particle size distributions. The resulting fragment-size dispersal information can then be used in models developed by Sparks (1986), and Carey and Sparks (1986) to identify eruption columns of particular intensity.

Plinian Eruption Dynamics

Recall from Chapter 7 that Plinian volcanic clouds may be divided into two components; a buoyant *column* ballistically propelled upward at its base, and a wind-blown *plume* (Fig. 8.1). Plumes include both the diffuse horizontal bands of gases and particulate matter that drift downwind at high altitudes from the tops of Plinian columns and the secondary buoyant ash clouds that ascend from active PDCs. Plinian columns will change entirely to plumes as eruptions wane and columns collapse. Let's take a closer look now at the dynamics of ascending and collapsing columns.

THE RISE OF CONVECTIVE PLINIAN COLUMNS

The external features of a Plinian eruption column is immensely complex as it grows above an active volcano (Fig. 8.2) (Kaminski & Jaupart 2001). Bulbous “cauliflower” projections



N

Fig. 8.1 Sarychev volcano in eruption, Matua Island, central Kurils, as photographed by International Space Station astronauts on June 12, 2009. This sub-Plinian column has only risen to about 8 km above the volcano at this time, but eventually reached altitudes of 15–20 km. The white cap is called a pileus cloud, and is formed from condensing air trapped above the ascending column. Note the active pyroclastic flow descending the volcano's flanks (arrow), co-ignimbrite clouds rising from an older PDC to north, and an ash plume from earlier explosion drifting off to the southwest. NASA image ISS020-E-9048, courtesy of the Earth Sciences and Image Analysis Laboratory, NASA Johnson Space Center.

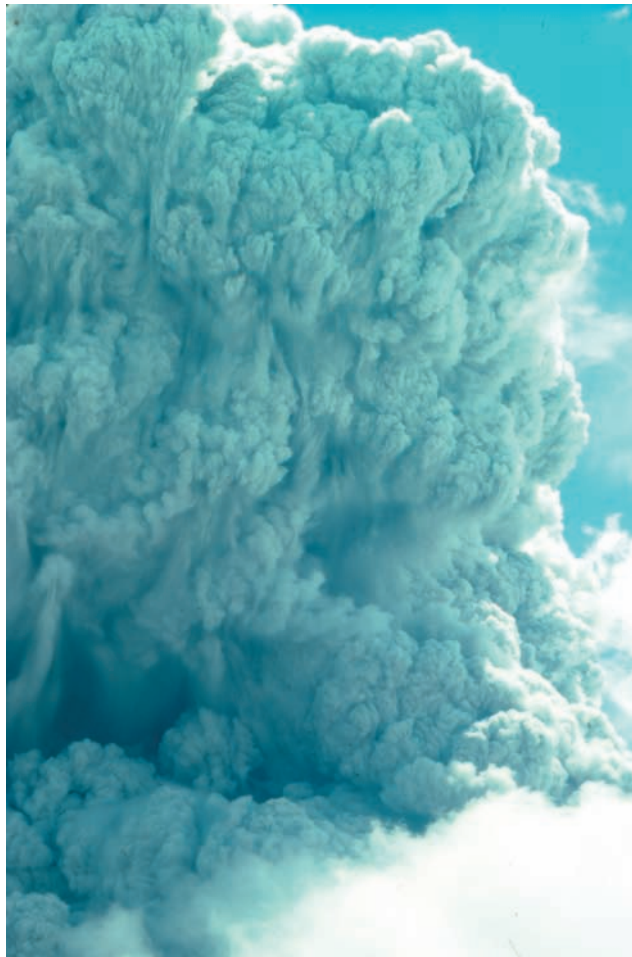


Fig. 8.2 Detail of sub-Plinian convective column arising from Mt Pinatubo volcano, July 4, 1991. The rapid, dynamic variations in column expansion during ascent must be seen to be appreciated! USGS photo by J. P. Lockwood.

churn rapidly upwards, and shoot laterally out of the column. Many are initially black with ash as they emerge from cloud interiors – because they are above 100°C in temperature, and visible steam cannot form – until they cool somewhat and turn to white or grey. The column may be ringed by bizarre skirt clouds that form and disappear quickly. Electrical charge imbalances within and between the columns and surrounding ground create near-constant lightning – which can form a near-continuous din. The roaring of the eruption and constant cracking of electricity can make conversations difficult, and if close enough the “whoomp-whoomp” sounds of falling blocks ejected from the base of a column can be heard.

When Sparks et al. (1973) first proposed their model for the formation of Plinian eruption deposits, much less was known about how Plinian columns are generated and dissipate than we know now. Subsequent well-observed Plinian and sub-Plinian eruptions (e.g. Mount St Helens [27], 1980, El Chichón [45], 1982, Mt Pinatubo [104], 1991, Mt Spurr [22], 1992, Soufrière Hills [60], 1996) have taught us much, but volcanologists have also created their own model eruptive columns and plumes, both numerically with computers and experimentally in tanks of water (which are reasonably safe research environments). Modelers have greatly benefited from the concepts of **fluid dynamicists** – the people who study how gases and liquids flow. Not only Plinian columns but the weaker and somewhat more variable Vulcanian clouds have been intensively studied (see, e.g., Clarke et al. 2002).

Plinian and sub-Plinian eruption columns consists of three vertically-stacked regions (Fig. 8.3), each dynamically distinctive, with variable ascent speeds and density relative to the adjoining atmosphere. Note that the **gas thrust region** is denser than air but does not collapse owing to the powerful inertial discharge of its mass from the vent (Fig. 8.4). Entrainment of air enables the gas-thrust region to undergo transformation into the **convective region**, which remains lighter-than-air up to the altitude of neutral buoyancy (H_B). At that level, atmospheric density and density within the rising column match, owing to lowered temperature, ingestion

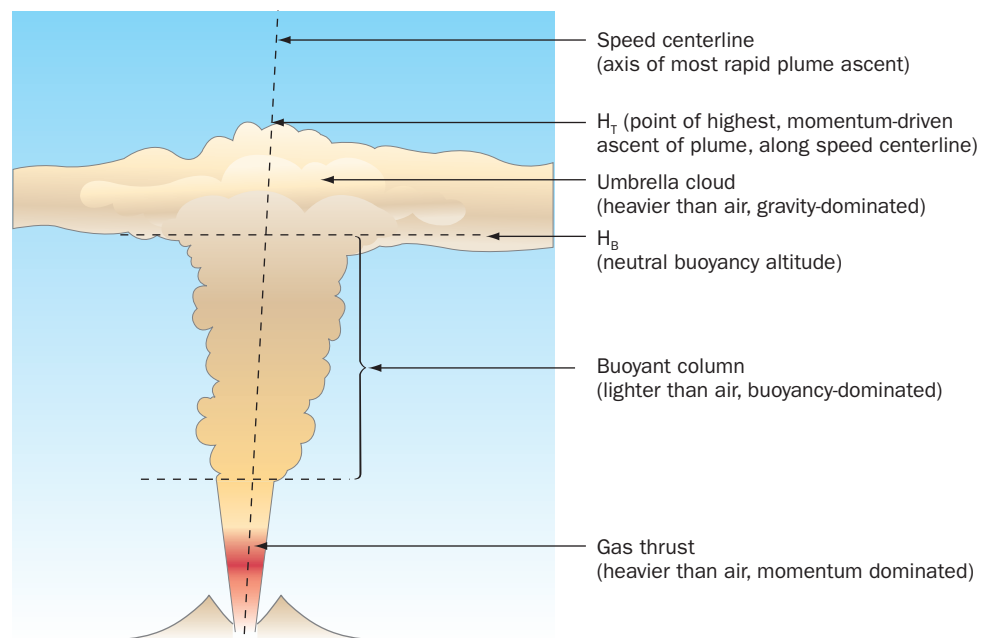


Fig. 8.3 Plinian column structure.



Fig. 8.4 Plinian eruption column rising from the decapitated summit of Mount St Helens volcano on May 18, 1980, about three hours after the onset of Plinian activity – view to east. The convecting column has risen at this time to about 20 km above the volcano. “Gas thrust” upward motion dominates the left side of the column, but minor downward movement of billowing ash is occurring on the right side. USGS photo by Austin Post.

of ever larger volumes of air, and dispersion of ejecta as the column expands in response to reduced high-altitude air pressure. The column still retains momentum, however, and will continue to rise a bit further to its maximum height (H_T), all the while spreading to form the **umbrella region** (Fig. 8.5). As a representation of this momentum, Sparks (1986) observed that the ratio $(H_T - H_B)/H_T$ for most Plinian eruption columns lies in the range 0.25 to 0.3.

The transition from a jet thrust into a convective column is a critical one, acting as a filter for fragments that fall out of the eruption column as the jet thrust loses momentum, but before it starts accelerating again with the ingestion of a critical amount of heated air. Woods (1988)

Fig. 8.5 Top of sub-Plinian eruption column from Galunggung volcano, Indonesia – August 16, 1982. The cloud top has reached a point of neutral buoyancy at about 12 km altitude, and is beginning to spread out to form an umbrella top, USGS photo by J. P. Lockwood.

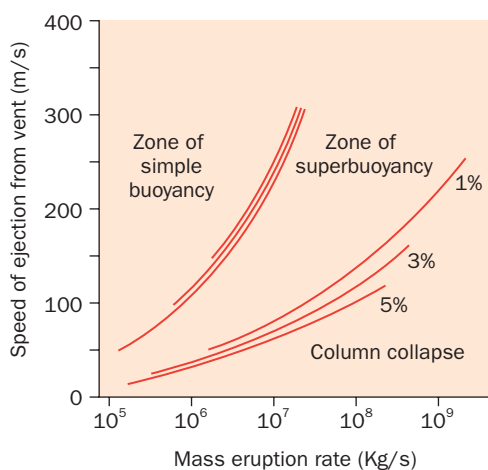


Fig. 8.6 Relationship of eruption discharge, speed of discharge, and water vapor content of eruption column (in 1, 3, and 5 weight percents) to buoyancy properties. Convective columns will become established only in the zone of superbuoyancy. After Bursik and Woods (1991).

and Wilson (1993) refer to the jet-thrust lifting of ejecta as **simple buoyancy**, and air-related convective lifting as **superbuoyancy**. The transition between these states of eruptive buoyancy is related directly to two aspects of an eruption; the speed at which material leaves the vent (m/s), and the mass discharge of material from the vent (kg/s). For example, eruption columns that erupt rapidly but contain low concentrations of particles fail to become superbuoyant, because they cannot inject and heat air from the surrounding atmosphere very effectively. Likewise, if an eruption column leaves the vent slowly, and it contains a high concentration of particles, it is bound to collapse before ascending very far. The best combination of circumstances for maximum column buoyancy is a moderate rate of ascent, with a moderate level of mass discharge (Fig. 8.6). The water vapor content of columns also plays a role in their ascent, with wetter clouds able to capture air slightly more

effectively than dry ones mixed solely with magmatic gases.

Temperature differences, density of erupted material, and most of all, rate and intensity of magma discharge are key determinants for the heights of eruption columns and the levels at which they flatten out into umbrella clouds (Sparks 1986; Odgen et al. 2008). This is illustrated in (Fig. 8.7), which also equates volume to mass of magma being discharged. Note the slight inflection points in the sets of lines drawn for both tropical (20°S–20°N) and temperate latitude cases. These inflections are caused because the atmosphere does not change gradationally all the way out to the fringe of Space, but is itself stratified into layers having slightly different physical and chemical properties. The atmosphere is thicker, less dense, and moister at tropical latitudes than in temperate, making it slightly easier for columns to rise there.

Of further interest is how *fast* columns ascend. Ascent rate depends not only on a combination of buoyancy factors, but also on initial momentum of the jet region. The written

description of Pliny the Younger of the opening phase of the 79 CE Vesuvius eruption (p. 193) suggests that the kilometers-high column appearing above the Bay of Naples developed in just a few minutes. He was not exaggerating. Eye-witness accounts of the initial Mount St Helens 1980 Plinian column by airline pilots indicate that the cloud reached 18 km height in about 5 minutes (Rosenbaum & Wait 1981). Modeling by Sparks (1986), reinforce the point, made earlier, that entrainment of air, buoyancy, magmatic heat and pressure–temperature changes in the atmosphere all play essential roles in determining the ascent speeds of columns. The results of their theoretical studies can be diagrammed to show how ascent speed changes in a column as it rises. The nest of curving lines shown in Fig. 8.8 each relates to a different numerically predicted column. Column (a) for example, erupts from the vent at an ascent rate of 300 m/s; a very powerful eruption even by Plinian standards. By the time it rises to 5 km the top of the column has slowed to about 140 m/sec, and at 10 km, near the tropopause in temperate climates, it has slowed to about 100 m/sec. Plots of two observed eruption column ascents, one for tropical Soufrière volcano [62] in the Caribbean (Sparks & Wilson 1982), and the other for temperate latitude Mount St Helens (Sparks 1986) are also shown. The matches with turbulence modeling are fair, though note the acceleration of the Mount St Helens column above 10 km does not match theoretical models well – perhaps a combined influence of strong upper level winds and unaccounted for stratospheric properties (Zimbelman & Gregg 2000; Ishimine 2006).

Most particles that exceed 20 mm in diameter, excepting highly porous pumices, drop out of the sides of columns as they convect upward (Sparks et al. 1992). For the most powerful “Ultraplinian” columns, as much as 60 percent of the bulk weight of solids can be very fine ash (less than 63 μm) capable of spreading hundreds of kilometers from the column axis in an expanding umbrella cloud (Walker 1981).

Observations and laboratory experiments indicate that the radial speed of umbrella expansions decrease as a function of radii, so that as speed declines, progressively smaller particles fall out to contribute to the growing tephra dispersal field below. In other words, the dispersal of fall ejecta can be regarded as a “map” of a slowing eruption umbrella. Carey and Sparks (1986) calculated estimates of original column heights for prehistoric eruptions. The highest eruption column is that estimated for the 186 CE Taupo [135] Phreatoplinian eruption in New Zealand – 51 km (Walker 1980), which is described further below.

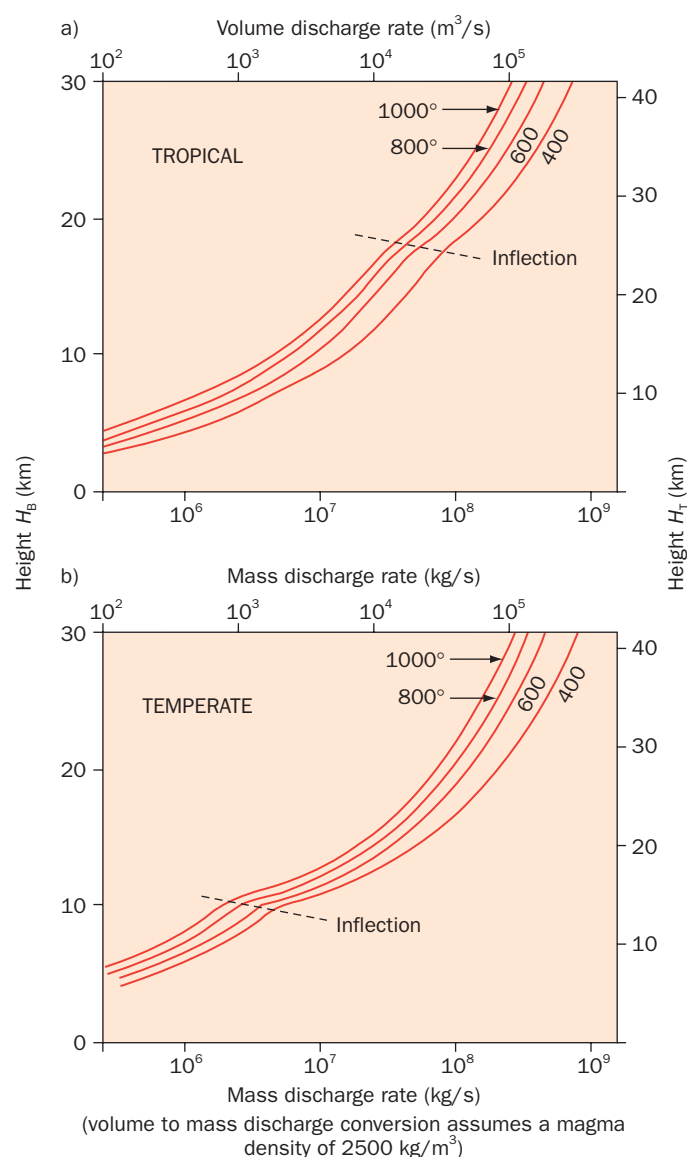


Fig. 8.7 Changes in neutral buoyancy levels (HB) with changing volumetric or mass discharge rates, for Plinian columns of varying source magma temperatures. Note the differences for eruptions under tropical (a) and temperate (b) conditions. After Sparks (1986).

Fig. 8.8 Theoretical variations of eruption column speed with height in the column, as measured at the centerline axis for columns of differing initial ejection speed (given at height = 0). Data for two historical eruptions are also plotted – Soufrière, from Sparks & Wilson (1982), and Mount St Helens from Sparks et al. (1986).

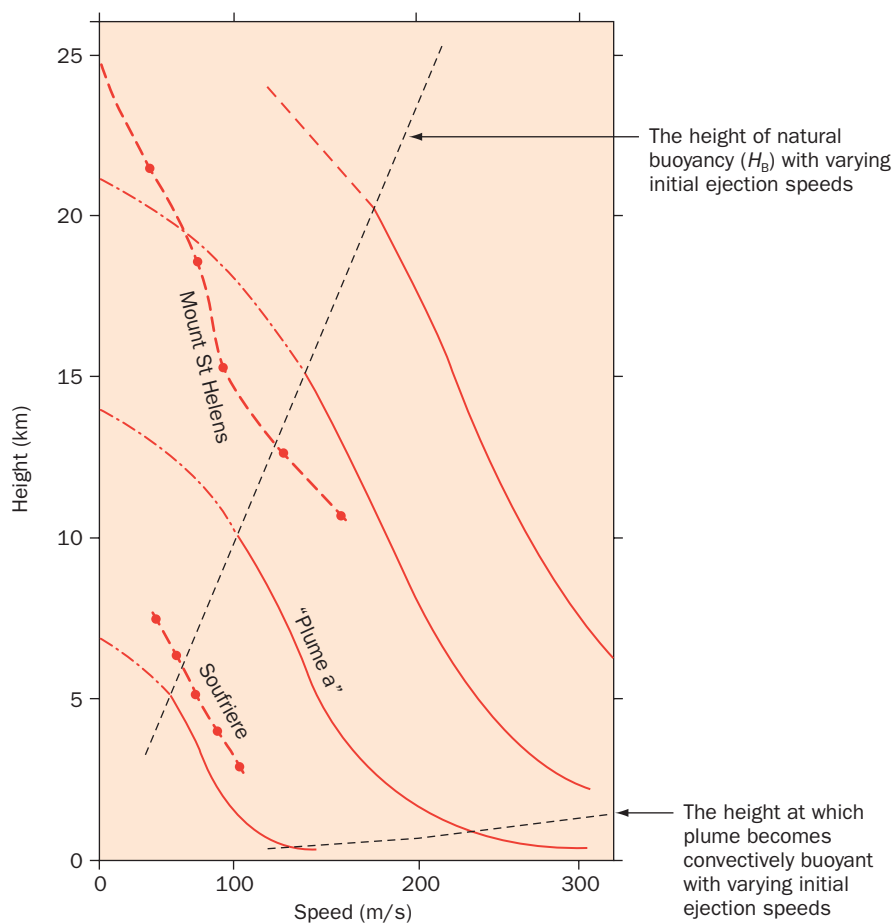
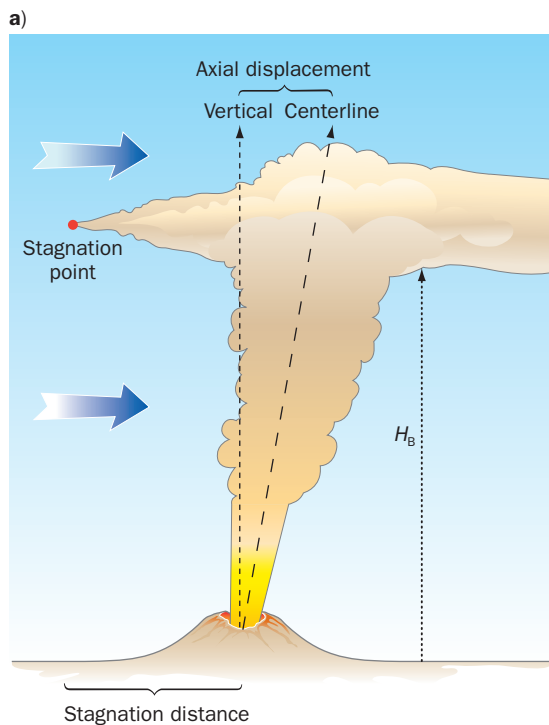


Fig. 8.9 Wind, Plinian columns, and air fall dispersals: a) Geometric parameters.



Wind, of course, will modify the simple radial distribution of tephra deposits according to grain size around a vent. If a strong atmospheric wind is blowing, the upwind spread of the umbrella cloud will cease where the spreading speed of the umbrella matches that of the opposing wind. This position is called the stagnation point. At a right angle to the wind direction, the umbrella will spread as though moving through still air, while downwind the cloud will, of course, propagate faster and farther (Wilson 1993). The distance the center of the eruption column is displaced by wind from its position directly above the vent at H_b is termed the column's **axial displacement**, and this is directly related to the stagnation point, depending upon the altitude and the wind speed (Fig. 8.9). This means that airfall deposits can serve as paleo-wind direction indicators. Carey and Sparks (1986) used the degree of ellipticity of wind-distorted airfall isopachs to estimate the high-altitude windspeeds occurring during a number of well-studied explosive eruptions. In some cases this can indicate the yearly season in which eruptions have occurred.

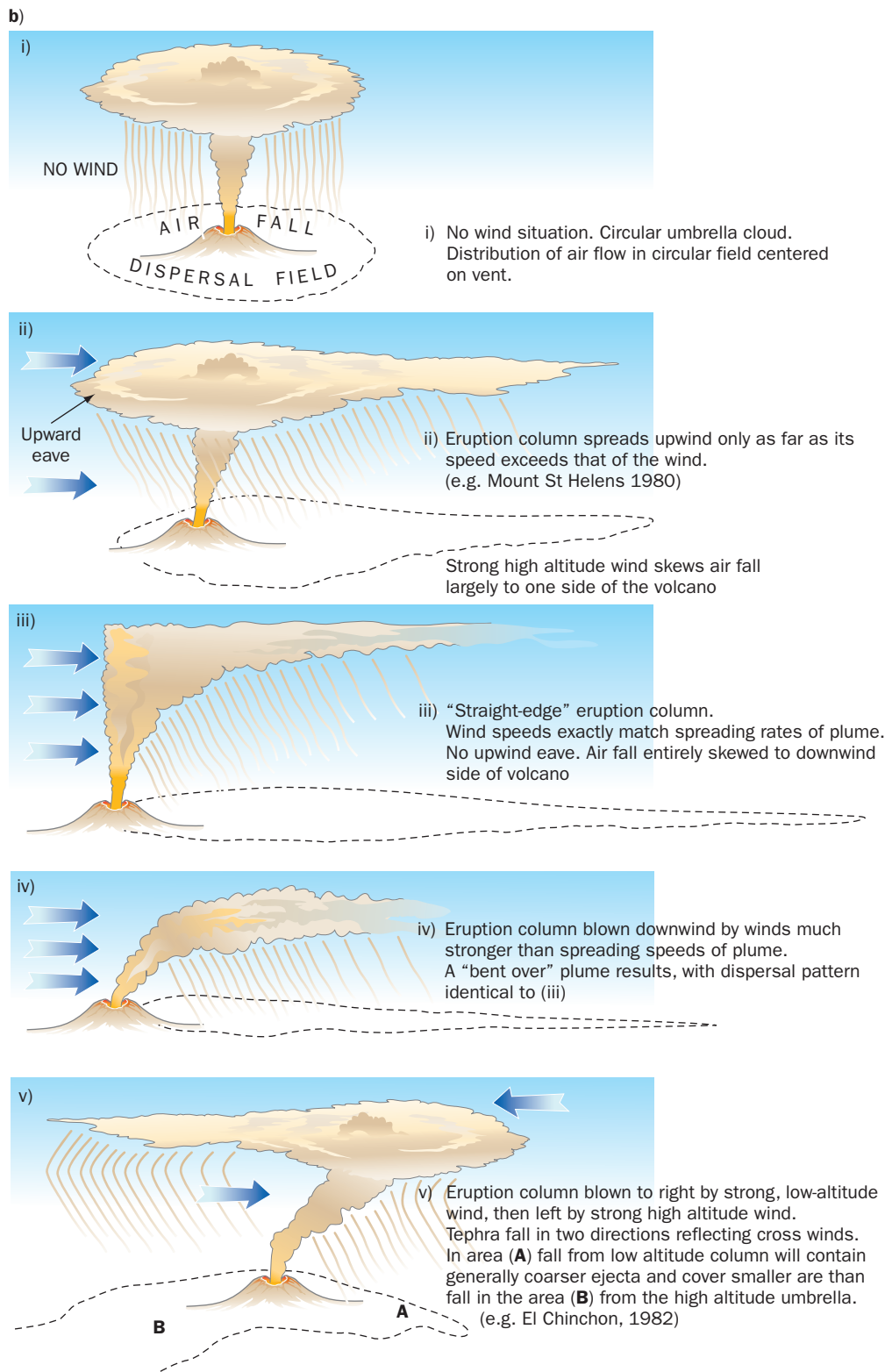


Fig. 8.9 (cont'd)

b) Cases.

In their 1989 study, Carey and Sigurdsson (1989) found that most of the 45 Plinian deposits they catalogued were preceded by pumice falls, but only when this early pumice exited the vent at calculated intensities in excess of 2.0×10^8 kg/s were major PDCs and caldera collapse also likely to occur. Bursik and Woods (1996) have more recently concluded that the most extensive pyroclastic flow activity develops during eruptions with intensities greater than 10^9 kg/s, with column activity persisting for approximately 20 minutes to over 30 hours. PDCs are certainly possible at lower intensity levels, but these are likely to be small, with attendant caldera formation improbable. Carey and Sigurdsson (1989) have also compared the calculated intensities to the magnitudes in their data set, coming up with minimal eruption durations of from 1.1 hours for a simple (observed) Plinian pumice fall, to 208 hours for the gigantic caldera-forming Los Chocoyos ash and pumice eruption in Guatemala (Rose et al. 1987).

Intensities and magnitudes, it turns out, correlate closely enough to be significant (Fig. 8.10). Larger magma chambers develop higher overpressures, and so produce higher intensity eruptions (Valentine & Wohletz 1989). Ogden et al. (2008) further suggest that steady levels of high overpressure will stimulate oscillatory column rise and collapse, accounting for the periodic generation of PDCs recorded in many Plinian eruption deposits. Another important variable influencing eruption rate, quite independent of magma overpressure, is **vent diameter**. Wilson et al. (1980) modeled the relationship between vent radius (r) and mass eruption rate (M) as follows:

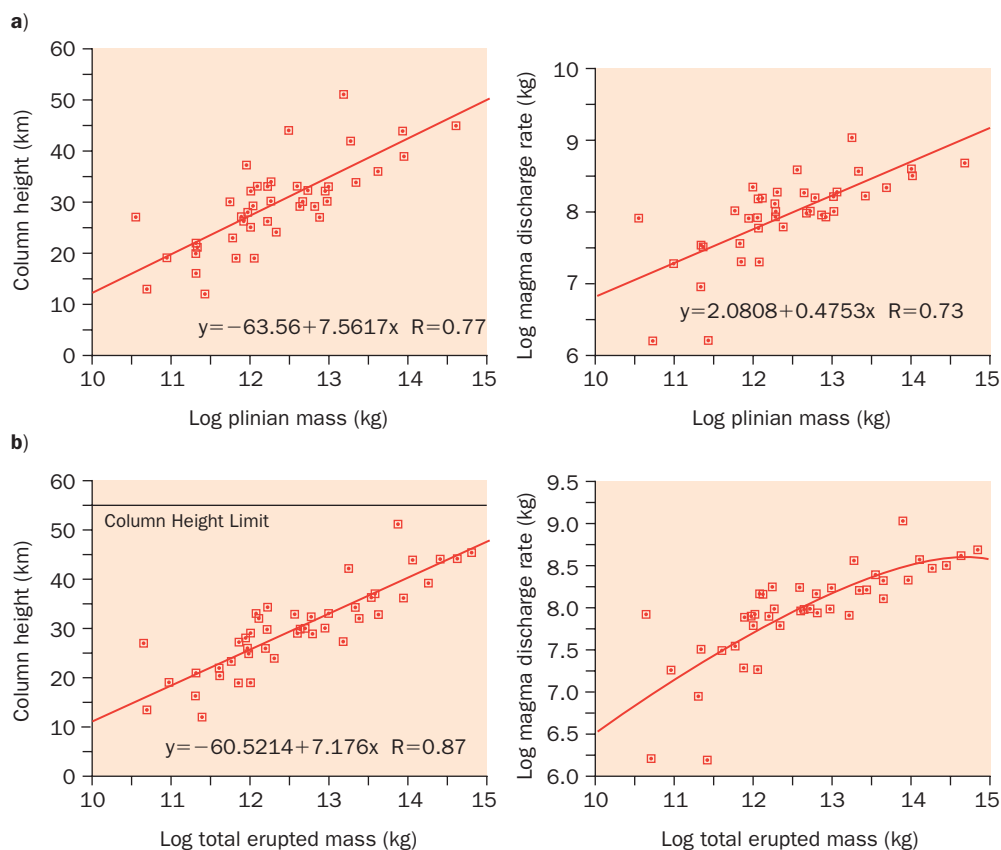


Fig. 8.10 Correlations of various eruption parameters calculated for 45 Plinian deposits by Carey and Sigurdsson (1989).

$$M = [(\pi r^4 g \rho_m (\rho_{cr} - \rho_m)) / 8\mu] \quad (8.1)$$

where ρ represents densities for both magma (m) and crust (cr), and μ is magma viscosity. Mass eruption rate is thus extremely sensitive to vent diameter, varying as the fourth power of the vent radius.

Field observations of graded air fall deposits suggest that many Plinian eruptions increase significantly in intensity shortly after initial venting, as indicated by reverse grading in pumice fall beds. Carey and Sigurdsson (1987), for example, inferred a greater than one-order of magnitude increase in the intensity of the early to middle stages of the 79 CE Vesuvius eruption, based upon differences in pumice sizes in the reversely graded Pompeii pumice fall. Perhaps the most reasonable explanation for this commonly inferred increase is that vents widen during eruptions. Erosive widening of a vent by particle abrasion and hydraulic weakening from fluctuating gas pressures certainly occurs in all explosive volcanic outbursts, as shown by the abundance of accessory and accidental fragments in their deposits. This is especially true for long-sustained, high-intensity eruptions. Higher intensity eruptions also have greater magnitudes, which must be supplied by larger volume magma chambers.

Not all Plinian fall deposits show reverse grading – many are ungraded or show normal grading. Systematic enlarging of vents, plainly, is not the only factor involved in affecting deposit characteristics. A further complication is the recirculation of pyroclastic material. Ejecta falling within a few kilometers of the base of a large convective column may, depending upon its coarseness, largely be reincorporated by the column via powerful atmospheric updrafts acting at the column edge (Fig. 8.11). There is also the complicated turbulence resulting from the fall back of pyroclasts into the top of the convective region from the umbrella cloud itself. Despite these caveats, the basic results of modeling provide a useful picture of the overall dynamics of Plinian eruption columns.

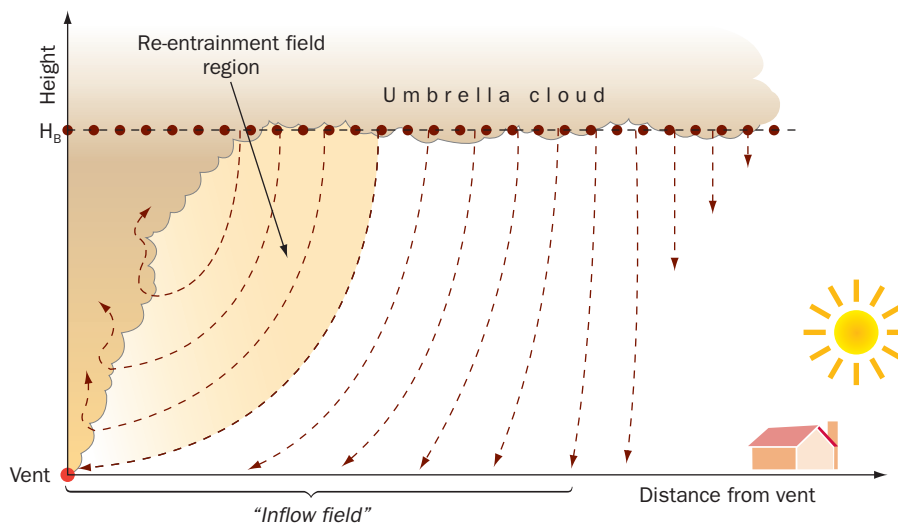


Fig. 8.11 Re-entrainment of falling tephra into Plinian columns. Air rushing back toward the vent to replace that which is sucked up into the column deflects fall pyroclast trajectories (dashed lines) so that some particles may become re-entrained and recycled – repeatedly. Modified from Bursik et al. (1992).

THE FALL OF PLINIAN COLUMNS

A Plinian eruption column may partially collapse when the ratio of solid particles to gases and trapped air greatly increases density at any fixed intensity level, potentially generating PDCs on volcano flanks. This could be due either to decreasing volatile content or to increasing solids content in the column, or to both factors operating at once. Rising column density, whether due to increased particulate content, volatile loss, or to cooling, contributes to eventual column collapse. Historically recorded accounts of Plinian column collapse indicate that it may take just a few minutes for some columns to fall apart, although more typically it can take several hours and involve numerous cycles of growth and collapse (Scott et al. 1996; Clarke et al. 2002). Some columns may collapse only on one side, or collapse in a sloppy, piecemeal fashion.

Wilson et al. (1980) calculated the physically important factors controlling column collapse (Fig. 8.12). Note that the speed at which material exits the vent (which should not be confused with eruption intensity and mass discharge rate) is also critical (Neri & Dobran 1994). Water vapor content also plays a key role in governing column collapse, and consideration

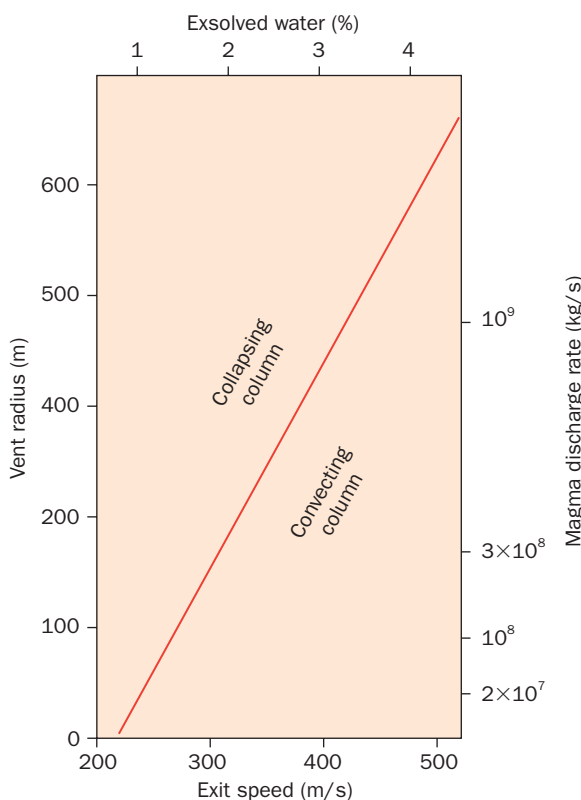


Fig. 8.12 Factors governing the collapse of convective columns. Wilson et al. (1980).

of this factor becomes especially important in comparing Phreatoplinian with drier Plinian eruptions (Wilson & Walker 1987). At a given level of vent discharge, steam-rich columns ingest far more air than dry ones do, and so might be expected to lack the critical particle-gas density balance needed to climb very high. Plumes whose conditions lie close to the dividing line between pure convection and collapse may experience short-lived pulses of collapse and recovery, as observed at Mount St Helens during its 1980 eruptions (Rowley et al. 1981). Sparks et al. (1978, 1997) concluded from density considerations that most column collapses begin at levels not exceeding about 10 km altitude, given a reasonable range of vent radii from 50–600 m.

Carey et al. (1988) set up a series of experiments to investigate how eruption columns collapse. Their basic idea was simple: They filled a large tank with slightly salty water, acting as a proxy for Earth's atmosphere. Into this they injected lower density fresh water through a narrow jet at the tank's bottom containing various concentrations of fine particles – analog Plinian columns, which they filmed. They varied the parameters of injection, including particle concentration and size and rate of injection to observe differences. Because the bulk (overall) density of a column of rising hot gases increases with particle concentration, they were able to simulate eruption columns ranging from highly buoyant (low particle concentration) to neutrally buoyant (high particle concentration). They compared their work with theoretical equations developed by fluid dynamicists (see, e.g., Turner 1986) to determine the extent to which their experiments reflected theory. Four basic modes of column collapse were observed, each dependent upon different levels of particle concentration and to a lesser extent particle

size. Eruption rates had no apparent bearing on the style of collapse. The most dilute columns shed a continuous veil of enclosing fine particles after reaching their maximum heights, each creating a deposit of uniform width around the vent. With increasing particle concentration, the cascading veils became more prominent and small eddies of particle-rich column material began appearing along the column edges, slowly propagating downward and merging with the falling ejecta. Carey et al. (1988) noted eruptive analogs of their experimental observations from the April 1979 eruptions of Soufrière volcano [62] on the Caribbean island of St Vincent:

These [dilute] flows originated high in the eruption column about 10 min after the eruption began, when the column had reached 18 km in height . . . They descended as a curtain down the slopes of the volcano and out to sea. People who were overrun by the flow reported no sensations of high temperature, and there was no destruction associated with their passage. A thin layer of ash was the only trace of this type of activity. Such dilute flows provide a new mechanism for the deposition of fine ash in the proximal regions of explosive volcanoes.

In their water-tank experiments, Carey et al. (1988) could cause many variations in collapse style by varying particle size and density, and if the “eruption” supply was suddenly shut off, the supported column of particle rich fluid would collapse all at once, creating a capping fall bed. The heavy ash falls witnessed by Pliny at the end of the 79 CE eruption possibly accompanied column collapse (p. 198). Smaller Plinian eruptions may simply involve the development of convective columns followed shortly by whole-column collapse. A bed of airfall pumice topped with a thin ash layer may be all there is to record such an eruption.

Pyroclastic Density Currents (PDCs)

As noted in previous chapters, PDCs are the deadly, ground-hugging torrents of hot ejecta mixed with gases that can pour down volcano flanks on many different scales, from the minor ones described at Galunggung (Chapter 1) to devastating outpourings that blanket thousands of square kilometers with deposits hundreds of meters thick. They are potentially the most devastating phenomena generated by large explosive eruptions, and can be produced by a range of eruption types (Table 8.1). Because of their violence,

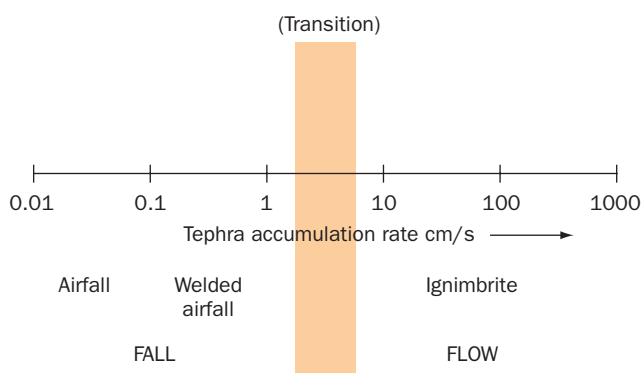
TABLE 8.1 RELATIONSHIP OF PDCs TO STYLES OF ERUPTION.

Eruption type	Commonly observed pyroclastic currents
Hawaiian, Strombolian, Ultravulcanian	None. Ballistic ejection of fragments only
Vulcanian	Block-and-ash flows, base surges
Plinian	Ash flows, Ground and ash-cloud surges
Hydrovolcanic	Base and blast surges

geologists cannot directly observe the internal processes involved, but can only infer them from external field observation of active currents, through modeling, and by careful study of their deposits.

All PDCs are highly dilute, heterogeneous mixtures of gas and fragmental material. Most only flow in response to gravitational forces on volcano flanks, but some may be initially driven by explosive forces. Their high content of expanding gases makes all of them highly fluid. Complete gradations exist between pyroclastic density current dynamic styles, and Branney and Kokelaar (2002) have shown that PDCs can change their characteristics during flow. As discussed in Chapter 7, there are two primary PDC types – the relatively higher particle concentration **pyroclastic flows** (typical of Plinian eruptions), and lower-density **pyroclastic surges** (common products of hydrovolcanic activity). What is “high” and what is “low” in terms of solids concentrations remains largely a relative question, however, since no one has been able to measure these values directly. Work with sediment cascades in shallow liquids and other modeling suggest that pyroclastic flows may contain “tens of percent solid particles” mixed with gases, while the percentage of suspended solid material must be as low as 1 to 3 percent for surges to form (Sparks and Wilson 1976; Bursik and Woods 1996). To initiate a PDC most erupting gases must not separate from pyroclastic material, and conditions must be favorable for the incorporation of atmospheric air. This requires rapid admixing of fragments with gases, which can take place either within vigorously vesiculating magma at the tops of conduits, or in and around the lower levels of a collapsing convection column. If fall ejecta around the

Fig. 8.13 Theoretical relationship of ashfall (tephra) accumulation rates to generation of pyroclastic flows. Flows will form when ashfall, as around the margin of a collapsing column, is especially heavy. After Wilson (1993).



column accumulate fast enough to thicken a deposit at a rate of at least 1–5 cm/s, then it may begin trapping air and magmatic gas in large volumes, resulting in pyroclastic currents (Fig. 8.13). Too much water vapor in a Plinian or Phreatoplinian eruption column can hinder PDC development, however, owing to the buoyancy of steam. The critical level of “too much” steam in this regard depends in large part upon the speed with which material is ejected from a vent but work by Koyaguchi and Woods (1996) suggests that in many cases less than about 15 weight percent water vapor is required in order for a column to remain buoyant.

THE ORIGINS OF PDCs

Pyroclastic flows and related pyroclastic surges (see later in this chapter) can originate in several ways – all of which involve the rapid release of pressure on high-level magma bodies and subsequent volatile exsolution, the rapid admixture of expanding gases with fragmental rock material, the entrainment of surrounding air, and gravitational flowage downslope. There are four principal types of volcanic activity that can generate PDCs. The most frequent pyroclastic flows and surges are generated by the repetitive collapse of growing volcanic domes (Figs. 8.15a; 8.14). Large dome collapse events may depressurize underlying magma chambers and trigger explosive blasts with major PDC activity, as has been well demonstrated during the long-lived eruption of Soufrière Hills volcano, Montserrat (Fig. 8.16; Chapter 9). The sudden decompression of cryptodomes as shallow magma chambers caused by sector collapse (Fig. 8.15b; Chapter 11) are uncommon but lead to far more violent explosive activity. The most

dangerous sources of high volume PDCs (primarily pyroclastic flows) are major Plinian or Vulcanian eruptions that involve boiling magma chambers and production of explosive Plinian columns followed by column collapse (Fig. 8.15c; Sparks and Wilson, 1976) and/or summit “biolover” phenomena (Fig. 8.15d; p. 242). Smaller PDCs are also associated with initial phases of directed-blast phenomena (Fig. 8.15e), and can also be generated by the secondary mobilization of primary PDCs or collapse of thick silicic flow fronts (Fig. 8.15f; Stoiber & Rose 1970).



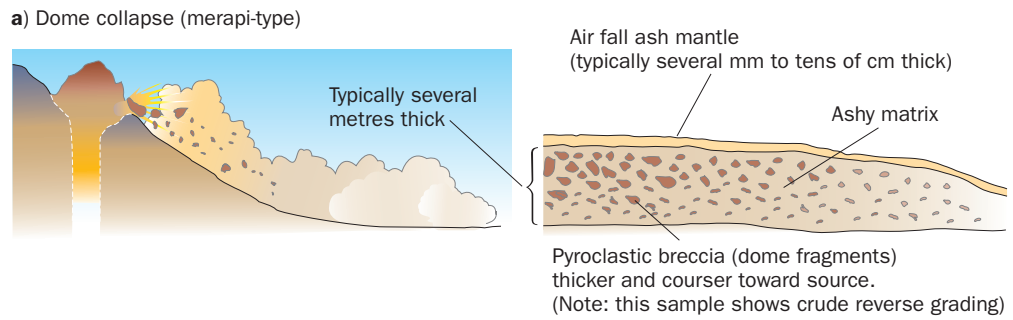
a)



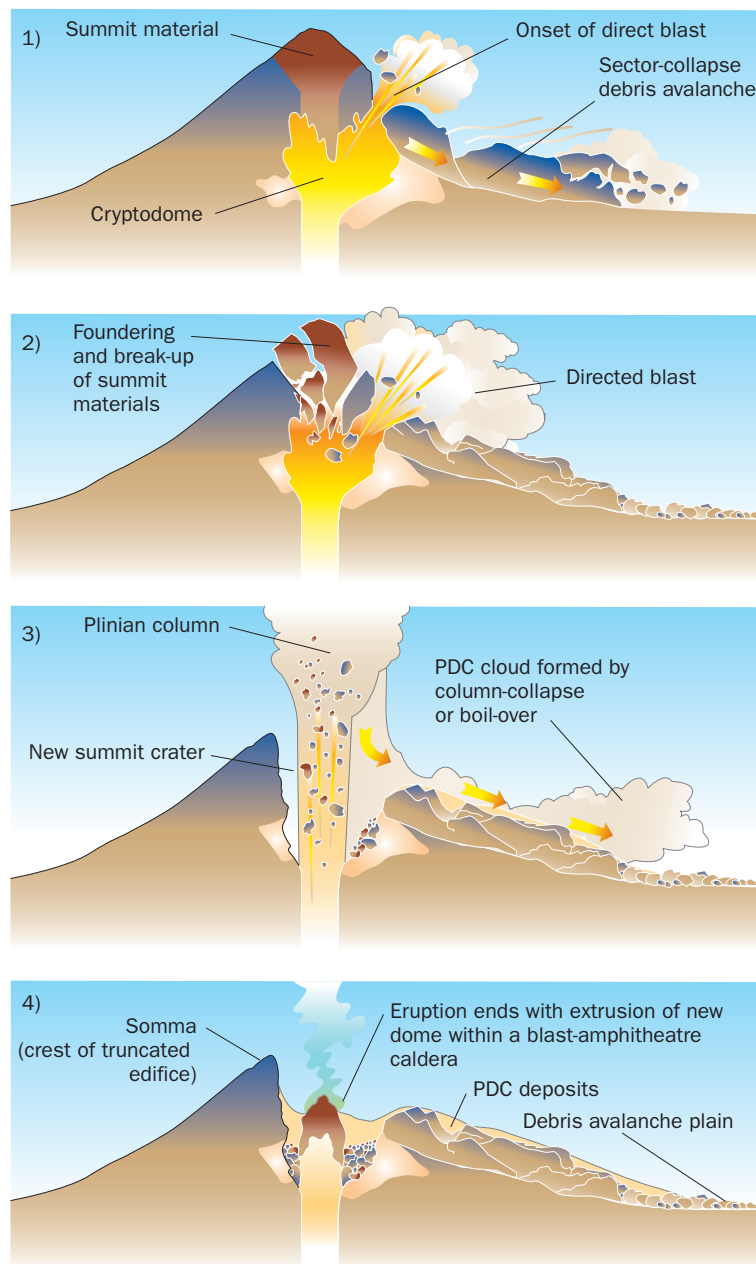
b)

Fig. 8.14 Merapi volcano, Indonesia. a) Profile view from south, showing fuming dome at summit. b) Close-up view of growing dome, October, 1982. The dome was growing at a rate of almost 100,000 m³/month at this time, and sending small pyroclastic flows and rockfall avalanches down the Gendol River several times per day. The magmatic SO₂ emissions from actively growing domes is usually intense. USGS photo by J. P. Lockwood.

Fig. 8.15 Various PDC formations showing associated deposits.

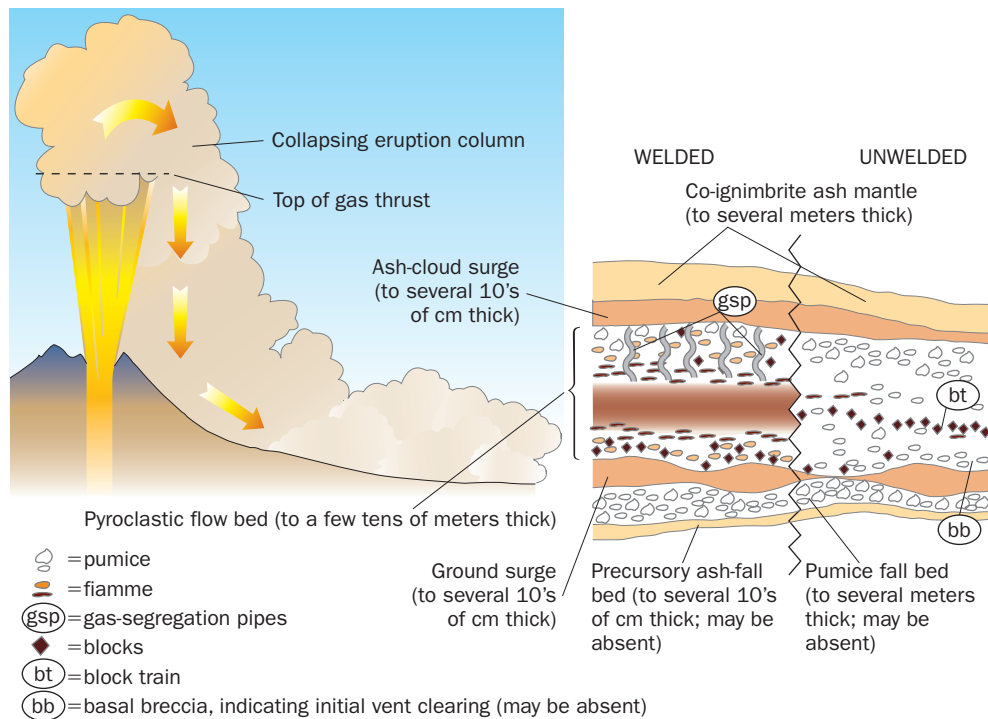


b) Sector-collapse, followed by magma decompression, directed-blasts and Plinian activity, as at Mount St. Helens in 1980



c) Column-collapse (“fountain-fed”) ash flows

Fig. 8.15 (cont'd)



d) Boil-over ash flows (with or without an eruption column)
Deposits similar to those of “column-collapse” ash flows

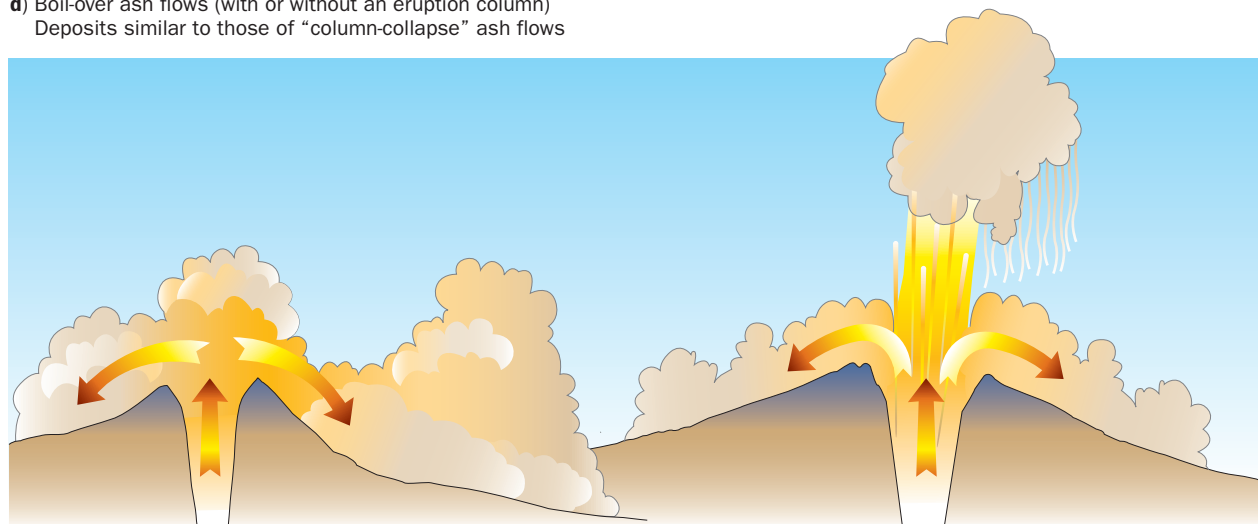
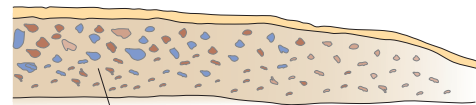
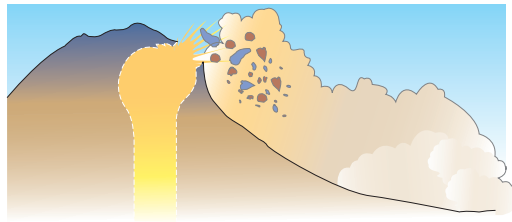
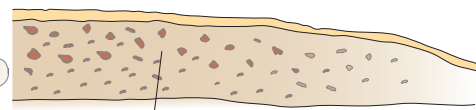
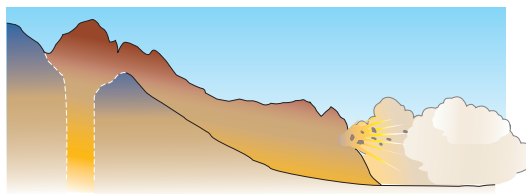


Fig. 8.15 (cont'd)**e) Cryptodome explosion**

Similar to ordinary dome or silicic flow explosion deposit, but enriched with accidental ejecta from volcanic edifice

f) Silicic flow front collapse

Similar to dome-collapse flow bed, above, but may show higher concentration of ash, fewer blocks

Fig. 8.16 Soufrière Hills volcano, Montserrat, viewed from the northeast, showing the growing summit dome on February 9, 1999. Voluminous pyroclastic deposits extend 3 km down the Tar River valley and several kilometers offshore on submarine slopes. Pyroclastic flows have reached the sea on both east and west coasts of Montserrat and caused great destruction since 1996. Photo by Simon Young, British Geological Survey, © NERC.



Because pyroclastic flows are characterized by lamellar, non-turbulent flow at their bases, they generally do not substantially erode the underlying surface, in contrast to highly turbulent pyroclastic surges. Pyroclastic flows are beautiful to watch (from safe distances!), so long as they are not flowing towards populated areas. They are extremely “well-lubricated” by their high gas content, and move almost silently as they speed downslope. Small pyroclastic flows that I (JPL) have witnessed at close range (p. 13) make almost no noise as they travel by – only faint whistling sounds – much like the rustling of leaves. Their beauty is tempered, however, by the knowledge that they are commonly extremely hot inside, and even momentary exposure to their hot gases will result in near-instant death. The people surrounded by dilute pyroclastic flows during the 1991 eruption of Unzen volcano [108] (including our friends Maurice and Katia Krafft and Harry Glicken) were burned beyond recognition with only a few minutes exposure; those at the very margins of the flows only survived for a few days, as their throats and lungs were horribly seared while they gasped for air.

Far more fortunate was Frank Perret (Chapter 1) during the 1929–32 eruptions of Mt Pelée [63] on the island of Martinique. In order to view the growth and collapses of Pelée’s active summit dome, Perret had a single-room wooden shack installed as a field station on a ridge 2 km below the volcano’s summit. The station overlooked the valley of the River Blanche, through which most pyroclastic flows he witnessed traveled harmlessly below him to the sea. On the evening of April 15, 1931, Perret was in his shelter, when:

I had one of those harrowing experiences which the volcanologist has to expect in close-range observation of an actual eruption . . . A huge spine had grown up near the west side of the dome summit. It was unstably poised and its fall seemed imminent. Just at the close of the swiftly passing tropical twilight, in the dead calm between day and night winds, an unusual sound brought me to the cabin door. The whole mass had fallen, leaving a great scar on the dome from which poured forth an ash-cloud of inky blackness, expanding upward as it rushed down the talus slope . . . At the same instant an explosion on its eastern summit shot out a second avalanche with rising cloud white as snow; two mighty parallel columns, ominous, terrifying, moving straight toward the station. I shall not attempt to describe all the sensations I felt, nor the thoughts that swept through my mind at that moment. My first thought was of instant flight. With a distance of 2.5 kilometers between me and the crater, it might be four minutes before the clouds reached me, but a moment’s reflection indicated that this could not be enough to escape the wide path of the cloud. I decided to risk the protection of the frail shack. Doors, windows, cracks, and holes were hastily closed and the onset awaited. Escapes from many former perils helped to allay my fears, but there was still the thought that this might be my last. I recall a sense of utter isolation; awe in the face of overwhelming forces of nature so indifferent to my feeble self. The track of the avalanche lay to the side of the station or these lines could never have been written. The chief dangers were heat and gas from the cloud. There was still a minute left. I peered out from the rear of the station. A sublime spectacle! Two pillars of cloud a thousand feet in height, apparently gaining in speed every instant and headed straight for my shelter. As I darted within, the blast was upon me – not a terrific shock as the reader might think, but swirling gusts of ash-laden wind, bringing a pall of darkness that might indeed be felt. The dusty air [that] entered every crevice of the shack was hot but not scorching. I felt the gases burning and parching my

Survival Tips for Field Volcanologists:

Whenever approaching an active volcano, always choose routes that “keep to the high ground.” Unexpected hazards like PDCs, lahars, and dense CO₂ accumulations will flow to low ground. Not only are ridge tops safer than valley bottoms – there are more likely to be cool breezes up there!

throat and then came a feeling of weakness (carbon monoxide?). It all lasted for half an hour, but it was nearly an hour before the feeling of suffocation was relieved by a kindly wind.

Painful as the experience had been – and still was – I had been granted an opportunity, from a situation only 200 or 300 meters from the direct path of the avalanche, to observe that marvelous manifestation of volcanism. During the whole time of its passage . . . there was a condition of absolute silence, broken only by the occasional slide of older lava blocks as they were thrust aside in its resistless sweep. (Perret 1935, pp. 61–2)

As Perret’s account indicates, pyroclastic flows have very low densities at their dilute margins owing to their low content of solid material, and will in some instances flow around fragile structures without damaging them. I (JPL) remember finding a soda bottle that remained upright on a charred table outside a home at the edge of a Galunggung pyroclastic flow. Although not toppled by the hot ejecta cloud, the glass had begun to melt and deform.

Small pyroclastic flows may pour down a mountainside at a relatively “slow” 20–30 m/s, while very large flows may reach speeds of 50 or even 100 m/s across wide areas (Freundt & Bursik 1998). The climactic Taupo, New Zealand pyroclastic flow possibly attained supersonic speeds of as much as 500 m/s close to its vent (Legros & Kelfoun 2002)! While mostly guided by gravity and topographically confined, fast moving ash flows have enough momentum to overtop ridges hundreds of meters high that stand in the way. For example, the 50 km³, 3400-year-old Aniakchak ash flow [9], Alaska, surmounted slopes as high as 700 m 20 km from its source vent (Miller & Smith 1977).

BOILOVER PYROCLASTIC FLOWS

Boilover pyroclastic flows originate in tops of magma conduits in a zone of magma boiling that produces relatively dense mixtures of gases and particles, mixtures that lack the buoyancy to ascend far above crater rims. Wolfe (1878), as quoted in Ross and Smith (1961), described the 1877 Cotopaxi [52] pyroclastic flows thus: “It is indeed one of the singular features of this eruption that the lava [*pyroclastic flows*] poured out of the crater not in one or several streams, but symmetrically in all directions, over its lowest edge as well as its highest points” and “that it flowed out over the highest crater edges like the foam from a boiling over rice-pot [*überwallenden Reistopfes*].” Taylor (1958) described the formation of boilover pyroclastic flows in his observations of the 1951 Mt Lamington [121] eruption:

On several occasions the discrete explosive events of the spear-head type gave way to a mass effect. Successive explosions fountained rapidly and extensively from many parts of the crater floor and filled the crater bowl with a massive, convoluted cloud of fragmental lava and gas. The cloud usually showed little tendency to rise. The heavy, yet buoyant mass seemed to behave as a layered hydrostatic column raised (sic) in the bowl of the crater. The heavier fractions poured out through the low gaps in the crater wall; the lighter fractions poured over the crater rim.

Macdonald (1972) refers to boilover pyroclastic flows as **overflowing glowing clouds**; Fisher and Schminke (1984) speak of them as **low-pressure boiling-over** flows. It is indisputable that many pyroclastic flows form in this manner, and that both column collapse and boilover mechanisms may operate during the same eruption. For example, Rowley et al. (1981) showed that “most pf’s [pyroclastic flows] originated [as] bulbous masses of ash, lapilli, and blocks [that] rose only a short distance above the inner crater and spread laterally” during the 1980 eruptions of Mount St Helens, though some also resulted from column collapse. Pyroclastic flows did not commence at Mount St Helens until nearly 4 hours after a Plinian column had risen to more than 20 km altitude at the beginning of the May 18 eruption. In contrast, during subsequent eruptions flows began to spill out of the crater *before* explosive columns were well-developed. In another instance, the PDCs of the June 15, 1991 climactic eruption of Mt Pinatubo originated from gravitational collapse of the basal portions of a Plinian column coincident with heavy tephra fall (Scott et al. 1996). And in the ongoing eruptions of Soufrière Hills volcano, Montserrat many pyroclastic flows have developed from crater overflows of low eruptive columns, and not from column collapse (Druitt & Kokelaar 2002).

In contrast to boilover flows from wide conduits where magma can release gas at shallow depths; deeper boiling in narrower conduits favors the development of the high-speed ejecta jets that result in the rise of pyroclastic material to great elevation above vents and the development of column-collapse-style pyroclastic flows. Lower volatile content in the boiling magma froth might well be another factor; the greater density of such mixtures would inhibit ascension into ascending Plinian clouds and predispose direct overflow of crater rims.

DEPOSITIONAL MECHANICS OF PYROCLASTIC FLOWS

Pyroclastic flows fed by Plinian eruptions, whether formed by column collapse or boilover processes, exhibit similar characteristics once they leave source areas. How such flows come to rest and form their deposits is not well-known. Some researchers have interpreted massive pyroclastic flow beds as resulting from the *en masse* settling of fragmental loads (Carey 1991). This indeed happens near the distal ends of many PDCs, and perhaps throughout most of the reach of smaller, denser currents such as block and ash flows in their final moments. Rheologically, such sudden deposition is characteristic of a type of non-Newtonian fluid (Chapter 4) called a **Bingham body** in which below a certain yield stress the moving mass behaves almost like a solid. Individual particles do not change their positions much relative to one another within the transporting current prior to sudden deposition. Internal shearing can also occur. Particles near the bottom of the moving mass tend to stop first, frozen into place by frictional drag, while particles higher up in the deposit keep moving, setting up strong shear stresses.

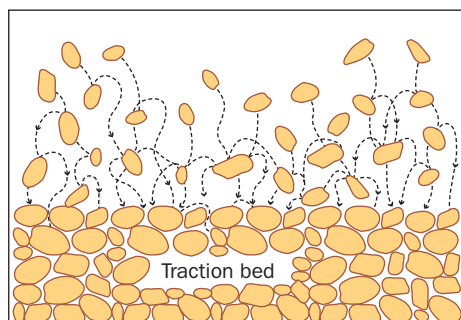
The notion that larger pyroclastic flow bodies such as ash flows settle by *en masse* deposition has been challenged by Branney and Kokelaar (1997, 2002), who argue such massive deposits develop primarily by **aggradation**, a process of gradual accumulation and build-up of fragments into a thick layer as dilute mixtures of gas and fragments move erratically across the depositional surface. Good cases can be made for aggradation during deposition of the Mazama Tuff around Crater Lake, Oregon, and Alaska’s Valley of Ten Thousand Smokes ignimbrite, especially by the common texture called **imbrication** (Mimura 1984; Fierstein

Fig. 8.17 Imbrication of pumice lapilli in the Tumalo Tuff, a Pleistocene ignimbrite west of Bend, Oregon. Pyroclastic flow moved left to right during deposition. Scale in cm. USGS photo by J. P. Lockwood.

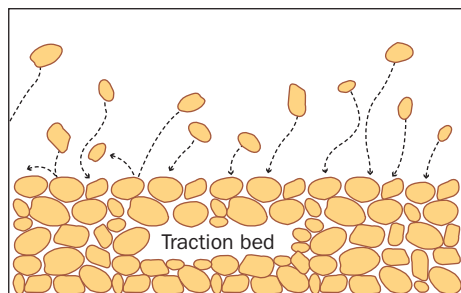


Fig. 8.18 PDC fabrics are a function of the way in which the constituent particles settle from their gaseous transport medium.

and Hildreth 1992). Imbrication, a common feature of pebbles in river bed deposits, is the stacking of platy or elongate fragments swept along by a fast-moving current under turbulolaminar or laminar conditions (Fig. 8.17). The clasts pile atop one another so as to slope back toward the source of the current. A process similar to aggradation and imbrication takes



Grain collisional interference during aggradational settling=Flows



Free settling of grains during aggradational=Surges

place in the traction deposition of pyroclastic surges, suggesting that there is, in fact, a complete spectrum in transport behavior between pyroclastic flows and pyroclastic surges (Druitt et al. 1982; Druitt 1996).

If aggradation, imbrication, and basal traction bed development occur in both pyroclastic flows and surges, we are left once again dealing with the question of what accounts for the striking difference in the appearance of flow and surge deposits. Brown and Branney (2004) suggest that the critical defining factor has to do with the suspended particle concentration just above the surface of the traction bed right at the moment of deposition. If the particles are so closely spaced that they *interact and hinder one another* in their final settling, a massive texture characteristic of pyroclastic flows will develop. If fragments are *too*

widely spaced to collide and lock one another into position in the moments before settling, surge-style bedding forms instead. Brown and Branney envision flow texture-determining particle interactions as taking place in a narrow gradational zone separating the emplaced basal bed from the still moving current cloud above (Fig. 8.18).

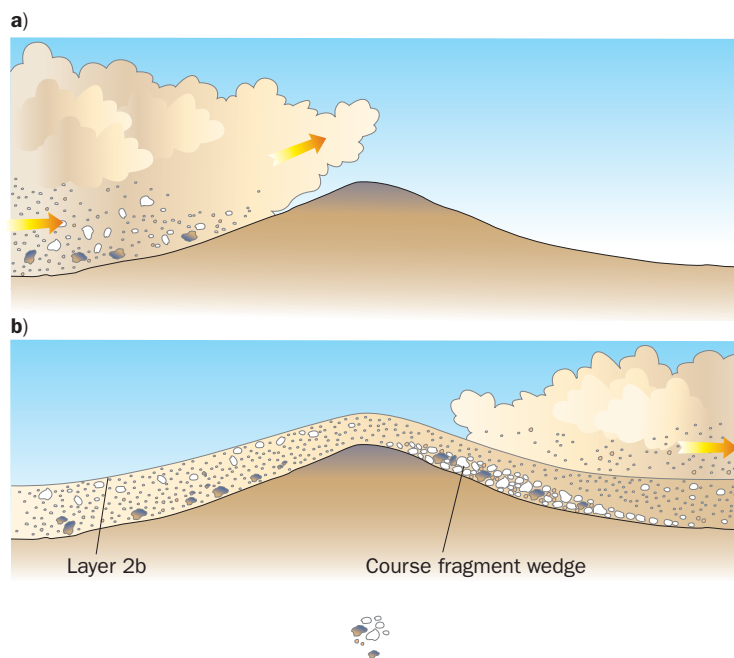
ASH ELUTRIATION AND FINES DEPLETION

Where an ash flow streams across the crest of a hill or ridge a pocket of air may be trapped on the lee side into which coarser pumice fragments fall, the lighter-weight material continuing to be swept on (Fig. 8.19). The resulting pumice-rich wedge may extend for tens of meters before pinching out in the direction of ash-flow movement. Walker (1983) referred to such deposits as being **finer-depleted**, because they lack the high concentrations of ash seen throughout most of the rest of the ignimbrite.

Another common agent of fines depletion is the escape of gases and trapped air through the top of a settling ash flow. The finest particles of ash are filtered out (**elutriated**) by the gas, which tends to escape via gas segregation pipes (Chapter 7). Well-sorted, tell-tale concentrations of coarse pumice and lithic fragments that lagged behind during elutriation allow one to distinguish gas pipes quite readily in eroded cross-sectional cuts (Fig. 8.20). They may extend vertically for many meters. Most are far better sorted than the surrounding ash flow deposits, illustrating the effectiveness of a high-density gas stream in filtering grain sizes. Many of them occur in clusters reflecting high concentrations of escaping gases from deeper in the deposit, in some cases derived from buried streams, marshes, and ponds. Some have more unusual origins. In the immediate aftermath of the May 18, 1980 eruption of Mount St Helens, gas segregation pipes developed in pyroclastic flows from the embedded carbonized remains of stems and branches, pieces of the tree blown-down and swept up by the pyroclastic current. The heated wood released gases into the overlying bed as it was being distilled to charcoal, gases that were concentrated enough to carry bits of charcoal upward for tens of centimeters (Druitt 1992). Most segregation pipes extend all of the way to flow surfaces, where the gas escapes through fumaroles following an initial burst of fine ash – a miniature eruption in and of itself. Some of these bursts are strong enough to scallop out shallow craters in the soft beds of late stage fall deposits. Later hydrothermal alteration of included fragments by the concentrated flow of vapors gives some of them a distinctive ochre or red color.

As large pyroclastic flows move downslope, tremendous amounts of material can periodically elutriate and jet from their advancing fronts, which is alternately (or simultaneously) entraining and releasing great amounts of surrounding air owing to their high turbulence and speed. These **flow**

Fig. 8.19 The launch-ramp effect for development of fines-depleted coarse particle concentrations on the leeward side of topographic highs crossed by ash flows.



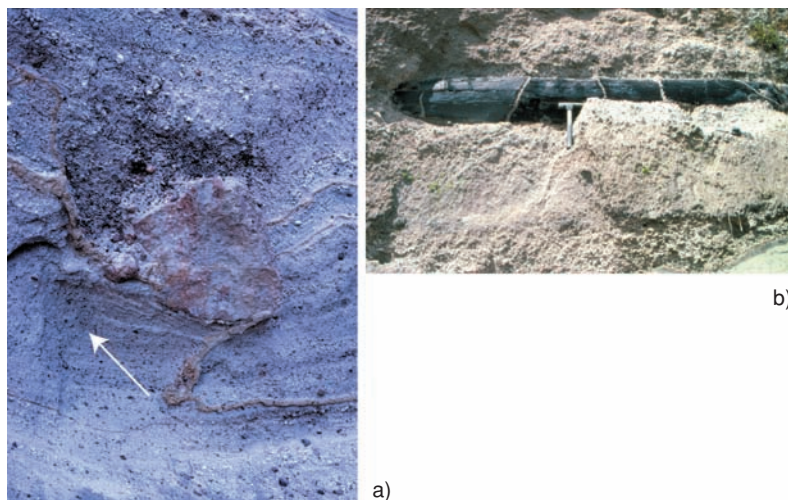


Fig. 8.20 Pyroclastic flow features. a) Ash elutriation features associated with a small lithic block (15 cm diameter) that impacted a freshly emplaced ash flow bed, El Cajete member of the Bandalier Tuff, New Mexico. The elutriation pipe initiated below block (arrow). The brown veins are caused by secondary alteration. Photo by R. W. Hazlett. b) Carbonized log preserved in the Taupo ignimbrite, New Zealand. Note the mobility of the ash – which penetrated the log as it carbonized and shrank after pyroclastic flow emplacement. USGS photo by J. P. Lockwood.

and surface of the flow deposit, leaving a zone of concentrated charcoal logs and rounded pumice clasts behind (Walker et al. 1980).

Ash flows may not continuously deposit material as they travel across surfaces. Such non-deposition is termed **bypassing** (Brown & Branney 2004). Bypassing, accompanied by significant erosion of the ground, may be common over distances of several kilometers on proximal slopes, where PDCs can be expected to move most rapidly. Scouring and erosion during bypassing probably provides a larger quantity of accidental and accessory ejecta to ash flows than is commonly appreciated. Later pyroclastic deposits, however, may bury bypassed areas, making their identification and interpretation difficult.

Work by Calder et al. (2000) on the relatively small Soncor ignimbrite from Láscar volcano [58] in northern Chile reveals that as the initially turbulent ash flow traveled, it laid out a bed of coarse breccia closest to its vent with finer lithic breccia farther downslope, and finally, lobate pumice deposits at the terminus (Fig. 8.21). The formation of basal breccias that thin distally, and pumice rich upper layers and distal margins is common in many ash flows (Chapter 7; Fig. 8.22). Experimental work by Choux and Druitt (2002) provides some insight into the nature of particle separation during dilute, turbulent transport. They used a water flume in which particles of two distinct densities, one light (pumiceous) and the other heavy (lithic) were immersed. They varied the volumetric particle concentration in experimental runs from between .06 percent and 23 percent. At concentrations of less than a few percent, light and dense particles responded in the same way to the currents – they had **hydrodynamic** (or **aerodynamic**) **equivalence**, meaning that they had the same settling speeds. Above about 5 percent particle concentration the behaviors of light and dense particles became separate. Heavier particles developed settlement patterns resembling the co-ignimbrite lag breccias mentioned in Chapter 7, while lighter particles accumulated atop the deposit and swept off to pile up at the distal end in a manner reminiscent of the Soncor pumices.

CO-IGNIMBRITE (CO-PDC) ASH PLUMES

As a pyroclastic flow travels, the gas-particle mixture at the top of the flow and at its terminus becomes lighter than the surrounding atmosphere owing to the fallout of larger and heavier fragments. Turbulent convecting clouds of fine elutriated ash, called **co-ignimbrite ash plumes**

head elutriation jets consist not only of fine ash, but also lumps of pumice and even occasionally denser lithic fragments. A spectacular example of fines depletion related to this process, somewhat similar to the Mount St Helens example cited above, occurred during eruption of the Taupo ignimbrite. Where this enormous ash flow overrode moist woodland, plants and trees were swept up and mixed in with the ash and pumice. Instantaneous combustion released large quantities of vapor that gushed upward through the ash. The elutriating ash-vapor mixture jetted from the advancing flow front

may ascend kilometers above moving PDCs. Fallout from these plumes commonly produces the thick, well-sorted ash beds seen capping many ignimbrites. Similarly formed ash beds atop pyroclastic flows having a high initial concentration of coarse ejecta, such as block and ash avalanches are typically thin. In other instances the volumes of co-ignimbrite ash may equal or even exceed the volumes of associated ignimbrites in other instances, indicating that the original ash flows must have been especially gas-rich (Freundt & Bursik 1998). In some cases, as at Montserrat, PDC-related ash plumes become strongly convective, and may even dwarf the heights of source eruptive columns.

Eye-witness accounts show that co-ignimbrite ash plumes rise directly from the turbulent front of advancing flow masses where air is easily entrained, and from places where the pyroclastic flow encounters changes in slope (Fig. 8.23). At Merapi volcano [101], pyroclastic flows in November 1994 reached the base of the 30° slope of the cone where their dense basal masses continued moving downhill while the turbulent ash clouds rising from their surfaces detached to form plumes as much as several kilometers high (Bourdier & Abdurachman 2001). Likewise, where ash flows cross hills or ridges, deposition of coarser ejecta in the pockets of relatively calm air on the downwind sides of each obstacle enhances the buoyancy of the remaining gas-particle mass, forcing the development of conspicuous ash plumes (Fig. 8.24). To distinguish

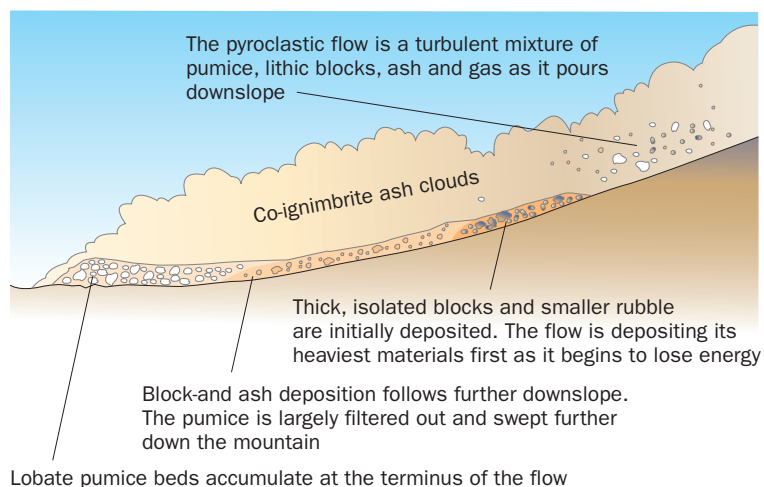


Fig. 8.21 Depositional facies of the Soncor pyroclastic flow, Lascar Volcano, Chile. After Calder et al. (2000).



Fig. 8.22 A remarkable concentration of pumice blocks marks the terminus of a small, late-stage pyroclastic flow erupted from the crater of Mount St Helens (MSH) on May 18, 1980. A grain dispersive sorting mechanism may have been at play to account for this concentration. View toward the MSH crater source, 5 km away. (USGS photo by Don Swanson)



Fig. 8.23 Pyroclastic flow pouring onto the sea off south coast of Montserrat Island, following a collapse of the Soufrière Hills volcano summit cone in September 1996. Note co-ignimbrite plume ascending over flow base, and discolored water from previous flows. Photo by Simon Young, British Geological Survey.

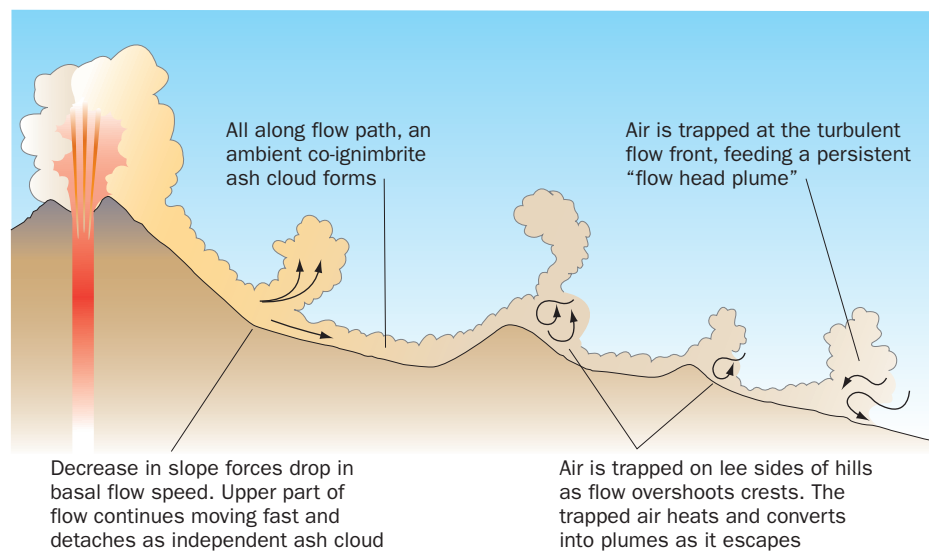
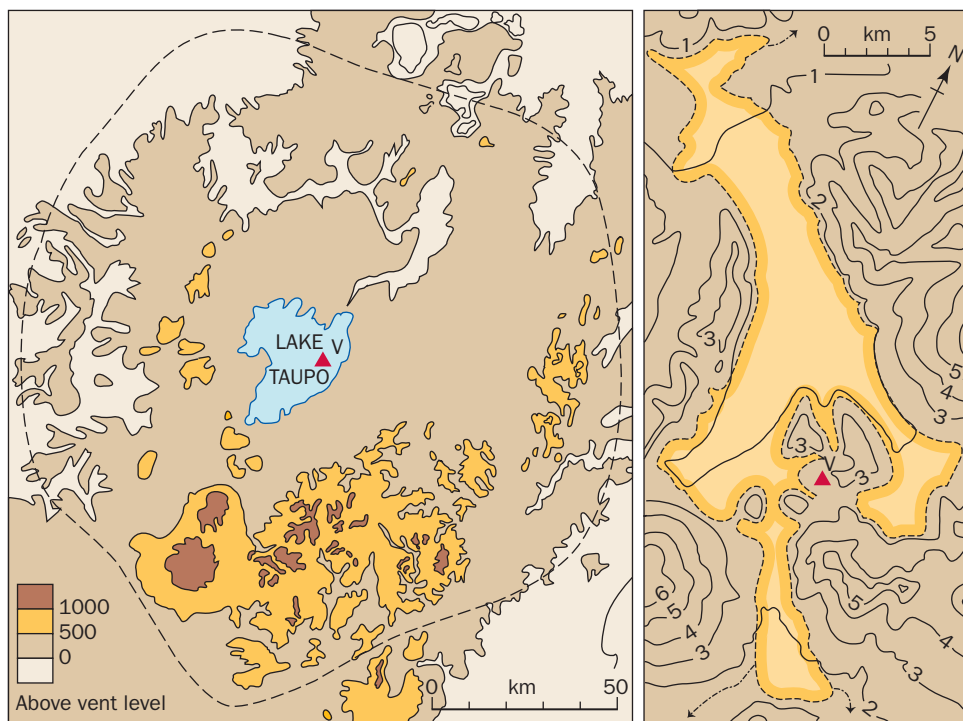


Fig. 8.24 Secondary, or "phoenix" plumes from pyroclastic flows.

these from the ordinary eruption clouds generated directly above a vent, some volcanologists have called them **phoenix plumes** (Dobran et al. 1993), alluding to the mythological Greco-Phoenician bird whose body “rose from the ashes.”

IGNIMBRITE ASPECT RATIOS AND CRITICALITIES

Walker (1983) distinguished two categories of ash-flows. He termed the deposits of conventional ash flows **high-aspect-ratio ignimbrites** (HARIs), and characterized them as being emplaced “quietly and passively in valleys,” typically by *en masse* dumping of pyroclastic loads, in contrast to the **low-aspect-ratio ignimbrites** (LARIs) representing ash flows with the “remarkable ability to scale mountains and cross open water.” An example of the former is the 1912 Novarupta [17] deposit in the Valley of Ten Thousand Smokes (VTTS) (Fig. 7.28). Examples of the latter include the above-mentioned Aniakchak Tuff [9], the Taupo and Oruanui [136] ignimbrites in New Zealand, and indeed virtually all Phreatoplinian eruption deposits (Fig. 8.25). **Aspect ratios** of ignimbrites (or lava flows) are measured by dividing the average thickness of the flow by the area encompassed by a circle with a radius equal to the farthest reach of a flow from its source – that is, its maximum thickness divided by the travel (**run-out**) distance. Walker measured an aspect ratio range of from 1/400 (VTTS) to 1/100,000 (Taupo).



Taupo ignimbrite, New Zealand, (coverage within the dashed line)

The Valley of Ten Thousand Smokes ignimbrite (orange) is high-aspect ratio. (Contours in 100m intervals)

Fig. 8.25 LARIs and HARIs examples. Source vents shown by red triangles. After Walker (1983).

The main current of the Taupo ash flow was indeed fast moving. Wilson (1985) found patches of veneer facies on the slopes of Ruapehu volcano [134], 60 km south of the source vent and 1500 m higher than the surrounding hummock plain. To climb this high at such a distance from the source, the current must have converted all of its available kinetic into potential energy according to:

$$U = (2gh)^{1/2} \quad (8.2)$$

where $h = 1500$ meters, and U the speed of the flow – an astonishing 170 m/s in this case. It is on the basis of calculations such as this that Wilson believes emplacement of the Taupo ignimbrite took only a matter of minutes, and estimates a speed of 170 m/s 60 km from the vent, and approaching 500 m/s near the Lake Taupo caldera source from an eruptive column on the order of 10 km in diameter.

Based on theoretical considerations, Bursik and Woods (1996) categorized ash flows into two categories somewhat differently than Walker's HARI and LARI characterization. They define **subcritical ash flows** as relatively slow (10–100 m/s) and relatively thick, with turbulent suspension loads puffing up to more than 1–3 km above the surface. **Supercritical flows** are faster (100–200 m/s) and thinner (500–1000 m). In general, subcritical ash flows decrease their volumes at a constant, linear rate as they spread away from vents, whereas supercritical ash flows entrain more air and become progressively more voluminous. The entrainment of large amounts of air also means that supercritical ash flows tend to produce larger and more numerous co-ignimbrite plumes, some of which may climb as high as 20–40 km, dwarfing related Plinian columns. As much as 20–40 percent of the ejecta in a supercritical ash-flow, primarily in the form of fine ash, may be removed through plume activity (Sparks & Walker 1977), and flow run-out may be significantly reduced due to loss of kinetic energy during plume generation. Because subcritical ash flows show less plume activity they tend to travel farther than their supercritical counterparts, even though slower moving.

Ash-flow speeds rise with increasing eruption intensities, hence larger Plinian eruptions (10^9 – 10^{10} kg/s) tend to generate supercritical ash flows in which air entrainment dominates the development of the flows (Bursik & Woods 1996). For subcritical flows, air entrainment is less important than sedimentation rate in terms of governing how the flows move, and how far they travel.

Single ash-flows may behave supercritically at some points along their paths, and subcritically at others. Woods (1988) investigated topographic effects on moving ash-flows, suggesting that a supercritical ash-flows approaching opposing ridge crests would expel air and gases, perhaps through co-ignimbrite plume generation, and become subcritical. But after crossing the ridge crest, the ash flow could entrain large amounts of air as it launches into the atmosphere for a short distance, as off a ski jump, and becomes supercritical again. The distance an ash-flow can travel depends significantly upon the degree to which it is in a subcritical or supercritical mode. For instance, an ash flow generated in a high-intensity eruption with an initial gas mass fraction of 0.1 wt. percent and mean particle size of 1 mm can travel 20–25 km down a valley 2 km wide in a supercritical state before stopping, whereas a subcritical flow will travel much further, up to 50–60 km. But on an open plain, given the same pyroclastic current conditions, a subcritical flow will only travel 15–20 km (Bursik and

Woods, 1996). In general, low-aspect ratio ash flows behave as supercritical flows. However the local impacts of topography on current dynamics, as introduced above, prevent a strict equivalence between the concepts of ash-flow aspect ratio and criticality. (Likewise, the concept of “criticality” as applied to ash flows must not be equated with Reynolds and Froude number “criticalities” to be introduced in different contexts later, though each applies to conditions of flow.)

THE ORIGIN OF PYROCLASTIC SURGES

Cold War era atmospheric testing of nuclear weapons produced an unexpected benefit for volcanology – revealing a new phenomena associated with near-surface explosions. During the July, 1946 underwater test of the 20 kt atomic bomb “Baker” at Bikini Atoll (south-western Pacific), a ring of steam and debris raced out across the lagoon at the base of a ascending mushroom cloud in all directions, at an average speed of 33 m/sec. Observers termed this cloud a **base surge**. Nuclear testing at the Nevada Test site in the 1950s demonstrated that base surges formed whenever explosions were focused at or near ground level (Fig. 8.26).

In 1952–3, an eruption of Barcena volcano [39], on an island off the west coast of Mexico produced a similar eruption column and base surge, leading geologists to suggest that



Fig. 8.26 “Priscilla” 37 kt atomic blast test at the Nevada Test Center, Nevada, June 24, 1957. Note well-developed base surge, expanding from the base of the ascending “mushroom cloud.” Photo courtesy US Department of Energy.

the physics of both were the same (Richards 1959). This was confirmed in 1965, when Taal volcano [105] in the Philippines erupted explosively through a submerged vent along the shore of a caldera-filling lake. The blast effects of the Taal base surge closely resembled those of some nuclear tests. The 100°C expanding surge cloud initially spread at 50 m/s, totally destroying trees within a kilometer of the vent, and plastering objects with hot ash out to a distance of 8 km. Moore (1967) described the effects of the eruption and popularized the term *base surge* to describe both the eruption and its deposits.

Base surge eruptions are most powerful when abundant water is involved, and are characteristic of many hydrovolcanic eruptions – a confirmation of Walker's (1973) assertion that “steam means power” when it comes to volcanic explosions. Their origins are also remarkably shallow: Rohrer (1965) related base surge run out to explosive power, noting that the distance traveled varies as one-third the power of the explosion yield, given an “optimal” explosion depth of only 10–15 m for a one-kiloton charge. Such an explosion would produce a gas-expansion-type base surge traveling 2.5 km. Moore (1967) applied these calculations to derive the explosive yield of the Lake Taal base surge, finding that a surge moving 6 km would require a 16 kt blast originating at a depth of “several meters.” Mastin and Witter (2000) went further in using energy equations to constrain the size of the Taal explosive body. Working with fuel-coolant ratios of 1 : 3 to 1 : 5, the range observed in hydrovolcanic eruptions (Wohletz, 1986), and assuming an efficiency of 10 percent in converting thermal to mechanical energy, they found that on the order of $1\text{--}2 \times 10^6$ tons of explosively interacting magma and water would be required to generate the Taal surge, equivalent to a vent 50 m in diameter volatilizing to a depth of 500–1000 m.

By the early 1970s comparison of recent base surge deposits with older features in the geological record showed that surge-like bedding could result from range of processes other than simply powerful Taal-style hydroexplosions. All shared in common the aspects of powerful, water or gas-rich ground-hugging energy dispersal. Sparks and Wilson (1976) introduced the term **pyroclastic surge** for this family of related phenomena. Pyroclastic surges tend to be cooler than pyroclastic flows, and many involve condensed water, as evidenced by the presence of accretionary lapilli in many deposits. Although many surges are emplaced “dry” (above condensation temperature of water), there is never evidence of welding in their deposits. Surge currents, although highly dilute, are characterized by extremely turbulent flow, and commonly cause mechanical erosion of earlier layers. In addition to base surges, **ground surges** and **ash-cloud surges** are also recognized (Wohletz 1998). **Directed blasts** have also been considered as a type of surge by some volcanologists, though their deposits imply more complicated emplacement mechanics, and they will also be discussed in the following sections.

Most base surges are relatively local in their effects, rarely extending more than 1 km from hydrovolcanic source vents. Surge processes can be integral components of larger sub-Plinian and Plinian eruptions though, and dry surge phenomena are contemporaneous with pyroclastic flows in most large explosive eruptions. The El Chichón eruption in March and April of 1982 (Chapter 14) illustrates the characteristics of dry surging, where hot air and dominantly magmatic gases rather than a dominance of steam drove PDC generation.

El Chichón is a heavily eroded dome complex in the jungle of southern Mexico (Fig. 14.1), which had erupted explosively in the eighth, fourteenth, and mid-nineteenth centuries, but despite this record had largely been ignored as a potentially dangerous volcano, because the gaps

between its eruptions were so lengthy. The onset of the 1982 eruption was sudden, and major loss of life took place. Pyroclastic currents, some moving as rapidly as 100 m/s, destroyed nine villages that could not be evacuated on time, with over 2000 fatalities. The six-day long eruption fluctuated between steam-rich Vulcanian, phreatomagmatic and Plinian phases (Macias et al. 1997). Sigurdsson et al. (1987) describe the initiation of two of the surges:

[Activity] began with an explosion which produced a low, incandescent eruption cloud around the summit of the volcano . . . From this cloud issued the first pyroclastic surge, which devastated the flanks of the volcano and spread in all directions, but mainly to the south up to 8 km from the crater. Minor pyroclastic flows and debris flows from the disintegrating dome also accompanied the first stage. Immediately following the surge a Plinian eruption column developed, from which [a] fallout layer . . . was deposited. From the distribution of lithic [fragments] in the fall deposit, it is clear that this eruption column was the most energetic of the El Chichón eruptions, with an average column height of 24 km. The . . . Plinian event also had the highest mass eruption rate, at 6×10^7 kg/s, producing a total of 0.39 km^3 [of ejecta] . . . The Plinian stage was followed by a second pyroclastic surge . . . which spread laterally from the crater and covered 104 km^2 . Because of the sequence of events from a Plinian column to a surge, we propose that the second surge originated during column collapse. It was accompanied by pyroclastic flows.

The depositional fabric of the El Chichón surge beds provides further detailed information about surge dynamics. In the lower halves of surge beds, materials coarsen upward – reversely graded – and the lee sides of sand waves face the distal ends of the deposits. Such a fabric is to be expected as long as the speed of the current is increasing throughout deposition. Heavier material is being plucked up by the strengthening current, and dune crests are migrating vigorously down slope. Just the opposite pattern occurs in the upper half of surge deposits, however, with material fining upward and lee sides of sand waves facing back toward the vent. The late-stage vent-ward migration of sand waves indicated by the reversal of slopes implies that a ground-level counterflow of hot gas and air back took place back toward the vent to equalize atmospheric pressure.

Late-stage vent-ward winds are not the only explanation for regressive shifting of sand waves. This can also happen if an eruption suddenly becomes much wetter, with cohesive wet ash accreting to the stoss sides of dunes, or if current speed rapidly accelerates to a high level (Schmincke et al. 1973; Allen 1982; Barwis & Hayes 1985; Cas & Wright 1987). Waters and Fisher (1970) termed the latter category of dunes **antidunes**. In a general way, what happens when antidunes form is that high speed currents abrasively erode the proximal surfaces over which they flow, plastering sand against the opposing sides of obstacles in the bed further downstream, which grow into mounds continuously shifting their crests backwards into the face of the oncoming current. The antidunes themselves will set up internal waves within the current that help shape and maintain additional, regularly spaced antidunes in a smoothly-flowing, fully developed system.

In the vicinity of vents, fresh pyroclastic surges roaring down slopes can be highly erosive. In the base surges of Taal and Barcena volcanoes, and even in the 79 CE surge deposits of Vesuvius, proximal erosion channels with U-shaped cross-sectional profiles are common.

At Koko Head, a Surtseyan tuff cone on the southeastern coast of Oahu in the Hawaiian Islands, these U-shaped channels range in width from 0.4 m to 5.5 m, with depths of 1 to 3 m. They occur low in the surge deposit, suggesting that they were scoured during the initial, highest-power portion of the eruption, only to be filled by subsequent surge layers as the speed and energy of surging waned. Fisher (1977) believes that some of these channels, in fact, began as normal fluvial runnels cut into soft ash, which repeated surging later sculpted into deeper and wider troughs. Elsewhere the connection between U-shaped channel cutting and pre-existing drainage is not evident. Fisher also suggested that cutting of furrows on slopes might be specifically correlated with the formation of particle-rich lobes frequently seen extending from the advancing fronts of base surges. The dynamic origin of such lobes is unknown, but at high speeds the segregation of particles into narrow funnels and channels is also seen in some experimental turbulent suspensions.

GROUND AND ASH CLOUD SURGES

Many ignimbrites are immediately underlain by patchy to widespread surge beds, which because of their basal position constitute **ground surge** deposits. Ash-cloud surge beds immediately overly many ignimbrites too, and in many cases are much more extensive and thicker than related ground surge features. Ground and ash-cloud surge layers tend to be fines-depleted, with a very high concentration of crystal fragments. Lacking much glass, they are largely impervious to the welding that may take place in adjacent ash-flow deposits (Wohletz 1998).

Several hypotheses have been discussed regarding the origin of ground surges. The simplest one asserts that ground surges initially form when an eruption column collapses, since the falling debris incorporates large amounts of air (Fisher 1979). The surging precedes in advance of a denser, flow-forming ash cloud, and hence lays down a ground pad for it to bury. Others believe that the scattered and localized occurrences of ground surge deposits and their highly fines-depleted compositions require a different mode of formation. Possibly they result from pockets of turbulence, trapped air masses, at the base of advancing ash flows which create locally dilute conditions (Valentine and Fisher 1986). Or perhaps, as in the case of the forest that was overwhelmed by the Taupo ignimbrite, they represent elutriations of dilute, turbulent ejecta from the swiftly advancing turbulent fronts of ash flows. If this latter interpretation is correct, the surges must spasmodically squirt forward, perhaps energized by blast waves, and disperse mere seconds before being covered by the slightly slower pyroclastic flows (Wohletz et al. 1984).

PDCs AND FLUID MECHANICS

As already discussed, particle transport in pyroclastic flows is regarded as being dominantly laminar, while in pyroclastic surges turbulence dominates. **Laminar flow** is a sheet-like movement of material in which separate particles maintain parallel directions of motion, though not necessarily at the same speeds. Roughly speaking, the ice crystals in a moving glacier shift down slope this way, with those closest to the base and the margins of the glacier moving more

slowly than those at the surface, near the central axis of the ice stream. **Turbulent flow** involves a chaotic movement of particles, all moving in different directions, and in some instances at different speeds. Flow paths are mostly curvilinear. Water molecules in a swiftly flowing stream or river show turbulence. A fluid may flow in a laminar manner at one time, and then become turbulent later. What determines mode of flow in an open channel is summarized by the **Reynolds equation**:

$$\text{Re} = (\rho R U_f) / \mu \quad (8.3)$$

Where Re is the **Reynolds number**; ρ is the fluid density; R is the ratio A/P, with A equaling the cross-sectional area of the channel through which the flow is pouring and P the length of contact between the flow and channel floor and banks (“wetted perimeter”); U_f is the speed of the fluid, and μ is the fluid viscosity. Reynolds numbers of magmas and gases moving through conduits are calculated somewhat differently, but that shouldn’t concern us here. The Reynolds number is *directly proportional to the speed and inversely proportional to the viscosity of a moving fluid*, with viscosity greatly increasing at higher particle concentrations. If the Reynolds number in an open channel is greater than about 2000, flow will be turbulent. If less than about 500 it is laminar, and if it is in the range 500–2000 a transitional motion occurs which is described as **turbulolaminar**.

Pyroclastic surges behave as **inertial flows** in which the moving masses may initially act like a homogeneous Newtonian fluid, then quickly split into two layers – rather as the engineers have observed in gas-particle experiments. One of these is fast and turbulently agitated, with widely-spaced particles buoyantly overriding the pull of gravity (see Kunii & Levenspiel 1969). The other is slower, with concentrated grains that shift elastically as a basal drag or traction load that may also be present, as we have seen, in ash flows (Lowe 1982). As a result of this dynamic division, Valentine (1987) refers to pyroclastic surges as **stratified currents**. The traction load forms the surge deposits we eventually see after everything comes to rest. In general, it grows at the expense of the upper, gas-rich stratum as a surge blasts along, although the gas-rich part of the surge widely erodes and redistributes basal materials locally, creating the wide variety of structures and textures that so distinctively characterize surge deposits.

The greater role of turbulence and interstitial gases in pyroclastic surges provides for better sorting than in grain-supported pyroclastic flows. Ash, lithic fragments, and pumice will sort out with maximum grain sizes at different ϕ -levels in different parts of the surge cloud. For example, coarser fragments may move almost exclusively within the traction load, intermediate-sized particles may move both by being embedded within the load, or by skipping and jumping along its surface. And finer particles may settle out largely after turbulence dissipates according to their terminal velocities in free air, a process Lowe (1982) refers to as **suspension deposition**.

Directed Blasts

When a shallow magma conduit suddenly depressurizes, molten rock and gases can rapidly escape by taking the path of least resistance to the surface. That path may be sideways through

the flank of a volcano, rather than vertically through its summit. The effects of this type of blast were first observed after the 1956 eruption of Bezymianny volcano [128] by Georgii Gorshkov, who visited this remote wilderness location following the eruption and coined the term “directed blast” to describe the phenomena involved (Gorshkov 1959, 1963). The first opportunity to document a directed blast by eye-witness accounts and film did not come until 1980, however, during the initial phases of the May 18, 1980 eruption of Mount St. Helens. Since the documentation of this eruption and its effects (Lipman & Mullineaux 1981) has had revolutionary impacts on the study of explosive volcanism, a review of this eruption and events that preceded the directed blast is in order.

CASE HISTORY OF A DIRECTED BLAST – MOUNT ST HELENS, 1980

The first signs of unrest at Mount St Helens (MSH) began with onset of an earthquake swarm on March 20, 1980, alerting geophysicists to the possibility of an eruption at this volcano for the first time in over a century. Sure enough, small Vulcanian ash bursts commenced on March 27. A shallow intrusion of dacitic magma was working its way into the northern flank of the volcanic cone, but the earliest minor explosive activity ejected only old rocks as magma ascended closer to the surface. The volcano’s northern flank bulged outward over a period of two months as the magma pressure built up within, moving an area of over 2 km² as much as 40 meters northward – at rates of up to 2 m/day (Lipman et al. 1981). Deformation extended far down the north flank, and tilt changes of up to 50 microradians/hr were noted at Timberline, 3 km from the MSH summit, causing visible displacement of level bubbles in survey equipment. The intrusion had formed a classic subsurface *cryptodome* (Chapter 9) and was primed with mounting gas pressure to produce a directed blast. Although similar swelling had preceded the 1956 directed-blast eruptions of Bezymianny volcano [128], Kamchatka (Gorshkov 1959), this example provided only one of several possible outcome scenarios, and most volcanologists on site thought a dome might extrude from the side of MSH without seriously destabilizing the edifice. Most believed that associated ash eruptions probably wouldn’t exceed in violence those which had occurred during the volcano’s lightly documented Goat Rocks period of activity a century and a half earlier. Although the potential hazards were not fully understood, a risk to visitors *was* recognized, and the area north of MSH was closed to public access – resulting in the saving of hundreds or perhaps thousands of lives on the morning of May 18.

Early on that morning, a magnitude-5 earthquake triggered a collapse of the volcano’s northern flank, producing a massive debris avalanche that cascaded northward. Dorothy Stoffel, observing from a light plane coincidentally flying above the mountain at the time, described the northern side of the mile-high cone as quivering like jelly in the moment leading up to sliding. Depressurized magmatic gases burst from the evolving slide scarp almost at once, jetting horizontally owing to the fact that the avalanche had opened a vent to one side, rather than on top, of the volcano’s magma column. Within about 15 seconds the blast cloud, moving at a speed of 90–110 m/s overtook the advancing front of the avalanche and then killed a promising young US Geological Survey volcanologist, David Johnston, who was posted

directly in the directed blast path, 6 km to the north-northwest (Voight 1981). He barely had the time to signal a warning by radio before being overwhelmed, and his body was never found. Lateral expansion of the blast cloud increased its speed to 325 m/s, and it retained enough momentum to overtop an opposing 380 m high barrier, now known as Johnston Ridge, at an estimated 235 m/s (Moore & Rice 1984). Blast materials reached supersonic speeds as they accelerated during flow (Kieffer 1981a, b) and quickly overtook and outran the initial debris avalanche.

Rosenbaum and Waitt (1981) record the testimony of some campers caught near the edge of the directed blast surge in forested highlands, an extraordinary 20 km to the west-northwest:

A very strong wind, which blew flames from the campfire flat along the ground and held braids of hair out horizontally, preceded the blast cloud by about 10–15 seconds. The witnesses were able to move about in the wind with little trouble, and no trees were toppled by it. No noise was associated with the approach of the cloud, and no concussion or loud noise was noted prior to the cloud's arrival. When the cloud arrived, it became totally black and all the trees seemed to come down at once. The witnesses were instantaneously buried in a combination of timber and "ash" and probably fell into the root ball of a blown-over tree. They could talk to each other but could see nothing. After perhaps 10 seconds it got very hot. At this time they could hear their hair "start to sizzle" as it was singed. One witness, who is a baker, estimated the heat to be "like a 300°F oven." Pitch boiled out of trees and remained hot enough to cause minor burns several minutes later. The sky cleared suddenly after several minutes and remained clear for a few more minutes. Then a dense ash fall began.

As the blast cloud reached the limit of its flow, the gases in the cloud abruptly became buoyant, shedding its remaining particle load as a poorly sorted, thin ash bed within a wide zone of trees with singed leaves. Local topography played an increasingly important role in influencing deposition with distance from the vent. In many watersheds, small, locally-generated, unusually fine-grained pyroclastic flows modified and buried initially emplaced surge layers. These weak PDCs lacked the energy to topple trees, in contrast to the original directed blast, but did transfer large masses of material into low lying areas, greatly thickening the deposits already accumulated there. The directed blast traveled at supersonic speeds in places, and completely devastated an area of about 600 km² (Fig. 8.27). Trees were uprooted, sheared off, charred, and carried away inside the blast cloud within a broad proximal zone (Fig. 8.27a), where temperatures were in excess of 350°C (Moore & Sisson 1981). Further out trees were merely blown down (Fig. 8.27b), and temperatures were much lower. In the outermost zones trees were not blown down but only singed by hot gases.

Hoblitt et al. (1981) studied the deposits left behind after the passage of the May 18 directed blast, and found them extremely complex, involving features attributed to pyroclastic flows, pyroclastic surges, and airfalls. Kieffer (1981) studied the dynamics of the May 18 directed blast and concluded that most of the blast gases and debris were discharged in the first 10–20 seconds from the exploding magma reservoir at around 100 m/sec, but that lateral speeds rapidly increased owing to expanding gases as the directed blast moved radially outwards. Total thermal energy release during this short-lived event is estimated at 24 megatons of TNT equivalent.

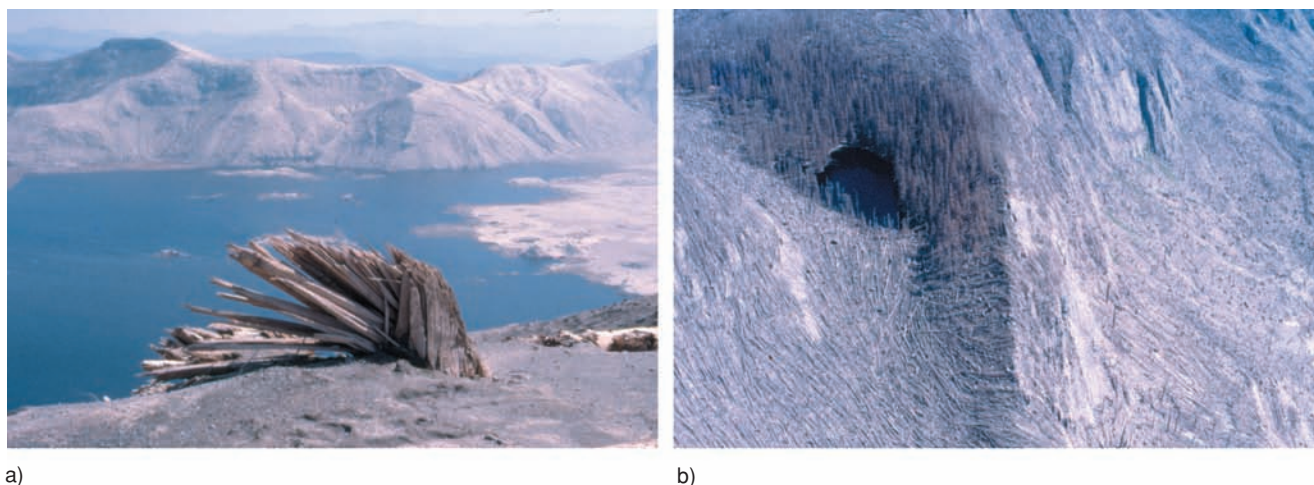


Fig. 8.27 Effects of the directed-blast eruption at Mount St Helens on May 18, 1980. a) Shattered tree stump 8 km north of the blast source. Stumps like this are all that remains of a dense forest that once covered the west edge of Spirit Lake (in the background). Note abrasion on the blast source side. b) Blown-down trees about 20 km northwest of the MSH blast source. Note the trees that were protected by a ridge and survived blow-down as the surge passed overhead. A few people survived the blast in such locations. USGS photos by J. P. Lockwood.

A comparison of directed blast deposits from three different volcanoes in three very different regions has demonstrated that their pyroclastic stratigraphy is quite similar, implying that very similar processes of transport and deposition operate for all such events (Belousov et al. 2007). Directed blasts are clearly the most violent phenomena associated with smaller, non-caldera-forming eruptions, and we are indeed fortunate that these occur so infrequently! Violent as they are, however, they are much less destructive than the much larger and more catastrophic “Super-eruptions”, to which we now turn our attention.

“Super-Eruptions”

“**Super-volcano**” is not a well-defined scientific term proposed by volcanologists; it is a term coined in 2000 by the writers of a popular BBC science program (*Horizon*) to describe volcanoes capable of “Super-eruptions.” In the words of the BBC narrator of the program, **Super-eruptions** were cataclysms that could “plunge the world into a catastrophe and push humanity to the brink of extinction.” The new term *Super-volcano* and the popularization of the older term *Super-eruption* caught the public imagination, and volcanologists were suddenly being asked to discuss the potential for such catastrophic events. Volcanologists quickly adopted these terms to describe such potentially catastrophic, yet extraordinarily rare explosive eruptions, and these words are now well-established in the geologic literature. Miller and Wark (2008) discuss the origins of these terms and the nature of “Super-eruptions” in more detail than will be possible here.

There is no standardized definition of what constitutes a Super-eruption, although any eruption with a VEI greater than 8 has been widely considered to qualify. Concerned about problems with eruptive column and volumes estimates, however, Mason et al. (2004) rejected

the VEI system, proposing to classify Super-eruptions strictly upon the basis of total *mass* ejected. Using a logarithmic scale approach like the VEI, they distinguish Super-eruptions as those producing log eruptive masses (“M”) greater than 10^{15} kg ($M > 8$). Thus defined, they identified 42 Super-eruptions that have occurred over the past 36 million years. The largest Super-eruption known to have ever taken place, and the only one with M greater than 9.0 (erupted mass more than 10^{16} kg), was the Oligocene La Garita caldera eruption of the Fish Canyon Tuff in southwestern Colorado (Chapter 11). More recently, Self (2006) defines Super-eruptions as having produced erupted magma volumes >450 km³ (ejecta volume >1000 km³).

No super-eruption has ever been witnessed by modern man – none have occurred within Holocene time. The most recent one took place in New Zealand about 26,500 years ago (see discussion below), and only five have happened in the past million years according to Mason et al. (2004). One of the largest Quaternary super-eruptions, from the Toba caldera [97] of Sumatra, produced over 2800 km³ of pyroclastic material and had major climatic impact on the entire Earth about 75,000 years ago (Chesner et al. 1991) (Fig. 8.28). This $M = 8.8$ eruption possibly caused a major decline in human populations (Chapter 13), and may have also stimulated an onset of continental glaciation. It covered about 1 percent of Earth’s surface with tephra to a depth of 10 cm or more – enough to collapse roofs and sink ships in modern terms (Mason et al. 2004).

Many individual calderas have produced multiple (2–4) Super-eruptions in the past, and are known to be underlain by active magmatic systems capable of large eruptions in the future. Some of these calderas remain geologically restless today, producing volcanic earthquakes, ground deformation and geothermal changes (Newhall & Dzurisin 1988; Lowenstern et al. 2006). Because Super-eruptions occur so infrequently, however, and because so little is known about their precursory activity, volcanologists have little ability to issue credible warnings in time for mass evacuations to take place. Lest anyone “lose any sleep” over the prospect of a Super-eruption occurring in their lifetime, however, we can take solace in the remote odds of such an event. Although the infrequency and probable non-random time distribution of such eruptions in the past precludes precise statistical calculations, Mason et al. (2004) suggest the probability of a M greater than 8 super-eruption occurring in the next million years is about 75 percent, with only a 1 percent chance of such an event taking place in the next 7200 years! Nonetheless, it is important to reflect on the words of Sparks et al. (2005):

There may be several super-eruptions large enough to cause a global disaster every 100,000 years. This means super-eruptions are a significant global humanitarian hazard. They occur more frequently than impacts of asteroids and comets of comparable potential for damage. Several of the largest volcanic eruptions of the last few hundred years, such as Tambora

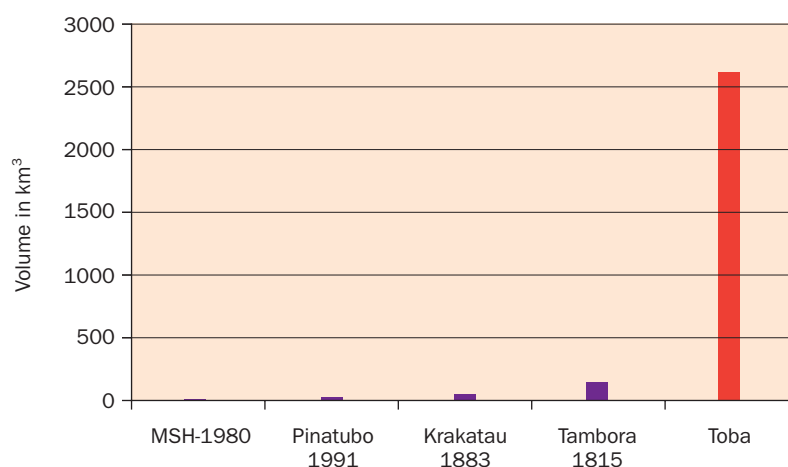


Fig. 8.28 Comparison of total ejecta volumes (km³) produced by historical eruptions with volumes produced by the “Super-eruption” of Toba volcano, 75,000 years ago.

(1815), Krakatoa (1883), and Pinatubo (1991) have caused major climatic anomalies in the two to three years after the eruption by creating a cloud of sulphuric acid droplets in the upper atmosphere . . . However, super-eruptions are up to hundreds of times larger than these, and their global effects are likely to be much more severe. An area the size of North America can be devastated, and pronounced deterioration of global climate would be expected for a few years following the eruption. They could result in the devastation of world agriculture, severe disruption of food supplies, and mass starvation. These effects could be sufficiently severe to threaten the fabric of civilization.

SUPER-ERUPTION CASE STUDY: THE ORUANUI, NEW ZEALAND PHREATOMAGMATIC ERUPTION

The Taupo Volcanic Zone is a northeast-southwest linear corridor of stretching, sinking crust in the central part of New Zealand's North Island, underlain by a supply of subduction-related magmas that have been continuously active for at least the past 2 million years. The central part of the Taupo Volcanic Zone, an area measuring 115 by 60 km, is one of the Earth's most active silicic volcanic fields (Wilson et al. 1995). Eight calderas ranging from 10–40 km in diameter lie within the zone, each related to past Plinian eruptions (Fig. 8.29). The southernmost caldera, occupying 140 km², formed 26,500 years ago during eruption of the Oruanui Tuff (Wilson 2001; Wilson et al. 2006). It has since been the location of about two dozen eruptions, mostly small, with the exception the previously described Taupo eruption of 186 CE. As impressive as the Taupo eruption was, the Oruanui event dwarfed it in comparison, being perhaps 15 to 20 times larger. The Oruanui eruptive episode was one of the two largest volcanic events in the past 250,000 years, the other being the eruption accompanying the Toba, Sumatra eruption 75,000 years ago which produced about twice as much volcanic material.

In contrast to the Taupo eruption, whose culminating phase probably lasted less than ten minutes, the Oruanui episode was protracted, involving ten independent eruptions, mostly phreatomagmatic, perhaps spanning several years in time. The episode began mildly enough, simply as a sub-Plinian pumice eruption followed by an ash fall. The hiatus that followed was sufficient for soil development on the early deposits. Several additional short-lived outbursts followed by pauses took place, and then the main part of the episode began, perhaps from several simultaneously erupting vents. As it developed it grew in intensity and magnitude, ultimately incinerating and burying most of the North Island – fortunately long before Polynesian explorers populated New Zealand.

The Oruanui deposits and the proximal portion of the later Taupo ignimbrite (for example, the Hatepe and Rotongaio Ashes) share many characteristics of ordinary wet surge blasts. Waveform facies development, accretionary lapilli, and other evidence of steam-magma involvement occur at several stratigraphic levels. The overall emplacement temperature of the Oruanui Tuff, despite thicknesses approaching 200 m in some sections, was no greater than 150–200°C, suggesting intensive cooling by trapped water, perhaps by eruption through a deep lake. To cool an ordinary Plinian eruption sheet of this size down to such a temperature would require boiling off as much as 50–100 km³ of water (Wilson 2001).

The sorting of the Oruanui Tuff differs distinctively from that of drier PDC deposits, which commonly show little distinctive change in sorting with increasing distance from source, apart from localized topographic influences and partitioning of lithic fragments and pumices described earlier. In the Oruanui Tuff, however, overall sorting *decreases* with distance from the source. A similar deterioration of sorting occurs in the deposits of the 1870 Askja [73], Iceland, eruption, which also began at the bottom of a lake. This shows up most strikingly at distal margins, where only coarse fragments are well-sorted while matrices are packed with particles of many shapes and sizes. Such peculiar arrangement is called **coarse-tailing**. Something filtered out the finer particles in an irregular way to create such a dispersal pattern, and that could well have been dense, highly turbulent steam. Booth and Walker (1973) observed that flocculated ash aggregates blown out by steam blasts issuing from a new vent on Mt Etna [82] in 1971 fell to the surface far sooner than they would have in dry air. As a result, ash accumulated in well sorted beds impacted by ballistic fragments close to the vent. Possibly a similar mechanism operated on a much larger scale during the Oruanui and Askja eruptions, selectively and irregularly removing fine ash which otherwise would have contributed to more uniform sorting throughout their deposits (Self & Sparks 1978).

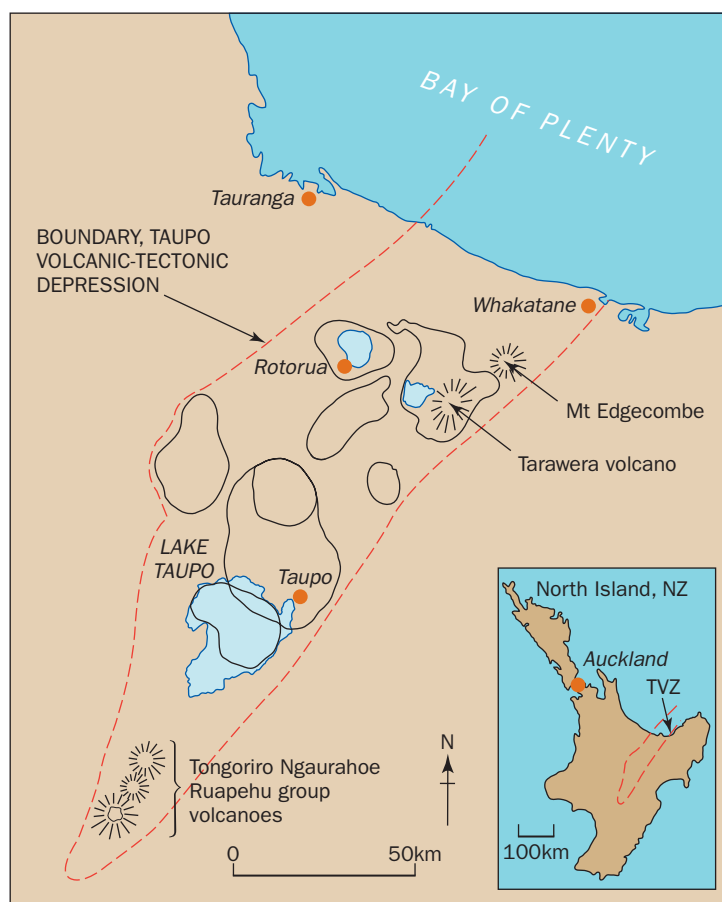


Fig. 8.29 Taupo Volcanic Zone (TVZ) on the North Island of New Zealand. Borders of major (overlapping in places) indicated by solid lines; major volcanoes shown by hatchures calderas (Modified from Gravley 2004).

FURTHER READING

- Freundt, A. (2001) *From Magma to Tephra: Modelling Physical Processes of Explosive Volcanic Eruptions*. North Holland, Elsevier Publishing, 334 p.
- Gilbert, J. S. and Sparks, R. S. J. (eds.) (1998) *The Physics of Explosive Volcanic Eruptions*. London, The Geological Society of London Special Publication vol. 145, 186 p.
- Miller, C. F. and Wark, D. A. (2008) "Supervolcanoes and their explosive super-eruptions." *Elements*, 4, 11–15.
- Sparks, R. S. J., Bursik, M. I., Carey, S. N. et al. (1997) *Volcanic Plumes*. New York, John Wiley and Sons, 590 p.

Chapter 8

Questions for Thought, Study, and Discussion

- 1 How do we measure the sizes of Plinian eruptions?
- 2 Describe the dynamic structure of an active eruptive column.
- 3 What is implied if the prehistoric tephra fall deposit of a particular eruption is skewed to one side or another of a source vent?
- 4 What explains the fact that many Plinian pumice fall deposits are reversely graded? And what might normal grading in the upper part of a pumice deposit indicate?
- 5 How and why do pyroclastic flows and surges form?
- 6 How do pyroclastic flows and surges move?
- 7 Why are deposits of pyroclastic flows and surges so different?
- 8 Describe the ways that local topography can effect the movement and deposition of PDCs.
- 9 What is the evidence for ash elutriation, both during eruptions and within the deposits that these eruptions leave behind?
- 10 What is ignimbrite “aspect ratio,” and why might this be a significant parameter?
- 11 How do directed blast deposits differ from those of ordinary PDC eruptions?
- 12 What are Super-eruptions, and should we be worried about them? Explain.





PART IV

VOLCANIC

LANDFORMS

AND SETTINGS

Volcanoes come in all sizes and shapes, not all of which look like the “typical” volcanoes of cartoons and tourist postcards. This Part discusses the many landforms created by volcanoes, from towering symmetrical cones, vast lava sheets, craters large and small, to the remote volcanoes beneath the sea and on distant planets. **Chapter 9** describes the **positive** landforms created by volcanoes, including vast lava plains, gigantic lava shields, and the “pointy volcanoes” characterized by the scenic conical structures most people associate with volcanoes. **Chapter 10** describes the perhaps less dramatic **negative** volcanoes, those marked for the most part by large depressions in the landscape – including the all-important, gigantic craters known as **calderas**, sites of the Earth’s most powerful eruptions. **Chapter 11** describes the processes that can suddenly tear volcanic edifices apart – massive landslides and volcanic mudflows. **Chapter 12** describes the unseen submarine volcanoes of the Earth and those of extraterrestrial worlds.

Chapter 9

Constructional (“Positive”) Volcanic Landforms

It is at once evident that repeated eruptions cannot fail to load the surface of the earth around their source with a mountainous excrescence of a magnitude proportional to the quantity of matter thrown up.
(George Poulett Scrope, 1862)

Volcanoes erupt vast quantities of lava and/or ash at the Earth’s surface, and most construct “positive” topographic features. These range from lava plains, plateaus, and shields to majestic composite volcanoes, and to smaller domes and pyroclastic cones. Some volcanoes are just “holes in the ground,” however – we’ll discuss those “negative” volcanoes in Chapter 10. We begin our descriptions of these positive landforms with a look at the most voluminous volcanoes on Earth – the Large Igneous Provinces (LIPs).

Large Igneous Provinces

Large Igneous Provinces are regions in which especially voluminous amounts of volcanic material (more than 50,000 km³) have erupted in long-lived eruptions that mantle large areas of the Earth’s surface. They may be sub-classified by the compositions of their dominant products (e.g., Large Basaltic-Rhyolitic Provinces (LBRPs), and Large Andesitic Provinces (LAPs)), or by their tectonic environments, including continental interior, back arc, rift or plate margin, and oceanic settings (Bryan et al. 2002; Sheth 2007). LIPs include the vast flood basalt tablelands, such as the Columbia River Plain (Chapter 6), caldera-studded ignimbrite plateaus such as the Sierra Madre Occidental in Mexico, the Great Basin in the western United States, and continental hot spot tracks such as the Yellowstone–Snake River Plain that trend across

Volcanoes: Global Perspectives, 1st edition. By John P. Lockwood and Richard W. Hazlett. Published by Blackwell Publishing Ltd.

TABLE 9.1 SOME WELL-PRESERVED, GEOLOGICALLY YOUNG LIPS. THESE PROVINCES CONSIST LARGELY IF NOT ENTIRELY OF FLOOD BASALTS. NOTE THE RELATIONSHIP TO HOT SPOTS.

Province	Location	Area (millions of km ²)	Volume of eruptives (millions of km ³)	Age (millions of years)	Associated hot spot
Columbia River	Pacific Northwest, USA	0.164	0.175	16.5–14.5	Yellowstone
Afar	NE Africa, Red Sea area	2.0	n/a	31–29	Afar
North Atlantic	Greenland, Iceland, NW Europe continental shelf	1.3	n/a	62–58	Iceland
Deccan	India	1.8	8.6	66	Reunion?
Madagascar	SW Indian Ocean	1.6	4.4	90–84	Marion
Caribbean-Columbian	Caribbean Basin	1.1	4.5	90–87	Galapagos
Ontong Java	SW Pacific	1.9	44	94–86	Louisville?

Source: Ernst et al. (2008).

southern Idaho (an LBRP in the above nomenclature). Some 35 LIPs have been erupted in the past 250 million years, and at least 240 others are known from Earth's older geologic record (Ernst et al. 2008; Table 9.1). A general view among earth scientists has been that many, if not all, LIPs represent the focused upwelling of hot mantle, in some instances plainly related to plume “hot spot” activity (Table 9.1; Chapter 2). The initial impingement of an ascending mantle plume on the underside of the lithosphere may introduce especially large amounts of heat and partial melting to the crust. Intensive, highly explosive silicic volcanism can be superseded by vast outpourings of unusually hot basaltic lava as rifting sets in later on. This appears to be the case, for example, in the Yellowstone–Snake River Plain volcanic region.

Of the LIPs, by far the largest occur on the sea floor. This is no accident. Oceanic lithosphere is thinner than continental, and rifts more easily, permitting the eruption of vast amounts of mantle partial melts that otherwise might underplate or intrude thicker continental crust without erupting. The submarine Ontong Java LIP is the largest flood basalt province in the world, having an area about the size of western Europe. It rises some 2000 meters above the adjacent ocean floor, showing much greater relief than its terrestrial counterparts. In addition to lava flows erupted from deep sea vents, parts of the plateau include deposits of phreatomagmatic pyroclastic material, possibly indicating occurrence of eruptions in shallow water or above sea level as development of the plateau culminated. Most basalt apparently was fed by widespread submarine fissure eruptions (Fitton et al. 2004).

In contrast to the submarine realm, most, if not all continental flood-basalt provinces originate as lavas spread out across broadly subsiding basins. For example, the Columbia River Plain is built of approximately 300 individual lava flows increasing in cumulative thickness toward the center of the province, with the deepest flows now buried as much as 3500 meters. This suggests that the underlying continental crust subsided as flows accumulated, or perhaps that the crust was rifting open as eruptions took place. While the base of the volcanic pile sank, the top of the flows formed a low-level plain or basin floor that was frequently resurfaced by freshly erupted lavas.

One of the reasons the word “flood” appears in “flood basalt province” is because of the way rapid and voluminous effusions of lava cover pre-existing topography (Chapter 6). The Columbia River lavas buried mountainous landscapes with a relief of over a kilometer. The output of lava is not regular in most flood basalt provinces, but rather spikes dramatically at one point or another during the period of volcanism. In the Columbia River Plain, eruptions of lava took place over an interval of 11–12 million years. But more than 90 percent of the total volume erupted in only about a million years – that is, less than 10 percent of the province’s lifespan. The crescendo in activity came early on – within the first two million years. After that, volcanism in the province gradually tapered off. Six great groups of flows erupted, each representing numerous individual eruptions (Swanson et al. 1979). The flows within each group share similar chemical make up but have mineralogical differences, suggesting that each had a distinctive mantle source (Tolan et al. 1989). Despite the impressive sizes of individual flows and total volume of lava erupted, soils, watercourses, and wildlife re-established themselves in the periods between some eruptions, as indicated by fossiliferous sedimentary deposits interbedded with lava flows in many places. Centuries often passed before another flood of lava covered the landscape.

In most areas of flood basalts the flows are mainly sheet-type pāhoehoe, though minor amounts of a`ā may also be present. Most flows are less than 10 m thick, but in places, individual flows have thicknesses of many tens of meters – even in excess of 100 m – and are commonly underlain by beds of shattered, glassy volcanic debris called **hyaloclastite** (“broken-glass rock”). These features represent the filling of river canyons with lava, or so-called **intercanyon flows**. Many intercanion flows show especially well-developed entablature jointing, though entablatures are not exclusive to this environment (Chapter 6).

The relationship of intercanion flows to their basal hyaloclastite deposits seems quite straightforward. As lava pours into a river channel, sudden quenching by cold water causes the perimeter of the active flow to shed countless flakes of sand and silt-sized grit. This matter piles up at the foot of the lava and then the flow overrides it. Steam explosions may wrench loose larger angular fragments that also mix in with the fine debris. Where the lava enters deep pools, hyaloclastite beds may grow to many meters thickness, and may include detached lava pillows or interfingers of long, contorted pillows extending from the flow. Many hyaloclastite beds become oxidized to a reddish or red-brown color or alter to yellow-brown palagonite as the lava travels across them and boils away pore water.

In some places, intracanyon flows fill dry river gorges, or follow watercourses with very little water. In such cases, little or no hyaloclastite will form, but a bed of rounded stream boulders and cobbles preserved directly beneath the flow indicates the presence of the watercourse. Along some very well exposed reaches of buried streams, the presence of pools and riffles may be preserved at the flow base as alternating pods of hyaloclastite and stream sediment.

WHAT A YOUNG FLOOD-BASALT PROVINCE LOOKS LIKE

The eastern portion of the Snake River Plain is a small (5×10^4 km²) flood basalt province in southern Idaho, in parts so young (a few thousand years) that its original, nearly featureless topography is nearly intact. I. C. Russell (1902, pp. 102–3) described its surface: “On the plain the lava spread out and formed what may be termed a lake of liquid rock . . . the

margin of the lake is approximately a contour line . . . No eye can observe that it is not a perfect plain.”

This surface is not so flat in detail; it was actually formed by many flows from numerous, widely separated vents. Around each vent, the outpouring of highly fluid lava built broad, nearly flat cones or lava shields (next section) with slopes for the most part less than 1°. These individual shields are typically 30–60 m high and several kilometers across at the base. At the summit of any particular shield a small spatter cone, a row of cones, or a spatter rampart may be found – features easily eroded away from older flood basalts. From the evidence of effusive eruptions seen elsewhere (e.g., in Hawai‘i), it seems likely that each shield vent grew along an early-formed fissure covered by lava later in the eruption. At Craters of The Moon National Monument, near Arco, Idaho, a well-preserved fissure set and spatter ramparts support this interpretation.

On the Ethiopian and Harar plateaus, flood-basalt flows radiate from some 40 overlapping shield volcanoes, much larger in scale than the modest edifices of the Snake River Plain. Some shields rise as much as 4000 m above surrounding lowlands, and the Semain shield volcano alone contains 1×10^4 km³ of lava. Deep erosion indicates that even at this scale, dikes whose orientations were controlled by regional tectonic stresses fed the shield-forming eruptions (Mohr and Zanettin 1988). This mode of shield volcano development does not extend throughout the whole of the Ethiopian flood basalt-province, however, perhaps because the shield lavas are alkalic in composition, and were probably somewhat viscous as they flowed away from their vents. Other flood basalts in the region are tholeiitic, and no doubt were more fluid. The most voluminous subaerial flood basalts are found in the Deccan Volcanic Province of southwestern India where more than 500,000 km³ are covered with basalt flows that were emplaced 64–65 million years ago. The total volume and locations of major vents for these basalts is not known as much of the Province is downfaulted beneath the Indian Ocean, but the volume could be more than a million km³ (Bondre et al. 2004). Perhaps K. G. Cox (1988, p. 239), a well-known Oxford petrologist is right: “Every continental flood basalt province has its own peculiar flavor.”

Erosional dissection of the basaltic plains commonly results in the formation of a step-like topography on the sides of the valleys, caused by the variable erosion resistance of different parts of the lava flows (Fig. 9.1). These steps gave rise to an old name for these basalts, which were once widely known as **traps** or **trap rocks**. In the United States the term is now almost obsolete, but it is widely used elsewhere. Where the beds have been tilted the treads of the steps may be inclined, or a series of sharp ridges marking the eroded edges of resistant beds, termed **hogbacks** or **cuestas**, may be formed.

Shield Volcanoes

As described in the previous section, vast, high-discharge outpourings of basaltic lava can build up flood-basalt provinces. In contrast, where lower-discharge, smaller volume effusions of very fluid lava occur, centered over a shallow magma chamber, a different type of landform develops. This is a gently sloping (up to or less than 15°) mountain with a broadly-rounded cross-sectional profile called a **shield volcano** (Fig. 9.2). The term “shield,” derives from a



fancied resemblance, in Iceland, to an early Germanic warrior's shield laid concave-side up on the ground. About 15 percent of the subaerial volcanoes on Earth are shield volcanoes (Suzuki 1977).

To illustrate the great variety of shield volcanoes and their fine-scale features, let's explore some examples from around the world.

Fig. 9.1 Flood-basalt traps of the Columbia River series.

Photo: Vic Camp.

SHIELD VOLCANOES OF HAWAI'I

The world's largest and most famous shield volcanoes are those of the Hawaiian Islands, whose eruptions we have already described in Chapters 1 and 6, but we shall take a closer look at their construction here.

The floor of the central Pacific has a mean depth of about 4200 m. Hawaiian volcanoes originate on the floors of this stygian deep. The youngest Hawaiian volcano is a 3000 m tall seamount, named Loihi [16]. It has almost 1000 m to grow before breaching the waves 30 km south of the island of Hawai'i (Malahoff 1987). The slopes of Loihi are as much as 10–15° steeper than those of the shields above sea level, where the land is inclined at angles of only 2–12°. This is partly due to landslide modification, and also because submarine lava flows do not usually travel as far as subaerial flows. The lower slopes of Loihi are composed mostly

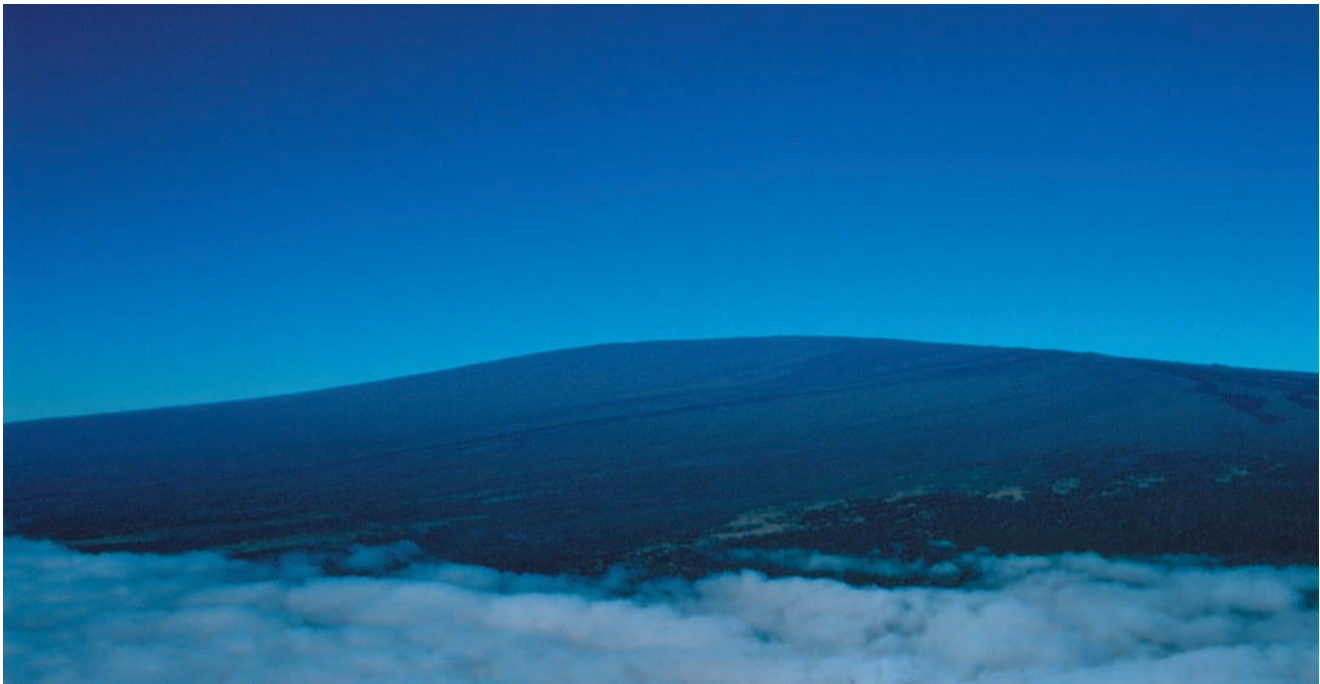
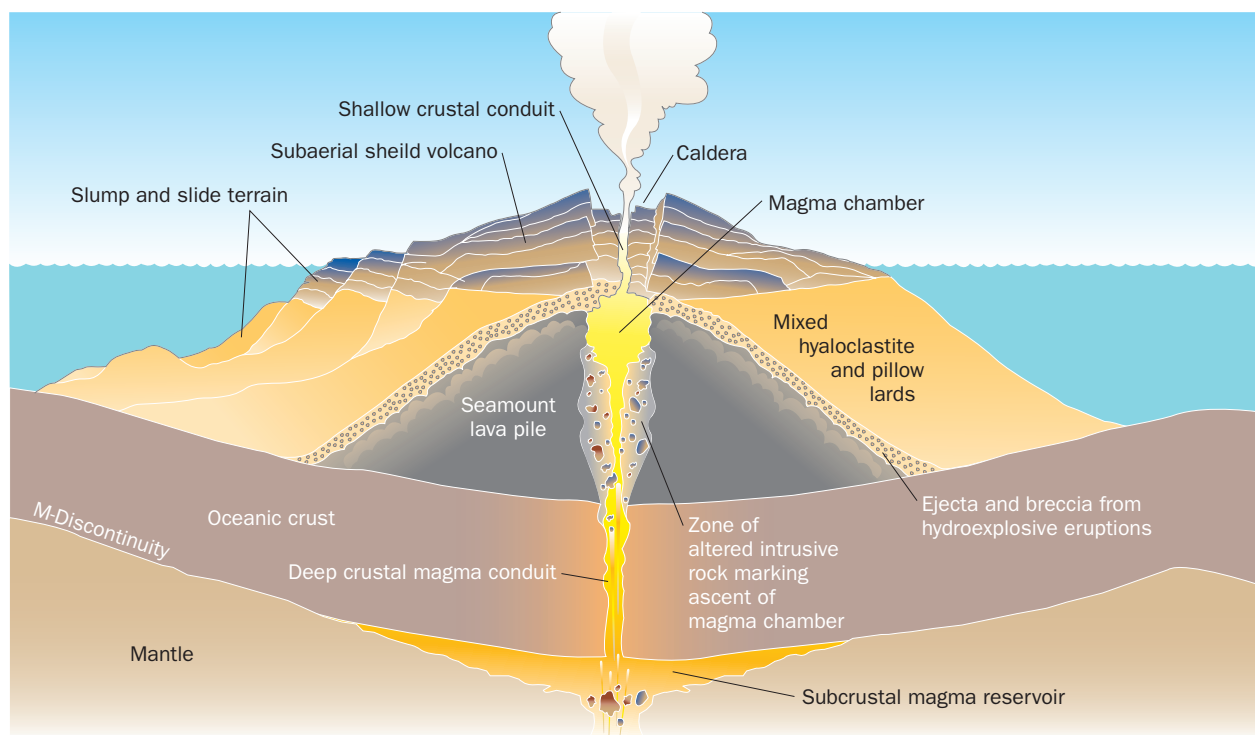


Fig. 9.2 Shield shape of Mauna Loa volcano, Hawai'i, viewed from the southeast. Only the upper 3 km of this shield is visible in this photo – another km of subaerial shield lies below the clouds, and another 5 km lies beneath sea level. Photo by J. P. Lockwood.

of breccia where numerous landslides have occurred. `A`ā and pāhoehoe form more stable flanks. Toward the summit, slopes become more gradual. A broadly arching crest marks the top, where a small caldera has formed. From the caldera two rift zones radiate, one stretching northward about 8 km, the other to the south 25 km.

Rift zones are among the outstanding features of Hawaiian volcanoes, resulting in dike-fed fissure eruptions, some of which evolve into focused lava lake, edifice-building activity that may persist for months or years. At fullest development there may be as many as three rift zones radiating from the summit of a Hawaiian volcano, with angles of about 120° between them. Usually, however, two of the rift zones are more active than the third. Gravitational stress plays a critical role in determining the orientation of any given rift zone, especially where one shield volcano grows against the flank of another (Chapter 4). Where a shield volcano grows from level seafloor, isolated relative to its closest neighbors, flank fissure eruptions still occur, but dikes radiating all points of the compass from the summit magma chamber feed these and no well-defined rift zones tend to develop. West Maui is one example of such a volcano. The basal outline of each Hawaiian shield is the direct result of the orientation and degree of development of each of its rift zones.

Building up to within a few hundred feet of sea level, a young Hawaiian volcano enters a zone of water shallow enough for explosive phreatomagmatic activity to become the dominant eruptive style. Eruptions generate vast amounts of hyaloclastite, which build a platform for an island to grow once summit vents build above sea level (Fig. 9.3). Hyaloclastite production continues all along the coast of the new island, wherever lava flows pour into the ocean, so that in time this debris envelops the older seamount formed during the initial stage of shield growth, creating a substantial (not-altogether-stable) foundation for the subaerial portion of the volcano.



Eventually, Hawaiian shields become so massive that they isostatically depress the underlying oceanic lithosphere to form a moat around the islands as much as 800-m deep – the Hawaiian Deep. At present, the youngest parts of the island of Hawai`i are sinking as fast as 2.5 cm every 10 years, flooding coastal real estate and roads in a few places. The mean rate of young shield growth is about double this, however, meaning that the island is growing higher at about the same rate its bottom is subsiding (Moore and Thomas 1988). The smallest of the Hawaiian Islands rise nearly 5 km above their bases; and Mauna Loa [13] and Mauna Kea [14] on the island of Hawai`i have absolute heights of about 10 km. Measured from the sunken bases of their volcanic piles, these mountains are even bigger, possibly representing accumulations of lava over 15 km thick! The volume of Mauna Loa alone is at least a hundred times greater than that of typical composite volcanoes such as Mount St Helens [27] or Vesuvius [79]. It is unlikely that mountains much bigger than these can grow on oceanic crust, given the weakness of Earth's lithosphere.

Young Hawaiian shields build up from repeated eruptions perhaps averaging 20–30 per century for many hundreds of thousands of years. Individual eruptions may last for years at a time, and growth rates are quite rapid, geologically speaking. For example, about 95 percent of the 30 × 65 km land area of Kilauea has been re-surfaced by fresh lava within the past 1500 years. To the northwest, Kilauea's giant neighbor Mauna Loa has had 90 percent of its slopes surfaced with lava flows less than 4000 years old. Within the past 170 years alone, 13 percent of Mauna Loa's surface has been buried by fresh lava (Lockwood and Lipman 1987). This activity contrasts with the very short lifespans and eruptive brevity of the small Icelandic and Cascadian shields.

Fig. 9.3 Schematic cross section of a typical Hawaiian shield volcano in the main (pre-alkalic) stage of development.

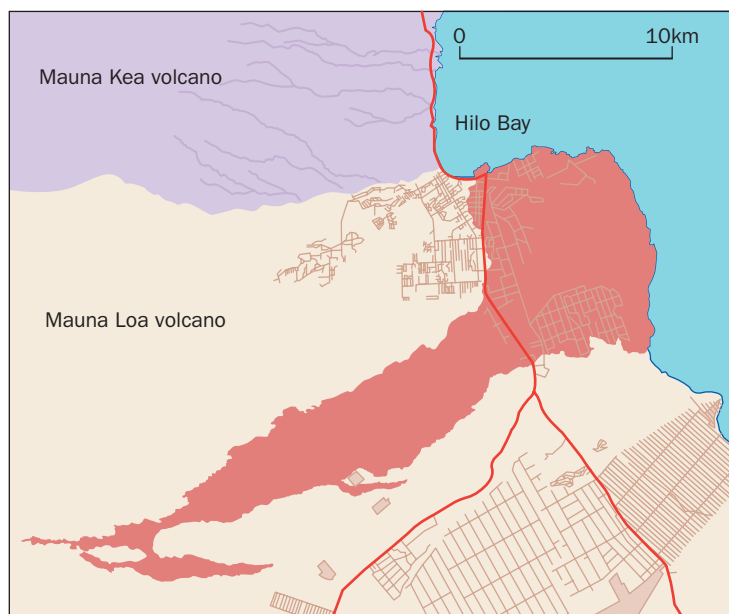


Fig. 9.4 Outline of the 1200 year-old `Panaewa Flow on the northeast slope of Mauna Loa volcano, Hawai`i. The flow remained narrow near its 1600 m elevation source vent, but widened downslope as it reached gentler terrain and encountered the Pacific Ocean – forming a lava delta and Hilo Bay. Modern roadways shown for reference. Shaded relief map modified from Trusdell and Lockwood (2009).

vents are located high on the volcano’s flanks. Flows from such vents are relatively narrow relative to length, and are supplied by central lava channels or pyroducts (Chapter 6). Because they are narrow, and initial lava production rates are relatively high, they may flow long distances (tens of kilometers) in the first few days. As eruptions continue, production rates commonly begin to wane as advancing pāhoehoe flows reach flatter terrain. On more level ground flows will begin to extend laterally and surface channels will become less common, as fluid lava is supplied by injections of lava beneath solidified crusts. Lava flows will commonly inflate vertically (Hon et al. 1994) and flow advance will mostly be in the form of “leakages” at the margins of flows (Chapter 6). Pāhoehoe flows are thus typically more narrow near their sources on relatively steep slopes, but will become broader as they reach more gentle slopes. On island volcanoes, contact of advancing lava with the sea may impede forward motion of the flow (by freezing barriers of water-quenched lava) and lava will extend laterally, forming “lava deltas” (Fig. 9.4).

The smooth profiles of most Hawaiian shields undergo considerable modification, owing to gravitational collapse of flanks in massive slumps and slides, most of which are rooted far underwater. These mass-wasting features are probably the largest, if not most impressive on Earth. In some instances as much as one-third of the landmass of individual islands have disappeared into the ocean as volcanic flanks have failed, playing a significant role in the development of Hawai`i’s spectacularly rugged topography. The Nuuanu slide, which broke from the flank of Koolau volcano on the island of Oahu almost 2 million years ago, had enough momentum to spread 160-km across the sea bed, most of the way climbing a gentle slope! The debris field from the slide is over 35-km wide, and contains pieces of volcanic shield as much as 35-km long and 1.5 km thick – as large as many stand-alone seamounts. This catastrophe must have created a gigantic tsunami all around the Pacific Rim. A smaller slide from the flank of Mauna Loa about 105,000 years ago raised sea waves that washed up over 600-m on the coast of Lanai, an island 150 km to the northwest.

Eruptions occur more frequently at the summits of Hawaiian shields than on the flanks, although those tend to be smaller. Eruptions within summit calderas take place from fissures that cross the caldera floor and often extend up the caldera walls and beyond onto the upper slopes of shields.

The flattened profile of the upper part of Hawaiian shields is due to a combination of summit caldera collapse and the fact that the most copious discharges of lava are from flank vents. If it were otherwise, the slope would remain constant to the edge of the caldera, or even become steeper because the same number of flows of the same width and thickness would cover a greater proportion of the circumference of the shield near the summit than farther downslope. The summit region would consequently build up faster than the middle flanks.

On typical basaltic volcanoes, most eruptive



Fig. 9.5 View east along the southeast coast of Kilauea volcano, Hawai'i, showing the step-faulting that has developed along this unsupported flank of the Kilauea shield. Such faulting is common wherever oceanic island volcanoes border deep oceans. USGS photo by J. G. Griggs.

Some Hawaiian volcanoes do not collapse all at once, as happened during the Nuuanu slide. Instead, their flanks gradually slump into the ocean. This sort of flank failure is presently active across most of the southern flank of Kilauea (Fig. 9.5). It is not clear whether slumps such as these are precursory to catastrophic land slides. But some geologists believe that the great mass-wasting events on Hawaiian volcanoes – indeed, on most oceanic shields – take place *during the time of volcanic primacy*, when poorly supported flanks are under the greatest strain from intrusions, and subject to intense loading from the accumulation of frequently-erupted lava flows. Lowering of sea level during times of continental glaciations may also be an important factor.

ICELANDIC SHIELD VOLCANOES

In Iceland, where geologists first studied shield volcanoes, the volcanic shields are all quite small relative to those in Hawai'i, ranging in basal diameter from only a few hundred meters across to about 15 km and in height up to 1000 m above their surroundings. Each is built by effusions of thin, fluid basalt pāhoehoe flows from a pipe vent or a very short segment of a fissure, and consequently each is nearly circular in ground plan. In the crater atop most shields, lava accumulates as a molten pond from which overflows build up gentle surrounding slopes. Some flows extend well beyond the bases of the shields, a record being a lava flow from the Trolladyngja shield that is 100 km long (Williams and McBirney 1979). Few of these flows exceed a meter in thickness, because the lava is extremely hot and fluid as it erupts.

Perhaps the best known of Icelandic shields is the type example Skjaldbreiður volcano [74] near Reykjavik – 500 m high and 10 km in diameter, with slopes averaging 7 to 8°. Nearby

shield volcanoes have slopes of only 2 to 3°, similar in profile to the very low shields around the vents of some flood eruptions, as in the Snake River Plain. Most of the Icelandic shields formed quickly during single eruptions. It is probable that even the biggest shield, Skjaldbreiður, grew up within a period of less than 10 years (Cas and Wright 1988). This is implied by the rapid growth of Surtsey [66], a new volcanic island which formed off the southern coast of Iceland in 1963–7. After the vent of Surtsey sealed itself off from contact with seawater, fluid flows poured out, building up a low shield on the new island. In all, about two cubic kilometers of lava issued, comparable in volume to smaller shields on the Icelandic mainland. Judging by the numerous extinct, eroding volcanoes that form rocky islands in the vicinity of Surtsey, it seems unlikely this young shield will ever return to life. In the past 11,000 years, about two dozen shields have formed in Iceland.

SHIELDS IN VOLCANIC ARCS

Composite cones, domes, and cinder cones are the predominant types of volcanic edifices in volcanic arc settings, but shield volcanoes can be found as well. As you might expect, these shields have significantly different character and composition from those in Hawai'i and Iceland.

Ambrym [132] is the largest active volcano in the Vanuatu (New Hebrides) island arc in the southwestern Pacific. It forms an island 30 by 50 km long, rising 1270 m above sea level. Atop the volcano is a 11 km wide caldera rimmed with inner slopes in places as much as 400 m tall. Ambrym typically erupts once every 5 to 10 years, with lava lakes episodically active in two of its caldera pits, Benbow and Marum. Overflows from the lakes have covered much of the caldera floor with fresh lava. Ambrym has an unusual history. The lower portion of the edifice is a broad shield volcano built up of basaltic pāhoehoe flows; its slopes measure only 2–3°. About 2,000 years ago, a sub-Plinian eruption broke out at the summit, triggered by intersection of magma with a shallow aquifer. Sixty to 80 cubic kilometers of ash, lapilli, and other ejecta erupted, forming a thick cap of pyroclastic debris ranging in composition from dacite at the bottom to basalt at the top. The outer slopes of the explosive deposits rimming the summit caldera are inclined at 10–20°. The caldera itself formed during eruption of this ejecta, but its mode of formation was not solely collapse, as is the case with calderas on most volcanoes. Its walls are not vertical, but are made up almost entirely of pyroclastic material lying at the angle of repose, suggesting that powerful explosions played the most important role in shaping the basin. The structure of Ambrym's summit resembles that of a gigantic tuff cone (Robin et al. 1993).

Some shield volcanoes occur adjacent to volcanic arcs, in slight back-arc positions. Mayor Island volcano [137], near the northeastern coast of New Zealand is one example. Unlike most shields, Mayor Island is built almost entirely of pantellerite (highly fluid, alkali-rich rhyolite), an uncommon rhyolitic lava type that characteristically forms in back-arc or intraplate tectonic settings. Eruptions of normal calc-alkaline rhyolite tend to be much more voluminous than their peralkaline counterparts, and typically erupt as ignimbrites, domes, or thick dome-fed flows. The 15 km wide shield of Mayor Island began to form by eruption of thick pantellerite lava flows (Fig. 9.6). Emerging above the sea, these flows issued in Hawaiian-style fissure eruptions and from more explosive cinder cones. Then, about 36,000 years ago, the summit



of the volcano began collapsing piecemeal, developing a caldera. The latest major subsidence occurred about 6000 years ago. Eruptions showed especially great variety throughout the period of collapse. On typical volcanoes, one might expect these differences in eruptive style to be related to changes in magma chemistry, or to changing volumes of erupted material. This is not the case on Mayor Island volcano – chemical variations are minimal, and no correlation can be drawn between eruption volume and eruption type. Instead, the manner in which molten rock rose and degassed inside the volcano appears to have varied greatly, for unknown reasons, over a geologically short interval of time (Houghton et al. 1992).

Two shield volcanoes much larger than Mayor Island (Newberry volcano [34] and the Medicine Lake Highland) also lie along the back-arc edge of the High Cascades in northern California and Oregon (Chapter 2). Though these volcanoes do not lie directly within the arc, they erupt essentially the same lavas as the main calc-alkaline arc volcanoes, including basaltic andesite and andesite. Structurally the shields lie within a region of extensional faulting called the Basin and Range, which covers much of the interior western US. Basin and Range faults guided the shallow intrusion and eruption of magma at both shields.

Medicine Lake volcano [32] began growing about a million years ago, atop a flood basalt plain called the Modoc Plateau (Fig. 9.7). The shield grew to a diameter of 25–30 km, and a volume of about 500 km³. Eruptions were dominantly Hawaiian with some Strombolian activity. Vents opened in widely scattered positions along roughly north-south trends parallel to

Fig. 9.6 Thick shield-building pantellerite flows on the northwest coast of Mayor Island, New Zealand (cliff is 110 m high). Flows are separated by soil zones that indicate substantial time elapsed between eruptions. Their bases are marked by quenched obsidian zones that were prized as weapon sources by Maori warriors. USGS photo by J. P. Lockwood.

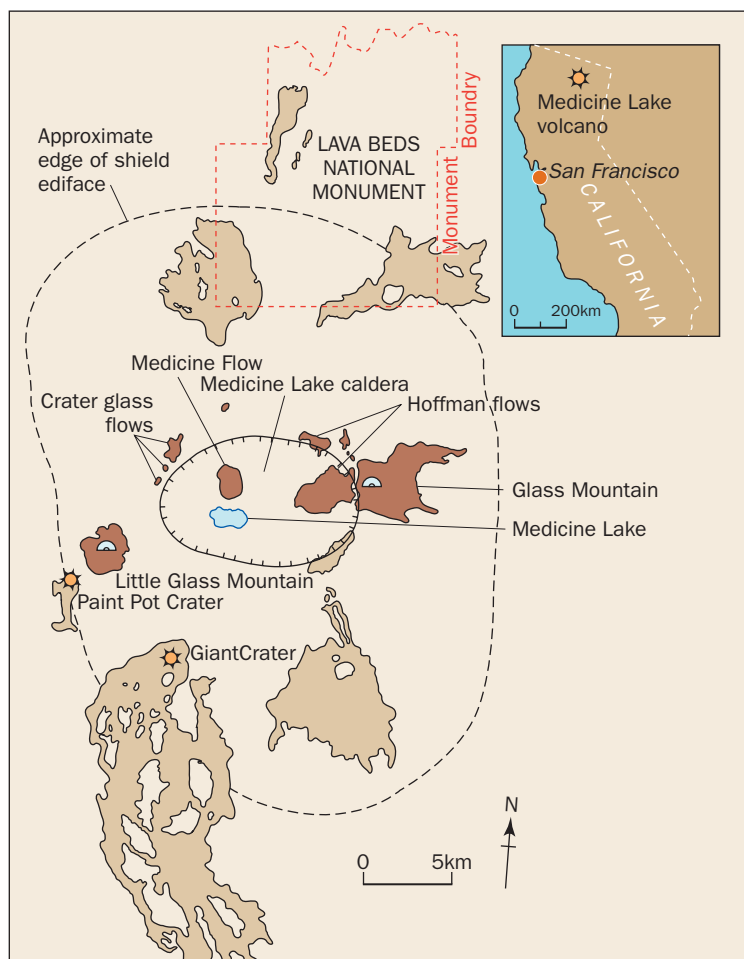


Fig. 9.7 Medicine Lake shield volcano, California. light brown = young basaltic and andesitic lava flows; red-brown = young glassy rhyolite and dacite lava flows. Remainder of the area is older forest and grassland. Modified from Donnelly-Nolan (1988).

around a pyroclastic core. Within any given shield, the blocky flows are strikingly homogeneous, though the compositions of adjacent shields may be distinctly different. Lack of significant chemical variation within shields suggests that they must have grown very rapidly, possibly during single eruptions lasting no more than a few years.

INTRAPLATE SHIELD VOLCANOES IN EASTERN AUSTRALIA AND NEW ZEALAND

Though lacking any historical eruptions, one of the world's largest and still potentially active volcanic regions extends 4200 km along the Great Dividing Range, the eastern edge of Australia (Fig. 9.8). In places the volcanic zone is 550 km wide. The nearest active plate boundaries now lie 2000–2800 km away. Much of the volcanic activity here began 80 million years ago, around the time continental rifting led to opening of the Tasman Sea and the separation of Lord Howe Rise from Australia, and later with the opening of the Coral Sea. Although rifting has ended, volcanic activity still continued, with an eruption at Mt Gambier [119] in South Australia occurring only 4600 years ago (Johnson & Taylor 1989).

underlying bedrock faults. A 6 by 10 km caldera had formed by 10,000 years ago. Around the caldera perimeter, at least 10 rhyolite obsidian domes extruded (Donnelly-Nolan 1988). A small ash eruption may have occurred in 1910 at the largest dome, Glass Mountain, showing that the volcano remains potentially active. A complex multi-chambered magma system underlies the Highland, fed by melts from both mantle and crustal sources (Chapter 4).

Much smaller shields are more typical of the Cascades; and these, like the shields in Iceland, are the result of single eruptions occurring from single point sources. On most shields, a prominent, steep-sided cinder cone marks the crest, giving them a shape that is distinctive even from a great distance. Good examples are Table and Badger Mountains on the northern boundary of Lassen Volcanic National Park, Goosenest not far from Medicine Lake volcano (Fig. 2.9), and the Whaleback near Mt Shasta [26]. The largest shields are no more than 600–1000 m high, and 10–15 km across at the base – comparable in scale to Skjaldbreiður. But unlike the Iceland shields, which are made up of fluid basaltic flows, these small Cascades volcanoes are composed of more viscous basaltic andesite and andesite lava spread

Several hypotheses explain the persistence of volcanic activity in Australia: Large, polygenetic volcanoes, including many shields similar to the Medicine Lake Highland described above, occur in a chain that grows younger toward the south. Numerous lava fields fed by small, monogenetic lava shields and cinder cones also occur along this line. We favor the explanation that the chain formed as Australia drifted northward over a melting source presently positioned in Bass Strait not far from Tasmania (Duncan & McDougall 1989); but slow relaxation of the lithosphere in response to early Tertiary rifting has also been suggested to explain this volcanism (Wellman 1989).

The monogenetic lava shields of Australia resemble those found in Iceland and the Snake River Plain of Idaho. They are gently-sloping central vent shields made up of piled up thin flows. They are extremely abundant; of the 400 volcanoes found in the Newer Volcanics field of South Australia, fully one half are shields or related lava cones (Joyce 1975). The largest probably did not exceed 16-km in diameter prior to erosion. In contrast, the larger polygenetic shields of Australia have extremely complex magmatic histories, reflecting the fact that their source melts derive from continental crust as well as the mantle.

The Australian hot-spot shields resemble shield volcanoes found in the northern part of the Kenya Rift Valley (Middlemost 1985). Webb and Weaver (1975) refer to these as **Turkana-type shields**. The African shields are generally trachytic in composition, with slopes of only about 5°. Basal diameters may reach 40 km, with smooth slopes surmounted by a rugged summit region of plugs and cones arrayed around a caldera. Their Australian counterparts show more compositional variation, but are comparable in size and structure. Most are less than 1000 km³ in volume.

Rangitoto [133], the best known intraplate shield volcano in New Zealand, forms a small island in the harbor of the country's largest city, Auckland. The volcano began erupting around 1200 CE (Brothers & Golson 1959), heralded by phreatomagmatic explosions as it built up to sea level. A small fragmental cone, not unlike those found on the monogenetic Cascades shields, grew at the summit as activity drew to a close.

Farther south in New Zealand a group of large intraplate shield volcanoes form peninsulas along the east coast of the South Island. One of the largest is the Dunedin shield, formed 10–13 million years ago. This volcano stretches 25 km across at the base and rises nearly 800 m. It has a polygenetic history, resembling that of the Australian hot spot shields. Erupted lavas include basalt, trachyte, and phonolite. Not only flows but extensive pyroclastic deposits,



Fig. 9.8 Locations of eastern Australian shield volcanoes mentioned in the text. Large volcanic edifices are shown by starred circles. Volcanic ages generally decrease to the south with the most recent eruptions occurring about 4600 years ago in the Newer Volcanics region of Victoria. Modified from Johnson (1980).

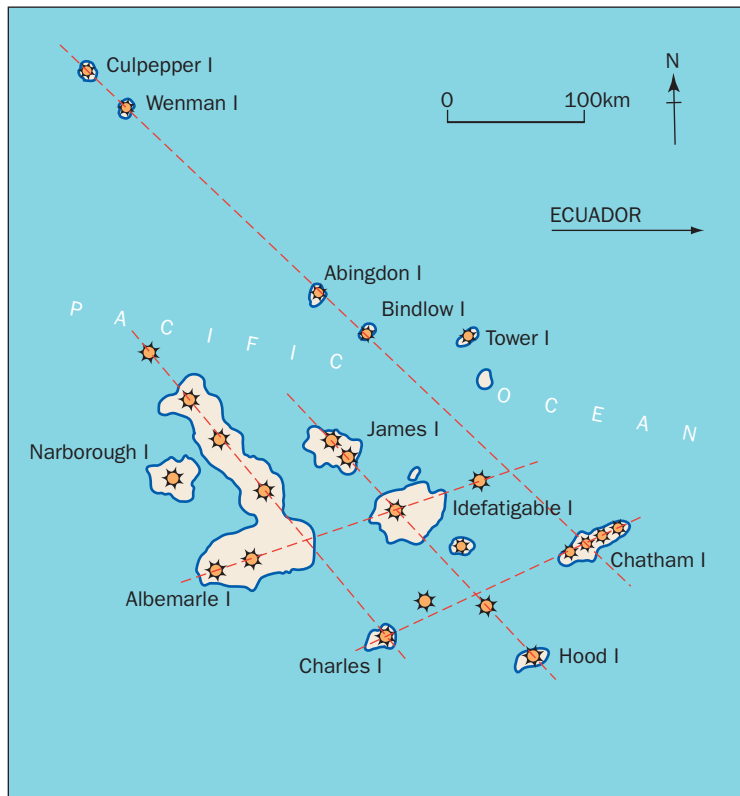


Fig. 9.9 The Galapagos Islands. Starred circles mark volcanic summits (some of which are submerged). Dashed lines show alignments of volcanoes along some sort of crustal fracture or fault grid. Modified from Ollier (1969).

even during the stage of vigorous shield growth. Tholeiitic and alkali basalt flows are intermixed, reflecting fundamental differences in the degree of melting or composition of the mantle beneath the two regions. Vincenzi et al. (1990) believe that the lavas develop by mixture of magma derived in part from the Galapagos hot spot and from the nearby Galapagos Rise, which drifted across the hot spot 8 million years ago.

Unlike the Hawaiian shields, the Galapagos volcanoes lack distinct rift zones, although radial fissure systems do occur, with linear arrays of cinder cones indicating sites of small Strombolian eruptions on lower flanks. In profile, these mountains are much steeper than young Hawaiian volcanoes, having middle slopes averaging about 25° . Otherwise, there are superficial similarities; lower slopes flatten out to meet the coast, and summit areas are broad and flat-topped (Simkin 1972). The calderas are much larger than those in Hawai'i. They are distinctively enclosed with concentric fracture systems, many of which have served as conduits for erupting lava. Spatter cones and ramparts mark sites of eruptions along most long fractures. Flows from these vents spread both down the steep outside flanks of the volcanoes and into the calderas themselves, partially filling them between repeated episodes of collapse. Williams and McBirney (1979) speculate that the volcanoes began growth with eruptions occurring primarily at centralized summit vents. Later, with formation of large calderas, the main site of effusive activity shifted to the circumferential ring fractures. In contrast to Hawaiian shields, the proportion of intrusions to effusive lavas may be considerably greater in typical Galapagos volcanoes.

Another reason the Galapagos shields differ so strikingly from their Hawaiian counterparts may be that these volcanoes are more widely spaced, proportionate to their volumes.

including base surge beds make up the flanks. Trachyte domes roughened the smooth profile of Dunedin's shield prior to erosion (Cas 1989).

SHIELD VOLCANOES OF THE GALAPAGOS ISLANDS

The basaltic shield volcanoes of the Galapagos Islands, also in an intraplate setting, differ in both general form and structure from those of the Hawaiian Islands to which they might be expected to show close resemblance (McBirney & Williams 1969). In ground plan, they are generally circular to somewhat elongate, ranging from 40 to over 70 km across at sea level, and rising as high as 3750 m above the ocean. The volcanoes are positioned at the intersections of tectonic fracture or fault systems on the sea floor, with no age-progressive pattern similar to that observed along the Hawaiian hot spot track (Fig. 9.9). In general, the Galapagos lavas are more alkaline than those of the Hawaiian Islands,

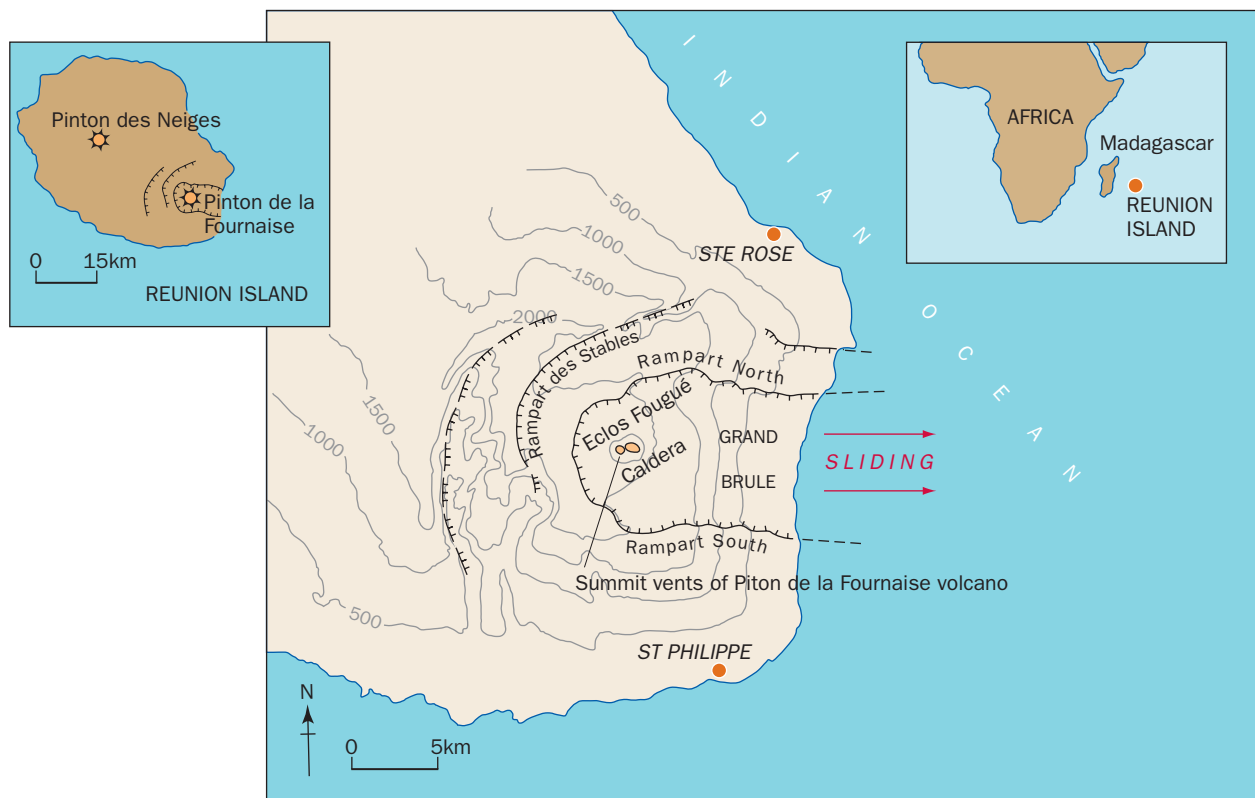
Gravitational instabilities are less likely to arise from the growth of one volcano up against the steep flank of another. There is no evidence of detachment faults underlying the flanks of the volcanoes, as at Kīlauea. Because a typical Galapagos volcano is structurally stable, it may be that magma reservoirs can more easily develop concentric dikes dipping in toward centralized summit chambers rather than swarms of dikes underlying rift zones. Circumferential vents enclosing Hawaiian calderas are rare, but do exist.

Similar to Hawaiian volcanoes, the Galapagos shields experience a change in the frequency and character of eruptions as they age. Outbursts become more explosive and less numerous in time, gradually building a steep cap of pyroclastic debris and short flows, which eventually inundate calderas and mantle upper slopes. The surfaces of some shields, such as Floreana, are dominantly composed of ejecta (Bow & Geist 1992). Erosion of the Galapagos shields is not as fast as it is in Hawai`i, given the drier climate.

SHIELD VOLCANOES ON LA REUNION ISLAND

The 50 by 65 km wide Island of Reunion, in the Indian Ocean 1100 km from the east coast of Africa, represents still another variation on the theme of shield volcanism. It is the youngest of the Mascarene Islands, which rise atop a hot spot melting source less active but almost as old as the one beneath Hawai`i (Bonneville et al. 1988). The island grew from the coalescing of two shield volcanoes (Fig. 9.10). The dormant shield of Piton des Neiges forms the

Fig. 9.10 Map of Piton de la Fournaise volcano, Reunion Island, southwest Indian Ocean. Major faults, with teeth toward downthrown blocks, enclose complex area of collapse in the volcano’s eastern flank. Like Stromboli, this collapse includes the summit vent area. Modified from Duffield et al. (1982).



northwestern half of the island, rising over 3000 m. The history of this volcano may have begun about five million years ago with initial eruptions on the deep sea floor, but the subaerial portion exposes rock no more than 2.1 million years in age. Radial fissure vents as well as summit fissure eruptions were numerous throughout the vigorous shield building stage of activity, which ended about 430,000 years ago. No well-developed rift zones formed. As in the Hawaiian and Galapagos Islands, a brief spasm of post-erosional activity commenced, creating a small cluster of alkali basalt and trachyte summit structures 350,000–12,000 years ago (Benard & Krafft 1986; Deniel et al. 1992). Multi-stage caldera collapse occurred throughout this interval of time. This contrasts with the development of calderas on Hawaiian volcanoes, which *preceded* late-stage alkalic volcanism.

The smaller southeastern neighbor of des Neiges is 2650 m tall Piton de la Fournaise [95]. Lying directly over the Reunion hot spot, this is the most active volcano in the Indian Ocean basin, and one of the most active in the world. Over 130 eruptions have occurred here since historic records began in 1644 CE. There are no well-formed rift zones, but radial vent eruptions are frequent, with some breaking out below sea level. Lavas are extremely fluid, producing spatter cones and ramparts and a few cinder cones. Similar to the Hawaiian shields, enormous sliding is taking place in the steep, seaward flank of la Fournaise, facing the southeast. Here the submarine slope drops off to a depth of nearly 4400 m. The unstable land mass has grown to engulf the entire summit of la Fournaise with its large pit craters, Dolomieu and Bory. Dolomieu crater had a major collapse in April, 2007, as underlying magma drained away to feed a voluminous flank eruption. Multiple east-facing arcuate scarps have developed indicating a long history of episodic summit collapse (Duffield et al. 1982). Enclos Foque, the still active scarp that closely encompasses the main vent of the volcano on three sides may have become active only 5000 years ago (Zlotnicki et al. 1990). Its seaward continuations are two huge normal faults bounding a sector of collapse – the main axis of the Grande Brule slide corridor. Because the volcano is deforming most rapidly in the direction of the slide, its effusive flank eruptions are concentrated in the Grande Brule. (Bachelery et al. 1983). Recent drilling of a nearly one-kilometer deep hole near the east coast suggests that sliding may have initiated from slippage in a bed of olivine crystals accumulating on the floor of a magma chamber.

The failure of part of the flank of Piton de la Fournaise is an excellent example of **sector collapse**; the sliding away of a large, wedge like slice of an active volcano. Sector collapses are not unique to shield volcanoes. They are even more common on composite volcanoes (next section), and will be discussed further in Chapter 11.

SUMMARY

Shield volcanoes form in a variety of geological settings, including intraplate, mid-ocean ridges and continental volcanic arcs. Shield volcanoes share the common aspect of having gentle slopes made up almost entirely of lava around a centralized vent area overlying a magma chamber or conduit. They range in composition from low-viscosity alkali-rich rhyolites and trachytes to basalt, though most are basaltic. Flows tend to be fluid enough to spread over considerable areas.

Most shield volcanoes are moderate-sized structures created during single eruptions. However the biggest mountains on Earth are also shield volcanoes that develop at mid-ocean

hot spots, where they form groups of islands. Large shield volcanoes commonly have summit calderas and radial fissure vents extending down their flanks. Cinder or spatter cones, lava shields, domes and coulees may grow up around some vents. A large, gravitationally unstable shield volcano typically has rift zones, and may experience gigantic landslides. On other more stable shields there is a tendency for circumferential vent systems to develop around summit calderas instead, and rift zones do not form. These shields tend to be steeper-sided, and more circular in shape than the elongate rift-zone shields.

Composite Volcanoes

These are the volcanoes most people regard as “typical”, and include the world’s most beautifully photogenic, snow-capped cones – the ones like Mt Fuji [113] (Fig. 9.11) that are featured on postcards and travel brochures from circum-Pacific areas. They are the great scenic volcanoes of the Earth (the “grey volcanoes”), made up of interbedded lava flows and layers of ash and cinder (Fig. 9.12). They are also referred to as **stratovolcanoes**, but shield volcanoes also consist of strata (beds) of lava, and we prefer to call those consisting of both lava and ejecta **composite volcanoes**.

Large composite volcanoes typically have complex eruptive histories, and their rocks record multiple periods of *construction* by Strombolian and Vulcanian summit eruptions, associated with outpourings of short lava flows, and *destruction* by mass wasting and sector collapse. Egmont volcano (Mt Taranaki) is a classic composite cone on New Zealand’s North Island. The present edifice (Fig. 9.13) is entirely composed of eruptive products less than 10,000 years old, but the volcano is surrounded by an immense ring of volcanic debris that records a volcanic history of growth and destruction that goes back well over 100,000 years. Vince Neall (2001) writes that “While much of the current Egmont cone is of Holocene age, the ring plain is 10 times as old and voluminous, containing the deposits from many previous pre-Egmont



Fig. 9.11 Mt Fuji, Japan, viewed from the east. Fuji (3776 m), which last erupted in 1707, is one of the world’s most beautiful composite volcanoes, yet remains active and potentially dangerous for a large population west of Tokyo. The satellite cone and crater formed in the 1707 eruption is seen just at snowline. Photo by Joseph R. Smyth.

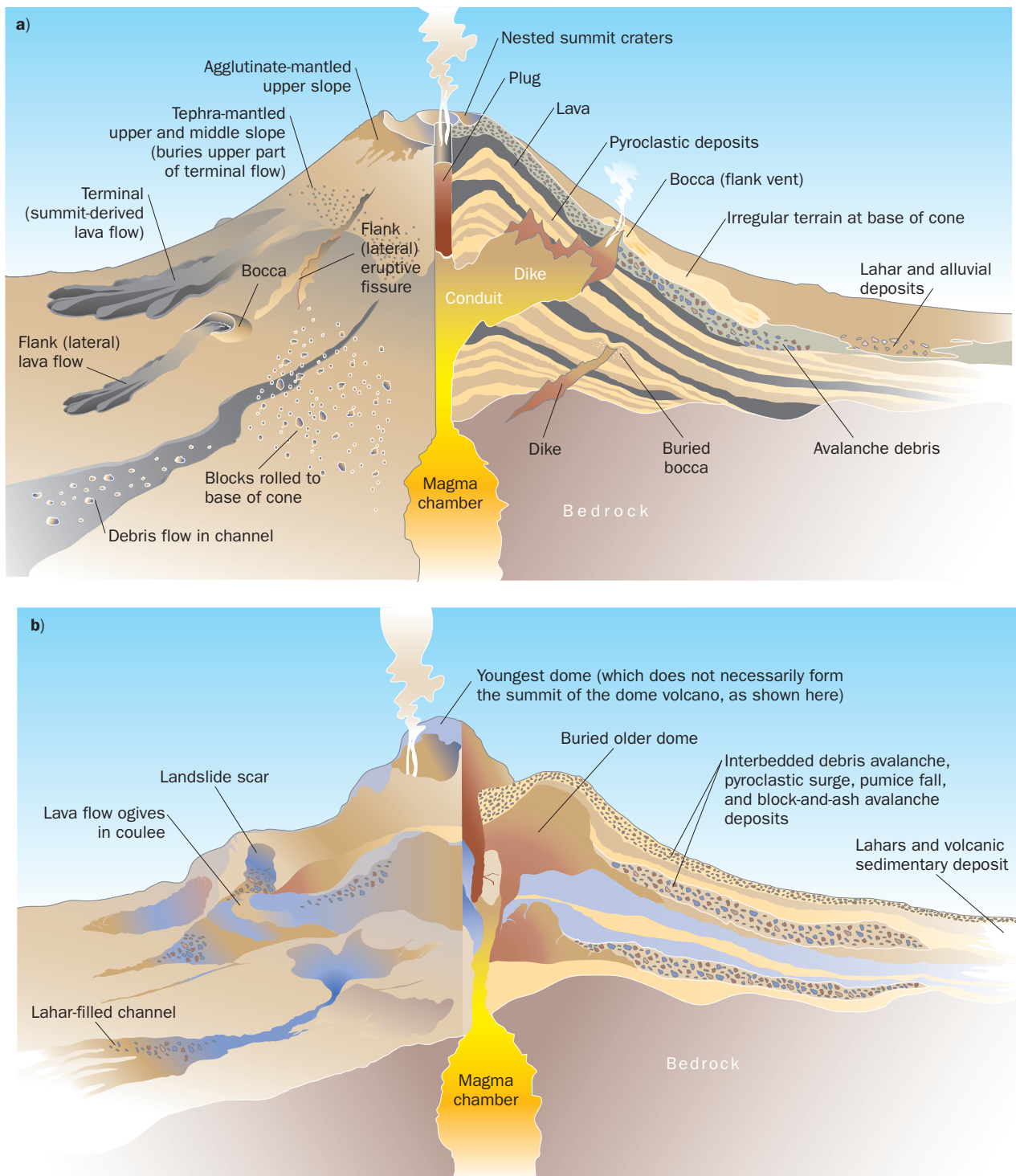


Fig. 9.12 a) Anatomy of a composite volcano. (This example does not include siliceous domes.) Many composite volcanoes show aspects of both this structure, and that shown in b). b) A composite volcano made up of high-silica domes, pyroclastics, and related debris is a structurally very complex mountain, lacking graceful symmetry.

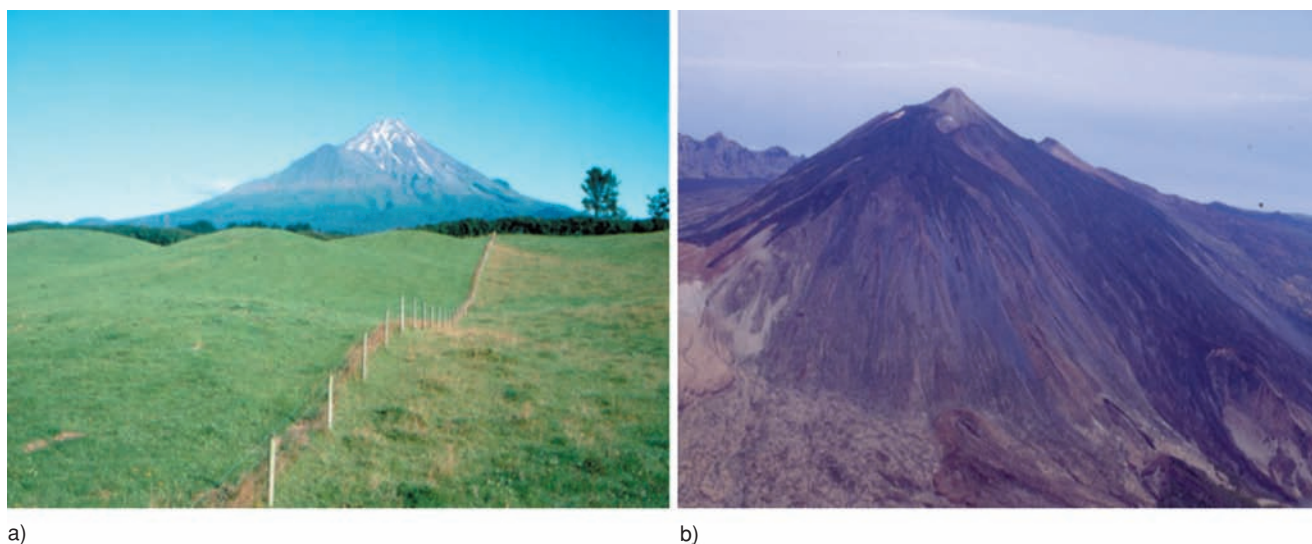


Fig. 9.13 Composite volcanoes have complex histories. a) Mt. Egmont (Taranaki) volcano, New Zealand, viewed from the southwest. This 2518 m high composite volcano records repetitive episodes of growth and destruction – surrounding deposits from debris avalanches and lahars are perhaps ten times the volume of the present edifice. Photo by J. P. Lockwood. b) Teide volcano, on the island of Tenerife, Canary Islands viewed from the north. Teide (3,718 m) is the tallest mountain in Spain and in the Atlantic Ocean, and is the youngest major volcanic edifice constructed on Tenerife over the past three million years. Photo by J. R. Losada.

cones that collapsed in the past.” Teide volcano (Fig. 9.13B) on the island of Tenerife, has a long and complex history of growth inside Las Canadas caldera, Canary Islands. It has not erupted at its summit in over 3,000 years, although several historical eruptions have occurred elsewhere on this volcanically active island. Mount St Helens was a classically symmetrical cone prior to the eruption of May 18, 1980, before it was decapitated in a few minutes by sector collapse and magmatic evisceration (Fig. 9.14).

Sub-Plinian and plinian eruptions often accompany such infrequent and self-destructive flank failures (Chapter 11) Ejecta may make up as much as 70 or 80% of some composite edifices, but in others, an equally large percentage of lava flows may be present (Cas & Wright 1988). The lava flows are most commonly blocky `a`ã , but they may rarely be spiny `a`ã, or even pāhoehoe. The ejecta is usually cinder or ash, but small amounts of agglutinate may also be present. Depending on the viscosity of the magma erupted, the lava flows may be thin and long or thick and short. Glassy domes are also common. Many large, dangerous composite volcanoes, such as Mt Pinatubo [104] in the Philippines and Montserrat in the Lesser Antilles, consist of an aggregation of domes, block-and-ash flow deposits, and ash and cinder fall beds. These volcanoes have highly irregular, lumpy profiles that hardly resemble the popular image of such “classic” composite volcanoes as Mt Shasta [26] or Mt Fuji [123], and because of this may not even be recognized as potential sources of peril. Block-and-ash flow debris is common on composite volcanoes, but lahar and debris flow deposits are even more common on lower slopes and the surrounding plains (Chapter 11). Dome growth characterizes the late stages of volcanism at many composite volcanoes, but at others like

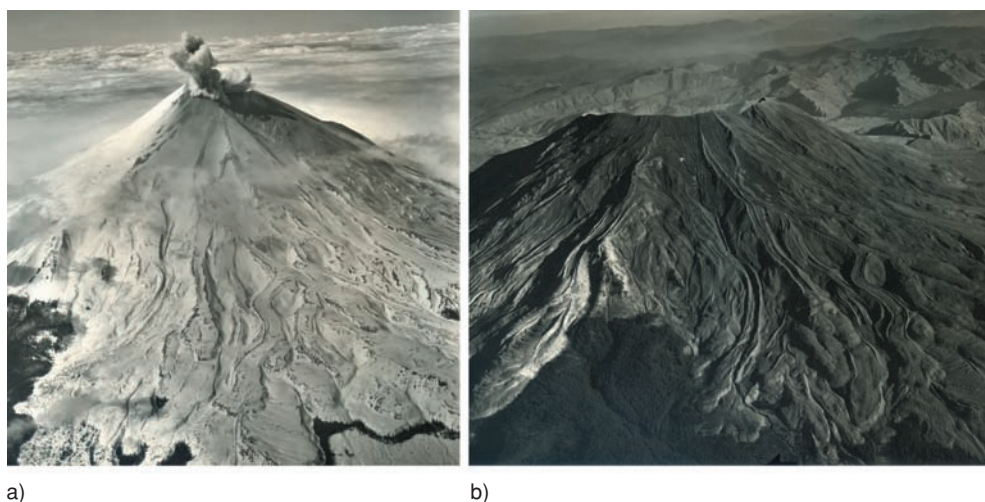


Fig. 9.14 Mount St Helens, before and after May 18, 1980. a) View to the northwest, April 10, 1980 as an awakening, snow-covered MSH was emitting steam and ash from the summit. b) View to the north-northwest, September 10, 1980 after this classic composite volcano literally “blew its top” and lost 400 m of its summit. The “X” marks show the same point for reference. Note the ‘a’ā flows with their well-developed lava channels that illustrate how prehistoric summit eruptions formed the volcano. USGS photos by Austin Post (a) and Robert Krimmel (b).

Survival Tips for Field Volcanologists:

Climbing **up** steep composite volcanoes is a lot more work than coming **down**, but descending them is much more dangerous than ascending. “Angle of repose” slopes require special caution – especially if partially mantled by poorly consolidated pyroclastic material. Several geologists (especially students!) have been killed descending composite volcanoes when their exuberance exceeds their caution.

Pinatubo and Montserrat, dome-related Vulcanian and even Plinian blasts take place through a large part of the history of the volcano. The growth of a dome is not sufficient justification to regard the volcano as approaching extinction.

Composite volcanoes range in height from a few hundred to several thousand meters, and in basal diameter up to about 30 km. As noted earlier, some display stunningly symmetrical cones such as Kronotsky [127] and Klyuchevskoi [129] in the Russian Far East (Fig. 1.13). Others such as Mt Pinatubo [45] and El Chichón [104] consist of irregular, non-majestic mountains that may not even be recognized as volcanoes until they burst to life. Most are built by eruptions that come principally from a single central pipe conduit, and consequently their ground plan is roughly circular. This may be greatly modified, however, where considerable proportions of their eruptions have been from lateral vents, termed **boccas** (Italian for “mouths”). “Double volcanoes” such as Mt Shasta and Shastina, or even a line of several quasi-independent cones may form from the same magma reservoir when the main vent shifts its position. The departure from circularity in ground plan is even greater in the rare cases where composite volcanoes are built around lengthy fissure vents. One of the outstanding examples of the latter is Mt Hekla [67] in Iceland. Hekla is a composite volcano built around a fissure 5–7 km long, and the basal plan of the mountain is an oval about 10 km long and only 5 km wide. Viewed in a direction parallel to the fissure, Mt Hekla has the general form of a typical composite volcano, but viewed at right angles to the fissure it appears as a broadly rounded dome resembling a shield.

On many composite cones the upper parts have uniform steep slopes near angles of repose (about 35°) and climbing is difficult (Fig. 9.15). The upward steepening of composite volcano slopes reflects the fact that most eruptions are relatively small (Fig. 9.16), and most



Fig. 9.15 Upper slope of Mayon Volcano, Philippines. The steep slope is at the angle of repose (35°) and little material can accumulate during eruptions. The lava flow in the background is about 40 cm thick; most erupted lava tumbles downslope to accumulate at lower elevations. Photo by J. P. Lockwood.



Fig. 9.16 Klyuchevskoi volcano in typical eruption, 1987 – view from west. Klyuchevskoi, in central Kamchatka, towers to over 4800 m elevation, and is the tallest and largest volcano in Eurasia. Photo by Aleksei Ozerov.

Fig. 9.17 Mayon volcano (2462 m) rises about 2 km above the surrounding plain of Albay Province, Philippines. This is one of the world's most scenic, yet dangerous volcanoes. More than 2000 people have been killed by lahars and pyroclastic flows on the flanks of Mayon in the past few hundred years. Photo by J. P. Lockwood.



pyroclastic debris falls near the central vent. At their bases, slopes typically flatten gradually to near horizontality. The less steep flanks are due to several factors: flank eruptions may have occurred at lower elevations, loose debris high on slopes will be eroded and deposited at bases by rainwash, streams, and lahars, and lava flows that emanate from the summit become thicker as they become more viscous further from vents. Lower flanks of composite cones are commonly comprised largely of lava flows and lahar deposits, whereas upper parts are mantled by pyroclastic debris from frequent small explosions. In humid regions, particularly in the tropics, the amount of loose material brought to lower volcano flanks by lahars is typically immense. At Mayon volcano [106] (Fig. 9.17), nearly the entire broad, gently sloping skirt of the cone is composed of lahar deposits with only minor amounts of ash fall beds.

Large masses of agglutinated spatter and even remnants of lava flows may accumulate on upper cone flanks near crater rims. In some cases craters do not exist at all, but instead the summit merely tapers to a gently rounded, hydrothermally altered crest mantled with ejecta. In other instances one or more domes completely fill the crater, giving the cone a steep, craggy top. The vents of some composite volcanoes remain fixed in position throughout the growth of the volcano, but more commonly vent positions shift somewhat during growth, in large part due to the plugging of older vents, or to change in position and configuration of the underlying magma reservoir – or both. In many cases the multiple vents marked by craters line up, reflecting the control of a basement fault or fracture on magma ascent. On other volcanoes, multiple summit craters of different ages are distributed in a random cluster across the mountaintop.

Gradual rebuilding of composite cones that have experienced sector or caldera collapse may proceed until only the highest rim of the former stump of the mountain remains uncovered by younger volcanic material. This collar-like relict of the older volcano is termed a **somma ridge** (or simply a **somma**) after Monte Somma, Italy which formed when a former edifice of

Vesuvius collapsed 17,000 years ago, leaving a cliffy, dike-laced rampart to the north of the modern cone. Eventually, a renewed edifice may grow large enough even to bury its somma, or sommas, completely, leaving no clue in its shape to a history of former catastrophe(s).

While the lifespans of individual shield volcanoes range from just a few years in Iceland, to as much as a one or two million years for large mountains such as Mauna Loa, lifespans estimates of composite volcanoes are less wide-ranging. Some (e.g., Mazama, Oregon; Hakone [114], Japan; Mt Pelée [63], Martinique) have eruptive histories extending back 400,000 years or so. Santorini volcano [84], Greece, may date back over a million years. Most composite volcanoes appear to be less than 100,000 years old, however; and many of these are probably in the waning stages of their activity (Wadge 1982). Quite a few composite volcanoes occur in overlapping proximity to one another (**volcanic complexes**), in which one volcano falls extinct while a neighbor just a few kilometers away starts growing. In this manner, individual volcanic complexes may remain active for millions of years. One example is the island of Martinique, a volcanic complex composed of at least six discrete, coalescing volcanoes that has existed for about 20 million years (Cas & Wright 1988).

Unlike small cinder cones and shield volcanoes, all composite volcanoes are polygenetic. Some, such as Stromboli, may be in nearly continuous eruption for thousands of years. Others experience as much as several thousand years between their eruptions. Some exhibit regular intervals between volcanic outbursts. Others appear to have random timing in their activity. Wadge (1982) estimated that on average the duration of quiescence on active composite volcanoes is more than double the duration of their eruptive activity.

A few composite volcanoes pursue essentially a single type of eruptive behavior throughout their lifetimes. Many others alternate or change their behaviors drastically. For example, beneath the edifice of Mt Mazama, a very explosive composite volcano, lies a basaltic shield which certainly represents an early stage of effusive volcanism in the very same area. Volcanologist Robert Decker likened volcanoes to people; each has its own “personality,” and each may experience its own “life changes,” some of them traumatic.

Mount St Helens, the most active and explosive volcano in the Cascade Range is a good example of a young composite volcano with a variegated eruptive history. Eruptions began in the area of Mount St Helens about 40,000 years ago. These were not mild effusions. From the start, PDCs, Plinian or sub-Plinian eruptions, and lahars spread debris widely across the region. Three early cycles of this kind of activity took place: The earliest, called the *Ape Canyon Period*, 40,000–35,000 years ago, was followed by an apparent hiatus of 15,000 years. While there could have been some eruptions during this long break, they must have been small as they left no traces. From 20,000–18,000 years ago, during the *Cougar Period*, renewed pyroclastic outbursts took place. This was followed by the similarly explosive *Swift Creek* (11,000–6000 BCE) and *Smith Creek* (2000–1000 BCE) eruptive periods. Then, beginning about 2500 years ago, the compositions of eruptive products abruptly became more diverse. Initially the volcano had erupted only andesite and dacite, almost entirely as ejecta. Now basalt also appeared, and fluid lava flows together with more silicic domes began playing a major role in building the composite cone. Lava flows and related radial dikes reinforced the cone, allowing it to grow taller than it could have had it been built solely of pyroclastic debris and dome rubble. Vigorous volcanic activity occurred between 2500–1600 BCE, 1200–800 BCE, and 400 BCE–300 CE. The current period of activity began 520 years ago,

culminating in the great blast of May 18, 1980. It is tempting to regard each of these discrete volcanic spasms as the expression of the rise of a distinct batch of magma into chamber beneath the volcano, though this is not certain. It is difficult to know what the geologically recent introduction of basaltic melt into the Mount St Helens conduit means for the future of the volcano.

SUMMARY

There is a continuous morphological spectrum between broad shield volcanoes and “pointy” composite ones. The primary difference between these end members relates to magma composition: “red” volcanoes almost always erupt low viscosity basaltic lava flows that travel far, forming shields; “grey” volcanoes typically erupt higher viscosity intermediate to silica-rich lavas that do not travel far or explosively disintegrate on eruption to form ash-covered composite cones. Composite volcanoes, like shields, show considerable variation in their features. In general, however, there is a range between those composed of relatively thin lava flows and tephra, with little or no history of self-destructive behavior, and those composed largely of aggregated domes and stubby, thick lava flows with an extremely violent history of construction alternating with self-destruction. Like shield volcanoes, composite volcanoes may experience changes in magma compositions and eruptive behaviors over time.

Minor Volcanic Landforms

Although massive shield volcanoes like Mauna Loa or large, scenic composite volcanoes like Mayon in the Philippines, Mt Fuji in Japan, or Mt Shasta in California are the ones most commonly envisioned by people as “ordinary” volcanoes, the reality is that most of the world’s volcanoes are quite small – typically less than a kilometer in diameter. These “minature volcanoes” are primarily located out of sight on the ocean floor (Chapter 12), but tens of thousands of others are found on land too – not only as satellite structures on larger volcanoes, but more commonly as independent edifices, resulting from single eruptions that may have lasted no more than a few months or years.

CINDER CONES

One of the most familiar of all volcanic structures is the **cinder cone** – a cone-shaped small mountain typically truncated with a bowl-shaped summit crater (Fig. 9.18), built almost entirely of lapilli-sized cinder with lesser amounts of volcanic bombs and blocks ejected around vents during Strombolian eruptions. Cinder cones are mostly of basaltic composition, and so tend to be quite dark when young, though high-temperature oxidation may turn their slopes and summits brick red. They range in size from a few tens to a few hundreds of meters in height, with diameters typically 3–5 times their heights. Their slope angles are the result of loose fragments rolling or sliding downwards during eruptions until they attain equilibrium, and are initially close to the angle of rest for piled up irregular fragments (the **angle of repose**



Fig. 9.18 Pu'u ka Pele cinder cone in the “saddle” between Mauna Kea and Mauna Loa volcanoes, Hawai'i. This 95 m-high, late Quaternary cone was formed by a flank eruption of Mauna Kea, but is being surrounded and will be eventually buried by younger Mauna Loa flows. The summit crater is 400 m in diameter. Hualalai volcano in background. Photo by J. P. Lockwood.

– around 30–35°). As crater walls are eroded with time, however their slopes will become more gentle, and this geomorphic evolution may be used to evaluate their rough age (Hooper & Sheridan 1998).

The craters at the tops of cinder cones are typically smoothly bowlshaped. In some cases slopes meet in the center to form pointed funnels, but on most the craters have rather flat floors formed by late-stage lava effusion or by material washing or blowing in to form level, clay-rich soils. In high-rainfall climates lakes may form in older craters.

The crater may consist of a single depression, indicating a single vent active at the end of the eruption, or it may consist of several depressions, each surrounding a former vent. Multiple craters are commonly aligned, as on some composite volcanoes, reflecting arrangement of the vents along a fissure. Where multiple craters are present during early stages of the eruption, they may be buried and replaced during later stages by a single crater when all but one of the vents become inactive (Fig. 9.19). The crater is largely the result of the construction of the surrounding rims, the area of the vent being kept relatively clear of falling ejecta by the force of the escaping gas. To some extent, however, it may also partly result from collapse at the end of an eruption, the lowering of the magma level in the conduit removing some support and allowing the overlying material to subside and the loose material of the crater walls to slide to



Fig. 9.19 Quarry wall cross-section of a late Holocene, forest-covered cinder cone in northern California, southern Cascade arc, USA. This cone, near Medicine Lake volcano, is one of many prehistoric monogenetic vents in the region. The line separating the steeply dipping layers on the right from the gently sloping strata on the left is called an angular unconformity, which in this case resulted from a shift in eruptive focus during growth of the cone. Note the large number of volcanic bombs scattered randomly in the beds of cinder. Photo by R. W. Hazlett.

a new position of rest. Sometimes the resulting collapse is very extensive and greatly alters the shape of the crater and even of the whole cone, but often it is comparatively minor and the original constructional form of the cone is little modified. Young cinder cones consist almost wholly of loose material, but with the passage of time groundwater moving through them may deposit calcium carbonate or some other type of cement that binds the fragments together.

Cones are constructed of superimposed layers formed by successive showers of fragments tossed out by successive explosions. The first layer forms a low mound-like rim on the ground around the vent, and each succeeding layer forms a mantle draped over the one below, sloping from the crest of the growing crater rim both outward away from the vent and inward toward it. On the outer slope of the cone, the layers commonly are quite regular, and individual layers extend over large segments of the cone. Within the crater the layers are generally very irregular, distorted and discontinuous, owing to truncation of their lower edges by succeeding explosions and resultant slumping of material on the side of the crater downward toward the vent.

Within individual cinder layers, the size of the fragments typically decreases upward, because in general during any one explosion the larger fragments are thrown less high, fall faster, and strike the ground sooner than the smaller ones. The size of the fragments (from less than a centimeter to as much as 30-cm across) depends in part on the strength of the explosion, more violent expansion of the gas tending to blast the magma into smaller shreds. Commonly, individual cinder cones are characterized by a range of more or less uniform size of fragments – mostly fairly coarse, or mostly fairly fine throughout – resulting from nearly uniform explosiveness of the entire eruption. However, it is also common to find a systematic increase in the size of fragments in the uppermost layers resulting from decreasing explosiveness toward the end of the eruption. It is also common to find occasional bombs embedded in a haphazard manner in finer cinder.

Fusiform and spindle bombs are often associated with the cinder, though generally in very minor proportion, and in some cones they are lacking. Typically, they are most abundant in the outer portion of the cone, and this also seems to result from a decrease in the gas content of the erupting magma and, consequently, in the explosiveness of the last stages of the eruption. The impacts of the larger bombs often form distinct pits, in places as much as a half-meter deep or more, in the surface of the cone, which may rupture the underlying layers or bend them downward as bomb sags. Sometimes, though comparatively rarely, the explosiveness decreases to such a degree that the ejecta changes from cinder to spatter, and a layer of welded spatter may form over the crater rim or even over a large part of the outer slope of the cone. Spatter accumulating on the crater rim may build a nearly vertical wall crowning the cone. Such cones have been called **ruffed cones**, because of the fancied resemblance to a seventeenth- or eighteenth-century ruff, or collar.

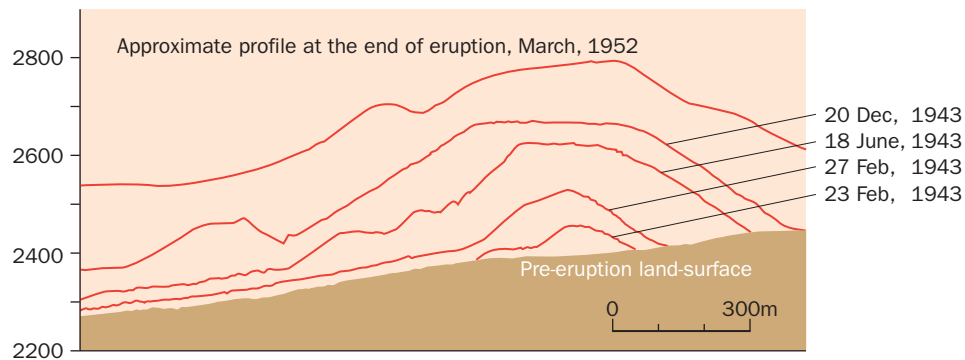
Cinder cones range in height up to 500 m. Seldom do they get much higher, apparently because even if the eruption continues, the instability of the piled up loose material causes it to slide and slump instead of building vertically, and also because of a common change of eruptive style. Basaltic monogenetic eruptions that begin with high fountaining commonly transition to effusive activity during later eruption phases, and are the source of lava flows (Fig. 9.20). As the eruptive style changes from gas-rich fountaining to lava production, the more dense molten lava extrudes through the enclosing low-density cinders to form a bocca at the cone base. First, wisps of fume start to rise from a small area on the side of the cone, then the area starts to glow and sometimes bulges slightly, and finally the molten lava stream emerges. The extrusion deforms the cone, and may carry away large fragments of collapsed cone flank on the flow surface – far downstream of the cone itself. Macdonald (1978) described portions of a cinder cone within Haleakala Crater, Hawai'i that were rafted more than 2 km from the source cone. Pieces as large as 30 m in diameter survived lava rafting virtually intact. Although Parícutín cinder cone [45] in Mexico reached a height of about 375 m within the first year of the eruption, it changed little in height during the following 8 years of activity as `a`a lava flows developed (Fig. 9.21). More about Parícutín later.

Many cinder cones are nearly circular in ground plan. Wood (1980) found that they typically range between 0.25 and 2.5 km in diameter, with a mean width of 0.9 km. The heights of the cones are usually about one-fifth of the width, given the ordinary angle of the slopes. Because crater rims are narrow, this also means that crater widths are typically about 40% that of the total cone diameter.

Fig. 9.20 SP Mountain is a classic late Holocene cinder cone with an associated lava flow in the northern part of the San Francisco volcanic field, Arizona. The cone is 25 m high and 1200 m in diameter; the basaltic andesite flow extends 7 km to the north and is up to 50 m in thickness. View to north. Photo by Wendell Duffield.



Fig. 9.21 Growth of Parícutín cinder cone, Mexico, 1943–52. Modified from Luhr & Simkin (1993).



Where the source vents are elongate, the cones are also elongate; fissure vents may be bordered by a row of partly coalescing cinder cones or by a long ridge of cinder. Some cones are almost perfectly symmetrical, but most are lower on one side than on the other, and in some cases the notch on the low side extends all the way to the base of the cone so that the edifice is horseshoe-shaped in ground plan. Such asymmetrical cones may result from nonuniform building because of inclined explosive jets that deposit more material on one side of the vent than on the other, or because of strong winds during the eruption that blew the majority of the ejecta in one direction. At other times, molten lava shoves its way through cone walls, as mentioned above, taking away a whole cone sector. More commonly cones have



Fig. 9.22 Typically horseshoe-shaped spatter cone forming on Kilauea volcano's East Rift Zone, April, 1983. Lava fountains are about 40 m high. The cone is kept open by a flowing river of lava that carries away clastic material falling on its surface. USGS photo by J. P. Lockwood.

a breached appearance simply because a stream of lava poured out from one side of the cone throughout much or all of its formation; cinders or spatter falling on the surfaces of the lava streams are immediately swept away, maintaining openings in horseshoe-shaped edifices (Fig. 9.22).

A few cinder cones have formed in historical times. One of the most recent and famous cases is that of Parícutín. Foshag and Gonzalez-Reyna (1956) interviewed Dionisio Pulido, the Mexican farmer who witnessed the birth of the cinder cone in his cornfield, 320 km west of Mexico City, on February 20, 1943. The eruption began as Dionisio was preparing to plow his field for spring sowing. His tale is re-quoted from Luhr and Simkin (1993, p. 56):

In the afternoon I joined my wife and son, who were watching the sheep, and inquired if anything new had occurred, since for two weeks we had felt strong tremors in the region. Paula [my wife] replied, yes, that she had heard noise and thunder underground. Scarcely had she finished speaking when I, myself, heard a noise, like thunder during a rainstorm, but I could not explain it, for the sky above was clear and the day was so peaceful, as it is in February. At 4 p.m. I left my wife when I noticed that a [large hole] had . . . opened on one of the knolls of my farm, and I noticed that [a] fissure . . . passed through the hole . . . and continued in the direction of Canicjuata, [about 1 km due west]. Here is something new and strange, thought I, and I searched on the ground for marks to see whether or not it had opened in the night, but could find none; and I saw that it was a kind of fissure that had a depth of only half meter. I felt a thunder, the trees trembled, and I turned to speak to Paula; and it was then I saw how, in the hole, the ground swelled and raised itself two or 2.5 meters high, and a kind of smoke or fine dust – gray, like ashes – began to rise up in a portion of the crack that I had not previously seen near the [hole]. Immediately more smoke began to rise, with a hiss

or whistle, loud and continuous; and there was a smell of sulfur. I then became greatly frightened and tried to help unyoke one of the ox teams. I hardly knew what to do, so stunned was I before this, not knowing what to think or what to do and not able to find my wife or my son or my animals. Finally my wits returned and I recalled the sacred Señor de los Milagros, which was in the church in San Juan Parangaricutiro and in a loud voice I cried, "Santo Señor de los Milagros, you brought me into this world – now save me from the dangers in which I am about to die," and I looked toward the fissure whence rose the smoke; and my fear for the first time disappeared. I ran to see if I could save my family and my companions and my oxen, but I did not see them and thought that they had taken the oxen to the spring for water. I saw that there was no longer any water in the spring, for it was near the fissure, and I thought that the water was lost because of the fissure. Then, very frightened, I mounted my mare and galloped to [the village of] Paricutín, where I found my wife and son and friends awaiting, fearing that I might be dead and they would never see me again.

The initial vent of Paricutín was quite small, no more than about 30 cm in size, but as the ground distended and lava continued to push up from below, the sides of the vent collapsed and widened. Six or seven hours after Dionisio fled his farm, the eruption became markedly more violent, with incandescent cinder now being ejected in great quantity for the first time, and lightning playing in the ash-laden Vulcanian eruption column. In a few days, activity became Strombolian, and by the end of the first week the cone was 140 m high. Within two months it grew to 310 m high, nearly its full size.

Jorullo cinder cone [42], some 160 km farther southeast in Mexico, commenced its eruption in 1759 with phreatic or phreatomagmatic explosions that continued for about 10 days before the activity became more purely magmatic. In six weeks, the cone grew to a height of 250 m. The first recorded "birth of a volcano," in contrast to the opening of boccas on the side of larger composite or shield volcanoes, took place in the Phlegraean Fields, not far from the ancient villa of Pliny near Vesuvius, in 1538. The cinder cone, known as Monte Nuovo (New Mountain), is only 135 m high, but was wholly built within 7 or 8 days.

ASH AND TUFF CONES

Phreatic and phreatomagmatic eruptions often produce another group of small monogenetic edifices, characterized by the accumulation of ash around vents, usually lying about at sea level or in low country with shallow water tables. These are called **ash cones**, or, if well-cemented and mineralized by palagonite into hard rock, **tuff cones**. Where moderately to very abundant blocks are imbedded in the ash, they are called **block-and-ash cones**. They are especially common around the margins of oceanic islands, where ascending magma encounters seawater near coasts, resulting in explosive eruptions that form landmarks such as the well known Diamond Head (Leahi), O'ahu Island, Hawai'i. As ascending magma quenches along conduits and is better and better isolated from seawater, eruptions will become less explosive and lava is commonly erupted in a final eruptive phase (Fig. 9.23).

Ash and tuff cones may closely resemble cinder cones in form. In the case of basaltic eruptions, explosion foci are so shallow that ejecta is blown out at a low angle rather than pitched



Fig. 9.23 Unnamed prehistoric tuff cone on the southeast coast of Anatahan island, Northern Marianas. This prehistoric tuff cone, about 500 m in diameter (a) has been eroded by the sea, revealing the feeder dike that fed a late stage lava flow that covered the crater floor (b). USGS photos by J. P. Lockwood.

high into the air, and the fragments accumulate at a considerable distance from the vent. As a result, ash and tuff cones commonly have much lower and broader profiles than cinder cones, and their craters are more like saucers than bowls or funnels. Typical profiles are shown in Fig. 9.24. Very broad, steep-sided ash (tuff) cones are sometimes referred to as **ash (tuff) rings**. They result from especially powerful, short-lived steam explosions. Many enclose steep-sided, shallow maar craters, typically filled with water. Most maars lack ash beds dipping inward

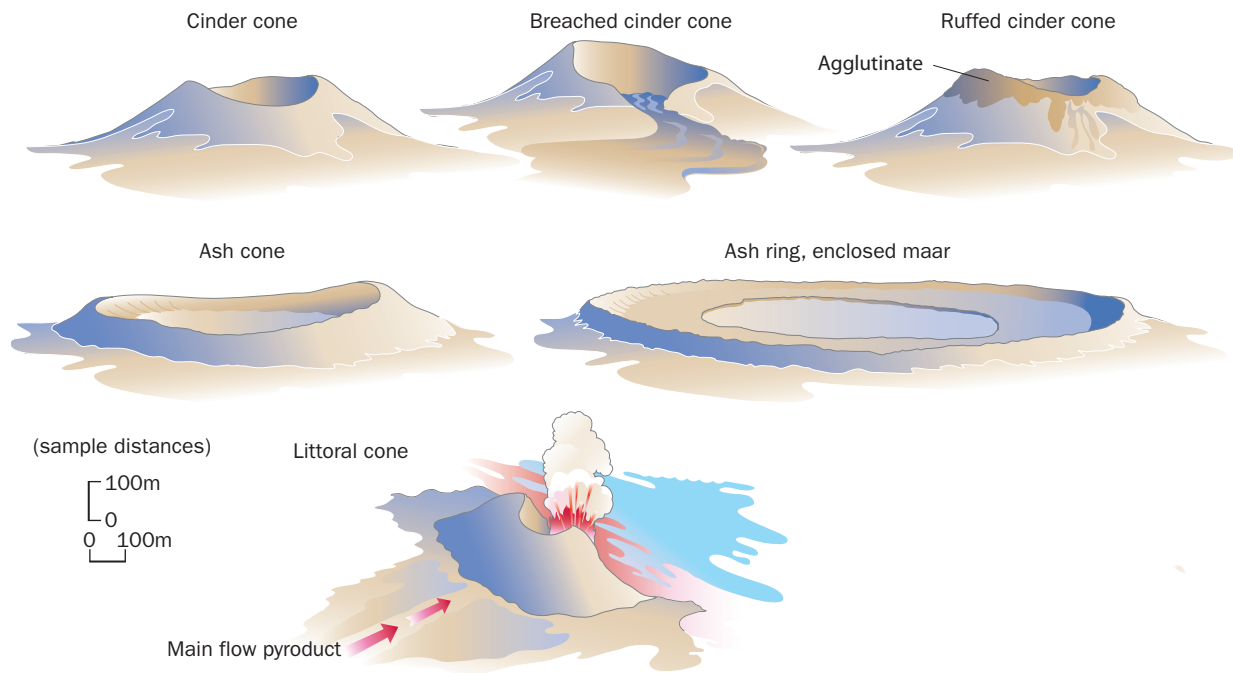


Fig. 9.24 Types of volcanic cones.

toward their centers. Instead each is delineated by a circular vertical scarp which may reveal the interior structure of the surrounding ash ring. Maar craters range in diameter from mere meters to several kilometers.

Ash cones may begin forming either under shallow water or on land. In the former case the cone commonly grows above water level, the base of the cone forming subaqueously and the upper part subaerially. The subaerial part of the cone consists partly or wholly of ash fall deposits, with regular bedding on the flanks, mantle bedding arching over the crater rim, and both normal and reverse graded bedding. Sorting ranges from poor to good. The thin beds which result from the fall of ash from small to moderate explosions are generally moderately to well-sorted, the degree of sorting increasing with distance from the vent. Thick, massive beds formed close to the foci of strong explosions may have very poor sorting. Slumping constantly distorts the bedding on the crater side of the rim, and less commonly on the outer slope. Falling bombs and blocks cause compaction and distortion of the beds, forming bomb and block-sags. Many ash layers, especially toward the base of the cone, show structures indicative of pyroclastic surging, including base surges (Chapter 8).

In the subaqueous portion of the cone the beds may show typical sedimentary features, and are apt to be better sorted than those of the subaerial part. Normal graded bedding, with the grains in each bed becoming finer upward, is often present and may be conspicuous. Underwater avalanches of fine sediment, termed **turbidity currents**, may disturb some layers, while redepositing others (Fisher & Waters 1970).

LITTORAL CONES

Unlike other kinds of volcanic edifices, littoral cones do not form around volcanic conduits but develop where lava flows enter large bodies of water. The water, reacting with lava, will quickly

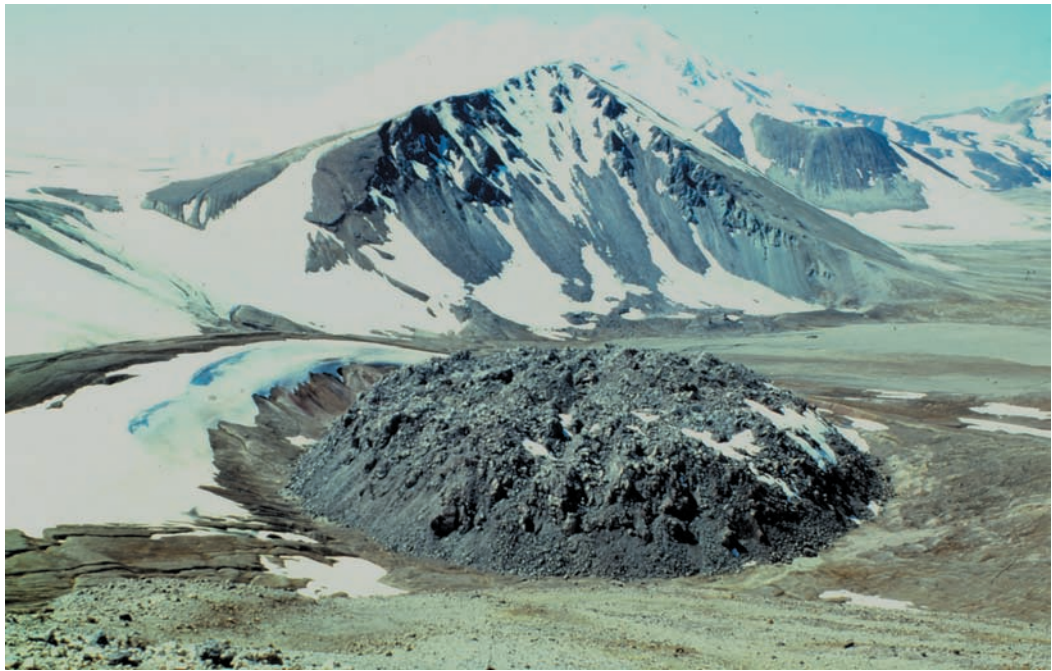
generate steam explosions, blasting out showers of solid and semi-solid fragments derived from the outer part of the flow, and liquid clots and droplets derived from the still-molten center. Most littoral explosions are caused by *`a`a* flows, because their advance usually is so slow that the amount of very hot lava newly exposed to the water within a small area at any one time is insufficient to generate a large, concentrated, and continuous volume of steam. More rarely they are caused by pāhoehoe flows, which are encased within a fairly continuous skin that serves to insulate most of the very hot portion of the flow from the water. But small littoral cones can form where the main feeder channels of pāhoehoe flows advance across turbulent surf zones. If the channels are openly exposed or have fragile crusts easily broken by the surf, strong steam blasts can take place, even generating cypressoid eruption clouds.

The larger clots of molten material expelled by littoral explosions solidify into bombs and lapilli. Generally, the bombs are irregular and rather dense, and characteristically their surfaces show a rather finely meshed shallow breadcrust-like cracking. At Pu`u Hou Hawai`i, a large littoral cone formed during the 1868 eruption of Mauna Loa, some of the bombs were still sufficiently fluid to flatten out into cow-dung morphology on impact. The smaller drops of liquid spray freeze to little rounded pellets and irregular fragments of glass. Sand-size material of this sort may be washed along shore to accumulate as beaches of black glass sand, with only minor amounts of stony debris or coral bits. Phenocrysts of green olivine may be winnowed out by longshore currents to collect in their own rare, and beautiful green sand beaches.

Where littoral explosions continue for more than a few days at fixed locations, they build cones that may reach 60 m in height and more than a kilometer in breadth at the base. Pu`u Hou reached a height of over 80 m during the 5 days that lava flowed into the ocean. Such cones are commonly built on the surfaces of the lava flows at the edges of the main feeding channels, where the contact of hot lava with the water is most continuous. A large percentage of the ejecta commonly falls into the sea and is washed away, so the cone is semicircular in plan with only the landward portion remaining. It may be quite regular in form with a single rim; or, as in the case of at Pu`u Hou, explosions at a series of different centers may build a complex cone with several rims. Often, two separate cones are built at the two sides of the lava channel; or if more than one lava channel entered the water in the same general area, three or more closely spaced cones may grow. Mantle bedding arches over the rims of cones, but bedding and sorting of the material is typically quite poor. Some beds are nearly pure ash, but others contain numerous lapilli and bombs. Where the lava was very fluid, the ejecta may be partly agglutinated in portions of the cone close to the site of the explosions. Local unconformities and slump structures are common in the cones.

It may be difficult or impossible to be sure whether a given prehistoric cone at or near the shoreline was formed above a primary vent or by a littoral explosion. The ash grains in a littoral cone are usually denser than ordinary vitric ash formed by juvenile magmatic explosions and show fewer arcuate forms resulting from the rupturing of vesicles. The difference results from the fact that the ordinary ash is formed by disruption of the magma from within by expansion of its own contained gas bubbles, whereas the littoral ash is formed by the blasting apart of the magma by gas (steam) that originates outside it. The degree of contrast depends on the amount of gas that is still contained in the lava when it reaches the shore. Where the lava has flowed

Fig. 9.25 Novarupta dome, on the Alaskan Peninsula, viewed from southwest. This 65 m high, 400 m wide lava dome was formed during the major Katmai [19] eruption of 1912. Photo by R. W. Hazlett.



for a long way and lost most of its gas, the fragments produced by the littoral explosion are quite dense. On the other hand, where gas is still exsolving from the lava and forming still-expanding vesicles, as it is in pāhoehoe flows, the fragments may be moderately vesicular.

VOLCANIC DOMES

Where highly viscous lava erupts to the surface, it has great yield strength (Chapter 4) and flows with such difficulty that it tends to pile up forming a steep-sided hill directly over and around a vent (Fig. 9.25). Such hills are known as **domes**, although the term “dome” is also used for other types of geological structures, especially tectonically domed strata. Domes that consist of new lava erupted onto the surface are termed **exogenous**. Some domes are formed by the uplifting of older rock as magma is intruded from below but never reaches the surface, and are termed **endogenous**, or **cryptodomes**. Most of the examples discussed in this chapter are exogenous domes, but other domes, such as Showa Shinzan which we discuss later, are formed mostly of endogenously uplifted material. One rare class of volcanic domes results from the upheaval of the plug filling the upper part of a pipe-like volcanic conduit, the semisolid to solid material being pushed up like a cork from the neck of a bottle. These are called **plug domes** or **spines**.

Most domes are comprised of very viscous lava, and when deeply exposed by later erosion, may show well-developed columnar jointing formed in their cores as they cooled. Some domes form by extrusion of viscous lava through an opening near their crest, the growth taking place by the piling up of one short flow over another. More commonly, however, new lava being squeezed up through the vent simply distends the mass above it, so that the growth is like that of



Fig. 9.26 Growing dome on the floor of Mount St Helens crater, ringed by its own talus, 1982. USGS photo by Lyn Topinka.

an expanding balloon. But the amount of stretching that the cooling skin of the dome can sustain without rupturing is limited. Most domes grow by a combination of internal and external accessions of lava with internal development predominant. The rims of growing domes are generally unstable, and are usually marked by borders of talus (Fig. 9.26) and large blocks (Fig. 9.27).

The degree to which the edges of a growing dome spread out from the margin of the vent depends on the viscosity of the liquid. Some spread very little. Others spread out to several times their height, and they grade into the short, thick coulee flows described in Chapter 6. Occasionally, part of a growing dome breaks away and forms a short lava flow. Most domes are of silicic composition, with rhyolite, dacite, and trachyte most common. Domes of andesite are far less common, and domes of basalt are rare.

Ferdinand Fouqué (1879) provided among the first – and most eloquent – detailed descriptions of a growing volcanic dome while studying to an effusive silicic eruption at Santorini volcano [84] Greece in 1866. Subsequent episodes of dome growth on Nea Kameni, the island



Fig. 9.27 The “Federal Building”, a 13 m diameter block that rolled off the Mount St Helens dome in 1982. USGS photo by Joe Walder.

at the center of Santorini’s mostly submerged caldera, occurred in 1925–8, 1939–41, and in 1950. The probability of future similar extrusions at Santorini is high, gradually filling in the island’s volcanic anchorage (Pyle & Elliott 2006).

Other historically well-documented dome eruptions took place at the summit of Mt Pelée [63] on the island of Martinique early in the twentieth century. T. A. Jaggar (1904) observed the growth of a new dome that began to grow about a week and a half after the deadly May 1902 eruption:

On the summit of the cone was seen a most extraordinary monolith, shaped like the dorsal fin of a shark, with a steep and almost overhanging escarpment on the east, while the western aspect of the spine was curved and smooth in profile. The field glass showed jagged surfaces on the steeper eastern side, and long smooth striated slopes on the western. Other horn-like projections from the cone could be discerned with difficulty on the slopes lower down.

This spine grew to almost 300 m in height after Jaggar left, but crumbled to rubble in 1903. Lacroix, who also documented this feature, estimated that without the loss of material from



Fig. 9.28 Fast-growing dome at the summit of Soufrière Hills volcano, Montserrat on April 27, 2007. Note the dust trails left by blocks tumbling down flanks of dome. Photo © NERC/ Government of Montserrat by Graham Ryan.

constant collapses, it might have grown to an ultimate height of 800 m. Localized spines only a few meters or tens of meters tall are very common on volcanic domes, and many domes bristle with. They are formed by the toothpaste-like extrusion of rapidly solidifying viscous magma through ruptures in the solid to semisolid shell of the dome. Such small spines continue to be extruded for only a few hours, but larger domes may grow for many months. Internal fracturing as they cool causes them to collapse into spectacularly massive breccias, sometimes accompanied by block-and-ash flows. Spines are highly ephemeral phenomena.

The best studied volcanic domes are those currently growing within the craters of Mount St Helens and Soufrière Hills [60] volcanoes (Fig. 9.28). After the May 18, 1980 eruption of Mount St Helens, relatively small domes repeatedly formed then were blown apart by explosions, but the volcano remained generally inactive for 18 years after dome growth ceased in 1986 (Fig. 9.29). Then, in October, 2004, dome growth resumed and remained vigorous until January, 2008, when activity again paused. The 2004–8 resurgence of dome building included the extrusion of giant fin-shaped spines that disintegrated within a few months (Figs. 9.30 and 9.31). (Comparisons with similar dome growth at Bezymianny volcano, Kamchatka [128], now active for over 50 years, suggest that dome growth at Mount St Helens is far from over.)

The 1975 dome at La Soufrière volcano [62] on St Vincent island took a little less than a half year for initial growth, beginning its formation exogenously. The dome developed rapidly during its first 20 days of life, then declined gradually through a phase of mostly endogenous growth over the next 130 days (Huppert et al. 1982). Likewise, the Mount St Helens dome, which began forming in the avalanche caldera shortly after the 1980 blast, grew initially by piling one exogenous lobe atop another, but then showing both modes of development as the magma entering the dome grew cooler and more viscous (Swanson & Holland 1990).



Fig. 9.29 Mount St Helens dome at the cessation of dome growth in 1986. The dome was unstable, and produced large landslides like the one in the foreground, but except for minor seismic activity and occasional steam venting, MSH showed no activity for the next 18 years. USGS photo by Lyn Topinka.

Possibly the most common dome-related explosions occur around the base of the dome and around spines on the dome. The surfaces of separation between the dome and the surrounding rocks, and between the spine and the crust of the dome, constitute zones of weakness which allow gases to escape from below and within the dome. In studying the dome that formed on Santorini in 1925 (named Fouque Kameni after the pioneer student of domes), H. S. Washington observed jets of gas issuing around the base of the dome like the spikes of a crown, and to these he gave the name **coronet explosions**. Explosions of this sort can cause the collapse of a spine above them and undermine the side of a dome, allowing it to collapse and add to the mass of crumble breccia. Some 350–650 years ago, explosions at the base of the Chaos Crags domes just north of Lassen Peak resulted in collapse of part of the domes, forming great rock avalanches that rushed 5 km down the valley and as much as 100 m up the opposite mountain slope. The blocky deposit left by the avalanches is known as the Chaos Jumbles.

Some domes have an internal structure consisting of a series of concentric layers like the shells of an onion. These appear to result from gradual expansion from within of a mass of



Fig. 9.30 Aerial view of the Mount St Helens dome complex from the northwest on February 22, 2005, after renewal of dome growth in 2004. Note the spectacular growing spine, called the “Whaleback” during its brief life. This spine is nearly 400 m long and rises about 200 m above the crater floor. USGS photo by Steve Schilling.

somewhat non-homogeneous magma—outer parts glassier, perhaps, and inner portions more microlite rich. Much more commonly, however, domes are either essentially structureless except for the gradual inward gradation from a brecciated outer part to a massive interior, or show divergent structures, fan-like in cross-section with the ribs of the fan radiating upward from the vent. Surfaces of domes are often marked by a series of concentric ridges resembling the ogives on coulees and blocky `a` flows. The internal flow structures may be nearly horizontal around dome bases, gradually changing to verticality near centers. It appears easier for a growing dome to expand upward than sideways, because of the confining action of its own shell and the increasing mass of crumbled breccia.

We conclude our discussion of domes with a case history from Japan where an eruption produced both endogenous and exogenous dome growth between 1944 and 1945 (modified from a summary by Macdonald, 1972). This eruption of the Showa Shinzan domes occurred during the Second World War, when a news blackout kept all but local citizens and a few Japanese scientists from knowing about this volcanic eruption of Usu volcano [118] on the northern island of Hokkaido, at the southern edge of Lake Toya caldera (Minakami et al. 1951). Usu is situated at the southern edge of Lake Toya caldera. A large endogenous dome (called a “yaneyama” or “roof mountain”) formed here in 1910, but for more than 30 years there was no activity. Then, in late 1943, earthquakes began to be felt in the area. A village postmaster, Masao Mimatsu, kept a meticulous, hand-illustrated journal of events. The volcano was fortuitously visible from his post office window, and throughout the eruption he kept track of the changing shape of the mountain by outlining its profile on a piece of paper he attached to the window (Fig. 9.32).



Fig. 9.31 The fast-changing morphology of growing domes within the Mount St Helens crater is shown by this view from the northwest on September 28, 2005. A new dome is growing to the west of the remnants of the Whaleback spine – which has completely disintegrated. USGS photo by John Pallister.

The first earthquake of the pre-eruption series was felt on December 28, 1943, and was followed by many more during the next few days. Within a few days, more than 500 earthquakes had been counted at Toya Hot Springs, and quakes continued in increasing number and intensity. At first they were felt most strongly at the northwestern base of the Usu edifice, but after 6 January they became strongest at the eastern base of the volcano. Past the eastern base of Usu, the Sobetsu River flows southward, and parallel to it ran irrigation canals, roads, and a railroad. Late in January, the ground surface near the southern base of the Usu began to rise. Cracks appeared in the roads and the banks of the canals, and water began to flow less rapidly through the canals. Wells and springs in the rising area dried up, while those in nearby areas flowed more abundantly. By early April the rising area was roughly circular and about 4 km across, and its central part had risen about 16.5 m. Then the center of the uplift suddenly shifted nearly a kilometer northward with its summit very close to the village of Fukaba. Magma was obviously shifting near the surface, but was still underground. In mid-June more than 100 severe earthquakes were being felt each day, and on June 22 the number reached 250. The ground surface had by then risen about 45 m. The villagers of Fukaba were literally being taken for a ride!

Then, at about 8:30 on the morning of June 23, a column of steam was seen rising from a field nearby. Steam discharge increased gradually over the next couple of hours, and at 10 a.m. an explosion hurled out mud, sand and blocks of rock, creating a crater about 45 m across.

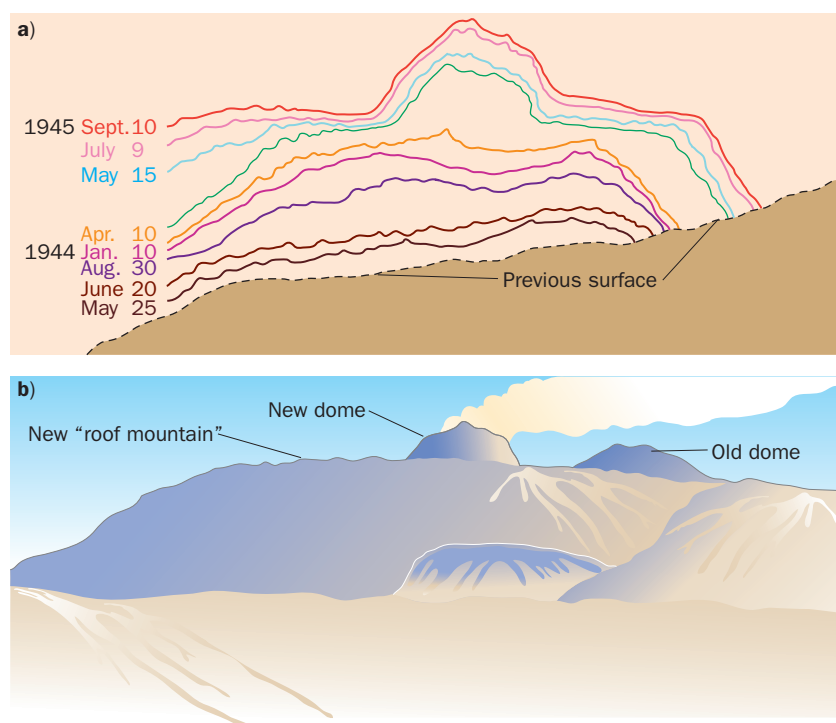


Fig. 9.32 The growth of Showa Shinzan dome, as sketched by Masao Mimatsu in 1944–5. Courtesy of Saburo Mimatsu.

A stream of mud flowed out of the crater and formed a steaming pool in a nearby hollow. Then, after a few hours of quiet, steam again began to rise, followed by another series of explosions. Similar series of explosions continued at short intervals throughout the next 3 months, some of the explosions throwing blocks of rock a 1500 m into the air. Other craters formed near the first one.

On July 2, a phreatic explosion expelled 2 million tonnes of debris, and lithic ash resulting from the pulverization of older rocks. The falling ash did much damage to forests and cultivated fields. A similar large explosion occurred on July 3, and the villagers of Fukaba finally abandoned their homes. By late September, seven separate craters had been formed in a group 600 m west of Fukaba, the earliest craters being partly buried by the material ejected during formation of the later ones. Avalanches of ash rushed down the mountain slope but were not hot enough to set wooden houses on fire. By late October, the upheaved area formed a flat-topped, dome-shaped hill 140–175 m high and nearly a kilometer across.

The crest and flanks of the hill still consisted of the original soil and rock cover, though largely torn apart. This new dome was named Showa Shinzan – “New Mountain of the Showa Era.” The Sobetsu River had been dammed by the rising ground and now had formed a lake nearly a kilometer long. But in spite of the upheaval and numerous phreatic explosions, no new lava had appeared. The uplift could still be characterized as a cryptodome.

At last, in early November, viscous magma began to extrude from the top of the uplift, just to one side of the group of explosion craters. This newly eruptive dome was incandescent, with such high viscosity that it was almost solid. It gradually grew in height and diameter, but it carried on its top a cap of older rock, including stream gravel that had once accumulated on the nearly level surface west of Fukaba village. The temperature of the new



Fig. 9.33 Showa Shinzan cryptodome viewed from the southeast, Usu volcano summit in the background. The flanks of the exogenous dome (barren summit) is covered by an uplifted carapace of older sedimentary rocks. Photo by Hiromo Okada.

lava was at least 1000°C, and the heat baked the clay of the old rocks in the cap to a natural brick. Small pyroclastic flows descended from the north side of the dome, reaching as far as Lake Toya (Okada, 2008, pers. comm.) Growth of the 300 m-diameter extrusion finally came to an end about September, 1945, with its summit about 110 m above the top of the earlier cryptodome, and over 300 m above the original level of the ground (Fig. 9.33). The dome remains steaming to this day, and has become a popular tourist attraction.

Volcano Old Age and Extinction

No one knows much about how volcanoes die. There is no one path taken to extinction, and volcanoes presumed “extinct” have been known to arise from the dead (e.g., Chaitén volcano, Chile [55], which erupted in 2008 after almost 10,000 years of quiescence). Some volcanoes may end their lives in a burst of silicic explosivity, collapsing like Mt Mazama in Oregon while others may end with minor basalt eruptions. Some appear to simply decline gradually, eruptions tending to pass from Strombolian or Vulcanian rigor to anemic Ultravulcanian or phreatic blasts at the end. Many volcanoes begin their lives effusively, and become more explosive with age. Others, like Vesuvius and Mount St Helens, show explosive early histories and become more effusive in time. There seems to be no making heads or tails of it at present, and we have to leave it at that.

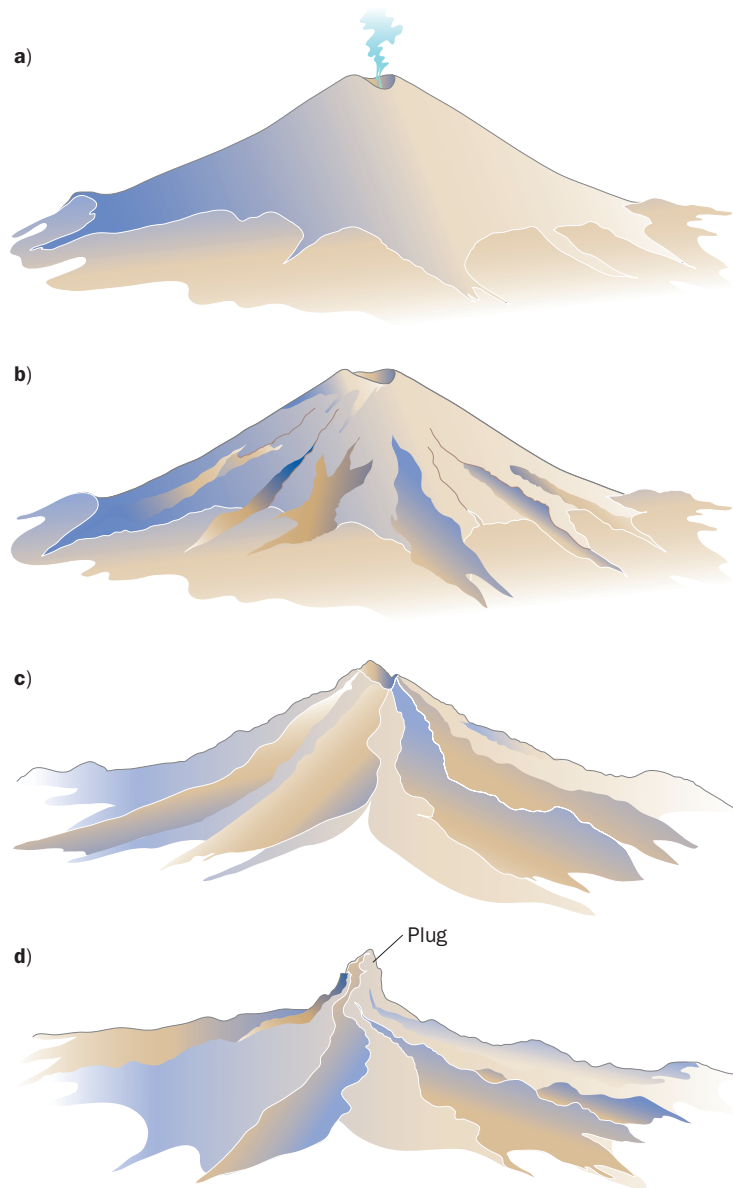


Fig. 9.34 Erosion of a composite volcano in a temperate to tropical latitude.

Even before most large volcanoes stop erupting, erosion begins to destroy their edifices. How erosion proceeds depends upon the type of volcano and the climate. The primary agents of erosion are flowing water and/or ice. Loose fragments of rock swept downslope by runoff acts as an abrasive tool which loosens other fragments. These materials scour the slope along favored paths for runoff, developing channels and gullies which grow wider as they deepen. Many composite volcanoes begin to grow on older, eroded land. As such volcanoes age, water running off slopes is funneled into the preexisting gullies and stream channels at volcano bases (Fig. 9.34). These channels gradually erode their way upward into volcano flanks, a process termed **headward erosion**. Within a few thousand years, volcanoes may pass into a stage of aging where the summit of the cone remains youthful and smooth, while lower flanks become deeply channeled. Large strips of uneroded cone flank may continue extending all the way to

Fig. 9.35 Mt Hood, Oregon, as viewed from the northeast. Glaciers have deeply sculpted this high volcano (3329 m), but the volcano remains active, and the conflict between fire and ice will continue to modify its shape in the future. Photo by J. P. Lockwood.



the base of the cone between the growing channels, but as the channels lengthen, deepen, and widen, these strips grow narrower and finally disappear. At last the channels work their way to the top of the cone, and the rims of the summit crater, if present, also disappear. At this time, the volcano becomes a roughly radial array of ridges and canyons all meeting at the position of the central conduit. Ten or twenty thousand years may have elapsed since the mountain last erupted. Continuing erosion lowers the ridgelines and channel beds, while also reducing their slopes. The conduit plug and dikes which reinforced the interior of the cone emerge as the surrounding, weaker edifice is stripped away, and become topographic prominences in the now rugged terrain of the old volcano. Erosion continues, perhaps for a few million years, until ultimately only the resistant plug and dike rock remain. Even these will weather away and disappear in time, leaving only a bedrock intrusive stock and dikes to mark the former presence of once majestic cones.

For high altitude or high latitude volcanoes, glacial ice may be the primary erosive agent on upper slopes, giving such volcanoes a particularly rugged, jagged appearance (Fig. 9.35). Intersection of glacial cirques as they expand summitward may sculpt the mountaintop to a sharp point in time. If late-stage eruptions happen to take place on glaciated volcanoes, the potential for lahars is extremely high, given the presence of enormous volumes of water in the form of ice, the steepness and weakness of the mountainsides, and the presence of unconsolidated glacial debris. This was tragically learned during the 1985 eruption of Nevado del Ruiz volcano [54], Colombia [58] (Chapter 14). Examples of other such potentially active and dangerous glaciated volcanoes include Mt Rainier, Washington [31]; Mt Shasta, California [26]; Iliamna, Alaska [20]; Koryaksky, Kamchatka [123], and Nevado Coropuna, the largest of the Peruvian volcanoes.

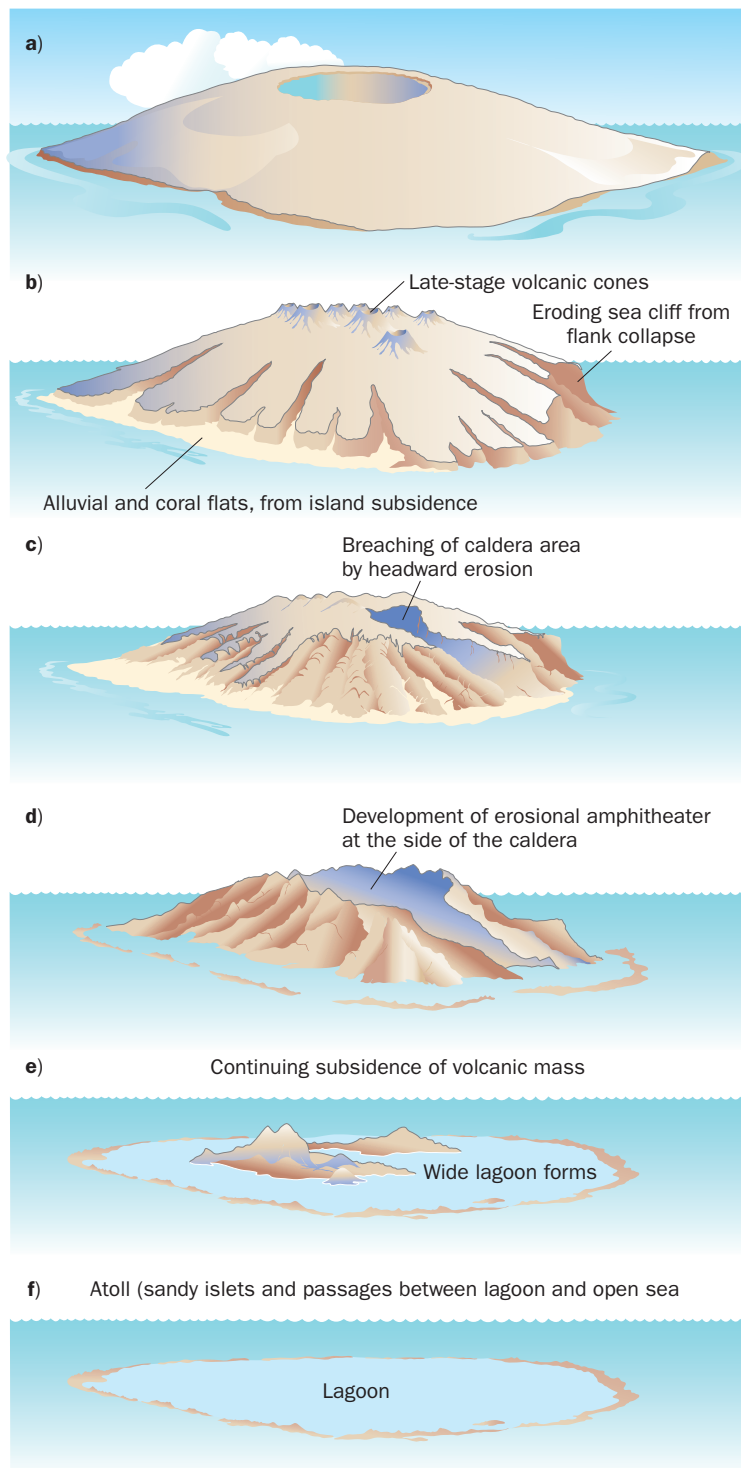
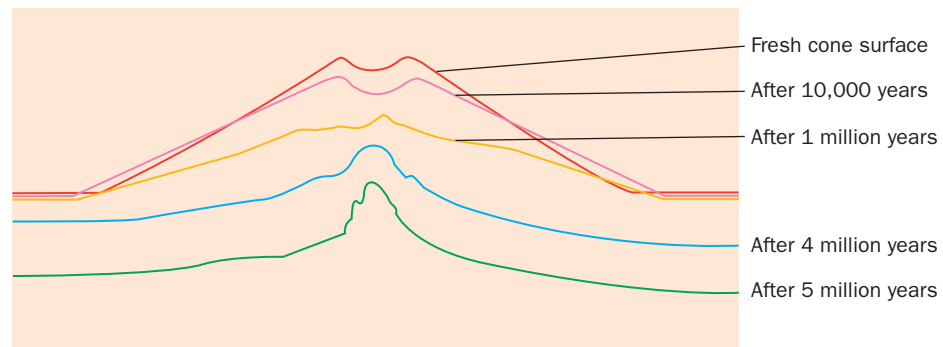


Fig. 9.36 Erosion and tectonic subsidence of an oceanic shield volcano.

Shield volcanic islands erode in a manner similar to composite volcanoes, but with some significant differences (Fig. 9.36). Headward erosion is triggered as runoff channels develop at the crests of shoreline cliffs, and water collects to flow into small embayments along young island shorelines, initiating channel development at the coast. The drainage system develops

Fig. 9.37 Changing profile of a cinder cone as it weathers and erodes away. From Kieffer (1971) and Cas and Wright (1988). Climatic conditions are those of Central France.

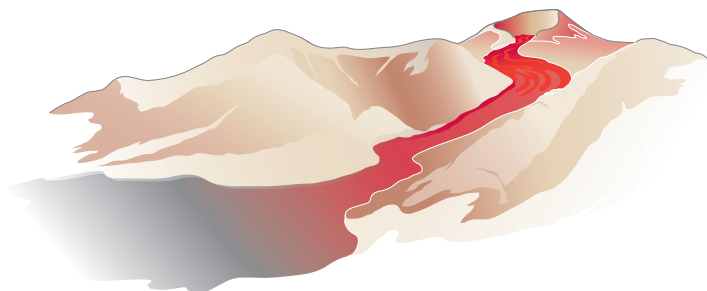


in the same manner described above for composite volcanoes. But, as they erode into caldera areas, streams may encounter weak, hydrothermally-altered rocks, which wear away much more readily than surrounding, more resistant lava flows. The streams quickly eat out the soft, clay-rich core of the volcano, until the perimeter of the former caldera becomes the high, cliffy rim of an erosional basin, usually with a horseshoe or spoon-shape. As erosion continues, the former caldera may retain its ridge crest outline for as long as several million years. In contrast to a composite volcano, whose summit crater completely disappears, Tectonic subsidence may submerge the volcano long before erosion planes it level with the sea.

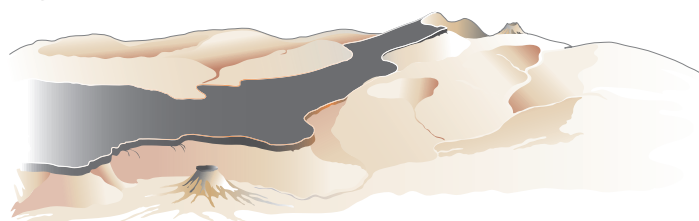
Cinder cones erode somewhat differently (Fig. 9.37). While they will show fine, grill-like channels in their flanks during the early stages of their erosion, the permeability of the loose cinder soaks up all but the heaviest rainfalls. Hence, channel development rarely progresses very deeply. The loose surface material of the cone is subject to mass wasting, and cinder often clogs channels, forcing occasional torrents of water to re-excavate them as erosion progresses. The net effect of this means that aging cinder cones may retain a generally smooth profile. At an advanced stage, the cinder cone may appear as nothing more than a red-brown, gently sloping knoll of oxidized cinder, its crater long wasted away. Studies by Kieffer (1971) of eroding cinder cones in the Massif Central of France indicate that it takes over 10,000 years for this level of decay to occur in that region. In the Big Pine volcanic field in east central California, similar development takes over 100,000 years and perhaps as much as 250,000 years, illustrating the influence of a climate that, for much of that time, has been more arid than in France. At the other end of the climate spectrum, Ollier (1969) reports erosion rates on Vulcan, the cinder and ash cone in tropical Rabaul Caldera [122], of as much as a meter of surface lowering over a 30-year interval, which works out to a rate of 30 m per 1000 years. In general, the steeper and longer a slope, the faster its surface at any fixed position erodes down. Eventually, a basaltic plug within the cone may be exposed, as in eroding composite volcanoes. The feeder dike beneath the cinder cone will also emerge as a wall of resistant rock as the landscape degrades.

Different types of volcanic deposits respond to weathering and erosion in strikingly different ways. Lava flows tend to be quite resistant to weathering, because of their fine textures and density, providing little opportunity for water penetration. The surrounding rocks usually weaken and erode away faster. In many regions, former canyon or valley-filling flows have become the caps of long, sinuous ridges after several million years of erosion. Many of the mesas and buttes of desert lands are capped by thin basalt flows (Fig. 9.38). The flows erode primarily by being undermined by erosion of the weaker rock beneath.

a) Young lava flow



b) Eroding landscape begins developing inverted topography (once low area of lava flow becoming high relative to surrounding landscape, owing to resistance to erosion)



c) Erosionally “old” landscape

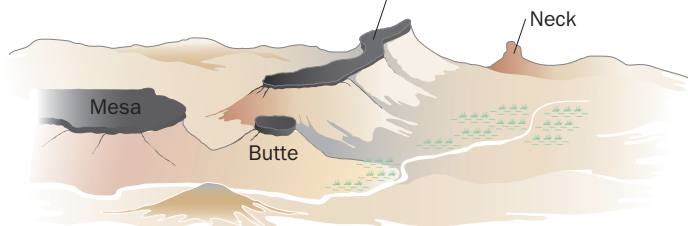


Fig. 9.38 Erosion of a temperate or desert landscape with a cinder cone and a lava flow.

Rocks that weather easily tend to develop gentle slopes, as rain water washes away detritus quickly – such rocks are commonly weak and cannot support steep faces. Steep faces indicate stronger rocks that weather slowly. Many ignimbrites illustrate this contrast well. The welded centers of the ash flows form dark cliffs, roughly partitioned by widely-spaced columnar joints. Their unwelded tops and bases are typically lighter in color, not being oxidized or baked, lack joints, and form gentle slopes. Where fumarolic pipes cemented by mineralization exist, these will rise as vertical pillars or chimneys through the unwelded upper section, since they effectively resist weathering.

Unwelded pyroclastic deposits erode quite easily, becoming laced with steep-walled channels (Fig. 9.39). The steepness of the channel walls isn't a result of resistance to weathering, but a testimony to the rapidity with which streams can abrade and cut straight down through the deposits. In contrast, lahars, thick with clays and often saturated with water, are not easily eroded, once they come to rest and de-water. Indurated lahar deposits, like lava flows, tend to form resistant, steep faced outcrops.

Fig. 9.39 Slot canyon formed where New York Creek cuts through the highly resistant, moderately welded portion of the 2050 year old Okmok ignimbrite, Umnak Island, Alaska. Note columnar jointing. The gentler slopes above this consist of the unwelded portion of the deposit and younger volcanic tephra layers. (Photo: Richard Hazlett).



FURTHER READING

- Huggett, R. (2007) *Fundamentals of Geomorphology*. London, Taylor and Francis Publishing, 472 p.
- Lu, Z. and Dzurisin, D. (2011) *INSAR Imaging of Aleutian Volcanoes*, Berlin, Springer Praxis, 300 p.
- Thouret, J.-G. and Chester, D. K. (2005) *Volcanic Landforms, Processes and Hazards*. International Association of Geomorphology (IAG) Working Group on Volcanic Geomorphology, *Zeitschrift für Geomorphologie, Supplementbände* vol. 140, 231 p.
- Tilling, R. I., Topinka, L. and Swanson, D. (1990) *Eruptions of Mount St. Helens; Past, Present, and Future*. US Geological Survey General Interest Publication, 56 p.

Chapter 9

Questions for Thought, Study, and Discussion

- 1 Why do some oceanic shield volcanoes have rift zones in their flanks, while others lack them?
- 2 Do each of the terms “shield volcano,” “composite volcano,” “cinder cone,” and “dome” necessarily also apply to underwater volcanoes too? Explain your answer(s).
- 3 Why are some domes endogenous, others exogenous, and some *both* during their construction?
- 4 If a volcano like Pinatubo appears from a distance merely to be a “non-majestic” group of hills in many places under heavy vegetation, how would you then determine that it is a potentially active volcano? Or would this even be possible?
- 5 How could you tell if a cinder cone was breached not by flank extrusion of lava late in the eruption, but rather by the continuous flow of lava away from the vent throughout the eruption?
- 6 Consider two composite cones; one with uniformly angled slopes and a small funnel shaped crater on top; the other with slopes that grow much steeper toward its broad summit, which lacks a crater and is approximately level – though quite rough in places. What might explain the differences in the slope aspects of these two cones?
- 7 Why is rejuvenated volcanism of such short duration on aging Hawaiian shield volcanoes?
- 8 Why are some composite volcanoes isolated edifices, while others occur in overlapping clusters (volcanic complexes) or in closely-spaced alignments?
- 9 Compare the erosional decay of an extinct composite volcano of moderate size built on a landscape near sea level in the tropics with one in the subarctic also built near sea level, and one in a temperate latitude desert. How and why do these three differ in appearance as erosion progresses?

Chapter 10

“Negative” Volcanic Landforms – Craters and Calderas

Craters of large-scale mountainous volcanoes, instead of marking the site of eternal constructive energy, mark rather the place of sudden withdrawal of lavas which sank back into the depths before their complete solidification.

(Alphons Stübel, 1903 [Quoted in Jaggar, 1947, p. 360])

Volcanic craters form in many different ways and come in many different sizes and shapes. Some (mostly smaller) craters form by the construction of rims around eruptive vents or by the explosive ejection of rim-forming material. Many involve both construction and collapse mechanisms in their origin. The small cup-shaped craters atop cinder cones and the broader ones of ash cones exemplify such “constructional” craters, and typically span a few tens of hundred meters in diameter or meters. Others (including the largest craters on Earth) form primarily by collapse above magma chambers. The largest collapse craters are termed **calderas**, and will be a major focus of this chapter, since their formation commonly accompanies the most violent and devastating eruptions known. Although geologically active calderas pose a risk to millions of people, they are also beneficial to human society, since younger ones host vast reserves of geothermal energy, and older ones are the hosts for rich metallic ore deposits (Chapter 15). We’ll not only discuss calderas from a morphological perspective in this chapter, but also summarize what has been learned about the mechanics of their formation.

Volcanoes: Global Perspectives, 1st edition. By John P. Lockwood and Richard W. Hazlett. Published by Blackwell Publishing Ltd.

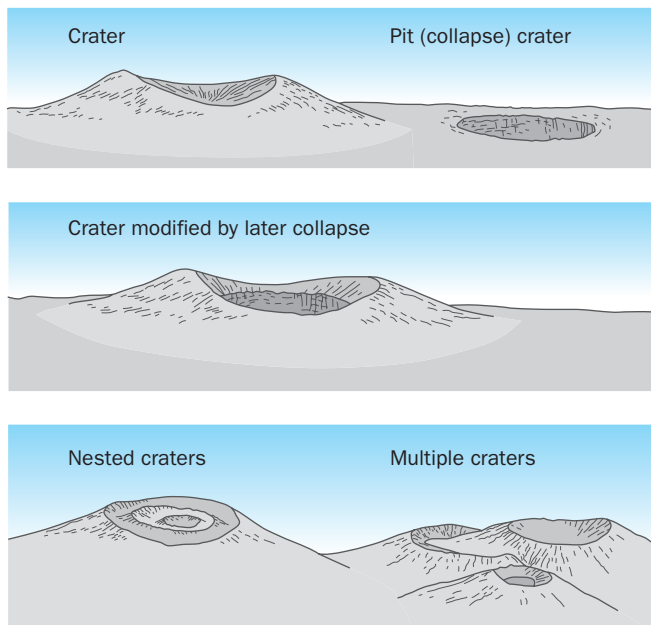


Fig. 10.1 Types of volcanic craters.



Fig. 10.2 Phreatomagmatic eruption during the formation of the eastern Ukinrek maar, April 6, 1977. The formation of these maars on the Alaska Peninsula, 60 km from the 1912 Katmai eruption, was the first historical volcanic activity in this area. Initial explosive activity formed this 300 m-diameter crater, which was later filled by growth of a basaltic dome. USGS photo by Juergen Kienle.

Small Craters

Many eruptions vary in intensity, so that one crater rim may be destroyed as blasts widen the crater or as the crater enlarges by collapse; or outer rims may be left to enclose younger crater rims developed by smaller blasts at a later time. Small-diameter crater rims lying within wider ones form **nested craters**. They are common on composite volcanoes, and on some cinder cones. **Multiple craters**, which overlap one another, develop where foci of explosions shift during an eruption or from one eruption to the next. Only the youngest crater in a coalescing set will show complete development of a rim (Fig. 10.1).

EXPLOSION CRATERS

Some craters form by purely hydrothermal explosive activity – where no magmatic activity is directly involved, and crater rims are formed by the ejection of older country rock blasted out by the action of violent gas explosions. Fluid lava flowing over swampy ground created a vast field of phreatic “pseudo-craters” in the Myvatn area of Iceland. Other good examples are the explosion craters found in many geothermal areas – where violent phreatic blasts excavate the landscape. Numerous examples of such features are found in Yellowstone National Park, USA, where prehistoric hydrothermal explosion craters as much as 2 km in diameter have been identified (Muffler et al. 1971). Some of these explosions evidently resulted from the rapid depressurization of shallow hydrothermal systems when overlying lakes suddenly drained. More recent examples were formed on the Alaska Peninsula in the spring of 1977, when violent phreatomagmatic explosions formed two craters (Ukinrek maars [10]). The initial phreatic explosions sent ash clouds as high as 6 km, and ash drifted as far as 160 km (Kienle et al. 1980). A lava dome was constructed by later magmatic activity in the larger eastern crater, but this has now been covered by a lake (Fig. 10.2). The maars formed in an area of known CO_2 mofettes, and gas emission continues. It has been proposed that CO_2 , as well as H_2O was a major component of the phreatic volatiles involved in the 1977 explosions.



Fig. 10.3 View to north of Dolomieu Crater, at the 2631 m summit of Piton de la Fournaise volcano, Reunion Island. The floor of this kilometer long caldera collapsed in April, 2007 to form a 330 m deep pit as lava drained out to form a major flank eruption. Photo ©Paul-Edouard Bernard De Lajartre.

Explosion craters are typically bounded by low, gently sloping rims that form as the largest fragments and the largest proportion of fragments of all sizes fall closest to the vent. Circular explosion craters with low rims of ejecta may resemble meteorite impact craters, and field-work may be necessary to resolve their origins.

COLLAPSE CRATERS

In contrast to craters formed by construction of their rims, **collapse craters** lack ejecta rims and tend to have very steep walls, with talus-filled floors that may taper to a point at the center of the crater. The roof rocks that drop as such craters form normally shatters. Collapse craters are all formed by the drainage of magma from underlying shallow magma chambers or other intrusive bodies (Fig. 10.3).

Pit crater is the generic name for small collapse craters less than a kilometer or so in diameter (Fig. 10.4). Pit craters are common in the rift zones of young Hawaiian shield volcanoes, especially near summits where magma withdrawal to supply flank eruptions at lower elevations can easily remove support from the shallow crust.

In some instances, the subsiding roof block in an opening crater descends all as one piece, like a piston moving through a cylinder, perhaps tilting as it does so. This happened, for example, in Lua Poholo Crater at the summit of Mauna Loa, where a level floor that formed when a flow poured into the crater after its initial formation tilted on one side during later subsidence, forming a **trap-door crater** (Fig. 10.5). Roche et al. (2001) did experimental studies of pit crater formation using silicone molds. They determined that if the source

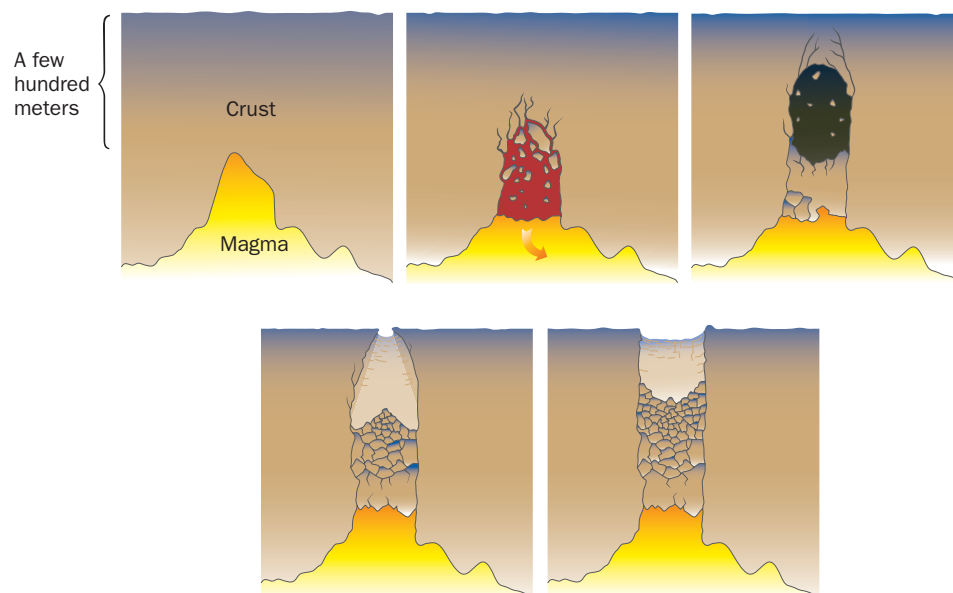


Fig. 10.4 Pit crater origin, caused by drainage of magma and upward stopping of collapse cavity.



Fig. 10.5 Lua Poholo, a 300 m diameter, 70 m deep pit crater on the northeastern floor of Mokuaweoweo caldera, Mauna Loa volcano, Hawai'i is a good example of a "trap-door" crater. The floor of this crater tilted during collapse as a small underlying magma chamber drained in 1880, feeding an eruption lower on Mauna Loa's flank. Photo © G. Brad Lewis.

cavity is quite shallow – less deep underground than it is wide – the roof will tend to collapse as a coherent block, as in Lua Poholo Crater. If the cavity is somewhat deeper than this, then the roof tends to fall by stoping from beneath – that is, by piecemeal collapse – and will develop a pit with initially overhanging walls and a small opening at the surface.

On some composite volcanoes, summit craters have deep, pipe-like pits in their centers, indicating that eruptions have a two-stage behavior; an early phase of shallow-focused explosive activity followed by a later stage of magma withdrawal. But where does draining magma go in a composite volcano? In part, the decline simply reflects the volume decrease in the underlying magma as exsolution occurs. But as in shield volcanoes, the molten rock also commonly feeds intrusive dikes or sills into the flanks. Radial dike intrusions can lead to large flank eruptions, draining enough melt to stop all but gas emissions at the summit. These emissions can be quite powerful, forming “Vesuvian”-like gas streams that core out the conduit, not only through direct blasting, but by abrading conduit walls with loose rubble, like sediment scouring a stream bed. Toward the ends of many explosive eruptions, the volume of gaseous magma lost through pyroclastic ejection exceeds the volume of fresh melt and volatiles ascending from below. Thus explosion foci and the tops of magma columns drop as eruptions progress. At the end of the activity, a large pit may remain which simply represents the emptied top of the conduit. Dome growth from the remaining, sluggishly ascending magma may later fill this pit to overflowing, leaving no trace of it behind.

Maars (Chapter 9) are another example of craters whose formation commonly combines aspects of both explosions and collapse. Their early phreatic or phreatomagmatic explosive phase may be followed by an episode of collapse, exposing the wide top of the conduit. Most maars fill with water, since their bottoms generally lie below the surrounding water table. On island volcanoes the intersection of rising magma along radial vents reacts explosively with seawater commonly to form maars in coastal areas. Since many maars form where CO₂-rich diatreme magma intersects the surface, they may continue to leak magmatic carbon dioxide through their floors for thousands of years after their formation (Chapter 4). The 10,000-year old Laacher See maar in northwestern Germany is famous for its springs of carbonated mineral water, CO₂ leaking into the 200 m deep Lake Nyos maar [77], set the stage for a tragic releases of lethal CO₂ in 1986 (Chapter 14).

Calderas

The term **caldera** has several meanings in volcanology, which has resulted in considerable confusion as to how the term should be used. These are the largest craters of all, by definition exceeding about 1–2 km in diameter. Although now used only to describe large volcanic craters formed by roof collapse above magma chambers, the word was originally proposed to describe any large depression on the summits or flanks of volcanoes, without regard to genetic origins, whether formed by summit collapse or by other processes such as mass-wasting, regional tectonic faulting, or the erosion of weak rocks within the hearts of volcanoes. The term means “kettle” in Spanish, and was popularized by von Buch after a feature called “La Caldera de Taburiente” on the island of La Palma (Lyell 1855). We now know that this particular “caldera” was mainly formed by erosion at the head of a giant sector-collapse landslide (Chapter 11), and would not be described as a caldera today.

Howell Williams, working at Crater Lake [29], Oregon, began our modern understanding of calderas with his classic book *Calderas and their Origin* (Williams 1941). Further insights

into the relationships between caldera formation and ignimbrites came in the 1960s and 1970s, largely inspired by the work of R. L. Smith (1960, 1979).

There are various kinds of calderas, but ambiguities about the individual histories of most makes rigid classification systems uncertain. Although some authors have proposed dividing these features into “erosion calderas” and “collapse calderas” (e.g., Karatson et al. 1999), that distinction is difficult as many if not most older features recognized as calderas have been extensively modified by erosion since geologic activity and their initial origins may be debatable. We will here restrict the term **caldera** to those volcanic features caused by collapse of volcanic roofs above underlying magma chambers, although we recognize that their original boundaries may be blurred by subsequent erosion. Another complexity is that the term caldera is rightfully used to describe volcanic features that may no longer have any original topographic expression, but instead refer to the deeper levels of collapse revealed by millions of years of erosion. As an example, the classic caldera complex of the San Juan Mountains, Colorado is now largely preserved as high-standing mountainous terrain, although major caldera interiors remain as low-lying areas within the high ranges after nearly 30 million years of erosion (Lipman 1984). In the rugged mountain ranges of the American Southwest, geologists may discern ancient calderas only by the presence of arcuate faults enclosing thick, light-colored tuffs and megabreccias that now stand out in the flanks of mesas and in canyon walls. Detailed geologic mapping and rock compositional analyses are generally required to identify the caldera sources for ancient ash flows in such older terrains, though in many instances finding a source is simply no longer possible due to post-eruption erosion and burial.

Most collapse calderas form near the summits of polygenetic volcanoes, directly over or near underlying magma chambers, and are of two general classes. One class, which we call **drainage calderas**, includes those caused by the lateral drainage of underlying magma chambers, typically within basaltic oceanic volcanoes. These calderas form when magma drains to lower elevations, often submarine, causing roofs over those chambers to collapse. The second class, which we refer to as **explosive calderas**, are associated with violent pyroclastic eruptions (Chapters 7, 8), and are caused by the subsidence of magma chamber roofs as magma is explosively erupted directly above or close to caldera boundaries. This second type of caldera is typically associated with silicic volcanoes of continental or island-arc areas. Marti et al. (2009) further divide such calderas on the basis of field relations.

DRAINAGE CALDERAS

Classic examples of drainage calderas include the summit calderas of Mauna Loa, Hawai‘i, and Fernandina [47], Galapagos (Simkin & Howard 1970). Mauna Loa’s caldera, Mokuaweoweo, formed by collapse about 1200 years ago as magma drained away to feed a large flank eruption 35 km away and 2500 m lower on the volcano’s East Rift Zone (Lockwood & Lipman 1987). It has subsequently enlarged by piecemeal collapse and undergone repeated periods of filling and drainage. Mokuaweoweo presently measures 5 by 3 km, with rims up to 180 m high (Fig. 10.6). It appears to have developed by incremental, passive subsidence, and doubtlessly overlies many older, buried caldera structures stacked atop one another and partially digested during the growth of the giant shield over hundreds of thousands of years. The arcuate shaped rims of many collapse calderas suggest that they form by coalescence of smaller, discretely formed pit craters, as shown in the walls of Mokuaweoweo (Fig. 10.7).



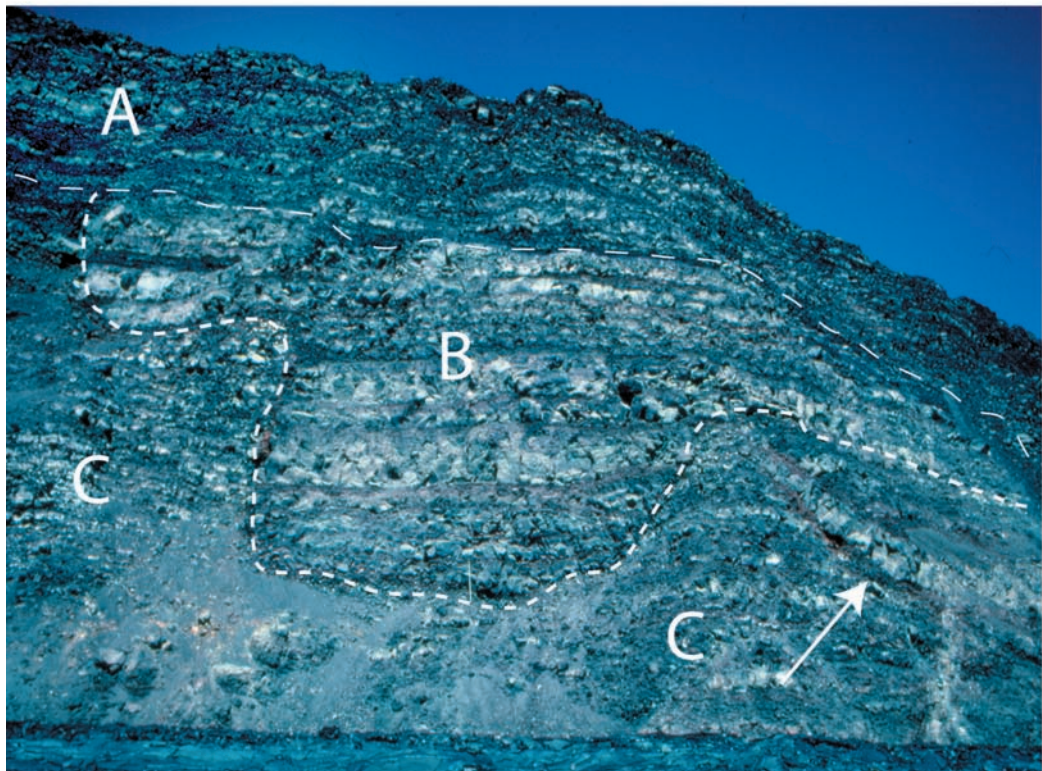
Fig. 10.6 View northeast across Mokuaweoweo caldera, Mauna Loa, Hawai'i. The caldera is 4.5 km long and 2.5 km wide, but this foreshortened view across the long axis gives a distorted perspective. Mauna Loa last erupted in 1984; the 1984 eruptive fissure extends across the length of the caldera and 1984 lavas cover the foreground and most of the caldera floor. The present caldera rim is up to 180 m high, but the caldera was estimated to be about 365 m deep when first observed by explorers in 1794. Because lava flows can now flow out of the caldera at either end it cannot become filled up to higher levels. Photo by J. P. Lockwood.

The *smallest* calderas tend to occur on the *largest* volcanic edifices – the intraplate basaltic shields. Although explosive calderas associated with continental volcanoes are much larger, the topographic edifices associated with them may be unassuming. As a basaltic volcano like Mauna Loa inflates with magma and grows through intrusions in its rift zones, the summit is subjected to tremendous tensile stress, which can facilitate summit collapse. Actual collapse is associated with drainage of the magma chamber, which removes support for the summit. Many such caldera collapse events may result in very little explosive activity, except in cases where high level water tables allow explosive interaction between groundwater and heated rocks.

One of the best documented recent caldera collapse events occurred at Miyakejima volcano [115], Japan in 2000. Miyakejima is a small island volcano along the Izu-Ogasawara island arc system about 200 km south of Tokyo. Seismic activity indicated that magma began to drain from a chamber beneath the volcano's summit in late June along a dike below the west flank,

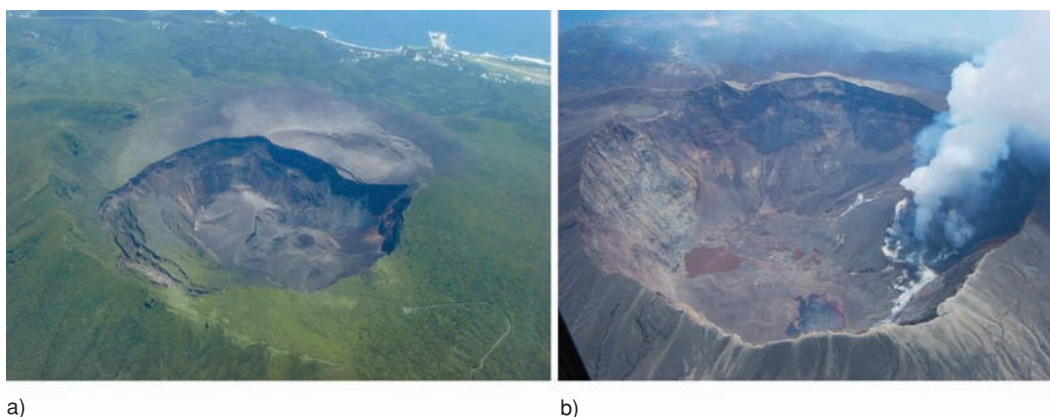
Fig. 10.7 The northwest wall of Mokuaweoweo caldera, Mauna Loa, Hawai'i. The lavas exposed in the 160 m-high vertical wall record the complex caldera history.

a) The youngest (about 1200 year-old) caldera overflows from a high-standing lava lake (above thin dashed line); b) Thick flows that completely filled a pit crater ("Lua Piha" – outlined by thick dashed line) on the flank of an earlier caldera; c) Earlier caldera overflows. The arrow points to a laccolith intruded into the flanks of an earlier caldera, fed from below by a dike at lower right corner. USGS photo by J. P. Lockwood.



and fed a submarine eruption 2 km off the island coast, prompting an evacuation of all island residents. Miyakejima's summit began to collapse on July 8 and to form a caldera that continued to enlarge, as phreatomagmatic and pyroclastic surge eruptions devastated the volcano's upper flanks (Fig. 10.8). The caldera collapse volume was about $600 \times 10^6 \text{ m}^3$, but only about $9 \times 10^6 \text{ m}^3$ of pyroclastic material erupted, showing clearly that drainage of magma was responsible for caldera formation (Nakada et al. 2005).

Fig. 10.8 Formation of Miyakejima caldera, Japan. a) July 9, 2000, as caldera collapse began in response to magma chamber drainage. b) June 4, 2001, following caldera formation and accompanying eruptive activity. Photos by S. Nakada and T. Kaneko.



EXPLOSIVE CALDERAS

Relatively small calderas are typically associated with the summits of composite volcanoes; larger calderas form from magmatic systems that may have originally supplied multiple volcanoes. Explosive silicic eruptions, typically Sub-Plinian or Plinian in character, accompany the origin of most. A well-studied example is the collapse of Mt Mazama, Oregon [28] and formation of Crater Lake caldera (Williams 1942). Mt Mazama is a name given to a petrologically complex group of overlapping low to intermediate shields and composite cones that began to form a high mountain in the central Cascades range about a half-million years ago (Bacon 1983). Volcanism continued as late Pleistocene glaciation modified the volcano’s shape and deposited extensive moraines on Mazama’s flanks. Between about 27,000 and 8000 years ago, rhyodacitic magma erupted north of the summit of Mt Mazama to form a series of flank cones, domes, and coulees as much as 300 m thick. This period of activity remains preserved as Llao Rock, Grouse Hill, Redcloud Cliff, and other prominences. Then, about 7700 years ago, immediately following emplacement of the Cleetwood rhyodacite flow, the climactic, caldera-forming eruption began (Bacon & Lanphere 2006). Bacon calculated that about 30 km³ of rhyodacitic magma initially erupted as tephra and ash flows from a single vent on the volcano’s north flank – before caldera collapse began – with ejecta falling as far away as Alberta, Canada. Another 20–30 km³ of magma then erupted from ring faults as Mazama’s entire summit area (an estimated 40–50 km³ of material) sank into the underlying, partly evacuated chamber, forming the present Crater Lake caldera (Fig. 10.9). Pyroclastic flows ejected during collapse rushed down preexisting canyons, burying glacial moraines, and extended as much as 70 km from their vents. While the ash flows continued to erupt, the composition of the magma changed from rhyodacite to andesite and gabbroic crystal mush, and the color of the pumice

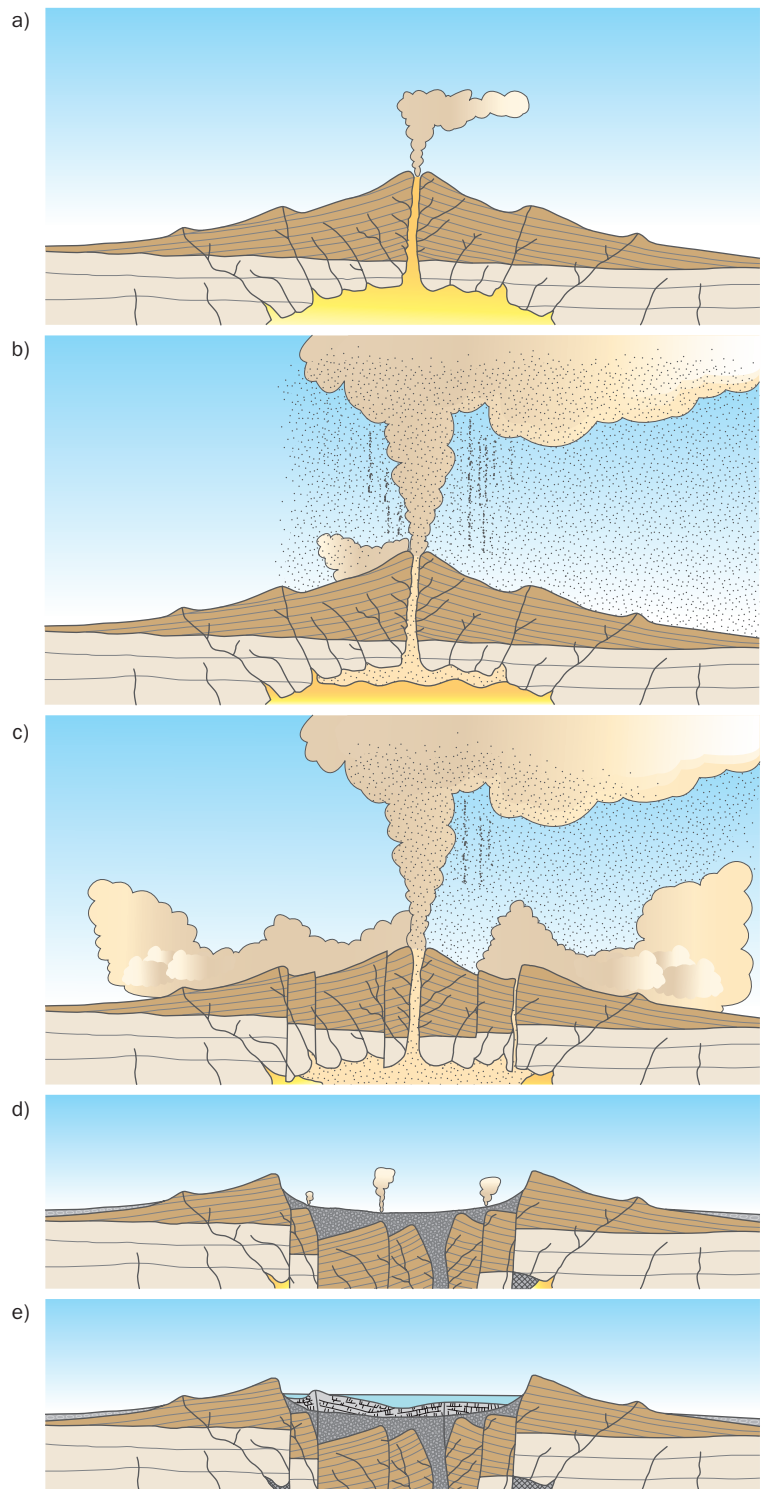


Fig. 10.9 Cross-sections showing the step-by-step collapse and partial regrowth of Mt Mazama to form Crater Lake, Oregon. Modified by C. R. Bacon after Williams, 1942).



Fig. 10.10 Eastern rim of Crater Lake caldera – view to north. Relatively thin andesitic and basaltic flows in the lower slope are capped by much thicker glassy dacitic coulées above, which erupted from the side of Mt Mazama shortly before caldera collapse. Their extrusion signified the impending destabilization of the underlying magma reservoir. The eroded volcanic neck of Mount Thielsen, known as the “Lightning Rod of the Cascades” by regional mountain climbers, is on the horizon. Thielsen was last active 100,000–250,000 years ago (Harris 2005). Photo by R. W. Hazlett.

changed from pale to dark gray. Since its formation, the caldera has partly filled with water from rain and melting snow, and also partly by material from andesitic eruptions, one of which built the cinder cone and blocky flows of Wizard Island (Fig. 10.10). Another large post-caldera cone is wholly submerged in the lake. The late-stage eruption of low-silica magma into continental calderas that formed during powerful silicic eruptions is a common occurrence, and further evidence for the role of mafic melts in initiating these eruptions.

Most composite volcanoes never experience large collapse calderas like Mt Mazama, though many will form smaller avalanche calderas and somma rings. This may be because the magma chambers underlying composite volcanoes are generally too deep and small to collapse. A critical ratio, as in the case of pit craters, relates the width of a magma chamber to the thickness of its roof. If this ratio is less than 1:1, the roof will be strong enough to support long-lasting composite volcanoes. If greater than this – that is, if the magma chamber has a very thin roof – then a major volcanic edifice may not develop at all. Composite cones such as Mt Mazama possibly represent volcanoes whose underlying magma chambers come to lie at some depth close to this critical ratio. This remains to be demonstrated geophysically, but is a hypothesis with some support from analog modeling (Acocella et al. 2001).

Very large, shallow magma chambers develop the largest calderas of all, the Cenozoic record being held by 75,000 year old Toba [97] caldera in Sumatra, which measures 40 by 105 km

(Chesner et al. 1991). Such vast calderas typically form independently of any single large volcano. Many, if not all, appear to form in association with volcanic complexes and fields (Chapter 1) Eventual caldera collapse destroys these edifice clusters, though volcanic eruptions may continue afterwards to rebuild many. The area of subsidence corresponds roughly to the maximum diameter to which the underlying magma reservoir grew as it evolved, though it may be somewhat smaller (Fig. 10.11).

Volcanic fields related to large-volume caldera collapse may be found in almost every conceivable volcanic setting. They are especially common in some continental volcanic arcs and back-arc environments. Fisher caldera [6] in the Alaskan-Aleutian volcanic arc includes a typical example of a recently formed caldera-related volcanic field. The caldera lies between two very large, independently formed composite volcanoes, Shishaldin [7] and Westdahl [5], near the terminus of the Alaska Peninsula. Measuring 12 by 18 km, Fisher is the largest of the dozen Holocene calderas within the arc. A ridge largely encloses the caldera, having gentle outer flanks and steep inner slopes. The ridge largely consists of the remains of small volcanoes that existed prior to caldera collapse. Because collapse and subsequent volcanic activity in and around the caldera disrupted stream drainages, two large lakes have formed on the caldera floor.

The oldest discernable episode of volcanism at the site of Fisher Caldera consisted of widespread basaltic lava effusions between 450,000 and 200,000 years ago, building up the tableland on which the present-day volcanic field partly lies (Stelling et al. 2005). A long erosional hiatus ensued, with activity beginning anew around 40,000 years ago. Eight small composite cones grew between then and about 9000 years ago, each no wider at the base than 2–3 kilometers. The cones formed in a ring defining the outline of the future caldera, with most of them clustered on the west side. These signified incipient fracturing in the roof of a young, shallow level magma body, probably different than the one related to the earlier outpourings of tableland lavas. Magma exploited the roof fractures during intervals of over-pressurization to build the cones. Pressure in the chamber apparently pushed the roof straight upward, partly decoupling it from the surrounding crust. Evidence of a similar **pre-caldera stage** of development also occurs at many other caldera-related volcanic fields, and at collapsed composite volcanoes such as Mt Mazama (Fig. 10.9). The pre-caldera Glass Mountain obsidian domes along the eastern side of California’s Long Valley caldera [37], source of the Bishop Tuff (Chapter 4) are an especially visible and accessible example. Along the eastern edge of Yosemite National Park not far to the north of Long Valley, the 6000 to 400 year-old Mono Domes form an arc quite likely enclosing what may become a future caldera.

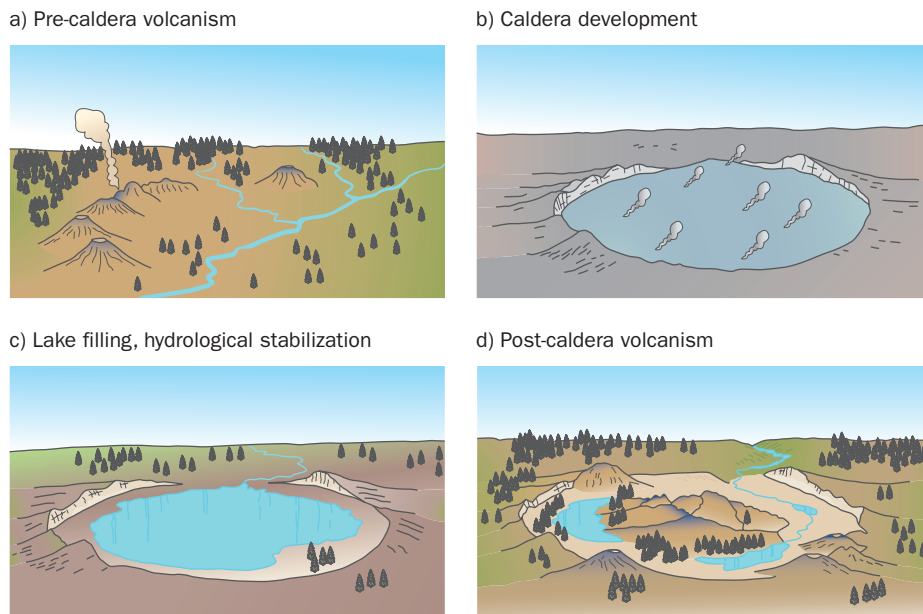


Fig. 10.11 Four common stages in the development of a large continental caldera with an associated volcanic field.

The pre-caldera phase of volcanism at Fisher Caldera ended abruptly 9100 years ago. Next events may have begun as a point-source eruption at one of the ring cones, or perhaps from a new vent centered in the midst of the pre-caldera volcanic field. In any case, the eruption was Plinian in character, in contrast to the milder activity of the pre-caldera stage. Collapse ensued concurrent with this violent eruption, and in a period of time probably not exceeding a few days, some 70 km³ of material spewed out as pumice-rich ash flows that traveled northwest to the Bering Sea – more than double the volume of the 1883 Krakatau [98] eruption (Stelling et al. 2005). The spreading pyroclastic currents were powerful enough to overtop Tugamak Ridge, more than 500 m high, 15 km from the vent (Miller & Smith 1977). Finer ash fall drifted hundreds of kilometers farther and covered thousands of square kilometers.

What must such a vast area of total devastation look like soon after a major pyroclastic eruption? One can possibly imagine by reading the account of Robert Griggs upon discovering the fresh ignimbrite plain (“Valley of Ten Thousand Smokes”) of the 1912 Katmai, Alaska [19] eruption in 1916, an area where pyroclastic flows inundated a mere 100 km² area (Griggs, 1922, pp. 191–2; Fig. 7.28):

The whole valley as far as the eye could reach was full of. . . literally tens of thousands . . . of smokes curling up from its fissured floor . . . Some were sending up columns of steam which rose a thousand feet before dissolving . . . After a careful estimate, we judged there must be a thousand whose columns exceeded 500 feet . . . It was as though all the steam engines in the world, assembled together, had popped their safety valves at once and were setting off surplus steam in concert . . . Some of the fumaroles were seen to be closely grouped in lines along common fissures; others stood apart . . . In some cases the steam issued from a large deep hole; in others there was no opening at all – the vapors simply escaped through the interstices of the soil particles . . . There was no relation between the size of the vent and its output. Some of the largest jets had very narrow throats, while from some cavernous holes there issued only faint breathes of steam. In many cases steam poured from the sides of the drainage gullies, where it did not break through the more compact surface layer of (ash) . . . The ground was hot in places where no visible exhalation was being given off, as we found to our dismay when we sat down on a bank seemingly safe enough.

The development of a caldera by no means ends the life of the source magma chamber. Influxes of new melt from below usually continue, re-pressurizing the reservoir and forcing new eruptions during the **post-caldera stage** of development. After a period of tens or several hundreds of thousands of years other Plinian eruptions associated with renewed chamber collapse may occur from different magmatic sources in the same area, creating new calderas overlapping or lying within the older one. Nested and overlapping (**compound**) calderas show that two or three caldera-forming events may originate from individual magma reservoirs during their lifetimes, as has been well-documented in the San Juan caldera cluster of Colorado (Lipman 2006) (Fig. 10.12). The La Garita caldera depicted in Figure 10.12 formed during a single initial eruption pulse about 28 million years ago, but with multiple subsidence segments forming concurrently. Eruption of the resulting Fish Canyon Tuff, comprising at least 5000 km³ of ash flows and tephra is the most voluminous pyroclastic eruption yet documented anywhere on Earth. An additional 2500 km³ of unaccountable ash and pumice may have deposited

as air fall debris downwind. Over the next 1.1 million years, an additional seven calderas formed within the giant basin of La Garita (Lipman, pers. comm. 2008).

Much younger than the San Juan volcanics, the Yellowstone Plateau [40] of Montana–Wyoming encloses a compound caldera some 60 km in diameter formed during three Plinian eruptions, 1.8, 1.2, and 0.6 million years ago (Christiansen 2001). Hydrothermal activity, including hot springs, geysers, and travertine deposition, has developed around the margins and within the caldera area, apparently heated by still restless magma. Calderas make excellent “chimneys” for the circulation of mineralizing fluids following their formation, and many of the world’s most important metallic ore deposits are associated with caldera-fill rocks (Chapter 15).

As explosive calderas form, pyroclastic flows and tephra commonly fill the developing depression simultaneously with roof collapse, and typically rush over the rims to bury vast areas. This indicates that Plinian eruption and surface collapse is a culminating, not precipitating event in caldera collapse. By the end of the eruption so much ejecta may accumulate that no crater may be present. Instead, a gently arching plateau of steaming pyroclastic debris may occupy the site of the caldera, although usually some topographic depression remains to entrap water if the climate and water table allow. It is important to note that the *visible* depth of a caldera is usually less than the *actual* amount of structural subsidence, in some cases by an order of magnitude, owing to pyroclastic infilling synchronous with bedrock collapse. Steep caldera rims commonly disintegrate simultaneously with primary foundering of caldera roofs, shedding huge volumes of country rock that can be preserved as megabreccias or mesobreccias embedded in pyroclastic deposits (Fig. 10.13).

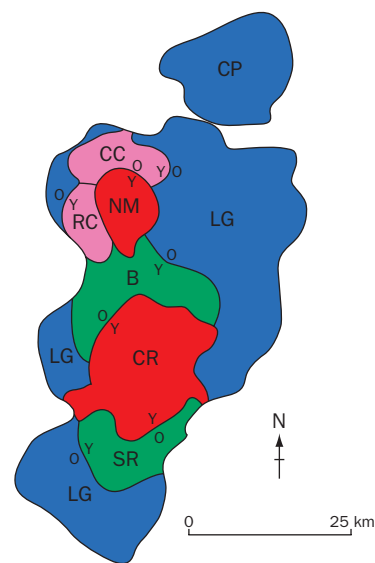


Fig. 10.12 Geometry of giant calderas in the San Juan caldera cluster, southern Rocky Mountains, Colorado. These overlapping calderas formed over a period of less than a million years in Oligocene time (Lipman and McIntosh 2008). LG, La Garita (source of the giant Fish Canyon Tuff), CP, Cochetopa Park, which preceded formation of the later smaller calderas: B, Bachelor; CC, Cebolla Creek; CR, Crede; NM, Nelson Mountain; RC, Rat Creek; SR, South River. Younger calderas in brighter colors; y/o indicates younger vs. older contact relations. Modified after Lipman (2006).



Fig. 10.13 Caldera-fill mesobreccia (“meso” means “medium-sized”). Abundant large clasts of Precambrian granite in matrix of weakly welded Sapinero Mesa Tuff (28.3 Ma), western San Juan Mountains of southwestern Colorado. This tuff, interleaved with megabreccia derived by slump failure from caldera walls, accumulated within its source caldera to a thickness of several kilometers, concurrently with subsidence. USGS photo by P. W. Lipman.

SUBCALDERA INTRUSIONS

Since the early twentieth century, structural geologists have been intrigued by a peculiar class of intrusions known as **ring complexes** (e.g., Anderson 1936). Where exposed by deep erosion, these consist of dikes which describe arcs or have circular outcrop patterns many kilometers in diameter. The dikes may be divided into two groups. **Ring dikes** extend vertically into the earth, or may flare outward with depth, away from the centers of the rings that they form at the surface. **Cone sheet** dikes taper downward toward a common point. Both kinds of intrusive structure typically coexist in the same complex, showing orientation around common centers, and both appear to be related to caldera development, the former principally with magma drainage and collapse, and the latter with build up of intrusive pressure (Fig. 4.5). The degree to which ring dikes and cone sheets develop depends in part upon magma chamber geometry (e.g., Gudmundsson et al. 1997), and in part on pre-existing crustal structure (e.g., Schirnick et al. 1999).

Bailey et al. (1924) called the Loch Ba ring dike on the Isle of Mull, Scotland, the “most perfect known example” of a ring dike. It forms a nearly continuous oval 5.8 by 8.5 km in diameter. The maximum width of the dike is about 300 meters. Stratigraphic correlation indicates that the bedrock inside the ring complex subsided about 150 m (Lewis 1968), suggesting that the ring dikes intruded along active faults concurrently with downfaulting. Their great widths in many places and their compositional diversity (Sparks 1988) suggest that they began forming a long time – perhaps many thousands of years – before any associated caldera collapse.

Research at Rabaul caldera [122] on New Britain Island in Papua New Guinea (Fig. 10.14), supports the notion of gradual ring fracture weakening and dike intrusions. Nine by 14 km wide Rabaul caldera surmounts a low volcanic shield, and is mostly flooded by the Bismarck Sea across a drowned eastern rim. Matupit Peninsula, next to the regional airport, marks a

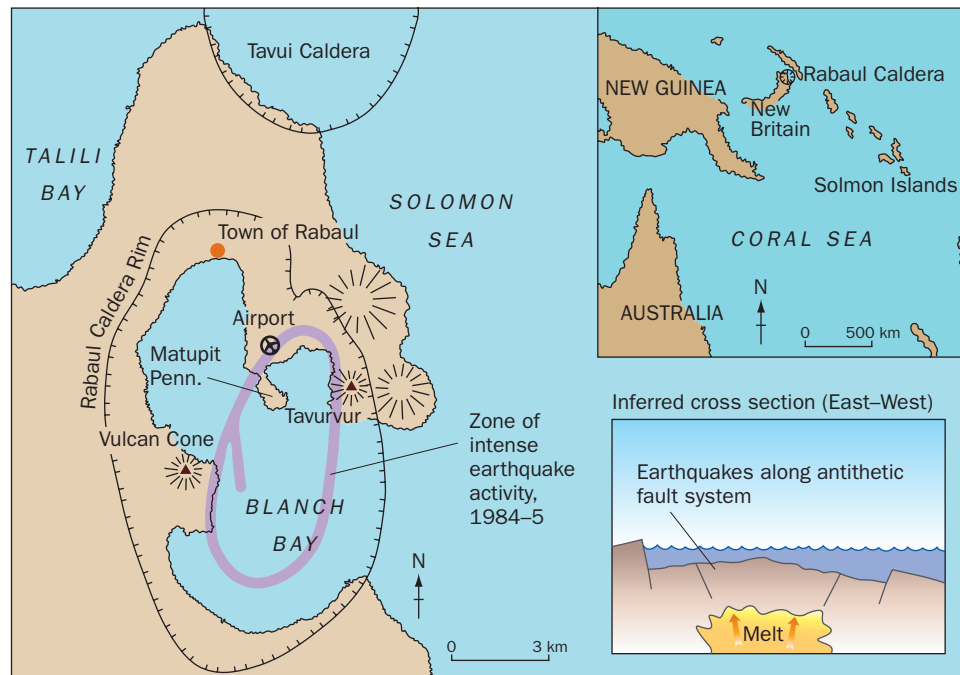


Fig. 10.14 Rabaul caldera, Papua New Guinea.

center of caldera resurgence. Like most major calderas, Rabaul is a compound feature. Its last major collapse 3500 years ago was accompanied by the ejection of 11 km^3 of pyroclastic debris – almost as much material as thrown out by the 1912 Katmai, Alaska eruption. Two polygenetic cones, Vulcan and Tavorvur lie 7 km apart along the perimeter of a zone of intense, shallow seismicity which forms an epicentral ellipse in the southern floor of the caldera. Hypocenters deeper than about 2 km lie slightly farther from the center of the ellipse than most hypocenters above that level, indicating a zone of crustal failure dipping outward with depth. This is the anticipated pattern of a developing ring fracture system, but with a bit of a twist: Many earthquakes less than about a kilometer deep define inward-dipping fault surfaces, the reverse of the pattern observed for deeper quakes. Saunders (2001) attributes these to **antithetic faulting** (Fig. 10.14) a type of normal faulting that essentially cuts off the corners of crustal blocks slipping along larger, opposite-dipping normal faults. Magma and hydrothermal fluids are exploiting this fracture system, as shown by recurrent and occasionally simultaneous eruptions of Tavorvur and Vulcan, most recently in 1994. Continuing eruptive and hydrothermal activity along the Tavorvur (east) side of the seismic zone, with quiescence on the Vulcan (west) side, indicates that deformation is taking place asymmetrically around the caldera.

Under prolonged tension in the shallow crust, ring dikes can form wide, complex networks, ranging in width from a few hundred meters to over a kilometer. They are usually coarse grained and grade from very mafic gabbros and peridotites to granite. The centers of the ring complexes are commonly occupied by coarse-grained plutonic rocks of the same composition to the ring dikes. In places, ring intrusions extend upward into volcanic rocks in eroded exposures (Macdonald 1972). In contrast, a cone sheet tends to consist of only one or a few dikes at any given point along its ring. Individual dikes may be thin, seldom exceeding 5 m in width, and many are fine-grained and basaltic.

Several hundred cone sheets, most enclosing others, lie in Devonian ring complexes on the Isle of Mull and on the nearby Ardnamurchan Peninsula in Scotland. The outermost sheets dip inward at angles of only 35 to 45° , but those closer toward the centers of the complexes dip more steeply – up to 75° . Projections of the dips of the cone sheets converge toward a focus at a depth of about 5 km beneath the middle of each complex. The structural geologist E. M. Anderson (1937) explained this pattern by suggesting the dikes formed when the upward pressure of a magma body at that focal depth lifted the roof above it at least 300 meters, producing upward-diverging fractures that were injected with melt.

Post-caldera Resurgence

The post-caldera stage of volcanism is commonly characterized by uplift of caldera floors, as the underlying magma chamber reinflates. This uplift, which may range from just a few meters to over a thousand meters, is termed **caldera resurgence**, and is typically accompanied by small eruptions that form minor cones and lava flows as illustrated by Okmok [4] (Fig. 10.15) and Aso [110] (Fig. 10.16) calderas. Resurgent activity results mostly from replenishment of gas-depleted magma reservoirs with fresh batches of magma after caldera formation. Marsh (1984) also cites increased water pressures in maturing, caldera-confined aquifers as a causal agent for minor resurgences.



Fig. 10.15 Okmok summit caldera is a classic collapse caldera on Umnak island, along a string of active volcanic islands along the Aleutian island arc, 1400 km west of Anchorage, Alaska. The caldera is almost 10 km in diameter, and formed about 2400 years ago. For much of its history the caldera was filled with a deep lake, so that most of the resurgent cones on its floor have formed in the presence of water. A month-long eruption that began on July 12, 2008 sent ash plumes as high as 12 km. USGS photo by Cyrus Reed.

Acocella et al. (2001) modeled caldera resurgence using layered sands to represent the crust and silicone to represent magma. They found that two modes of resurgence appear to be typical, depending upon the previously mentioned aspect ratio of magma chamber width to crustal roof thickness (Fig. 10.17). At an aspect ratio of around one (1 : 1), a large domical uplift in the crust takes place, surmounted by a smaller capping mound. Inward-dipping and steepening reverse faults trim the base of the main uplift, while normal faults fringe the summit rise. Crustal layering within the area of uplift is little disturbed, and may remain largely congruent with surrounding flat-lying bedding. Melt may work its way up along the outer fault system, feeding small volcanic eruptions within the so-called caldera **moat** – the area between the central uplift and caldera perimeter. A wide variety of domes, cinder cones and – if a lake is present – maars and tuff cones may develop. Virtually all of these landforms are monogenetic, though they can nearly grow atop one another in places. The Italian islands of Ischia and Pantelleria are examples of this kind of resurgence lifting the centers of shallow, largely submerged calderas above the sea.

Modeling studies show that for even shallower magma bodies, with chamber width more than double the thickness of its roof crust, resurgence takes on a different character. Central



uplift again occurs, and the area of resurgence is also fringed with inward-dipping reverse faults. But layering within the uplift tends to dip away toward the base, and the crest of the uplift may subside in time. The area of subsidence can simply be a circular, dimple-like depression, but if regional crustal extension prevails, this may modify the stress imposed by upwelling magma to create a graben whose orientation lies perpendicular to the direction of regional extension. Post-caldera volcanism not only occurs within the moat, but also in the graben or dimpled center of the uplift as well.

Outstanding examples of the latter kind of caldera resurgence include Jemez caldera, New Mexico, and Long Valley, California. Fisher Caldera (p. 327) probably also belongs within this class. Following its collapse 9100 years ago, a period of quiescence lasting several thousand years allowed a prehistoric lake in Fisher Caldera to accumulate over six meters of clays. Then, after resurgence began, two small polygenetic cones and at least seven monogenetic vent structures grew within the caldera. Resurgence drained much of the original lake water, with several square kilometers of clay beds and a maar now exposed above water. During this time, one poly-genetic cone and a solitary monogenetic edifice also grew outside, though close to, the Fisher Caldera rim. The volcanic field at Fisher Caldera will probably continue to develop over the next few thousand years.

Fig. 10.16 Aerial view of the 25 × 18 km diameter Aso caldera, Japan, looking north. The caldera was formed during four major explosive eruptions, the most recent about 90,000 years ago. The resurgent cones in the center of the caldera include Nakadake (fuming), one of the most active volcanoes in Japan. Photo by Yasuo Miyabuchi.

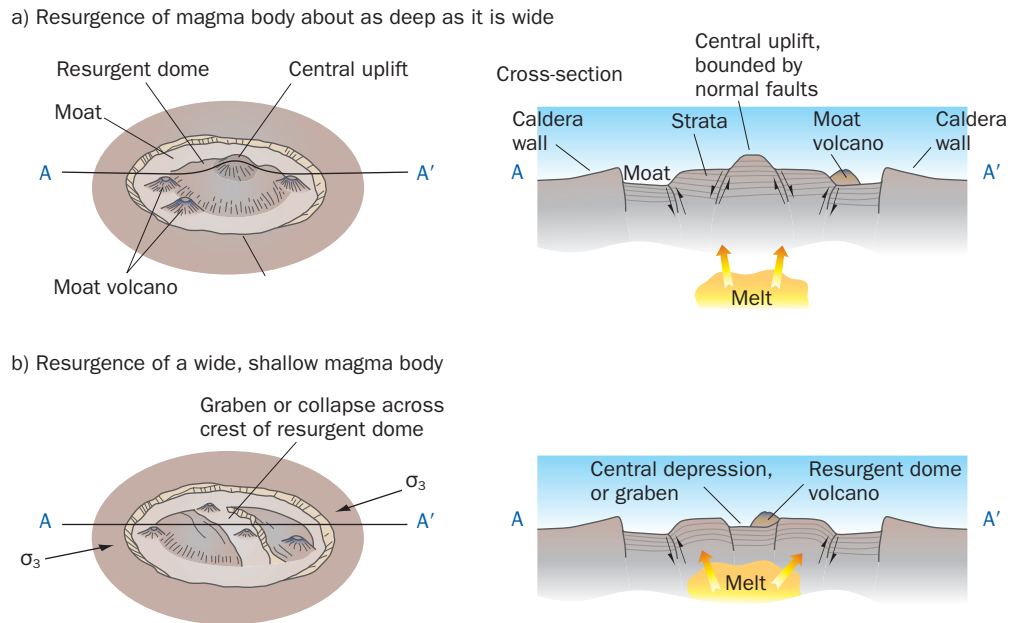


Fig. 10.17 Types of caldera resurgence. After Acocella et al. (2001).

What explains differences in these modes of resurgence? In the case of Ishcia and Pantelleria, the rising melt was able to displace the block of crust upward without causing significant internal deformation. The block was simply too thick to lose its coherency relative to the width of the rising magma body. At Jemez, Fisher, and Long Valley, this apparently was not the case. The thin roof block fractured internally during uplift, permitting the ascent of magma through the center of the caldera floor to the surface. The subsidence or collapse at the center of the uplift simply resulted from stretching of the crustal block beyond its tensile strength. Experimental work by Walter and Troll (2001) suggests that a complete gradation of caldera structures exists between these two styles of resurgence.

During resurgence, eruptions can be highly effusive, often involving lavas of the same or similar composition as the magma that erupted during caldera formation, as for example, at Yellowstone caldera. Here, over the past 640,000 years, numerous chemically evolved rhyolite flows have poured into the area of most recent collapse (Wicks et al. 2006). Post-caldera resurgent activity may also involve eruption of low-silica lavas, as at Crater Lake, described above. Within the 760,000-year old Long Valley caldera, crystal-poor rhyolite lava erupted as resurgence began 700,000–600,000 years ago, but following uplift of the central caldera floor, cooler, crystal-rich silicic flows spilled into the moat at roughly 200,000 year intervals (500,000, 300,000, and 100,000 years ago). The eruptions took place in clockwise succession around the area of resurgent uplift. Scattered basaltic eruptions may also occur around the fringe of resurgent silicic calderas, revealing the involvement of mafic magma in the reservoir system. Some erupted lavas may even contain evidence of basalt-rhyolite mingling at depth.

Caldera Formation Mechanisms

Anderson (1937) referred to the processes of caldera formation as **cauldron subsidence**, but he could not prove the relationship with surficial volcanism. That relationship is now well-established, and it has been noted that eroded mid-Tertiary calderas in the San Juan volcanic field serve as analogues for structures that must underlie major active volcanic fields in the Andes (Lipman & McIntosh 2008). Caldera collapse mechanics and geometries vary widely, however, and it can be said that no two calderas form in exactly the same way. Collapse geometries are controlled by three principal factors: 1) the size and geometry of underlying magma chambers; 2) regional stress fields and pre-existing tectonic structures; and 3) the nature and strength of rocks in the subsiding cover. Lipman (1997) described five types of caldera collapse geometries, adding that examples exist which show structural gradation between each:

- 1 **Plate** or **piston** calderas, first proposed by Anderson (1937), involve floor crust which remains intact as it drops along enclosing ring faults, in the manner described above. Single, high volume Plinian eruptions take place during this process, commonly breaking out along eruptive fissures rimming the **whole edge** of the dropping block. The La Garita caldera in the San Juan Mountains of Colorado, mentioned earlier, appears to belong to this group. The La Garita roof block dropped over 2.5 km simultaneously during eruption of the mammoth Fish Canyon Tuff.
- 2 **Piecemeal calderas** have floors broken into blocks which have subsided to different degrees. They resemble the "chaotic-collapse calderas" described by Scandone (1990), but rather than resulting from a single collapse and eruption event, piecemeal calderas are the result of multiple subsidences and eruptions, resulting in compound or nested caldera features.
- 3 **Trapdoor calderas** result from eruption and collapse along one side of a ring fracture system, with floors sloping at an angle toward the location of maximum subsidence (Steven & Lipman 1976). Fisher Caldera formed in a trapdoor manner, as did the La Pacana caldera, Chile [64], which has among the world's largest resurgence structures (Lindsay et al. 2001). Trapdoors may display pre-caldera stage vents only on the collapsed margin (Steven & Lipman 1976).
- 4 **Down-sag calderas**, originally described by Walker (1983), overlie magma bodies which are nearly too small or deep to form calderas. The land simply sinks without rupturing. Down-sag calderas are not as common as the other types discussed above.
- 5 **Funnel calderas** may be even less common. Funnel calderas are small calderas whose enclosing faults converge downward into wide pipe-like conduits. Lipman (1997) believes that many funnel calderas have been misinterpreted, owing to retreat of caldera rims by syn-eruptive landsliding to produce inward-sloping structural boundaries. Most are probably piston calderas. Nevertheless, some true funnel calderas such as Nigorikawa in Japan exist, where exploration drilling has demonstrated the subsidence of roof rocks several kilometers downward into a narrow vent. Funnel calderas are typically small depressions, only a few kilometers across. They lack the related resurgence structures and volcanic fields of larger calderas.

All of these caldera types are quickly modified by landsliding of caldera rims soon after or contemporaneously with caldera collapse, so that the **rim diameters** of calderas always exceeds

the **structural diameters** of the original collapse boundaries. No matter how they form, recent advances in high-precision radiometric dating have revealed that major, complex caldera systems can develop their entire cycles of collapse, multiple eruptions, and resurgence in 50,000–100,000 years (Lipman & McIntosh 2008). Though most silicic calderas form coincidentally with explosive eruption of large amounts of tephra and PDCs, not every such caldera shows this association (e.g., Gilbert et al. 1996; Giannetti 2001). As is well documented by petrologic and field studies, the ultimate cause of the magmatic instability that culminates in caldera formation is probably related to input of heat from ascending basaltic melts (Fig. 10.18) (Bachmann et al. 2002).

Caldera Roots – Relationships to Plutonic Rocks

The magma chambers once present beneath all calderas are doubtless never completely evacuated, and frozen remnants of these once molten bodies can be found beneath all calderas – if erosion exposes deep enough levels, and if these plutonic rocks are not made unrecognizable by subsequent magmatic activity or metamorphism. Very large granitic batholiths are widely exposed by erosion on the world's continents (Fig. 2.7), and it is probable that most of these once-molten magmatic bodies at one time connected to overlying volcanic systems and in all likelihood were associated with calderas, of which traces rarely remain. The problem in understanding the relationship between caldera formation and plutonism is mostly a matter of identifying areas where identifiable calderas have been eroded to sufficient depths to expose their roots – but not so deeply as to have erased the volcanic–plutonic connections (as in the case of the Scottish ring complexes discussed above). Such areas do exist in many parts of the world, and are especially well-exposed in the South American Andes, and in western North America, as described by Lipman (1984). Bachmann et al. (2002, pp. 1469–503) note that the great, dominantly dacitic ignimbrite sheets that also occur in these regions act as “a link between the plutonic and volcanic realms. Indeed, they resemble erupted batholiths in the sense that they have comparable volumes, occur in the same tectonic settings, and are characterized by high phenocryst contents (~40–50%)” erupted close to crystallization temperatures. Hildreth (1981) refers to these products of continental caldera eruption as the “Monotonous Intermediates,” because they lack evidence of compositional zonation, much like the vast bulk of intermediate and silicic plutons found in the same regions.

Volcano-tectonic Depressions

The term **volcano-tectonic depressions** has been used to describe very large grabens or composite grabens, best displayed in continental areas stretching along the axes of volcanic arcs (Chapter 2). Regional stresses associated with plate convergence and heating from deep-seated magma generation and emplacement lead to the development of these major landforms. They enclose multiple volcanic edifices and centers, and allow for the build up of thick sequences

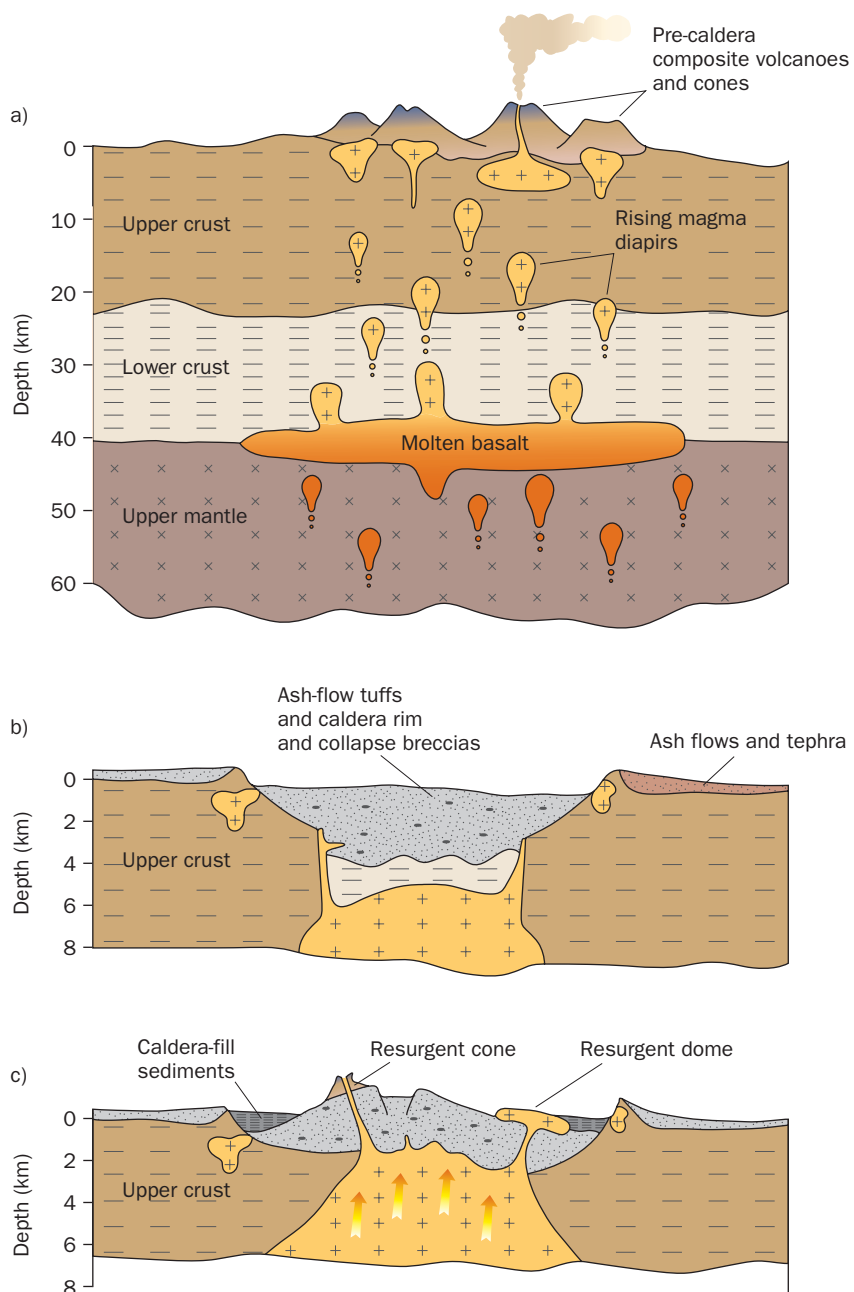


Fig. 10.18 Model for the origin of silicic ash-flow calderas. After Lipman (1984, 1988). Depths shown are schematic approximations.

a) Pre-caldera activity, showing a cross-section of continental crust and upper mantle. A lens of molten basalt from differential melting sources deeper in the mantle is accumulating at the Mohorovicic discontinuity. This hot basalt causes melting and mobilization of overlying crust and the formation of magma diapirs that move upward to supply surface volcanoes and ever-larger shallow magma chambers.

b) The explosive eruption of immense volumes of ash-flow tuffs and tephra has caused the magma chamber roof to collapse along steep marginal faults as the eruption proceeds. The steep walls rimming the caldera collapse, widening the caldera surface diameter as the eruption continues, forming extensive wallrock breccias that mix with erupting tuffs to partially fill the new caldera.

c) As new magma rising from below continues to inflate the sub-caldera magma chamber, this relatively low-density material causes uplift of the caldera floor and feeds resurgent volcanic activity.



Fig. 10.19 Map of Kagoshima volcano-tectonic depression, Kyushu Japan. Modified from Okuno et al. (1998).

of volcanic and sedimentary material in their floors. Some authors have also associated the term with single very large calderas or volcanic complexes (e.g., Toba, Yellowstone), but we believe that this is an erroneous use of terminology. Volcano-tectonic depressions are bigger features than calderas, and as mentioned above, result from broader crustal stress than imposed by any single magma reservoir – hence the presence of “tectonic” in the term. Individual volcano-tectonic depressions range up to 800 km in length and may be as much as 150 km wide. Boundary faults generally involve both extensional (normal) and strike-slip movements. Sedimentation and erosion may obscure these faults in places, but elsewhere, they form prominent scarps stretching hundreds of kilometers. Large water bodies such as lakes Managua and Nicaragua in Central America and Kagoshima Bay in Japan result from flooding of depression floors (Fig. 10.19). The development of most if not all continental volcano-tectonic depressions coincides with intensive ash flow eruptions, many of the sort described in the previous section (e.g., De Silva et al. 2006).

FURTHER READING

- Baer, R. B. and Siegel, L. J. (2000) *Windows into the Earth: The Geologic Story of Yellowstone and Grand Teton National Parks*. Oxford, Oxford University Press, 242 p.
- Bove, D. (2001) “Geochronology and geology of Late Oligocene through Miocene volcanism and mineralization in the Western San Juan mountains, Colorado.” US Geological Survey Professional Paper 1642, 30 p.
- Gottman, J. and Martí, J. (2008) *Caldera Volcanism: Analysis, Modelling, and Response*. North Holland, Elsevier, 516 p.
- Van der Pluijm, B. and Marshak, S. (2003) *Earth Structure: An Introduction to Structural Geology and Tectonics*. New York, W. W. Norton, 672 p.

Chapter 10

Questions for Thought, Study, and Discussion

- 1 What is the fundamental difference between eruptions that create nested craters and those creating multiple craters?
- 2 In what essential, physical, respects does a crater formed by volcanic explosions differ from one formed by collapse?
- 3 A volcanic crater consists of an upper rim of loose ash and blocky debris, while the bottom of the crater consists of a cylindrical shaft of vertical walls made up of interlayered pyroclastic material, breccia, and solid, vesicle-poor lava. What kinds of eruptions have taken place at this volcano, and how did this crater form?
- 4 What physical characteristics distinguish drainage from explosive calderas?
- 5 How might the "pre-caldera stage" in the history of a typical continental volcanic field differ from the "post-caldera stage," or, in fact, is it even meaningful to speak of these stages?
- 6 What geologic circumstances favor development of trapdoor calderas as opposed to piston calderas?
- 7 What evidence exists to suggest that vast areas of ignimbrite sheets along continental margins may be underlain at depth by granitic plutons?

Chapter 11

Mass-wasting Processes and Products

Although volcanoes have collapsed many times in history, it was Mount St Helens in May, 1980 that really made volcanologists aware that an entire flank of a volcano could fail.
(Peter Francis, 1993)

For all of the awesome power of their eruptions, volcanoes are inherently weak structures, their interiors broken by fractures and weakly consolidated zones of breccia, and their internal cores commonly altered into soft, putty-like clays by hydrothermal activity. Volcanic edifices are continuously stressed by intrusions and the steady influence of gravity, and inherently become less stable as they grow higher. Almost all large volcanoes have significant histories of falling apart from time to time as they grow – ongoing struggles between the eruptions that build them higher and the sometimes catastrophic gravitational mass-wasting failures that suddenly may tear away their flanks and obliterate their summits. Because the slopes of composite “grey volcanoes” are typically mantled by poorly consolidated ash and other loose material, the erosive powers of rainfall and volcanic mudflows (lahars) are also potentially catastrophic agents of volcano destruction.

Landslides, Avalanches, and Sector Collapses

The great English boxer Robert Fitzsimmons (1863–1917) popularized the phrase “the bigger they are, the harder they fall,” and what is true for boxers is also true for volcanoes! The largest landslides known on Earth, many of them submarine, are derived from the flanks of

Volcanoes: Global Perspectives, 1st edition. By John P. Lockwood and Richard W. Hazlett. Published by Blackwell Publishing Ltd.

great volcanoes, and although infrequent, such landslides are an ever-present hazard. Volcano landslides are of several varieties and sizes. They form at composite volcanoes, at dacitic dome complexes, and as vast submarine deposits on the flanks of oceanic shields.

The general term **mass wasting** refers to the sudden collapse and sliding away of mountainsides, and can take place in a variety of ways. **Block-glide landslides** tend to be at the small end of the volcano mass wasting scale, in which a layer of hard, surficial rock breaks free high up on the side of a cone and slides semi-coherently downhill across underlying weaker material. If the slide plane cuts across many layers, however, the detached mass will rotate during movement. Some of the largest mass wasting features on volcanoes are giant **rotational slides** of this nature. Rotational slides tend to move more slowly than another category of even more violent mass movement – avalanches.

An **avalanche** is a detached mass that breaks into many smaller fragments on its way down slope. They are very common on composite cones. For example, numerous small block-glide avalanches took place during the April, 1944 eruption of Vesuvius [79] triggered by the collapse of fresh lava flows deposited atop loose ejecta on the upper slopes of the volcano. Earthquake activity associated with a subsequent explosive phase of the eruption evidently triggered the failure. Each avalanche lobe, though completely fragmentary, shows a general layering of clasts and grit reflecting the stratigraphic structure of its source area upslope. In other words, little relative mixing of fragments took place during transport (Hazlett et al. 1991). None of the 1944 flows presently can be traced upslope to their points of origin.

Larger landslides may form **debris avalanches** as they spread out. Debris avalanche deposits are very large, chaotic units lacking any clear reflection of source area stratigraphy. Further downslope, debris avalanches may transform into lahars (volcanic debris flows) as they incorporate more water and mud. This happened, for instance on the flanks of Ontake volcano, Japan [11], in 1984 when an $M = 6.8$ earthquake triggered an avalanche that changed to a debris avalanche and then to a lahar as the mass traveled 13 km down the volcano's southern flank (Endo et al. 1989; Fig. 11.1a).

Far more devastating than landslides, which affect small sections of volcanoes, are the huge collapses of entire volcano flanks, termed **sector collapses**. Some collapses may be piecemeal and incremental. An example is provided by Stromboli [83] in the Tyrrhenian Sea north of Sicily. Gravitational stress on the volcano is greater on the west side of the volcano, which faces unbuttressed deeper sea. Destabilized by the near continuous intrusion of fresh magma high into the volcano and by the weight of erupted material, this side of the mountain has experienced at least seven episodes of incremental collapse over the past 100,000 years (Tibaldi 2001). The wedge-shaped **sector** prone to failure begins underwater and extends on-land up to Stromboli's summit. Romagnoli et al. (1993) estimate that $4.7\text{--}6.1\text{ km}^3$ of landslide debris accumulated at the submarine base of this sector. Glowing ejecta and occasional small flows from the classically Strombolian eruptions are channeled down the channelway of the failing sector, which is called the Sciara del Fuoco ("Ski-slope of Fire").

The Stromboli example is small compared to the terrifyingly sudden collapses of cubic kilometers of mountainsides typical of most sector collapse events, as at Mount St Helens [27] in 1980 (Chapter 8) or at Unzen [108] in 1792 (Fig. 11.1b). An even larger sector collapse debris avalanche took place about 7200 years ago at Socompa volcano [57], which towers 2050 m above the high Atacama Desert in the Andes of northern Chile (de Silva & Francis 1991).



Fig. 11.1 Mass-wasting effects. a) Landslide scar and debris flow deposits on the southeast flank of Unzen volcano, Japan. This landslide was triggered by a M=6.8 earthquake in 1984, forming debris avalanche and lahar deposits that traveled 13 km downslope – causing great property damage and loss of life. Photo provided by T. Kobayashi; © Otaki Village Office. b) Aerial photograph of Unzen volcano, Japan, showing sector collapse scar on the south flank of Mayuyama dome, source of a major sector collapse in 1792 that destroyed Shimabara and generated a major tsunami that surged across Shimabara Bay, killing almost 15,000 people on the opposite shore. Active Fugendake dome in background. Photo courtesy Japanese Ministry of Land, Infrastructure, and Transport (MLIT).



The 36 km³ of avalanche deposits spread across 600 km² of land. The largest blocks of detached edifice material are several km long and up to 450 m high! The combined sector collapse and directed blast tore a 70° wedge out of the flank of Socompa – 12 km wide at the mouth and over 400 m deep in places. Only about 20 percent of the volume of the avalanche consists of



Fig. 11.2 Prehistoric debris avalanche deposit on the southwest flank of El Misti volcano, Peru. Note the subangular shapes of boulder clasts and the variety of clast sizes. Photo by J. P. Lockwood.

material from the edifice; the rest is from underlying ignimbrite, gravel, and salt flat deposits that evidently failed under the weight of the growing volcano, essentially squirting from beneath its base all at once and causing the failure of the volcano above (van Wyk de Vries et al. 2001). Socompa had the misfortune of trying to grow atop a weak and actively deforming substrate.

Debris avalanche deposits are typically poorly sorted, with pulverized, variably fractured angular to subangular rock fragments (Fig. 11.2), many of them quite large (Fig. 11.3). Some older debris avalanche deposits have been mistaken for the ground moraines left by ancient glaciers (Ponomareva et al. 1998), or for other types of chaotic sedimentary

rocks, but their distinctive internal characteristics usually make recognition straightforward (Ui 1983). Whole slices of volcanic edifices, as blocks measuring hundreds of meters across may be present. Called **toreva blocks** (Reiche 1937), these mega-fragments are large enough to form substantial hills or ridges in debris avalanche deposits (Fig. 11.4). Breakup during transport is sustained until the moment the avalanche comes to rest, which takes place quite suddenly since many of the grains in the shifting body interlock, giving the mass a fairly high yield strength once inertial momentum subsides. Debris

Fig. 11.3 Block in the prehistoric “Ten Thousand Hills” debris avalanche deposit, Tasikmalaya, Indonesia. This subrounded fragment shows the internal fracturing typical of large blocks carried by debris avalanches – in this case about 25 km from its source within Galunggung volcano. USGS photo by J. P. Lockwood.



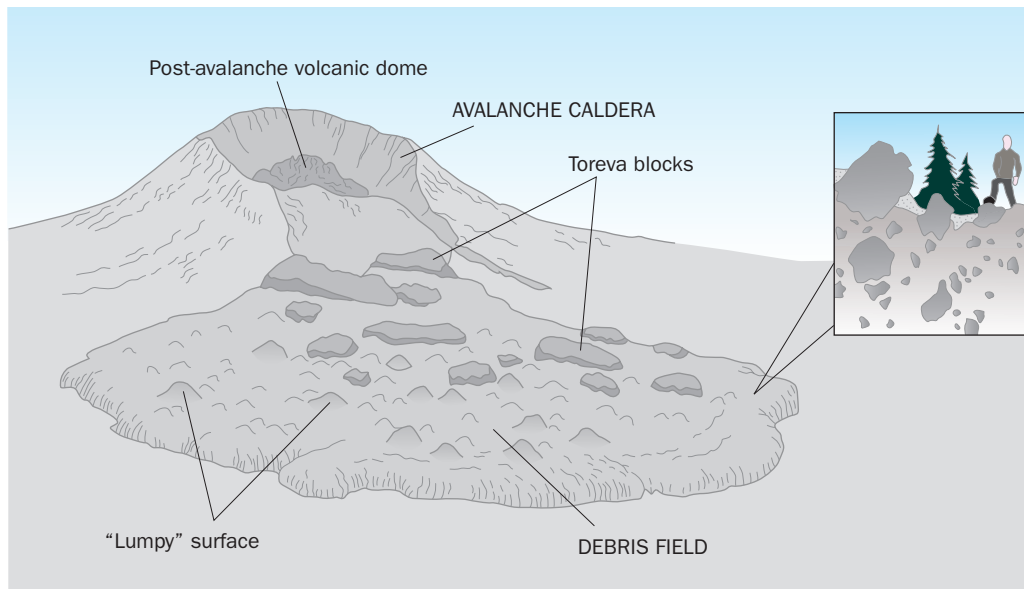


Fig. 11.4 Common volcanic debris avalanche features.



Fig. 11.5 View of the west flank of Ruapehu volcano, North Island, New Zealand. The debris avalanche deposits in the foreground formed during a sector collapse of Ruapehu’s north flank 9500 years ago. Such hummocky surfaces are characteristic of debris avalanche deposits all over the world. Photo by J. P. Lockwood.

avalanches may spread out across lowlands around volcanoes at speeds as high as 40 m/s, forming a roughly level terrain broken by numerous large, steep-sided rises and mounds. Subsequent ash eruptions may subdue these rugged landscapes, but debris avalanche landforms, even where mantled by younger deposits, are typically unmistakable for thousands of years (Fig. 11.5).

Debris fields or **debris plains** may extend for tens of kilometers from the source volcano, and be nearly as wide as they are long, depending upon pre-existing topography.

Cavities left in the mountainside by large sector collapses are called **sector collapse scars**. At volcanoes such as Mount St Helens or Galunggung [99] (Fig. 1.6), open craters kilometers wide and hundreds of meters deep mark former summits and flanks which failed catastrophically during debris avalanching, and once-symmetrical cones may be transformed into giant, horseshoe-shaped craters. Where debris avalanches enters large bodies of water major local tsunami may be generated, as at Unzen volcano [108] in 1792 (Chapter 14). The 1792 collapse of Mayuyama dome was apparently triggered by deformation within the adjoining Fugendake dome, which had erupted a month earlier. Catastrophic sector collapse events may be followed by even more devastating **directed blasts** (Chapter 8), as high-standing magma chambers are de-pressurized and explode violently.

Catastrophic sector collapses in many cases are pre-conditioned by hydrothermal weakening of volcano flanks. This is certainly the case at Nevado del Toluca [44], Mexico, where a highly-fluid Pleistocene debris avalanche resulted from collapse of a hydrothermally weakened slope, traveling down a graben and then out across a plain to a distance of 55 km from the mountainside. Blocks in the flow deposit range up to 15 m in diameter, and the deposit itself is from 15 to 40 m thick (Capra & Macias 2000). Several major prehistoric debris avalanche deposits on the flanks of volcanoes in Oregon and Washington, including Shasta [26], McLoughlin [25], Rainier [31], and Mount St Helens, involved failure of the north slopes of these volcanoes, possibly reflecting the fact that the northern flanks are subject to more sustained snow and ice accumulation, and are more vulnerable to hydrothermal weakening due to erosion and ground water infiltration. Sector collapse of composite volcanoes can also be triggered by earthquakes, by the intrusion of magma (Ellsworth & Voight 1995), and simply by the inherent gravitational instability of growing volcanoes, which become internally unstable as more and more material is added to their edifices by ongoing eruptions.

The failure of actively growing domes is also a major source of debris avalanches. The active, snow-clad volcano Shiveluch [130], Kamchatka, has produced 13 large debris avalanches in the past 4500 years, most recently in 1964. The intervals between these avalanches range from 30 to 340 years. Each collapse has been followed at once by an explosive eruption – a cycle of dome extrusions terminated by large-scale failures of dome flanks (Ponomareva et al. 1998). The 1964 debris avalanche began as a series of ordinary rock falls from an active dome that rapidly accelerated into wholesale dome and sector collapse. One and a half cubic kilometers of debris roared downslope, covering 98 km² out to a distance of 16 km from the vent (Gorshkov & Dubik 1970). The avalanche triggered a modest phreatic dome explosion followed by a powerful Plinian eruption. The volcano has been erupting almost continuously since 1980, generating several small debris avalanches, pyroclastic flows, lahars and Plinian eruptions – in what is fortunately a remote and unpopulated area.

Dormant or inactive volcanoes can also produce debris avalanches. Forested Casita volcano [49], Nicaragua, for example, with deeply eroded valleys on all flanks, hardly resembles a volcano in profile, and had not erupted since at least the sixteenth century. Hydrothermal activity is widespread across Casita's summit and upper eastern flank, however, and the combination of perched, high-standing ground water and mineral alteration has led to deformation of the edifice and steepened slopes that frequently sent small landslides into adjacent

valleys. As Hurricane Mitch blew across the region in 1998, heavy rainfall destabilized the head wall of one very large, prehistoric landslide on the south flank, causing a debris avalanche that covered 12 km² of mostly rich agricultural land, devastated two towns, and killed 2500 people (Kerle & van Wyk de Vries 2001). At least seven major Quaternary debris avalanche deposits have been identified in Guatemala (Vallance et al. 1995), and hundreds more have been identified world-wide, especially in the past two decades as their features have become better known. Sector collapses and resultant debris avalanches are usually unpredictable, and pose great risks to populations anywhere in the world where steep volcanic slopes stand above populated regions.

Lahars

Catastrophic mudflows cascading down the slopes of composite volcanoes and onto the surrounding plains have been responsible for great loss throughout the world, and have probably killed more people than any other volcano-related phenomena worldwide (Blong 1984). They are referred to by the Indonesian word **lahar**, a term restricted to mudflows originating on volcanoes. A 1988 Geological Society of American Penrose Conference broadly defined lahars as “A general term for a rapidly flowing mixture of rock debris and water (other than normal streamflow) from a volcano” (Smith & Fritz 1989). The same phenomena are termed **debris flows** where mudflows originate from other sources. For example, debris flows plague the Los Angeles metropolitan area, far from any active volcano. Most of these are triggered by intense rainfall and rapid erosion of steep, fire-burned slopes of mountains above the city. In many parts of the world, hydraulic mining, overgrazing, clear-cutting of timber and the construction of roads high on mountainsides also frequently trigger debris flows. The term lahar also includes the more dilute sediment-laden flows called **hyperconcentrated flows**, which commonly derive from more dense lahars as these mixtures of water and sediment flow downslope onto gentler terrain.

Lahars are major agents of mass-wasting, and transport large amounts of massive rock debris down volcano slopes. They commonly transition into more dilute but equally destructive floods as they extend farther from their volcano sources, depositing a variety of beds that are perhaps best studied using the tools of sedimentology rather than of volcanology. Many processes can initially trigger lahars, including eruptions, earthquakes, heavy rainfall, snow melt, or landslides (Table 11.1). By whatever processes that initiate them, large amounts of water must combine with fine-grained clay size material high on the volcano slopes in order to generate high-density fluids capable of eroding and transporting vast amounts of mud, water, and loose rock debris downslope. Lahars may contain over 65 volume percent of entrained sediment (80 percent by weight), which greatly raise their bulk densities, allowing them to pick up and transport huge boulders. The increasing erosive effects of these bulked-up mudflows have a snowball effect as they roar downslope, entraining evermore mud and debris as they increase in volume. Because of their bulk density and the ramming effect of entrained massive boulders, a vigorous lahar can sweep away bridges and obliterate massive buildings with ease (Fig. 11.6) – they are far more mechanically destructive than PDCs (Chapter 8) – which at least usually leave the burned shells of buildings in their wake.

TABLE 11.1 CAUSES OF LAHARS.

General category	Specific examples
Volcanic activity	<ul style="list-style-type: none"> • Hot ejecta or dome collapses spread onto snow or ice covered slopes • Debris avalanches or sector collapses • Failure of crater MMS • Surtseyan ejection of crater lake waters onto snow and ice covered slopes, or onto slopes laden with fresh, loose volcanic ash
Seismic activity and volcano deformation	<ul style="list-style-type: none"> • Landslides from shaking or oversteepening of deforming slopes, entering stream drainages or snow and ice covered slopes
Heavy rainfall	<ul style="list-style-type: none"> • Heavy regional rainfall onto volcanic slopes newly mantled with ash
Melting of snow and ice	<ul style="list-style-type: none"> • Thaw of snow on volcanic slopes covered with fresh mantles of ash during the winter months
Crater lake eruptions	<ul style="list-style-type: none"> • Volcanic crater lakes contain large volumes of water that can be mobilized by eruptive activity or may be released suddenly if crater rims fail
Deforestation	<ul style="list-style-type: none"> • Removal of vegetation on volcanic slopes by logging, agriculture, or fires that exposes loose soils and volcanic materials to heavy rainfalls. (Many ordinary debris flows in non-volcanic setting such as suburban Los Angeles originate this way.)

Lahars produce runoff that far exceeds the ordinary discharge capacity of streams and rivers draining a volcano's slopes. The term **stream discharge** refers to the amount of water moving per unit time past a particular point along a stream channel. For example, the average annual discharge of the Amazon River, the largest river in the world, is some $2 \times 10^6 \text{ m}^3$ of water per second, while the Mississippi River has a discharge about one tenth of this value. The discharges of lahars range up to $10^6 \text{ m}^3/\text{s}$ – comparable to the Amazon – and they move as fast as 5–20 m/s, even faster on steep slopes (Pierson 1995).

To watch an active lahar descending a volcano's flanks is an incredible experience. The fast-moving lahars that coursed down rivers below Galunggung's summit crater in 1982 flowed like serpentine rivers of viscous lava – only much faster than lava would on similar slopes. Their surfaces roiled with standing waves of mud, and their great density became evident when giant boulders boiled up out of the flow and then re-submerged, repeatedly being brought to the flow surface as the lahars moved downstream. After lahars had passed by the river channels were difficult to cross because of the deep deposits of sticky mud that they left behind.

Lahars may be part of a sequence of flowing material that begins as muddy water floods near volcano summits and bulks up as they roar downslope, incorporating more water, mud and rock debris through their increasing erosive power. But, they always begin to deposit material as they slow and spread out on the volcano flanks. As they slow down and drop out entrained sediment, they commonly transition to hyperconcentrated flows, a special type of lahar that contains much lesser amounts of entrained sediment than do denser lahars, then eventually transitions to “muddy water” at their distal ends after all coarser material has been deposited upstream (Pierson 2005). A key feature of lahar flows is the large proportion of clay-sized suspended load, which gives them the high density required to suspend and transport huge boulders. Indonesian geologists use a “tongue-test” to identify lahar deposits and to



Fig. 11.6 The ruins of Armero, Colombia, after it was destroyed by lahars on the night of November 13, 1985. The lahar from Ruiz volcano was channeled by the Lagunillas River in a narrow flow up to 35 m deep (inset) but was less than 3 m deep where it widened and flowed through the city. The lahar contained entrained boulders more than a meter in diameter, however, which acted like battering rams, destroying three-story-high concrete buildings, of which only the foundations remain. More than 23,000 people perished in Armero that night – but none of the victims would have needed to walk more than 150 m to higher ground and salvation. USGS photos by J. P. Lockwood.

distinguish them from ordinary alluvial sediments – one’s tongue will stick to samples of clay-rich lahar matrices, but not to the interstitial material of other sedimentary deposits (this doesn’t work for hyperconcentrated flow materials).

In outcrop, lahar deposits are seen to be non-bedded, poorly sorted with a high-proportion of clay- and silt-size matrix, and most lack the boulder-to-boulder clast-supported internal structure characteristic of conglomerates and landslide breccias (Fig. 11.7). Larger fragments show slight to extensive rounding due to abrasion during transport, but finer clasts (sand and gravel size) are typically angular. Because of the typical high proportion of clay in matrices, deposits are commonly well-indurated and may form stable cliffs in outcrop. Pumice is readily pulverized in debris flows, so any pumice clasts in the initial flow may be missing, although fine depositional matrices can have considerable glass components derived from pumice fragmentation. Lahar deposits commonly show variation in clast composition with distances from source areas, reflecting the incorporation of non-volcanic material eroded from streambeds beyond the volcanic edifice. The boulders that destroyed Armero, Colombia

Fig. 11.7 Prehistoric lahar deposit on the west flank of Ruapehu volcano, New Zealand. Note the mud matrix and that the boulder clasts are “matrix-supported” – they are not “clast-supported” as would be the case in fluvial conglomerates. Photo by J. P. Lockwood.



in 1985 were of gneiss and granite from basement rocks exposed kilometers from the base of Ruiz volcano; it was difficult to find any volcanic clasts in lahar deposits.

Causes of Lahars

There are many ways in which lahars can be generated, including volcano deformation, eruptive activity and dome growth, heavy rainfall, melting of snow and ice, crater lake explosions, earthquakes, and human impacts (Table 11.1). More than one of these processes commonly contribute together to form the deadly conditions required for lahar initiation.

ONGOING ERUPTIVE ACTIVITY AND DOME GROWTH

Explosive eruptive activity can cover the slopes of volcanoes with vast amounts of unconsolidated, unstable tephra that can be re-mobilized to form lahars, as happened for more than a decade after the 1991 eruption of Pinatubo, Philippines [104]. Dome growth, for example at Mount St Helens or Bezymianny [128] results in minor collapse events and related explosions that commonly generate lahars.

SEISMIC ACTIVITY AND VOLCANO DEFORMATION

As volcanoes grow through intrusive activity, they will change their shapes (deform) and can exert regional stresses on surrounding parts of volcanic complexes. Over-steepened slopes can



Fig. 11.8 Forest devastation after massive 1982 tephra fall – Galunggung volcano, Indonesia. Note the erosive rills beginning to develop – such small sources provided the material that fed massive, destructive lahars downstream. USGS photo by J. P. Lockwood.

lead to sector collapse, debris avalanches, and lahars (e.g., Unzen volcano 1792). Because volcanoes are inherently weak structures, large earthquakes can trigger landslides that quickly turn into deadly lahars, as was noted above for Ontake volcano (Fig. 11.1a). Lahars triggered by an $M = 6.4$ earthquake near Huila volcano, Colombia [53] in 1994 killed several hundred people. The fact that a major regional earthquake may be “overdue” in the Washington State/ British Columbia area poses an indirect threat to populated areas because of the large amounts of snow, ice, and hydrothermally weakened rocks that loom high on the slopes of Mt Rainier [32].

HEAVY RAINFALL

Following explosive eruptions, tephra deposited on steep slopes provide vast amounts of loose sediment for rainfall to mobilize. Water falling on wooded hillsides is ordinarily captured by vegetation and held within forest litter to slowly percolate into the ground below, evaporate, or evapotranspire through living plant tissues. A large pyroclastic eruption, however, strips a forest of leaves, even blowing down and sweeping away large trees to render the land bare (Fig. 11.8). Covers of loose pumice and ash accumulate, and may develop crusts as much as a centimeter thick. Rainfall cannot percolate through this crust, and immediately runs downslope in rivulets soon laden with abrasive ash and gravel pellets. The rivulets scour the tephra cover into **rills** – narrow, vein like channels characteristic of rapidly eroding landscapes. As they merge into streams, the potential for generating lahars greatly increases. This origin for lahars is especially common on tropical composite volcanoes, because they are seasonally subjected to heavy rainfall. For example, precipitation from Typhoon Yunya and other monsoonal rains produced devastating lahars in the hours and days following the June 15, 1991 eruption of

Mt Pinatubo [104] (Newhall & Punongbayan 1996) Heavy rainfall can also saturate loose or weakened material on slopes of inactive volcanoes, producing devastating lahars unrelated to eruptive activity, such as those derived from a debris avalanche on Casita volcano (discussed above). Rainfall can make accumulations of tephra and loose rock susceptible to mass movements in two ways: it increases the weight of the mass, and also can increase internal pore pressures – a major factor in the triggering of landslides as well as ash slumping.

Not all of the rain causing lahars is necessarily the product of regional weather systems. Eruption columns, too, can generate their own rainfall. Large amounts of steam carried to high altitudes in eruptive plumes will condense and may fall near volcanoes as muddy rain, generally in the waning stage of column development. The shock waves of volcanic blasts, some traveling at supersonic speed, can also force condensation of moisture as they propagate from a vent. Shock-generated vapor clouds formed in advance of, and were overtaken by the 1980 Mount St Helens blast surge, adding moisture to that pyroclastic density current. Lahars were among the final events of the 79 CE Vesuvius eruption that destroyed Pompeii and Herculaneum, and may have been generated by water condensed from the cooling plume above.

MELTING OF SNOW AND ICE

The sudden melting of snow and ice, caused by eruptive activity, heavy warm rains, or accelerated geothermal activity can cause small water floods that quickly transition to major lahars as they travel downslope. Though not as common as rainfall-generated lahars, these lahars are among the largest, longest, highest discharge-rate flows in the world, especially those originating from subglacial eruptions, considered further in Chapter 13. Major and Newhall (1989) documented more than 40 world-wide volcanoes that have generated lahars and floods through the melting of snow and ice by eruptive activity in historical times. They point out that most of these eruptions are at volcanoes located at latitudes higher than 35° or with summits exceeding 4000 m elevation.

While rainfall generated lahars may take place months or even years after a volcanic eruption, lahars related to melting snow and ice caps are a more immediate consequence of eruptions, typically forming less than a month following initial activity. Even small eruptions beneath glaciated volcanoes can generate devastating lahars, as was demonstrated by the devastating 1985 Ruiz eruption, which was only a moderate sized summit pyroclastic outburst.

Mt Rainier [31], WA is an example of a snow and ice-covered volcano that has produced major lahars in the past. Deeply scoured and capped by 23 major glaciers with 13.6 million m³ of ice, this deceptively beautiful mountain is potentially the most dangerous volcano in the United States (Driedger & Kennard 1986). The volumes of Rainier's lahar deposits exceed by far all other products of the volcano for the past 10,000 years. Rainier was especially active between 6500–4500 years and 2500–2000 years ago, when sector collapses generated major debris avalanches and very large associated lahars. The 5700 year old Osceola mudflow has a volume of about 8 km³, traveled over 100 km from Rainier, and blanketed about 300 km² of landscape, most of it in the now crowded Puget Sound lowlands. The lahar followed the course of the White River, scooping up stream-side granitic boulders as much as 10 m in diameter. As it burst from the Cascade Range it spread as widely as 12 km across the surrounding plain, burying at least one Native American camp site and probably some local residents as well

(Harris 2005). The 500-year old Electron mudflow is not nearly as voluminous as the Osceola mudflow, but did travel more than 50 km from Rainier down the Puyallup River, almost to the present-day city of Tacoma. It mostly consists of hydrothermally-altered material derived from the weak western flank of Mt Rainier (Crandell et al. 1979). Much has been learned about how to mitigate lahars risk through public education and engineering methods – these will be described in Chapter 14.

CRATER LAKE ERUPTIONS

Many volcanic craters on active volcanoes, floored with impermeable hydrothermal clays and other volcanic detritus, quickly fill with water and may become hot, highly acidic pools with submerged active fumaroles. Renewed intrusive activity beneath these lakes can suddenly expel large amounts of water onto upper volcanic slopes, owing to hydrovolcanic explosions, infilling of lake basins with pyroclastic material, overflow and rapid erosion of low points in their rims – or some combination of these events (Fig. 11.9). Mixing with loose ash, soil, rocks, and downed vegetation, such floods may transform quickly into lahars. Lahars from draining crater lakes typically flow out at speeds as high as 2–8 m/s (Pierson 1995). Although not as common as other forms of lahar generation, such eruptions within Kelut, Indonesia [102] and Ruapehu,

Fig. 11.9 Ice-covered summit of Mt Rainier volcano, Washington (4392 m), looking west, with the Emmons glacier just right of center. The last well-documented magmatic eruption of Mt Rainier was about 900 CE. Damaging lahars could be triggered by future eruptions or by major earthquakes in this tectonically active region. USGS photo by Rocky Crandell, courtesy of Tom Sisson.





Fig. 11.10 Scene of train wreckage a short time after the 1953 Tangiwai (Whangaehu River) Ruapehu lahar disaster, New Zealand. Photo courtesy of Archives New Zealand/ Te Rua Mahara o te Kāwanatanga/Wellington Office [Archive ref. AAVK W 3493 D-1022].

New Zealand [134] crater lakes have killed thousands of people. On Christmas Eve, 1953 an explosive eruption generated a lahar that rushed down the Whangaehu river and washed out a bridge just as train was crossing. The train plunged into the lahar and killed 151 people (Fig. 11.10).

Lahar Dynamics

Before discussing the ways in which lahars, hyperconcentrated flows and other mixtures of sediment and water move, a brief discussion of fluid behavior is in order. As discussed in Chapter 4, pure water is a Newtonian fluid, that is it has no yield strength and will continue flowing readily down slopes. In contrast, Non-Newtonian fluids exhibit yield strength, and will come to rest with measurable thicknesses. Because pure water has no strength it cannot suspend dense particles like sand or gravel – these will fall to the bottom of flowing water. When water is mixed with sufficient clay- and silt-size particles, however, its bulk density will increase,

it develops yield strength, no longer behaves as a Newtonian fluid, and may suspend large amounts of coarse sand and gravel in the moving flow. When flows contain more than around 70 to 80 percent by weight of suspended sediments, bulk densities can increase 1.6 to 2.1 times that of pure water. Particles partially support each other during transport, preventing much turbulence; flows are “cohesive” and flow much like wet concrete (Pierson et al. 1996).

Fluids at rest may be described in terms of their density, viscosity, or yield strength, but when they are moving an additional parameter, **criticality** governs behavior. Fluids, whether water or lahars, behave differently as they flow at different speeds through different types of conduits or channels. Water cascading through rapids, for example, behaves very differently than water flowing placidly down a river. In the former case the water flows chaotically and somewhat unpredictably, driven mainly by inertial forces, and is said to behave **supercritically**. Slow-moving river waters are responding only to gravitational forces in predictable ways, and are behaving **subcritically**. As mixtures of mud, rock, and water flow down the slopes of volcanoes they may exhibit both super- and sub-critical behavior in different areas depending on their speeds and channel geometries. For the open-channel conditions that concern us fluid criticality can be determined by calculating a **Froude Number (Fr)**, a dimensionless value that depends only on flow speeds (V) and channel dimensions (Eqn 11.1).

$$Fr = \frac{V}{\sqrt{g \cdot D}} \quad (11.1)$$

where V = fluid speed (m/sec); g = acceleration of gravity (m/sec/sec); D = “Hydraulic depth” of channel (cross-sectional area of channel/channel width).

When Fr is greater than 1 moving fluids will exhibit supercritical behavior, tend to flow *around* obstacles in their paths rather than wash over them, and exhibit standing waves and hydraulic jumps (sudden thickening of current with upstream back-wash) wherever flow speeds slow suddenly downslope. Such phenomena help mix particles and contribute significantly to scour and erosion of underlying beds. Many dense lahars (debris flows) will behave as supercritical fluids during much of their flowage, especially on steep slopes, though they may transition in and out of this condition as they move along.

When Fr is less than 1 moving fluids will exhibit subcritical behavior, tend to flow *over* obstacles in their paths, with little lateral displacement or hydraulic jump behavior. Subcritical lahars tend to be somewhat less erosive than supercritical flows, even though they still transport very high concentrations of particles. Most hyperconcentrated flows and water floods behave subcritically, except when their speeds are high or their channels very wide and shallow (i.e. Fr greater than 1) (Fig. 11.11). Hyperconcentrated flows contain lesser amounts of clay-size particles than do the denser, mostly supercritical lahars, are “incohesive” and cannot suspend their loads when they come to rest. Particles have more room to move about during transport, and flow tends to be turbulent rather than laminar. Gravitational forces become dominant in guiding the flow, permitting the heaviest particles to settle quickly to the bottom as in an ordinary stream.

Dense, muddy lahars may stop suddenly, with their particle loads “freezing” in place with only minor adjustments in position of individual grains as the bed settles – similar to the *en masse* deposition of block and ash flows that we described in Chapter 8. Such poorly sorted,

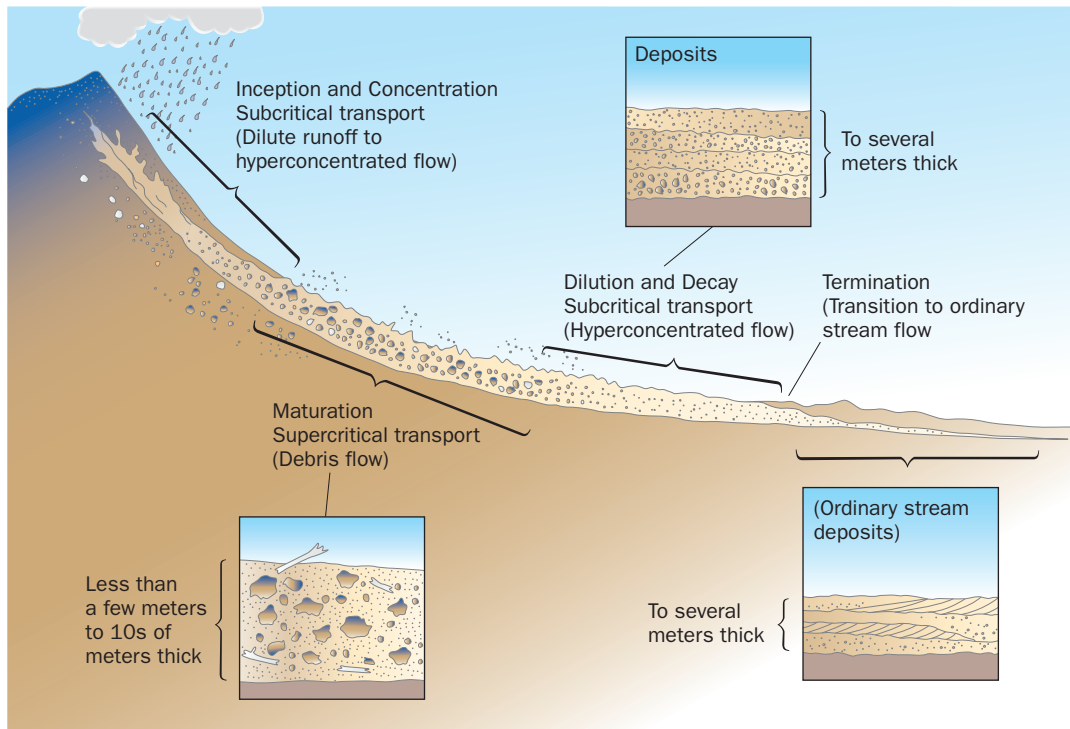
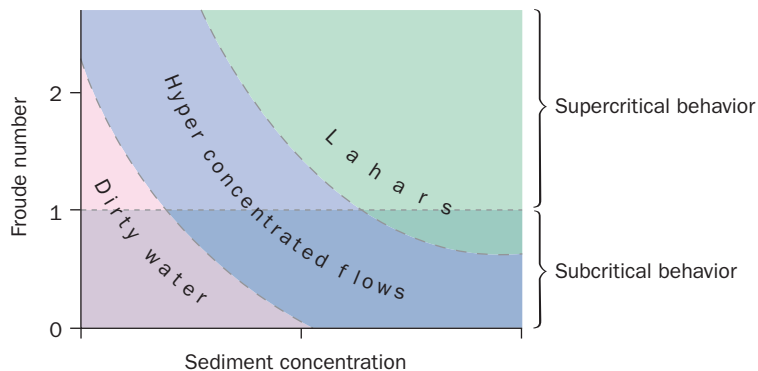


Fig. 11.11 The relationship of lahars, hyperconcentrated flows, and water floods as a function of sediment concentration and criticality.

clay-rich lahars commonly form well-consolidated, cliff-forming deposits around the eroded flanks of many volcanoes. Hyperconcentrated flow lahars are less clay-rich, however, and their moderately-sorted deposits are not cliff-forming.

Lahar Destructiveness

Fig. 11.12 Evolution of lahar facies during flow.



Most lahars are initiated as dilute, subcritical flows high on volcano slopes, but quickly increase their volumes as they incorporate sediment along travel paths (Fig. 11.12). Lahars cannot deposit sediment on steeper slopes, where they are highly erosive to stream bottoms and banks – streamlining their own channels. These supercritical flows are capable of transporting very large boulders and logs, which are especially effective tools for shattering bridges, walls, and other obstacles in their way (Fig. 11.13). The lahars that flowed into Armero on November 13, 1985 carried boulders up to a meter in diameter into the city, which acted like inertial battering rams, destroying major concrete buildings (Fig. 11.6). Geology student Jose Luis Restrepo was in Armero that night on a university fieldtrip. Jose and the other students knew Ruiz volcano was erupting, because ash had started falling

in the afternoon, but they had no idea that lahars had already begun flowing down the flanks of the volcano toward them. Here are translated excerpts from what he told me (JPL) two weeks afterwards:

About 11:30 all the lights went out as Armero's generating plant was inundated and the flow arrived a few minutes later. It was only about 2 meters deep as it entered town, rushing down streets, and the only lights were from the headlights of cars being tumbled about by the flow. We ran to our hotel and three of us climbed to the third floor terrace, thinking this would be a safe place since the walls were of concrete.

Lower-standing buildings around us were swept away as the flood kept rising. I felt great shocks as rocks slammed into the hotel and suddenly it all crashed down. The screams of people were terrible and I was sure I was going to die a horrible death, but with four companions we climbed into a concrete water cistern that had come from the hotel roof. We were swept along with debris and screaming people, as burning gas tanks lit up the terrible scene. We saw a high wave of mud coming at us, but somehow our tank stayed afloat. Some mud was warm – but most was cold. We crashed against a standing tree. There were many people around us stuck in the mud, but we were unable to help them. We dragged one man into our tank, but his legs had been amputated and he was in great pain. When morning came, we saw that we were only 50 m from the edge of the mud, but when I saw the terrible devastation behind us I lost all control and cried – Armero was gone – except for our little island of trees. About 300 people were able to struggle through the mud to a small hill – the Armero cemetery – where we waited amongst the tombstones for rescue.

More than 23,000 residents of Armero perished that night, and of the 32 students in Jose's group, only 19 survived.

The destructive potential of lahars changes dramatically after their transition to subcritical flow. Subcritical, hyperconcentrated flows are not harmless, but they don't knock buildings over – they bury them (Fig. 11.14). Like any large, fast-moving flood, they are effective at eroding river banks, undermining foundations and depositing large amounts of sand-size sediments in a short amount of time. Repeated hyperconcentrated flows following the 1991 eruption of Pinatubo blanketed perhaps 300,000 hectares of rich Luzon farmland with deposits up to 25 m thick, and destroyed the homes of more than 50,000 people. Efforts to dam or divert these hyperconcentrated, sediment rich flows have cost hundreds of millions of dollars, but have been largely ineffective.

As we have seen, volcanic edifices are susceptible to gravitational failure by massive landslides and by rapid erosion; they are relatively ephemeral geomorphic features and few last as significant topographic forms for more than a few million years after they have ceased



Fig. 11.13 Gigantic lahar boulder near Mulaló, Cotopaxi volcano, Ecuador. This boulder, which weighs at least 3000 tonnes, was carried about 20 km down the west flank of Cotopaxi by a massive, devastating lahar in 1877. The boulder came to rest when the lahar was no longer able to transport it because of diminishing velocity and thickness. The bus is about 10 m long. Photo by J. P. Lockwood.

Fig. 11.14 Burial of homes in 1982 by hyperconcentrated flow deposits alongside Cibanjara River, 8 km below lahar sources, Galunggung volcano, Indonesia. Roof tiles have been salvaged from the abandoned homes. USGS photo by J. P. Lockwood.



activity. Their histories typically involve long battles between the eruptive processes that build them higher and the gravitational processes that tear them down. For most extinct volcanoes their one-time glory is best preserved in surrounding sedimentary deposits – deposits that commonly far exceed the original volumes of the largest volcanic edifices that produced them.

FURTHER READING

- Committee on Natural Disasters, Division of Natural Hazards, National Research Council (1991) *The Eruption of Nevado del Ruiz Volcano, Columbia, South America, November 13, 1985, Natural Disaster Studies: A Series*. National Academies Press, 128 p.
- Jakob, M. and Hungr, O. (2005) *Debris-Flow Hazards and Related Phenomena*. New York, Springer Praxis Publishing, 739 p.
- McGuire, W. J., Jones, A. P. and Neuberg, J. (1996) “Volcano instability on the Earth and other planets.” *Geological Society of London Special Paper* 110, 388 p.
- Pierson, T. C., Janda, R. J., Umbal, J. V., et al. (1992) “Immediate and long-term hazards from lahars and excess sedimentation in rivers draining Mt Pinatubo, Philippines.” *US Geological Survey Water Resource Investigations Report* 92-4039, pp. 1–35.

Chapter 11

Questions for Thought, Study, and Discussion

- 1 Volcanoes do not always experience sector failures because of inherent weaknesses within their edifices. In some cases other geologic factors can contribute to that failure. Explain.
- 2 How would you distinguish a debris avalanche deposit from that of a typical lahar?
- 3 How and why are many lahar deposits also related to debris avalanches?
- 4 What gives a lahar energy and increases its capacity to erode as it travels?
- 5 What happens where a lahar starts, and what happens where a lahar stops?
- 6 Why are lahars just as destructive (if not more so) than most PDCs?
- 7 On what bases would you highlight areas of extreme lahar risk if you were making a map of potential danger around a grey volcano to advise local authorities? Also, what criteria would you use to designate evacuation routes for a local population?

Chapter 12

Volcanoes Unseen and Far Away

Представляется весьма вероятным, что вулканизм мог играть определяющую роль в формировании внешних оболочек многих космических тел.
(Yevgenii Markhinin, 1985)

[It appears highly likely that volcanism might play a defining role in the formation of the outer shells of many cosmic bodies.]

Half a century ago, the science of volcanology was for the most part focused only on subaerial volcanoes of the planet Earth. Although submarine eruptions had been documented as the causative phenomena responsible for shallow water explosive volcanism, volcanologists had no inkling that submarine volcanism was the *dominant* manifestation of volcanic activity on Earth, nor that active volcanism was taking place anywhere else in our solar system. There were theories that volcanic activity had occurred on the Moon and Mars, but the extent or complexity of this volcanism was unimagined. **Subglacial** volcanism was widely recognized, principally from observations in Iceland, but much fieldwork was needed to document its extent and to understand the processes involved, and a new term **glaciovolcanism** has been coined to describe these phenomena.

All of this “unseen” volcanism gradually came into view with the advent of new technologies, including specialized cameras, deep sea manned submersibles, sonar, high resolution telescopes, satellites and related instrumentation. We are still exploring new volcanic terrains with these tools and continue to gain fresh insights about volcanism in environments that are physically hostile to humans. We have even been fortunate enough to glimpse actual eruptions

Volcanoes: Global Perspectives, 1st edition. By John P. Lockwood and Richard W. Hazlett. Published by Blackwell Publishing Ltd.

taking place on the sea floor and other worlds. Far from being restricted to Earth's dry land surface and coastal waters, we now appreciate that volcanoes are truly a cosmic phenomenon. These "unseen volcanoes" are discussed in this chapter in two sections – the first will document the previously unseen volcanoes of Earth, and the second will explore the volcanism that has accompanied formation of the inner rocky planets and the current cryptovolcanic activity that is ongoing in the far reaches of the solar system.

Submarine and Subglacial Volcanoes – The Meeting of Fire, Water, and Ice

SUBMARINE ERUPTIONS

Although submarine volcanism, which has been estimated to account for over 80 percent of all volcanic activity on Earth (Crisp 1984) poses no threats to human life, this underappreciated activity is a manifestation of the principal dynamic forces acting on the Earth's crust, and an understanding of these phenomena is critical to an understanding of many terrestrial mineral deposits (Chapter 15) and perhaps to an understanding of life itself (Chapter 13). Although this section refers to "submarine" eruptions, the same physical processes apply to volcanoes that erupt beneath any water cover, including the relatively uncommon interaction of "fire and water" on the floors of freshwater lakes. We will first discuss *where* submarine volcanism occurs (and is probably occurring somewhere at this moment as you read these words, deep beneath the ocean's surface) and then describe the details of *how* these unseen volcanoes erupt.

TECTONIC ENVIRONMENTS

Mid-Ocean Ridge

Oceanographers discovered the Mid-Ocean Ridge (MOR) in a piecemeal fashion over a century, and for many decades researchers believed that there were multiple discrete ridges on the sea-floor (hence the historical pluralization "Mid-Ocean Ridges"), when in fact the MOR is a single, albeit sinuous planetary feature (Chapter 2). The misnomer goes even deeper than that, however, since the MOR only really bisects one ocean basin, the Mid-Atlantic – though small spurs also symmetrically divide the Gulf of California, Red Sea, and other very young seaways. The MOR is the principal locus where oceanic plates are pulled apart by deep convective forces, new crust is born, and young volcanic rocks are directly exposed on the oceans' floors. A great deal of oceanographic work has been carried out on the MOR in the past few decades as petrologists have sampled and characterized the uniquely primitive volcanic rocks erupted at many localities, naming them MORBs – Mid-Ocean Ridge Basalts (Blatt et al. 2006) (Chapter 3). We now know that MORBs cover over half of Earth's surface, though in most places they are veneered by a thin layer of deep marine muds.

Mantle upwelling and heating elevates the MOR an average of about 500 m relative to the surrounding deep sea floor, with gently inclined flanks stretching as much as 25–50 km to either side of the crest (Fig. 12.1). Elongate magma chambers as shallow as 1–4 km and

10 km wide underlie the crest, fed from mantle sources as deep as 75 km (Kent et al. 1990; Boudier et al. 2000; Mencke et al. 2002; Singh et al. 2006). The gross morphology of the MOR is greatly influenced by spreading rates – how fast new crust is formed along its axis and thus how fast the flanks are spreading away from the axial rift zone (Fig. 12.2). The MOR can be regarded virtually as a single “mega-volcano” – the largest on Earth, because its crest almost everywhere overlies shallow pockets of magma fed by a single source – Earth’s upper mantle, and eruptions can occur practically anywhere along its length.

Gentle effusive activity from fissures is dominant in the MOR axial rift. Highly fluid lava pours out as pāhoehoe, commonly forming flow fields that look remarkably like their counterparts on land. Close to eruptive fissures where initial eruption rates are high, broad sheet lava fields form. Lava channels and pyroclasts similar to terrestrial analogs occur in many places, and collapse features associated with fissure drainback or other types of drainage also rupture flow surfaces (Fornari et al. 1980; Fornari et al. 2004; Garry et al. 2006). Unlike terrestrial flows, however, the interiors of deep submarine pāhoehoe flows contain numerous shallow, complex voids resulting from entrapment and boiling of seawater under thin lava crusts. Later collapse of roof crusts reveals that the pockets beneath are supported by pillars which probably grow as large amounts of heated seawater continue to flush through the flow interiors as the lava advances and inflates (Chadwick 2003; Perfit et al. 2003; Fig. 12.3).

At the margins of advancing lava flows where output rates are slower, sack-like piles of basaltic **pillow lava** are a characteristic feature (Fig. 12.3). Pillow lavas were first recognized in exposures on dry land of ancient, uplifted submarine basalts. They have been observed forming by divers in shallow water off the island of Hawai‘i, who report that their formation is a remarkably gentle process: Cylindrical lava

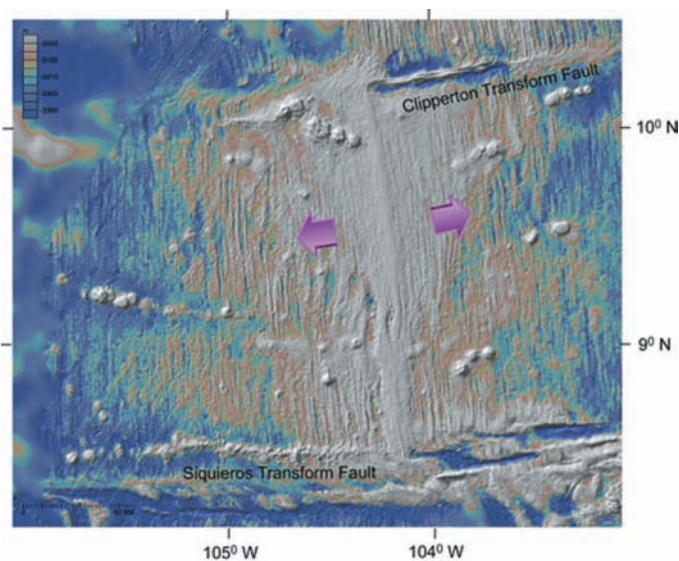


Fig. 12.1 Detailed bathymetry of a well studied Mid-Ocean Ridge spreading section, the East Pacific Rise near 10°N, off the coast of Central America. Note the ridge offsets along transform faults and the large number of “off-axis” submarine volcanoes, which indicate the upwelling of magma on the flanks as well as the center of the ridge crest. The figure is 275 km across; scale is in the lower left corner. Compiled by Dan Fornari from the Marine Geoscience Data System database (<http://www.marine-geo.org/>) using GeoMapApp software.

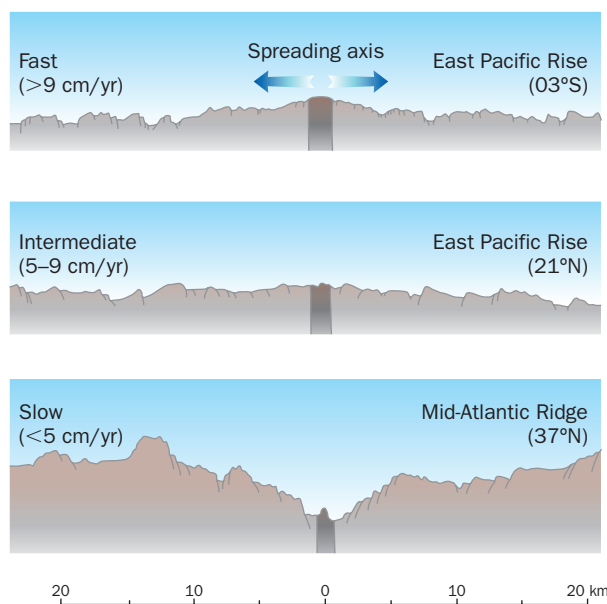


Fig. 12.2 Profiles across Mid-Ocean Ridge spreading centers, showing characteristic morphologies associated with differing spreading rates. Zones of most active volcanism shown by dotted areas. After Macdonald (1982).



Fig. 12.3 Typical pillow lavas, as seen through the porthole of a submersible (US Navy DSV *Sea Cliff*) diving in volcanic terrain off the west coast of Hawai'i Island. These pillows, at about 800 m depth are lightly dusted with calcareous planktonic ooze, showing that they are prehistoric, but probably no more than 2–300 years old. USGS photo by J. P. Lockwood.

toes swell into pillows that can break free and tumble down slope into deeper water, accumulating in a bed of glassy lava fragments with other sediments. Some pillows may expand to the point of rupturing, feeding the growth of new offshoot pillows as they continue to grow (Yamagishi 1985). Pillows commonly trap steam and exolving gases in their cores, and at times highly vesicular, steam-filled pillows forming in shallow water may break off their source feeders and rise to the surface (Fig. 12.4). They do not float for long, however, as they become waterlogged when the interior steam condenses, and sink back into the depths. Such “floating pillows” have been observed forming in the Azores as well as Hawai'i, and may be a more common phenomenon than previously appreciated.

The insulating character of quenched flow crusts coupled with the effect of high H_2O heat capacity and the efficient circulation of cold, deep seawater is demonstrated by a recently documented eruption along a portion of the East Pacific Rise near $9^{\circ} 50' N$ latitude, south of Acapulco, Mexico (Soule et al. 2007). This area is one of the most intensely studied mid-ocean ridge systems in the world, and a

dozen ocean bottom seismometers (OBSs) had been deployed along the ridge axis in 2005 at 2500 m depth to monitor seismic activity along this fast-spreading ridge segment. The plan was to recover these OBS instruments later for data retrieval, but when a surface crew arrived in 2006 they were only able to recover four instruments – the others had apparently been engulfed by fresh lava! Five of the OBS units were never found and were apparently buried by lava, but three were still able to transmit acoustic signals – but did not rise to the surface on command – they were apparently “stuck” in lava. OBS No. 212, however, was eventually found almost 100 m away from its point of initial deployment – where it had ridden atop a lava flow after being partially engulfed. The OBS had survived its wild ride in good condition, but was thoroughly embedded, and the lava needed to be carefully broken away by the arms of the remotely-operated vehicle Jason-2. A delicate plastic flag was still attached to the seismometer casing less than half a meter above the flow top, showing that water temperatures above the moving lava had never been very hot (Fig 12.5). A similar wild ride was taken in 1998 by another ocean floor monitoring instrument on Axial seamount, an active volcano on the Juan de Fuca ridge west of Oregon. This instrument contained a pressure sensor, which showed that it was uplifted more than 3 m as new lava flowed beneath it and inflated, but the temperature of surrounding seawater only rose $2^{\circ}C$ (W. Chadwick, 2008, pers. comm.).

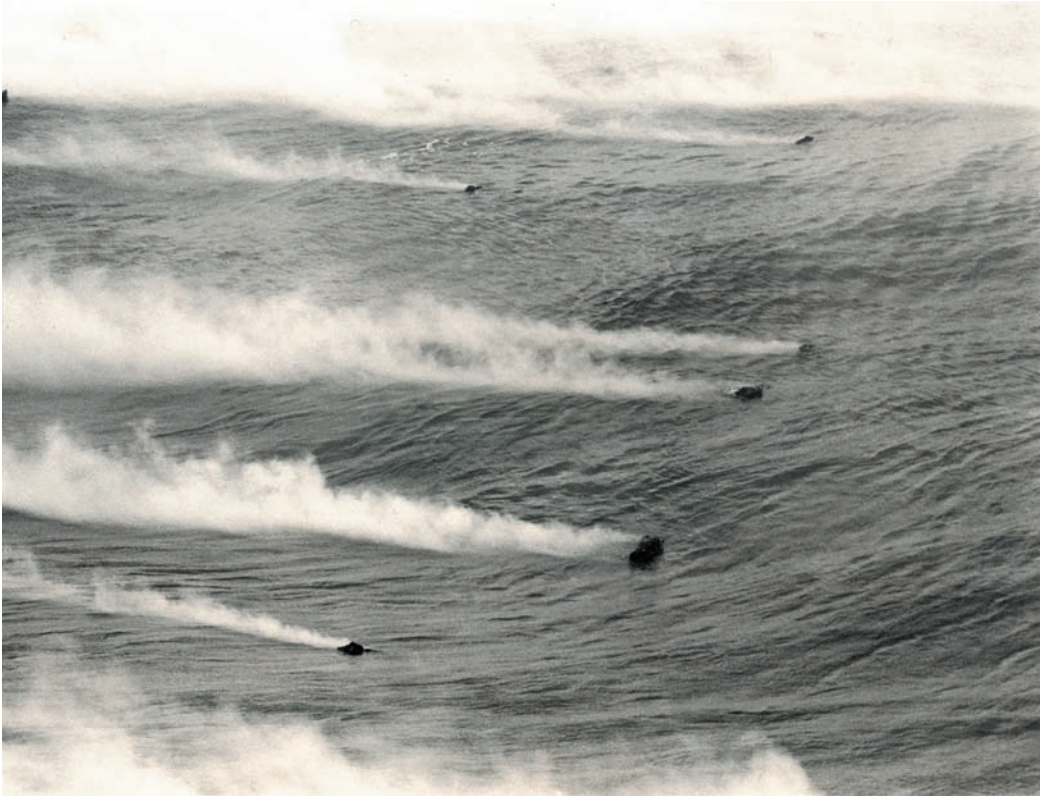


Fig. 12.4 Discrete pillows floating above a site where pāhoehoe lava was flowing into the ocean on the south flank of Kīlauea volcano, Hawai‘i in 1989. The pillows were derived from “buds” on active submarine pillow lavas flowing 25 m below the surface. USGS photo by J. D. Griggs.

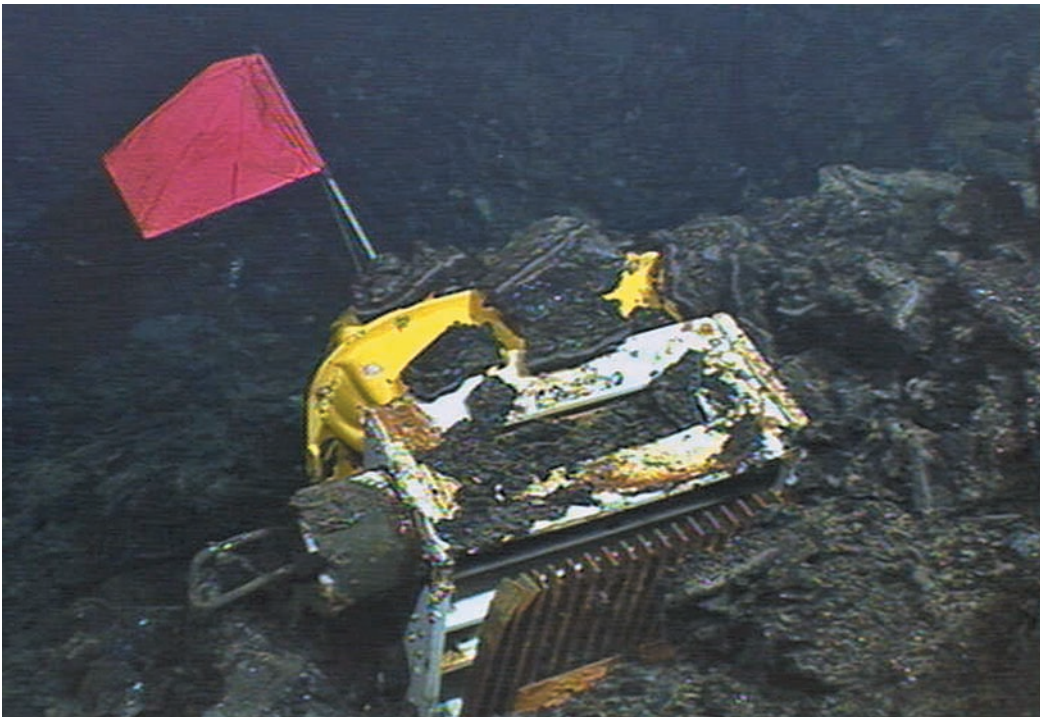


Fig. 12.5 An ocean-bottom seismometer (OBS) trapped in a slabby pāhoehoe lava flow during the 2005–6 East Pacific Rise eruption at around 2540 m depth. The OBS was found to be partly enveloped by lava and had been transported almost 100 m by the flow. The acoustic command components were still functional, which facilitated location and recovery of the OBS. Note the undamaged plastic flag. Jason2 Remotely Operated Vehicle (ROV) photo courtesy of the Woods Hole Oceanographic Institution, National Deep Submergence Facility – ROV Group, the National Science Foundation – Ridge 2000 Program, and the scientific party of cruise AT15-17, E. Klein, Chief Scientist.

As scientists became aware of the critical role of the MOR system in the origin of the oceanic crust, they first assumed that most of the world's numerous undersea volcanic peaks (**seamounts**) developed there too, only to be carried away from their sites of origin by sea-floor spreading. Subsequent detailed study of these volcanoes show that with few exceptions volcanic seamounts originate where discrete magma sources erupt on the flanks of the MOR, and not along its crest. Large volcanic edifices stand little chance of growing in an axial rift valley because of diffuse eruption loci, rifting and faulting (Chapter 2). Most form within 100 km of MOR axes, and with the exception of hot-spot volcanoes, the occurrence of new volcanism on oceanic crust diminishes as the lithosphere grows thicker and older with distance from the Ridge (Batiza 1981; Hillier 2007).

These off-ridge volcanoes come in many shapes and sizes – from small isolated monogenic volcanoes a hundred meters or less in height to true mountains tens of kilometers wide at their bases and 3–4 km high (Gardener et al. 1984). Smaller seamounts typically have conical shapes, but larger ones have more complex forms, with summits either flattened or dimpled with submarine calderas. The lava flows they produce can be far traveling. Individual flows more than 60 km long have been observed off Hawai'i and near the base of seamounts associated with the East Pacific Rise (Fornari et al. 1985; Holcomb et al. 1988).

Harry Hess (Chapter 2) discovered a number of flat-topped seamounts in the north-central Pacific during wartime bathymetric surveys, and as you may recall, named these features **guyots** (Hess 1946). Hess correctly surmised that the flat summits of many guyots represent volcano-fringing coral reefs – atolls – drowned by tectonic submergence. The coral polyps that flourish in warm, sunlit water could not maintain upward reef construction fast enough to compensate for sinking of their volcanic foundations. For a time this persuasive argument convinced oceanographers that all flat-topped seamounts formed in this way – biogenically as well as geologically, but the distribution and variable depths of their tops, and the fact that some guyots lack coral caps, demonstrated that this can't be the whole story. As some submarine volcanoes grow large, magma infiltrating their interiors can more easily erupt from the flanks than from the summit, building up extensive flanks so that the summit acquires a more flattened profile (Fornari et al. 1985). Volcanoes may also develop flat tops by growth from circumferential vent systems, as is shown by subaerial volcanoes of the Galapagos Islands (Simkin 1972). Like oceanic volcanoes that project above the surface of the sea, large submarine volcanoes are also inherently unstable; their summits can collapse and major flank failures may blanket surrounding ocean floors with extensive debris flows.

Oceanic plateaus and hot spot tracks

The most voluminous volcanic eruptions ever to occur on Earth formed the extensive basaltic sheets referred to as Large Igneous Provinces (LIPs) (Mahoney & Coffin 1997). Although these include the great subaerial flood basalt plateaus (Chapter 9), we now know that the world's largest LIPs formed on ocean floor (Taylor 2006). Oceanographic research and deep-sea drilling programs over the past few decades have revealed the enormous size of these high-standing submarine basalt plateaus, which may rise more than a kilometer above the surrounding seafloors. The Ontong Java Plateau, which underlies the Solomon Islands covers an area of 2 million km², and may have a volume as high as 60 million km³, the most

voluminous LIP on Earth (Fitton & Godard 2004). Radiometric dating shows that the massive LIPs in the western Pacific formed in two episodes during Late Cretaceous time. The impact of these voluminous eruptions may have led to major chemical changes in ocean waters and to mass extinctions of marine fauna (Kerr 1998; Chapter 13).

Many submarine seamount volcanoes are aligned in linear chains that may extend thousands of kilometers across the seafloor, and commonly show no indication that they ever formed subaerial islands. Some of these volcanic chains show age progressions that suggest they formed above intra-plate hot-spots, (Chapter 2) but others trend at angles to known plate motions and may have formed above linear zones of weakness or in the oceanic crust, or may indicate deep-seated linear melting anomalies. Radiometric dating has shown that most of the intraplate submarine volcano chains in the Pacific are of Cretaceous age, and are chronologically related to the widespread magmatic processes responsible for the formation of the above-mentioned oceanic plateaus – spasms of tremendous heat release from Earth's interior (Rea & Vallier 1983).

Shallow water explosive submarine eruptions

While effusive eruptions predominate in the deep sea, explosive eruptions are also capable of taking place there. In fact, detailed seafloor exploration by manned submersibles and remotely-operated vehicles (ROVs) have shown that explosive volcanism can occur at *any* water depths, although such eruptions tend to be larger and more violent in shallower water.

Eruptive vents that open at water depths of less than a few hundred meters, where hydrostatic confining pressures are low, readily trigger Surtseyan eruptions. Over a period of days or weeks these may lead to emergence of new volcanic islands (Chapter 7). But most new islands do not survive the erosive power of tides and waves for long. Three factors are necessary for long-term survival: First, the eruption rate has to be fast enough to build a natural dam around the vent, keeping out the surrounding water so that effusive activity may ensue. Then, after effusive activity has begun, lava flows or welded agglutinate must mantle enough of the loose fragmental base of the island to defend it against erosion. Finally, if the island is to grow large enough to become a substantial platform for life, follow up eruptions must take place with a short enough repose interval to increase overall land area or simply to replace land that eroded away in the time since the last volcanic activity.

The historic record contains numerous instances of “wannabe” volcanic islands that never made it. A good example took place in 1831, in the midst of a Mediterranean conflict between Great Britain, France and the Italian Kingdoms. In July of that year a strange event happened off the southwest coast of Sicily, in waters claimed by all three powers. The surface of the sea boiled, ash and rocks were blasted upwards, dead fish were noted, and the smell of sulphur was strong in Sicily and North Africa. By August a small island had risen above the sea and a British crew landed, claiming the new land for England. They named it Graham Island. The Sicilians, wanting this fresh speck of land for themselves, sent a crew there, pulled down the Union Jack, claimed it for Sicily and renamed it Ferdinanda in honor of their Neapolitan king. Graham Island/Ferdinanda grew to 65 m above sea level and had an area of 4 km² at one point – potentially sufficient for a naval outpost (Fig. 12.6). The French also attempted to claim the

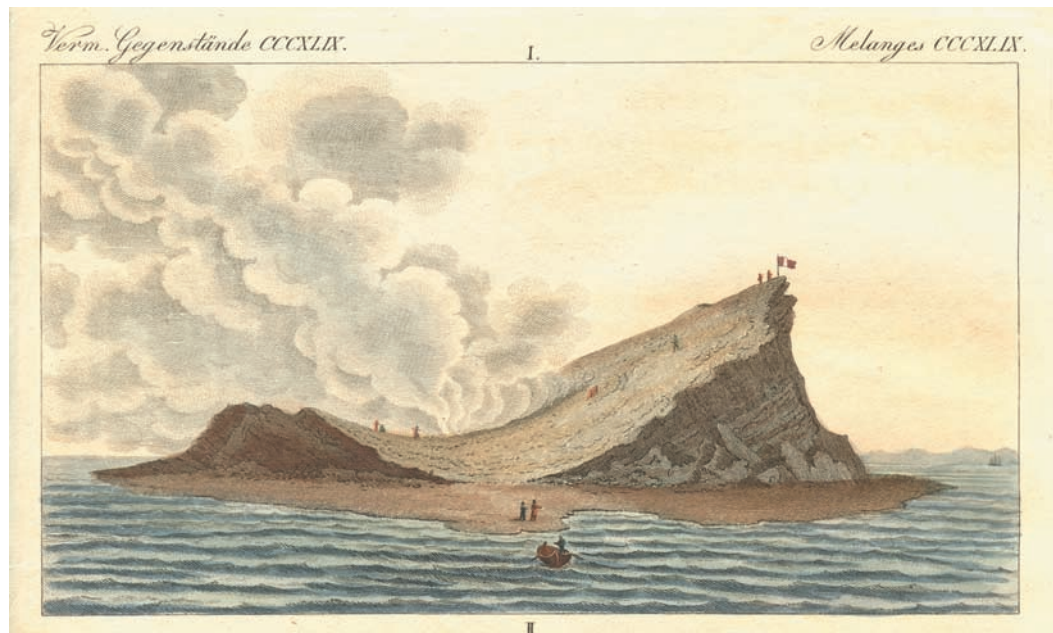


Fig. 12.6 Ferdinandea, the “ephemeral island” as sketched in 1831. Engraving from the *Bilderbuch für Kinder*, Bertuch, 1849, courtesy of Stephan Kempe.

island, but volcanic activity stopped and the disputed territory quickly disintegrated and washed away. By December, 1831 it was no more. Another eruption briefly rebuilt an island in 1863, but the site is now represented only by a shoal – the top of a large submarine volcano. The volcano became seismically active again in 2006, and will no doubt again build new land above the sea one day. (Who will claim it then?)

Shallow submarine eruptions are perhaps more common than generally recognized, and several are recorded each year, especially along island-arc chains. A typical submarine eruption is heralded by large areas of persistently discolored water, caused by the convective rising of ash-laden hot water above an active vent (Chapter 7). Jagged Surtseyan clouds may later burst above the sea, but whether events progress that far or not is unfortunately unpredictable, as shown by the tragic case of Myōjin-Shō [116] in 1952. Myōjin Shō is a submarine volcano rising some 500 m high above the surrounding seabed, located about 450 km south of Tokyo on the Izu-Ogasawara Ridge, a chain of volcanic islands and submarine volcanoes. Numerous submarine eruptions had been recorded from this area for almost a century, and on September 17, 1952 a fishing vessel reported a new eruption 12 km NE of the Bayonnaise Rocks. The reawakened volcano was named after the fishing boat (the *Myōjin Maru*), and ships and aircraft rushed to the scene to investigate the eruption. On September 24, a Japanese research ship, the *Kaiyo-Maru No. 5* had the misfortune to be conducting a marine survey **directly over** the active vent, some 50 m below, when an extremely violent hydrovolcanic explosion occurred. The 10 m-long vessel was completely destroyed and the 31 scientists and crew aboard were all killed – the worst disaster in the history of Japanese oceanographic research. Periodic explosions continued for the next year, and a new island as much as 100 m high formed and disappeared repeatedly (Minakami 1956). After 1953 no reappearances of land occurred, but submarine volcanic activity continued, and was studied using a pioneering unmanned radio operating survey boat, the *Manbou* (Sunfish), which for the first time utilized the SOFAR

(Sound Fixing and Ranging) channel to listen safely to the volcano's underwater rumblings. Eruptive activity only finally tapered off in 1970.

Subsequent studies have revealed that Myōjin-Shō is a resurgent volcano on the northeast rim of a 5.6 km wide, extensively mineralized submarine crater, now called the Myōjin Knoll caldera, whose floor lies 1100 m below sea level. The resurgent volcanism within and at the margins of the caldera has been extensive and is characterized by voluminous accumulations of silicic pumice that appear to have been erupted underwater at over 500 m depth (Fiske et al. 2001). Despite its low density most of this pumice likely never reached the sea surface, but became water-logged and sank soon after formation.

With more shallow vents, pumice from some silicic eruptions can rise all the way to the surface, forming great rafts that persist for months (Chapter 7). An underwater eruption at Tonga's Home Reef volcano [1] in the summer of 2006 (Fig. 12.7) produced an 8 km wide raft of floating dacite pumice, parts of which reached northeastern Australian beaches over 4000 km away by the spring of 2007. The frequency of small to moderate-sized silicic submarine eruptions is so great in the Tonga–Kermadec island arc that similar pumice rafts are reported once every 5 to 15 years.

Deep water explosive eruptions

The “conventional wisdom” (a dangerous thing!) that was accepted by all volcanologists not so long ago was that the high hydrostatic pressures of the deep oceans would prevent the

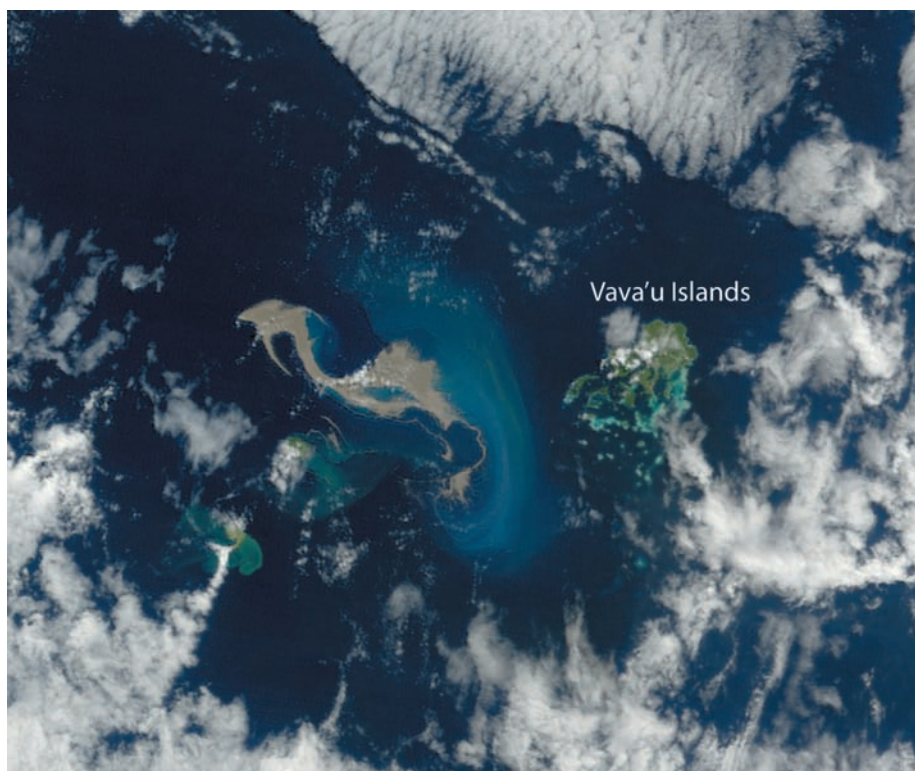


Fig. 12.7 Floating pumice raft from the submarine eruption of Home Reef volcano [1] as seen from space. The raft is over 75 km long and over a meter thick in places. NASA MODIS image T20066222-15200 (August 10, 2006)

explosive eruptive activity so characteristic of shallow-water eruptions. The assumption was that phreatic explosions could only take place at very shallow depths (less than 100 m). Submersible studies over the past two decades have shown however, that pyroclastic deposits are widespread in all submarine volcanic environments – regardless of water depths. It was also erroneously assumed that high confining pressures on the deep sea floor would prevent dissolved magmatic gases from exolving and contributing to pyroclastic activity, but that was quickly disproved by the observation that vesicles are present in lava samples recovered from all depths. The realization that deep sea explosive volcanism was an important phenomenon was given economic impetus by the realization that many of the Earth's largest metallic ore deposits (Kuroko-type, Chapter 15) are associated with pyroclastic rocks that are clearly marine in origin (Burnham 1983). Proof-positive, real-time eye-witness evidence that explosive eruptive activity occurs on the deep sea was recently provided by submarine exploration of active volcanoes in the Northern Marianas arc, when ROV operators in 2004 discovered ongoing explosive activity near the 555 m deep summit of NW Rota-1 volcano [120], 175 km northwest of Guam (Fig. 12.8) (Embley et al. 2006). Video of the ongoing eruption showed cauliflower-shaped white clouds pulsating up to 50 m. above the small volcanic vent named “Brimstone Pit,” roiling plumes that rained down large blocks of highly vesicular basaltic andesite and blobs of molten sulfur. Similar phenomena were documented in 2005, and in 2006 incandescent lava was observed being ejected from the vent – the first-ever direct observation of high-temperature submarine volcanism (W. W. Chadwick, 2008, pers. comm.). The flanks of the 16 km-diameter NW Rota-1 volcano are mantled with pyroclastic debris from these on-going summit eruptions, which appear to be continuous phenomena during the periods of observation.

Submarine eruptive activity in island arc environments is much more common than previously assumed. In May 2009, an interdisciplinary survey team discovered an active eruption at 1200 m water depth (by far the deepest active eruption site ever studied), at W. Mata volcano in the Lau basin – a backarc environment 200 km southwest of Samoa. Observations from the tethered ROV Jason-II showed spectacular eruption of gas rich magma from at least two vents, which both produced pulsating explosions from the tops of 10 m high vent edifices, and vesicular pillow lavas near their bases (K. Rubin, 2009, pers. comm.).

Explosive submarine eruptions involve two separate processes that contribute to the fragmentation of lava and to the formation of deep sea pyroclastic rocks. Simple quenching of hot lava results in differential stresses and fracturing that produce angular fragments of broken rock – hyaloclastite – as is normal when lava flows pour into the sea. But recent studies of submarine pyroclastic deposits also indicate that *actual lava fountains* have operated on the deep seafloor – producing primary vitric ejecta that clearly erupts as globules of molten rock – in the form of delicate fragments of glass bubbles and “Pele's tears” (Chapter 6). How can lava fountains operate under the great pressures existing on the deep sea floor, at depths where “steam” (gaseous water) cannot exist? Beneath about 3000 m, water at high temperature becomes “super-critical” and two fluid phases can coexist at high temperature (Wohletz 2003), although neither of these fluids have the potential for the great volume expansion that drives shallow-water and subaerial explosive volcanism. Explosive eruptions at these depths must be driven by exolved magmatic gases contained within the erupting lava (Perfit et al. 2003). The concentration of these gases (in large part CO₂) is not normally sufficient to drive explosive



Fig. 12.8 Eruptive plume above an active vent at 550 m depth on NW Rota-1 submarine volcano in the Mariana volcanic arc, located 100 km north of Guam. Note basaltic lava bombs falling out of plume. ROV photo by the NOAA Ocean Exploration Program, and NOAA Vents Program – courtesy of W. W. Chadwick.

activity, but pockets of such gases may be formed by magmatic processes before they are erupted (Head & Wilson 2003).

SUBGLACIAL ERUPTIONS

Many of the Earth's most active volcanoes are covered by snow and ice, and when these volcanoes erupt, unusual processes generate unique features and hazards. The specialized field of **glaciovolcanology** first developed in Iceland, a country where the concentration and frequency of subglacial eruptions is greatest. Subglacial historical eruptions have occurred in Antarctica, and eruptions have taken place beneath snow-capped volcanoes on all continents except Australia. Where these eruptions occur, molten lava probably never touches ice directly, or if so not for long, as liquid water and steam form an interface between the lava and ice near instantaneously, and cooling lava may produce ten times its volume in melted water. Many of the rock structures that form where "fire and ice" meet (pillow lavas and hyaloclastites) are thus similar whether formed beneath glaciers, in lakes, or beneath the sea. Volcanic hazards associated with these eruptions differ greatly from subaqueous volcanism, however, because of the exceptionally large volumes of water or lahars that may suddenly be released across populated lands down slope.

Distribution

The Earth's glaciers are divided into two types: the thick "continental" ice sheets, which cover vast areas of land (and sea) in polar regions, and the smaller "montane" glaciers, which form on high mountain at any latitude. Of the former, the Antarctic ice sheet is Earth's largest, and

accounts for about 90 percent of all the world's glacial ice. Almost two dozen volcanoes are known from Antarctica (Simkin & Siebert 1994), extending from the continuously active Mt Erebus [131], across West Antarctica, and down the Antarctic Peninsula. Erebus is one of the most active volcanoes in the world, but its lava lake is confined to a crater perched well above the closest glacial ice. The other Antarctic volcanoes are entirely or largely covered by glaciers, including the active Deception Island volcano [64], which last erupted from its caldera margins in 1967–70, destroying buildings and forcing evacuation of resident island research personnel (Smellie 2002). The Antarctic ice sheet is very thick, and some volcanoes are deeply buried. Recent ice-penetrating radar studies (Corr & Vaughn 2008) have documented a major volcanic eruption (VEI = 3–4) that occurred near the coast of the West Antarctic ice sheet and blanketed an area of over 20,000 km² with tephra about 2200 years ago. This tephra layer now lies buried beneath 100–700 m of ice, and was derived from a subglacial volcano that stands about a kilometer above the glacial bedrock. There is evidence that this and nearby volcanoes remain thermally active, and a concern that subglacial heating may be contributing to the well documented thinning and accelerated sliding of the adjacent Pine Island glacier.

Although not on a continent, “continental” glacier ice fields cover almost 10 percent of Iceland and bury several active volcanoes. The large Vatnajökull glacier (8100 km²) has long been known for its geothermally-heated lakes that overlie Grímsvötn [70], one of the world's most frequently active volcanoes with over two dozen eruptions recorded over the past thousand years of Icelandic human history (Simkin & Siebert 1994). Grímsvötn is characterized by a large, ice-filled caldera athwart the Icelandic eastern rift zone, and is related to the fissure system that fed the great Laki [71] eruption of 1783–4 (Chapter 6). Melting of ice above the Grímsvötn magma chamber sustains a subglacial warm-water lake whose water level is constantly monitored because of the threat of **jökulhlaups** (glacial lake outburst floods), which increases as lake levels rise. A subglacial fissure opened just north of Grímsvötn on September 30, 1996, and provided an excellent opportunity for scientists to make a detailed study of subsurface eruptive phenomena and magma-ice thermal exchange beneath Vatnajökull. The eruption (named Gjálp) eventually produced 0.8 km³ of basaltic hyaloclastites, but only an estimated 2–4 percent of this material erupted through the ice sheet into the atmosphere. The eruption melted more than 2.5 km³ of ice at the base of the glacier, at an initial rate of about 500,000 m³/day. This could be calculated by measuring the volume of a large down sag and collapse in the overlying glacial surface (Gudmundsson et al. 2004). Meltwater poured into the adjacent Grímsvötn caldera lake, and was stored there until sufficient hydrostatic pressure at the lake bottom exceeded the ice overburden pressure. At that point the water began wedging its way downslope along the ice–bedrock interface. It probably also melted new passageways by release of heat. Although the Gjálp eruption stopped on October 13, the meltwater did not reach the edge of Vatnajökull, 50 km away, until November 5, when it explosively burst forth, creating a jökulhlaup that destroyed bridges, roads, and powerlines while depositing house-size blocks of ice kilometers from the glacier's ruptured margin. The torrential floods formed lahars that added several km² of new land to the coast of Iceland. The initial discharge rate of jökulhlaup water was over 45,000 m³/sec – much greater than the average flow rate of the Mississippi River!

Grímsvötn returned to life beginning in the summer of 2003 with heightened seismic activity accompanied by caldera uplift. Icelandic scientists increased their monitoring in

preparation for a likely eruption. Earthquake activity suddenly jumped to a more intense level on October 25, prompting a public warning of impending volcanism. Meanwhile, meltwater input from the surrounding ice increased, and the caldera lake level rose to the point where the base of the surrounding glacier could retain it no longer. On October 28, the lake began draining again, and a jökulhlaup took place the next day in the nearby Skeidara River watershed. Prior experience had demonstrated that drop in lake level by roughly 10–20 meters could trigger an explosive eruption by reduction of pressure on the underlying magma chamber. So alerted, the scientists warned the Volcanic Ash Advisory Centre in London on October 29 of a possible tephra cloud that might threaten air traffic (Chapter 14). Sure enough, a swarm of intense volcanic earthquakes and tremor began on November 1, 2004, announcing the beginning of the eruption, which soon sent ash to altitudes of more than 10 km (Fig. 12.9). All air traffic was safely rerouted by then (Vogfjord et al. 2005).

Wherever volcanoes rise to sufficient height and precipitation is adequate (even near the Equator) they will be covered with snow and ice. This is true for most of the high Cordilleran volcanoes of North and South America, and for volcanoes of the Aleutians and Kamchatka. Although the volumes of meltwater and resultant floods caused by volcanic melting of these much smaller montane glaciers and snowfields are generally much less than that produced by eruptive activity beneath continental glaciers, these volcanoes too can produce disastrous jökulhlaups and lahars. A tragic case in point involves the 1985 eruption of Ruiz volcano [54] (Colombia). The summit of Ruiz (5321 m) was covered by a small glacier only about 30 m thick on the evening of November 13 when hot pyroclastic material blasted up through deeper ice and overlying snow that filled Arenas crater. The initial pyroclastic surges formed deposits



Fig. 12.9 Eruption of Grímsvötn volcano on November 2, 2004, triggered by the drainage of a subglacial lake (view from south). The column of ash and steam is about 700 m wide at the base and was rising to over 11 km at this time. This vigorous explosive phase lasted for about 30 hours and was followed by minor explosive activity until the eruption was over on November 6. Note the black ash ejecta at the plume base – which is black not because of increased ash content, but because its temperature is over 100°C, and steam has not yet condensed. Photo by M. Gudmundsson.

that consisted mostly of angular ice clasts with sparse lithic debris (Fig. 12.10). Little meltwater was apparently produced by this initial explosive activity, but subsequent pyroclastic flows melted snow overlying the glacier and triggered small lahars that incorporated unconsolidated pyroclastic and water-saturated sediments to form the massive debris flows that devastated cities as far as 50 km away (Chapters 11 and 14; Pierson et al. 1990).

The Kamchatka peninsula (Chapter 2) is home to over 100 volcanoes, at least a dozen of which have been active in historical time. All of these are covered with snow and ice most of the year, and Kamchatka volcanologists are very accustomed to observing the interactions between fire and ice. When these volcanoes send lava or pyroclastic flows down their flanks, abundant steam hides much of the activity (Fig. 12.11), but because lava and PDC's are much more dense than snow, flows tunnel beneath thick snow banks, melting large volumes of water as they proceed. These quickly melt the overlying snow and generate small lahars downslope. While mapping a fluid prehistoric lava flow on the slopes of Gorelli volcano [2] I (JPL) encountered extensive pillow lavas at basal contacts where the flow had tunneled under a snowfield. The pillows had been quenched so quickly by the surrounding meltwater that the mat of underlying tundra plants had only been carbonized in a few places! Mee et al. (2006) describe distinctive fracture patterns in lava flows quenched at snow-lava contacts on a Chilean volcano. Prehistoric lava flows near the summit of Mauna Kea volcano [14] show similar fracturing in pillowed basalt formed where they flowed beneath summit glaciers which have long since melted away (Fig. 12.12) (Porter 1987). The sudden release of subglacial meltwater caused by these flows generated a major jökulhlaup that caused extensive erosion of river channels as far away as Hilo, some 40 km downstream (J. P. Lockwood, unpublished mapping). Volcanic eruptions beneath glaciers can also incorporate large blocks of ice in pyroclastic flows, which may generate phreatic explosions, as occurred after the 1980 eruption of Mount St Helens (Fig. 12.13).

Landforms

As we discussed above, subglacial effusive eruptions occurring beneath thick ice fields produce large volumes of meltwater that will enclose the erupting lava in a watery interface. If lava supply rates are very high, and hydrostatic pressures relatively low, extensive fragmentation of quenched lava will occur and extensive subglacial hyaloclastite deposits can be formed; if effusion rates are slower and the hydrostatic pressure is higher, pillow lavas similar to those formed in submarine environments will be formed instead (Gudmundsson et al. 2004).

The recession of once more-extensive Icelandic ice sheets has revealed distinctive flat-topped mountains, called by Icelanders **table mountains**, which are characterized by pillow lavas at their bases and hyaloclastic deposits at their summits reflecting change in depth of ice-water cover during edifice growth. The steep flanks of most table mountains exist because of original confinement by ice, while the flat tops represent eruption into the floors of overlying meltwater lakes. Because of the confusion with the more common table mountains that are formed by the erosion of flat-lying resistant sedimentary beds or lava flows in arid terrains around the world, however, the term **tuya** is now preferred to describe these distinctive features, after Tuya Mountain in British Columbia (Fig. 12.14).



Fig. 12.10 Pyroclastic surge ice breccias on the rim of Arenas crater, north of the summit of Ruiz volcano, Colombia, formed during the eruption of November 13, 1985. This subglacial eruption produced pyroclastic deposits with similar structures to lithic breccias – but most of the angular clasts were of ice. Later phases of the brief eruption produced hot pyroclastic flows that overrode earlier surge deposits. USGS photo by J. P. Lockwood.

In some parts of Iceland during the last ice age, long eruptive fissures such as that of the Eldgjá–Laki eruptions (Chapter 6) developed beneath the ice sheet that covered most of the island. These ancient flood-basalt eruptions are recorded by the presence today of long, steep-sided ridges of hyaloclastite, commonly altered to brownish palagonite (Fig. 12.15). Termed **hyaloclastite ridges**, these features are now major topographic divides as much as 44 km long. In a well-studied part of Iceland’s western Volcanic Zone, there are almost

Fig. 12.11 Lava flowing down north-west slope of Klyuchevskoi volcano, Kamchatka in April, 2007. Flowing lava is more dense than snow and commonly flows beneath a short-lived snow cover. Klyuchevskoy (4750 m), is the largest and most active volcano in Eurasia. Photo by Yurii Demyanchuk.



Fig. 12.12 Subglacial pillow lavas formed at the contact between a prehistoric lava flow and ice at 4050 m elevation on Mauna Kea volcano, Hawai'i. This large, glassy pillow was later abraded by subsequent glacial movement after the flow cooled. Note hammer for scale. Photo by J. P. Lockwood.

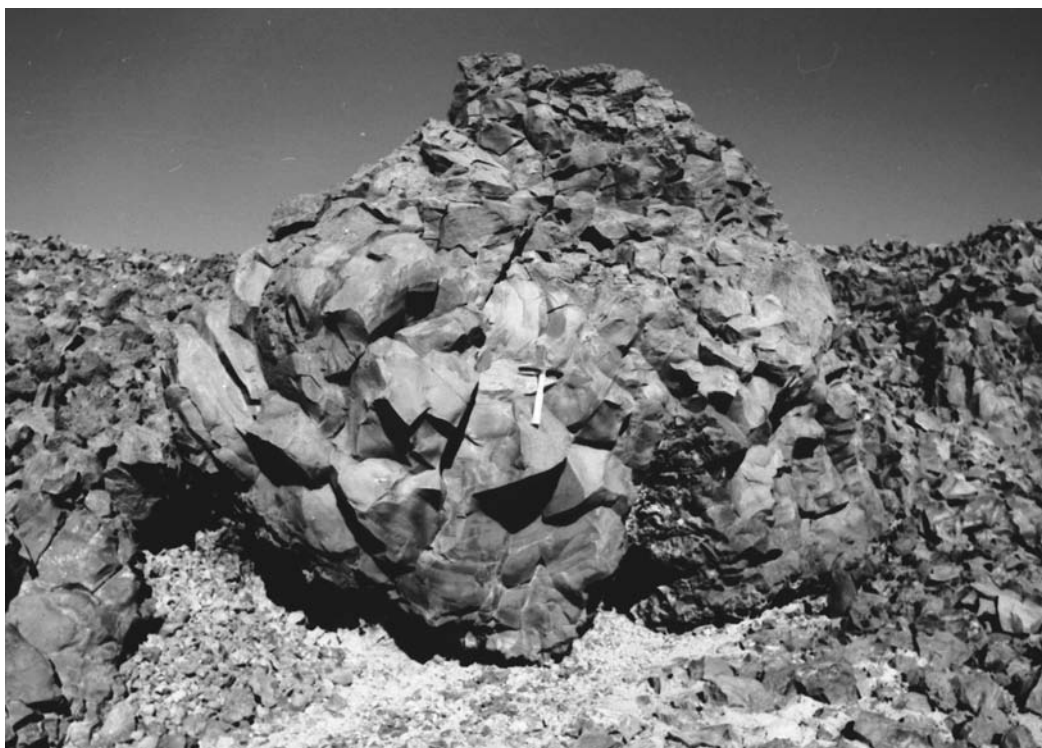




Fig. 12.13 Steam explosions in pyroclastic flow deposits on the 1980 “Pumice Plain” near the southwest corner of Spirit Lake, Mount St Helens, Washington. These phreatic explosions were caused by the melting of large blocks of glacial ice embedded in the hot pyroclastic flow deposits, and continued for months after the May 18, 1980 eruption. Note the phreatic explosion craters from previous events. USGS photo by Dan Dzurisin.

twice as many hyaloclastite ridges as there are tuyas (Zimbelman & Gregg 2000). A new hyaloclastite ridge developed along a 6 km fissure during the 1996 Grimsvötn eruption. Radio echo soundings and gravity surveying have since helped map the ridge, still covered by Vatnajökull glacier, which at highest point rises some 450 m above the pre-eruption bedrock, with a maximum width of some 2 km. The original thickness of the ice into which this ridge developed was 550–750 m (Gudmundsson et al. 2002).

Extraterrestrial Volcanoes

Volcanoes are not unique to Earth. Our neighboring planets in the Solar System have spectacular volcanoes, and it may well be a universal rule of thumb that all the inner, rocky planets and satellites more than a few hundred kilometers in diameter have produced effusive



Fig. 12.14 Tuya Butte, British Columbia, viewed from the south. This is the type locality for **tuyas**, the distinctive flat-topped volcanic features that form beneath thick glaciers. This tuya formed during the Pleistocene within a glacier estimated to be almost 1 km thick, and is about 400 m high, having a volume of 2–3 km³. Tuyas and other subglacial volcanic features are widespread in British Columbia where subglacial volcanism has been extensively studied. Geological Survey of Canada photo by Cathy Hickson.



Fig. 12.15 Late Pleistocene hyaloclastite formed beneath glacial ice about 40 km east of Thingvellir, Iceland. The mechanical pencil is 16 cm long. Photo by R. W. Hazlett.

TABLE 12.1 PLANETS AND SATELLITES IN THE SOLAR SYSTEM KNOWN TO HAVE VOLCANOES.

Planet or moon[†]	Still volcanically active?	Major source(s) of heating	Major kinds of volcanic landforms	Known or possible types of volcanic eruptions*
Earth	Yes	Radiogenic	Composite cones, shield volcanoes, lava shields, basalt plains, Plinian calderas, cinder cones, domes	Flood basalt; Hawaiian; Strombolian; Vulcanian; Plinian; Surtseyan
Venus	Probably	Radiogenic	Shield volcanoes, lava shields, basalt plains, coronae, paterae, montes, canali	Flood basalt Hawaiian
Moon	No	Early radiogenic, impacts	Shield volcanoes(?), lava shields, basalt plains, cinder cones, rilles	Flood basalt Hawaiian; Strombolian
Mars	Probably not	Early radiogenic	Shield volcanoes, lava shields, basalt plains, cinder cones(?), paterae, tholi, montes	Flood basalt Hawaiian Strombolian(?) Vulcanian(?) Plinian
Io	Yes	Solid tidal	Shield volcanoes, paterae	Flood basalt(?) Hawaiian; Vulcanian(?) Sulfur plume
Enceladus	Yes	Solid tidal	None	H ₂ O plume
Triton	Yes	Solar	None	N ₂ plume

[†] Saturn's largest Moon, Titan, may also exhibit signs of active water- or methane-based volcanism.

* Applying terrestrial eruption classifications to other worlds is somewhat misleading, because planetary atmospheres and gravity fields differ greatly. Explosive eruption behavior in particular differs significantly. Take the fifth column of this table somewhat with a grain of salt!

volcanoes similar to those on the Earth at one time in their histories (Table 12.1). The basic role of all volcanoes, no matter their chemistry is to help cool worlds (Chapter 2). Most rocky planets and moons have high temperature origins, and all continue to produce heat through radioactive decay, gravitational adjustments, and tidal stresses. In general, the bigger a rocky planet, the greater its ability to sustain internal heat production through self-generated radiogenic decay, and with that the continuation of volcanism (Chapter 3). While volcanic activity remains widespread on Earth, for example, it died out on the much smaller Moon hundreds of millions of years ago (Spudis 2000).

Not all volcanoes erupt silicate or carbonate-based magmas: the outer, icy planets also produce volcanoes of very different sorts from those of Earth. Some volcanoes further out in the Solar System erupt much cooler matter, including water and nearly freezing gases! We certainly have not seen all of the permutations of volcanic activity possible in Nature, but what we have seen expands imagination and understanding far beyond what would have been possible had we remained strictly Earth-bound.

THE MOON – FLOOD BASALTS IN SPACE

Most cultures have names for the pattern of dark patches on the white face of the full Moon. Consider for example “the Man on the Moon” many of us learned to identify as children, or the giant rabbit pattern familiar to people in eastern Asia. Whatever the image evoked, we are actually looking at tholeiitic flood basalt plains across 400,000 km of Space when we view these dark patches. Most of these dark fields of lava accumulated between 4.2 and 3.1 billion years ago. Termed **maria**, the lunar flood fields cover 16 percent of the otherwise brightly reflective lunar surface (Fig. 12.16). Curiously, they are distributed almost entirely on the hemisphere that permanently faces Earth. Were the “far side” of the Moon to face Earth instead we’d hardly have a clue as to their existence, apart from satellite observations made in recent decades.

The wide range of ages in the maria flows suggest that melting in the mantle was episodic, probably mostly triggered by the shock of giant meteorite impacts. When a meteorite of more than a few hundred meters diameter strikes, a pressure pulse shoots through the crust at speeds of kilometers per second. Almost at once this is followed by intensive tensional relaxation as the lithosphere and underlying mantle rebound, much of the superficial material spreading as tendrils of showering ejecta extending for hundreds of kilometers. This **rarefaction** event, accompanied by transient heating to several million degrees, can instantaneously melt a large volume of impacted bedrock. Intensive fracturing extending kilometers beneath and around the new crater can also trigger decompression melting and open up pathways for molten rock to ascend well after the dust has settled. In some craters a conspicuous central peak stands above a plain of slightly younger lava, illustrating the connections between impact, rebound and volcanism (Wilhelms et al. 1987; Wilhelms 1993).

Since the heyday of maria formation, the surface of the Moon has gradually stabilized into its present sterile configuration. The planet is too small to have any significant atmosphere, and is now too cold to generate volcanic activity. The youngest radiometric age for a sample of lunar lava is about 800 million years, with the vast majority of volcanic products issuing billions of years earlier (Spudis 2000).

VENUS – A “MANTLE PLUME WORLD”

It might be expected that Venus, our closest planetary neighbor, would show many similar geological characteristics to Earth, including plate tectonics, hot spot tracks, continents, and ocean basins, even in the absence of liquid water. But despite the similarity in the sizes and mean densities of Earth and Venus – the diameter of Venus is only 330 km less than that of Earth – the two planets lose their heat in remarkably different ways and have very different physical surfaces. While large, ancient masses of intensely fractured, elevated crust superficially resemble continents set in a global ocean basin, there is no evidence for plate tectonics on Venus, such as subduction zones, alpine-style mountain ranges, and hot spot tracks. In fact, of the approximately 1750 volcanoes (greater than 20 km in diameter) that have so far been identified, few are aligned whatsoever, in striking contrast to the linear belts of volcanoes found on Earth (Crumpler & Aubele 2000). Neither is there any evidence that the crust of Venus has differentiated into “oceanic” and “continental” components. The continent-sized, highly



Fig. 12.16 The Earth-facing surface of the Moon, showing the scattering of dark volcanic maria, which for the most part plainly fill large, impact related basins. Photo: NASA.

fractured and faulted highland plateaus of Venus, termed **tessarae**, appear to be made up of ordinary basaltic crust, crumpled and uplifted from powerful compressive forces. The tessarae cover about 15 percent of the surface of Venus; the rest is basaltic lowland spotted with volcanic structures and uplifts, in places complexly rifted and fractured (Cattermole 1994; Crumpler 1996; Moore 2002).

The surface conditions of Venus are inhospitable in the extreme, with mean atmospheric temperatures of 430°C , and pressures equivalent to what one would expect at a depth of a kilometer beneath the sea on Earth, roughly one-hundred times Earth's sea-level atmospheric pressure. The "air" in this oven-like environment is mostly carbon dioxide (97 percent), with clouds of sulfuric acid droplets forming a permanent layer 45–60 km above the surface. Carbon dioxide and sulfur dioxide are certainly important volcanic gases, and though no actual eruptions have been observed on Venus to date, it seems probable that the atmosphere is almost entirely a product of volcanic exhalations persisting into geologically recent times. The relative lack of meteorite impact craters on Venus and the fresh appearance of most volcanic structures support this conclusion (Bougher et al. 1997; Moore 2002).

The distribution of volcanoes on Venus is non-uniform. One hemisphere, including the Beta, Alta, and Themis regions, contains several times the global average concentration of vents (Head et al. 1992). This area of the planet is also somewhat elevated, though not as high as the tessarae, and is deeply cut by faulted rift blocks and fractures indicating that the surface has stretched and ruptured throughout. The lithosphere of this part of the planet is unusually hot and possibly supported by an enormous bulge of upwelling mantle (Bindschaller & Parmentier 1990). Lightly cratered lava covers virtually the entire surface of the planet (Strom et al. 1994; Basilevsky & Head 1996).

Soviet Venera landers sampled the surface of Venus in the 1980s, demonstrating that the crust of the planet, at least in the lowlands, consists mostly of tholeiitic basalt, the same composition making up Earth's ocean floor (Barsukov 1992). Hence it should be little surprise that lava shields and small (less than 20 km across) shield volcanoes are common volcanic landforms (Guest et al. 1992). Flood basalt plains and plateaus, many deeply fractured and faulted, abound, and fields of small lava shields are the most common planetary volcanic feature. Larger shield-like volcanoes with compound elements also occur, in many cases exceeding 100 km in diameter; larger than any volcano found on Earth. These are the highest landforms on Venus other than the tessarae themselves (Head et al. 1992).

Not everything appears purely basaltic however. Flattened, circular dome-like masses, termed **farr** (singular: **farrum**) or **pancake domes**, which somewhat resemble the rhyolite and dacite domes found on Earth, occur in rare scattered clusters (Fig. 12.17). The largest farrum so far observed is 65 km in diameter, and its steep, rough margin rises nearly a kilometer. Whether these masses are highly siliceous, like most domes on Earth, is unknown. If so, their presence implies that some shallow reservoirs of Venusian magma have undergone a high degree of chemical differentiation. Many Venusian domes and other volcanoes have large landslide scallops in their sides, and some closely resemble the catastrophic sector collapses observed on Earth (Chapter 11; Basilevsky & Head 2003).

Sinuuous channels, termed **canali**, wind tortuously across many gradually sloping Venusian surfaces. These channels superficially resemble the unroofed drainage channels of especially large basalt flows seen on Earth. But they are much larger than similar terrestrial features, being as much as several kilometers wide, hundreds of meters deep, and hundreds of kilometers long. (The longest canal stretches 1400 km) canali remain enigmatic features more closely resembling meandering river beds than unroofed pyroclasts, perhaps related to some poorly understood process of thermal or mechanical erosion occurring during large-volume flow under atmospheric conditions very different from Earth's (Gregg & Greeley 1993).

Many Venusian volcanoes occur in dense clusters, localized atop areas of domically uplifted crustal "hot spots". Hot spots are also indicated by the presence of **coronae**, calderas tens of kilometers in diameter bordered by concentric ring fractures (Fig. 12.18). In addition to the ring structure, radial fractures commonly extend hundreds of kilometers from each corona. Some fractures mark the courses of enormous dikes fed at shallow depths, showing that the Venusian lithosphere is weak and vulnerable to point-source dike injection beneath areas of tens of thousands of square kilometers (Ernst et al. 1995). In many cases, the radiating fractures curve into the trends of regional tectonic fracture sets, giving the overall fracture pattern the appearance of a giant spider with curving legs. Planetary geologists refer to these particular coronae as **arachnoids** (Stofan et al. 1992). Unlike terrestrial calderas,

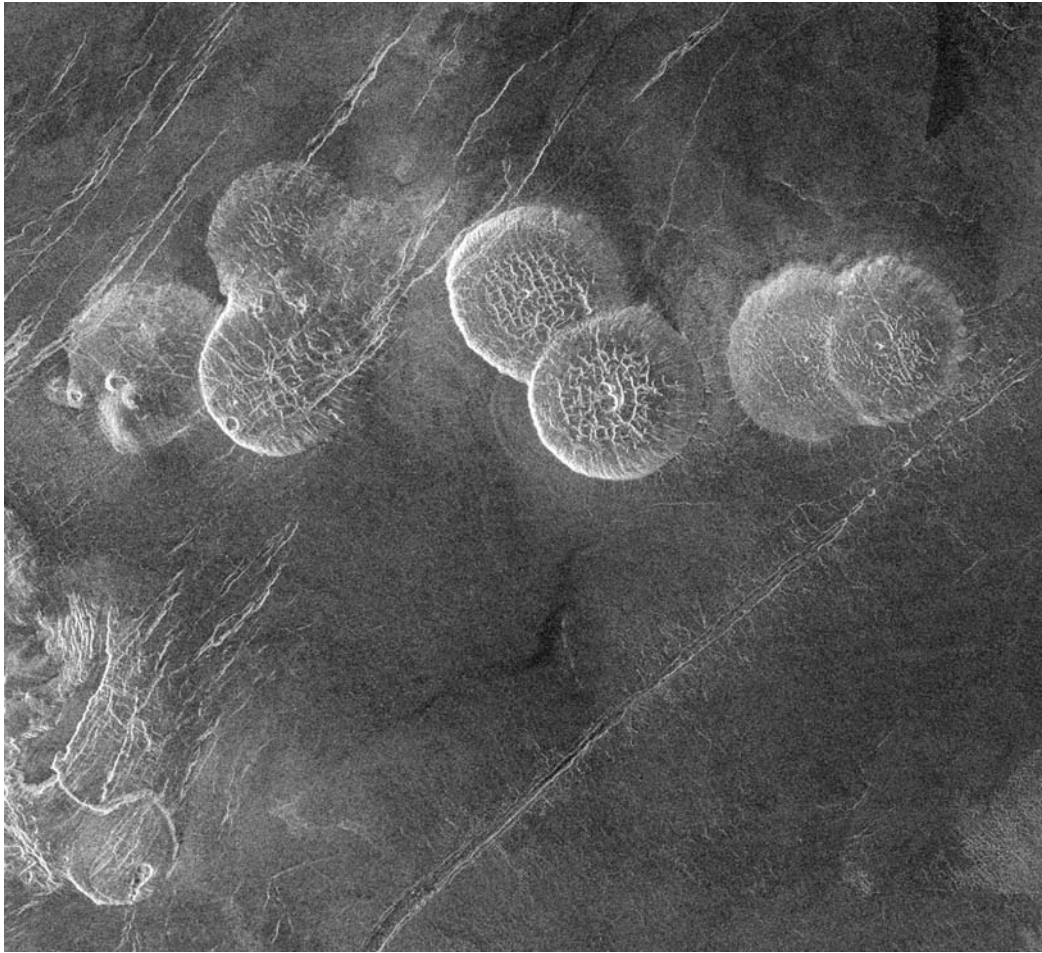


Fig. 12.17 A chain of farra (“pancake domes”) partly cut by younger fractures on a lava plain, Venus, imaged by Magellan Mission radar. The largest farrum is about 25 km in diameter and 700 m thick – much larger than any silicic flow on Earth. Light areas represent rougher radar-reflective surfaces, darker areas are smoother. Photo NASA, JPL/Caltech. NASA Archive PIA00215[1].

coronae lack associated widespread deposits of pyroclastic ejecta. In fact, the great pressure of the Venusian atmosphere discourages explosive eruptions, including anything approaching a Plinian outburst. Some coronae calderas show little evidence of erupting anything, in fact, and probably form simply from collapse of rising, stretching crust. In other cases, effusive eruption plainly accompanied corona development, in many places through vents on the flanks of coronae-crowned uplifts (Crumpler & Aubele 2000).

Radiating networks of grabens that are likely to overlay shallow dikes, form starburst patterns hundreds of kilometers in diameter in some locations. No accompanying volcanism or uplift accompanies these structural magmatic or radial fracture centers. Each structural magmatic center probably marks the initial impingement of a rising plume of hot, partly molten mantle at the base of the lithosphere, which could in time evolve into a fully developed corona. In fact, all states of gradation are seen between structural magmatic centers and coronae. They tell us that mantle plumes and hot spot volcanism play a primary role in facilitating heat release from Venus (Soloman et al. 1992).

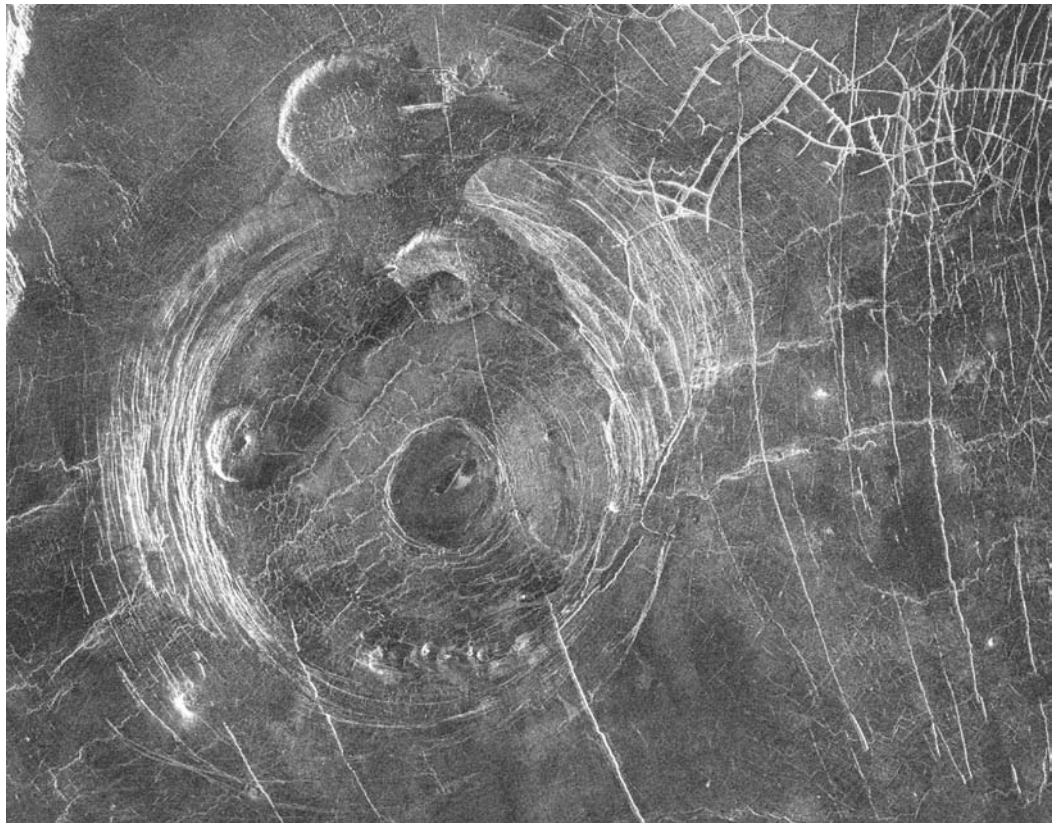


Fig. 12.18 Aine Corona, a partly collapsed area of magmatic uplift on the surface of Venus displaying related concentric fractures and farra. Photo NASA, JPL/Caltech. NASA Archive PIA00202[1].

On the Earth's Precambrian crustal cratons, remnants of giant radiating dike swarms are preserved in several regions, implying that Earth too once produced some now distinctly Venusian volcanic features (Ernst et al. 1995). If this is so, what accounts for the change in the paths these two planets took? More particularly, why does Venus lack the vigorous plate tectonic dynamic now helping keep Earth cool?

One possible answer to the above question leads us back to the oppressively thick and hot Venusian atmosphere. While a surface temperature of 430°C is well below the melting point of basalt, it does keep the underlying surface significantly warmer than it would be under terrestrial conditions. Ascending magma would not lose heat as rapidly as it does at equivalent depths inside Earth. More importantly, the very high air pressure at the surface means that levels of neutral buoyancy are much shallower in the Venusian crust. In fact, it is likely that molten rock penetrating the lithosphere of the Venusian lowlands remains buoyant all the way to the surface, and fails to form substantial, long-lasting magma chambers. This is supported by the fact that lava shield fields dominate lowlands, while larger shields, complex volcanoes, and coronae are more abundant at higher elevations. It is simply easier for magma to escape from the Venusian surface than on Earth – or at least on Earth's continents (Head et al. 1992; Grosfils et al. 1999).

The floor of Earth's oceans, at a mean depth of over 2 km, has a pressure more than double that of the atmosphere of Venus, and it is certainly easier for magma to issue here

than elsewhere on Earth's surface. The thousands of seamounts scattered across the ocean floor form what may be regarded as enormous volcanic fields, far larger than any seen on Venus with the arguable exception of the Beta-Alta-Themis Regiones. In other words, plate tectonics may largely be a manifestation of our planet's surface environment, just as mantle plume volcanism may be stimulated by the Venusian atmosphere. Sea water too, plays another critical role by providing the source fluid for substantial volatile flux during subduction, described in Chapter 2 as vital for creating arc volcanism. The recycling of water in Earth's mantle and lithosphere leads to the development of important continent-building suites of rocks that simply have no chance of forming on a world as anhydrous and hot as Venus.

MARS – LARGE VOLCANOES ON A SMALL PLANET

Larger than the Moon, but only about a third of the diameter of Earth or Venus, Mars has a volcanic history that blends aspects of volcanism from all three of these neighboring worlds. Being intermediate in size, Mars has substantially fewer volcanoes than either Venus or Earth, but certainly more than have been identified with certainty on the Moon. There are only about two dozen named, notable volcanoes on the Martian surface, but these include some volcanic giants, the biggest known volcanic features in the Solar System (Zimbelman 2000).

Like Venus, Mars shows no evidence of plate tectonics. As befits the smallness of this planet, the atmosphere is tenuous and thin. Though water once played across the planet's surface, this world is now drier than anyplace on Earth. Volcanism there appears to have resulted from primarily two forces of nature: the impacts of enormous meteorites, and plume-like upwelling from the deep interior.

Perhaps two or three billion years ago (dating Martian eras is quite uncertain), an enormous impact scoured out the 2100 km wide Hellas Basin, which quickly flooded with a smooth plain of fluid, homogeneously cooling lava. Intense impact fracturing opened up a northeast-southwest line of weakness to either side of the Basin through which molten rock erupted to construct the four Hellenic volcanoes, Amphitrites, Hadriaca, Peneus, and Tyrrhena. These belong to a special morphological group, termed **paterae**, which in fact makes up almost half of the large Martian volcanoes, and a number of volcanoes on Venus and the Jovian moon Io as well. A typical patera consists of a single large caldera that may have collapsed in multiple stages, perched at the nearly level crest of a very gently sloping (up to 1°) volcanic rise. The diameters of the Hellenic paterae range from 120 to 180 km, with summits no more than a kilometer above the surrounding older terrain. Individual calderas range up to 30 km across. Like other ancient volcanoes on this part of Mars, the Hellenic paterae are deeply gullied and furrowed, and quite possibly constructed of easily eroded ejecta generated by massive Plinian-style eruptions.

Paterae continued to form long after the Hellenic impact. The largest, Alba Patera, has a diameter of 450 km, and rises 4 km above an adjoining flood lava plain. The shallow central caldera is a hundred kilometers across – the biggest volcanic crater on Mars. Alba Patera appears to be made up mostly – if not entirely – of lava flows morphologically resembling ordinary *ʻaʻā* and *pāhoehoe*. Individual flows are truly enormous, perhaps as much as an order of magnitude greater than the largest flows on Earth.

Alba Patera is but one of a cluster of enormous volcanoes, for the most part shields, in the Tharis region of Mars (Figs. 12.19 and 12.20). The biggest of them all is Olympus Mons, with a diameter of 500 km and a surface area equal to that of the State of Arizona. With slopes not exceeding 5° in most places, Olympus Mons rises 27 km above its base. The top of the volcano is so high that atmospheric pressure is only 2 percent of what it is in the nearby lowlands. The summit caldera, a composite of at least five major and probably minor collapses, measures 90 by 60 km and is as deep as 3 km – comparable in scale to reconstructions of the largest calderas on Earth (Chapter 10). Episodes of lava lake infilling, interspersed with renewed collapse have created a complex, terraced caldera floor, well preserved because erosion is such a very slow process on Mars (Mouginis-Mark & Robinson 1992). One of the most striking aspects of Olympus Mons is the scarp enclosing the foot of the mountain, a fault cliff 3–6 km high which faces outward, away from the volcano. Large landslides shed from the scarp created debris fields and lobate masses in some cases stretching hundreds of kilometers onto the surrounding plain. Some deposits resemble the sea floor debris fields formed by the catastrophic collapse of Hawaiian shields (Lopes et al. 1980). The scarp clearly developed late during the growth of the volcano, but the presence of numerous unbroken flows draped across its face indicate that eruptions continued for awhile after it developed. The basal scarp of Olympus Mons is one of the large-looming mysteries of Martian topography.

Unlike Earth's Moon, volcanic activity may be far from over on Mars. Detailed photographic studies by NASA's Global Surveyor starting in 1997, and the Mars Express High Resolution Stereo Camera, which began orbiting Mars in December of 2003, provide evidence of effusive volcanism perhaps as young as 2–2.5 million years, with flows mantling the flanks of Olympus Mons erupted mostly within the past 200 million years. It cannot be assumed that Mars is now internally cold and volcanically dead, and in fact, volatile efflux may still be in progress.

IO – AN “INSANELY ACTIVE” VOLCANO WORLD

When Galileo Galilei first turned his new telescope to look at the giant planet Jupiter in 1610, he quickly spotted four large moons circling that body which have since been named the **Galilean Moons**. There are over 60 known satellites orbiting Jupiter, but most are small, irregular bodies, little more than giant, icy rocks trapped in the Jovian gravity field. The Galilean moons are notably larger, however, comparable in diameter to Earth's Moon, or the planet Mercury. Listed in order of their distance from Jupiter, the four are named Io, Europa, Ganymede, and Callisto.

The first spacecraft to explore this system, Voyagers I and 2, flew past the Galilean Moons in the spring and summer of 1979. Observers had expected to see small, dead worlds, but were instead surprised as they collected data showing the presence of interior oceans on at least two of the moons thought to be too cold to sustain liquid water – Europa and Callisto. Even more stunning was Io, the innermost moon, which was volcanically active almost beyond imagination.

The heating of the Galilean moons derives in large part from the tidal forces acting on them as they orbit Jupiter, the largest body in the Solar System other than the Sun itself (Peale



Fig. 12.19 Based upon cratering density and estimates of growth rates, this trio of shield volcanoes in the Tharsis region of Mars probably formed on the order of 700 million–3 billion years ago: At the lower left is Arsia Mons (oldest of the group), with Pavonis Mons in the center, and Acraeus Mons (the youngest) in the upper right. The spaces between the volcanoes are each about 700 km. The volcanoes lie at the crest of a gently sloping lava-covered uplift some 10 km high – the Tharsis Bulge. In the lower right is the head of the 4000 km long, 6–7 km deep Valles Marineras, a tectonic rift valley probably related to early growth of the Bulge. Photo: NASA, JPL/Caltech. NASA Archive PIA02987[1].

et al. 1979). The continuous flexing of the moons by intense tidal forces generates great frictional. The surface of Io rises and falls a hundred meters with each tidal cycle, compared to a mere 0.1–0.4 m on Earth. This is all the more impressive, considering that Io is only about the size of our Moon.

In March of 1979, Voyager 1 photographed a powerful volcanic cloud shooting 300 km into space from the volcano Pele, seen on the horizon of Io. In the moon's low density sulfurous atmosphere (nine orders of magnitude less dense than Earth's atmosphere) the cloud

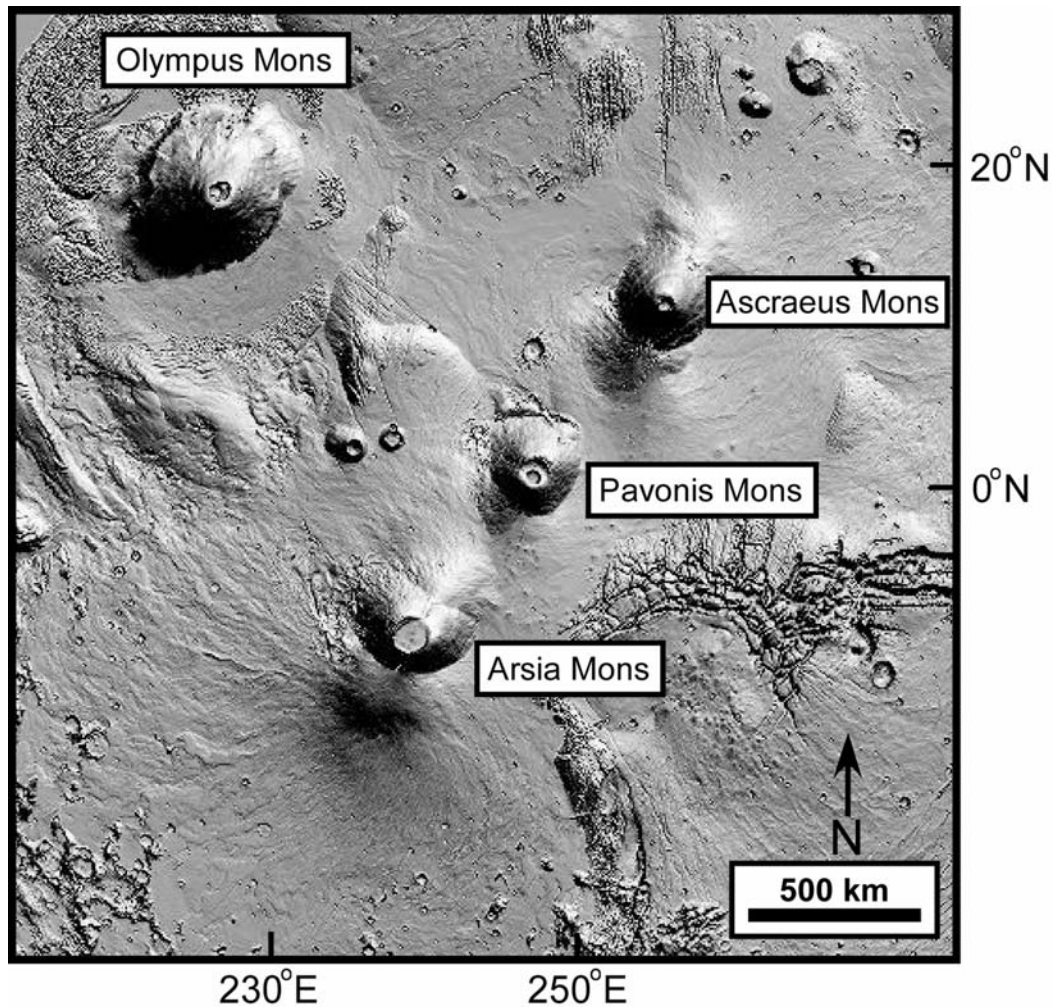


Fig. 12.20 Shaded relief map showing Olympus Mons and other large shield volcanoes in the Tharsis Region on Mars (vertical exaggeration about 3x). Illumination is from the northeast. From Garry et al. (2007).

resembled a giant opened umbrella. Its fall ejecta ultimately covered 10,000 km² of the moon's surface. To add to the excitement, eight additional volcanic clouds were quickly discovered during the Voyager fly-bys, and spacecraft thermal sensors showed that nine other volcanoes were "hot," perhaps ready to erupt or recently having done so. With the return of the Galileo Mission in 1996 and the later Cassini mission (2000–1), many changes in the surface could be precisely documented. These included the outpouring of fresh lava flows exceeding 100 km in length, and the apparently continuing eruption at a number of volcanoes, including Prometheus, Loki Patera, and Pele, all active in 1979. The Galileo spacecraft photographed ten additional eruption clouds, and brought the total number of known active volcanoes on Io up to 74, with dozens of additional hot spots (Fig. 12.21) (McEwen et al. 1998).

One of Io's most striking and telling aspects is its color. The surface is yellow, red, and orange, mottled with white, black and dark grey patches (Fig. 12.22). This coloration, together with spectrographic analyses of plumes, initially led observers to believe that only sulfur or sulfur-related compounds erupt from Io's volcanoes, and that these materials have coated virtually the whole moon, with the exception of the white patches, which are likely to be sulfate frost condensing out of the frigid atmosphere. (The surface temperature on Io is a chilly

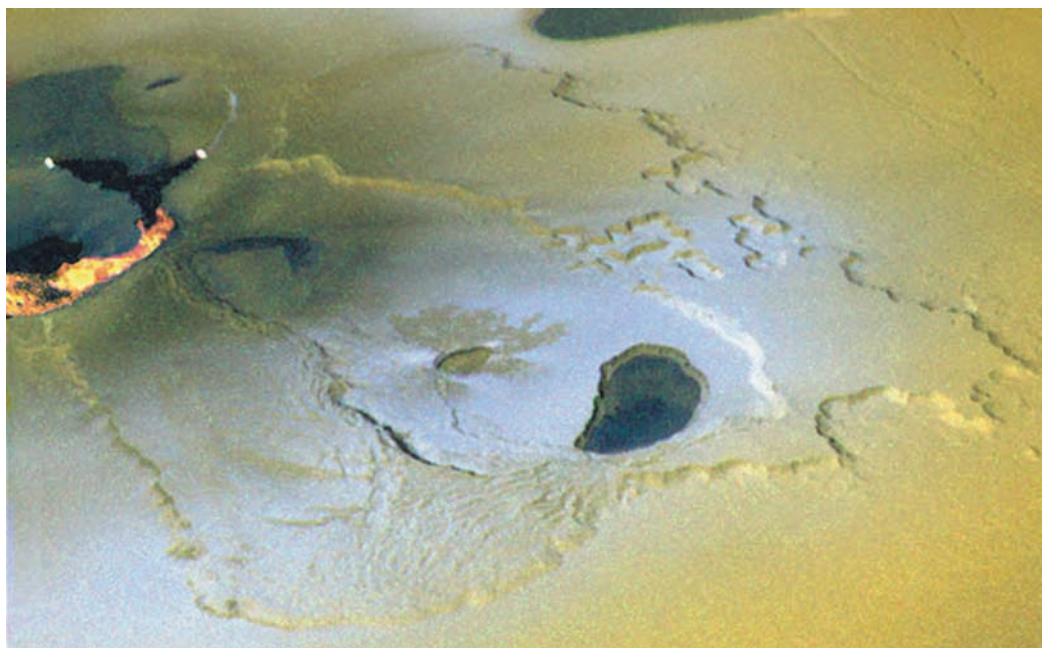


Fig. 12.21 The scalloped (possibly sapped) volcanic tableland and compound caldera features of Tvashtar patera, Io, with an on-going effusive eruption highlighted to the left. The frame is roughly 200 km across, left to right. Volcanic activity in this area has been observed by spacecraft on two other occasions. In 2000, the Galileo spacecraft imaged a 25 km-long eruptive fissure with lava fountaining as high as 1 km, which subsequently cooled to form the dark strip just to the right of the active area. Tvashtar was erupting again at the time of the New Horizons spacecraft Jupiter fly by in 2007, when a massive plume was observed. Photo: NASA Archive PIA02550[1].

–143°C.) Astronomer Carl Sagan pointed out most of the colors, especially the warm ones, could signify the presence of different forms of molecular sulfur known to absorb light at different wavelengths according to their temperature. However, subsequent thermal measurements by infrared detectors on Earth-based telescopes and on the Galileo spacecraft have shown that the temperatures at active volcanic vents are typically consistent with silicate volcanism (Johnson et al. 1988; Veeder et al. 1994). Values as high as 1500°C have been measured, indicating that substantial volumes of silicate lava must also pour from Io’s volcanoes (Keszthelyi et al. 2006; Davies, 2009). Indeed, some fresh flows retain their dark coloration too long to be composed of sulfur; and larger volcanoes, as high as 18 km, are likely to be composed mostly of silicate rock – stronger natural construction material. We now know that mafic to ultramafic silicate magmas, as on planets closer to the Sun, are the primary drivers of Io’s volcanoes.

Ionian volcanoes take a wide variety of forms. Large areas of the surface are covered in extensive lava flows, some with visible pyroclastic systems. One of the longest known lava flows in the Solar System, erupted from Amirani volcano, extends 500 km. Patera calderas occur by the hundreds, set into flat plains and squat mesas, some of which contain active lava lakes. The biggest, most powerful volcano is Loki Patera, the vent of which is marked by a restlessly molten lava lake with an area of over 20,000 km²! Io’s volcanoes individually erupt vastly larger volumes of lava than their terrestrial counterparts (Ashley Davies, pers. comm. 2009; Davies 2009).

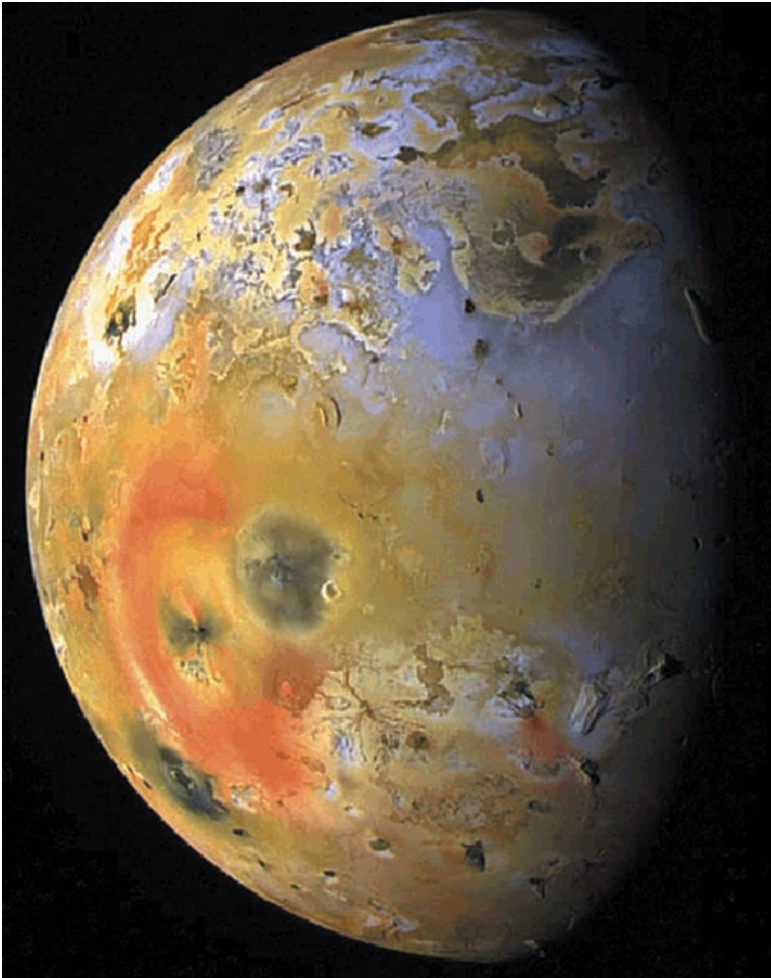


Fig. 12.22 The surface of Io, the lava flows and other surface features of which are coated with dark smudges of pyroclastic debris – localized around volcanoes – and brightly-colored, globally distributed gas sublimates. The mineralized, nearly complete red ring to the lower left is centered around the volcano Pele. The ring resulted from the explosive eruption and deposition of a sulfurous plume in the very tenuous Ionian atmosphere. When first imaged by the Galileo Orbiter, the ring was complete. But between the 7th and 10th orbit of the spacecraft around Jupiter, the 400 km wide Pillan patera grew to cover its upper right section – stark testimony to the vigor of volcanic activity on this strange world. Photo taken in 1999: NASA Archive PIA01667).

body in the Solar System and its sulfur-rich lithosphere is being continuously recycled. Amongst the material escaping from Io, a fine mist of sulfur particles escapes into Space, cast there by the larger sulfur plumes spraying from Io's surface. Some of it coats the neighboring moon, Amalthea, painting it red and orange. The rest escapes to form a diffuse ring, or **torus**, orbiting Jupiter. Io is exceptional for bodies its size, thanks to powerful external forces. It is a world seemingly on the verge of tearing itself apart.

Eruptions commonly issue Hawaiian-style from fissures – often generating massive volcanic clouds whose deposits cover large portions of Io's surface as sulfur-rich "snowfalls." Vent-derived clouds are rich in sulfur (S_2) and may shoot as far as 500 km into Space before spreading and settling out. They originate where ascending silicate magma melts deeply buried deposits of sulfur and sulfur dioxide in volcanic conduits at temperatures well above surface boiling points. (The same principal acts to explain water geysers on Earth.) The great heights of these columns may be attributed to the low gravity and very tenuous atmosphere of Io (with about one billionth the atmospheric pressure at sea level on Earth). Were such eruptions to occur from a terrestrial volcano, their columns would rise only a few kilometers. Additional, less substantial volcanic cloud development takes place where silicate flows snake across the ordinarily frigid landscape, boiling adjacent sulfate-rich ices. Lava flows made of molten sulfur also almost certainly form as a result of thermal interaction with hot silicate lava (Geissler 2003; Davies 2009).

Like the Earth's moon, Io keeps one face continuously toward Jupiter, 440,000 km away. While volcanoes are scattered across Io's entire surface, they are concentrated at roughly the $165^\circ W$ and $352^\circ W$ meridians, theoretical points of maximum tidal stress on opposite sides of the moon (Schenk et al. 2001).

Io shows no evidence of plate tectonics. The satellite's lithosphere has to be at least 30 km thick in order to support its highest mountains. Volcanic activity is apparently resurfacing Io faster than any other planetary

DEEPER SPACE – COLDER VOLCANOES

Deeper in space, volcanic activity takes the form of erupting water and gasses, a non-magmatic phenomenon called **cryptovolcanism**. So far cryptovolcanic eruptions have been observed on only two worlds beyond the orbit of Jupiter; Enceladus, a moon of Saturn; Triton, a moon of Neptune; and are probable on larger non-planetary objects in the Kuiper Belt – such as Charon, a moon of Pluto.

Enceladus is a small moon with a diameter of only 500 km – barely the diameter of Olympus Mons on Mars. Planetary bodies of this size barely maintain a spherical shape, and in fact Enceladus is slightly oblong. Moderately cratered water ice covers the northern hemisphere, where crater counts suggest that freezing took place at least 10–100 million years old. Not much has happened since then. In the south, however, surface conditions are much different – and far more dynamic. A fresh veneer of tectonically disrupted ice covers the region, laced with a network of light blue fractures termed “tiger stripes” similar to the leads crisscrossing broken river ice after refreezing. Infrared spectrometer measurements reveal that the ice in the tiger stripes is about 15°C warmer than the surround ice “plates,” indicating that relatively warm matter, probably liquid water, is active below.

The south pole of Enceladus shows the most extreme tectonic deformation. Fractures and broken platelets, some heaved and thrust aside, and boulders of ice from 10 to 100 m diameter lie strewn across the dim, blue-white landscape (Porco et al. 2006). In 2005, the Cassini spacecraft observed a spectacular geyser of water shooting up 500 km and dissipating into the oxygen-rich E-ring circling Saturn. Enceladus was feeding matter into one of Saturn’s rings! A sprawling system of fluid pockets beneath the polar surface, hardly above freezing temperature, may have supplied the high-pressure jet of liquid water (Spencer et al. 2006). But what caused the eruption? Like the Galilean worlds that orbit Jupiter, Enceladus experiences tremendous tidal forces exerted by Saturn, and possibly also by a neighboring satellite, Dione. There is also some evidence to suggest that the orbit of Enceladus is librating (oscillating), causing tidal stress to heat up its interior (Hurford et al. 2009). In any event, this world seems to defy the “small planet – no heat” equation.

Triton is a much bigger world, with a diameter of 2700 km, almost matching Io. Being even farther from the Sun as it orbits Neptune, frozen gases and ice also cover the surface. Floating high in a tenuous, nitrogen-rich atmosphere, wispy clouds of nitrogen ice crystals provide weak daylight shade. Perhaps these clouds are residues of volcanic plumes. In August, 1989, Voyager 2 swept close past Triton, and photographed jets of dark matter shooting from two locations in the southern hemisphere. Each column rose about 8 km above Triton’s surface, then flattened out and spread downwind about 150 km before dissipating. Eruptions like this must be commonplace on this Neptunian moon, since Voyager recorded the dark ejecta blankets of more than a hundred other, earlier plumes (Geissler 2000).

Triton’s surface temperature is –235°C, only a bit above absolute thermodynamic “zero.” On Earth, the physics of matter interactions at this temperature can only be studied in a laboratory. We know that gases such as nitrogen, carbon dioxide, and methane, all found on Triton, freeze when it gets so cold. But nitrogen will sublime at –225°C, not much above an average day’s temperature on that world, so it seems likely that it would take only a little bit of heating to generate violent nitrogen gas eruptions from the frozen crust. One proposal

is that carbon particles trapped in the shallow, translucent crust capture weak sunlight seasonally, then re-radiate this energy in thermal infrared wavelengths. This **solid-state greenhouse effect** heats the surrounding nitrogen ice just enough to turn it into gas. Like water flashing to steam, vaporizing nitrogen expands with great force – about a hundredfold per unit volume. Voyager happened to pass Triton’s southern hemisphere at a time when that region was nearing summer solstice – the optimal moment for such heating, and rare good fortune indeed given that the length of one year on Triton is equivalent to 165 years on Earth.

From what we’ve observed on Enceladus and Triton, it would be surprising if other worlds in the outer fringes of our Solar System were not also volcanically active. Perhaps gas eruptions take place unseen on Titan, Saturn’s largest moon, which is permanently obscured in a thick, smog-like atmosphere. Recent surveying by the Cassini spacecraft has detected glaciers resembling lava flows, ice shields, and even ice calderas on that world (Elachi et al. 2005; Kerr 2005). Maybe Pluto will prove to have nitrogen plumes also, much like those on Triton. The common occurrence of volcanic activity throughout our solar system virtually assures that volcanism must be taking place on planets around other suns in our galaxy and beyond.

Earth’s terrestrial eruptions “get all the press,” especially ones in populated areas and those easy for reporters to access. Although these are the ones we know most about, eruptions from the unseen volcanoes are far more numerous and voluminous. We have recently begun to learn about them, and to document those occurring in far more remote reaches of our solar system. Volcanism clearly plays a fundamental role in the redistribution of heat on massive bodies, and widespread volcanic activity must be commonplace throughout the Universe. Even if we can’t be sure that life exists on other worlds, we *can* be sure that volcanoes do!

FURTHER READING

- Davies, A. G. (2009) *Volcanism on Io: A Comparison with Earth*. Cambridge, Cambridge University Press, 355 p.
- Lopes, R. M. C. and Carroll, M. W. (2008) *Alien Volcanoes*. Baltimore, The Johns Hopkins University Press, 176 p.
- White, J. D. L., Smellie, J. L. and Clague, D. A. (eds.) (2003) *Explosive Subaqueous Volcanism*. Washington, DC, American Geophysical Union, 379 p.

Chapter 12

Questions for Thought, Study, and Discussion

- 1 Would you expect to find a composite volcano like Mount St Helens on the deep ocean floor? Why or why not?
- 2 What is the origin of the Earth's many submarine seamounts?
- 3 What factors are most important for building a long-lasting volcanic island?
- 4 Some shallow submarine eruptions take place without developing Surtseyan eruption clouds. Yet we still can see evidence of their taking place. How can this happen?
- 5 How does the flow of pāhoehoe erupted from vents along the MOR differ from that of subaerial pāhoehoe erupted from, say, the flank of Kīlauea?
- 6 For many years, earth scientists presumed that explosive volcanic eruptions could not take place in water more than a few hundred meters deep. Why were they wrong?
- 7 How and why do volcanic landforms formed subglacially differ in appearance from volcanoes formed subaerially?
- 8 Why do many large impact craters on the Moon have central peaks, with floors of basaltic lava?
- 9 How and possibly why do the volcanoes of Venus appear so different from those of the Earth, a world that is otherwise very similar in terms of its density and overall size?
- 10 Intensive volcanic activity is confined (as far as we know) to only smaller planetary satellites in the outer solar system. Why, and how does this volcanism differ from that of the inner solar system?





PART V

HUMANISTIC

VOLCANOLOGY

This Part discusses the interactions of human society and volcanism – the important ways in which volcanoes have affected the Earth’s life, have impacted human safety, and provided society’s necessary mineral and energy resources. **Chapter 13** discusses the climatic and biological impacts of volcanism and the role of volcanism in human evolution and history. **Chapter 14** describes the nature of volcanic hazards and risks and the ways in which that risk can be lessened through volcano monitoring and crisis management. **Chapter 15** discusses the role volcanoes play in the concentration of metallic ores and geothermal resources critical to modern civilization.

Chapter 13

Volcanoes: Life, Climate, and Human History

Le volcanisme contribue au développement de l'humanité; il ya un revers à la médaille: les volcans tuent, provoquent parfois d'effroyables catastrophes et à l'occasion, perturbent le climat.

(Patrick Barois 2004)

[Volcanism contributes to the development of humanity; but on the other side of the coin: volcanoes kill, sometimes cause horrible catastrophes, and on occasion disrupt the climate.]

Volcanoes and the Origin of Life

Volcanoes likely played an essential role in the origin of life early in the Earth's history. From the time of Darwin's idea of a "warm little pond" as a natural nursery for life, scientists have speculated that organic molecules, life's building blocks, could form under natural conditions, perhaps aided by phenomena such as lightning and volcanic activity. In 1953, Stanley Miller and Harold Urey replicated Earth's primitive, reducing atmosphere in a pressure flask – a mixture of methane, ammonia, water and hydrogen instead of carbon dioxide, nitrogen, oxygen and water. Subjecting this brew to electrical discharges, the two chemists produced glycine and alanine as well as (quite likely) other amino acids (Miller 1953). Yevgennii Markhinin (1980) later coined the term **biovolcanology** to describe the possible interactions of volcanic activity and biology, and discussed the unique chemical environments primordial volcanoes could have provided for the development of life. He proposed that before free oxygen appeared in the Earth's atmosphere, lightning from Plinian eruption clouds may

Volcanoes: Global Perspectives, 1st edition. By John P. Lockwood and Richard W. Hazlett. Published by Blackwell Publishing Ltd.

have catalyzed the formation of organic molecules from the Precambrian atmospheric soup of CH_4 , H_2 , H_2O , CO_2 , and N_2 . In the same vein Johnson et al. (2008), using an apparatus also coincidentally developed by Miller in the 1950s, modeled a steam rich, electrically active eruption column to produce some 22 amino acids and 5 amines. They demonstrated that a reducing global atmosphere wasn't necessary to build these molecules. Localized prebiotic chemical synthesis could take place even in an atmosphere more like today's, noting:

In . . . volcanic plumes, HCN, aldehydes, and ketones may have been produced, which, after washing out of the atmosphere, could have become involved in the synthesis of organic molecules. Amino acids formed in volcanic island [arc] systems could have accumulated in tidal areas, where they could be polymerized by carbonyl sulfide, a simple volcanic gas that has been shown to form peptides under mild conditions.

Recent discoveries of simple life forms (bacteria) living within hydrothermal vents on under-sea volcanoes – so called **hyperthermophilic environments** – has stimulated exciting new thinking about the possible range of volcanic settings in which life might have arisen (see, e.g., Huber & Wächtershäuser 2006). Perhaps instead of Darwin's warm little pond or tidal pool, a "warm little sea" (or at least a portion of that Sea) hosted the world's first biological ecosystem instead.

In any event, none of these discoveries tells us with certainty what provided the "spark" that got life going. Whether this magic spark was struck under the guidance of a Higher Power or was a natural happening is best left for religious authorities and philosophers to argue, but either way, volcanism is one likely provider of the crucibles in which life first began. Further important thoughts about how **abiotic** chemistry may have transitioned to *biochemistry* were given by Miller and Orgel (1974).

Once established, natural processes of selection will favor the most successful life forms, and it has been suggested that volcanoes accelerate evolutionary processes even today, by creating isolated ecological niches where limited numbers of individuals and restricted gene pools magnify the importance of random mutations in forcing evolutionary adaptation (Carson et al. 1990).

Volcanoes, Atmosphere, and Climate

Economist Kenneth Boulding (1968) popularized the concept of "Spaceship Earth," which asserts that our planet's life-support system is based upon natural cycles of matter and energy that are fully interlocking. One component of the system cannot change without all others ultimately being affected. Life developed and evolved through exploiting these cycles. It modified them favorably, if perhaps unwittingly, in the process. Because of the integration of life with natural fluxes, Earth System scientists, who study Spaceship Earth holistically, refer to these fluxes as **biogeochemical cycles**.

A good example of a biogeochemical cycle is the natural flux of water, which geologists call the **hydrological cycle**. This flux is powered by solar energy and gravity: Water evaporates

from water bodies, rises over high land, cools and precipitates to feed streams and rivers or groundwater which eventually return the water to places where it can evaporate again. Water is essential for life, being a vital ingredient in the transport of nutrients and construction of cells, tissues, and other organic structures. Irrespective of how the water is ingested, it does not remain long in any given organism. Plant leaves, for example, continuously yield water vapor via evapotranspiration, which contributes significantly to the notable haziness seen above many forests.

Volcanoes play a critical role in biogeochemical cycling. It is fair to say, in fact, that Earth's life as we know it might not exist without volcanic activity. It is beyond the scope of this book to explore fully the reasons for this, but it is worth surveying two examples; the **carbon** and **sulfur cycles** to illustrate the point (Fig. 13.1).

CARBON DIOXIDE

Carbon dioxide is a **greenhouse gas**, meaning that it acts to make the atmosphere warmer than it would be if sunlight re-radiated directly back into space after reaching Earth's surface. The ground converts many wavelengths of solar energy to infrared radiation, which we feel as heat. Escaping back into the air, the infrared radiation is absorbed and re-radiated by various gases, so that atmospheric residence time of this energy is prolonged, making conditions warmer. Though present in only 390 ppm in the atmosphere, but increasing at 2 ppm/yr (largely reflecting human combustion of fossil fuels), carbon dioxide is one of the most effective gases in this regard, and one whose CO₂ concentration is greatly sensitive to changes in the **carbon cycle**, which is the continuous exchange of CO₂ between the atmosphere, oceans, and life. Volcanoes are major sources of CO₂, and as such are an important factor in this global balancing.

Carbon dioxide combines with water through metabolic reactions to make organic compounds. Photosynthesis by plants is a very straightforward example of this. Hence, much CO₂ that otherwise would end up in the air is instead stored in organisms, especially vegetation. CO₂ is also absorbed by seawater. The colder the seawater, the greater its capacity for retaining dissolved carbon dioxide. Much of the deep-marine carbon storage may take the form of methyl hydrate crystals, the possible mining of which concerns many environmental scientists.

In epochs when temperatures are great, rates of evapotranspiration and biochemical reactions increase, favoring blossoming of plant life and greater storage of carbon dioxide. Greater biomass mitigates warming by reducing greenhouse retention of heat – a negative feedback process that has been vital throughout the latter part of Earth history. However, warmer atmosphere also means warmer seas, so that oceanic degassing can lead to an enhanced level of CO₂ in the atmosphere despite the increase in biological activity. Ice ages have come and gone at least 17 times over the past 2.4 million years, forced in large part by changes in Earth's orbital revolution, tilt, and albedo. During the most recent ice age temperatures were 4–5°C cooler than at present, terrestrial biomass was considerably reduced, and atmospheric CO₂ levels were less by about 120 parts per million. Ocean–atmosphere interaction has also been important throughout this period.

Volcanoes are critical as an abiotic source of “new” CO₂ for atmospheric balance. As life respire or dies and decays, CO₂ returns to Earth's atmosphere, completing the carbon cycle. But the cycle is far from perfect owing to the fact that dead organisms require oxygen to decay.

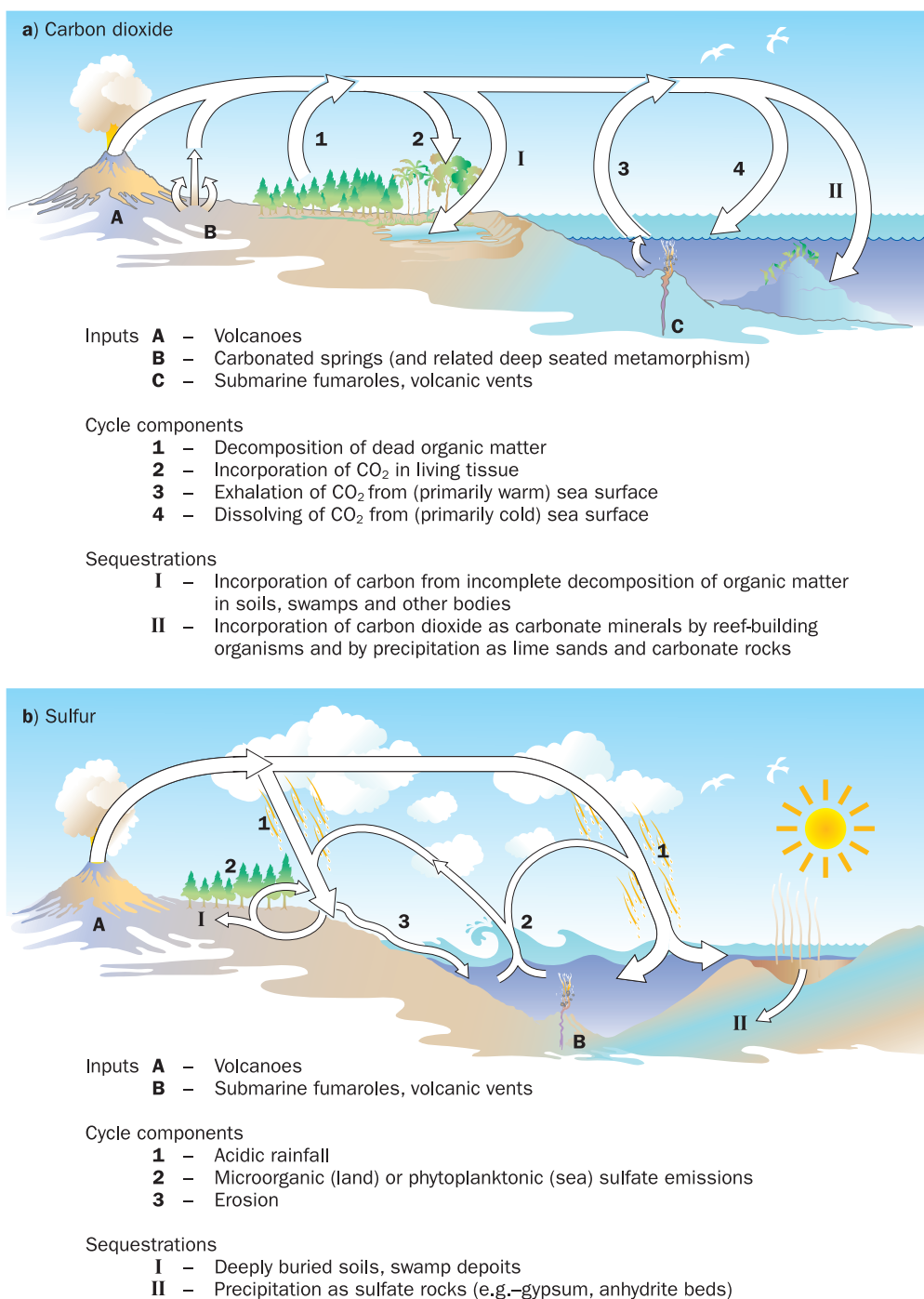


Fig. 13.1 The role of volcanoes in the global biogeochemical cycles of carbon dioxide and sulfur.

Beneath piles of litter or sediment in deep, stagnant water, organic remains accumulate, ultimately converting to coal, petroleum, gas, or limestone. Along convergent plate margins, much of this material – especially limestone – is subducted. Weathering of silicate minerals also removes CO₂ from the atmosphere. Hence, carbon dioxide is “scrubbed” from the system. In fact, Holland (1978) calculated that without replenishment the atmosphere would lose all

of its carbon dioxide in only about 10,000 years – and within the oceans in about 500,000 years, at given current rates of natural removal. Metamorphism, volcanic outgassing, and other important natural feedbacks step in to replenish the supply. Contemplate this for a moment, and one appreciates more deeply the ecological and physical balances of Boulding's "Spaceship Earth."

Of course, the rate of volcanic CO₂ production has not been constant through long spans of geologic time – or even on a decadal basis. The late Cretaceous period, around 65–80 million years ago is a notable contrast to the present. At that time the continents were arrayed in such a way that no Arctic Ocean existed. Warm equatorial waters could mix with polar seas to produce a higher mean ocean temperature than at present. This contributed significantly to the build up of CO₂ in the atmosphere. Moreover, the super-continent of Pangaea had broken apart as heat trapped beneath this enormous landmass finally weakened the lithosphere, stimulating intensive sea-floor spreading. The level of volcanism worldwide was considerably greater than the average for at least the past half-billion years. This activity, too, augmented the large amount of CO₂ in the atmosphere – perhaps four times greater than the current level. Since it is conceivable that human industrial activity could add just as much carbon dioxide to the air we breathe over the next few centuries, it is worth reflecting that during late Cretaceous time temperatures at the North Pole were not unlike those of Washington State today. Conifers flourished around the pole and tropical flora existed above the Arctic circle (Flannery 2001).

SULFUR

Like carbon dioxide, the annual global production of volcanic sulfur is something for which we humans may be grateful, since it facilitates protein development in our bodies and that of all other living organisms. The sulfur cycle is considerably more complex than the carbon cycle in large part due to the multivalent nature of sulfur. Volcanic sulfur is released primarily as SO₂, which can adhere to ash particles or dissolve in atmospheric moisture to precipitate later as acid rain or mists containing a mixture of H₂SO₄, H₂S, and sulfate ions (SO₄⁻²). Ultimately, then, volcanogenic sulfur becomes an important component of soil and soil pore water. Sulfate ions are also the dominant form of sulfur where it is present in water bodies and seas.

The fates of sulfur on land and in the sea differ significantly. On land, nutrient recycling by growing and decaying vegetation maintains a reservoir of sulfur to support ecosystems. Deforestation and erosion can disrupt this supply. Microorganisms are important for breaking down sulfur-bearing compounds from decaying organic matter, making sulfur available for living plants to rescavenge. Sulfates may be returned to the air as a part of this microorganic activity, so recycling is not 100 percent efficient. In the oceans, too, marine life incorporates sulfur, primarily through processing by phytoplankton which is then consumed at higher levels in the food chain. Shallow sea temperatures and nutrient supply in turn regulate phytoplankton activity. High surface temperatures dampen nutrient upwellings that nourish marine life. But in counterbalance, phytoplankton releases sulfur back to the air in the form of dimethylsulfide (DMS), which drifts inland as wave-tossed sea spray to fertilize coastal soils, and plays an even more important role, perhaps, by nucleating water droplets to form clouds.

This in turn helps cool the atmosphere by increasing reflection of sunlight back out into Space. DMS production, together with the thermal properties of water helps explain the moderating effects of oceans on the global environment.

As in the case of the carbon cycle, natural mechanisms exist to sequester sulfur and prevent the build up of an intolerably acidic atmosphere through continuing volcanic activity. On land, organic decay in oxygen poor swamps and bogs is incomplete and considerable amounts of sulfur end up locked in plant remains, eventually to form sulfur-rich coal deposits such as those found in southern China. Since sulfate is the second most abundant dissolved ion in the oceans (after carbonate), evaporation in warm, shallow gulfs and lagoons, called **sabkhas**, forces precipitation of sulfate minerals such as gypsum and anhydrite. At certain times in geologic history, truly enormous supplies of these minerals have accumulated. The sulfate beds of the Delaware Basin, formed by evaporation of a shallow Permian sea in western Texas 250–280 million years ago is one example. More recently, repeated evaporation of the Mediterranean at the close of Miocene times (5–7 million years ago) produced gypsum beds as much as a kilometer thick. Volcanism counteracts this sequestration of sulfur, while biological activity acts to modulate the level of sulfur build-up in the atmosphere at any one time, generally at levels that favor the continuation of life.

Vast amounts of sulfate aerosols produced by Plinian or flood basalt eruptions may penetrate the tropopause at the base of the stratosphere. On the laterally moving air masses at this level in the atmosphere, aerosols from a single great eruption may spread worldwide. Distribution largely depends on the latitude of the eruption. At high latitudes a volcano might lie pole-ward of the subtropical jet stream, and since mixing of the air masses to either side of a jet stream is sluggish, its aerosols are likely to be restricted mostly to the hemisphere (north or south) in which it lies. Large eruptions near the equator are more likely to spread their sulfates worldwide because of trans-hemispheric circulation.

Volcanoes are also major sources of significant quantities of sulfur gases that do not reach stratospheric levels. Most active volcanoes emit some sulfur continuously through fumarolic activity (Chapter 3). Kilauea volcano [16] is particularly productive, and is currently (2009) erupting an average of 1250–1500 tonnes of sulfurous gases daily. The sulfur is emitted from two primary sources, one directly over Kilauea's summit magma chamber (Halema'uma'u crater) and Pu'u O'o – a lateral vent on the volcano's East Rift Zone (Fig. 13.2). It is estimated that the world's volcanoes produce between 1.5 and 50 Tg SO₂ per year, varying because of episodic explosive eruptions that insert much larger amounts into the stratosphere (Texter et al. 2004).

The lower stratosphere does not readily mix with the convective air masses closer to Earth's surface. Hence, hazes of volcanic aerosols introduced by great Plinian and flood basalt eruptions may persist at this high altitude (15–20 km near the equator, 10 km in polar regions) for as long as several years. Like ordinary water clouds, volcanic aerosols increase Earth's albedo (reflectivity), cooling the atmosphere so much that they have significant impacts on global climate (Rampino & Self 1984). Because large volcanic eruptions are not frequent, these impacts are historically noteworthy. As mentioned in Chapter 6, for example, the largest historical flood basalt eruption took place in south-central Iceland with opening of the 57 km long Eldgjá fissure in 934 CE. More than 19 km³ of basalt lava poured out episodically over a period of 3–8 years, forming flows as long as 40 km, and as wide as 20 km. Degassing of these

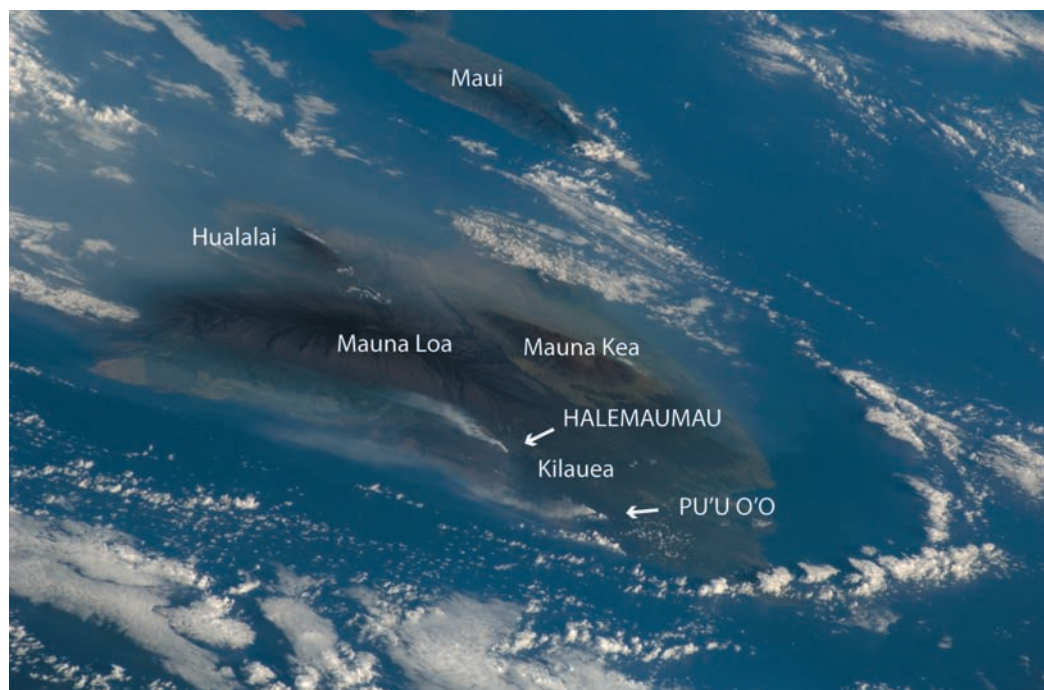


Fig. 13.2 Volcanic gas emissions from Kīlauea volcano, Hawai‘i, as viewed by astronauts from the Space Shuttle Atlantis on May 13, 2009. View to northwest shows Maui island in background, and conversion of H_2O and SO_2 plume from Halema‘uma‘u and Pu‘u O‘o vents to brown particulate-rich “vog” as it collects downwind of Hawai‘i Island, and circles around north side of island. Note “bow wave” of clouds forming upwind of island. Photo courtesy of Image Science and Analysis Laboratory, NASA-Johnson Space Center (STS-125-E6569).

flows produced about 35 megatons of SO_2 , all of which remained within the lower atmosphere around Iceland. The sulfur output directly from eruptive vents was much greater, and had widespread climatic impact. Thordarson et al. (2001) estimate that the vents dumped 185 megatons of SO_2 into the upper troposphere and stratosphere. Combined with water, this corresponds to a potential yield of 450 megatons of H_2SO_4 aerosol. Reports of moist dust and sulfur particle fogs came from Europe and the Middle East in 934–9 CE) as the fume from the eruption spread across the Atlantic. In China, half way around the world, a string of intensely hot summers simultaneously killed hundreds in Luoyang, capital of the Later Tang Empire, and in the four years following the eruption, severe winters and locust-plagued summer droughts starved many thousands, leading to collapse of the central government (Fei and Zhou 2006).

Two factors muted the potential impact of the Eldgjá gas release. One is the extreme northerly location of Iceland. Sulfates were apparently swept up in the westerly jet stream and largely confined above $30^\circ N$ latitude (Lamb 1970). The other is that the Eldgjá eruption took place over several years, allowing atmospheric mixing to reduce sulfate concentrations below the levels that would have occurred had the volcanic activity taken place all at once. Thordarson et al. (2001) calculate that an instantaneous release of 185 megatons of sulfur compounds to the lower stratosphere would cause global atmospheric cooling of about $1.2^\circ C$. To put things in perspective, the difference between current mean atmospheric temperature and that near the close of the last Ice Age is only about $4\text{--}5^\circ C$.

The 1600 CE eruption of Huaynaputina volcano in southern Peru was perhaps the largest eruption of the past 500 years, also had major global impact, which has so far received little scientific attention. It produced almost 20 km^3 of tephra, which blanketed an area of

Image not available in the electronic edition

Fig. 13.3 Norwegian painter Edvard Munch's *The Scream* – possibly influenced by the atmospheric effects of the 1883 Krakatau eruption. Reproduced with permission from Erich Lessing/Art Resources, New York; National Gallery, Oslo, Norway.

at least 300,000 km² (de Silva & Zielinski 1998), depositing ash and sulfuric acid aerosols in Antarctica and probably aerosols in Arctic ice too. Tree ring analyses and historical accounts suggest that this eruption caused the coldest summers in the past several hundred years, compounding Little Ice Age cooling trends.

The more recent eruptions of Tambora [103] (1815), Krakatau [98] (1883), and Pinatubo [104] (1991) each caused major global cooling. These were equatorial, highly explosive eruptions, each injecting the stratosphere with millions of tonnes of fine ash, aerosols, and sulfate particles. Each eruption was also less energetic, though more powerful than the Laki [71] outbreak. The Krakatau eruption, in particular, impressed European observers with remarkable, smog-like, sunsets and silvery midday skies. This inspired a number of paintings, possibly including the lurid sky in Edvard Munch's famous work *The Scream*, which he painted in 1893 (Fig. 13.3). In Poughkeepsie, New York and New Haven, Connecticut, fire companies were turned out by local alarms from panicked citizens misconstruing lurid volcanic sunsets for large fires (Simkin & Fiske 1983). For over an hour after sunset the western skies continued to show a bright yellow, orange, or red band from sunlight reflecting off high-altitude aerosols, a phenomenon known as **noctilu-**

cence. Sunrises were also affected, and over three months after the May 20 eruption, Reverend Sereno Bishop in Honolulu related the following observations from friends in the Caroline Islands (Simkin & Fiske 1983, pp. 155–6):

They state that, while they were dressing their children on the morning of September 7, the natives came anxiously asking what was the matter with the sun, which rose over the mountains with a strange aspect. It was cloudless, but pale, so as to be stared at freely. Its colour Dr. Pease called a sickly greenish-blue, as if plague stricken. Mrs. Pease's journal described it as "of a birds-egg blue, softened as this colour would be by a thin gauze. Around the sun the sky was a silvery-gray. At the altitude of 45° the sun appeared of its usual brightness, but resumed its pallid green aspect as it declined in the west."

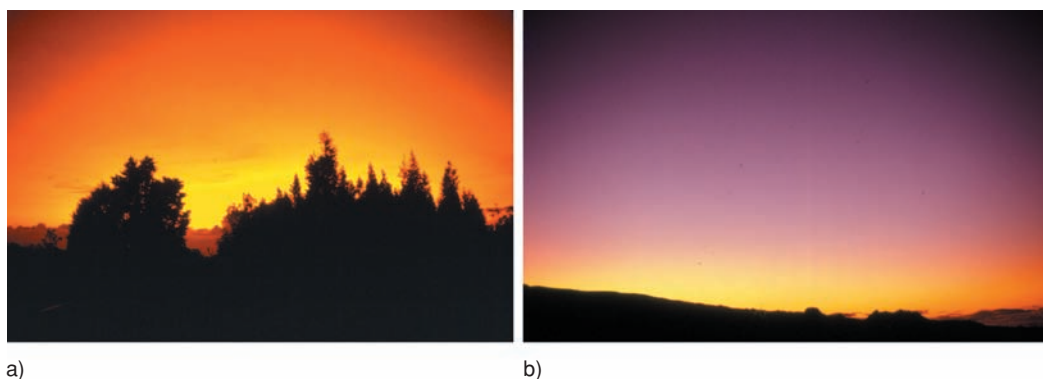


Fig. 13.4 Atmospheric effects of the April 4, 1982, El Chichón eruption, as observed from Hawai'i two weeks later. This eruption released abnormally large amounts of SO_2 into the stratosphere, causing anomalous conditions that persisted for many months in the northern hemisphere. Photos by J. P. Lockwood.

Reverend Bishop also made the first, and perhaps most literary descriptions of another optical affect of Krakatau's volcanic aerosols, a corona or circular patch of hazy white or bluish-white light enclosing the sun. The coronas Bishop observed extended to an angular distance of as far as 20° from the sun, and were fringed with a faint ring of red, brown, pink, or orange color, now termed a **Bishop's ring**. Bishop's rings were most intense a year following the Krakatau eruption, but continued to be seen for as long as three years. The radius of Bishop's rings, and of the corona they enclose, is inversely proportional to the size of the aerosol particles which produce them by means of diffraction and reflection of incident sunlight (Bary & Bullrich 1959). Similar, but much less dramatic visual displays were associated with the 1982 and 1991 eruptions of El Chichón [45] (Rampino & Self 1984) and Pinatubo volcanoes (Fig. 13.4).

Given the well-known short-term climatic impacts of these large historical volcanic eruptions, is it possible that much larger prehistoric eruptions had much greater impacts? This question tempts scientists seeking to explain various mass extinctions observed in the fossil record. Of particular interest are the gigantic flood-basalt eruptions that formed the Deccan Traps in central India and the even more voluminous submarine Large Igneous Province (LIP) eruptions of the late Cretaceous. Much of this intensive volcanism took place within a million years of the extinction of the dinosaurs and most other large animal species living at the end of Mesozoic times. The extinctions created huge niches in the environment ultimately filled by mammals and birds. Was so much sulfur released by this volcanism that the world plunged into an altered climatic regime – a prolonged “volcanic winter”? Only a few years of cooler temperatures imposed on a tropical world could have had devastating impacts through disruption of reproductive cycles, photosynthesis, and food chains. Acidification of rainfall and atmospheric moisture would be especially hard on photosynthesis, while polluted waters could impact terrestrial and even marine biota (Officer & Drake 1983). The correlation between these great volcanic events and the extinction of the dinosaurs is compelling, and certainly reinforced by the fact that as *individual* phenomenon, LIP eruptions show strong correlations with four other major extinction events between 300 and 150 million years ago. The eruption of the Siberian Traps of eastern Russia, mammoth flood basalt eruptions at the end of the Permian period 250 million years ago, coincides with the largest-known mass extinction in Earth history, when 90–95 percent of all living species became extinct (see, e.g., Morgan et al. 2004; Rampino & Strother 1988). But the case is not watertight. For one thing, younger LIP events *cannot* be related to die-backs (Wignall 2005). Eruption of the voluminous

Columbia River basalts between 16 and 18 million years ago, for instance, produced no discernable breaks either in the North American or global fossil records. In addition, the Chicxulub meteor impact off Yucatan 60 million years ago, with its well-documented global impact (Alvarez & Zimmer 1997) clearly was catastrophic for the world of the dinosaurs. Improved paleontological data for the Cretaceous–Tertiary transition reveal that extinctions of both flora and fauna increase in severity toward its 100 km wide crater, now largely buried by younger limestone (Hildebrand et al. 1991; Flannery 2001). Perhaps the most that may be said with respect to the closely antecedent Deccan and mid-Pacific volcanism is that these eruptive episodes possibly stressed existing biota so that when the Chicxulub strike occurred shortly thereafter (geologically speaking), extinctions were worse than may otherwise have been (Frankel 1999; Arens & West 2008).

Volcanic Influence on Soil Fertility and Agriculture

Fertile soils have attracted human populations since the dawn of the agriculture nearly 11,000 years ago. Initial farming and grazing could take place in a wide range of environments, but depletion of soil nutrients by overplanting of crops and erosion has rendered, and continues to render, many of these areas sterile – a problem of mounting global concern that undermines the highly-applauded Green Revolution. In only a few geologic environments does natural replenishment of nutrients readily take place, often sustaining very fertile soils. One such environment includes the world's floodplains, such as that of the Huang He River in eastern China, the Euphrates-Tigris breadbasket of Iraq, and the Egyptian Nile. The other regions of renewable fertility are associated with the grey volcanoes of volcanic arcs, where frequent ash falls create fertile soils allowing in some cases for as many as three crop harvests per year. On train rides across the countryside of Java, one observes that the wealth of the towns (as measured by numbers of bicycles or quality of homes and clothing) increases wherever the train approaches a volcano – indicating the prosperity provided by farming in these areas. The most productive tea plantations in Java grow on ash-derived soils, and indeed about one tenth of the human population lives upon the soil products of volcanoes, especially around the Pacific Rim (Chapter 14). Many early civilizations, too, drew their wealth and power from the fertility of volcanic soils, including the Aztec, Inca, and Highland Maya in the Americas, and the Mataram of central Java (Newhall et al. 2000).

Rock and rock fragments contain almost all of the nutrients that plants and animals need to thrive, but the nutrients are locked up in crystalline minerals or glasses inaccessible for biological exploitation. Residual soils form in the same places as their original source materials through chemical weathering. They characteristically develop three main layers (A-B-C) over time, with the rate of layer development dependent upon the climate and rock type. In the humid temperate climate of northern Japan, the topmost fertile A-horizon may start to develop from a bed of volcanic ash within a century, and the underlying B-horizon, also a source of soil fertility within 100–500 years. The complete sequence, A-B-C is usually in place after about a thousand years, though development of a rich organic component in ash-soils (≥ 10 percent by weight carbon) may take 4000–5000 years (Wada & Aomine 1973; Ugolini & Zasoski 1979). Slower rates of weathering and soil development occur in other non-volcanic temperate regions,

and it may take as long as 20,000–100,000 years for clays – valuable primary nutrient sources – to form fully (Gibbs 1968).

Although rich in mineral nutrients, juvenile volcanic soils contain little nitrogen, but they yield abundant crops given appropriate fertilization. A key factor in their natural fertility may be the high, unsaturated water content of the soil, which helps promote rapid cation exchange. Volcanic ash soils (**andosols**) commonly support a wide range of crops, even within the same region. But the response of agriculture to fresh ash fall is not always positive. If tephra accumulation amounts to less than a few centimeters, the addition of ash will rejuvenate the soil by adding new nutrients without damage. Heavier accumulations bury the soil so deeply, however that without intensive tilling farmers must abandon their fields and wait for weathering to restore the land. That can take a long time indeed – possibly well past a lifetime. In the third-century CE, the explosive eruption of Ilopango volcano [48], El Salvador deposited tephra exceeding a meter thickness as far as 77 km from the eruption focus. Sheets (1979) estimated that it may have taken as much as two centuries for the land in the devastated area to recover to its pre-eruption productivity.

Tephra fall not only impacts, for better or worse, the agriculture of a region, but may greatly alter fisheries as well, with harmful implications for populations dependent upon them. Workman (1979, p. 346) notes:

Red salmon were beginning their annual run when Katmai [Alaska] erupted in June 1912. Salmon already in the streams of Afognak Island stayed there until they suffocated with their gills filled with liquid mud. About 4000 perished in the Litnik Stream Hatchery. Rains kept the lakes and streams muddy, preventing or delaying salmon from reaching their spawning grounds. A heavy rain in mid-August put so much ash in the water that salmon suffocated. . . . In this later run salmon were observed ascending the polluted streams a short way, going back to sea, then trying to ascend again, repeating erratic movement a number of times.

In the following year, however, salmon populations exploded, perhaps in response to the input of nutrients from volcanic ash entering their waterways.

Volcanoes have also provided unexpected resources for biologists who study the ecology and rates of forest growth. Dating of individual prehistoric lava flows that cross climatic zones governed by elevation, temperature, and rainfall have provided a boon to biologists who can evaluate details and rates of forest succession processes as a function of differing environmental factors (Vitousek et al. 1995).

Volcanoes and Human History

Volcanoes in the East African Rift System forged the ecological cradles in which primates began to walk upright and human species evolved. Although primates lived throughout much of Eurasia and the Americas throughout the Tertiary Period, it was only in the African East Rift System where hominid species evolved, and where modern humans first appeared. Volcanic activity in the East Rift frequently stressed the resident proto-humans there, isolated small populations, and together with tectonic deformation created new environmental niches, where

restricted populations needed to rapidly adapt in order to survive (WoldeGabriel et al. 2000). Fresh lava flows there also were a source of easily worked glassy rocks where tool-making could be learned, critical to the evolution of human intelligence and social structures. Volcanism played a vital role in our evolution.

It was also volcanism that possibly almost ended the human evolutionary experiment, when a catastrophic eruption 8000 km east of Africa caused worldwide climactic changes in Late Pleistocene time. The Ultraplilian super-eruption of Toba volcano [97] on Sumatra, 75,000 years ago (Chapter 8) injected vast quantities of ash and volcanic aerosols into the upper atmosphere, causing a volcanic winter that probably lasted for several years (Strothers 1984). Mitochondrial DNA studies have conclusively shown that human populations were drastically reduced about this time, and that only a few thousand individuals survived as ancestors of the billions of humans who inhabit the Earth today (Rampino & Self 1993; Ambrose 1998; Rampino & Ambrose 2000). The exact cause of this population “bottleneck” is not known, but the fact that the timing approximately correlates with the Toba eruption suggests that catastrophic climatic change may have been responsible for a famine that drastically reduced our ancestral populations.

Social Impact of Volcanic Eruptions

Volcanoes impact society in many ways. Their psychological influence throughout history extends beyond fear or respect for the unknown (which in some traditions motivated human sacrifices and religious worship) but also generates artistic respect for their beauty. Perhaps the first depiction of an erupting volcano is of Hasan Dagi [89], a now-dormant volcano on the Anatolian Plateau of central Turkey – from a fresco recovered in the ruins of 6200 year old Çatal Höyük, one of the world’s oldest known cities. Likewise, classical Japanese artists are renowned for their portrayals of Mt Fuji [113]. Volcanoes remind us that primal forces of nature are still operating in the world to change and create anew.

The physical impacts of volcanic eruptions can have major societal repercussions and displace or kill thousands of people. In 260 CE, a thriving, sophisticated Mayan culture occupied the highlands of what is now El Salvador when the above mentioned Ilopango Plinian eruption took place, forcing perhaps hundreds of thousands of survivors to flee to coastal Guatemala and Belize. The catastrophe shifted native trade routes far to the north, possibly bringing new wealth and power to such Lowland Mayan centers as Tikal in Guatemala and drastically altering the whole course of Mayan history (Sheets 1979).

Similar speculations have been made about the impact of the 1645–1625 BCE caldera-forming eruption of Santorini volcano [84] on the Minoan civilization (McCoy & Heiken 2000). Some archaeologists have proposed that this moderately violent (VEI = 6) late Bronze Age eruption, with its attendant tsunami and pyroclastic activity, so devastated Minoan power that a vacuum developed, stimulating the rise of Mycenae and the later Greek City States (Nixon 1985). Caldera collapse during the eruption probably submerged the center of the strategically central Aegean island of Thera, of which present-day Santorini is but a remnant, and with it buried the thriving Minoan settlement of Akrotiri – the “Minoan Pompeii.” The eruption possibly inspired the legend of Atlantis described by Plato, who wrote his dialogs

1300 years later (Friedrich 1999). Consider the following 1871 translation of Professor Benjamin Jowett (University of Oxford) from Plato's *Timaeus*:

Now in this island of Atlantis there was a great and wonderful empire which had rule over the whole island and several others, and over parts of the continent . . . This vast power, gathered into one, endeavored to subdue at a blow our country . . . but [then] there occurred violent earthquakes and floods, and in a single day and night of misfortune all [the] warlike men [of Atlantis] in a body sank into the earth, and the island of Atlantis in like manner disappeared in the depths of the sea. For this reason the sea in those parts is impassible and impenetrable, because there is a shoal of mud in the way, and this was caused by subsidence of the island.

Likewise, frequent explosive eruptions of Merapi in the eighth-tenth centuries CE apparently forced abandonment of the giant temple and political center of Borobodur and encouraged the decline of the Mataram culture (Newhall et al. 2000). Such impacts have ripple effects through all of subsequent human history.

The competition for volcanic resources has also had impacts on human affairs. Eastern Aleut peoples often fought wars over precious obsidian for spear points and other implements to use in their subarctic island outposts. They mined sulfur from fuming craters to use in starting fires – an important task in that wet, wood-deprived region – and used volcanic hot springs to cook fish, edible roots, and the meat of sea mammals (Workman 1979). The mining of magmatic silver from Laurion helped provide Athens with the wealth it needed to defeat the Persians at the Battle of Salamis. Likewise, the metals fashioned from subvolcanic ores in southern Spain financed and equipped the Carthaginians in the Second Punic War, which very nearly ended the Roman Republic. Renaissance Spain rose to power on a tidal wave of gold, plundered from American native peoples who had retrieved it from volcano-related placer deposits.

Perhaps the most archeologically important eruption in all of human history was the 79 CE outburst of Vesuvius [79], which buried the cities of Pompeii and Herculaneum, the port of Stabiae, and countless villas, farms, and fields within 20 km of the volcano. As though thrown into a time capsule, a portion of Roman society was preserved beneath thick Plinian tephra and PDC deposits (Fig. 13.5). The story of how these ruins were “found” after over 1500 years of burial is worth recounting. Digging of a canal in 1592 accidentally brought the first artifacts from Pompeii to light, but serious excavation did not begin until 1710 when Austrian Prince D’Elboeuf obtained statuary from a well dug by a peasant on land atop the site of Herculaneum. D’Elboeuf purchased the well site without realizing that a Roman city lay beneath his bucolic countryside property. But with mixed success in finding further statues, and continuing difficulty in digging through hard mudstone and tuff, he soon lost heart. Bullard (1976, pp. 204–5) describes what happened next:

The political fortunes of Italy now changed, and in 1735 Naples and Sicily came under Spanish rule. The eldest son of the King of Spain, 19-year-old Charles of Bourbon, became the absolute monarch of the Two Sicilies. The royal youth, much interested in fishing and hunting, acquired for his pastime the house that had formerly belonged to the Prince

Fig. 13.5 Temple of Jupiter, Pompeii, with Mt Vesuvius volcano in the background. Built in the second century BCE, this temple and the entire city of Pompeii was buried in 79 CE. The central areas of Pompeii were excavated during the nineteenth century, but unfortunately none of the original pyroclastic deposits that buried Pompeii were preserved until later cooperative work between archeologists and volcanologists. Photo by J. P. Lockwood.



*d'Elboeuf. Still in the house were many of the statues which d'Elboeuf had recovered from his diggings. In 1738, young King Charles married Maria Amalia Christini, whose father, Augustus III of Saxony, was a great patron of the arts . . . When the king brought his young queen to Naples, she was fascinated by the ancient statuary . . . and she begged her husband for more pieces. He organized a digging force, and work was started at the original well which d'Elboeuf had taken over from the peasant. The first discovery consisted of three pieces of a statue of a huge bronze horse. Next they found the torsos of three marble figures in Roman togas and another bronze horse. As work progressed, a flight of stairs was discovered, and on December 11, 1738, a plaque bearing the inscription *Theatrum Herculanensem* was unearthed. Thus, by sheer luck, it appears that d'Elboeuf had unwittingly hit upon the front of the stage of a theater, on which had collapsed, under the impact of the mudflow, the wall which served as wings and background, with its marble facing and numerous statues. This was one of the few spots, perhaps the only one, where sculpture was literally piled one piece upon the other. Thus Herculaneum was discovered.*

These archaeological discoveries strongly inspired writers, artists, architects, scholars of history, theologians and philosophers throughout the Western World. Such finely detailed artifacts as wall frescoes and graffitti, Roman glassware and plumbing, prepared foods, ornamented doors, furniture, tiled bathrooms, medical equipment, and the body molds of many people, and some of their pets, came to light in subsequent excavations. Many frescoes are practically as good as photographs in their depiction of Roman dress, manners, hobbies, mythology, taste, religious practice, and industry. As tragic as the 79 CE eruption was, had it not occurred this “voice” from the past would be missing, and our appreciation of early Roman

society would be much less personal and clear. Unfortunately, for the first two centuries of archeological exploration the pyroclastic deposits that buried these cities were only regarded as “dirt” to be removed and there was no volcanological effort to understand the nature of the 79 CE eruption (Chapter 7). This has now changed, much of that “dirt” is now being preserved (Fig. 13.6), and studies by Italian volcanologists, working in cooperation with archeologists, have led to much greater understandings of this tragedy and the details of the eruption, which involved precursory earthquakes, early Plinian tephra fall, and later devastating PDCs (Scandone et al. 1993).



Fig. 13.6 Human body preserved in pyroclastic surge deposits of the 79 CE eruption of Mount Vesuvius, at Pompeii. Note that the surge deposits formed a dune structure downcurrent from the body, which formed an obstruction to the PDC. Photo by J. P. Lockwood.

Dozens of archeological sites buried by volcanic pyroclastic deposits are now known in addition to Akrotiri and Pompeii, including the more recent discovery of a sixth-century Mesoamerican agricultural village known as Joya de Cerén, El Salvador (Sheets 2002), built in an area devastated by the large eruption of Ilopango 200–300 years previously. Cerén was itself destroyed (and preserved) by a small eruption from Loma caldera volcano, only 600 m north of the village. The on-going archeological investigations at Cerén, in cooperation with volcanologists, sociologists and agricultural experts, has provided a detailed insight into the daily lives and culture of these rural people, who lived on the edge of the Mayan empire. The village and surrounding fields were buried by about 4 m of tephra, which preserved household belongings and even food supplies. The well-preserved crops showed that the eruption occurred in mid-summer, probably on an August evening as villagers were finishing their meals. The eruption was probably preceded by large earthquakes and explosions that caused the residents to flee to safety, without any known victims. Volcanoes not only change history, but they preserve our past, and will likely continue doing so as future eruptions occur in an ever more populated world.

FURTHER READING

- Fisher, R. V., Heiken, G., and Hulen, J. B. (1997) *Volcanoes: Crucibles of Change*. Princeton, Princeton University Press.
- McCoy, F., and Heiken, G. (2000) *Volcanic Hazards and Disasters in Human Antiquity*. Boulder, Geological Society of America.
- Robock, A. and Oppenheimer, C. (2003) *Volcanism and the Earth's Atmosphere*. Washington, American Geophysical Union.
- Sheets, P. D. and Grayson, D. K. (1979) *Volcanic Activity and Human Ecology*. New York, Academic Press.

Chapter 13

Questions for Thought, Study, and Discussion

- 1 The environmental benefits of atmospheric carbon dioxide and sulfur compounds are very different. Explain.
- 2 In what ways can volcanic eruptions modify global climate?
- 3 Suppose that Earth lacked volcanism. How would our planet be different?
- 4 Look up and describe the biological role of amino acids.
- 5 Discuss the balance between beneficial and destructive impacts of volcanic eruptions.
- 6 Why are areas devastated by prehistoric eruptions sought out by archeologists for research excavations?

Chapter 14

Volcanic Hazards and Risk – Monitoring and Mitigation

*Los desastres naturales no existen.
Se presenta un desastre, no por causa de la Naturaleza,
sino por la falta de preparación por parte de la Sociedad.*
(Hugo Delgado Granados)

*[There's no such thing as natural disasters.
Disasters take place, not by Nature's hand,
but by the lack of preparation on the part of Society]*

For lower forms of life on Earth, volcanic activity must be of little long-term concern – eruptions either do or do not destroy them, they may or may not be able to flee their fates, and life goes on. For human beings, however, our higher awareness makes volcanic activity of long-term concern, since eruptions can alter our environment and impact our societies in dramatic ways. Modern science and technology have revealed that volcanic activity is a manifestation of natural processes and not the work of gods, and as such is subject to rational observation and limited control – in the sense that the detrimental impact of volcanic eruptions on human society can be greatly reduced (mitigated) by public education, advance planning, and in some circumstances by direct intervention in volcanic processes.

For me (JPL) volcanology was initially a “fun” career, and I regarded eruptive activity as “entertaining” and “beautiful” phenomena. Those perspectives changed dramatically one day in late November, 1985, when I was dropped by a helicopter with USGS colleagues on the outwash plains of lahar deposits about 5 km downstream from the ruins of Armero, Colombia

Volcanoes: Global Perspectives, 1st edition. By John P. Lockwood and Richard W. Hazlett. Published by Blackwell Publishing Ltd.

– a city that had been obliterated by lahars two weeks earlier. Human bodies are less dense than lahar sediments, float to the surface, and we were surrounded by the rotting remains of hundreds of the 23,000 people who had perished here on 13 November. I shall never forget the horrors of that day, nor the sudden realization that although eruptions may indeed be “beautiful,” they can also be deadly, and that “deadly” is not merely an abstraction involving ink on paper. Real people live on and near volcanoes, and their lives may well depend on the work we do as volcanologists. Volcanology can be “fun” but it is also serious business, and no matter what aspect of volcanology we pursue, we should never forget that the ultimate value of our research and study will be the contributions that allow our colleagues who may be faced with life and death situations to make better decisions, based on better understandings of “how volcanoes work.” Peterson (1996) estimated that nearly 10 percent of the world’s population lives on or near active volcanoes. The volcanic risk to most of these people is very low, but risks change as volcanoes become restless, and awareness of risk is important for public well-being. For these reasons, this chapter on volcanic hazards and risks is the most important of our entire book – this is the essence of “applied volcanology” – the interface between volcanology and the Society we all ultimately serve.

Hazards and Risk

The terms **hazards** and **risks** are too often used synonymously, but in fact they have very different meanings. “Hazards” describe natural or man-made processes that have the potential to wreak havoc whether humans are threatened or not, whereas “risk” describes the effects that those hazards may pose for people, property, or other features within a threatened area. A large eruption at a remote volcano may thus involve many **hazards** such as lava flows and explosive behavior, but if the area were unpopulated, there would be no **risk** to humans. Volcanic hazards are natural phenomena that will occur no matter what humans do, whereas volcanic risks are caused by humans who are “in the wrong place at the wrong time.” Hazards are usually described in general terms, such as “Hazards at X volcano include pyroclastic flows and lahars,” whereas risks are what most concern people, and are best expressed in semi quantitative terms, such as “The risk of lava flows impacting X area is about 35 percent / 1000 years.” Nothing much can be done to control volcanic hazards, but a great deal can be done to lessen volcanic risk to human populations and to their infrastructures through better planning and public education. Reducing volcanic risk and the losses caused by volcanic hazards is one of the most important challenges facing those volcanologists who deal with active volcanoes.

Active, Dormant, and Extinct Volcanoes

Volcanologists use various terms to describe the eruptive state or potential of a volcano. These terms are hardly “standardized,” however, and inconsistent use has led to scientific as well

as to public confusion. For most volcanologists, an **active volcano** describes a volcano that has erupted in humanly recorded history and has the potential to do so in the future. The problem with this definition is that the history of human observation varies greatly from place to place – from over 3000 years of written documentation in the Mediterranean area to less than 400 years for the preservation of oral traditions in places like Hawai`i. Other geologists consider any volcano that has erupted in the past 10,000 years to deserve being called “active” (Simkin 1984). For most of the public, however, an “active” volcano refers to a volcano that is presently erupting.

Dormant volcanoes are ones that have not erupted in historic times, but are known to have prehistoric eruptive recurrence intervals greater than the elapsed time since their last eruption. Dormant volcanoes may hide their potentials for eruptive activity very well, however, and may not even be recognized as volcanoes by local people, especially in tropical regions where heavy rainfall causes deep erosion, and vegetation grows quickly, obscuring signs of past activity. Examples include El Chichón volcano [45] (Fig. 14.1) in Chiapas, Mexico (which was considered extinct by many before a deadly eruption in 1982) and Mt Lamington [121] in Papua, New Guinea, which was not even recognized as a volcano prior to its catastrophic eruption in 1951 (Taylor 1958). **Extinct** volcanoes are those which are not expected to ever erupt again and show no signs of seismic nor fumarolic activity. To determine that a volcano is safely extinct, however, requires field mapping to determine past eruptive history. If a volcano can be shown to have not erupted for periods of time *much*

longer than its past eruptive recurrence intervals, it is safe to call it extinct. A critical problem, however, is that most of the world’s volcanoes have not been mapped in sufficient detail to determine their past histories. Simkin and Siebert (1994) noted that “Some of the most calamitous eruptions of recent decades have been from volcanoes with no previously known



a)



b)

Fig. 14.1 El Chichón volcano, Chiapas, Mexico a) before the 1982 eruption, b) after the 1982 eruption had destroyed the cone. The 1982 explosive eruptions destroyed the preexisting summit lava dome, formed a crater about a kilometer wide and 300 meters deep, and formed devastating pyroclastic flows that killed about 2000 people in the villages surrounding the volcano. The volcano was not recognized as such by the local people living in this area. Photos a) by Paul Damon and b) by R. I. Tilling.

historical volcanism,” and showed that of the 16 largest eruptions of the past 200 years, 12 had no previously known historical activity! As an example of a “lurking” volcano, Chaitén (southern Chile) [55], had not erupted in over 9000 years and was thus considered to be extinct, but came back to life with little warning in May, 2008, with a VEI = 3 eruption that caused widespread damage. Connor et al. (2006) warn that “It is incorrect to assume that volcanoes that have not been active during the Holocene are incapable of future eruptions.”

Volcanic Hazards

Volcanic hazards can be divided into two classes: **Primary Hazards** – eruptive phenomena directly related to volcanic activity, and **Secondary Hazards** – those phenomena indirectly related to the eruptions themselves. Secondary hazards may be triggered immediately by eruptive activity, or may develop many years or even decades after eruptive activity has ceased.

PRIMARY VOLCANIC HAZARDS

Lava flows, volcanic gases, and localized airfall of spatter and other tephra are the primary hazards associated with effusive activity of “red volcanoes” (Fig. 14.2). Primary hazards associated with explosive “grey volcanoes” include pyroclastic density currents (flows and surges), the widespread deposition of airfall tephra, and the threats posed by volcanic ash to aviation. Most of those primary hazards associated with volcanic eruptions have already been discussed at

Fig. 14.2 View of Goma, eastern Democratic Republic of Congo, after fluid lavas poured through the city in 2002. Nyiragongo volcano, source of these lavas, looms over the city in the background. Highly fluid pāhoehoe lavas flowed around and through buildings, but ‘a`ā flows crushed any structures they encountered. Photo by J. P. Lockwood.



length in Chapters 6, 7, and 8, and will not be further described in this section. We turn instead to aviation hazards.

Volcanic ash hazards to aviation

Explosive eruptions can send large amounts of volcanic ash and aerosols as high as 40 km into the stratosphere, where it may persist for weeks and completely circle the globe (Chapter 7). Volcanic ash was not a major problem for commercial aviation prior to the jet age, since internal combustion engines ingest less air and operate at lower temperatures than do jet turbines, and prop-driven aircraft fly at lower altitudes and speeds. As introduced in Chapter 1, the new risks to commercial aviation were first driven home to me (JPL) in 1982, when I inspected a damaged B-747 at Jakarta airport after it had made an emergency landing there, following direct encounter with an eruption plume from Galunggung volcano. The windshield of the aircraft was completely frosted and leading edges of the wings and engine nacelles were stripped of paint. Each of the engines had failed in flight before re-starting, and each had to be replaced. Two 747 aircraft entered the unseen plumes and were surrounded by static electrical discharges and filled with fine ash and sulfur gases as they flew into Galunggung ash clouds at night that summer, terrorizing the almost 500 passengers aboard these flights (Tootell 1985). Each 747 lost power in all four engines, each was able to restore power only after losing several kilometers of altitude, and each made emergency landings at Jakarta after heroic pilot efforts. Apart from the externally visible damage of impact abrasion from ash particles, more serious damage occurred within the jet turbine engines themselves, which operate at temperatures exceeding the melting point of silicic ash. Besides severe abrasion effects, ingested ash was melted within combustion chambers and redeposited in cooler areas, which caused the engine failure at high altitudes. Sulfur gases cause more insidious metallurgical damage that can result in weakened metals and subsequent failure. Besides the threat to aircraft and passengers, ash-producing eruptions can shut down airports for many days, disrupting air traffic and damaging ground facilities.

The international aviation community was greatly alarmed by the realization that this previously unrecognized severe hazard could cause future disasters. That fear was realized in 1989 when another B-747 flew into an ash cloud from Redoubt volcano, Alaska [21], lost all four engines, descended almost 5 km without power before restarting engines and making an emergency landing in Anchorage (Miller & Casadevall 2000).

International air routes are located downwind of hundreds of potentially explosive volcanoes throughout the world (Casadevall & Thompson 1995). The urgent need for an effective warning system, highlighted by the near disasters in Indonesia and Alaska, motivated extraordinary international cooperative efforts to warn pilots about inflight ash hazards and to predict the movement of ash plumes, which can remain threatening for thousands of kilometers downwind of erupting volcanoes. These efforts, largely led by the International Civil Aviation Organization (ICAO) with critical input from volcanologists, has resulted in the establishment of nine Volcanic Ash Advisory Centers (VAACs) around the world for around-the-clock operations to link volcano observatories, meteorologists, satellite monitoring agencies, and air traffic control centers. These VAACs must coordinate input from these agencies and provide inflight warnings to threatened pilots in near real-time, since explosive eruption ash plumes can reach the 9–11 km high altitudes at which jets travel in only a few minutes, and can jeopardize hundreds of flight operations downwind of these volcanoes within a few hours.

SECONDARY VOLCANIC HAZARDS

Volcanic eruptions commonly cause secondary hazards that are much worse and more widely destructive than the direct actions of the eruptions themselves. The list of secondary hazards is long, and includes the following:

- 1 **Lahars** (Chapter 11) have caused more loss of life than any other volcano-related hazard. Although lahars are not produced directly by eruptions themselves, they may be regarded as volcanic hazards because they generally require the presence of unstable pyroclastic material on steep volcanic slopes left by previous volcanic activity, or the presence of structurally weakened volcanic edifice rocks. Ash and other unconsolidated volcanic debris may be converted to lahars during eruptions by the melting of snow and ice, or may be mobilized by heavy rainfall or seismic activity years after the eruption (or eruptions) have “set the stage” for subsequent disasters.
- 2 **Debris avalanches and catastrophic sector collapses** (Chapter 11) are another major, but infrequent volcanic hazard caused by the fact that steep “composite” volcanoes are inherently weak and unstable edifices, vulnerable to gravitational collapse. Such collapses may be triggered by eruptive activity that deforms the volcanic edifice beyond the point of stability (e.g., the initial collapse of Mt St Helen’s [27] north flank on May 18, 1980) or could be triggered by large earthquakes unrelated to any volcanic activity.
- 3 **Tsunami** are deadly hazards mostly caused by submarine earthquakes unrelated to volcanic activity, but may also be caused by large submarine eruptions (e.g., Krakatau [98], 1883), or by massive volcanic debris avalanches or PDCs that enter the ocean or large lakes (e.g., Unzen [108], 1792). Tsunami are discussed in more detail later in this chapter.
- 4 **Floods** caused by failure of dams created by lava flows, debris avalanches, or pyroclastic deposits.
- 5 **Catastrophic carbon dioxide release** from limnic overturn of volcanic lakes – and other CO₂-related hazards. This subject is discussed in more detail later in this chapter.
- 6 **Climate change and atmospheric pollution** caused by large volcanic eruptions can cause disease and famine over great distances – even globally (e.g., Laki [71], 1783, Tambora [103], 1815). The relatively high content of fluorine salts absorbed on tephra has caused devastating mortality of grazing livestock after pyroclastic eruptions in Iceland (Blong 1984) and acid rainfall and fumes associated with eruptions can cause major damage to agricultural crops, as can the blanketing effect of fine tephra. SO₂ is a particularly destructive volcanic gas associated with both eruptive and quiescent periods, and has caused widespread damage to crops in Hawai`i and Nicaragua (Delmelle et al. 2004). Magmatic gases from active volcanoes undergo chemical changes as they migrate downwind, forming acids and particulate haze that may exacerbate respiratory diseases. Lava flows that contact seawater can cause hazardous secondary steam eruptions and liberate dangerous halogen gases.
- 7 Public health effects owing to **gas emissions** or the **inhalation of fine ash** are potential risks associated with eruptions of any volcano in populated areas, and include largely underappreciated mental health effects on stressed populations (Buist & Bernstein 1986).

Since lahars, debris avalanches, and climatic effects are discussed elsewhere in this book (Chapters 11 and 13), we now consider the hazards of volcano-related tsunami, floods, magmatic CO₂ emissions, and volcanic lakes.

Volcanogenic tsunami

While only 8 percent of the 7900 historically reported eruptions have occurred from submarine volcanic vents, they have caused about 20 percent of all recorded volcano fatalities (Mastin & Witter 2000). **Tsunami** (Japanese for “great harbor wave”) are giant sea waves, so large that their wave movements extend downward to the ocean floor. The depth of the sea, in fact, controls their speed. Individual wave sets may travel through the open ocean as fast as 800 km/hr (compared to a maximum speed of about 100 km/hr for ordinary wind-driven waves). The wavelengths of tsunami are as much as 160 km, with amplitudes of only a few tens of centimeters far out at sea (Dudley & Lee 1998). Hence, passengers on ships at sea might not notice the passage of tsunami waves beneath them. Near shore, however, all of this enormous energy is concentrated, causing wavelengths to shorten and wave crests to rise. In inlets and bays additional wave funneling creates abnormally high waves that may run kilometers up coastal valleys as they dispense their energy before receding. Most tsunami result from undersea tectonic earthquakes that cause vertical displacements of the seafloor or generate submarine landslides. These great waves will be generated only when the morphology of the seafloor below changes suddenly.

Volcanogenic tsunami are generated when large volumes of seawater are suddenly displaced by submarine or littoral eruptions or by collapse of volcanic edifices beneath or adjacent to the sea (Fig. 14.3). History records over 90 volcanogenic tsunami beginning with Pliny the Younger in his account of the 79 CE Vesuvius [79] eruption, who reported that water “withdrew” from the shore of the Bay of Naples, stranding fish and other marine creatures before a resurgence of the sea. During the May 8, 1902 eruption of Mt Pelée, Martinique [63], the pyroclastic flows that obliterated the city of St Pierre also entered an adjoining bay, generating small tsunami that entered the harbor of Fort de France, 25 km away.

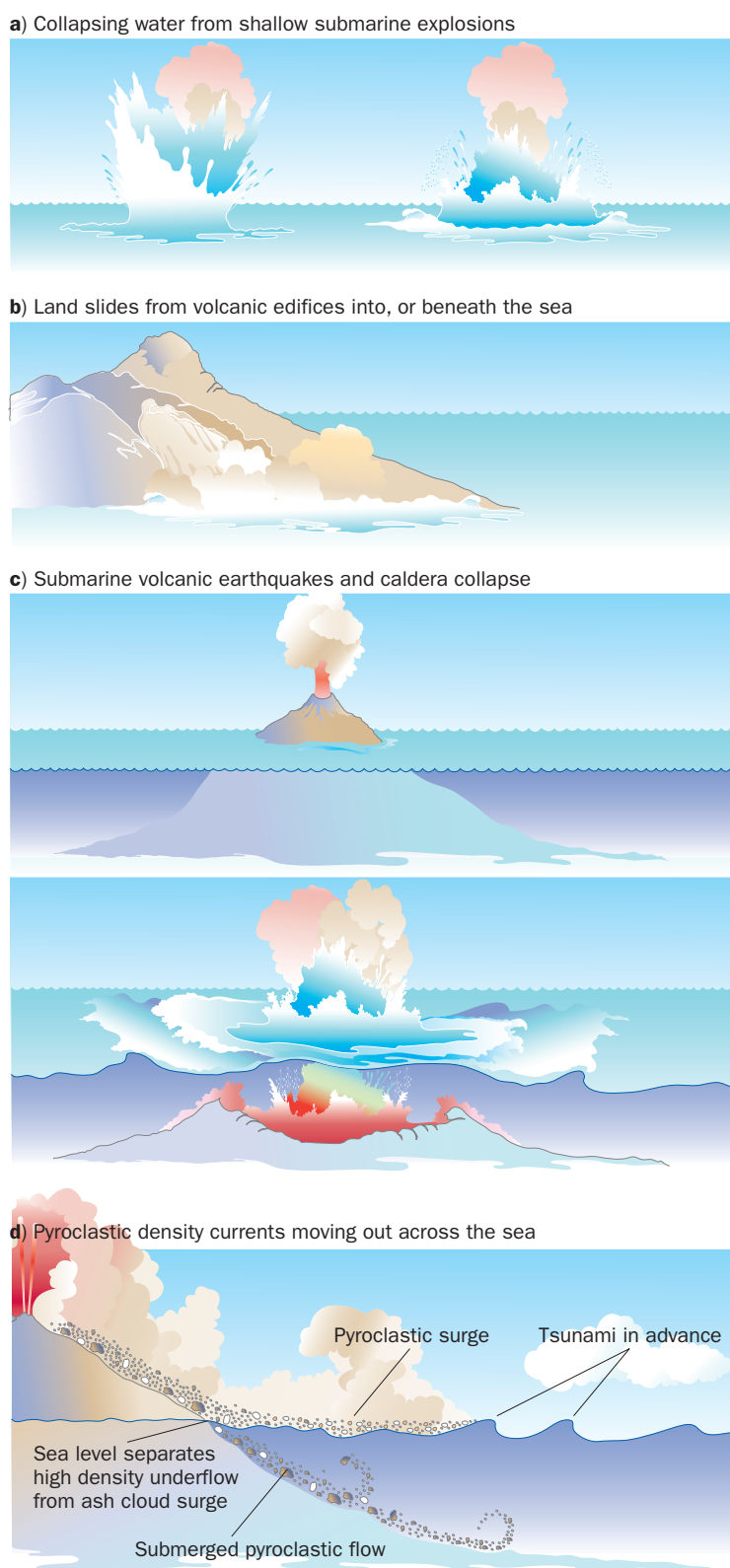


Fig. 14.3 Some causes of volcanic tsunami.

Of the approximately 60,000 tsunami fatalities related to historical volcanic activity, most were caused by two events. In May, 1792, after nearby eruptive activity, a steep dome making up part of the Unzen volcano complex in southern Japan partially collapsed (Chapter 11) forming a voluminous debris avalanche that reached the sea, setting up a series of giant tsunami waves. The waves destroyed 17 seaside villages, mostly across a bay from the destroyed town of Shimabara (Fig. 11.16). Damage was worsened by the fact that the disaster coincided with a spring high tide. 15,000 people died, and 80 km of coastline were devastated. In some inlets, wave heights reached nearly 60 m above mean sea level, a record for known volcanic tsunami (Dudley & Lee 1998).

An even more disastrous volcanic tsunami occurred during the 1883 Krakatau eruption in Indonesia. On August 26–27, when the culminating phase of the eruption took place, gigantic waves pounded the shorelines of the Sunda Strait, killing more than 36,000 people, all of them living near the coast or close to the coast. One of the loveliest ports-of-call on the marine route from Europe to Australia was Anjer, a colorful trading center with a dominantly Sundanese, Chinese, and Arab population on the west coast of Java, about 40 km from the volcano. The town was built at the end of a bay constrained by two ranges of hills, with a low agricultural plain stretching inland; a fine tsunami funnel in other words. On a Sunday afternoon, Plinian activity began, causing loud concussions and ground shaking throughout Anjer and other districts rimming the Strait. A black eruption column could be seen rising off the distant island, which soon spread to darken the sky directly above the town. One resident on the Java coast reported what happened a few hours later (quoted from Simkin & Fiske 1983, p. 73):

Before daybreak on Monday, on going out of doors, I found the shower of ashes had commenced, and this gradually increased in force until at length large pieces of pumice-stone kept falling around. About 6 a.m., I was walking along the beach. There was no sign of the sun, as usual, and the sky had a dull, depressing look. Some of the darkness of the previous day had cleared off, but it was not very light even then. Looking out to sea I noticed a dark object through the gloom, traveling toward the shore. At first sight it seemed like a low range of hills rising out of the water, but I knew that there was nothing of the kind in that part of the Sunda Strait. A second glance – and a very hurried one it was – convinced me that it was a lofty ridge of water many feet high, and worse still, that it would soon break upon the coast near the town. There was no time to give any warning, and so I turned and ran for my life . . . In a few minutes I heard the water with a loud roar break upon the shore. Everything was engulfed. Another glance around showed the houses being swept away and the trees thrown down on every side . . . Struggling on, a few yards more brought me to some rising ground, and here the torrent of water overtook me. I gave up all for lost, as I saw with dismay how high the wave still was. I was . . . taken off my feet and borne inland [by the current] . . . I remember nothing more until a violent blow aroused me. Some hard firm substance seemed within my reach, and clutching it . . . I found myself clinging to a coconut palm-tree. Most of the trees near the town were uprooted and thrown down for miles, but this one . . . had escaped and myself with it . . . The huge wave rolled on, gradually decreasing in height and strength until the mountain slopes at the back of Anjer were reached, and then, its fury spent, the waters gradually receded and flowed back into the sea. The sight of

those receding waters haunts me still . . . As I clung to the palm-tree, wet and exhausted, there floated past the dead bodies of many a friend and neighbor. Unless you go yourself to see the ruin you will never believe how completely the place has been swept away.

This tsunami disturbed tide gauges as far away as La Havre, France, 16,000 km distant. Its debris, including trees packed with pumice and human remains, washed up on shorelines as far as 4000 km from Krakatau for months following. But what caused this calamity? Volcanologists have been divided about the matter. There are several possibilities. One obviously is the fact that over half of the island of Krakatau vanished at this time, engulfed by caldera collapse that created a large crater on the seafloor. Perhaps huge landslides off the scarp of Rakata volcano, the truncated remnant of the island, or submerged vertical fault rupture and mass wasting also played a role, as did the impact of pyroclastic flows on the sea surface (Latter 1981). At 15 localities around the Strait, including Anjer, the initial shoreline water movement was toward land, not the withdrawal that would be expected from seawater suddenly flooding a cavity opening in the seafloor. This suggests to some that the outward displacement of the ocean by submarine explosions caused the big waves. But not all localities showed initial tsunami insurgence (Dudley & Lee 1998). In fact, the Dutch engineer Verbeek (1885) described shoreline water as initially receding in many places, with currents flowing toward the volcano in the open Strait. One modern view suggests that the eruption's pyroclastic activity, as at Mt Pelée, was the main cause (Yokoyama 1981). Because of density differences, the dense basal ash flow components may sink and travel submerged along the sea bed, displacing large amounts of water like a submarine landslide, while the lighter ash cloud surge races out across the surface, also shoving water ahead of it like a powerful wind fan (Fig. 14.3d), while generating large amounts of steam. How far can a pyroclastic surge race across water? It is certain that a huge amount of ash and pumice traveled at least 10 km laterally from the vent, forming two temporary islets in water originally 35–40 m deep (Verbeek 1883). At Katimbang on the southeast cape of Sumatra 40 km from Krakatau, a Dutch official and his family barely escaped with their lives while the ordeal in Anjer was unfolding. With 15 m high tsunami striking the shore, they fled inland and took refuge in a mountain hut, but were seriously burned by scalding ash gushing through openings in the floor of the shelter. Given their account, it seems certain that an energetic surge traveled across the sea the 40 km between the vent and Katimbang, ultimately ending on the flanks of Raja Bassa mountain where the Dutch official and his party had taken shelter (Self 1992; Simkin & Fiske 1983; Yokoyama 1981). Despite questions about the exact origin of the Krakatau tsunami, it is certain that underwater volcanic explosions, in fresh water lakes as well as the sea, have the potential to generate tsunami (Mastin & Witter 2000).

Carbon dioxide hazards

This section on CO₂ hazards may seem over-emphasized, in light of the fact that other volcanic processes kill many more people most years. The dangers of CO₂ emissions are, however, greatly underappreciated by most volcanologists and others who work around active volcanoes, and we feel the risks involved are worth discussion. Dozens of people are poisoned by CO₂ around volcanoes each year, but the causes of their mysterious deaths are commonly unrecognized, or are incorrectly attributed to “asphyxiation”. More than 150 people were killed

by CO₂ on the Dieng Plateau, Indonesia [100] in 1979 (LeGuern et al. 1982), and at least 1800 people died in 1984 and 1986 downslope from Lakes Monoun and Nyos [77], Cameroon, when deep volcanic lakes overturned and released vast amounts of CO₂ (see following section).

Although CO₂ is an essential minor component of the Earth's normal atmosphere, critical to regulate pulmonary functions in animals, and is an energy source for plants, it is poisonous to plants and animals when concentrated. It normally comprises about 0.4 percent of the atmosphere, although its concentration is slowly increasing, owing to human activities. At atmospheric concentrations above 3–4 percent serious physiological effects are noted in humans, and the Immediately Dangerous to Life or Health (IDLH) concentration has been set at 40,000 ppm (NIOSH 1994). The anesthetic properties of carbon dioxide have long been noted by anesthesiologists, and humans will lapse into unconsciousness when CO₂ exceeds about 6 percent of the air they breathe. At CO₂ levels above 8–10 percent (varying with individuals) neurological reactions will cause respiratory failure and death. People who unwittingly venture into areas of concentrated CO₂ and die are thus not “asphyxiated,” since there is adequate oxygen available – they are poisoned.

CO₂ is one of the three most abundant volatile constituents of magmas – along with H₂O and SO₂ (Chapter 3). It is a highly mobile gas, and normally diffuses harmlessly to the atmosphere over the surfaces of volcanoes either by dispersed migration through rocks and soil, or as a fume component at eruptive vents and fumaroles. So long as the CO₂ is dissipated over a wide area no hazard is created, but when emissions are concentrated or the gas is dissolved in the waters of deep lakes, hazardous concentrations may result. Concentrations of CO₂ in fumaroles or solfataras are usually low enough not to form significant hazards. CO₂ is the dominant gas in the less common fume vents called **mofettes**, however, where it may constitute more than 90 percent of the gases released. Mofette gases are typically cool, usually as cool as the surrounding air. When no wind or breezes are present, CO₂ may accumulate in hollows or small valleys, since it is a heavier-than-air gas, 1.5 times as dense as normal atmosphere. Because CO₂ is a colorless, odorless gas it may not be recognized as a hazard until too late.

Animals wandering into such pools of CO₂ may quickly lose consciousness and die (Fig. 14.4). A modern “death gulch” of this sort was found by early geological explorers in the Absaroka Range near Yellowstone National Park, and described by Thomas Jaggar in one of his early publications. Although wind circulation cleared out the CO₂ before the men entered the gulch, the bodies of several grizzly bears indicated the deadly potential of the place. More recently, the shallow rise of magma under Mammoth Mountain Volcano in east-central California, next to a popular ski resort, increased CO₂ content in the soils from an ambient level of 1.5 volume percent of soil gas to 30–90 percent, killing the forest in places, and leading to nausea and dizziness for people staying in local mountain cabins (Chapter 3). Three skiers were killed on Mammoth Mountain in 2006, when they fell through snow into a concealed mofette. Excavations near or beneath volcanoes are especially dangerous, and many people are killed in such places by accumulations of CO₂, most recently beneath Teide volcano [75] in the Canary Islands, where six people perished while exploring water tunnels beneath that volcano. Volcanic craters are especially hazardous places on windless days because they are closed depressions where CO₂ can concentrate, and dozens of people have been killed exploring craters within volcanic cones in Japan and at Rabaul volcano [122].



Fig. 14.4 Skeleton of dog in mazuku on the slopes of Nyamuragira volcano, Democratic Republic of Congo. Skeletons of vultures and other carrion-eating animals were also abundant. USGS photo by J. P. Lockwood.

Carbon dioxide mofettes are widespread along the East African Rift Zone, and are called **mazuku** in Swahili. The mazuku are places known for “evil winds” by local people, and are low-lying areas where dense CO_2 accumulates on windless days. Mazuku are frequently associated with sources of water, and in East Africa the myth of “Elephant Graveyards” is based on the fact that bones of elephants and other large mammals have been found in large concentrations in areas where mofettes are associated with volcanism. Mazuku are common around Nyiragongo [88] and Nyamuragira [87] volcanoes in the eastern Democratic Republic of Congo, and similar mofettes are also deadly places in Indonesia and Kamchatka (Fig. 14.5). On windless days carbon dioxide concentrations of up to 90 percent have been measured in these low-lying areas. Where not mixed by breezes the contact between the denser CO_2 and overlying air is commonly sharp, and one can see such boundaries because of the change in refractive index, and feel the higher density and viscosity of the gas. Because of its density, only places near the ground may be affected. Adults were able to safely walk across ground with flowing CO_2 currents at Dieng [100] in 1979, while most children collapsed and died, as did parents who stooped to save them. Intentionally breathing from a Kamchatka mofette (Dolina Smerti “Valley of Death”) in 1990 (while a friend stood by to retrieve me!) I (JPL) quickly became dizzy and almost lost consciousness, but breathing normal air revived me immediately. Volcanologist Tom Miller had his encounter with CO_2 poisoning in the summer of 1977 a few months after the Ukinrek maar [10] eruption, at a nearby place called “Gas Rocks” known for CO_2 mofettes. While squatting down next to a CO_2 “soda spring” he suddenly lost consciousness, but was saved by colleagues standing nearby. He writes: “What surprised me in particular was how fast and with no warning this all took place!” (Miller, 2008, pers. comm.).

Fig. 14.5 Carbon dioxide mofettes can be deadly places. Despite warning signs many people die in these low-lying places every year. a) Warning sign above a Nyiragongo volcano “mazuku” on outskirts of Goma, Democratic Republic of Congo. b) Warning sign below mofettes on the Dieng Plateau, Indonesia, in an area where 149 people were killed in 1979. Photos by J. P. Lockwood.



Local residents learn where mazuku are located and how to avoid them, but during the Rwandan refugee crisis of 1994, many passing travelers lost their lives in mazuku when looking for a place to sleep. Normal breezes will quickly dissipate the CO₂ and make the mazuku temporarily safe, but if the wind dies down, these places become deadly. Basements can also accumulate hazardous levels of CO₂ in volcanic areas, and one enterprising factory owner I met near Goma controlled rats by throwing food scraps into a deep hole excavated into soil beneath his basement!

Survival Tips for Field Volcanologists:

Craters or other closed depressions on young volcanoes can become “death traps” on windless days if substantial CO₂ has accumulated. CO₂ is a colorless and odorless gas and gives few warnings of toxicity. Whenever descending into craters or closed depressions on windless days – be careful!

Hazards associated with volcanic lakes

There are three principal types of volcanic lakes: those formed by the damming of streams or rivers by lava flows, debris flows, or PDCs; those occupying maars or other old, inactive craters; and those occupying the summit craters of active volcanoes. The first type form on the flanks of volcanoes, and pose hazards of flooding and lahars as vast amounts of impounded waters may be suddenly released when these dams are overtopped by rising waters. Pyroclastic surge deposits that dammed a pre-existing stream in Cameroon impound 50×10^6 m³ of water on the edge of Lake Nyos maar, and pose a significant hazard to populated areas downstream (Lockwood et al. 1988). Maar lakes pose a special problem because they are commonly associated with sources of magmatic carbon dioxide and may entrap and dissolve large amounts of CO₂ in their deep waters. This is not a problem in temperate climates, since seasonal temperature changes cause annual lake overturning that will release stored CO₂ before it builds to dangerous levels. In tropical climates however, especially near the equator, the lack of seasons may preclude natural lake overturning, and quasi-stable lakes may allow dissolved gas to build up to dangerous levels, posing the threat of catastrophic release of lethal amounts of poisonous CO₂. The 1986 gas release from Lake Nyos maar, Cameroon (Fig. 14.6) is a tragic example that killed more than 2000 people (Kling et al. 1987). Lakes that occupy the summit craters of active volcanoes are the most hazardous volcanic lakes of all. Summit crater lakes are particularly important to understand because they serve as chemical traps above magmatic systems, and may accumulate the heat and magmatic volatiles that would normally be released to the atmosphere. Such lakes are commonly extremely acidic, because of the ingress of SO₂ and HCl gases from the underlying magmatic systems (Fig. 14.7). Eruptive activity that might result in minor explosions and degassing activity at dry craters may result in the expulsion of



Fig. 14.6 Lake Nyos, Cameroon, eight days after the tragic overturn of August 21, 1986. More than 1500 people were killed by massive amounts of carbon dioxide gas that flowed downslope into populated areas after being released by overturning of the lake waters. The brown color of the water is caused by oxidation of the iron-rich deep waters that mantle the lake surface. Note the bare cliffs in the background, scoured of vegetation by water fountains and seiches that accompanied the overturn event. USGS photo by J. P. Lockwood.

large volumes of lake water and the generation of massive lahars – of the sort that have killed thousands of people on the flanks of Kelut volcano [102], Indonesia and Ruapehu Volcano [134], New Zealand. Means to mitigate the risks associated with each of these three lake types are discussed later in this chapter.

Volcanic Risk

Since 1700 CE, more than a quarter of a million people have perished in volcanic eruptions, almost a third of them during the past century (Simkin et al. 2001). However, volcanic eruptions, despite their violence, are not at the top of statistical lists of hazards. Traffic accidents in the United States alone usually kill many more people every year than volcanoes do worldwide! Although the risk to human life posed by volcanic eruptions appears to be less than that of other hazards such as earthquakes, tsunami, and floods, that perception is based

Fig. 14.7 Maly Semyatchik crater lake, Central Kamchatka. Lakes in the summit craters of active volcanoes trap ascending acid gases, and owe their blue colors to extremely high acidity. The white objects are small ice blocks. Photo by R. W. Hazlett.



on the human experience of only the past few hundred years – the period of modern communications. No “Super-eruptions” (Chapter 8) have occurred near large population centers during this time, yet such infrequent events will surely occur in the future, and have the potential to claim millions of lives, while altering the earth’s climate in disastrous ways (Chapter 13). Over 100 million people now live within areas that have been devastated by prehistoric pyroclastic flows adjacent to large calderas. If not forewarned and evacuated there will be no survivors when the next large caldera-forming eruption takes place in a populated region,

Volcanic risk to humans and their property is expressed by most people in relatively subjective terms, e.g.: “People shouldn’t live there – that volcano could erupt at any time,” or “I think it’s safe to build a town there – the volcano hasn’t erupted in hundreds of years.” But, volcanologists must describe risk in more quantitative terms for officials and emergency planners, and methods for more rigorous evaluation of risk is the subject of this section.

Fournier d’Albe (1979) suggested that volcanic risk could be evaluated according to three general, qualitative parameters:

$$\text{Volcanic risk} = \text{Hazard} \times \text{Value} \times \text{Vulnerability} \quad (14.1)$$

Hazards are the various volcanic phenomena, discussed previously, that could possibly impact a given area (lava flows, tephra fall, lahars, etc). Assuming volcanologists have been able to evaluate the volcano’s past eruptive history, this factor in the above equation is potentially the best known of the above parameters. The odds that any particular hazard will affect any

particular area over a particular time span are best discussed in terms of **probabilities**, which we'll soon consider further.

Values are relatively straightforward for property in the area of interest, but also include the subjective value of human lives at risk and of social stability, and must consider the cultural, economic, and political importance of the people and property at risk.

Vulnerability relates to the ability of the area in question to withstand the impact of likely volcanic hazards. In their analyses, New Zealanders call this **fragility**. Are the buildings strong enough to survive ash fall loads? Are the residents capable of evacuating the area if needed? This parameter is of most concern to volcanologists and society, as it is here that human intervention can play a major role in reducing volcanic risk. Reduction of vulnerability (**risk mitigation**) is feasible, and should not be all that difficult to accomplish once threatened people realize that they are at risk. To emphasize the importance of risk mitigation, the above Fournier d'Albe equation should be re-written as follows:

$$\text{Volcanic risk} = \text{Hazard} \times \text{Value} \times (\text{Vulnerability} - \text{Risk mitigation efforts}) \quad (14.2)$$

STATISTICAL ANALYSIS OF VOLCANIC RISK – PROBABILITIES

Geologic studies of a volcano's past history are essential for evaluations of volcanic hazards, but by themselves are of little applied use unless those studies result in analyses of future risk. Insurance companies have a great need to quantify risk, in order to establish insurance rates. Land use planners, government officials, and emergency service providers also need to quantify risk in order to plan for future disasters. For these purposes, the determination of **probabilities** is critical – in order to calculate the chances (the odds) that a certain area will be impacted by future events over specific time periods.

Some volcanologists may prefer to leave the preparation of statistics to trained statisticians, but despite what statisticians may claim, statistical analysis is almost always based on subjective decisions of what data are to be analyzed, and it is much less dangerous for volcanologists to learn “a little statistics” than it is for statisticians to learn a “a little volcanology.” For this reason, a discussion of simple probability theory is in order.

Any statistical analysis of future volcano behavior must be based on the assumption that the past activity of that volcano will characterize future behavior. The reliability of the analysis is a function of 1) how long a history of eruptive activity is known for the volcano in question, and 2) how many events (eruptions, tephra falls, lahars, or whatever) have occurred over this period. A volcano with a well-documented, long history of many eruptive events will yield much better statistical projections than will a volcano with a short history and few documented eruptions.

If the past eruptions of the volcano appear to be randomly distributed in time, then the relatively simple tools of **Poisson analysis** may be used to evaluate the probabilities of future activity. Probably no eruptive phenomena are truly **random**, but unless non-random patterns can be quantified, Poisson techniques are most appropriate. It is important to consider the possibility that eruptions have not occurred randomly, but instead may be increasing or

decreasing in frequency over time, or that the eruptions may be clustered in periods of increased activity, or may show periodic, non-random behavior. There are many tests available to analyze the temporal distribution of past events for random behavior (Davis 1986; Mader et al. 2006).

If the distribution of volcanic events in time does not appear completely random, then **deterministic** (non-random) factors need to be taken into account in statistical evaluations of future probabilities. But analyses then become much more complex and subjective (Turner et al. 2008). Because of the inherent complexities of eruptive processes, rigorous deterministic analyses are mostly fraught with interpretative judgments, and in most cases Poisson analyses may still substantially be useful, if the most recent span of a volcano's history has shown random behavior, and at times may simply be the best that we can do.

When past eruptions appear to have occurred randomly over time and Poisson analytical tools are to be employed, the following conditions (modified from Davis 1986) must be assumed:

- 1 Each future eruption will occur independently, and will not be related to the timing of previous eruptions (there is no "recharge" time).
- 2 The probability that an eruption will occur in a future time interval will not change with the passage of time.
- 3 The probability that an eruption will occur in a particular time interval is proportional only to the length of that interval.
- 4 The probability of more than one eruption occurring in the same time interval is very small.

If these conditions are assumed then the following equation may be used to determine the statistical probability (P) that a hazardous volcanic event will occur over a certain time period in the future:

$$P = 100 (1 - e^{-t/T}) \quad (14.3)$$

where t = probability evaluation window (yrs), and T = event recurrence interval (yrs).

Although it may be of scientific interest to calculate the probabilities that an eruption of any type will occur somewhere on a particular volcano in the future, for practical purposes it is of more use to stakeholders to calculate the probabilities that a particular area on the volcano (perhaps a city or an area being evaluated for development) will be impacted by a particular hazard. A professional volcanologist may be asked the following question by a developer or insurance company in need of evaluating volcanic risk: "What are the probabilities that my project area could be covered by a lava flow (or impacted by some other hazard) in the future?" In order to provide the needed answers, a geologic map of the area in question must be made if none is available, and the ages of lava flows or timing of other hazardous events in that area determined. Selection of the area to be studied is not simple – the area must be large enough to reveal the typical flux of lava flows into areas near the property of interest, but not so large as to generalize regional hazard probabilities that do not reflect the specific risks to the area in question.

In the box on p. 429 we consider how probabilities can be calculated to evaluate the risk of lava flows that could impact one particular landscape – in this case on the flank of a "red volcano" on the island of Hawai'i.

Hualālai [12], one of three active volcanoes on the island of Hawai`i, has erupted more than 75 lava flows over the past 5000 years (Moore & Clague 1991); no area on its slopes is completely devoid of volcanic risk. A developer on the western flank of the mountain needs to answer a general question for economic analysis: “What are the odds that my proposed project will be impacted by a lava flow in the future?” To answer this question, it will be first necessary to prepare a geologic map of all the lava flows that had come close to this facility in the past. “Close” was arbitrarily defined as any lava flow that came within about 5 km of the site (Fig. 14.8). Six radiocarbon-dated lava flows were later determined to have entered the area over the past 4700 years in a temporally random fashion (Fig. 14.9). The “recurrence interval” for lava flow impact (T) is thus 783 years. The probabilities (P) that flows will enter this area again in the future for various future time intervals (t) may be calculated from the statistical probability equation above, and are given in Table 14.1.

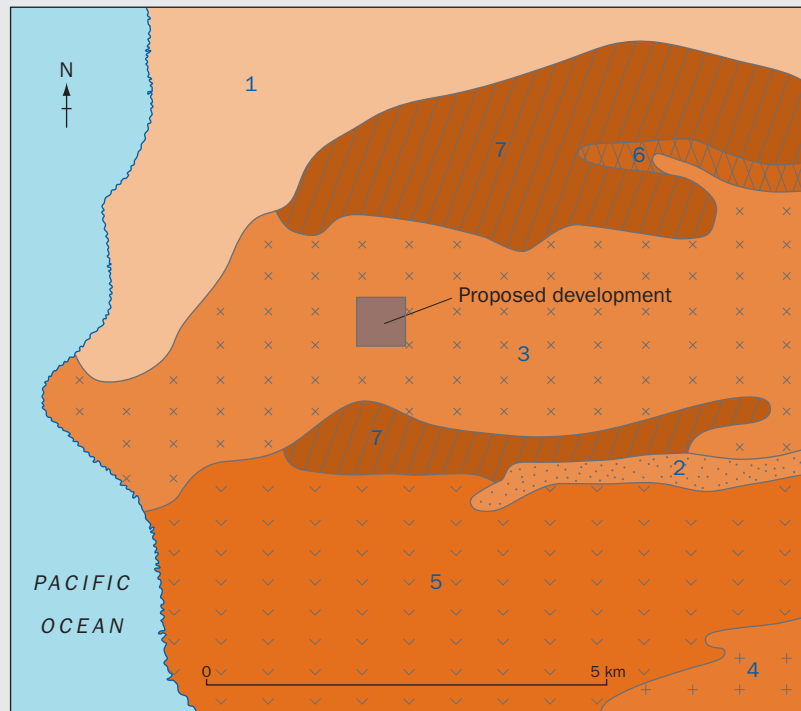


Fig. 14.8 Geologic sketch map of lava flows surrounding proposed development.

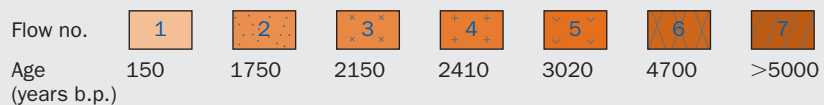


Fig. 14.9 Age distribution of lava flows entering Hualālai test area.

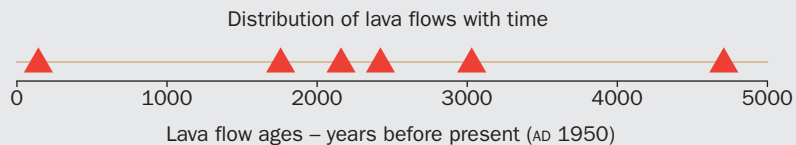


TABLE 14.1 SIMPLE POISSON PROBABILITIES THAT THE HUALALAI TEST AREA WILL BE IMPACTED BY FUTURE LAVA FLOWS OVER VARIOUS FUTURE TIME INTERVALS.

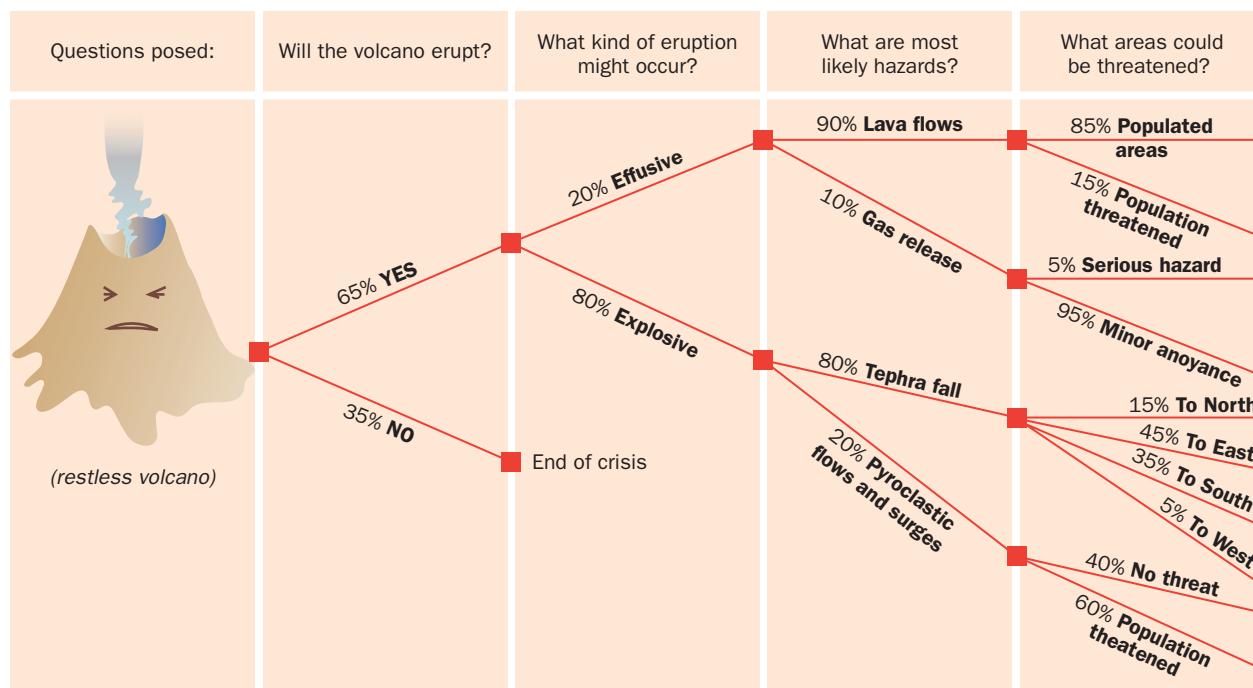
	Future time interval t (years)					
	10	50	100	250	500	1000
Probability P (%)	1.3	6.2	12.0	27.3	47.2	72.1

NON-QUANTITATIVE ASSESSMENTS OF VOLCANIC RISK

Fig. 14.10 “Event-trees” are important tools to represent schematically the “odds” of possible scenarios developing during volcanic unrest, and are easily understood by the public. As a volcanic crisis unfolds, the “odds” of future developments continually change as new information becomes available, and branches of the tree become outdated by actual events.

During a volcanic crisis there may not be time for a meaningful statistical analysis of risks. Instead, volcanologists on the scene may be asked “What do you think the volcano is going to do?” The embarrassing reality is that volcanologists never *really* know what the future holds on a day-to-day basis (volcano gods are capricious and always have the potential to deliver surprises!), but scientists do have their “best guesses” based on long experience, and need ways to semi-quantitatively express those opinions. Excellent tools for this are **probability trees** or **probabilistic event trees** (Newhall & Hoblitt 2002; Marti et al. 2008), which diagrammatically assign informal probabilities of future events as answers to specific questions – e.g. “What are the probabilities that the volcano will erupt?”, “If the volcano erupts, what are the probabilities that the eruption will be large or small?”, “What are the probabilities that lahars – or lava flows – or tephra fall will be involved?” (Fig. 14.10). In this manner volcanologists on-scene can reach a consensus about their “best guesses,” so as to better advise authorities and to more credibly communicate to public groups about what is most *likely* to happen.

The development of probabilistic event trees has evolved to include statistical evaluations of the inherent uncertainties involved, and these methods have become sophisticated tools to present the odds for various eruptive outcomes. This is a most important tool in the situations where government officials must make difficult social and economic decisions regarding the need for mass evacuations of threatened populations (Woo 2008). When major economic and political issues are involved in responses to long-lived periods of volcanic unrest,



volcanologists may be called on to rigorously defend their assessments before investigative panels or courts of law as expert witnesses. For such forensic purposes the assumptions that lead to those assessments require a defensible evaluation of all evidence involved, by the techniques Willy Aspinall et al. (2003) call “Evidence-based Volcanology.”

MITIGATION OF VOLCANIC RISK

Public education, land-use planning, and geologic studies are all essential for reduction of volcanic risk to people and to the built environment. Direct intervention in volcanic processes is also a possible risk mitigation strategy in certain situations.

Public education

Volcanic disasters always involve people or structures that are “in the wrong place at the wrong time,” but unfortunately human memories are short and understanding volcanic hazards and risk are not high priorities in determining where people choose to live. Mitigation (reduction) of volcanic risk for vulnerable populations should not be difficult to accomplish, but how much that risk can be reduced depends on how much is known about the hazards involved, and how great an effort societies will undertake to reduce their exposure. In theory, the first steps are relatively easy – people residing near active volcanoes must become aware of the risks they face, and must learn what they can do to reduce them. In the real world, however, the realities involved in public education are often very complex, especially in rural communities where general education levels may be relatively low, and religious beliefs and cultural traditions may be very strong. Sociological studies to identify the degree of awareness about volcanic hazards and the willingness to heed warnings are an important way to mitigate risk (Gregg et al. 2004).

Although public understanding of ways to reduce volcanic risk to people and their property seems like an obvious virtue (especially to outside “experts”), there are often intertwined local economic and political vested interests fearful that awareness of risk may reduce property values or somehow threaten economic stability of the involved communities. Despite these complexities, much has been learned about the most effective ways to disseminate reliable volcanic risk information to vulnerable communities, and thousands of lives have been saved by timely dissemination of warnings (e.g., the 1991 Mt Pinatubo [104] eruption). Failures to effectively deliver credible warnings (e.g., the 1985 Ruiz [54] eruption, where tens of thousands of lives were needlessly lost), weigh heavily on the minds of volcanologists, however, and efforts to improve communications between volcanologists, government authorities, and the public remain one of our most important obligations.

The most critical need for conveying hazards and risk information to the public is to make the information available in terms that are readily understood by ordinary citizens. Color-code systems have long been used to indicate risk levels and to alert the public as to the level of danger. **Green-yellow-red** schemes are most easily understood, as volcanic threats increase. Mexican agencies prepared an excellent “traffic-light” scheme used around Popocatepetl volcano, based on universal familiarity with traffic light colors (Fig. 14.11). This poster tells people what the different colors mean and how to respond to different alert levels.

SEMÁFORO DE ALERTA VOLCÁNICA
VOLCÁN POPOCATÉPETL

El Sistema Nacional de Protección Civil ha desarrollado y aplicado el Sistema de Alertamiento llamado "Semáforo de Alerta Volcánica" para informar a la población sobre la actividad del volcán y las medidas generales de prevención correspondientes a cada etapa.

NORMALIDAD (Verde)
Desarrolla tus actividades normalmente

Fase 1

El volcán está en calma

- Mantente informado
- Memoriza:
Rutas de Evacuación
Sitios de Reunión
Refugios Temporales
- Asiste a pláticas de orientación
- Participa en los Simulacros

Fase 2

El volcán presenta fumarolas
Actividad sísmica local

ALERTA (Amarillo)
*Permanece atento a la información oficial
Debes prepararte para una posible evacuación*

Fase 1

Sismicidad volcánica local frecuente
Fumarolas de vapor o gas
Emisiones ligeras de ceniza
alrededor del volcán

- Mantén atención a la información que difundan las autoridades locales
- Ten guardados y a la mano documentos importantes
- Ensaya desplazamientos a sitios seguros, sitios de reunión y albergues
- Sigue las instrucciones de las autoridades y mantente alerta
- Debes de prepararte para una posible evacuación

Fase 2

Actividad explosiva de escala baja a intermedia
Lluvias de ceniza leves a moderadas en poblaciones cercanas
Posibilidad de flujos piroclásticos y flujos de lodo de corto alcance

Fase 3

Actividad explosiva de escala intermedia a alta
Creclimiento de domos y posible expulsión de magma
Explosiones de intensidad creciente
Lluvias de cenizas notorias sobre poblaciones cercanas

ALARMA (Rojo)
Tú y tu familia deben de estar listos para la evacuación

Fase 1

Actividad explosiva de escala intermedia a grande
Explosiones que pueden lanzar fragmentos de material volcánico
Flujos piroclásticos y lodos que pueden alcanzar poblaciones cercanas e intermedias
Lluvias de cenizas importantes en poblaciones y ciudades lejanas

- Sigue las instrucciones de las autoridades
- Debes prepararte para una posible evacuación
- Dirígete con tu familia a los sitios de seguridad o a los sitios de reunión para ser trasladado a los refugios temporales o sitios seguros
- Si puedes evacuar por tus propios medios, debes de hacerlo
- Mantente continuamente informado sobre la evolución del fenómeno

Fase 2

Registro de actividad explosiva de escala grande a extrema
Columnas eruptivas de gran alcance y posibles derrumbes del edificio volcánico
Flujos masivos piroclásticos o de escobros
Grandes lahares de efectos desastrosos
Lluvias intensas de ceniza, arena y fragmentos sobre poblaciones a distancias mayores
Graves daños al entorno incluyendo zonas demarcadas en el mapa de peligros volcánicos

Secretaría de Gobernación
Coordinación General de Protección Civil
Centro Nacional de Prevención de Desastros
Dirección General de Protección Civil

Control de vicio, información sobre la actividad del volcán Popocatepetl,
Tel. 52-05-16-38 (24 hrs)
Sit. de la Red: 01-800-123-31-30

Centro Nacional de Comunicaciones (CENAPRED)
de la D.G.P.C. de la S.G.O.B.
Tel. 56-16-00-42 / 16-00-44-85
Sit. de la Red: 01-800-00-41-33

www.cenapred.gob.mx
www.proteccioncivil.gob.mx

Fig. 14.11 Semaforo de Alerta Volcanica (Volcanic Traffic Light Alert System) poster as distributed to populations at risk from future major eruptions of Popocatepetl, Mexico (de la Cruz-Reyna & Tilling 2008). This poster explains possible alert levels, what risks to expect, and what actions to take.

The 1985 Ruiz disaster (Chapter 11; p. 458) caused increased awareness of volcanic hazards throughout Latin America, especially in Ecuador, Colombia's southern neighbor. Cotopaxi [52], south of Quito, is one of the most dangerous active volcanoes in the Andes, and has claimed many thousands of lives over the past centuries. Volcanologists prepared a volcanic risk map to document volcanic hazards for local government authorities (Miller et al. 1978). Ecuadorian emergency agencies, in cooperation with local geologists then prepared simplified posters to inform vulnerable residents in plain language about those risks (Fig. 14.12). Similar posters have now been prepared for distribution around many hazardous volcanoes throughout the world by local civil defense agencies, and are invaluable public education tools.

Land-use planning

Appropriate zoning regulations can be designed and enforced to prevent populations and critical facilities from being established in high-risk areas. This depends ultimately in the credibility of governments, which in turn depends largely on the reliability of volcanological information that is provided to authorities.

Geologic studies

Geologic mapping and associated radiometric dating studies (Chapter 6) are essential to decipher a volcano's past eruptive history and to better understand the potential for future eruptions. Geologists conduct their field studies in order to recognize patterns of past volcanic behavior that are critical for interpreting the present behavior, and for looking into the future. James Hutton's assertion that "The

present is the key to the past” is true, but must be inverted when it comes to volcanology: “*The past is the key to the present – and to the future*”!

VOLCANIC RISK MAPS

Geologic maps are critical for understanding a volcano’s history and for determining the recurrence intervals for hazardous eruptive events, but by themselves are of relatively little use to the emergency managers and land-use planners who must make decisions about volcanic risk. For these officials, **volcanic risk maps** are essential (Fig. 14.13) and are best prepared by the geologists who have conducted the geologic mapping of the particular volcano in question. As was tragically learned during the 1985 eruption of Ruiz volcano, Colombia, however, (see section on Volcanic Crisis Management below) even well-designed risk maps may not be understood by laymen residents, and more graphical warnings, such as were described above, must be prepared for popular distribution and use.

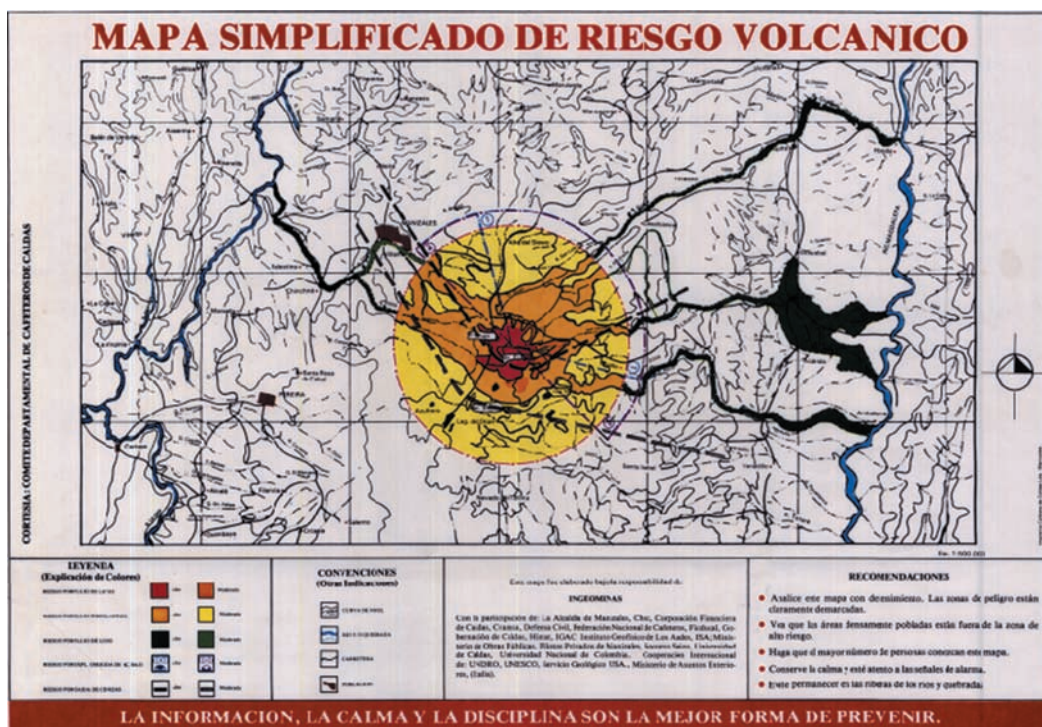
DIRECT INTERVENTION

Humans may directly intervene in volcanic processes to lessen the impact of associated hazards through engineering means or individual efforts in various ways – depending on the hazard involved. The three principle volcanic hazards that are amenable to human modification to reduce risk are tephra falls (Chapter 7), lahars (Chapter 11), and lava flows (Chapter 6) – each will be discussed separately. Pyroclastic surges and flows (PDCs) overwhelm most structures in their paths, however, and no direct intervention means to protect lives or property from these hazards have been proposed or seem feasible at this time.



Fig. 14.12 Lahar hazards poster, Cotopaxi volcano, Ecuador. This widely distributed poster depicts the areas and municipalities that could be threatened by future lahars and provides easily understood information about the nature and dangers of lahars, the areas at risk, the locations of evacuation centers, and basic information on where to obtain warnings and what to do in case alarms are sounded. Poster created by Patricia Mothes of the Ecuadorian Geophysical Institute, National Polytechnic School in cooperation with the Ecuadorian National Office of Civil Defense.

Fig. 14.13 Volcanic hazards map published on October 7, 1985, showing areas susceptible to lahar inundation by lahars on the flanks of Ruiz volcano, Colombia. This map proved extremely accurate in defining these areas, but was never understood by the thousands of people who perished needlessly on November 13. (INGEOMINAS, 1985).



Tephra fall risk reduction

Falling volcanic ash can be a rather beautiful sight at first, as it is commonly a gentle process, sounds are deadened, and the soft light that may soon turn to total darkness casts an eerie, peaceful ambience over the land as verdant landscapes are quickly transformed into uniform grayness (Chapter 1). Any admiration for the esthetic aspects vanishes quickly however, as the fine ash penetrates all manner of mechanisms (including the engines of automobiles and aircraft), and breathing may become difficult. The first steps are obvious as people scurry to cover their heads and faces with umbrellas or newspapers, and will soon seek particle masks or damp clothes to facilitate breathing and to limit lung damage. The next steps are not so obvious, and rushing inside homes to avoid the ash may not be a wise move if the ashfall is heavy and prolonged. Many people who sought shelter inside the homes of Olongapo, Philippines during the 1991 eruption of Mt Pinatubo perished when roofs collapsed under the weight of water-soaked ash. Major buildings at Clark Air Force Base at the foot of Pinatubo also collapsed (Fig. 14.14), but aircraft and personnel had been evacuated before the climatic 15 June eruption. Unless roof pitches are steep – not common in the tropics (!), roofs may collapse under as little as 15 cm of ash – especially if wet (Spence et al. 1997). Individuals can greatly reduce damage to their homes and business buildings by removing ash before it builds up to dangerous levels – a sometimes difficult process when ash is still falling. Day may have suddenly turned to night, and lightning may be crackling overhead. During the 1982 eruption of Galunggung [99] volcano, many villagers returned daily to their homes to remove accumulated ash (Fig. 14.15), but where ash was not removed, roofs collapsed, completely

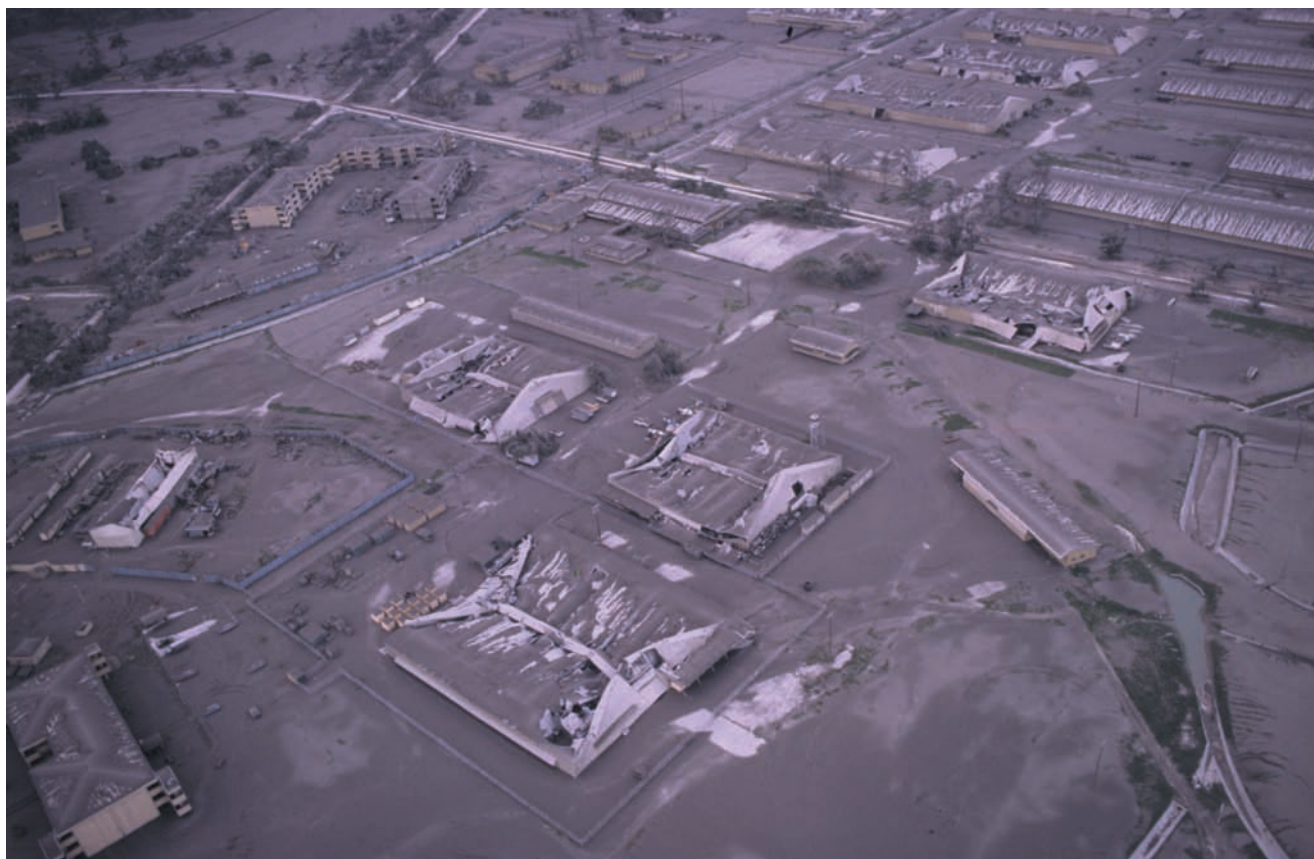


Fig. 14.14 View of Clark Air Force Base, 25 km east of Mount Pinatubo, Philippines, after the eruptions of June, 1991. The hangars in the foreground were destroyed by the weight of accumulated airfall tephra, and hundreds of millions of dollars in damage were caused to this important facility. Fortunately, owing to timely warnings from volcanologists, all aircraft were removed from these hangars and flown to safety before the paroxysmal eruption of June 15. After major Plinian ashfall events, everything is grey – this is a color photograph. USGS photo by Rick Hoblitt.

destroying homes (Fig. 14.16). Ash removal from city streets and airport runways is also critical, and must be done repeatedly if the tephra fall is on-going.

Lahar Risk Reduction

Lahar risks can be reduced through major engineering efforts in advance of eruptive activity or before the rainy seasons that frequently trigger them. Techniques used to lessen lahar damage (known as **sabo** engineering in Japan) are focused on three principal strategies:

- 1 channelization of lahars by reinforcing and augmentation of natural or man-made pathways;
- 2 impounding of lahar debris by the construction of dams and basins; and
- 3 removal of large boulders from flowing lahars by massive grates that trap the largest boulders (Fig. 14.17).

Fig. 14.15 Villager removing accumulated ash from his roof in Cikasasah between eruptive episodes of Galunggung volcano in 1982. People who returned to their homes after eruptive episodes to remove ash generally were able to save their homes from destruction. USGS photo by J. P. Lockwood.



Fig. 14.16 Ruins of home destroyed by the weight of accumulated ash near Cipanas, Galunggung volcano, Indonesia. Note trees in background – defoliated and killed by falling ash. USGS photo by J. P. Lockwood.

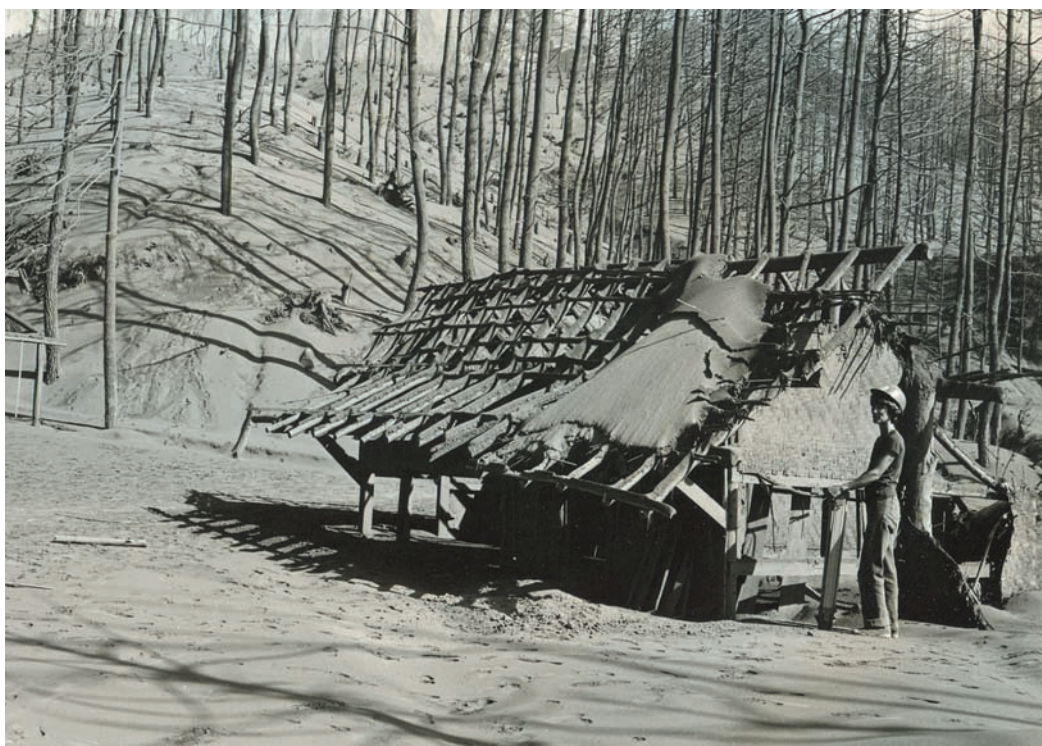




Fig. 14.17 Sabo dam for retarding lahars across the Mizunashi River system below Unzen [108] volcanic dome, Japan (in background). Dome growth in 1991 caused pyroclastic flows to move repeatedly down this river and set the stage for lahars and debris avalanches that remain a hazard at present. The sabo dam, 290 m wide and 10 m high, is designed to impound lahar deposits and to remove large lahar boulders by “filtering” them from lahars that may overtop the sabo. The lahar catchment basin above the sabo must be continuously excavated of debris to accommodate future lahar material. Photo courtesy of Etushi Sawada, Unzen Restoration Work Office, Nagasaki.

This last strategy is to eliminate the ramming effect of entrained boulders that can destroy even the strongest buildings at risk downslope.

A problem with lahar mitigation efforts is that they are mostly temporary, as repeated lahars can overwhelm any human-built structures with time. Lahar mitigation efforts are most sophisticated and extensive in Japan, although the maintenance of these extensive sabo systems involves huge costs, as accumulation basins have to be repeatedly excavated, and lahar diversion structures rebuilt.

Fig. 14.18 San Juan Parangaricutiro Church, projecting through lavas erupted in 1944 from Parícutín [45] volcano (seen on skyline), Michoacan State, Mexico. The Parícutín eruption began in a farmer's cornfield on February 20, 1943 and lasted for 9 years. Church steeples seem to commonly survive when lower-standing structures are buried by lava flows and lahars in volcanic areas. Photo by J. P. Lockwood.



Lava flow risk reduction – lava diversion

When lava flows through towns, destruction is usually complete, although it is of interest to note that in some cases only churches may remain standing (Fig. 14.18). Although taken by some to demonstrate the religious sensitivities of lava, this actually reflects the fact that those churches are usually the most imposing and strongest built structures in rural towns, and also are frequently constructed on hills!

Like lahar risk, the risks of lava flow impact can be best reduced or eliminated by careful advance planning, so that cities and vulnerable structures are built away from or above likely lava flow paths. But for many reasons, notably the attractiveness of flat land close to water, many communities in volcanic areas are sited in drainages subject to lava inundation. People rarely plan for low-probability future events, so that wherever effusive eruptions occur in populated areas, human-built structures are commonly threatened.

Lava flows are fluids, albeit much more viscous than lahars, and by and large flow down-slope following the easiest paths. Under certain circumstances human intervention may be employed to alter those “easiest paths” and divert them away from destructive courses. Efforts to change those directions or geometry of active lava flows are known as **lava diversion** and have been employed with varying success for several centuries. The earliest recorded attempt to change the path of a lava flow occurred during the 1669 eruption of Etna [82] volcano, when citizens attempted to divert a lava flow from inundating the important port city of Catania. Macdonald (1972, pp. 419–20) described the attempt:

Under leadership of a man named Diego Pappalardo, 50 or so men from Catania covered themselves with wet cowhides for protection against the heat and dug a channel through the wall of hot lava at one edge of the flow. At first the operation was successful. Molten lava escaped through the gap thus created and flowed away at an angle to the path of the original flow, reducing the amount of lava moving toward Catania. However, the new stream was headed toward the town of Paterno, and 500 indignant citizens of that town armed themselves and drove the Catania men away. The channelway in the main flow wall [levee] soon clogged up and the flow continued toward Catania, where it came up against the feudal city wall. For several days the wall withstood the flow and diverted it around the city toward the sea, but eventually the lava broke through a weak place in the wall and flooded part of the city. Thus, the 1699 eruption provides examples of lava diversion both by destroying the flow wall and by turning the flow with an artificial barrier.

Although the 1669 efforts were ultimately unsuccessful, evolving technology (the invention of bulldozers, airplanes, and powerful water pumps) has given society powerful new tools to divert lava flows, and humans have had considerable success in changing the direction or limiting the spread of advancing flows during the twentieth century. Diversion of flowing lava is only appropriate to consider in special, uncommon circumstances, where terrain is appropriate, sufficient time is available, economic benefits outweigh potential costs, and the threatened populations and governments are willing to consider “messing with nature”. Techniques that have been successfully utilized to alter the courses of lava flows or to impede their progress include: 1) construction of earthen barriers; 2) application of large volumes of water to solidify advancing flows; and 3) use of explosives to disrupt active pyroclasts and flow channels.

Earthen barriers

Relatively small lava diversion barriers were built to attempt lava flow diversion during the 1906 eruption of Vesuvius and the 1955 and 1960 eruptions of Kīlauea [15]. None of these barriers worked, because they were viewed as dams to stop the advance of flows and were far too small to achieve their objectives. The barriers built to protect the town of Kapoho in 1960 (Macdonald 1962) were constructed of highly vesicular, low density pāhoehoe, and were simply floated away by lava flows of greater density. The most successful lava diversion barriers to date were built during the 1983 and 1992 eruptions of Etna volcano. During the 1983 eruption, massive berms up to 14 m high were built and successfully diverted flows around a valuable resort and threatened astronomic facilities (Fig. 14.19) (Colombrita 1984; Lockwood and Romano 1985). Lava barriers were built directly across flow paths in 1992 in order to temporarily delay flow advance and protect the town of Zafferana, while efforts to explosively disrupt pyroclasts upslope were being carried out (Barberi et al. 1992). Experience has shown that lava diversion barriers can never “stop” lava flows except temporarily as they will eventually be overrun if an eruption continues long enough. They can only be successful if designed to change the direction of lava flow paths, but only where sloping terrain allows diverted lava to readily flow downslope away from the barrier. Lava diversion barriers can also be constructed

Fig. 14.19 Diversion of an active `a`a flow above the Sapienza resort and tramway complex, Etna Volcano, Sicily in May, 1983. A 25 m wide `a`a flow is being diverted by a 10 m-high lava barrier, which is being built higher as this photo was taken. The barrier, built from 100,000 m³ of transported rocks in 10 days as lava piled up against it, crosses an earlier flow that had nearly overwhelmed the Sapienza buildings a week before the diversion effort began. The barrier successfully diverted the flows about 100 m laterally from their natural terrain path and saved the vital Sapienza structures. USGS photo by J. P. Lockwood.



in advance of eruptive activity to protect valuable facilities from anticipated future lava flows, as has been done in Iceland, Japan and Hawai`i (Fig. 14.20).

Water cooling

During the 1960 Kīlauea eruption, firefighters noted that small amounts of water sprayed on advancing pāhoehoe flows could temporarily stop thin flows by freezing immobile crusts over liquid interiors. The amounts of available water were too small to have any lasting effect in this case, and it was not until 1973 that water application was shown to be a viable lava diversion technique. In that year a new volcano erupted on the island of Heimaey, Iceland, just upslope from the island's only city. Icelandic emergency officials ordered enormous volumes of seawater to be pumped and sprayed on advancing `a`a flows to quench molten lava and to cause those flows to thicken and slow their advance (Williams & Moore 1983). The heroic efforts of Icelanders at Heimaey, utilizing massive water pumps and diversion barriers, saved much of the city and spared the economically invaluable harbor from closure by advancing lavas (Fig. 14.21). About six million m³ of seawater were pumped onto the advancing flow over a five month period, and it was found that roughly a cubic meter of water was required to solidify and immobilize a cubic meter of flowing lava. Water application is most feasible where advancing lava flows are close to large bodies of water, although small amounts of water may suffice to freeze small flows that threaten to overtop barriers.

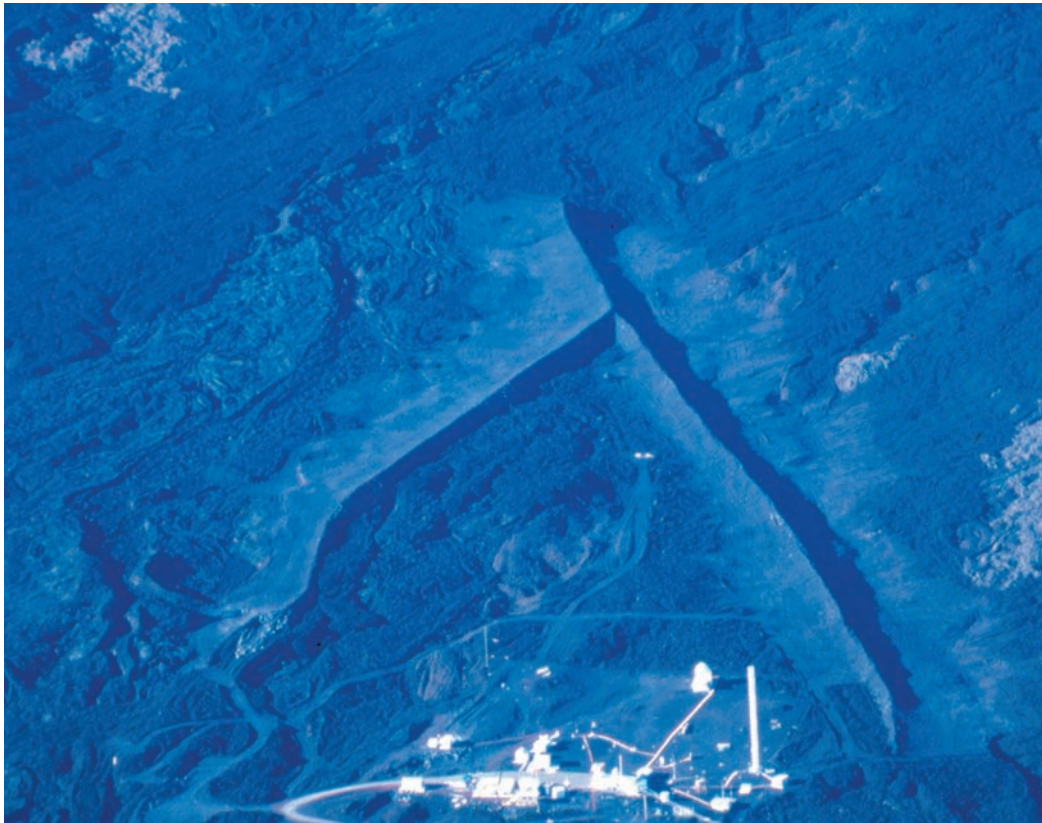


Fig. 14.20 Lava diversion barrier, constructed to divert future lava flows around the NOAA Mauna Loa Observatory on the north slope of Mauna Loa volcano, Hawai'i. The longest arm of the 5–7 m-high barrier is about 700 m long. This NOAA facility is of global importance, as it maintains the longest complete record of atmospheric CO₂ monitoring in the world, and protection from future lava flows is essential. The 'a'a flows surrounding the Observatory were erupted in 1843. Photo © G. Brad Lewis.



Fig. 14.21 Pumping seawater to solidify and stop the advance of lava down a Vestmannaeyjar street, Heimaey, Iceland in March, 1973. The flow, here about 8 m thick, was slowed and greatly thickened by the cooling operation, and was successfully blocked. By July, 1974 the lava had been completely removed and the street had been returned to use. Photo courtesy of Sveinn Eiriksson.

Explosives

Explosives have been used several times to attempt lava flow diversion in Hawai'i (Mauna Loa [13] volcano) and Italy (Etna volcano). The Mauna Loa efforts in 1935 and 1942, conducted by US Army Air Corps bombers, used obsolete munitions and aircraft, and were not successful, although in 1942 levee walls were broken and a flow diverted for a short distance before it rejoined the original channel. Field experiments with modern delivery systems have shown that aerial bombing does have the potential to disrupt pyroducts and active lava channels (Lockwood & Torgerson 1980), but these modern techniques have never been employed on active flows.

Large quantities of explosives were successfully hand-emplaced in the walls of lava channels and pyroducts to disrupt supply conduits during 1983 and 1992 eruptions of Etna volcano (Lockwood & Romano 1985; Barberi et al. 1992), although the lava-diversion effects were short-lived. The use of explosives to divert lava flows has proven to be culturally controversial in Hawai'i, and is most appropriate to employ where target areas are remote, and where the negative impacts of unsuccessful efforts or unintended consequences are acceptable.

VOLCANIC LAKE RISK REDUCTION

Hazards from the three types of volcanic lakes mentioned earlier in this chapter are each amenable to different means of mitigation. Lakes formed by the blockages of pre-existing streams pose risk to downstream populations if they are overtopped by rising lake waters. To mitigate these risks drainage tunnels or canals can be excavated in erosion resistant rocks below the dam level, as was done successfully to keep the levels of a rapidly rising Spirit Lake stable at Mount St Helens in 1981–2. The second category of volcanic lakes, those known to contain dangerous and rising concentrations of CO₂ gas can be made safer by controlled de-gassing efforts, as is being done at “killer lakes” in Cameroon (Kling et al. 2005). Degassing is achieved by lowering a large diameter plastic pipe to CO₂-saturated lower levels of these lakes, initiating upward flow by lowering pressure in the pipe until the buoyant rise of bubble-filled water becomes a self-sustaining process and fountains of water and gas are released harmlessly to the atmosphere (Fig. 14.22). The controlled de-gassing of Cameroonian volcanic lakes has now been carried out since 2001, and has become an important example of successful human efforts to mitigate volcanic risk (Fig. 14.23).

The third category of volcanic lakes, those at volcano summits, are the most dangerous of all because of the interaction of water and eruptive activity, and have generated lahars that have killed thousands of people on the flanks of volcanoes (Chapter 11). Kelut volcano, in central Java, is one of Indonesia's most active volcanoes. Eruptions within its large central crater lake have ejected waters onto the outer slopes of the volcano many times in the past, forming lethal lahars. After a lahar-producing eruption in 1919 that killed over 5000 people, major efforts were initiated by Dutch engineers to lower lake levels by a series of tunnels through crater walls. These and subsequent tunneling efforts reduced the volume of the summit lake dramatically, and subsequent eruptions have produced much less damaging lahars.¹

1 A lava dome that began to grow in Kelut crater in November, 2007 has completely displaced the preexisting lake, thus eliminating the lake-lahar hazard – for the time being!

Volcano Monitoring

There are two purposes for volcano monitoring: 1) to understand better “how volcanoes work;” and 2) to provide public warnings of potentially harmful future activity. Prognostications about the future involve defining the terms **predictions** and **forecasts**, which are used to describe prospects for future events. *Predictions* are highly specific about the time, place and nature of future events, whereas *forecasts* are much more general. Wise volcanologists should never make predictions, however, for reasons well stated by Bob Decker in his important 1973 paper “State-of-the-art in Volcano Forecasting”:

Forecasting the time and place of volcanic eruptions is one of the major goals in volcanology. I could have used the title “Prediction of Volcanic Eruptions” [in my paper], but the word “prediction” sounds precise and deterministic, and the state-of-the-art in this field is far from precise. The practice of weather forecasting has introduced all of us to a more probabilistic and less precise notion of scientific prediction that is still most useful even if not perfectly precise. Choice of the term “forecasting” is an attempt to convey this same sense of useful though uncertain prediction of events which lie in the future.”

Volcanoes always seem to give some warnings before they erupt (at least in hindsight), and in an ideal world, there would be some means to monitor all of the Earth’s potentially active volcanoes – in order to provide early warning of impending eruptive activity that could threaten nearby populations, or could pose threats to aircraft that fly above or downwind of them. Unfortunately, there are far too many potentially dangerous volcanoes in the world to monitor on a routine basis. Of the 538 volcanoes known to have erupted during historic times (Simkin and Siebert 1994), less than half are under regular surveillance (McGuire 1995). As noted earlier, many active volcanoes have never even been mapped, and most have geologic histories that are poorly known. Even where routine monitoring of a particular volcano is taking place, the type and amount of instrumentation will likely be insufficient to provide a complete picture of volcanic activity. When a potentially hazardous volcano does become “restless,” equipment and personnel may need to be brought from thousands of kilometers away. At times such equipment may arrive after an eruption has already begun, too late to warn people

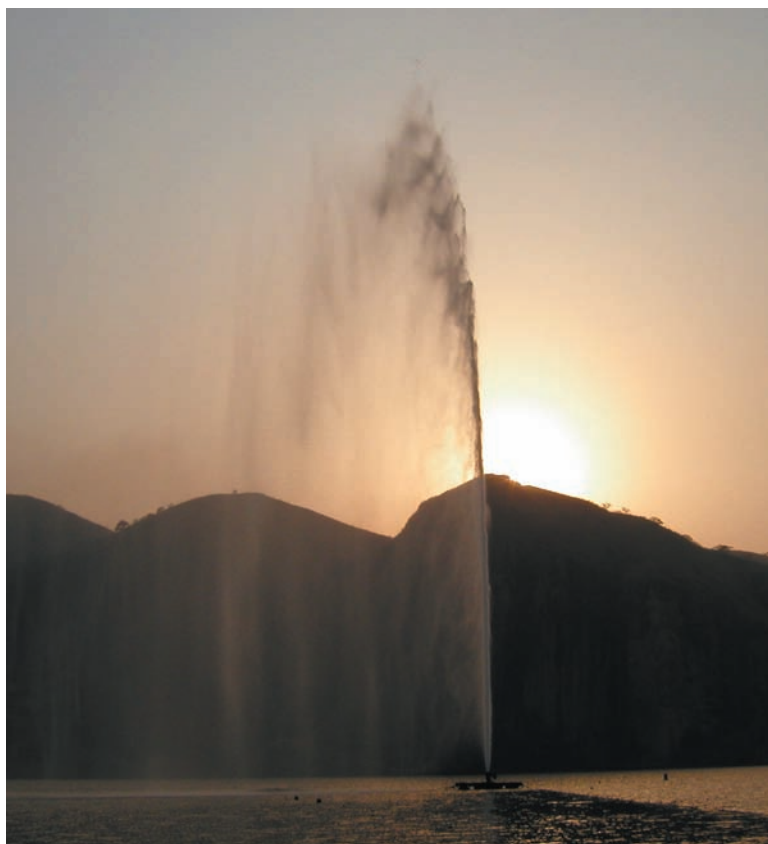
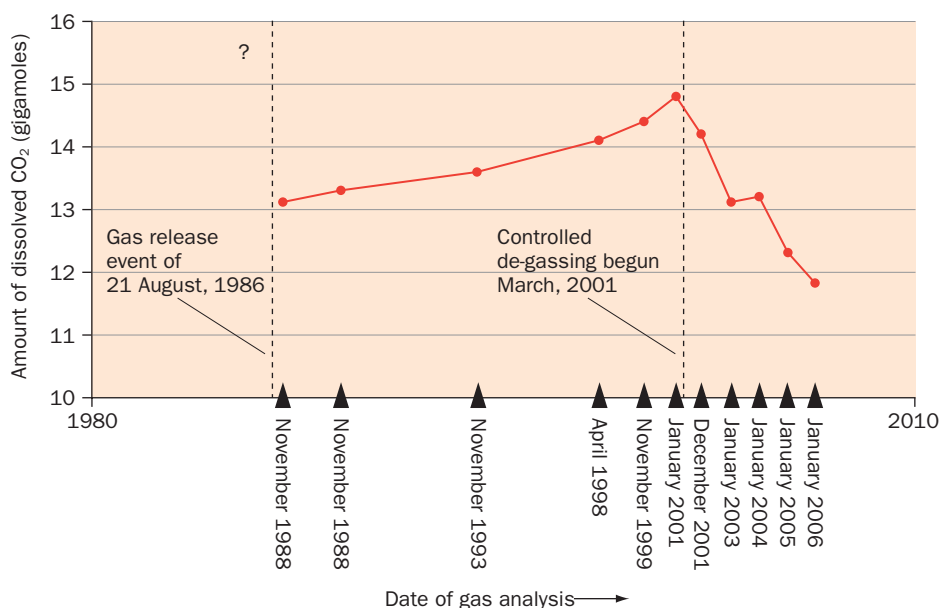


Fig. 14.22 Self-sustaining de-gassing of Lake Nyos, 2006. This fountain of water and CO₂ gas is being propelled upward about 40 m by the expansion of carbon dioxide gas in a 200 m long pipe whose intake is in CO₂-saturated waters near the bottom of Lake Nyos. USGS photo by W. C. Evans.

Fig. 14.23 Amount of carbon dioxide dissolved in the waters of Lake Nyos, Cameroon after the tragic lake overturn event of August 21, 1986, showing the effect of controlled de-gassing efforts. CO₂ content in gigamoles (1 gmole CO₂ = 44 × 10⁶ kg). CO₂ content before the August 21 event has been estimated at about 27 gmols. Controlled degassing efforts must continue to offset gas recharge rate and to make the lake safer. Data from Kusakabe et al. 2008.



in advance of impending trouble. Fortunately, the time between initially observed volcanic unrest and subsequent eruptive activity is commonly long enough for emergency monitoring and successful risk mitigation (e.g., Mount St Helens, 1980 and Mt Pinatubo, 1991). Unfortunately, the tragedy of the 1985 Ruiz eruption (Chapter 11) demonstrates that a long warning period by itself will not prevent disaster, if the links between scientists, emergency officials, and the endangered public are not forged well (see later section on Volcanic Crisis Management).

Although new technical developments are constantly improving our ability to understand volcanoes as time goes on, the increases of populations living in volcanically hazardous areas constantly boost the need for better monitoring. While volcanologists are now much more capable of providing warnings about volcanic risk, the overall threat of volcanic eruptions to populated areas has ironically never been higher. McGuire (1995) observes:

A major problem requiring solution is the fact that most unmonitored or poorly monitored volcanoes are located in developing countries where population numbers are rapidly increasing. Competition for the most fertile agricultural land is seeing the slopes of potentially destructive volcanoes becoming increasingly crowded, particularly in Southeast Asia, and in Central and South America.²

² In the South American Andes the processes of global warming are exacerbating the situation, since climatic changes are forcing potato farmers in the high volcanic Andes to cultivate their crops at ever-higher elevations, closer to potential eruptive centers.

Nonetheless, two of the most extensive volcano observatory systems in the world are located in less-wealthy countries (Indonesia and the Philippines). More lives have been saved by volcanologists in these countries than by volcanologists in all of the rest of the world combined! An appreciation of the magnitude of the volcano monitoring efforts in these countries is best obtained by being in the modern volcano observatories in Bandung or Manila and listening to the morning radio reports coming in from dozens of field posts located in remote locations all over these volcanic lands – some accessible only by footpaths. The observers at many of these observatories may not be highly-trained, and they may only have records from a single, smoke-drum seismograph to add to visual reports, but their great dedication to monitoring “their volcano” in order to protect the lives of villagers below is admirable and should never be forgotten. Volcano observatories, no matter their level of sophistication, are critical to understanding volcanic behavior. Some history about them follows.

VOLCANO OBSERVATORIES

History

The Vesuvius Volcano Observatory (Osservatorio Vesuviano – OV) is the world’s oldest volcano observatory, and was established by the King of Naples in 1841 on a heavily forested knob overlooking the port of Naples, halfway up the western side of Vesuvius. The hilltop location was close to the volcano, hence providing easy access to important field localities, while remaining topographically protected from the volcano’s frequent lava flows. It was also upwind of the heaviest historical ash falls from the volcano, which the builders knew could collapse roofs. The new institute was initially christened the Osservatorio Meteorologica Vesuviana, because the state of scientific knowledge about volcanoes at that time was so slim that learned people, following the suggestion of Aristotle (!) felt it was appropriate to lump volcanic eruptions together with weather phenomena. Earth magnetism was also considered appropriate to study at the OV – perhaps, for all anyone knew, it might turn out that volcanic eruptions were somehow related to changes in the Earth’s magnetic field, or *visa versa*. (In fact, shallow magma intrusions *can* have striking effects on local magnetic fields, but their eruptions are not triggered by changes in the strength of planetary magnetism). The OV has been a beacon for volcanologists because of its long history and proximity to the great variety of both effusive and explosive eruptive action characteristic of Vesuvius. Frank Perret (Chapter 1) made his first detailed volcanologic observations there (Perret 1924), and witnessed the devastating 1906 eruption – which also nearly destroyed the observatory. The OV had another close call during WWII, when it was alternatively occupied by German and Allied soldiers and reduced to the operation of a single seismograph – which Director Guiseppe Imbo kept in his home! Imbo was able to give early warnings about the eruption of March, 1944, the most recent eruption of this dangerous volcano.

The OV was the world’s only volcano observatory for over 70 years, as for the most part volcanoes elsewhere in the world were studied only *after* they erupted. This began to change after the widely publicized Mt Pelée disaster of 1902, when about 30,000 people perished. After viewing the carnage in St Pierre, Thomas Jaggar (Chapter 1) realized that continuous monitoring of volcanoes would be required to understand them and to warn vulnerable

populations of impending eruptions. He founded the Hawaiian Volcano Observatory (HVO), now operated by the U.S. Geological Survey, on the rim of Kilauea caldera in 1912. HVO set an example for many more observatories around the world, and many of the most important tools and techniques for volcano monitoring were developed there. The World Organization of Volcano Observatories (WOVO) now lists 79 observatories, located in 32 countries. These facilities come in many varieties, depending on available funding and the perceived threat of the volcano being monitored. Some observatories in developing countries consist of one or two technical observers manning a single seismometer. Others are much more sophisticated, centralized facilities, typically operated by governments or in some cases by universities, which bring together teams of multi-disciplinary monitoring specialists. The pioneering Vesuvius and Hawaiian observatories each monitor only a few local volcanoes. In contrast, the Alaska and Cascade Volcano Observatories in the United States, the Institute of Volcanology in Petropavlovsk, Kamchatka, the Center for Volcanology and Geological Hazard Mitigation in Indonesia, and the Philippine Institute of Volcanology and Seismology (PHIVOLCS) watch hundreds of potentially active cones, calderas, and volcanic fields, many in remote locations. Indonesia has more active volcanoes (129) than any other country on Earth, and maintains observatories or observation posts on 66 of them! Seventy-nine volcanoes have erupted in Indonesia in the past 400 years, and each of these has the potential to cause widespread death and destruction in this densely populated land, so that the work of the dedicated volcanologists and technicians at these facilities is essential for public safety. State-of-the-art observatories also monitor the volcanoes of France, Italy, Japan, and Russia. New facilities continue to develop, but long-term funding support for volcanological studies waxes and wanes in response to short-term volcanic crises. It is no surprise that satellite remote sensing and telecommunications have become so important for monitoring volcanoes in remote locations and for providing early warnings about volcanoes that are becoming restless. All major observatories maintain portable equipment that can be deployed quickly to unmonitored volcanoes when needed (“expeditionary monitoring”). The US Geological Survey has established a special unit, the Volcano Disaster Assistance Program (VDAP) to send specialized equipment and volcanologists to any area in the world where emergency monitoring is requested. Several volcano observatories have been established as temporary responses to particular eruptions and have evolved into first-class observatories with wide responsibilities. An example is the Montserrat Volcano Observatory, established in response to the 1995 eruption of the Soufrière Hills [60] volcano, Lesser Antilles, which is now the foremost volcano observatory in the Caribbean region.

Only a thousand or so practicing scientists and technicians staff the world’s volcano observatories, but millions of people living near active volcanoes depend on their monitoring efforts to warn them of impending danger. Research carried on at these observatories is improving our understanding of active volcanoes, and is thus contributing to public safety.

MONITORING METHODS

Volcano monitoring involves visual observations, eruption documentation, and instrumental surveillance. The instrumental monitoring efforts are each based on the need to detect changes in the underlying magma chambers and the migration of magma within the volcano. Most of these instruments either *listen* to the volcano (seismic monitoring), or *measure changes* in

volcano shape, gas output, or thermal or magneto-electrical characteristics. Volcanologists also study the chemistry and mineral compositions of erupted rocks for hints about changing magma properties, and collect samples for archiving. No single monitoring method can adequately determine a volcano's behavior. Successful monitoring requires an appreciation of all the various techniques that can be brought to bear, and even then will depend heavily on individual human talents of interpretation and intuition. Here are brief descriptions of some of the most important monitoring techniques.

Seismic monitoring

Seismic monitoring is the single most critical activity at any volcano observatory and commonly provides the earliest warnings of pending eruptive activity. When the strength of rocks is exceeded by stresses caused by magma movement, the rock responds by fracturing. This generates acoustic waves which we can detect instrumentally or feel as an earthquake. Lower frequency seismic events may also be generated by sudden development or collapse of gas bubbles in magma, by the flashing of hot water to steam, or by shear during the flow of highly viscous liquids (Chouet 1996).

Seismic studies on an active volcano are a monitoring challenge, because volcanic earthquakes tend to occur in swarms rather than as the isolated, infrequent events and aftershocks typical of most non-volcanic regions. Volcanic earthquakes are much smaller than the largest tectonic ones, with greatest magnitudes (M) less than 5.0. Most volcanic earthquakes have M less than 2.0, and are only detected instrumentally. Hundreds of such tiny earthquakes may be recorded each day by sensitive instruments, though most have M less than 0, and cannot be located.

Seismic waves are detected by **seismometers**, electro-mechanical devices that generate electrical signals as the earth in which they are embedded moves vertically and horizontally. **Seismographs** record these signals. Older seismographs depended on needles to swing back and forth across slowly-rotating paper-covered drums, but modern systems record and analyze seismic signals digitally. The resulting trace, whether recorded in analog or digital form is called a **seismogram**, and consists of abrupt onset waves followed by a slow decay known as a **coda**. Minakami (1960) recognized two basic classes of volcanic earthquakes: **A-type** and **B-type**. A-type earthquakes have clear P (pressure)- and S (shear)-wave phases, relatively high frequencies and are caused by deeper fracturing of the wall rock around magma conduits. P-phase waves, which travel faster and arrive earliest at seismographs are recorded first. Slower S-phase waves arrive later (Fig. 14.24). The time difference between arrivals of these two waves is proportional to the distance of the quake to seismometers. B-type earthquakes have lower frequency coda, lack clear S-phase components, and typically occur at shallow depths (less than 1 km). These low frequency quakes may result from the formation and collapse of gas bubbles in rising magma, from fluid movement, or if very shallow, from flashing of steam and tensile fracturing or shearing of rock (Chouet 2003). These two classes of volcanic earthquakes (A- and B-types) are now commonly referred to as **Volcano-tectonic (VT)** and **Long-period (LP)** earthquakes, respectively.

Two other types of seismic signals may be recorded at active volcanoes. **Explosion events** generate short, sharp, high-frequency codas, made up entirely of compressive P-waves which typically accompany an air-shock pulse. **Volcanic tremor** is perhaps of most concern to

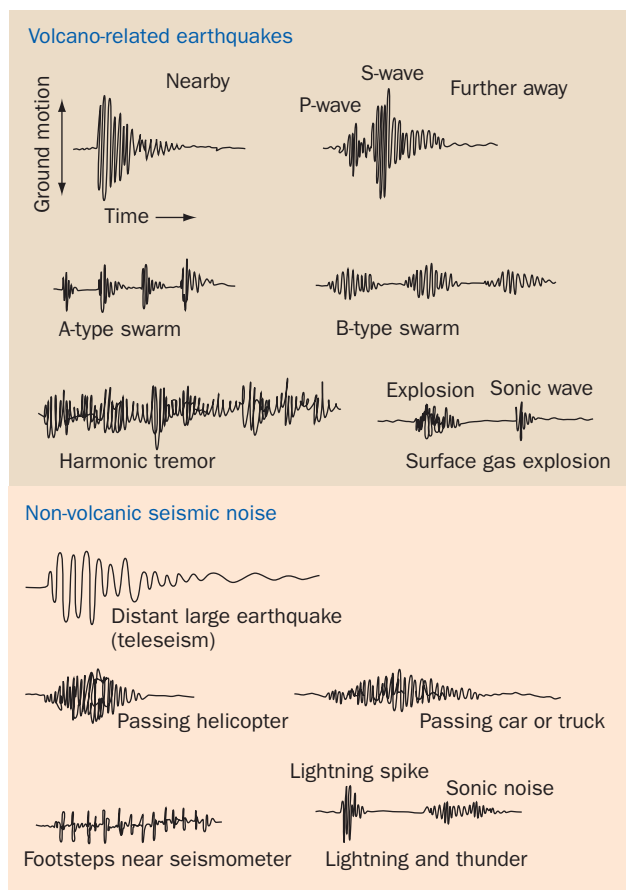


Fig. 14.24 Typical seismic signals that might be recorded on a volcano observatory seismograph. These are sketches – not actual seismic signal traces. From R. Y. Koyanagi (1974, pers.comm.) and other sources.

volcanologists, and appears as predominantly low-frequency harmonic coda that may persist for minutes, hours or days preceding or accompanying eruptive activity. This continuous vibration is often attributed to fluid moving under high pressure, in most cases by flowing magma, and commonly precedes or accompanies eruptive activity. Seismographs record many other types of signals at volcano observatories, some volcanic in origin, and some resulting from “noise” and distant non-volcanic events (Fig. 14.24).

As magma rises within 1 to 3 km of the surface, hours to a few months in advance of an eruption, the character of seismicity commonly changes. Newhall and Endo (1987) note that in 25 percent of the 192 eruptions they considered, high frequency (VT) quakes decline significantly before eruptive activity – an important “calm before the storm” signal. This might be due to intense shallow fracturing in the crust (McNutt 1996). Low frequency B-type (LP) earthquakes predominate in these pre-eruptive periods, often accompanied by volcanic tremor.

Seismic epicenters do not, however, always correspond to the locations of ensuing eruptions. For example, the precursory earthquake swarm at Pinatubo 1991 eruption began almost two weeks before the eruption – 5 km from the eventual outbreak site. Seismic activity declined at the original swarm site, then resumed directly beneath the impending eruption location, reflecting magma migration (Harlow et al. 1996).

At Kīlauea, an interval of intense summit deflation accompanied by strong harmonic tremor often begins tens of minutes to several hours before opening of the first eruptive fissures, especially when activity breaks out along one of the volcano’s rift zones. This enables volcanologists to warn local authorities in time to safely evacuate visitors from potentially threatened areas in the National Park (Chapter 1).

During the ensuing eruption, all types of volcanic earthquakes may be generated. Their relative abundances, frequency distribution, and times of onset provide important clues about eruption mechanics. At explosively erupting volcanoes where eruptions occur in a series, precursory seismicity may be strong for the initial outburst, but once the vent is cleared of obstructions little or no seismic precursors may precede further explosions. McNutt (1996) recommends careful and cautious monitoring around such volcanoes at least three to six months following an explosive event to make sure people are not caught by surprise. Following eruptions, episodes of renewed deep (5–15 km) high frequency seismicity commonly occur beneath many volcanoes, which Abe (1992) relates to readjustment in the crust as a result of the withdrawal of magma. These earthquakes may signify a return to volcanic quiescence, the true end of an eruption.

Computer data processing has opened new opportunities for analysis of volcanic earthquake swarms in recent years. The Real-time Seismic Amplitude Measurement (RSAM) system,

introduced by Endo and Murray (1991) averages the amplitudes of all earthquakes, irrespective of type, recorded at a particular seismic station over intervals of one to ten seconds, then presents the data in a time-amplitude diagram helping researchers see how the overall seismic energy of an earthquake swarm is changing. The Seismic Spectral Amplitude Measurement (SSAM) system (Stephens et al. 1994) takes a slightly different approach by analyzing the amplitudes of seismic waves for particular frequencies as recorded during fixed intervals of time at particular seismometers. These systems permit volcanologists to track the progression of the various kinds of volcanic activity in real-time immediately before an eruptive event; an important contribution of modern seismic technology to a better understanding of volcano dynamics.

McNutt (1994) developed another way of comparing seismic energy release with volcanic activity, studying the codas of volcanic tremor recorded at various seismic stations around erupting volcanoes. He showed that the energy released as volcanic tremor (primarily harmonic) is directly proportional to the intensity of eruptions, and to such eruption parameters as the amount of ejecta released and the heights of ash columns. By this method, were a strong eruption to take place at night with no visual observations or radar facilities nearby, tremor measurement alone could provide a general idea of potential aviation threat from rising ash plumes with a certainty of about 95 percent.

DEFORMATION MONITORING

As has been discussed elsewhere in our text, volcanic edifices are rather weak structures, mostly comprised of relatively brittle, easily fractured lava flows and loose accumulations of volcanic ash and breccia. Conceptually, it is useful to think of active volcanoes as balloon-like coverings over their underlying magma chambers, and one begins to conceptualize volcanic deformation this way when living on or near an active volcano! Whenever internal pressures within magma chambers change, or magma migrates to a different part of the volcano, volcano surfaces deform accordingly. The many geodetic techniques for monitoring these changes will be discussed briefly here, but are treated in much greater detail by Dzurisin (2007).

Deformation changes on an active volcano are usually very small and physically imperceptible to humans, and can only be detected by sensitive instruments. At times however, volcanic edifices deform rapidly due to the internal movement of shallow magma, such as at Showa Shinzan [132] in the early 1940s (Chapter 9), or at Mount St Helens in the early spring of 1980 (Chapter 7). Sakurajima [109], is a composite volcano rising 1100 m above the mostly submerged Aira Caldera in southern Japan (Chapter 10). The influential Japanese seismologist F. Omori studied its powerful 1914 eruption, and noticed that benchmarks around the mountain rose in elevation as magma moved toward the surface before the eruption, inflating the landscape over many square kilometers (Omori 1914). His observations were the first showing that changes in the level and slope of the surface could be used to discern subterranean magma movement. Ground deformation studies have since been applied to many active and erupting volcanoes worldwide, notably achieving refinement at Kilauea in Hawai'i, where eruptions are usually non-violent, access is easy, and the climate mild.

There are three basic parameters of volcano deformation that need to be monitored: horizontal distance, vertical elevation, and surface tilt. These three parameters are interrelated, and normally all three variables are involved as any volcano changes its shape. Until recently

each of these geometric variables were measured separately with different instruments and techniques, but increasingly capable, newly developed instruments, many involving earth satellite technology, have revolutionized geodetic studies and can simultaneously measure multiple parameters over large areas. The new instruments are relatively expensive, however, and time-tested traditional monitoring tools are still useful – especially for surveys of smaller areas.

Old-fashioned optical theodolites and stadia rods have been used to measure horizontal distances and elevations for over 200 years, and are inexpensive and useful tools for volcano deformation studies. They are still used for **leveling surveys**, which are the most versatile methods for precise measurement of elevation changes around the flanks of deforming volcanoes. Leveling depends upon a network of benchmarks that must be surveyed repeatedly to measure volcanic deformation over time. For reference to other surveys these networks must be tied into locations that surveyors assume represents “stable” ground. Such a reference benchmark ordinarily is not far from the base or summit of a volcano, since the ground heave associated with volcano inflation tends to be largely confined to the area of the edifice itself. On island volcanoes Mean Sea Level (MSL) is a handy reference point.

Although horizontal distances can be measured with theodolites, they have low precision compared to various types of Electronic Distance Meter (EDM) devices that have been developed over the past 40 years for precise measurements along lines of sight. Differences in vertical angle (elevation) as well as distance between benchmarks may be combined using modified EDM systems called **total field stations**. Total field instrumentation, as well as EDM equipment is somewhat expensive, but less sophisticated means of measuring tilt and leveling certainly lie within the means of low-budget volcano monitoring efforts. During the Mount St Helens activity in late 1980–2, ordinary steel tapes served to measure rapid ground deformation, permitting successful prediction of 13 dome eruptions (Swanson et al. 1982)

Tiltmeters record the slope of the ground. As the interior of a volcanic edifice inflates and fills with new magma, the flanks of the mountain ever so slightly steepen. **Wet tilt measurements**, largely superseded by electronic tilt measurement devices, utilize three water pots connected by hoses are arrayed in an equilateral triangle with sides approximately 15 meters long. The level of water in each pot, achieving equilibrium, changes as the slope of the ground changes, with water flowing into the lowermost pot. **Dry-tilt** measurements are a simpler alternative to wet tilt, involving theodolites and stadia rods. Tilt measurements are remarkably precise; a well-maintained tiltmeter can detect angular changes of less than a **microradian**, equivalent to the angular change of a kilometer long board lifted a mere millimeter at one end (Decker & Decker 1997).

The advent of satellite-based surveying using the Global Positioning Satellite (GPS) and other systems has revolutionized volcano deformation studies and largely replaced older conventional surveying methods at most modern observatories. GPS surveys allow real-time horizontal and vertical data to be remotely collected in hard to access places, and do not require lines of sight between survey points. Space-based **remote sensing** technology is providing even more capable tools for volcano deformation studies – these are described in a later section.

K. Mogi (1958) first provided a mathematical model relating ground deformation around active volcanoes to volume changes of underlying magma chambers. His work permitted

volcanologists to calculate depths to the sources of deformation. Mogi applied his new model to Omori's 1914 Sakurajima data, which showed that between 1895, when local benchmarks were emplaced, and 1914, during the eruption, a 60 km wide region centered around the middle of Aira caldera subsided by as much as a meter, while the immediate vicinity of Sakurajima rose by several meters. Mogi determined that the source of deformation lay 8–10 km beneath the center of Kagoshima Bay, about 10–15 km away from the volcano. Subsequent uplift in this broad region beginning in 1919 indicated replenishment of the caldera magma system, which culminated in another Sakurajima eruption and regional subsidence in 1946 (Murray et al. 1995). Several refinements of Mogi's equations to allow for analyses of more complex magma body geometries have subsequently improved the utility of ground deformation studies to interpret subsurface processes.

OTHER GEOPHYSICAL MONITORING TECHNIQUES

Geophysical monitoring techniques of many varieties complement seismic and ground deformation monitoring. Microgravity studies, for example, seek to detect changes in mass within volcanoes arising from shallow intrusions, although they must be combined with deformation monitoring to filter out elevation changes that also affect gravity. Gravity surveys are also useful for evaluating internal density structures of volcanoes, which can define caldera infill deposits, shallow conduits, and hydrothermally altered bedrock areas. Different kinds of volcanoes have different gravitational responses to intrusions. Changes in gravity are strongest, and in some respects most easily interpreted, around composite volcanoes. Eggers (1987) argued that this was due to displacement of high-density rock by vesiculating magma. An integrated approach to monitoring magma movement through simultaneous measurements of gravity and deformation changes shows promise for evaluating pre-eruptive behavior and may be useful for eruption forecasting (Rymer & Williams-Jones 2000; Williams-Jones & Rymer 2002).

A great variety of electrical methods may be utilized for volcano monitoring, and include measurement of the electromagnetic (EM) fields generated by volcanic activity, induced EM fields generated by large surface transmitters, surface measurement of electrical self-potentials, surface or subsurface studies of heat flow, and perturbation of Very-Low Frequency (VLF) radio signals by shallow magma conduits. VLF-EM studies at Kilauea volcano are now being used routinely to evaluate the flux rates of shallow magma movement in pyroducts (Kauahikaua et al. 2003). Volcanoes make lots of noise when they erupt, but most of their sounds are inaudible to human ears. Infrasound waves (<20 Hz) reveal a great deal about volcanic activity and eruption precursors. Infrasound monitoring is a valuable tool for volcano observatories – especially at night or during bad weather when visual observations are not possible (Garces et al. 1999, 2003).

Gas monitoring

As was discussed in Chapter 3, all magmas contain dissolved gases as important components, and as these magma bodies rise toward the surface or undergo cooling and crystallization, large

amounts of these gases are released and rise to the surface, Monitoring of these gases is an important component of overall monitoring efforts, and many techniques are in use. Those methods can be divided into three categories:

- 1 direct sampling of gases emitted from known fumaroles or soils – which can be done through field sampling for later laboratory analysis or continuous instrumental monitoring;
- 2 direct sampling of air, either through continuously-operated air quality monitors or from airborne sampling devices; and
- 3 remote-sensing techniques – either from satellite based monitors that categorize and track volcanic plumes as they migrate downwind of active volcanoes or by looking up at volcanic plumes from ground-based instruments. These techniques are discussed in the following section.

As has been mentioned earlier, the three most important volcanic gases emanating from volcanoes are water (H_2O), sulfur dioxide (SO_2), and carbon dioxide (CO_2), although many more volatile species are usually present in minor amounts. H_2O is the most visible gas, since it readily condenses to the steam seen as “smoke” above volcanoes and volcanic fumaroles. It is the least important gas to monitor, however, because it largely comes from secondary meteoritic sources, and does not tell much about underlying magmatic systems. SO_2 is much more important, as it is almost entirely derived from magmatic sources and is an atmospheric pollutant of concern (Chapter 13). Interpretations of SO_2 flux variations are made difficult by the fact that it is highly soluble in water, however, and its release from solfataras and fumaroles is greatly affected by rainfall and soil moisture. Nonetheless it is easy to monitor semi-quantitatively in volcanic plumes by remote sensing techniques (discussed later), and gives an important measure of magmatic production rates at active volcanoes. CO_2 is increasingly viewed as an important volcanic gas for study, since it is highly mobile, rises quickly to the surface from magmatic sources, is not greatly affected by surface water, and may be one of the best indicators of the emplacement of new magma beneath a volcano (Chapter 3). New analytical tools have made CO_2 flux monitoring much easier and applicable for volcano monitoring (Gerlach et al. 2002). Large declines in CO_2 emissions preceding each of three Plinian eruptions at Mount St Helens in 1980, detected by direct plume sampling, helped to forecast the eruptions of August 7 and October 16–18 (Harris et al. 1981).

VOLCANO REMOTE SENSING

In its broadest sense, remote sensing refers to any technique that allows observers to monitor volcanic activity from distant vantage points, and could include visual and photographic documentation. Since the development of Earth-orbiting satellites in the past half-century, however, the term has been increasingly associated with observations made from space (Mouginis-Mark et al. 2000). These new methods allow for global monitoring of volcanoes that are either too remote, or at times too dangerous for conventional ground-based study. Quantitative remote sensing methodologies can be deployed from three platform levels: ground, aircraft, and satellites.

Ground-based techniques

The earliest remote sensing studies involved the analyses of SO₂ emissions in volcanic fume clouds using a correlation gas spectrophotometer (COSPEC). Observers could breathe fresh air, well away from eruptive perils, from fixed points or by driving COSPEC-mounted vehicles back-and-forth beneath plumes to quantify daily emissions of sulfur. Newer techniques and instrumentation, including miniaturized UV-spectrometry (FLYSPEC), Fourier Transform InfraRed Spectroscopy (FTIR) and mini-Differential Optical Absorption Spectroscopy (DOAS) analyze the ratios and absolute amounts of a wide variety of gas concentrations issuing from volcanoes (Platt & Stutz 2008). Since such ratios can systematically change before, during, and after eruptions, these new techniques are powerful and relatively inexpensive tools for gas geochemists. Ground-based radar in support of civil aviation has proven remarkably effective in tracking the appearance and expansion of large eruption ash clouds when eruptions occur near major airports, as during the Mount St Helens eruptions (Chapter 8).

Airborne techniques

Airborne COSPEC monitoring is useful, though it is far more expensive than ground-supported studies, and cannot be repeated following the same precise routes. Thermal infrared multispectral scanning (TIMS) and the related multispectral infrared and visible spectrometer (MIVIS) system hold more promise for airborne applications, permitting researchers to map volcanoes in reconnaissance detail. TIMS work is especially useful in discriminating lava flows of different age based upon weathering and other aging characteristics (Kahle et al. 1988). Highly detailed and accurate mapping is also facilitated by topographic synthetic aperture airborne radar (TOPSAR), which creates digital elevation models (DEMs) of volcanoes. Francis et al. (1996) cite the example of the DEM mapping of a lava flow on Hekla [67] having a variable thickness of 5–33 m, with relief of up to 15 m on its surface. Ridge lines as small as 2 m high could be mapped remotely, with minutes of data collection and a few days of processing in the place of months or years of arduous ground work.

Satellite techniques

Satellite observation has proven to be a low-cost and effective alternative to ground monitoring for many remote volcanoes. The technology has yet to achieve its full potential, but is already showing exciting possibilities. The earliest non-military detection of volcanic heat from Space took place over Surtsey [66] volcano, Iceland, in 1967 (Williams & Friedman 1970). Since then, volcanic reconnaissance has become an important service of many different satellites. Five kinds of space platforms have demonstrated different kinds of utility (Francis et al. 1996):

- 1 High spatial resolution sensors, such as the LANDSAT thematic mapper (TM) and the French Systeme Probatoire d'Observation de la Terre (SPOT) sense visible and infrared

energy reflected or radiated from Earth's surface back into space. They can resolve the details of land forms down to the scale of 10–30 m, which can assist in large-scale study of volcanic landforms. De Silva and Francis (1991) scrutinized TM images of the central Andes to estimate the number of potentially active volcanoes in that region, based upon degrees of post-ice age erosion and volcanic deposition. The same locality may be observed by TM or SPOT cameras from once a week to once a month, depending upon the satellite and its orbit. This makes these sensors of little use in examining on-going eruptions, but they can provide the first information we get about volcanic change in little-visited localities. Rowland and Munro (1992) document a large intra-caldera avalanche and eruption within Fernandina [47] caldera in the Galapagos, which came to the attention of volcanologists thanks to SPOT reconnaissance. TM observations, together with those of the advanced very-high resolution radiometer (AVHRR) have also been the primary means of monitoring eruptions at Láscar [58] volcano, Chile (Francis & Rothery 1987; Wooster & Rothery 1997). Despite its name, the AVHRR lacks the fine resolution of TM and SPOT surveys. But this system can provide data at least four times a day for any volcano in the world, making it potentially valuable as a means of monitoring eruptions. It provides data changes in the heat emission of large bodies, including lava lakes (Wiesnet & D'Aguzzo, 1982), cooling lava flows (Oppenheimer 1991) and pyroclastic deposits (Harris et al. 1997). AVHRR images are wide-ranging – to 3000 km, and may be downloaded for study within ten minutes.

- 2 Environmental satellites, like high resolution sensors, detect visible light or infrared radiation, and can obtain multi-spectral images. Their spatial resolution is low (hundreds of meters), as they image large areas and can survey the entire globe. This makes it possible to spot volcanic plumes that might be missed by other, more narrowly-focused satellite scans. Such satellites travel in polar orbits, providing frequent repeat viewing of single locations. Hence it is easy to track the progress of eruption plumes to warn people downwind, including aviators. The total ozone mapping spectrometer (TOMS), aboard the Nimbus-7 and Meteor-3 satellites, is intended to monitor the condition of the ozone layer, but has also proven invaluable in monitoring sulfate aerosol injection of the stratosphere during big explosive eruptions. The Moderate Resolution Imaging Spectroradiometer (MODIS) instruments are carried aboard the Terra (EOS AM) and Aqua (EOS PM) satellites, and have replaced TOMS for volcanic plume monitoring.
- 3 Space Shuttle and related space vehicle photography has produced spectacular images of volcanoes and eruptions from Space, and are readily available from government facilities or private vendors. Unfortunately, such platforms are not in continuous operation, like most other satellites, and are only of use when subject volcanoes are cloud-free.
- 4 Synthetic aperture radar (SAR) methodologies, first developed for terrain mapping of remote or inaccessible areas from aircraft, can now be employed on satellites, which cover vast areas of the Earth. Rowland et al. (1993) used SAR data to examine Aleutian and Alaskan volcanoes, which, for other approaches, are often very difficult to study owing to inclement weather and shortage of daylight. Radar analysis enabled them to map volcanic deposits around Aniakchak [9] caldera, Westdahl [5] and Spurr [22] volcanoes. More impressively, perhaps, radar showed the presence of dimples in the ice cap of Veniaminoff [8] volcano, which may have marked the occurrence of recent subglacial eruptions. The Phased

Array L-band SAR (PALSAR) instruments carried on Japanese satellites are able to provide detailed terrain images through dense vegetation – very useful for geologic mapping of tropical volcanoes.

- 5 SAR **radar interferometry** has proven to be extremely useful for remote detection and analysis of volcanic deformation – for volcanoes not covered with deep vegetation, and also for volcanoes covered by ice (Scharer et al. 2008). The basic methodology was proven following the 1992 M7.3 Landers, southern California earthquake, when SAR images taken from almost 800 kilometers above the Earth were compared with images taken by happy chance not long before the seismic displacements. Wavelength analysis provided a precise measure of how distances had changed between satellite and ground as a result of the earthquake, leading to construction of an **interferogram**, or ground displacement map (Massonet et al. 1993). In just a few moments SAR had gathered data that would have taken years to collect using standard methods, and revealed patterns of strain that might never have become evident otherwise. Scientists quickly recognized that this technique also holds great promise for volcanic ground deformation monitoring. For example, interferometry showed uplift from renewed dike injection beneath the floor of remote Okmok [4] caldera in the Aleutian Islands following a 1997 eruption, with shifting loci of uplift tracking the migration of the shallow melt. Since no other means of closely monitoring the volcano existed at the time, SAR satellites became instant, low-budget “volcano observatories.” An example of an interferogram that demonstrates volcanic deformation on the island of Hawai‘i over a four year period (Fig. 14.25) demonstrates the utility of interferograms in monitoring volcano deformation over large areas. Interferograms are notoriously difficult to analyze however, and their interpretations may be ambiguous and dependent on the experience of the investigator involved. Conventional methods have the advantage of greater precision and simpler interpretation, and can be conducted at low cost with traditional survey equipment, but they only reveal changes at specific survey points.

Volcanic Crisis Management

Volcanic disasters are usually preceded by volcanic crises or premonitory activity, and this pre-eruptive period is the most crucial time period for scientists, emergency managers, and political authorities to coordinate their activities to avert preventable losses. Pre-eruptive crises involve complex interplays among the scientists themselves, and between scientists, emergency managers, and the political authorities who must ultimately make the difficult fiscal and humanitarian decisions required to protect lives. Successful management of volcanic crises and disasters is best achieved when there is a prior awareness of potential hazards by *all* the above, and the roles of these key players are well defined in advance. Unfortunately this is all too rarely the case, and in practice these relationships usually need to be established or refined after a volcano becomes restless or a disaster strikes. The most important factor in successful crisis management is the establishment and maintenance of effective channels of communication between each of these groups and with the media representatives who will ultimately convey most of the information to the affected public. As noted earlier, effective, ongoing public education about volcanic risk and hazards can facilitate this communication and enable timely

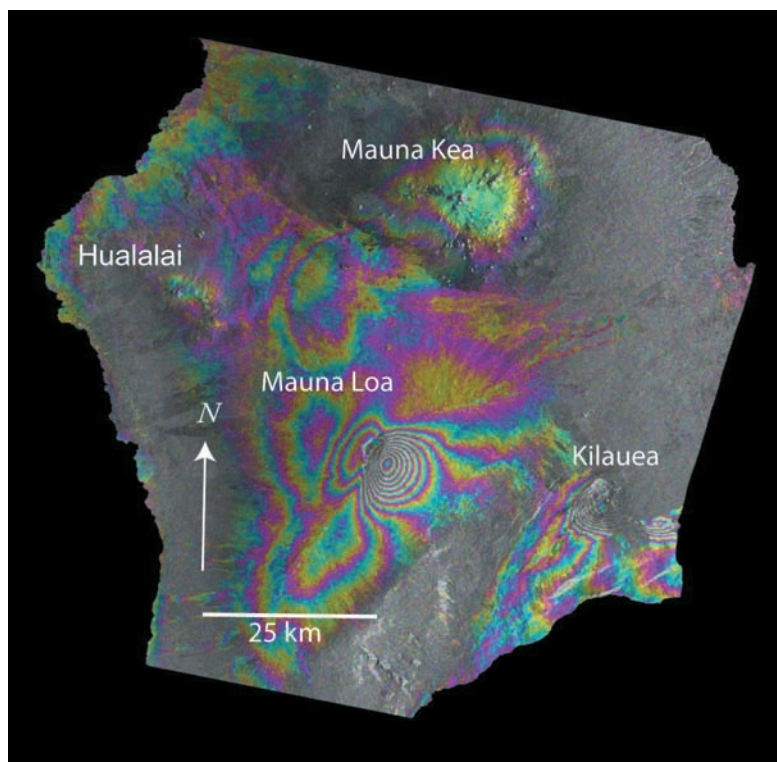


Fig. 14.25 SAR interferogram of part of Hawai'i Island, showing deformation of Mauna Loa and Kīlauea volcanoes over a four year period (January 27, 2003 to January 1, 2007). Surface deformation between those two time periods is represented by colored fringes. Each set of fringes represents 2.8 cm of deformation along the radar's line of sight, but because the radar's look angle is inclined from vertical (about 22 degrees in the above image), the observed deformation is a mix of vertical and horizontal motion. As a result, many deforming regions (for example, southeast of Mauna Loa's caldera) have an asymmetric appearance. A progression of fringes from pink to yellow to blue indicates decreasing range (distance) between the satellite and ground. The opposite fringe progression indicates lengthening distance between the satellite and ground. Fringes in the summit region of Mauna Loa indicate inflation, with the double-lobed pattern suggesting both a spherical magma reservoir at depth just southeast of the caldera plus a tabular magma body running the length of the caldera. Inflation is also occurring at Kīlauea's summit, although the East Rift Zone is deflating. The fringes around Mauna Kea and northwest of Mauna Loa are related to atmospheric distortion and not to deformation. Interferogram and caption by Mike Poland, USGS.

citizen responses to hazards alerts as they are issued. Scientists have the most critical roles to play during volcanic crises, as they initially have great public credibility. Maintaining that credibility is important, and depends on their professional behavior (IAV-CEI 1999). Fiske (1984) presents a particularly telling example of the interaction of volcanologists, government and the media in the case of two nearly simultaneous, close-by volcanic eruptions in the Caribbean. La Soufrière-Guadeloupe³ [61] is an eroded, 12 km wide composite volcano surmounted by a younger cone at the southern end of Guadeloupe Island, about 500 km southeast of Puerto Rico. About 72,000 people lived on the flanks of La Soufrière in 1976, most of them in the district capital of Basse Terre on the west coast of the volcano. Earlier seismic monitoring indicated that the base level earthquake count for La Soufrière is 1–10 shallow tremors a month. Between July 1975 and July 1976, however, this number steadily rose to over 200 events a month. Plainly magma was on the rise somewhere in the volcano, though little scientific attention was given to the matter. On July 8, 1976 the first of many explosions suddenly burst forth as dense clouds of ash and steam roiled from summit fissures. This triggered panic as local residents fled the mountainside. Over the next month intermittent ash outbursts continued while steam emissions increased and earthquake numbers remained high. On August 12, scientists declared that falling ash now included fresh glassy material, not the pulverized older rock fragments that had characterized the initial Ultravulcanian phase of the eruption. This suggested that magma had ascended to a shallow level beneath the summit and had begun discharging directly to the surface. To some of the scientists this

³ There are two volcanoes named "La Soufrière" in the lesser Antilles – this one more specifically referred to as "La Soufrière-Guadeloupe," and another 300 km to the south on the island of St Vincent.

indicated that dome growth and violent explosions were possibly imminent. Remembering the Mt Pelée volcanic disaster on nearby Martinique 74 years earlier (Chapter 1), these scientists urged the local governor to begin immediate evacuation of the tens of thousands of residents remaining in the area.

It later came as a shock for the governor and members of the public to realize that the volcanologists urging evacuation had spoken in haste. In fact, the fine glassy ash had been misinterpreted. Later study indicated that no juvenile material had been present. But the damage had been done. Organized evacuation of any large population is not only a logistical nightmare, made worse when pressured by immediate dangers, but an economic and social catastrophe as well. The population of Guadeloupe was not wealthy, depending heavily upon agriculture, fishing, and tourism for sustenance. These slim sources of income disappeared as people rapidly streamed from La Soufrière to safer quarters of the island. The government evacuated nearly a quarter of the endangered population within the first two days.

Meanwhile, more than a dozen other scientists converged on the island, mostly from France, and began work out of a hastily-assembled volcano observatory at Fort St Charles. There was little coordination between these scientific groups, and no single spokesperson who could speak for all of them. Instead, the observers haphazardly worked in separate groups, in two rival teams. Members of the press wandered freely in the field, including areas that were closed to the public. Ever eager for a story, media personnel hurriedly interviewed members of the different teams, amplifying scientific differences and speculations publicly. This deepened personal rivalries among some of the scientists, exacerbated public fears, and created needless tension for authorities who were trying to constrain the impact of the crisis. One group of scientists concluded that the eruption was not so dangerous as originally feared. The other held fast to the alarmist scenario. During the next few months, as volcanic activity gradually waned, public disagreements that should have been privately discussed in the setting of an organized team raged in public. In the end, the French government convened a special Committee, including foreign volcanologists, to develop a scientific “consensus” on the situation, based upon all available information. The Committee concluded that the doom-sayers had erred in their judgment. Careers were needlessly savaged, the economy of Guadeloupe wastefully disrupted, and the credibility of the volcanological community was greatly diminished.

Less than 3 years later another crisis struck the Caribbean when a different volcano, also coincidentally named Soufrière [62], began erupting on St Vincent island, about 300 kilometers south of Guadeloupe. This eruption occurred only 77 years after a tragic eruption in 1902 had killed almost 1700 people on the island, so there was great potential for panic. In this case, however, a well-established seismic monitoring and tiltmeter array operated by the University of the West Indies provided advance warning of impending activity and prevented panic as about 20,000 people evacuated from threatened areas. Only 5–7 scientists converged on the island during the eruption, organized under a single aegis at a volcano field station that was kept strictly off-limits to the press. A single scientific consensus presented by telephone or in writing reached the media through appointed representatives, while differences in scientific opinion were resolved privately. Although the explosive eruption caused great agricultural damage owing to tephra fall and formed a new dome, no lives were lost (Fiske & Sigurdsson 1982). The lessons from these eruptions have been learned, and have been effectively applied in many (though not all) volcanic crisis situations ever since.

Whims of fortune and judgment also play an important role in the “management” of every volcanic crisis. Had the volcanic ash on La Soufrière not been misidentified, and a major eruption had taken place, how would the situation have played out? Had a General in command of Clark Air Force Base in the Philippines not taken seriously the timely warning of USGS and PHIVOLC scientists to evacuate Clark Air Force Base before the climactic 1991 Pinatubo eruption, how many more people might have died there?

A bottom-line reality to keep in mind, is that volcanologists never know exactly what a volcano will do – no matter how sophisticated the available monitoring equipment and expertise deployed. At some point human judgment (“best guesses”) have to be made, and we each have to hope and pray that our assumptions are correct. When life and death decisions must be made as to whether people should be evacuated from threatened areas, how far they should be moved for safety, and how long they should stay away, the most important thing volcanologists can do is to first reach consensus amongst themselves. They must then convey consistent recommendations to the government authorities and agencies that will ultimately make the difficult decisions required to save lives. Those decisions depend not only on scientific forecasting, but also on critical economic, political, and social factors that must ultimately be considered.

This does not mean, however, that volcanologists can simply provide their factual observations and recommendations to government authorities and then walk away from all responsibility as to how and if their recommendations are acted on. The tragic 1985 eruption of Nevado del Ruiz (Colombia) was a type example of what can happen when knowledgeable volcanologists fail to concern themselves with the “end-use” of their findings. Ruiz gave ample warning of an impending eruption when small earthquakes and increased fume emissions were noted from the ice clad, 5300 m high summit crater in November, 1984 – a year before the climactic eruption. Local geologists, who had no previous experience dealing with restless volcanoes, realized the potential hazards involved, and alerted national Colombian officials about the potential risks to populated areas. John Tomblin of the United Nations Disaster Relief Organization (UNDRO) was invited by Colombian officials to assess the situation in March, 1985, and afterwards issued an international appeal for technical assistance (Mileti et al. 1991). Unfortunately, there was little response until a large phreatic eruption occurred on September 11, 1985, deposited ash around the volcano and sent a lahar almost 30 km downslope. UN-supported technical experts came to Colombia from Costa Rica, Ecuador, Italy, and the United States. They provided advice, some seismic monitoring equipment, and recognized the extreme risk to cities located along river valleys downslope, but made no efforts to see that their findings reached the people at risk. The Colombia Geological Survey (INGEOMINAS) took the lead in assessing the hazards, but had little success in convincing others about the gravity of the situation. INGEOMINAS published an excellent risk map in early October (Fig. 14.13), but made no major effort to contact threatened populations directly. The Colombian Civil Defense Agency and local authorities made uncoordinated efforts to educate people living in high risk areas, but were thwarted by sensational stories in Colombian newspapers, which in some cases accused government scientists of attempting to lower property values for personal gain. The excellent risk map published on 7 October was distributed to 17 different government agencies, but insufficient efforts were made to present the map to affected citizens, although the map was published by a national newspaper on October 9 (Herd and Comité de Estudios Vulcanológicos 1986).

As a result, 25,000 people died needlessly on the night of November 13. None of the victims would have needed to walk more than 150–200 m to higher ground that night to have survived – had they understood the risks involved and had they received credible warnings of their peril. “Top-down” volcanic crisis management works fine to assess risks and to coordinate agency responses, but to save lives successful crisis management requires “bottom-up” input and participation from the people whose lives are in jeopardy. Unless local citizens and their leaders are directly informed about their peril by credible scientists and trusted higher level authorities, and become personally involved in the means of their salvation, disasters like that of November 13 are bound to be repeated in the future. When effective communication channels are never established (ideally before disaster strikes), confusion and tragedy are likely to result (Fig. 14.26). Public education about volcanic hazards helps pave the way for such communication channels to open quickly and effectively as need demands. Consider, for example, that community-based education carried out by dedicated volcanologists from the Rabaul Volcano Observatory facilitated the timely self-evacuation of more than 10,000 people when Tavurvur volcano erupted in the middle of the night in 1994. Governments that tend to be paternalistic in nature assume that bureaucratic efforts alone can protect their citizens; but a well-informed population can take measures to save itself and avoid mass tragedy as soon as warnings pertaining to volcanic eruptions are issued.

Another very important aspect of volcanic crisis management concerns the relationships between volcanologists and the media. The media (newspapers, radio, and television) are the most important intermediary between scientists and citizens who are at risk. This is because the media are able to reach a much broader audience of potentially vulnerable people than feasibly could be reached by scientists through public meetings, and in many cases the media will have already established great credibility with their audiences. It is therefore critical that scientists know how to communicate effectively with media personnel and that a scientifically credible representative be chosen to act as a single spokesperson for scientific teams during a crisis. This person needs to understand and respect the special needs of reporters who can become either important allies – or harsh adversaries if good relationships are not carefully fostered.

There are generally two types of media representatives who attend press conferences and/or seek interviews with scientists during major volcanic crises or disasters; the approaches and needs of these two groups tend to differ greatly. **National and international reporters** are often interested in sensational headline-grabbing stories and may be prone to exaggeration in order to attract an audience. Depending on circumstances, they also face clear-cut deadlines that may vary significantly from those of the more laid-back local media. Such persons should be treated more formally, with a certain degree of caution to avoid misunderstandings and damaging mis-quotes. Reporters representing **local media**, however, fall into a second distinct category and are the most important messengers of critical information that local citizens need to understand for personal survival. These reporters usually have a vested interest in “getting the story right” and are the ones whose friendship and trust are best cultivated *before* a volcanic crisis develops. In an ideal situation, local volcanologists will have established relationships with these reporters long before the “outside” media descend during a major crisis. One can speak frankly with them about details that might be impossible or dangerous to discuss at formal press conferences when video cameras are rolling and tape recorders are turned on!

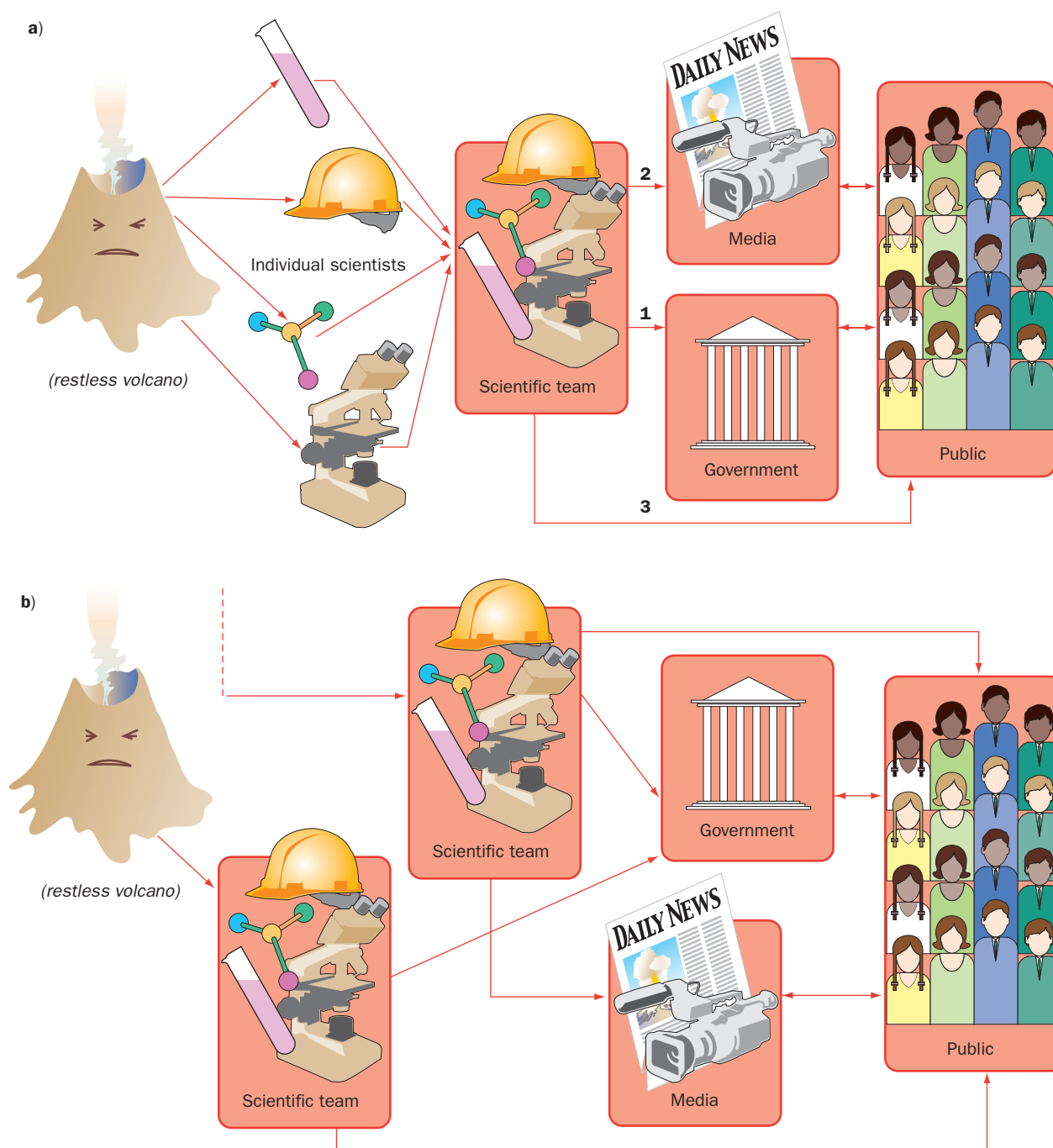
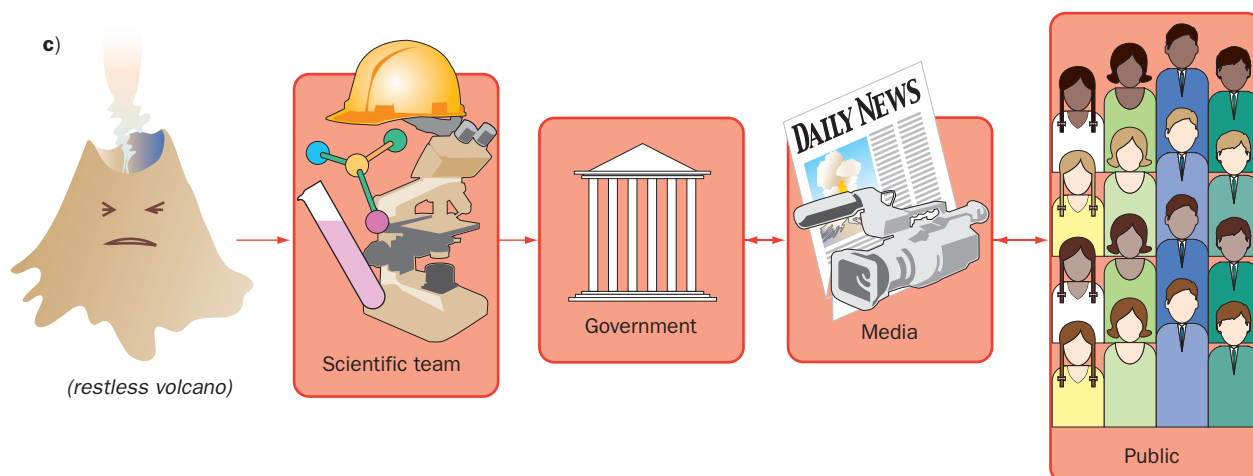


Fig. 14.26 Volcanic crisis management relationships flow sheet. a) Ideal relationships: 1) The volcano provides data to individual scientists; 2) The scientists form one team and speak with one voice; 3) The scientists first provide information to government authorities, then via press conferences to the media, then directly to the affected public via public meetings. b) La Soufrière-Guadeloupe experience (1976): 1) The volcano provides data to independent scientific teams; 2) The individual scientific teams contact the media, then the authorities with their individual opinions; 3) Mass confusion and misunderstandings result.



Another factor in crisis management involves the length of the pre-eruption crisis. Eruptions preceded by short, intense periods of forewarning activity (e.g., Galunggung – Chapter 1) are more easily dealt with by public officials than are those preceded by several months or years of pre-eruptive activity. People can too easily become used to dangerous pre-eruptive events if they occur over a long enough period, and the warnings of volcanologists may become less and less credible. The catastrophic May, 1980 eruption of Mount St Helens (Chapter 7) was preceded by less than two months of relatively low-level activity. What terrible loss of life might have occurred had “nothing much” continued to happen until the peak of the summer tourist season? Would public officials have continued to heed the warnings of scientists as political and economic pressures to open the area to the public increased?

Volcanic eruptions will always be accompanied by hazardous activity, and the risks to society posed by that activity are constantly growing, as populations increase near active volcanoes. To lessen those risks, new generations of volcanologists must continue to develop enhanced techniques to better understand volcano behavior and for volcano monitoring. The odds that a major caldera-forming eruption will occur in a densely-populated area in the near future are very low, but such an eruption could well occur one day, and one can hope that by then future volcanologists will have developed reliable eruption prediction tools that will allow credible warnings to be given before disaster strikes!

Fig. 14.26 (cont'd)

c) Ruiz experience (1985): 1) The volcano speaks to scientists, who form one team; 2) The scientists speak mostly to government authorities; 3) The media provides confusing reports to the public; 4) The public receives mixed messages that are mostly ignored – a mass tragedy results.

FURTHER READING

- Blong, R. J. (1984) *Volcanic Hazards: A Sourcebook on the Effects of Eruptions*. Orlando, Academic Press.
- Dzurisin, D. (2007) *Volcano Deformation: Geodetic Monitoring Techniques*. Chichester, UK, Springer-Praxis.
- Latter, J. H. (ed.) (1989) *Volcanic Hazards: Assessment and Monitoring*. Berlin, Springer-Verlag.
- Mader, H. M., Coles, S. G., Connor, C. B. et al. (2006) *Statistics in Volcanology*. London, Geological Society of London.
- Mouginis-Mark, P. J., Crisp, J. A., and Fink, J. H. (eds.) (2000) *Remote Sensing of Active Volcanism*. Washington, DC, American Geophysical Union.
- Scarpa, R. and Tilling, R. I. (eds.) (1996) *Monitoring and Mitigation of Volcano Hazards*. Heidelberg, Springer-Verlag.

Chapter 14

Questions for Thought, Study, and Discussion

- 1 What is the most important work a volcanologist can do – volcanic *hazards* evaluations, or volcanic *risk* mitigation? Defend your answer!
- 2 Does a volcano have actually to be in eruption to be considered active? Explain.
- 3 Why are dormant volcanoes especially dangerous?
- 4 What is the difference between “primary” and “secondary” volcanic hazards? Provide an example of each category.
- 5 Why are tropical maar lakes apt to be more dangerous than their counterparts in more temperate climates?
- 6 Under what circumstances are Poisson analyses appropriate for the evaluation of volcanic risks?
- 7 What are probability event trees, and how are they useful?
- 8 What is the value, and what are the limitations of volcanic hazards maps?
- 9 How can the hazards posed by lava flows, lahars, and volcanic lakes be mitigated through human intervention? Is “messing with Mother Nature” appropriate?
- 10 What are some easy-to-make mistakes in volcano crises, and what are some successful strategies to be considered?

Chapter 15

Economic Volcanology

Volcanoes are nature's forges and stills where the elements of the Earth, both rare and common, are moved and sorted. Some elements are diluted and some pass through unchanged, but many are transported and concentrated into those precious lodes that people seek for fortune or industry.
(Barbara Decker 1979)

Three basic activities separate the human species dramatically from the rest of the living world: agriculture, the ability to control fire (energy), and the utilization of metals (mineral ores). As we saw in Chapter 13, volcanoes are economically important because they provide nutrients for the rich growing soils of volcanic areas, but they also transport great amounts of exploitable heat energy to the Earth's upper crust, and are responsible for the formation of most mineral deposits. In this chapter we will focus on the role of volcanic energy in its many forms, and on the ways volcanic processes concentrate metallic elements and form other deposits of economic use to society.

Earth Energy Relationships

Measurements of increasing temperature with depth in drill holes and deep mines show that huge amounts of thermal energy are being transferred upwards to the surface of the Earth by conduction ("heat flow" – Chapter 3). Araki et al. (2005) estimate that the total amount of heat released from the Earth's surface by heat flow from below (to the atmosphere

Volcanoes: Global Perspectives, 1st edition. By John P. Lockwood and Richard W. Hazlett. Published by Blackwell Publishing Ltd.

and oceans) is around 3×10^{13} watts (9.8×10^{20} joules/year). The input of energy to the Earth's surface from absorbed solar radiation is much greater yet – estimated at 5×10^{24} joules/year (extrapolated from data of Li et al. 1997). The energy released by volcanic eruptions turns out to be miniscule relative to the overall Earth energy budget, and is estimated by Verhoogen (1980) at less than 8×10^{11} watts (2.6×10^{19} joules/year), or only about 2% of the conductive heat flow production! 8×10^{11} watts is still a staggering value, given the tiny relative areas of the vents and fissures through which all that energy escapes relative to the whole surface of the planet.

Volcano Energy

Volcanic eruptions release vast amounts of energy in several different forms, many not normally included in a review of this subject, but each important in its own way. We find it useful to separate volcano energy into two categories for the sake of discussion: 1) **Eruptive volcano energy**, which reaches the Earth's surface directly during eruptions and 2) **Stored volcano energy**, trapped within and beneath volcanoes as a result of intrusive and seismic activity.

ERUPTIVE ENERGY

Most eruptive volcano energy during effusive eruptions is released as thermal energy by cooling lava or ash brought to the surface during the eruptions. Kinetic energy is also released through physical impact as lavas rise and flow downhill, but this is rarely considered in calculating the total energy budget of an eruption. Thermal energy is almost entirely radiative as lava flow surfaces cool, but flows may also continue transferring energy conductively to percolating rainwater and to adjacent rocks – sometimes for many years in those rare instances where deep lava lakes are formed (Chapter 6).

The energy released during explosive eruptions is also primarily thermal in nature (Hedervari 1963; Sparks 1986; Pyle 1995). Other forms of energy may also be released, though they are ordinarily of lesser magnitude. These include the energy of shock waves transferred through the atmosphere (sonic waves) or water (tsunami waves), and the kinetic energy represented by movement of volcanic ejecta or mass wasting of the volcanic edifice or erupted products. In explosive eruptions, most of the released thermal energy is either transferred quickly to the atmosphere by buoyant clouds of ash and gas (Sparks et al. 1986), or more slowly by the cooling of PDCs. Phreatic eruptions are a special case – where the principal energy release may be kinetic rather than thermal (Shimozuru 1968).

COMPARISON OF ERUPTIVE ENERGY WITH OTHER FORMS OF NATURAL ENERGY RELEASE

To witness a major explosive eruption, where huge amounts of hot ash and gases are ejected from the Earth, or a large effusive eruption where millions of cubic meters of molten rock flow

across the land, one would naturally assume that volcanoes are one of the most important energy producers amongst all natural surface phenomena. But – is this true? The energy of explosive eruptions is usually more impressive and destructive than that of longer-lived effusive eruptions, since it is released in a much shorter period of time. In other words, explosive eruptions show much more **power** (where the term “power” signifies **rate** of energy expenditure). While a magnitude 8 earthquake pales in comparison to the energy of most larger volcanic eruptions, it is far more powerful than most eruptions, and in terms of kinetic energy release, potentially far more destructive.

Even then, most eruptions are dwarfed in terms of total energy release by other hazardous natural phenomena, which occur somewhere on Earth every year (large earthquakes, wildfires, and cyclonic storms). A plot of total energy versus power (Fig. 15.1) shows that, though the infrequent great eruptions of VEI greater than 7 (Chapter 8) can “compete” with other natural phenomena, the more frequent large earthquakes, hurricanes, typhoons and wildfires exceed most eruptions in these respects; and even average hurricanes are stronger than all but the largest eruptions in terms of energetics and power (Emanuel 1999).

Stored Energy: Geothermal Power

Although the amount of energy transferred directly to the Earth’s surface by volcanic eruptions is large (see Verhoogan’s estimate above), most volcanic energy is stored within and beneath volcanoes, and reaches the surface only by slow conduction or by upward migration of heated groundwater. Geothermal resources (in the form of hot springs) have long been used by humans for bathing and for cooking food, but the exploration for deeper, higher temperature resources that could be used to produce electricity only began in 1904, with pioneering efforts in the Larderello area of Italy in 1904 (DiPippo 1988). Geothermal production of electricity was insignificant until after the middle of the twentieth century, when increasing petroleum prices and evolving technologies allowed geothermal electric power production to accelerate rapidly (Fig. 15.2). The generation of electricity from geothermal resources has increased an average of 8.6 percent/yr according to Lund (2000), and he estimates that production will increase at faster rates in this century – in large part owing to the expected rise in economic and environmental costs of fossil fuel. Still, geothermal energy is only a bit player on the world energy scene – and is likely to remain so for the foreseeable future. Eighty-six percent of the world’s energy needs were met by burning fossil fuels and by nuclear power in 1998 and 14 percent was supplied from renewable resources (Fridleifsson 2003). Geothermal energy production accounted for only 2 percent of this latter total, while hydroelectric power provided

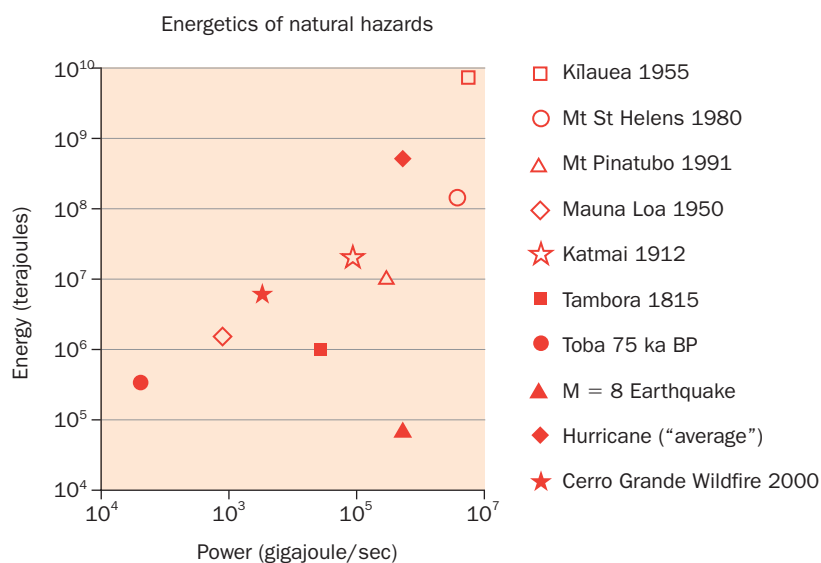


Fig. 15.1 Comparison of the energy and power of volcanic eruptions and other natural hazards. Data obtained from various sources, including Emanuel (1999), Kasahara (1981), and Pyle (1995). For reference, 1 terajoule is equivalent to the explosion of about 240 tons of TNT.

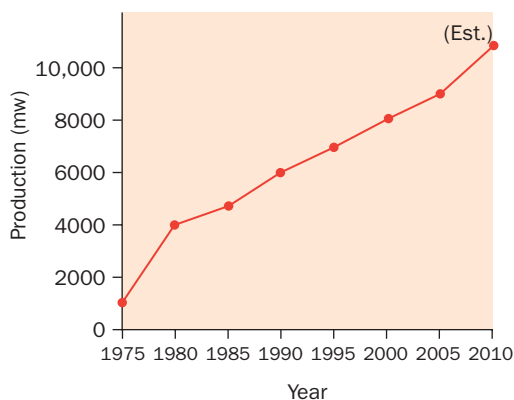


Fig. 15.2 History of worldwide geothermal power generation (Megawatts). Data from various Geothermal Energy Association informal reports.

92 percent of renewable sources. Estimated reserves of recoverable geothermal energy are immense, however, and as part of the world's energy budget, this non-polluting, renewable energy resource will certainly continue to increase in importance.

Most polygenetic volcanoes are underlain by magma chambers at some point during their active lives (Chapter 3), and direct energy recovery from these molten bodies has been frequently proposed (principally in the popular media). Tapping energy directly from a magma chamber might seem to be a promising proposition, but it appears such efforts are futile, however, since experimental placement of heat exchangers directly into magma (as into the Kilauea Iki lava lake – Chapter 6) shows they become immediately encased in an insulating

glassy selvage, making extraction of heat inefficient. Magma chambers do transfer vast amounts of thermal energy to adjacent rocks over long periods of time, however, together with dikes and other intrusive bodies (Chapter 4). Volcanic earthquakes and tremor that typically accompany or precede eruptive activity also provide heat energy (Cristofolini et al. 1987). The shallow crust beneath and within the volcanoes stores this heat effectively because of the low thermal conductivity of volcanic rocks. Individual volcanoes and their surrounding rocks can remain at elevated temperatures for tens of thousands of years after all eruptive activity has ceased.

Although the Earth's temperature increases with depth everywhere, only areas located near volcanic fields are characterized by the high-temperature rocks necessary to support commercially feasible, large-scale geothermal electrical energy production. Unfortunately, hot rock alone is not sufficient for energy production, as no technology exists for the direct conversion of hot rock or magma heat to power. To exploit volcanic heat from hot rocks, water must be present (either as hot water or steam) as an intermediate medium to transport heat to surface generation facilities, and the rocks themselves must be sufficiently permeable to allow this water to circulate. Three types of volcanic geothermal systems (Fig. 15.3) have proven to be commercially exploitable for the generation of electrical power: **Vapor-dominated systems**, where water is present as steam that can be used to directly power turbines; **water-dominated systems**, where hot water (usually above about 200°C) can be brought to the surface, partially flashed to steam to drive turbines; and **moderate-temperature water systems**, where water temperatures are too cool to directly drive turbines, but where another fluid with a lower boiling point can be vaporized to power turbines in binary fluid systems. The **vapor-dominated** systems are the most efficient and profitable geothermal fields, but are also the least common. An example is the Geysers field north of San Francisco, the world's largest, which has generated as much as 2000 megawatts (MW) of power in the past; poor steam reservoir management has now lowered current production to about 1000 MW, still enough to supply the energy needs of San Francisco. Experience at the Geysers has revealed the risks for non-sustainable overproduction of geothermal energy, but has also shown how to maintain long-term power production by careful production management and water reinjection – an essential technique at any geothermal field. **Water-dominated** systems are the most commonly developed geothermal fields in the world, with over 70 generation facilities in about 25 countries now producing over 9000 MW of electrical power worldwide (Bertani 2006). An example of such a field is the Coso geothermal area, being developed in a volcanic field

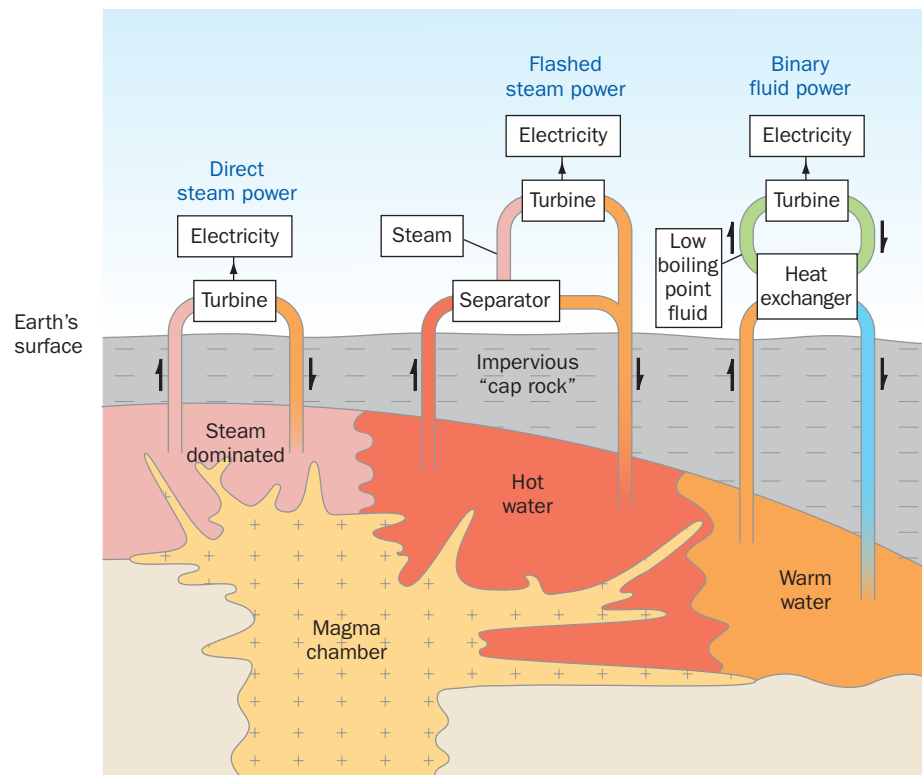


Fig. 15.3 Schematic diagram of three geothermal reservoir types and power generation facilities above a magmatic system.

250 km north of Los Angeles, California (Adams et al. 2000). **Moderate-temperature** geothermal systems (100–200°C) are most commonly developed to supply binary fluid power plants. A good example is in the Mammoth Lakes area of California, where three binary fluid power plants produce around 40 MW of power. Development of the Wairakei moderate-temperature geothermal field in the Taupo Volcanic Zone, New Zealand (Fig. 15.4), resulted in the second oldest large-scale geothermal power plant in the world (after Lardarello, Italy). Wairakei went on-line in 1958, expanded its resources to include exploitation of lower temperature fluids with a binary power plant in 2005, and now produces more than 180 MW annually, helping to make New Zealand one of the world's leaders in using renewable resources for power generation (Bixley et al. 2009).

DIRECT-USE APPLICATIONS

Large volumes of low-temperature warm water (less than 100°C) are a common byproduct of geothermal power generation in volcanic areas, and can also be obtained from non-volcanic areas of high heat flow or tectonic activity. These resources are also of great economic value, as they can be used for multiple agricultural, residential, and industrial uses – drying crops, heating buildings, running refrigeration systems, and supplying warm water to public baths. Iceland is a pioneer in development of geothermal resources for electrical energy production and direct-use applications, and now supplies almost all of its energy needs with sustainable geothermal and hydroelectric projects. The more recent development of geothermal heat pump



Fig. 15.4 Wairakei Geothermal Area, New Zealand, viewed from the north. Lake Taupo in the right corner background. Photo by J. P. Lockwood.

systems, where heat exchanger loops are buried within a few feet of the ground surface, are proving to be an economic alternative to conventional heating (and cooling) of residential buildings over much broader areas of North America and Europe.

Volcanoes and Ore Deposits

Modern technology depends on two natural resource pillars; fossil fuels and metals. Metals, in turn, come from a multitude of minerals that have formed in many different ways, and are divided into three classes: **iron** (modern society's most economically important metal), **base metals** (Cu, Pb, Zn, Sn, etc.) and **precious metals** (Au, Ag, Pt, etc). We will not discuss the common metals iron or aluminum, as their deposits are not generally related to igneous activity. Almost all of the world's deposits of base and precious metals are, however, directly related to volcanism or to intrusive processes, and will be the focus of this section.

Metallic **ore deposits** are defined as economically exploitable concentrations of metal-bearing minerals. Such deposits are not commonplace, nor can their occurrences be easily prospected, although new techniques in remote sensing, airborne geophysics, and geochemical prospecting provide powerful new tools for identifying and prioritizing exploration targets that would never have been suspected a few decades ago. Without metallic ore deposits, civilization would hardly have moved past its beginning. The terms "Iron Age," "Bronze Age," and "Industrial Age" record the incremental progress of technology and manufacturing enabled by metallic ore deposits throughout history.

Ore mineralization around a subvolcanic intrusion can take place in numerous settings and at different times as a magma body cools and crystallizes. Some mineralization may occur

TABLE 15.1 PLUTONIC ASSOCIATIONS. COMPILED BY KARL ROA (2008 INFORMATION).

Deposit Type	Host Rock	Examples (reference)	Average Grade
Porphyry Cu/Mo/Au	Granite, granodiorite and related breccias/stockworks	Chuquicamata, Chile (1);	0.55% Cu
	Dacite porphyry-intermediate sill complex	El Teniente, Chile (2); Grasberg, Indonesia (3);	1.31%Cu 1.04% Cu; 0.9 ppm Au
	Basalt/monzo-diorite dikes	Oyu Tolgoi, Mongolia (4)	1.25% Cu; 0.24 ppm Au
Epithermal Au/Ag	a. Low sulphidation Andesite/rhyodacite	Hishikari, Japan (5)	40 ppm Au
	b. Intermediate sulphidation Andesite	Fruta del Norte, Ecuador (6)	20 ppm Au
	c. High sulphidation Basalt-Rhyolite	Pueblo Viejo, Dominican Rep (7)	3.22 ppm Au
VMS Cu/Zn/Ag	Archean felsic meta-volcanics	Kidd Creek, Canada (8)	1.82% Cu, 5.61% Zn 54 ppm Ag

1: Camus (2002, pp. 5–21).

2: Cannell, et al. (2005, pp. 979–1003).

3: Underlying Value. Freeport McMoRan Copper & Gold Inc., Annual Report. 88 pp
<http://www.fcx.com/inrl/annlrpt/2006/FCX%20AR%202006.pdf>

4: Kirwin et al. (2005).

5: Izawa et al. (1990, pp. 1–56).

6: (Aurelian, private report).

7: Barrick Gold Corp web page. <http://www.barrick.com/GlobalOperations/NorthAmerica/PuebloViejoProject/default.aspx>

8: http://www.falconbridge.com/our_business/copper/operations/kidd_creek.htm

within the magma body itself. Much may occur within the volcanic cover overlying an intrusion (Table 15.1). Most can take place more broadly in the enclosing host bedrock facilitated by fluids set into motion by magmatic heat. Grateful commodities brokers might well view magmas as the agents by which they earn their livings! Weathering and erosion in turn can develop additional deposits of considerable value, for example, supergene copper deposits and placer gold.

The different ways that metallic ore deposits can develop may be divided into two general classes: those associated directly with high-temperature **magmatic processes**, and those associated with **hydrothermal activity** at or near the Earth's surface. An example of a purely magmatic ore deposit is given by the two billion year-old Bushveld Complex in the Transvaal region of South Africa. This immense saucer-shaped body may have originally included over a million cubic kilometers of molten rock, emplaced by multiple replenishments within a period of less than a hundred thousand years (Cawthorn and Walraven 1998). Most of the Complex is mafic in composition, suggesting that it may represent the feeding system for a Large Igneous Province that has long since eroded away (Hatton 1995). As repeated injections of mantle-derived melt entered the Bushveld magma reservoir and cooled, fractional crystallization laid down beds of platinum, gold, and chromium-rich ore. These extremely

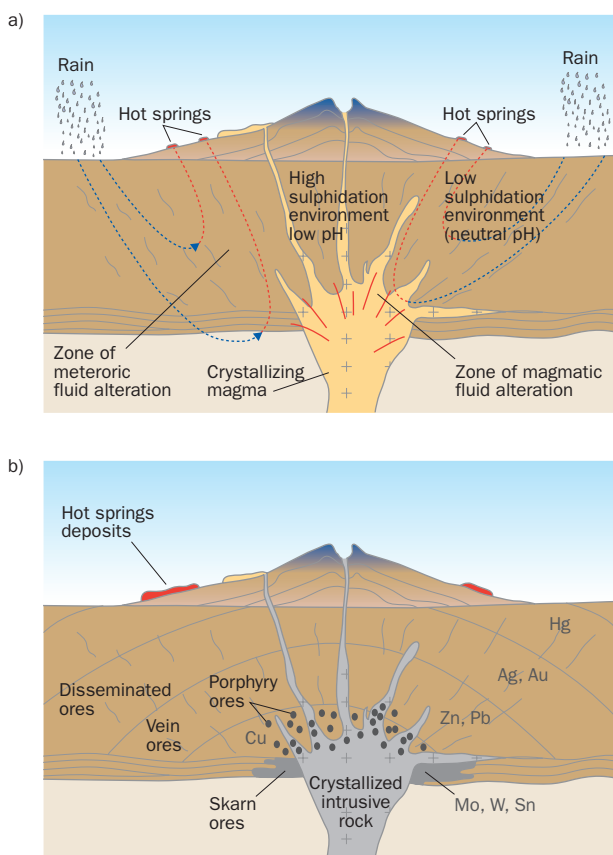


Fig. 15.5 Mineralization processes associated with volcanogenic systems and relationships with ore deposits. After an unpublished sketch by Hiroshi Ohmoto.

tion, acidities and chemical compositions of the transporting fluids, and on the chemistry and temperatures of the rocks these fluids encounter (Fig. 15.5). Valuable ore deposits formed by hydrothermal activity include gold and copper such as found at Bingham Canyon, Utah and Chuquicamata, Chile.

Researchers have long debated the question of whether the heated groundwater and associated ore metals come from magma itself or from surrounding country rocks, but isotopic data suggest that in the early stages of magma emplacement there can be a significant juvenile component. Some ore and gangue minerals trap tiny bubbles of the fluids from which they precipitate as they crystallize. Such **fluid inclusions** provide valuable information about processes that remove metals from magma. Gold, for example, appears to bond ionically with volatile chlorine, forming a compound that is soluble in high temperature solutions, but breaks down to precipitate native gold upon cooling. Many gold particles are rimmed or embedded in pyrite in a later stage of sulfide precipitation, to be followed finally by milky quartz.

Evidence for potential ore mineralization around the shallow conduits of some volcanoes may be seen in their accidental ejecta. Consider for example, the active conduit of Mt Vesuvius, which passes up through beds of limestone and calcareous marl that provide a foundation for the Campanian Plain in Italy. Xenoliths of these formations embedded in Vesuvian lavas and ejecta show that hot, acidic solutions emanating from the conduit have penetrated the surrounding fractured wallrock, dissolving some of the minerals encountered there while

valuable layers, termed **reefs** by local miners, may be individually traced across the rolling landscape as far as 70 km. These reefs contain a very large percentage of the world's mineable platinum and chromium, with the Merensky reef alone (Viljoen 1999) estimated to contain 17,000 tons of platinum in one widespread layer, commonly only about 25 cm thick.

Ores related to hydrothermal activity may consist of metals contributed directly by magma itself, or leached and concentrated from the enclosing host rock as fluids cool farther away from their heat sources. The fluids commonly travel through cracks and fissures in the rock, filling them with mineral deposits to form **ore veins**. Many vein-filled cracks may be related directly to intrusion and volcanic activity. A dense network of veins called a **stockwork** may develop directly over or close to the intrusion itself. Commonly minerals such as milky quartz and pyrite ("fools gold") precipitate with the ore. In and of themselves, these minerals are worthless, but as indicators of possible ore enrichment they are useful prospecting indicators and called **gangue minerals** to distinguish them. The host rock in the vicinity of veins may also break down and oxidize at shallow depths, transforming into masses rich in yellow clays, red to black hematite and golden brown limonite. Different metals will be deposited in different areas, depending on the temperatures, oxygenation

simultaneously precipitating others that are more stable at high-temperature, including minor ore deposits. Ore petrologists call this process **metasomatism**. The resulting calcium-rich metamorphic rock is a **skarn**. The envelope of skarn enclosing the Vesuvian conduit may be several hundred meters wide, given that fractured carbonate rocks are readily permeable. Two common products of skarn metasomatism are the minerals scheelite and wolframite, both calcium-tungstates. One of the largest tungsten mines in the world (now closed) lies along Pine Creek on the eastern side of the Sierra Nevada Range, California (Bateman 1965). The metasomatism there occurred sometime during the Mesozoic Era, when numerous granitic plutons doubtless fed an active chain of volcanoes above the levels where glaciated mountain crests rise today. Its operation was of strategic importance in winning World War II.

Aqueous solutions around sub-volcanic magma bodies can easily permeate bedrock beneath volcanoes for many kilometers beyond their bases. As they alter the crust through various mineral reactions and mix with the groundwater, they lose their acidity and volatiles. Where these fluids reach Earth's surface, hot springs, geysers, fumaroles, and related features develop. There are two general kinds of hydrothermal fields that permeate many active volcanoes. Those lying close to or upon volcanic edifices are characterized by highly acidic hot springs (pH 0.5–1.5), sulfur deposits, and high-temperature gas fumaroles. Hydrothermal fields farther away are characterized by hot springs whose waters have become neutral in acidity, and show little or no sulphur deposition. Geysers commonly form in this latter environment, partly because groundwater supplies are more stable than closer to active volcanoes. Geysers recycle water of entirely meteoric origin, though ultimately derive their heat from cooling magma. The famous geyser basins of Yellowstone National Park are an example of this latter kind of hydrothermal system.

Ore deposits may form within a few hundred meters of the surface in hydrothermal areas, though occurrences are notoriously spotty. Mining geologists call such ore bodies **epithermal** ("shallow-heated") **ores**. There are a few noteworthy examples of epithermal gold deposits in still active hydrothermal systems, including Mina Limón in Nicaragua, and Ladolam in Papua New Guinea. Miners of epithermal ores in active hydrothermal fields must deal with potential flooding and sweltering conditions underground, however, with mine walls greatly altered to hot, sticky mud by hydrothermal circulation.

PORPHYRY COPPERS AND RELATED ALTERATION

Copper is one of the most basic and oldest metals used by humans, and can form in various volcanic environments. For reasons yet unknown, veinlets and amygdules of pure copper formed late in the cooling of some Precambrian basalt flows on the Upper Peninsula of Michigan. It could be picked directly out of outcroppings with stone tools and patience, and stimulated metalworking and widespread trade among Native Americans throughout the region. In the Old World, copper deposits in the ancient basaltic sea-floor crust of the island of Cyprus sustained an important bronze industry throughout the Eastern Mediterranean, once smelting technology was developed. The name Cyprus, in fact, stems from *aes cyprium*, the Roman name for Cyprus, meaning "Island of Copper."

Deep erosion of low-grade, high-tonnage porphyry copper deposits in some parts of the world shows evidence for the passage of hydrothermal fluids in and around certain granitic

plutons. Each pluton was formerly a silicic magma chamber that stewed and underwent chemical transformation in its own volatile-rich residual “juice” as it cooled and hardened, producing concentric alteration shells that extend into the surrounding country rock for kilometres. The alteration often is centered in an upper portion of the pluton known as the **potassium-silicate alteration zone** that is enriched in reddish potassium feldspar and biotite. Farther out, the surrounding **sericite zone** includes rocks containing abundant hydrothermal quartz, calcite, sericite and pyrite; while even further away the most far-reaching alteration effects are displayed by rocks of the greenish **propylitic zone**, which contain abundant chlorite, epidote, and albite. The most productive occurrences of copper ores tend to occur in the potassium-silicate alteration zone, taking the form of scattered crystals of chalcopyrite and other cupriferous minerals embedded in granite, or as vein-filling minerals. The crystallized host rock also ordinarily contains especially large crystals of potassium feldspar, called **megacrysts**. The resulting texture, termed **porphyritic**, lends its name to this class of ores; **porphyry coppers**. As a bonus for miners, molybdenum, gold, tungsten, and tin may also be abundant in association with the copper. The American Southwest is noteworthy for its abundance of porphyry copper deposits. Their associated volcanoes and probable epithermal ore deposits have long since been destroyed, however, by the erosion of several kilometers of overburden.

NICKEL

Nickel plays a vital role in the manufacture of steel to make it harder, Like copper and gold, nickel ores are ultimately related to shallow magma chambers, but for the most part in far more unusual ways. One of the greatest nickel deposits in the world is the Sudbury intrusive complex in Ontario, Canada. This large body evidently formed in response to the impact of a **bolide** (large meteorite) during Precambrian times (Faggart et al. 1985). The meteorite blew an enormous hole in Earth’s crust, perhaps as deep as several kilometers and from 200–250 km in diameter! As matter blasted out of the crater, decompression of the underlying mantle triggered almost instantaneous melting, resulting in a gigantic body of basaltic magma that welled up into the shallow crust and possibly even into the crater itself to produce the terrestrial equivalent of a small lunar mare (Chapter 12). During ascent of the magma large pockets of immiscible sulfur-rich liquid developed within the dominantly silicate melt. Nickel concentrated within these pockets, bonding with the sulfur to form nickel-sulfide minerals such as pentlandite as the melt cooled. Subsequent erosion has exposed the ore, making the Sudbury complex one of only about a half-dozen major nickel mines in the world. Another great nickeliferous body of similar age, the Stillwater complex in Montana may be of similar origin.

Another very different kind of nickel ore occurs on the island of New Caledonia. Basalt lava flows there contain unusually nickel-rich phenocrysts of olivine. Although the fresh flows cannot be mined directly, since the phenocrysts are too few and far between, tropical weathering concentrates the nickel-bearing crystals in the lateritic soils forming from these flows. New Caledonia, like Sudbury, has become a major world supplier of nickel. Weathered serpentinites of Cuba were also once a major nickel source, but production has been halted owing to trade embargoes on necessary processing chemicals.

SEA-FLOOR MINERALIZATION

Ore mineralization is not restricted to terrestrial geological environments. The ocean floor proves to be a potent environment for ore development too. In many island arcs and at Mid-Oceanic Ridge, submarine volcanic eruptions and black smoker fumaroles release dark clouds of flocculating mineral precipitates laden with copper, zinc, gold, lead, and other metals into the sea. Research suggests that some of these metals come directly from ascending, degassing magma, whereas others are concentrated from the surrounding sea-floor crust aided by associated hydrothermal activity. There are usually no strong currents in the deep ocean to disperse the metal-bearing precipitates far, hence metal bearing minerals rain down onto the surrounding seabed to accumulate as white, yellow and dark-gray beds. Most of the metals bond with sulfur, forming various sulfide and some sulfate minerals. The influx of heat, acids, and chemicals from the submarine vents may force precipitation of minerals directly out of the sea water as well, including gypsum and anhydrite. The resulting **stratiform** ore deposits, known as **Volcanic Massive Sulphide (VMS)** deposits, are typically rich in copper, zinc and lead, and are economically important sources of gold, silver and lesser amounts of arsenic, cobalt, and tin (Figs. 15.6 and 15.7). VMS ore deposits have been found on all continents (except Antarctica – so far!). Because of their great economic importance, a great deal of geologic research has been devoted to interpreting their origins. Two types of VMS deposits exist: one is associated with ocean floor basalts and associated oceanic crustal rocks formed along divergent plate boundaries (Chapter 12); the other with felsic volcanic rocks erupted in shallow near-continental back-arc basins or along volcanic arcs (Chapter 2; Fig. 15.8). Japan, an island-arc nation, features some of the best examples of the latter type of ore deposit in the world. These are the classic **Kuroko-type deposits** (Ohmoto and Skinner 1983), where rich ores formed directly on the seafloor or in shallow dacite-thyolite domes (Fig. 15.9) Marine investigations have shown that similar VMS deposits are presently forming beneath submarine calderas along the Bonin Arc (Fiske 2001; Glasby et al. 2008).

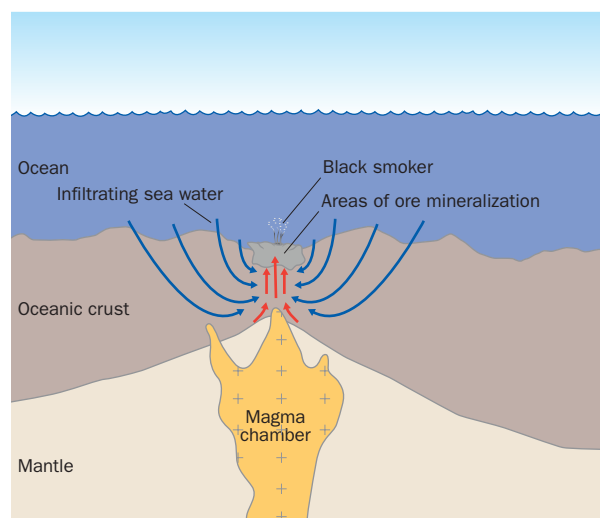


Fig. 15.6 Formation environment for Volcanogenic Massive Sulphide (VMS) deposits on the seafloor, where rising fluids from magmatic bodies create “heat engines” that drive the circulation of sea water through oceanic crust. Although this cross-section depicts a Mid-Ocean Ridge location, the same processes apply anywhere oceanic crust is undergoing extension, including active submarine calderas. Red arrows: ascending hot fluids; blue arrows: descending cool fluids.

Other Useful Volcanic Materials

Volcanoes produce many non-metallic resources of great economic importance. Not so glamorous as gold, silver, or diamonds, but more important to the infrastructure of society are the vast amounts of volcanic materials that are quarried for construction purposes, either as cut blocks or as aggregate and crushed rock. Fine-grained basalt is especially important for construction because of its strength and resistance to weathering, and quarries in the Eifel region of Germany have long provided building stones for cathedrals all over central Europe. Early Romans discovered that vitric tephra from Campi Flegrei volcano on the Bay of Naples had unique properties when mixed with calcinated lime [$\text{Ca}(\text{OH})_2$]. The lime reacts with

Fig. 15.7 Open pit Kidd Mine, Ontario, Canada. This is one of the world's largest VMS deposits, and produces over 100,000 tonnes annually of Cu, Zn, Pb, plus other metals. The pit is about 800 m long, 220 m deep, but was mined out in 1977. The mine's production is now entirely from underground sources, which extend to almost 3 km below the surface – the world's deepest sulphide ore mine. Photo courtesy Xstrata Copper.



Fig. 15.8 Side-scan sonar bathymetric view of the Brothers volcano, southern Kermadec Arc, New Zealand. This view to the north shows the 500 m-high rim bounding an 8 × 13 km caldera. The young post-caldera cone rises to within 1100 m of the sea surface, and is marked by active hydrothermal venting. This vent, along with vents on the NW caldera rim reach 300°C temperature, is associated with deposition of Cu, Zn, Pb sulphides, and indicates that subsurface VMS ore deposits may be forming today. Image courtesy of New Zealand American Submarine Ring of Fire 2007 Exploration, NOAA Vents Program, the Institute of Geological & Nuclear Sciences and NOAA-OE.

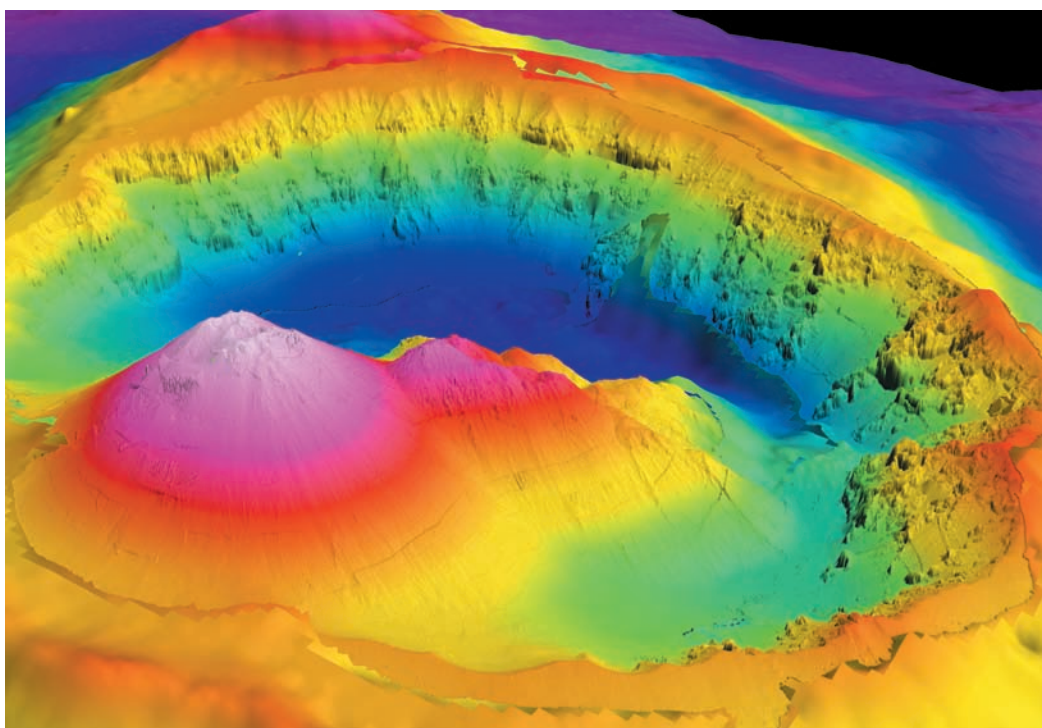




Fig. 15.9 Large polished outcrop sample (40 cm high) of classic Kuroko-type ore from the Fukazawa Mine, Akita Prefecture, Japan, showing original sedimentary structure indicative of seafloor deposition. The black ore layers consist of fragmental, fine-grained aggregates of sphalerite-galena with subordinate tetrahedrite and barite. Although primarily mined for Cu, Pb, and Zn, these ores also are rich in Au and Ag. Photo courtesy of Ryoichi Yamada, DOWA Holding Co.

volcanic glass to form calcium silicate, which forms a durable concrete when mixed with sand. This material, called **pozzolan** after the nearby city of Pozzuoli, was used as mortar and concrete in classic structures like the Pantheon and Colliseum of Rome, which are still standing after two millenia. Pozzolanitic volcanic tephra is a valuable commodity, which can enhance the qualities and lower the costs of concrete, and is being used to build durable roads and runway surfaces in many volcanic areas of the world.

Elemental sulfur deposits are found on most volcanoes of the world, and have been exploited by peoples for medicinal purposes since the dawn of civilization. The Chinese invention of gunpowder over a thousand years ago increased the demand for sulfur, and the European conquerors of the Americas were doubtlessly delighted to find so many volcanoes in Central and South America. These volcanoes enabled the conquistadores to manufacture gunpowder along their routes, and thus played an important role in the bloody conquest of Native Americans.

FURTHER READING

- Gibson, H. L. (2005) "Volcano-hosted ore deposits." In J. Martí and G. G. J. Ernst (eds.), *Volcanoes and the Environment*. Cambridge, Cambridge University Press, pp. 333–86.
- Heiken, G. (2005) "Industrial uses of volcanic materials." In J. Martí and G. G. J. Ernst (eds.), *Volcanoes and the Environment*. Cambridge, Cambridge University Press, pp. 387–403.
- Wohletz, K. H. and Heiken, G. (1992) *Volcanology and Geothermal Energy*. Berkeley, University of California Press, 432 p.

Chapter 15
**Questions for Thought, Study,
and Discussion**

- 1 From where does most of the Earth's energy come?
- 2 What the sources of most of the energy utilized by society for power generation?
- 3 How can volcano energy be best utilized?
- 4 Why are most of the world's metallic ore resources associated with igneous bodies and the roots of volcanoes?
- 5 Why have the interfaces between submarine volcanoes and seawater been places for ore deposition throughout the Earth's history?
- 6 Why are the Earth's geothermal energy production fields almost all associated with past volcanism?
- 7 What are the major types of geothermal resources, and how are they exploited to produce electrical power?

Epilogue: The Future of Volcanology

The future for volcanology is bright! Never before have volcanologists had such magnificent new tools to study volcanoes, and the need for volcanology to contribute to societal needs has never been greater.

For the first few thousand years of recorded history, humankind sought to explain volcanic activity in terms of religion or mysticism. Then, as the science of volcanology began to develop in the nineteenth century, studies focused on describing field relationships in new, universally accepted terms. Important tools were developed to extend our knowledge about the inner structure and dynamics of volcanoes early in the twentieth century, and volcanologists and petrologists began to understand the ways in which volcanic magmas form and evolve. The works of these pioneers form the foundations of our science, and future advances in volcanology will truly be built on their shoulders. The last decades of the twentieth century saw the development of remarkable new analytical tools, but were also marked by volcanic eruptions that claimed many lives, demonstrating that volcanology has not yet adequately bridged the gap between pure science and human social needs.

The twenty-first century has brought with it new challenges, as resource scarcities and enormous environmental issues loom over society, and the need for science to help formulate wise policy and political action deepens. Increasingly the public looks to science for help in clarifying and resolving these issues. Pure “ivory tower” research, although critical to the healthy advancement of science, cannot alone provide adequate justification for the increased funding that will be required to protect society more effectively from volcanic hazards and risk. Such new social responsibilities do not, however, mean that the roles of scientific curiosity and high quality research about the nature of volcanism should diminish. Indeed, a need to explain better the inner workings of volcanoes is *essential* to improving our ability to monitor

potentially dangerous volcanoes and to save lives. The increased emphasis on “Humanitarian Volcanology” will not only be driven by the fiscal realities of scientific funding opportunities, but also by the changing nature of the new students in dozens of countries around the world who are pursuing volcanology as a career. Volcanology (and most of science) was once considered a “man’s field,” and few women entered volcanology until the late twentieth century, but that has changed – much to the benefit of our science! Increasingly, idealistically-minded students from diverse backgrounds are asking “How can I contribute to a better world?” The realization that volcanology is not just a “rock course,” but also a means to “serve society through science” will attract new recruits and guarantee a healthy future for volcanology.

There are critical needs ahead for those future volcanologists to address. Most of the world’s active volcanoes have never been adequately studied in the field. High-quality geologic mapping of these little-known volcanoes is essential for an understanding of past eruptive behavior – a *sine qua non* requirement for forecasting of future behavior and for statistical evaluations of future risk. New ground-based and remotely-sensed monitoring techniques, enhanced data transmission capabilities, and advances in digital information technology, will make it possible to provide real-time information to volcanologists anywhere on Earth and to local emergency authorities, enabling them to provide advance warnings to threatened populations. Another challenge for future volcanologists will be to increase synergistic cooperation with other physical sciences such as biology, physics, chemistry, and atmospheric sciences, and to improve communications and understanding between volcanologists, emergency planners, social scientists, and the public at large.

The primary purpose underlying all volcanological research must be to continue our understanding of “how volcanoes work” and, thus contribute to the ultimate goal of reducing volcanic risk for the increasing numbers of people living in the shadows of active volcanoes. This is a noble goal for a career, and echoes the motivation that caused Thomas A. Jaggar (Chapter 1) to redefine his life after witnessing the needless loss of life caused by the 1902 Mt Pelée [63] eruption.

To repeat, the future of volcanology is bright! The challenges ahead are great, but the increased capabilities of the next generation of volcanologists give great hope. The final words of Gordon Macdonald to me (JPL) deserve repeating for future volcanologists: As we parted a few days before he died, he asked me to tell his friends to “*Carry on!*” – a message Rick Hazlett and I now pass on to you, patient reader, with all best wishes for your further learning in the field from volcanoes – *the best teachers you will ever have!*

References

- Abe, K. (1992) "Seismicity of the caldera-making eruption of Mt. Katmai, Alaska in 1912." *Bulletin of the Seismological Society of America*, 82, 175–91.
- Acocella, V., Cifelli, F., Funicello, R., et al. (2001) "The control of overburden thickness on resurgent domes: Insights from analogue models." *Journal of Volcanology and Geothermal Research*, 111, 1–4, 137–53.
- Adams, M. C., Moore, J. N., Björnstad, S., et al. (2000) "Geologic history of the Coso geothermal system." *Proceedings of the World Geothermal Congress 2000*, Kyushu-Tohoku, Japan.
- Aiuppa, A., Baker, D. R., and Webster, J. D. (2009) "Halogens in volcanic systems." *Chemical Geology*, 263, 1–4, 1–18.
- Aki, K. and Koyanagi, R. Y. (1981) "Deep volcanic tremor and magma ascent mechanism under Kilauea, Hawai'i." *Journal of Geophysical Research*, 86, 7095–109.
- Allen, J. R. L. (1982) *Sedimentary Structures: Their Character and Physical Basis*. New York, Elsevier.
- Allen, S. R. (2001) "Reconstruction of a major caldera-forming eruption from pyroclastic deposit characteristics: Kos Plateau Tuff, eastern Aegean Sea." *Journal of Volcanology and Geothermal Research*, 105, 141–62.
- Alvarez, W. and Zimmer, C. (1997) *T. Rex and the Crater of Doom*. Princeton, Princeton University Press, 185p.
- Ambrose, S. H. (1998) "Late Pleistocene human population bottlenecks, volcanic winter, and differentiation of modern humans." *Journal of Human Evolution*, 34, 6, 623–51.
- Anderson, D. J. and Lindsley, D. H. (1988) "Internally consistent solution models for Fe-Mg-Mn-Ti oxides: Fe-Ti oxides." *American Mineralogist*, 73, 714–26.
- Anderson, E. M. (1936) "Ring dykes and cauldron subsidence: The dynamics of formation of cone sheets." *Proceedings of the Royal Society of Edinburgh*, 56, 128–57.
- Anderson, E. M. (1937) "Cone-sheets and ring dykes: The dynamical explanation." *Bulletin Volcanologique*, 2, 1, 35–40.

- Anderson, J. L. and Smith, D. R. (1995) "The effect of temperature and oxygen fugacity on Al-in-hornblende barometry." *American Mineralogist*, 80, 549–59.
- Anderson, J. L., Barth, A. P., Wooden, J. L., et al. (2008) "Thermometers and thermobarometers in granitic systems." *Reviews in Mineralogy and Geochemistry*, 69, 121–42.
- Anderson, L. W. and Hawkins, F. F. (1984) "Recurrent Holocene strike-slip faulting, Pyramid Lake fault zone, Western Nevada," *Geology*, 12, 681–4.
- Arakami, S. and Ui, T. (1982) "Japan." In R. S. Thorpe (ed.), *Andesites: Orogenic Andesites and Related Rocks*. Chichester, John Wiley, pp. 259–92.
- Araki, T., Enomoto, S., Furano, K., et al. (2005) "Experimental investigation of geologically produced antineutrinos with KamLAND." *Nature*, 436, 499–503.
- Arens, N. C. and West, I. D. (2008) "Press-pulse: A general theory of mass extinction." *Paleobiology*, 34, 456–71.
- Arno, V., Bakashwin, M. A., Baker, A. Y., et al. (1980) "Geodynamic evolution of the Afro-Arabian rift system," *Atti dei Convegni Lincei Accademia Nazionale*, pp. 629–43.
- Aspinall, W., Loughlin, S. C., Michael, F. V., et al. (2002) "The Montserrat Volcano Observatory: Its evolution, organization, role and activities." *Geological Society of London, Memoirs*, 21, 71–91.
- Aspinall, W. P., Woo, G., Voight, B., et al. (2003) "Evidence-based volcanology: Application to eruption crises." *Journal of Volcanology and Geothermal Research*, 128, 1–3, 273–85.
- Atkinson, A., Griffin, T. J., and Stephenson, P. J. (1975) "A major lava tube system from Undara Volcano, North Queensland." *Bulletin Volcanologique*, 39, 2, 266–93.
- Avdeiko, G. P., Palueva, A. A., and Khlebrodova, O. A. (2006) "Geodynamic conditions of volcanism and magma formation in the Kurile-Kamchatka Island Arc System." *Petrology*, 14, 248–65.
- Bachelery, P., Chevallerier, L., and Gratier, J. P. (1983) "Caracteres structuraux des eruptions historiques du Piton de la Fournaise." *Comptes Rendus de l'Académie de Science Paris*, II, 296, 1345–50.
- Bachmann, O. and Bergantz, G. W. (2008) "The magma reservoirs that feed supereruptions." *Elements*, 4, 17–21.
- Bachmann, O., Dungan, M. A., and Lipman, P. (2002) "The Fish Canyon magma body, San Juan volcanic field, Colorado: Rejuvenation and eruption of an upper-crustal batholith." *Journal of Petrology*, 43, 1469–503.
- Bacon, C. R. (1983) "Eruptive history of Mount Mazama and Crater Lake caldera, Cascade Range, USA." *Journal of Volcanology and Geothermal Research*, 18, 1, 57–115.
- Bacon, C. R. and Lanphere, M. A. (2006) "Eruptive history and geochronology of Mount Mazama and the Crater Lake region, Oregon." *Geological Society of America Bulletin*, 118, 1331–58.
- Baer, R. B. and Siegel, L. J. (2000) *Windows into the Earth: The Geologic Story of Yellowstone and Grand Teton National Parks*. Oxford, Oxford University Press, 242p.
- Bailey, E. B., Clough, C. T., Wright, W. B., et al. (1924) "Tertiary and pre-Tertiary geology of Mull, Loch Aline and Oban." *Memoirs of the Geological Survey of Great Britain*. London, HMSO, 445p.
- Barberi, F., Carpezza, M. L., Valenza, M., et al. (1992) *L'eruzione 1991–1992 dell'Etna e gli interventi per fermare o ritardare l'avanzata della lava*. Rome, Giardini.
- Bardintzeff, J.-M. and McBirney, A. R. (2000) *Volcanology*, Sudbury, MA, Jones and Bartlet.
- Barois, P. (2004) *Guide Encyclopédique des Volcans*. Paris, Délachaux et Niestlé, 416p.
- Barsukov, V. L. (1992) "Venusian igneous rocks." In V. L. Barsukov, V. P. Volkov, and V. N. Zharkov (eds.), *Venus Geology, Geochemistry, and Geophysics: Research Results from the Soviet Union*, Tuscon, AZ, University of Arizona Press, pp. 165–76.
- Barwis, J. H. and Hayes, M. O. (1985) "Antidunes on modern and ancient washover fans." *Journal of Sedimentology*, 55, 907–16.
- Bary, E. de and Bullrich, K. (1959) "Zur theorie des Bishopringes." *Meteorologische Rundschau*, 29, 89.

- Basilevsky, A. T. and Head, J. W. III (1996) "Evidence for rapid and widespread emplacement of volcanic plains on Venus: Stratigraphic studies in the Baltis Vallis region." *Geothermal Research Letters*, 23, 1497–500.
- Basilevsky, A. T. and Head, J. W. III (2003) "The surface of Venus." *Reports on Progress in Physics*, 66, 1699–734.
- Bateman, P. C. (1965) "Geology and tungsten mineralization of the Bishop district, California." Washington, DC, US Geological Survey, Professional Paper 470, 208p.
- Bateman, P. C. and Eaton, J. P. (1967) "Sierra Nevada Batholith, California." *Science*, 158, 1407–17.
- Batiza, R. (1981) "Lithospheric age dependence of off-ridge volcano production in the North Pacific." *Geophysical Research Letters*, 8, 8.
- Behrens, H. and Jantos, N. (2001) "The effect of anhydrous composition on water solubility in granitic melts." *American Mineralogist*, 86, 14–20.
- Bell, K. and Simonetti, A. (1996) "Carbonate magmatism and plume activity: Implications from the Nd, Pb, and Sr systematics of Oldoinyo Lengai." *Journal of Petrology*, 37, 1321–39.
- Belousov, A. B., Voight, B., and Belousova, M. (2007) "Directed blasts and blast-generated pyroclastic density currents: A comparison of the Bezymianny 1956, Mount St Helens 1980, and Soufrière Hills, Montserrat 1997 eruptions and deposits." *Bulletin of Volcanology*, 69, 7, 701–40.
- Benard, R. and Krafft, M. (1986) *Au Coeur de la Fournaise, Nourault-Benard, Saint-Denis*. France, La Reunion, 220p.
- Bergantz, G. W. and Dawes, R. (1994) "Aspects of magma generation and ascent in continental lithosphere." In M. P. Ryan (ed.), *Magmatic Systems*. San Diego, Academic Press, 291–17.
- Bertani, R. (2005) "Worldwide geothermal power generation, 2001–2005." *International Geothermal Development*, May/June issue, 89–111.
- Bierwith, P. N. (1982) "Experimental welding of volcanic ash." Master's thesis, Monash University, Australia.
- Bindschalder, D. L. and Parmentier, E. M. (1990) "Mantle flow tectonics: The influence of a ductile lower crust and implications for the formation of topographic uplands on Venus." *Journal of Geophysical Research*, 95, 21, 329–44.
- Bixley, A. W., Clothworth, A. W., and Mannington, W. (2009) "Evolution of the Wairakei geothermal reservoir during 50 years of production." *Geothermics*, 38, 145–54.
- Blatt, H., Tracy, J., and Owens, B. E. (2006) *Petrology: Igneous, Sedimentary, and Metamorphic*, New York: Macmillan Publishing.
- Blong, R. J. (1984) *Volcanic Hazards – A Sourcebook on the Effects of Eruptions*. Orlando, Academic Press.
- Blower, J. D. (2001) "Factors controlling permeability-porosity relationships in magma." *Bulletin of Volcanology*, 63, 497–504.
- Blundy, J. and Cashman, K. (2006) "Reconstructing the 1980–86 Mount St. Helens magma reservoir using melt inclusions." American Geophysical Union Fall Meeting, San Francisco.
- Bobrowski, N., Hönninger, G., Galle, B., et al. (2003) "Detection of bromine monoxide in a volcanic plume." *Nature*, 423, 273–6.
- Bondre, N. R., Duraiswami, R. A., and Dole, G. (2004) "Morphology and emplacement of flows from the Deccan Volcanic Province, India." *Bulletin of Volcanology*, 66, 29–45.
- Bonneville, A., Barriot, J. P., and Bayer, R. (1988) "Evidence from geoid data of a hotspot origin for the Southern Mascarene Plateau and Mascarene Islands (Indian Ocean)." *Journal of Geophysical Research*, 93, B5, 4199–212.
- Bonney, T. G. (1899) *Volcanoes: Their Structure and Significance*. New York, G. P. Putnam and Sons.

- Bonnichsen, B. and Kaufmann, D. F. (1987) "Physical features of rhyolite lava flows in the Snake River Plain volcanic province, southwestern Idaho." In J. H. Fink (ed.), *The emplacement of silicic domes and lava flows. Geological Society of America Bulletin*, 212, 119–45.
- Booth, B. and Walker, G. P. L. (1973) "Ash deposits from the new explosion crater, Etna, 1971," *Philosophical Transactions of the Royal Society of London*, 274, 141–51.
- Boudier, F., Godard, M., and Armbruster, C. (2000) "Significance of gabbronorite occurrence in the crustal section of the Semail ophiolite." *Marine Geophysical Researches*, 21, 307–26.
- Bougher, S. W., Hunten, D. M., and Phillips, R. J. (1997) *Venus II: Geology, Geophysics, Atmosphere, and Solar Wind Environment*, Tucson, University of Arizona Press.
- Boulding, K. (1968) *Beyond Economics: Essays on Society, Religion, and Ethics*. Ann Arbor, University of Michigan Press, 281p.
- Bourdier, J. L. and Abdurachman, E. K. (2001) "Decoupling of small-volume pyroclastic flows and related hazards at Merapi Volcano, Indonesia." *Bulletin of Volcanology*, 63, 309–25.
- Bove, D. (2001) "Geochronology and geology of Late Oligocene through Miocene volcanism and mineralization in the Western San Juan mountains, Colorado." US Geological Survey Professional Paper 1642, 30p.
- Bow, C. S. and Geist, D. J. (1992) "Geology and petrology of Floreana Island, Galapagos Archipelago, Ecuador." *Journal of Volcanology and Geothermal Research*, 52, 83–105.
- Bowen, N. L. (1913) "The melting phenomena of the plagioclase feldspars." *American Journal of Science*, 35, 577–99.
- Bowen, N. L. (1928) *The Evolution of The Igneous Rocks*, Princeton, Princeton University Press.
- Boyd, F. R. (1961) "Welded tuffs and flows in the rhyolite plateau of Yellowstone Park, Wyoming." *Geological Society of America Bulletin*, 30, 41–50.
- Branney, M. J. and Kokelaar, B. P. (1994) "Volcanotectonic faulting, soft-state deformation and rheomorphism of tuffs during development of a piecemeal caldera." *Geological Society of America Bulletin*, 106, 507–37.
- Branney, M. J. and Kokelaar, B. P. (1997) "Giant bed from a sustained catastrophic density current flowing over topography: Acatlan ignimbrite, Mexico." *Geology*, 25, 115–18.
- Branney, M. J. and Kokelaar, B. P. (2002) *Pyroclastic Density Currents and the Sedimentation of Ignimbrites*. London, Geological Society of London.
- Brigham, W. T. (1909) "The volcanoes of Kilauea and Mauna Loa on the island of Hawai'i." *Memoir 2*, no. 4, Bernice Pauahi Bishop Museum, Honolulu, 222p.
- Brothers, R. N. and Golson, J. (1959) "Geological interpretations of a section of rangitoto ash on Matutapu Island, Auckland, New Zealand." *Journal of Geology and Geophysics*, 2, 569–77.
- Brown, G. C., Rymer, H., Dowden, J., et al. (1989) "Energy budget analysis for Poas crater lake: Implications for predicting volcanic activity." *Nature*, 339, 370–3.
- Brown, R. and Branney, M. (2004) "Bypassing and diachronous deposition from density currents: Evidence from the giant regressive bed form in the Poris ignimbrite, Tenerife, Canary Islands." *Geology*, 32, 445–8.
- Bryan, S. E., Cook, A., Evans, J. P., et al. (2004) "Pumice rafting and faunal dispersion during 2001–2002 in the Southwest Pacific: Record of a dacitic submarine explosive eruption from Tonga." *Earth and Planetary Science Letters*, 227, 135–54.
- Bryan, S. E., Riley, T. R., Jerram, D. A., et al. (2002) "Silicic volcanism; an undervalued component of large igneous provinces and volcanic rifted margins." *Geological Society of America Special Papers*, 362, 97–118.
- Buddington, A. L. and Lindsley, D. H. (1964) "Iron-titanium oxide minerals and synthetic equivalents." *Journal of Petrology*, 5, 310–57.

- Buist, A. S. and Bernstein, R. S. (eds.) (1986) "Health effects of volcanoes: An approach to evaluating the health effects of an environmental hazard." *American Journal of Public Health* 76, Supplement, March, 90.
- Bullard, F. (1976) *Volcanoes of the Earth*, Austin, University of Texas Press, 579p.
- Buller, A. T. and McManus, J. (1973) "Distinction among pyroclastic deposits from their grain size frequency distributions." *Journal of Geology*, 81, 97–106.
- Burnham, C. W. (1983) "Deep submarine pyroclastic eruptions." In H. Omoto and B. J. Skinner (eds.), *The Kuroko and Related Volcanogenic Massive Sulfide Deposits*. Littleton, The Economic Geology Publishing Company, pp. 142–8.
- Bursik, M. I. and Woods, A. W. (1996) "The dynamics and thermodynamics of large ash flows." *Bulletin of Volcanology*, 58, 175–93.
- Bursik, M. I., Sparks, R. S. J., Gilbert, J. S., et al. (1992) "Sedimentation of tephra by volcanic plumes. I. Theory and its comparison with a study of the Fogo A plinian deposit, Sao Miguel (Azores)." *Bulletin of Volcanology*, 48, 109–25.
- Calder, E. S., Sparks, R. S. J., and Gardeweg, M. C. (2000) "Erosion, transport and segregation of pumice and lithic clasts in pyroclastic flows inferred from ignimbrite at Lascar Volcano, Chile." *Journal of Volcanology and Geothermal Research*, 104, 1–4, 201–35.
- Camus, F. (2002) "The Andean porphyry systems." In D. R. Cooke and J. Pongratz (eds.), *Giant Ore Deposits: Characteristics, Genesis and Exploration*, Hobart, University of Tasmania, pp. 5–21.
- Cannell, J., Cooke, D. R., Walshe, J. L., et al. (2005) "Geology, mineralization, alteration, and structural evolution of the El Teniente Porphyry Cu-Mo deposit." *Economic Geology*, 100, 5, 979–1003.
- Capra, L. and Macias, J. L. (2000) "Pleistocene cohesive debris flows at Nevado de Toluca Volcano, central Mexico." *Journal of Volcanology and Geothermal Research*, 102, 149–68.
- Carey, S. N. (1991) "Transport and deposition of tephra by pyroclastic flows and surges." *Society for Sedimentary Geology*, SEPM Special Publication, 45, 39–57.
- Carey, S. N. and Sigurdsson, H. (1987) "Temporal variations in column height and magma discharge rate during the 79 AD eruption of Vesuvius." *Geological Society of American Bulletin*, 99, 2, 303–14.
- Carey, S. N. and Sigurdsson, S. (1989) "The intensity of Plinian eruptions." *Bulletin of Volcanology*, 51, 28–40.
- Carey, S. N. and Sparks, R. S. J. (1986) "Quantitative models of the fallout and dispersal of tephra from volcanic eruption columns." *Bulletin of Volcanology*, 48, 109–25.
- Carey, S. N., Sigurdsson, H., and Sparks, R. S. J. (1988) "Experimental studies of particle-laden plumes." *Journal of Geophysical Research*, 93, 15, 314–328.
- Carr, M. J., Feigenson, M. D., Patino, L. C., et al. (2003) "Volcanism and geochemistry in Central America: Progress and problems." In J. Eiler (ed.), *Inside the Subduction Zone Factory*, Washington, DC, American Geophysical Union, Geophysics Monograph Series, 138, pp. 153–74.
- Carroll, M. R. and Holloway, J. R. (1994) "Volatiles in magmas." *Reviews in Mineralogy*, 30, Chantilly, Mineralogical Society of America, 517p.
- Carson, H. L., Lockwood, J., and Craddock, E. M. (1990) "Extinction and colonization of local populations on a growing shield volcano." *Proceedings of the National Academy of Sciences, USA*, 87, 7055–7.
- Cas, R. A. F. (1989) "Eruptive centres." In R. W. Johnson (ed.), *Intraplate Volcanism in Eastern Australia and New Zealand*. Cambridge, Cambridge University Press, pp. 60–3.
- Cas, R. A. F. and Wright, J. V. (1987) *Volcanic Successions: Modern and Ancient*. London, Chapman and Hall.
- Cas, R. A. F. and Wright, J. V. (1988) *Volcanic Successions: Modern and Ancient*. London: Unwin Hyman.

- Casadevall, T. J. and Thompson, T. B. (1995) *World Map of Volcanoes and Principal Aeronautical Features*. US Geological Survey, Geophysical Investigations Map GP-1011.
- Cashman, K. V., Thornber, C. R., and Pallister, J. S. (2008) "From dome to dust: shallow crystallization and fragmentation of conduit magma during the 2004–2006 dome effusion of Mount St Helens, Washington." In D. Sherrod, W. Scott and P. H. Stauffer (eds.), US Geological Survey Professional Paper 1250, *A Volcano rekindled: The Renewed Eruption of Mount St. Helens, 2004–2006*, pp. 387–414.
- Cattermole, P. (1994) *Venus: The Geological Story*, Baltimore, Johns Hopkins University Press.
- Cawthorn, R. G. and Walraven, F. (1998) "Emplacement and crystallization time for the Bushveld complex." *Journal of Petrology*, 39, 1669–87.
- Chadwick, W. W. (2003) "Quantitative constraints on the growth of submarine lava pillars from a monitoring instrument that was caught in a lava flow." *Journal of Geophysical Research*, 108, B11, 2534.
- Chang, W.-L., Smith, R. B., and Wicks, C. (2007) "Accelerated uplift and magmatic intrusion of the Yellowstone Caldera, 2004 to 2006." *Science*, 318, 952–6.
- Chappell, B. V. and White, A. J. R. (2001) "Two contrasting granite types: 25 years later." *Australian Journal of Earth Science* 48, 489–99.
- Chappell, W. M., Durham, J. W., and Savage, G. E. (1961) "Mold of a rhinoceros in basalt, lower Grand Coulee, Washington." *Geological Society America Bulletin*, 62, 907–18.
- Chesner, C. A., Rose, W. I., Deino, R., et al. (1991) "Eruptive history of Earth's largest Quaternary caldera (Toba, Indonesia) clarified." *Geology*, 19, 200–3.
- Chouet, B. A. (1996) "New methods and future trends in seismological volcano monitoring." In R. Scarpa and R. Tilling (eds.), *Monitoring and Mitigation of Volcano Hazards*. New York, Springer, p. 841.
- Choux, C. M. and T. H. Druitt (2002) "Analogue study of particle segregation in pyroclastic density currents, with implications for the emplacement mechanisms of large ignimbrites." *Sedimentology*, 49, 907–28.
- Christiansen, R. L. (1979) "Cooling units and composite sheets in relation to caldera structure." In C. E. Chapin and W. E. Elston (eds.), *Ash-flow Tuffs*. Geological Society of America Special Paper 180, 29–42.
- Christiansen, R. L. (1984) "Yellowstone magmatic evolution – its bearing on understanding large-volume explosive volcanism." In *Explosive Volcanism: Inception, Evolution, and Hazards*. Geophysics Research Forum. Washington, DC, National Academy Press, pp. 84–95.
- Christiansen, R. L. (1987) "Rhyolite-basalt volcanism of the Yellowstone Plateau and hydrothermal activity of Yellowstone National Park, Wyoming." *Proceedings of the Rocky Mountain Sectional Meeting*, Geological Society of America.
- Christiansen, R. L. (2001) "The Quaternary and Pliocene Yellowstone Plateau volcanic field of Wyoming, Idaho, and Montana." US Geological Survey Professional Paper 729-G: 145.
- Christiansen, R. L. and Lipman, P. W. (1966) "Emplacement and thermal history of a rhyolite lava flow near Fortymile canyon, southern Nevada." *Geological Society of America Bulletin*, 7, 671–84.
- Christiansen, R. L., Foulger, G. R., and Evans, J. R. (2002) "Upper mantle origin of the Yellowstone hot spot." *Geological Society of America Bulletin*, 114, 1245–56.
- Church, A. A. and Jones, A. P. (1995) "Silicate-carbonate immiscibility at Oldoinyo Lengai." *Journal of Petrology*, 36, 869–90.
- Clague, D. A. (1987) "Hawaiian xenolith populations, magma supply rates and development of magma chambers." *Bulletin of Volcanology*, 49, 577–87.

- Clague, D. A. and Dalrymple, G. B. (1987) "Hawaiian-Emperor volcanic chain." In R. W. Decker, T. L. Wright and P. H. Stauffer (eds.), *Volcanism in Hawai'i: U.S. Geol. Survey Prof. Paper 1350*. US Geological Survey, pp. 5–54.
- Clarke, A. B., Voight B., Neri, A., et al. (2002) "Transient dynamics of Vulcanian explosions and column collapse." *Nature*, 415, 897–901.
- Clemens, J. (1998) "Observations on the origins and ascent mechanisms of granitic magmas." *Journal of the Geological Society of London*, 155, 8483–851.
- Cloos, H. (1941) "Bau und Tätigkeit von Tuffschloten." *Geologische Rundschau*, 30, 405–527.
- Coan, T. (1844) "Journey to Mauna Loa." *Missionary Herald*, 40, February, 44–7.
- Coan, T. (1857) "Volcanic action on Hawai'i." *American Journal of Science*, 73, 435–7.
- Coan, T. (1882) *Life in Hawai'i – An Autobiographical Sketch*. New York, Anson D. F. Randolph & Company.
- Coats, R. R. (1951) "Volcanic activity in the Aleutian arc." US Geological Survey, 35–47.
- Cohen, B., Vascancelos, P. M. D., and Knesel, K. M. (2004) "Tertiary magmatism in southeast Queensland." In J. McPhie and J. McGoldrick (eds.), *Past, Present, and Future*. Sydney, Geological Society of Australia, p. 256.
- Cole, P., Guest, J., Duncan, A., et al. (2001) "Capelinhos 1957–1958, Faial, Azores: Deposits formed by an emergent Surtseyan eruption." *Bulletin of Volcanology*, 63, 204–20.
- Colombrita, R. (1984) "Methodology for the construction of earth barriers to divert lava flows: The Mt. Etna 1983 eruption." *Bulletin of Volcanology*, 74, 4, 1009–38.
- Committee on Natural Disasters, Division of Natural Hazards, National Research Council (1991) *The Eruption of Nevado del Ruiz Volcano, Columbia, South America, November 13, 1985, Natural Disaster Studies: A Series*. National Academies Press, 128p.
- Condie, K. C. (1982) *Plate Tectonics and Crustal Evolution*. New York, Pergamon Press.
- Connor, C. B., McBirney, A. R., and Furlan, C. (2006) "What is the probability of explosive eruption at a long-dormant volcano?" In H. M. Mader, S. G. Coles, C. B. Connor, et al. (eds.), *Statistics in Volcanology*, London, Geological Society, pp. 39–46.
- Cooke, R. S. S., McKee, C. O., Dent, V. F., et al. (1976) "Striking sequence of volcanic eruptions in the Bismarck volcanic arc, Papua NG, in 1972–1975." In R. W. Johnson (ed.), *Volcanism in Australasia*. Elsevier, Amsterdam, 149–72.
- Corner, J. B. (1974) "Genesis of Jamaican bauxite." *Economic Geology*, 69, 1251–64.
- Corr, H. F. J. and Vaughn, D. G. (2008) "A recent volcanic eruption beneath the West Antarctic ice sheet." *Nature Geosciences*, 1, 122–5.
- Cox, K. G. (1988) "The Karoo Province." In J. D. Macdougall (ed.), *Continental Flood Basalts*. Dordrecht, Kluwer Academic, pp. 239–71.
- Craig, H. and Lupton, J. E. (1981) "Helium-3 and mantle volatiles in the ocean and oceanic crust." In C. Emiliani (ed.), *The Sea: Oceanic Lithosphere*, vol. 7. pp. 391–428.
- Crandell, D. R., Mullineaux, D. R., Miller, C. D., et al. (1979) "Volcanic-hazards studies in the Cascade Range of the Western United States," In P. D. Sheets and D. K. Grayson (eds.), *Volcanic Activity and Human Ecology*. New York, Academic Press, pp. 195–219.
- Crisp, J. A. (1984) "Rates of magma emplacement and volcanic output." *Journal of Volcanology and Geothermal Research*, 20, 177–211.
- Cristofolini, R., Gresta, S., Imposa, S., et al. (1987) "An approach to problems on energy sources at Mount Etna based on seismological and volcanological data." *Bulletin of Volcanology*, 49, 729–36.
- Crowe, B. M. and Fisher, R. V. (1973) "Sedimentary structures in base-surge deposits with special reference to cross-bedding, Ubehebe Craters, Death Valley, California." *Geological Society of America Bulletin*, 84, 663–82.

- Crumpler, L. S. (1996) "Venus." In J. Dasch (ed.) *Macmillan Encyclopedia of Earth Sciences*. New York: Simon and Schuster, pp. 1129–35.
- Crumpler, L. S. and Aubele, J. C. (2000) "Volcanism on Venus." In H. Sigurdsson, (ed.) *Encyclopedia of Volcanoes*. San Diego, Academic Press, pp. 727–69.
- Dana, J. D. (1852) "Note on the eruption of Mauna Loa." *American Journal of Science*, 2nd Series, 14, 1–4, 254–329.
- Davies, A. (2009) *Volcanism on Io: A Comparison with Earth*. Cambridge, Cambridge University Press.
- Davies, R. J., Brumm, M., Manga, M., et al. (2008) "The East Java mud volcano (2006 to present): An earthquake or drilling trigger?" *Earth and Planetary Science Letters*, 272, 3–4, 627–38.
- Davis, J. C. (1986) *Statistics and Data Analysis in Geology*. New York, John Wiley and Sons.
- Dawson, J. B. (1998) "Peralkaline nephelinite-natrocronatite relationships at Oldoinyo Lengai, Tanzania." *Journal of Petrology*, 39, 2077–94.
- Dawson, P. B. and Chouet, B. A. (1999) "Three-dimensional velocity structure of the Kilauea caldera, Hawai'i." *Geophysical Research Letters*, 26, 18, 2805–8.
- Day, S. J. (1993) "The structural evolution and mechanics of volcanoes and subvolcanic intrusions." *Journal of the Geological Society of London*, 150, 207–8.
- De Carolis, E. and Patricelli, G. (2003) *Vesuvius AD 79: The Destruction of Pompeii and Herculaneum*, Rome, Roberto Marcucci.
- De la Cruz-Reyna, S. and Tilling, R. I. (2008) "Scientific and public responses to the ongoing volcanic crisis at Popocatepetl volcano, Mexico: Importance of an effective hazards-warning system." *Journal of Volcanology and Geothermal Research*, 170, 121–34.
- De Rita, D., Di Filippo, M., and Rosa, C. (1996) "Structural evolution of the Bracciano volcano-tectonic depression, Sabatini Volcanic District, Italy." In A. W. J. McQuire, P. Jones and J. Neuberg (eds.), *Volcano Instability on the Earth and Other Planets*. London, Geological Society of London, p. 110.
- de Silva, S. L. and Francis, P. W. (1991) *Volcanoes of the Central Andes*. New York, Springer-Verlag.
- de Silva, S. L. and Zielinski, G. A. (1998) "Global influence of the AD 1600 eruption of Huaynaputina, Peru." *Nature*, 393, 455–8.
- de Silva, S., Zandt, G., Trumbull, R., et al. (2006) "Large ignimbrite eruptions and volcano-tectonic depressions in the Central Andes: A thermomechanical perspective." *Geological Society of London, Special Publications*, 269, 47–63.
- Decker, R. W. (1973) "State-of-the-art in volcano forecasting." *Bulletin Volcanologique*, 37, 3, 372–93.
- Decker, R. W. (1990) "How often does a Minoan eruption occur?" In D. A. Hardy, S. Keller, P. V. Galanopoulos et al. (eds.), *Thera and the Aegean World III*. vol. 2 (Earth Sciences), The Thera Foundation, London, 444–54.
- Decker, R. W. and Decker, B. (1979) *Volcanoes*. New York, W. H. Freeman, 244p.
- Decker, R. W. and Decker, B. B. (1991) *Mountains of Fire*. Cambridge, Cambridge University Press.
- Decker, R. W. and Decker, B. (1997) *Volcanoes: Third Edition*. New York, W. H. Freeman.
- Decker, R. W. and Kinoshita, W. (1971) *Geodetic Measurements: The Surveillance and Prediction of Volcanic Activity*. Paris, UNESCO.
- Decker, R. W., Wright, T. L., and Stauffer, P. H. (eds.) (1987) "Volcanism in Hawai'i." US Geological Survey Professional Paper 1350, 1667p.
- Delaney, P. T. and Pollard, D. D. (1981) "Deformation of host rocks and flow of magma during growth of minette dikes and breccia-bearing intrusions near Shiprock, New Mexico." *US Geological Survey*, 61.
- Delmelle, P., Stix, J., Baxter, P. J., et al. (2004) "Atmospheric dispersion, environmental effects and potential health hazard associated with the low-altitude gas plume of Masaya volcano, Nicaragua." *Bulletin of Volcanology*, 64, 6, 423–34.

- Deniel, C., Kieffer, G., and Lecointre, J. (1992) "New ^{230}Th - ^{238}U and ^{14}C age determinations from Piton des Neiges Volcano, Reunion: A revised chronology for the differentiated series." *Journal of Volcanology and Geothermal Research*, 51, 253–67.
- Devine, J. D. (1995) "Petrogenesis of the basalt-andesite-dacite association of Grenada, Lesser Antilles island arc." *Journal of Volcanology and Geothermal Research*, 69, 1–33.
- Dieterich, J. H. and Decker, R. W. (1975) "Finite element modeling of surface deformation associated with volcanism." *Journal of Geophysical Research*, 80, 4094–102.
- Dilek, Y. and Robinson, P. T. (eds.) (2003) *Ophiolites in Earth History*. London, Geological Society of London.
- DiPippo, R. (1988) "International developments in geothermal power production." *Geothermal Resources Council Bulletin*, 8–19.
- Dobran, F., Neri, A., and Macedonio, G. (1993) "Numerical simulation of collapsing volcanic columns." *Journal of Geophysical Research*, 98, 4231–59.
- Donnelly-Nolan, J. M. (1988) "A magmatic model of Medicine Lake Volcano, California." *Journal of Geophysical Research*, 93, B5, 4412–20.
- Dorn, R. I. (2009) *The Role of Climatic Change in Alluvial Fan Development*. New York, Springer-Verlag.
- Driedger, C. L. and Kennard, P. M. (1986) "Ice volumes on Cascade volcanoes: Mount Rainier, Mount Hood, Three Sisters, and Mount Shasta." *U.S. Geological Survey*, 28.
- Druitt, T. H. (1992) "Emplacement of the 18 May 1980 lateral blast deposit ENE of Mount St. Helens, Washington." *Bulletin of Volcanology*, 54, 554–72.
- Druitt, T. H. (1996) "Turbulent times at Taupo." *Nature*, 381, 476–7.
- Druitt, T. H. and Kokelaar, B. P. (2002) *The Eruption of Soufriere Volcano, Montserrat, from 1995 to 1999*. London, Geological Society of London.
- Druitt, T. H. and Sparks, R. (1982) "A proximal ignimbrite breccia facies on Santorini, Greece." *Journal of Volcanology and Geothermal Research*, 13, 147–71.
- Dubosclard, G., Donnadieu, F., Allard, P., et al. (2004) "Doppler radar sounding of volcanic eruption dynamics at Mount Etna." *Bulletin of Volcanology*, 66, 443–56.
- Dudley, W. and Lee, M. H. (1998) *Tsunami!* Manoa, University of Hawai'i Press.
- Duffield, W. A. (1972) "A naturally occurring model of global plate tectonics." *Journal of Geophysical Research*, 77, 14, 2543–55.
- Duffield, W. A., Stieltjes, L., and Varet, J. (1982) "Huge landslide blocks in the growth of Piton de la Fournaise, La Reunion, and Kilauea volcano, Hawai'i." *Journal of Volcanology and Geothermology Research*, 12, 1, 147–60.
- Duncan, R. A. and Clague, D. E. (1985) "Pacific plate motion recorded by linear volcanic chains." In A. E. M. Nairn, F. G. Stehli and S. Uyeda (eds.), *The Ocean Basins and Margins: The Pacific Ocean*, vol. 7b. New York, Plenum Press, pp. 89–121.
- Duncan, R. A. and MacDougall, I. (1989) "Volcanic time–space relationships." In R. W. Johnson (ed.), *Intraplate Volcanism in Eastern Australia and New Zealand*. Cambridge, Cambridge University Press, pp. 43–53.
- Dutton, C. E. (1884) *Hawaiian volcanoes*. Fourth Annual report of the US Geological Survey, 1882–83, Government Printing Office, Washington, DC, 75–219.
- Dzurisin, D. (1980) "Influence of fortnightly earth tides at Kilauea volcano, Hawai'i." *Geophysical Research Letters*, 7, 11, 925–8.
- Dzurisin, D. (2007) *Volcano Deformation: Geodetic Monitoring Techniques*. Chichester, Springer-Praxis.
- Easton, R. M. and Lockwood J. P. (1983) "'Surface-fed dikes' – the origin of some unusual dikes along the Hilina Fault Zone, Kilauea Volcano, Hawai'i." *Bulletin Volcanologique*, 46, 1, 45–53.

- Eaton, G. P. (1979) "A plate-tectonic model for late Cenozoic crustal spreading in the western United States." In R. E. Riecker (ed.), *Rio Grande Rift- Tectonics and Magmatism*. Washington, DC, American Geophysical Union, 7–32.
- Ebinger, C. J., Baker, J., Menzie, M. A., et al. (2002) "Volcanic rifted margins." Geological Society of America Special paper 362, 236p.
- Edmonds, M., Pyle, D. M., Oppenheimer, C. M., et al. (2003) "Trends in SO₂ fluxes 1995–2001 at Soufrière Hills Volcano, Montserrat, West Indies and their implications for changes in conduit permeability, hydrothermal interaction and degassing regime." *Journal of Volcanology and Geothermal Research*, 124, 23–43.
- Eggers, A. A. (1987) "Residual gravity changes and eruption magnitudes." *Journal of Volcanology and Geothermal Research*, 33, 201–16.
- Eichelberger, J. (1978) "Andesites in island arcs and continental margins: Relationship to crustal evolution." *Bulletin of Volcanology*, 41, 481–500.
- Elachi, C., Wall, S., Anderson, R., et al. (2005) "Cassini view the surface of Titan." *Science*, 308, 970–4.
- Ellsworth, W. L. and Voight, B. (1995) "Dike intrusion as a trigger for large earthquakes and the failure of volcano flanks." *Journal of Geophysical Research*, 100, 6005–24.
- Emanuel, K. A. (1999) "The power of a hurricane: An example of reckless driving on the information superhighway." *Weather*, 54, 107–8.
- Embley, R. W., Chadwick, W. W., Baker, E. T., et al. (2006) "Long-term volcanic activity at a submarine arc volcano." *Nature*, 44, 25 May, 494–7.
- Endo, E. T. and Murray, T. (1991) "Real-time seismic amplitude measurement (RSAM): A volcano monitoring and prediction tool." *Bulletin Volcanologique*, 53, 533–45.
- Endo, K., Sumita, M., Machida, M., et al. (1989) "The 1984 collapse and debris avalanches of Ontake volcano, Central Japan." In J. H. Latter (ed.), *Volcanic Hazards Assessment and Monitoring*. Berlin, Springer-Verlag, pp. 210–29.
- Enlows, H. E. (1955) "Welded tuffs of Chiricahua National Monument, Arizona." *Geological Society of America Bulletin*, 66, 1215–46.
- Epp, D. (1979) "Age and tectonic relationships among volcanic chains on the Pacific Plate, Hawai'i Symposium on Intraplate Volcanism and Submarine Volcanism," July 16–22, University of Hawai'i at Hilo, 121.
- Erlich, E. N., Melekestsev, I. V., Tarakanovsky, A. A., et al. (1973) "Quaternary Calderas of Kamchatka." *Bulletin of Volcanology*, 36, 1, 222–37.
- Ernst, R. E., Buchan, K. L., Aspler, L. B., et al. (2008) *Large Igneous Provinces Commission, LIP Record*. International Association of Volcanology and Chemistry of the Earth's Interior, available at: <http://www.largeigneousprovinces.org/record.html>.
- Ernst, R. E., Head, W. J., Parfitt, E. A., et al. (1995) "Giant radiating dike swarms on Earth and Venus." *Earth Science Reviews*, 39, 1–58.
- Faggart, B. E., Basu A. R., and Tatsumoto, M. (1985) "Origin of the Sudbury Complex by Meteoritic Impact: Neodymium Isotopic Evidence." *Science*, 230, 4724, 436–9.
- Fedotov, S. A. (1985) "Estimates of heat and pyroclast discharge by volcanic eruptions based upon the eruption cloud and steady plume observations." *Journal of Geodynamics*, 3, 275–302.
- Fedotov, S. A. and Masurenkov, Y. P. (1991) *Active Volcanoes of Kamchatka*. Moscow, Nauka Publishers.
- Fei, J. and Zhou, J. (2006) "The possible climatic impact in China of Iceland's Eldgjá eruption inferred from historical sources." *Climate Change*, 76, 443–57.
- Ferry, J. M. and Watson, E. B. (2007) "New thermodynamic models and revised calibrations on the Ti-in-rutile thermometers." *Contributions to Mineralogy and Petrology*, 154, 429–37.

- Fierstein, J. and Hildreth, W. (1992) "The Plinian eruptions of 1912 at Novarupta Volcano, Katmai National Park, Alaska." *Bulletin of Volcanology*, 54, 646–84.
- Fierstein, J. and Wilson, C. N. (2005) "Assembling an ignimbrite: Compositionally defined eruptive packages in the 1912 Valley of Ten Thousand Smokes ignimbrite, Alaska." *Geological Society of America Bulletin*, 115, 1094–107.
- Finlayson, D. M., Gudmundsson, O., Ikitarai, I., et al. (2003) "Rabaul Volcano Papua New Guinea; Seismic tomography imaging of an active caldera." *Journal of Volcanology and Geothermal Research*, 124, 153–71.
- Fisher, R. L. and Hess, H. H. (1963) "Trenches." In M. N. Hill (ed.), *The Sea*. New York, John Wiley and Sons, pp. 411–36.
- Fisher, R. V. (1961) "Proposed classification of volcanoclastic sediments and rocks." *Geological Society American Bulletin*, 72, 1402–14.
- Fisher, R. V. (1964) "Maximum size, mean diameter, and sorting of tephra." *Journal of Geophysical Research*, 69, 341–55.
- Fisher, R. V. (1977) "Erosion by volcanic base-surge density currents: U-shaped channels." *Geological Society of America Bulletin*, 88, 1287–97.
- Fisher, R. V. (1979) "Models for pyroclastic surges and pyroclastic flows." *Journal of Volcanology and Geothermal Research*, 6, 305–18.
- Fisher, R. V. and Schmincke, H. U. (1984) *Pyroclastic Rocks*. New York, Springer-Verlag.
- Fisher, R. V. and Waters, A. C. (1970) "Base surge bedforms in maar volcanoes." *American Journal of Science*, 268, 157–80.
- Fisher, R. V., Heiken, G., and Hulen, J. B. (1997) *Volcanoes: Crucibles of Change*. Princeton, Princeton University Press.
- Fisher, T. P., Burnard, P., Marty, B., et al. (2009) "Upper-mantle volatile chemistry at Oldoinyo Lengai volcano and the origin of carbonatites." *Nature*, 459, 77–80.
- Fiske, R. S. (1984) "Volcanologists, journalists, and the concerned local public – a tale of two crises in the eastern Caribbean." In N. R. C. Geophysics Study Committee, *Explosive Volcanism: Inception, Evolution, and Hazards*. Washington DC, National Academy Press, 170–6.
- Fiske, R. S. and Sigurdsson, H. (1982) "Soufrière volcano, St. Vincent: Observations of its 1979 eruption from the ground, aircraft, and satellites." *Science*, 216, 4550, 1105–6.
- Fiske, R. S., Naka, J., Lizasa, K., et al. (2001) "Submarine silicic caldera at the front of the Izu-Bonin arc, Japan: Voluminous seafloor eruptions of rhyolite pumice." *Geological Society of America Bulletin*, 113, 7, 813–24.
- Fitton, J. G. (1980) "The Benue Trough and Cameroon Line – a migrating rift system in West Africa." *Earth and Planetary Science Letters*, 51, 132–8.
- Fitton, J. G. and Godard, M. (2004) "Origin and evolution of magmas on the Ontong Java Plateau." In J. G. Fitton, J. Mahoney, P. J. Wallace, et al. (eds.), *Origin and Evolution of the Ontong Java Plateau*. London, Geological Society of London, pp. 151–78.
- Fitton, J. G., Mahoney, J. J., Wallace, P. J., et al. (2004) *Origin and Evolution of the Ontong Java Plateau*. London, Geological Society of London.
- Flannery, T. (2001) "The Eternal Frontier: An Ecological History of North America and Its Peoples." *Atlantic Monthly Press*, 368.
- Foit, F. F., Gavin, D. G., and Hu, F. S. (2004) "The tephra stratigraphy of two lakes in south-central British Columbia, Canada and its implications for mid-late Holocene volcanic activity at Glacier Peak and Mount St. Helens, Washington, USA." *Canadian Journal of Earth Sciences*, 41, 1401–10.
- Fornari, D. J., Batiza, R., and Allan, J. F. (1987) "Irregularly shaped seamounts near the East Pacific Rise: Implications for seamount origin and Rise axis processes." In B. H. Keating, P. Fryer,

- R. Batiza, et al. (eds.), *Seamounts, Islands, Atolls*. American Geophysical Union Monograph 43, pp. 35–47.
- Fornari, D. J., Ryan, W. B. F., and Fox, P. J. (1985) “Sea-floor lava fields on the East Pacific Rise.” *Geology*, 13, 6, 413.
- Fornari, D. J., Lockwood, J. P., Lipward, P. W., et al. (1980) “Submarine volcanic features west of Kealakekua Bay, Hawai‘i.” *Journal of Volcanology and Geothermal Research*, 7, 2, 323–37.
- Fornari, D. J., Tivey, M. D., Schouten, H., et al. (2004) “Submarine lava flow emplacement at the East Pacific Rise 9° 50′N – Implications for uppermost ocean crust stratigraphy and hydrothermal fluid circulation.” In *The Thermal Structure of the Ocean Crust and the Dynamics of Hydrothermal Circulation*. Geophysical Monograph 148, Washington, DC, American Geophysical Union, pp. 187–218.
- Foshag, W. F. and Gonzalez-Reyna, J. (1956) *U.S. Geological Survey Bulletin: Birth and Development of Parícutín Volcano, Mexico*. US Geological Survey, pp. 355–489.
- Fouqué, F. A. (1879) *Santorin et ses éruptions*. Paris, G. Masson.
- Fournier d’Albe, E. M. (1979) “Objectives of volcano monitoring and prediction.” *Journal of the Geological Society of London*, 136, 321–6.
- Francis, E. H. (1982) “Magma and sediment-I: Emplacement mechanism of late Carboniferous tholeiite sills in northern Britain.” *Journal of the Geological Society of London*, 139, 1–20.
- Francis, P. (1993) *Volcanoes: A Planetary Perspective*. Oxford, Oxford University Press, 443p.
- Francis, P. W. and Rothery, D. A. (1987) “Using the Landsat Thematic Mapper to detect and monitor active volcanoes.” *Geology*, 15, 614–17.
- Francis, P. W., Wadge, G., and Mouginiis-Mark, P. J. (1996) “Satellite monitoring of volcanoes.” In R. Scarpa and R. I. Tilling (eds.), *Monitoring and Mitigation of Volcanic Hazards*. Berlin, Springer, 841p.
- Freundt, A. (2001) *From Magma to Tephra: Modelling Physical Processes of Explosive Volcanic Eruptions*. North Holland, Elsevier, 334p.
- Freundt, A. and Bursik, M. I. (1998) “Pyroclastic flow transport mechanisms.” In A. Freundt and M. Rosi (eds.), *From Magma to Tephra: Modelling Physical Processes of Explosive Volcanic Eruptions, Developments in Volcanology 4*. New York, Elsevier, pp. 173–245.
- Freundt, A. and Schmincke, H.-U. (1986) “Emplacement of small-volume pyroclastic flows at Laacher See (East-Eifel, Germany).” *Bulletin of Volcanology*, 48, 39–59.
- Fridleifsson, I. B. (2003) “Status of geothermal energy amongst the world’s energy sources.” *Geothermics*, 32, 379–88.
- Friedrich, W. L. (1999) *Fire in the Sea – The Santorini Volcano: Natural History and the Legend of Atlantis*. Cambridge: Cambridge University Press.
- Fryer, P., Lockwood, J. P., Becker, N., et al. (2000) “Significance of serpentine mud volcanism in convergent margins.” In Y. Dilek, E. M. Moores, D. Elthon, et al. (eds.). *Ophiolites and Oceanic Crust – New Insights from Field Studies and the Ocean Drilling Program*. Colorado, Geological Society of America. Special Paper 349, pp. 35–51.
- Furman, T., Meyer, P. S., Frey, F. A., et al. (1992) “Evolution of Icelandic central volcanoes: Evidence from the Austurhorn Intrusion, southeastern Iceland.” *Bulletin of Volcanology*, 55, 45–62.
- Gamble, J. A., Price, R. C., Smith, I. E. M., et al. (2003) “⁴⁰Ar/³⁹Ar geochronology of magmatic activity, magma flux, and hazards at Ruapehu Volcano, Taupo volcanic Zone, New Zealand.” *Journal of Volcanology and Geothermal Research*, 120, 271–87.
- Garces, M. A., Harris, A. J. L., Hetzer, C., Johnson, J. B. Rowland, S. K., Marchetti, E., and P. Okubo (2003) “Infrasonic tremor observed at Kilauea Volcano, Hawai‘i.” *Geophysical Research Letters*, 30, 20, No. 2023.
- Garces, M. A., Iguchi, M., Ishihara, K., Morrissey, M., Sudo, Y., and Tsutsui, T. (1999) Infrasonic precursors to a Vulcanian eruption at Sakurajima Volcano, Japan, *Geophysical Research Letters*, 26 (16), 2537–40.

- Gardner, J. E., Thomas, R. M. E., Jaupart, C., et al. (1996) "Fragmentation of magma during Plinian volcanic eruptions." *Bulletin Volcanologique*, 58, 144–62.
- Gardener, J. V., Dean, W. E. et al. (1984) "Shimada seamount: An example of recent midplate volcanism." *Geological Society of America Bulletin*, 95, 855–62.
- Garry, W. B., Gregg, T. K. P., Soule, S. A., et al. (2007) "Formation of submarine lava channel textures: Insights from laboratory simulations." *American Geophysical Union*, 111, B3104, 1–21.
- Geissler, P. (2000) "Cryptovolcanism in the outer solar system." In H. Sigurdsson (ed.), *Encyclopedia of Volcanoes*. San Diego, Academic Press, pp. 785–800.
- Geissler, P. E. (2003) "Volcanic activity on Io during the Galileo Era." *Annual Review of Earth and Planetary Sciences*, 31, 175–211.
- Gerlach, T. M. (1991) "Present-day CO₂ emissions from volcanoes." *Transactions of the American Geophysical Union [EOS]*, 72, 249, 254–5.
- Gerlach, T. M., McGee, K. A., Elias, T., et al. (2002) "Carbon dioxide emission rate of Kilauea volcano: Implications for primary magma and the summit reservoir." *Journal of Geophysical Research*, 107, B9, 2189.
- Geze, B. (1964) "Sur la classification des dynamismes volcaniques." *Bulletin Volcanologique*, 27, 237–57.
- Ghiorso, M. S. and Sack, R. O. (1991) "Fe-Ti oxide thermometry, thermodynamic formulation and estimation of intensive variables in silicic magmas." *Contributions to Mineralogy and Petrology*, 108, 485–510.
- Giannetti, B. (2001) "Origin of the calderas and evolution of Roccamonfina volcano (Roman Region, Italy)." *Journal of Geothermal Research*, 106, 3–4, 301–19.
- Gibbs, S. H. (1968) *Volcanic ash soils in New Zealand*. Department of Science and Industrial Research, New Zealand, 39.
- Gibson, H. L. (2005) "Volcano-hosted ore deposits." In J. Martí and G. G. J. Ernst (eds.), *Volcanoes and the Environment*. Cambridge, Cambridge University Press, pp. 333–86.
- Giggenbach, W. F. (1987) "Redox processes governing the chemistry of fumarolic gas discharges from White Island, New Zealand." *Applied Geochemistry*, 2, 143–61.
- Gilbert, J. S. and Lane, S. J. (1994) "The origin of accretionary lapilli." *Bulletin of Volcanology*, 56, 398–411.
- Gilbert, J. S. and Sparks, R. S. J. (eds.) (1998) *The Physics of Explosive Volcanic Eruptions*. London, The Geological Society of London, Special Publication No. 145.
- Gilbert, J. S., Lane, S. J., Sparks, R. S. J., et al. (1991) "Charge measurements on a particle fallout from a volcanic plume." *Nature*, 349, 598–600.
- Gilbert, J. S., Stasiuk, M. V., Lane, S. J., et al. (1996) "Non-explosive, constructional evolution of the ice-filled caldera at Volcan Sollipulli, Chile." *Bulletin of Volcanology*, 58, 1, 67–83.
- Gill, J. B. (1981) *Orogenic Andesites and Plate Tectonics*. Berlin, Springer-Verlag.
- Glasby, G. P., Iizasa, K., Hannington, M., et al. (2008) "Mineralogy and composition of Kuroko deposits from northeastern Honshu and their possible modern analogues from the Izu-Ogasawara (Bonin) Arc south of Japan: Implications for mode of formation." *Ore Geology Reviews*, 34, 4, 547–60.
- Godchaux, M. M., Bonnichesen, B., and Jenks, M. D. (1992) "Types of phreatomagmatic volcanoes in the Western Snake River Plain, Idaho, USA." *Journal of Volcanology and Geothermal Research*, 52, 1–25.
- Gonnermann, H. M. and Manga, M. (2007) "The fluid mechanics inside a volcano." *Annual Review of Fluid Mechanics*, 39, 321–56.
- Gorshkov, G. S. (1959) "Gigantic Eruption of the Volcano Bezymianny." *Bulletin of Volcanology*, 20, 77–109.
- Gorshkov, G. S. (1963) "Directed volcanic blasts." *Bulletin of Volcanology*, 26, 83–8.
- Gorshkov, G. S. and Dubik, Y. M. (1970) "Gigantic directed blast at Shiveluch Volcano (Kamchatka)." *Bulletin Volcanologique*, 34, 261–88.

- Gottman, J. and Martí, J. (2008) *Caldera Volcanism: Analysis, Modelling, and Response*. North Holland, Elsevier, 516p.
- Gourgaud, A., Camus, G., Gerbe, M.-C., et al., (1989) "The 1982–83 eruption of Galunggung (Indonesia) – A case study of volcanic hazards with particular relevance to air navigation." In J. H. Latter (ed.), *Volcanic Hazards – Assessment and Monitoring*. Berlin, Springer-Verlag, pp. 151–62.
- Gravley, D. (2004) "Evolution and eruptive products of the Whangapoa Basin, Taupo Volcanic Zone." Doctoral dissertation, University of Canterbury.
- Greeley, R. (1971) "Observations of actively forming lava tubes and associated structures, Hawai'i." *Modern Geology*, 2, 207–23.
- Gregg, C. E., Houghton, B. F., Johnston, D. M., et al. (2004) "The perception of volcanic risk in Kona communities from Mauna Loa and Hualalai volcanoes, Hawai'i." *Journal of Volcanology and Geothermal Research*, 130, 179–96.
- Gregg, T. K. P. and Greeley, R. (1993) "Formation of Venusian canali: Considerations of lava types and their thermal evolution." *Journal of Geophysical Research*, 98, 10,873–82.
- Gregg, T. K. P. and Keszthelyi, L. P. (2004) "The emplacement of pahoehoe toes: field observations and comparison to laboratory simulations." *Bulletin of Volcanology*, 66, 381–91.
- Griggs, R. F. (1922) *The Valley of Ten Thousand Smokes [Alaska]*. Washington, DC, National Geographic Society.
- Grosfils, E., Aubele, J., Crumpler, L., et al. (1999) "Volcanism on Venus and Earth's Seafloor." In J. Zimbleman and T. K. P. Gregg (eds.), *Environmental Effects on Volcanic Eruptions*. New York, Plenum Press, pp. 113–42.
- Gudmundsson, A. (1986) "Formation of crustal magma chambers in Iceland." *Geology*, 14, 164–6.
- Gudmundsson, A. (1998) "Magma chambers modeled as cavities explain the formation of rift zone central volcanoes and their eruption and intrusion statistics." *Journal of Geological Research*, 103, 7401–12.
- Gudmundsson, M. T., Pálsson, F., Björnsson, H., et al. (2002) "The hyaloclastite ridge formed in the subglacial 1996 eruption of Gjalp, Vatnajökull, Iceland: present day shape and future preservation." In *Remote Sensing of Terrestrial and Martian Subglacial Features*. Geological Society of London Special Publications, 202, 319–35.
- Gudmundsson, M. T., Sigmundsson, F., Björnsson, H., et al. (2004) "The 1996 eruption at Gjalp, Vatnajökull ice cap, Iceland: Efficiency of heat transfer, ice deformation and subglacial water pressure." *Bulletin of Volcanology*, 66, 46–65.
- Gudmundsson, S. L. (2006) "Magma chambers, dyke injections and surface deformation in composite volcanoes," *Geological Research Abstracts, European Geosciences Union*. 8.
- Guest, J. E., Bulmer, J. L., Aubele, J., et al. (1992) "Small volcanic edifices and volcanism on the plains of Venus." *Journal of Geophysical Research*, 97, 15,949–96.
- Guffanti, M. and Weaver, C. S. (1988) "Distribution of late Cenozoic volcanic vent in the Cascade Range: Volcanic arc segmentation and regional tectonic considerations." *Journal of Geophysical Research*, 93, 6513–29.
- Gunnarsson, B., Marsh, B. D., and Taylor, H. P. Jr (1998) "Geology and petrology of postglacial silicic lavas from the southwest part of the Torfajökull Central Volcano, Iceland." *Journal of Volcanology and Geothermal Research*, 83, 1–45.
- Gurioli, L., Pareschi, M. T., Zanella, E., et al. (2005) "Interaction of pyroclastic density currents with human settlements: Evidence from ancient Pompeii." *Geology*, 33, 441–4.
- Halliday, W. R. (1998) "Hollow volcanic tumulus caves of Kilauea caldera, Hawai'i County, Hawai'i." *International Journal of Speleology*, 27B, 95–105.
- Hamilton, D. L., Burnham, C. W., and Osborn, E. F. (1964) "Solubility of water and effects of oxygen fugacity and water content of crystallization in mafic magmas." *Journal of Petrology*, 5, 21–39.

- Hamilton, W. L. (1973) "Tidal cycles of volcanic eruptions – fortnightly to 19 year periods." *Journal of Geophysical Research*, 78, 17, 3363–75.
- Hammarstrom, J. M. and Zen, E. (1986) "Aluminum in hornblende: An empirical igneous geobarometer." *American Mineralogist*, 71, 1297–313.
- Harlow, D. H., Power, J. A., and Laguerta, E. P. (1997) "Precursory seismicity and forecasting of the June 15, 1991 eruption of Mount Pinatubo." In C. G. Newhall and R. S. Punongbayan (eds.), *Fire and Mud: Eruptions and Lahars of Mount Pinatubo, Philippines*. Philippine Institute of Volcanology and Seismology and University of Washington Press: Quezon City, pp. 285–305.
- Harper, B. E., Miller, C. F., Koteas, C. C., et al. (2004) "Granites, dynamic magma chamber processes and pluton construction: the Aztec Wash pluton, Eldorado Mountains, Nevada, USA." *Transactions of the Royal Society of Edinburgh, Earth Sciences*, 95, 277–95.
- Harris, A. J. L., Butterworth, A. L., Carton, R. W., et al. (1997) "Low-cost surveillance from space: Case studies from Etna, Krafla, Cerro Negro, Fogo, Lascar, and Erebus." *Bulletin Volcanologique*, 59, 49–64.
- Harris, D. M., Sato, M., and Casadevall, T. J. (1981) "Emission rates of CO₂ from plume measurements." In P. W. Lipman and D. R. Mullineaux, *The 1980 eruption of Mount St. Helens, Washington*. Washington, DC, US Geological Survey. Professional Paper 1250, 201–7.
- Harris, S. L., (2005) *Fire Mountains of the West: The Cascade and Mono Lake Volcanoes*. Mountain Press, Missoula, MT, 454p.
- Harrison, T. N., Brown, P. E., Dempster, T. J., et al. (1990) "Granite magmatism and extensional tectonics in southern Greenland." *Geological Journal*, 25, 287–93.
- Hasse, K. M., Struncik, N., Garbe-Schnoberg, D., et al. (2006) "Formation of island arc dacite magmas by extreme crystal fractionation: An example from Brothers Seamount, Kermadec island arc (SW Pacific)." *Journal of Volcanology and Geothermal Research*, 152, 316–30.
- Hatton, C. J. (1995) "Mantle plume origin for the Bushveld and Ventersdorp magmatic provinces." *Journal of African Earth Sciences*, 21, 571–7.
- Hawkins, D. and Wiebe, B. (2007) "Construction of the subvolcanic Vinalhaven Intrusive Complex, coastal Maine, Abstracts with Program Volume, Twentieth Annual Keck Symposium in Geology." Twentieth Annual Keck Symposium in Geology.
- Hazlett, R. W. (1990) "Extension-related volcanism in the Mopah Range volcanic field, southeastern California." *Geological Society of America*, 174, 133–45.
- Hazlett, R., Buesch, D., Anderson, J., et al. (1991) "Geology, failure conditions, and seismogenic avalanches of the 1944 eruption at Vesuvius, Italy." *Journal of Volcanology and Geothermal Research*, 47, 249–64.
- Head, J. W. and Wilson, L. (1992) "Magma reservoirs and neutral buoyancy zones on Venus: Implications for the formation and evolution of volcanic landforms." *Journal of Geophysical Research*, 97, E3, 3877–903.
- Head, J. W. and Wilson, L. (2003) "Deep submarine pyroclastic eruptions – theory and predicted landforms and deposits." *Journal of Volcanology and Geothermal Research*, 151, 155–93.
- Head, J. W. I., Crumpler, L. S., Aubele, J. C., et al. (1992) "Venus volcanism: Classification of volcanic features and structures, associations, and global distribution from Magellan data." *Journal of Geophysical Research*, 97, 13,153–97.
- Heald, E. F., Naughton, J. J., and Lynus Barnes, I. (1963) "The chemistry of volcanic gases, 2, Use of equilibrium calculations in the interpretation of volcanic gas samples." *Journal of Geophysical Research*, 68, 2, 545–57.
- Hedenquist, J. W. and Aoki, M. (1991) "Meteoric interaction and magmatic discharges in Japan, and its significance for mineralization." *Geology*, 19, 1041–4.

- Hedervari, P. (1963) "On the energy and magnitude of volcanic eruptions." *Bulletin Volcanologique*, 25, 373–86.
- Heiken, G. (2005) "Industrial uses of volcanic materials." In J. Martí and G. G. J. Ernst (eds.), *Volcanoes and the Environment*. Cambridge, Cambridge University Press, pp. 387–403.
- Heiken, G. (2006) *Tuffs: Their Uses, Hydrology, and Resources*. New York, Geological Society of America.
- Heiken, G. and Bierwith, P. N. (1982) "Experimental welding of volcanic ash." Master's thesis, Monash University, Australia .
- Heiken, G. and Wohletz, K. (1992) *Volcanic Ash*. Ann Arbor, University of California Press.
- Heirtzler, J. R. (1968) "Sea-floor spreading." *Scientific American*, 219, 6, 60–70.
- Helz, R. T. (1980) "Crystallization history of Kilauea Iki lava lake as seen in drill core recovered in 1967–1979." *Bulletin of Volcanology*, 43, 3, 675–701.
- Helz, R. and Thornber, C. R. (1987) "Geothermometry of Kilauea Iki lava lake, Hawai'i." *Bulletin of Volcanology*, 49, 651, 668.
- Henry, C. D. and Wolff, J. A. (1992) "Distinguishing strongly rheomorphic tuffs from extensive silicic lavas." *Bulletin of Volcanology*, 54, 171–86.
- Herd, D. G. and Comité de Estudios Vulcanológicos (1986) "The 1985 Ruiz volcano disaster." *EOS (American Geophysical Union Transactions)*, 67, 19, 457–60.
- Hess, H. H. (1946) "Drowned ancient islands of the Pacific basin." *American Journal of Science*, 244, 772–91.
- Hess, H. H. (1960) "The Evolution of ocean basins." Princeton, Princeton University Department of Geology, Special Paper.
- Hibbard, M. J. and Hibbard, M. (2002) *Mineralogy: A Geologist's Point of View*. McGraw Hill, 576 p.
- Hildebrand, A. R., Penfield, G. T., Kring, D. A., et al. (1991) "Chicxulub Crater: A Possible Cretaceous-Tertiary boundary impact crater on the Yucatan Peninsula, Mexico." *Geology*, 19, 867–71.
- Hildreth, W. (1981) "Gradients in silicic magma chambers: Implications for lithospheric magmatism." *Journal of Geophysical Research*, 86, 10, 153–92.
- Hildreth, W. (2007) *Quaternary Magmatism in the Cascades: Geologic Perspectives*. Washington, DC, US Geological Survey.
- Hildreth, W. and Mahood, G. (1986) "Ring fracture eruption of the Bishop Tuff." *Geological Society of America Bulletin*, 97, 396–403.
- Hillier, J. K. (2007) "Pacific seamount volcanism in space and time." *Geophysical Journal International*, 168, 2, 877–89.
- Hoblitt, R. (1994) "An experiment to detect and locate lightning associated with eruptions of Redoubt Volcano." *Journal of Volcanology and Geothermal Research*, 62, 499–517.
- Hoblitt, R. P., Miller C. D., and Vallance, J. W. (1981) "Origin and stratigraphy of the deposit produced by the May 18 directed blast." In P. W. E. Lipman and D. R. Mullineaux (eds.), *The 1980 eruptions of Mount St. Helens, Washington*. US Geological Survey, Professional Paper 1250, 401–19.
- Holcomb, R. T., Moore, J. G., Lipman, P. W., et al. (1988) "Voluminous submarine lava flows from Hawaiian volcanoes." *Geology*, 16, 400–4.
- Holland, H. D. (1978) *The Chemistry of the Atmosphere and Oceans*. New York, Wiley Inter-Science, 352p.
- Hon, K. H. and Gansecki, C. A. (2003) "The transition from `a` to pāhoehoe crust on flows emplaced during the Pu`u O`o-Kupaianaha eruption." In C. Helliker, D. A. Swanson and J. T. Takahashi (eds.), *The Pu`u O`o-Kupaianaha Eruption of Kilauea Volcano, Hawai'i*. New York, US Geological Survey, 1676, 89–103.

- Hon, K., Kauahikaua, J., Denlinger, R., et al. (1994) "Emplacement and inflation of pahoehoe sheet flows: Observations and measurements of active lava flows on Kilauea Volcano, Hawai'i." *Geological Society of America Bulletin*, 106, 351–70.
- Hooper, D. M. and Sheriden, M. F. (1998) "Computer-simulation models of scoria cone degradation." *Journal of Volcanology and Geothermal Research*, 83, 3–4, 241–67.
- Houghton, B. (1993) "Wet explosive eruptions." *Explosive Volcanism: Processes and Products, Commission on Explosive Volcanism Short Course*. J. McPhie, Canberra, Australia, 3.1–3.8.
- Houghton, B. F. (1993) "Dry Explosive Eruptions: Processes and Products." *Explosive Volcanism: Processes and Products, Commission on Explosive Volcanism (IAVCEI) Short Course*, J. McPhie, Canberra, Australia.
- Houghton, B. F. and C. J. N. Wilson (1989) "A vesicularity index for pyroclastic deposits." *Bulletin Volcanologique*, 51, 451–62.
- Houghton, B. F., Weaver, S. D., Wilson, C. J., et al. (1992) "Evolution of a Quaternary peralkaline volcano: Mayor Island, New Zealand." *Journal of Volcanology and Geothermal Research*, 51, 217–36.
- Huber, C. and Wächtershauser, G. (2006) "Alpha-hydroxy and alpha-amino acids under possible Hadean, volcanic origin-of-life conditions." *Science*, 314, 630–2.
- Huff, W. D., Bergström, S. M., and Kolata, D. R. (1992) "Gigantic Ordovician volcanic ash fall in North America and Europe: Biological, tectonomagmatic, and event-stratigraphic significance." *Geology*, 20, 10, 875–8.
- Huggett, R. (2007) *Fundamentals of Geomorphology*. London, Taylor and Francis Publishing, 472p.
- Hulme, G. (1974) "The interpretation of lava flow morphology." *Geophysical Journal of the Royal Astronomical Society*, 39, 361–83.
- Huntingdon, A. (1973) "The collection and analysis of volcanic gases from Mount Etna." *Philosophical Transactions of the Royal Society of London, Series A. Mathematical and Physical Sciences*, 174, 119–27.
- Huppert, H. E., Shepherd, J. B., Sugurdsson, H., et al. (1982) "On lava dome growth, with application to the 1979 lava eruption of the Soufrière of St. Vincent." *Journal of Volcanology and Geothermal Research*, 14, 3–4, 199–222.
- Hurford, T. A., Bills, B. G., Helfenstein, P., et al. (2009) "Geological implications of a physical libration on Enceladus." *Icarus*, 203, 541–52.
- IAVCEI Subcommittee for Crisis Protocols (1999). "Professional conduct of scientists during volcanic crises." *Bulletin of Volcanology*, 60, 323–4.
- Imai, A., Listancio, E. L., and Fujii, T. (1993) "Petrologic and sulfur isotopic significance of highly oxidized and sulfur-rich magma of Mt. Pinatubo, Philippines." *Geology*, 21, 699–702.
- INGEOMINAS (1985) "Mapa Preliminar de Riesgos Volcanicos Potenciales del Nevado del Ruiz, Republica de Colombia." Ministerio de Minas y Energia, 7 October.
- Ishimine, Y. (2006) "Sensitivity of the dynamics of volcanic eruption columns to their shape." *Bulletin of Volcanology*, 68, 516–37.
- Izawa, E., Urashima, Y., Ibaraki, K., et al. (1990) "The Hishikari gold deposit: High-grade epithermal veins in Quaternary volcanics of southern Kyushu, Japan." *Journal of Geochemical Exploration*, 36, 1–56.
- Izett, G. A., Wilcox, R. E., Powers, H. A., et al. (1970) "The Bishop ash bed, a Pleistocene marker bed in the western United States." *Quaternary Research*, 1, 121–32.
- Jakob, M. and Hungr, O. (2005) *Debris-Flow Hazards and Related Phenomena*. New York, Springer Praxis Publishing, 739p.
- Jaggard, T. A. (1904) "The initial stages of the spine on Pele." *American Journal of Science*, 17, 97, 34–40.
- Jaggard, T. A. (1909) "The Messina earthquake – prediction and protection." *The Nation*, 88, 2271, 22–3.

- Jaggard, T. A. (1917) "On the terms aphyrolith and dermolith." *Washington Academy of Science*, 7, 10, 277–81.
- Jaggard, T. A. (1919) *Monthly Bulletin of the Hawaiian Volcano Observatory*, 7, 5 (May).
- Jaggard, T. A. (1945) *Volcanoes Declare War: Paradise of the Pacific*. Honolulu, Ltd.
- Jaggard, T. A. (1947) *Origin and Development of Craters*, Geological Society of America Memoir 21, 508p.
- James, M. R., Lane, S. J., Wilson, L., et al. (2008) "Degassing at low magma viscosity volcanoes: Quantifying the transition between passive bubble burst and Strombolian eruption." *Journal of Volcanology and Geothermal Research*, 180, 81–8.
- Jellenik, A. M. and DePaolo, P. (2003) "A model for the origin of large silicic magma chambers: Precursors of caldera-forming eruptions." *Bulletin of Volcanology*, 65, 313–81.
- Jellinek, A. M. and Ross, K. (2001) "Magma dynamics, crystallization, and chemical differentiation of the 1959 Kilauea Iki lava lake, Hawai'i, revisited." *Journal of Volcanology and Geothermal Research*, 110, 235–63.
- Jicha, B. R., Scholl, D. W., Singer, B. S., et al. (2006) "Revised age of Aleutian Island Arc formation implies high rate of magma production." *Geology*, 34, 661–4.
- Johnson, J. B., Aster, R., Jones, K. R., et al. (2008) "Acoustic source characterization of impulsive Strombolian eruptions from the Mt. Erebus lava lake." *Journal of Volcanology and Geothermal Research*, 177, 673–86.
- Johnson, R. W. (ed.) (1980) *Intraplate Volcanism in Eastern Australia and New Zealand*. Cambridge, Cambridge University Press, 408p.
- Johnson, R. W. and Taylor, S. R. (1989) "Preview—Introduction to intraplate volcanism." In R. W. Johnson (ed.), *Intraplate Volcanism in Eastern Australia and New Zealand*. Cambridge, Cambridge University Press, 408p.
- Johnson, S. E. and Schmidt, K. L. (2002) "Ring complexes in the Peninsular Range Batholith, Mexico and the USA: Magma plumbing systems in the Middle and Upper Crust." *Lithos*, 61, 187–208.
- Johnson, T. V., Veeder, G. J., Matson, D. L., et al. (1988) "Io: Evidence for silicate volcanism in 1986." *Science*, 242, 1280–3.
- Johnston-Lavis, H. J. (1885) "Some speculations on the phenomena suggested by the geological study of Vesuvius and Monte Somma." *Geological Magazine*, 2, 302–7.
- Joyce, E. B. (1975) "Quaternary volcanism and tectonics in southeastern Australia." *Quaternary Studies*, Wellington, Royal Society of New Zealand, 169–76.
- Jurado-Chichay, Z. and Rowland, S. K. (1995) "Channel overflows of the Pohue Bay flow, Mauna Loa, Hawai'i: Examples of the contrast between surface and interior lava." *Bulletin of Volcanology*, 57, 117–26.
- Jurado-Chichay, Z. and Walker, G. P. L. (2001) "Variability of Plinian fall deposits: Examples from Okataina Volcanic Center, New Zealand." *Journal of Volcanology and Geothermal Research*, 111, 239–63.
- Kahle, A. B., Gillespie, E. A., Abbott, M. J. et al. (1988) "Relative dating of Hawaiian lava flows using multispectral thermal images: A new tool for mapping of young volcanic terrains." *Journal of Geology and Geophysical Research*, 93, 15329–51.
- Kaminski, E. and Jaupert, C. (2001) "Marginal stability of atmospheric eruption columns and pyroclastic flow generation." *Journal of Geophysical Research*, 106, 21, 785–98.
- Kant, E., (1803) *Physische Geographie*, V. 2. Mainz, Gottfried Vollmer, 242p.
- Karatson, D., Thouret, J. C., Moriya, I., et al. (1999) "Erosion calderas: Origins, processes, structural and climatic control." *Bulletin of Volcanology*, 61, 3, 174–93.
- Kasahara, J. (2002) "Geophysics, tides, earthquakes, and volcanoes." *Science*, 297, 348.
- Kasahara, K. (1981) *Earthquake Mechanics*. Cambridge, Cambridge University Press.

- Kauahikaua, J., Sherrod, D. R., Cashman, K. V., et al. (2003) "Hawaiian Lava-flow dynamics during the Pu`u O`o-Kupaianaha eruption: A tale of two decades." In C. Heliker, D. A. Swanson and J. Takahashi, *The Pu`u O`o-Kupaianaha Eruption of Kilauea Volcano, Hawai`i: The First 20 Years*. US Geological Survey, Professional Paper, 1676, 63–88.
- Kavanagh, J. L., Menand, T., and Sparks, R. S. J. (2006) "An experimental investigation of sill formation and propagation in layered elastic media." *Earth and Planetary Sciences Letters*, 245, 799–813.
- Kempe, S. (2002) Lavaröhren (Pyroducts) auf Hawai`i und ihre Genese. *Angewandte Geowissenschaften in Darmstadt – Schriftenreihe der deutschen Geologischen Gesellschaft*. Darmstadt, W. H. Rosendahl, 15, 109–27.
- Kempe, S. (2008) "Immanuel Kant's remark on lava cave formation in 1803 and his possible sources." *Proceedings of the 13th International Symposium on Volcanospeleology, Jeju Island, Korea, Sept. 1–5*, 35–7.
- Kent, G. M., Harding, A. J., and Orcutt, J. A. (1990) "Evidence for a smaller magma chamber beneath the East Pacific Rise at 9°30N." *Nature*, 344, 650–3.
- Kerle, N. and van Wyk de Vries, B. (2001) "The 1998 debris avalanche at Casita Volcano, Nicaragua – Investigation of structural deformation as the cause of slope instability using remote sensing." *Journal Volcanology and Geothermal Research*, 105, 49–63.
- Kerr, A. C. (1998) "Oceanic plateau formation – A cause of mass extinction and black shale deposition around the Cenomanian-Turonian boundary." *Journal of the Geological Society of London*, 155, 619–26.
- Kerr, R. A. (2005) "Icy volcanism has rejuvenated Titan." *Science*, 308, 193.
- Keszthelyi, L., Self, S., and Thorvaldur, T. (2006) "Flood lavas on Earth, Io, and Mars." *Journal of the Geological Society*, 163, 253–64.
- Kieffer, G. (1971) "Aperçu sur la morphologie des régions volcaniques de Massif Centrale." Symposium Jean Jung: Géologie, Géomorphologie et Structure Profonde de Massif Central Français. Clermont-Ferrand, pp. 479–510.
- Kieffer, S. W. (1981a) "Blast dynamics of Mount St. Helens on 18 May 1980." *Nature*, 291, 568–70.
- Kieffer, S. W. (1981b) "Fluid dynamics of the May 18 blast at Mount St. Helens." In P. W. Lipman and D. R. Mullineaux, *The 1980 eruption of Mount St. Helens, Washington*. Washington, DC, US Geological Survey. Professional Paper 1250.
- Kienle, J., Kyle, P. R., Self, S., et al. (1980) "Unirek maars, Alaska I. April 1977 eruption sequence, petrology and tectonic setting." *Journal of Volcanology and Geothermal Research*, 7, 11–37.
- Kirwin, D. J., Forster, C. N., Kavalieris, I., et al. (2005) "The Oyu Tolgoi copper-gold porphyry deposits, South Gobi, Mongolia." In R. Seltmann, O. Gerel and D. J. Kirwin (eds.), *Geodynamics and Metallogeny of Mongolia with a Special Emphasis on Copper and Gold Deposit*. London, CERCAMS, pp. 1–14.
- Klein, F. W., Koyanagi, R. Y., Nakata, J. S., et al. (1987) "The seismicity of Kilauea's magma system." In R. W. Decker, T. L. Wright and P. H. Stauffer (eds.), *Hawaiian Volcanism Geological Survey Professional Paper 1350*, pp. 1019–185.
- Kling, G. W., Clark, M. A., Wagner, G. N., et al. (1987) "The 1986 Lake Nyos gas disaster in Cameroon, West Africa." *Science* 236, 169–85.
- Kling, G. W., Evans, W. C., Tanyileke, G., et al. (2005) "Degassing Lakes Nyos and Monoun: Defusing certain disaster." *US National Academy of Sciences, Proceedings*, 102, 40, 14185–90.
- Klug, C. and Cashman, K. V. (1994) "Vesiculation of May 18, 1980 Mount St. Helens magma." *Geology*, 22, 468–72.
- Klug, C. and Cashman, K. V. (1996) "Permeability development in vesiculating magmas: Implications for fragmentation." *Bulletin Volcanologique*, 58, 87–100.

- Kokelaar, B. P. (1983) "The mechanism of Surtseyan volcanism." *Journal of the Geological Society of London*, 140, 939–44.
- Koppers, A. A. P., Staudigel, H., Pringle, M. S., et al. (2003) "Short-lived and discontinuous volcanism in the South Pacific: Hot spots or extensional volcanism?" *Geochemistry, Geophysics, Geosystems: The Electronic Journal of the Earth*, 4, 1089.
- Koyaguchi, T. and Kaneko, K. (1999) "A two-stage thermal evolution model of magmas in continental crust." *Journal of Petrology*, 40, 241–54.
- Koyaguchi, T. and Woods, A. W. (1996) "On the formation of eruption columns following the explosive mixing of magma and surface water." *Journal of Geophysical Research*, 101, 5561–74.
- Kudo, A. M. and Weill, D. (1970) "An igneous Plagioclase geothermometer," *Contributions to Mineralogy and Petrology*, 25, 52–65.
- Kusakabe, M., Ohba, T., Yoshida, Y., et al. (2008) "Evolution of CO₂ in lakes Monoun and Nyos, Cameroon, before and during controlled degassing." *Geochemical Journal*, 42, 1, 93–118.
- Lamb, H. H. (1970) "Volcanic dust in the atmosphere: With a chronology and assessment of its meteorological significance." *Philosophical Transactions of the Royal Society of London*, 266, 1179, 425–533.
- Lassiter, J. C. (2006) "Constraints on the coupled thermal evolution of the Earth's core and mantle, the age of the inner core, and the origin of the ¹⁸⁶Os/¹⁸⁸Os 'core signal' in plume-derived lavas." *Earth and Planetary Science Letters*, 250, 306–17.
- Latter, J. H. (1981) "Tsunamis of volcanic origin: Summary of causes, with particular reference to Krakatoa, 1883." *Bulletin Volcanologique*, 44, 467–90.
- Latter, J. H. (ed.) (1989) *Volcanic Hazards – Assessment and Monitoring*. Berlin, Springer-Verlag.
- Le Bas, M. J., Le Maitre, R. W., Streckheisen, A., et al. (1986) "A chemical classification of volcanic rocks based upon the total alkali-silica diagram." *Journal of Petrology*, 27, 745–50.
- Lee, J. M. (2007) "Seismic tomography of magmatic systems." *Journal of Volcanology and Geothermal Research*, 167, 37–56.
- Lee, W.-J. and Wyllie, P. J. (1997) "Liquid immiscibility in the join NaAlSi₃O₈-CaCO₃ at 1GPa: Implications for crustal carbonates." *Journal of Petrology*, 38, 1113–35.
- LeGuern, F., Tazieff, H., and Faivre, P. R. (1982) "An example of health hazards: people killed by gas during a phreatic eruption: Dieng Plateau, Java, Indonesia." *Bulletin of Volcanology*, 45, 153–6.
- Lewis, G. B. and de Lajartre, P. B. (2007) *The Red Volcanoes [volcans rouges – à couer des montagnes de feu]*. London, Thames and Hudson.
- Lewis, J. D. (1968) "Form and structure of the Loch Ba ring-dyke, Isle of Mull." *Proceedings of the Geological Society of London*.
- Li, X., Baker, D. N., Temerin, D., et al. (1997) "Are energetic electrons in the solar wind the source of the outer radiation belt?" *Geophysical Research Letters*, 24, 923–6.
- Lindsay, J. M., Schmitt, A. K., Trumbull, R. B., et al. (2001) "Magmatic evolution of the La Pacana caldera system, Central Andes, Chile: Compositional variation of two cogenetic, large-volume felsic ignimbrites." *Journal of Petrology*, 42, 459–86.
- Lipman, P. W. (1976) "Caldera collapse breccias in the western San Juan Mountains, Colorado." *Geological Society of America Bulletin*, 87, 1397–410.
- Lipman, P. W. (1980) "Cenozoic volcanism in the western United States: Implications for continental tectonics." *Studies in Geophysics: Continental Tectonics*, 161–74.
- Lipman, P. W. (1984) "The roots of ash flow calderas in western North America – windows into the tops of granitic batholiths." *Journal of Geophysical Research*, 89, B10, 8801–41.
- Lipman, P. W. (1988) "Evolution of silicic magma in the upper crust, the mid-Tertiary Latir Volcanic Field and its cogenetic granitic batholith, northern New Mexico, USA." *Transactions of the Royal Society of Edinburgh*, 79, 265–88.

- Lipman, P. W. (1997) "Subsidence of ash-flow calderas – relation to caldera size and magma-chamber geometry." *Bulletin of Volcanology*, 59, 198–218.
- Lipman, P. W. (2006) *Geologic Map of the Central San Juan Caldera Cluster*. Southwestern Colorado, US Geological Survey.
- Lipman, P. W. and Banks, N.G. (1987) "A'a flow dynamics, Mauna Loa, 1984." In R. W. Decker, T. L. Wright and P. H. Stauffer (eds.), *Volcanism in Hawai'i*. US Geological Survey Professional Paper 1350, pp. 1527–67.
- Lipman, P. W. and McIntosh, W. C. (2008) "Eruptive and non-eruptive calderas, northeastern San Juan Mountains, Colorado: Where did the ignimbrites come from?" *Geological Society of America Bulletin*, 120, 7–8, 771–95.
- Lipman, P. W. and Mullineaux, D. R. (1981) *The 1980 Eruptions of Mount St. Helens. Washington, DC*, US Geological Survey Professional Paper 1250.
- Lipman, P. W., Moore, J. G., and Swanson, D. A. (1981) "Bulging of the north flank before the 18 May eruption – geodetic data." *The 1980 Eruptions of Mount St. Helens, Washington, DC*. US Geological Survey Professional Paper 1250, pp. 143–55.
- Lirer, L. and Vinci, A. (1991) "Grain-size distributions of pyroclastic depositis." *Sedimentology*, 38, 1075–83.
- Llewellyn, E. W. and Mangan, M. (2004) "Bubble suspension rheology and implications for conduit flow." *Journal of Volcanology and Geothermal Research*, 143, 205–17.
- Lockwood, J., Costa, J. E., Tuttle, M. L., et al. (1988) "The potential for catastrophic dam failure at Lake Nyos Maar, Cameroon." *Bulletin of Volcanology*, 50, 340–9.
- Lockwood, J. P. (1980) "Gordon Macdonald, 1911–1978." *Journal of Volcanology and Geothermal Research*, 7, 2, 177–88.
- Lockwood, J. P. and Lipman, P. W. (1980) "Recovery of datable charcoal beneath young lavas – lessons from Hawai'i." *Bulletin Volcanologique*, 43, 3, 609–15.
- Lockwood, J. P. and Lipman, P. W. (1987) "Holocene eruptive history of Mauna Loa." In R. W. Decker, T. L. Wright and P. H. Stauffer (eds.), *Volcanism in Hawai'i*. US Geological Survey Professional Paper 1350, pp. 509–36.
- Lockwood, J. P. and Romano, R. (1985) "Diversion of lava during the 1983 eruption of Mount Etna." *Earthquake Information Bulletin*, 17, 4, 124–33.
- Lockwood, J. P. and Torgerson, F. A. (1980) "Diversion of lava flows by aerial bombing – lessons from Mauna Loa volcano, Hawai'i." *Bulletin of Volcanology*, 43, 4, 727–41.
- Lockwood, J. P. and Williams, I. (1978) "Lava trees and tree molds as indicators of lava flow direction." *Geological Magazine*, 115, 1, 69–74.
- Lockwood, J. P., Tilling, R. I., Holcomb, R. T. et al. (1999) "Magma Migration and resupply during the 1974 summit eruptions of Kilauea Volcano, Hawai'i." *US Geological Survey*, United States Government Printing Office, 37p.
- Lofgren, G. (1971) "Spherulitic textures in glassy and crystalline rocks." *Journal of Geophysical Research*, 76, 5635–648.
- Lopes, M. R., Guest, J. E., and Wilson, C. J. (1980) "Origin of the Olympus Mons aureole and perimeter scarp." *The Moon and the Planets*, 22, 221–32.
- Lopes, R. M. C. and Carroll, M. W. (2008) *Alien Volcanoes*. Baltimore, The Johns Hopkins University Press.
- Lowenstern, J. B., Smith, R. B., and Hill, P. D. (2006) "Monitoring super-volcanoes – geophysical and geochemical signals at Yellowstone and other large caldera systems." *Philosophical Transactions of the Royal Society*, A, 364, 2055–72.
- Lu, Z. and Dzurisin, D. (2011) *INSAR Imaging of Aleutian Volcanoes*. Berlin, Springer Praxis, 300p.

- Luedke, R. G. and Smith, R. L. (1981) "Map showing distribution, composition and age of late Cenozoic volcanic centers in California and Nevada." US Geological Survey.
- Luhr, J. F. and Simkin, T. (1993) *Paricutin: The Volcano Born in a Mexican Cornfield*. Phoenix, Geoscience Press, 427p.
- Lund, J. W. (2000) "World status of geothermal energy use – overview 1995–1999." *Geothermal Resources Council Transactions*, 24, 383–8.
- Luongo, G. L., Perrotta, A., and Scarpati, C. (2003) "Impact of the AD 79 explosive eruption on Pompeii, I: Relations amongst the depositional mechanisms of the pyroclastic products, the framework of the buildings and the associated destructive events." *Journal of Volcanology and Geothermal Research*, 126, 201–33.
- Lyell, C. (1855) *A Manual of Elementary Geology* (5th edn). New York, D. Appleton and Company.
- Macdonald, G. A. (1962) "The 1959 and 1960 eruptions of Kilauea volcano, Hawai'i, and the construction of walls to restrict the spread of the lava flows." *Bulletin of Volcanology*, 24, 249–94.
- Macdonald, G. A. (1972) *Volcanoes*. Englewood Cliffs, Prentice-Hall.
- Macdonald, G. A. (1978) "Geologic map of the crater section of Haleakala National Park, Maui, Hawai'i." *I Map 1088*, US Geological Survey.
- Macdonald, K. C. (1982) "Mid-ocean ridges: Fine-scale tectonics, volcanic and hydrothermal processes within the plate boundary zone." *Annual Reviews of Earth and Planetary Sciences*, 10, 155–90.
- MacLeod, N. S. and Sherrod, D. R. (1988) "Geologic evidence for a magma chamber beneath Newberry Volcano, Oregon." *Journal of Geophysical Research*, 93, B9, 10, 067–79.
- Mader, H. M., Coles, S. G., Connor, C. B., et al. (2006) *Statistics in Volcanology*. London, Geological Society of London.
- Mahoney, J. J. and Coffin, M. F. (1997) *Large Igneous Provinces – Continental, Oceanic, and Planetary Flood Volcanism*. Washington, DC, American Geophysical Union.
- Major, J. J. and Newhall, C. G. (1989) "Snow and ice perturbation during historical volcanic eruptions and the formation of lahars and floods." *Bulletin of Volcanology*, 52, 1–27.
- Malahoff, A. (1987) "Geology of the summit of Loihi submarine volcano." *Volcanism in Hawai'i, The 1980 Eruptions of Mount St. Helens*. US Geological Survey Professional Paper 1350, pp. 145–55.
- Mangan, M. T. and Cashman, K. V. (1993) "Vesiculation of basaltic magma during eruption." *Geology*, 21, 157–60.
- Mangan, M. T. and Cashman, K. V. (1996) "The structure of basaltic scoria and reticulite and inferences for vesiculation, foam formation, and fragmentation in lava fountains." *Journal of Volcanology and Geothermal Research*, 73, 1–18.
- Markhinin, Ye. K. (1980) Вулканы и Жизнь [Volcanoes and Life]. Moscow, Mysl' Publishers, 196p.
- Markhinin, Ye. K. (1985) Вулканизм [Vulcanism]. Moscow, Nedra Publishing.
- Marland, G., Andres, R. J., Boden, T. A., et al. (1998) "Global, regional, and national CO₂ emission estimates from fossil fuel burning, cement production, and gas flaring, 1751–1996, DATASET NDPO30." Carbon Dioxide Information and Analysis Center (CDIAC), Oak Ridge National Laboratory, Oak Ridge, Tennessee.
- Marsh, B. D. (1984) "On the mechanics of caldera resurgence." *Journal of Geophysical Research*, 89, B10, 8245–51.
- Marshall, P. (1935) "Acid rocks of the Taupo-Rotorua volcanic district." *Transactions of the Royal Society of New Zealand*, 64, 323–66.
- Martí, J., Aspinall, W. P., Sobradeloet, R., et al. (2008) "A long-term volcanic hazard event tree for Teide-Pico Viejo stratovolcanoes (Tenerife, Canary Islands)." *Journal of Volcanology and Geothermal Research*, 178, 543–52.
- Martí, J., Geyer, A. et al. (2009) "A genetic classification of collapse calderas based on field studies, and analogue and theoretical modelling." In T. Thordarson, S. Self, G. Larsen, S. K. Rowland and

- A. Hoskuldsson, *Studies in Volcanology: The Legacy of George Walker*. London, Geological Society of London, 249–66.
- Martin, D. P. and Rose, W. I. (1981) “Behavioral patterns of Fuego volcano, Guatemala.” *Journal of Volcanology and Geothermal Research*, 10, 67–81.
- Martin, U., Németh, K., Lorenz, V., et al. (2007) “Introduction: Maar-diatreme volcanism.” *Journal of Volcanology and Geothermal Research*, 159, 1–3.
- Marty, B., Sano, Y. and France-Lanord, C. (2001) “Water-saturated oceanic lavas from the Manus Basin: Volatile behaviour during assimilation-fractional crystallisation-degassing (AFC/D)” *Journal of Volcanology and Geothermal Research*, 108, 1–10.
- Mason, T. P. and Smith, R. L. (1977) “Spectacular mobility of ash flows around Anakchak and Fisher calderas, Alaska.” *Geology*, 5, 173–6.
- Mason, B. G., Pyle, D. M., and Oppenheimer, C. (2004) “The size and frequency of the largest explosive eruptions on Earth.” *Bulletin of Volcanology*, 66, 735–48.
- Massonet, D., Rossi, M., Carmona, C., et al. (1993) “The displacement field of the Landers earthquake mapped by radar interferometry.” *Nature*, 364, 138–42.
- Mastin, L. G. (1994) “Explosive tephra emissions at Mount St. Helens, 1989–1991 – the violent escape of magmatic gas following storms?” *Geological Society of America Bulletin*, 106, 175–85.
- Mastin, L. G. and Pollard, D. D. (1988) “Surface deformation and shallow dike intrusion processes at Inyo Craters, Long Valley, California.” *Journal of Geophysical Research*, 93, 13, 221–35.
- Mastin, L. G. and Waite, R. B. (2000) “Glacier Peak – History and hazards of a Cascade volcano.” US Geological Survey Fact Sheet 058-00.
- Mastin, L. G. and Witter, J. B. (2000) “The hazards of eruptions through lakes and seawater.” *Journal of Volcanology and Geothermal Research*, 97, 195–214.
- Masurenkov, Y. P. (1991) “Hypsometric and lateral patterns of active volcanoes.” In S. A. Fedotov and Y. P. Masurenkov (eds.), *Active Volcanoes of Kamchatka*. Moscow, Nauka Publishers, pp. 54–66.
- Mather, T. A., Pyle, D. M., and Allen, A. G. (2004) “Volcanic origin for fixed nitrogen in the early Earth’s atmosphere.” *Geology*, 3, 905–8.
- Matthews, A. J., Barclay, J., and Johnstone, J. E. (2009) “The fast response of volcano-seismic activity to intense precipitation: Triggering of primary volcanic activity by rainfall at Soufrière Hills volcano, Montserrat.” *Journal of Volcanology and Geothermal Research*, 184, 405–15.
- Mauk, F. J. and Johnston, M. J. S. (1973) “On the triggering of volcanic eruptions by Earth tides.” *Journal of Geophysical Research*, 78, 3356–62.
- McBirney, A. R. (1965) “Volcanic history of Nicaragua.” *University of California, Berkeley Publications in the Geological Sciences*, 55, 1–65.
- McBirney, A. R. and Williams, H. (1969) “Geology and petrology of the Galapagos Islands.” Geological Society of America, 197p.
- McClelland, L., Simkin, T., Summers, M., et al. (eds.) (1989) *Global Volcanism 1975–1985*. Englewood Cliffs, Prentice-Hall and American Geophysical Union.
- McCoy, F. and Heiken, G. (2000) *Volcanic Hazards and Disasters in Human Antiquity*. Boulder, Geological Society of America.
- McCulloh, T. H., Fleck, R. J., Denison, R. E., et al. (2002) “Age and tectonic significance of volcanic rocks in the Northern Los Angeles Basin, California.” US Geological Survey Professional Paper 1669, 24p.
- McEwen, A., Keszthelyi, L., Geissler, P., et al. (1998) “Active volcanism on Io as seen by Galileo SSI 219.” *Icarus*, 135–81.
- McGee, K. A. and Gerlach, T. M. (1998) “Annual cycle of magmatic CO₂ in a tree kill soil at Mammoth Mountain, California: Implications for soil acidification.” *Geology*, 26, 463–6.

- McGuire, W. J. (1995) "Monitoring active volcanoes – an introduction." In W. McGuire, C. Kilburn and J. Murray (eds.), *Monitoring Active Volcanoes: Strategies, Procedures and Techniques*. London, UCL Press, 421p.
- McGuire, W. J., Jones, A. P., and Neuberg, J. (1996) "Volcano instability on the Earth and other planets." Geological Society of London Special Paper 110, 388p.
- McNutt, S. R. (1994) "Volcanic tremor amplitude correlated with the volcano explosivity index and its potential use in determining ash hazards to aviation." *Acta Vulcanologica*, 5, 193–6.
- McNutt, S. R. (1996) "Seismic monitoring and eruption forecasting of volcanoes: A review of the state of the art and case histories." In R. Scarpa and R. Tilling (eds.), *Monitoring and Mitigation of Volcano Hazards*. Berlin, Springer-Verlag, pp. 99–146.
- McNutt, S. R. and Davis, C. M. (2000) "Lightning associated with the 1992 eruptions of Crater Peak, Mount Spurr Volcano, Alaska." *Journal of Volcanology and Geothermal Research*, 102, 45–65.
- McPhie, J., Doyle, M., and Allen, R. (1993) "Volcanic textures: A guide to the interpretation of textures in volcanic rocks." Hobart, Centre for Ore Deposits and Exploration Studies, University of Tasmania, 198p.
- Mee, K., Tuffon, H., and Gilbert, J. S. (1994) "Snow-contact volcanic facies and their use in determining past eruptive environments at Nevados del Chillán volcano, Chile." *Bulletin of Volcanology*, 68, 363–76.
- Menand, T. (2007) "The mechanics of sills in layered elastic rocks and their implications for the growth of laccoliths and other igneous complexes." *Earth and Planetary Sciences Letters*, 267, 93–9.
- Mencke, W., West, M., and Tolstoy, M. (2002) "Shallow-crustal magma chamber beneath the axial high of the coaxial segment of the Juan de Fuca Ridge at the source site of the 1993 eruption." *Geology*, 30, 359–62.
- Mercalli, G. (1907) *I vulcani attivi della Terra*. Milan, Ulrico Hoepli.
- Middlemost, E. A. K. (1985) "Miocene shield volcanoes of New South Wales." Geological Society of Australia, New South Wales Div., Publication 1, 49–58.
- Mileti, D. S., Bolton, P. A., Fernandez, G., et al. (1991) *The Eruption of Nevado del Ruiz Volcano, Colombia, South America – November 13, 1985*. Washington, DC, National Academy Press.
- Miller, C. F. and Miller, J. S. (2002) "Contrasting stratified plutons exposed in tilt blocks, Eldorado Mountains, Colorado River Rift, NV, USA." *Lithos*, 61, 209–24.
- Miller, C. F. and Wark, D. A. (2008) "Supervolcanoes and their explosive super-eruptions." *Elements*, 4, 1, 11–15.
- Miller, C. F., Walker, B.A., Lowery, L., et al. (2005) "Construction of Plutons by Horizontal Depositional and Intrusive Sheets." *Geological Society of America Abstracts with Programs*, 37, 7, 130.
- Miller, S. and Orgel, L. E. (1974) *The Origins of Life on Earth*. Englewood Cliffs, Prentice-Hall Publishing, 229p.
- Miller, S. L. (1953) "A production of amino acids under possible primitive Earth conditions." *Science*, 117, 528–9.
- Miller, T. P. and Casadevall, T. J. (2000) "Volcanic ash hazards to aviation." In H. Sigurdsson (ed.), *Encyclopedia of Volcanoes*. New York, Academic Press, pp. 915–30.
- Miller, T. P. and Smith, R. L. (1977) "Spectacular mobility of ash flows around Aniakchak and Fisher calderas, Alaska." *Geology*, 173–6.
- Miller, W. F., Geller, R. J., and Stein, S. (1978) "Use of a bubble tiltmeter as a horizontal seismometer." *Geophysical Journal of the Royal Astronomical Society*, 54, 661–8.
- Mimura, K. (1984) "Imbrication, flow direction, and possible source areas of the pumice-flow tuffs near Bend, Oregon, U.S.A." *Journal of Volcanology and Geothermal Research*, 21, 1–2, 45–60.
- Minakami, T. (1956) "Report on volcanic activities and volcanological studies in Japan for the period from 1951 to 1954." *Bulletin Volcanologique*, 18, 39–76.

- Minakami, T. (1960) "Fundamental research for predicting volcanic eruptions, Part I." *Bulletin of the Earthquake Research Institute, Tokyo University*, 38, 4497–544.
- Minakami, T., Ishikawa, T., and Yagi, K. (1951) "The 1944 eruption of Volcano Usu in Hokkaido, Japan." *Bulletin of Volcanology*, 11, 45–160.
- Mogi, K. (1958) "Relations between eruptions of various volcanoes and the deformations of the ground surfaces around them." *Bulletin of the Earthquake Research Institute*, 36, 99–134.
- Mohr, P. A. and B. Zanettin (1988) *The Ethiopian Flood Basalt Province*. Dordrecht, Kluwer.
- Montelli, R., Nolet, G., Dahlen, F. A., et al. (2003) "Finite frequency tomography reveals a variety of plumes in the mantle." *Science*, 303, 5656, 338–43.
- Moore, H. J. (1987) "Preliminary estimates of the rheological properties of 1984 Mauna Loa lava." In *Volcanism in Hawai'i*, US Geological Survey Professional Paper 1350, pp. 1569–88.
- Moore, J. G. (1967) "Base surge in recent volcanic eruptions." *Bulletin. Volcanologique*, 30, 337–63.
- Moore, J. G. (1970) "Pillow lava in a historic lava flow from Hualalai Volcano, Hawai'i." *Journal of Geology*, 78, 239–43.
- Moore, J. G. and Sisson, T. W. (1981) "Deposits and effects of the May 18 pyroclastic surge." In *The 1980 Eruptions of Mount St. Helens*. US Geological Survey Professional Paper 1250, pp. 421–38.
- Moore, J. G. and Thomas, D. M. (1988) "Subsidence of Puna, Hawai'i inferred from sulfur content of drilled lava flows." *Journal of Volcanology and Geothermal Research*, 35, 165–71.
- Moore, P. (2002) *Venus*. London, Cassell.
- Moore, R. B. and Clague, D. A. (1991) "Geologic Map of Hualalai Volcano, Hawai'i." US Geological Survey, I Map 2213.
- Morgan, J. (1971) "Convection plumes in the lower mantle." *Nature*, 230, 42–3.
- Morgan, J., Reston, T. J., and Ranero, C. R. (2004) "Contemporaneous mass extinctions, continental flood basalts, and 'impact signals': Are mantle plume-induced lithospheric gas explosions the causal link?" *Earth and Planetary Science Letters*, 217, 263–84.
- Mouginis-Mark, J. and Robinson, M. J. (1992) "Evolution of Olympus Mons caldera, Mars." *Bulletin of Volcanology*, 54, 347–60.
- Mouginis-Mark, P. J., Crisp, J. A., and Fink, J. H. (eds.) (2000) *Remote Sensing of Active Volcanism*. Washington, DC, American Geophysical Union.
- Mueller, S., Scheu, B., Spieler, O., et al. (2008) "Permeability control on magma fragmentation." *Geology*, 36, 399–402.
- Muffler, L. J. P., White, D. E., and Truesdell, A. H. (1971) "Hydrothermal explosion craters in Yellowstone National Park." *Geological Society of America Bulletin*, 82, 723–40.
- Murai, I. (1961) "A study of the textural characteristics of pyroclastic flow deposits in Japan." *Bulletin of the Earthquake Research Institute of Tokyo University*, 39, 133–254.
- Murray, J. B., Pullen, A. D., and Saunders, S. J. (1995) "Ground deformation surveying of active volcanoes." In W. J. McGuire, C. Kilburn and J. Murray (eds.), *Monitoring Active Volcanoes: Strategies, Procedures and Techniques*. London, UCL Press, pp. 113–50.
- Myers, A. (2007) "Investigating volcano's plumbing system." *Bolletino del la Comunità Scientifica in Australasia*, April, 36.
- Nairn, I. A. and Cole, J. W. (1981) "Basaltic dikes in the 1886 Tarawera Rift, New Zealand." *Journal of Geology and Geophysics*, 24, 585–92.
- Nakada, S., Nagai, M., Kaneko, T., et al. (2005) "Chronology and products of the 2000 eruption of Miyakejima volcano, Japan." *Bulletin of Volcanology*, 67, 3, 205–18.
- Neall, V. E. (2001) "Volcanic landforms." In A. Sturman and R. Spronken-Smith (eds.), *The Physical Environment: A New Zealand Perspective*. South Melbourne, Australia, Oxford University Press, pp. 39–60.
- Neuville, D. R., Courtil, P., Dingwell, D. B., et al. (1993) "Thermodynamic and rheological properties of rhyolite and andesite melts." *Contributions to Mineralogy and Petrology*, 113, 572–81.

- Newhall, C. G. and Endo, E. T. (1987) "Sudden seismic calm before eruptions: illusory or real?" *Hawai'i Symposium on How Volcanoes Work* [abstracts volume]. US Geological Survey, Hilo, Hawai'i, 190.
- Newhall, C. G. and Dzurisin, D. (1988) *Historical Unrest at Large Calderas of the World*. New York, US Geological Survey.
- Newhall, C. G. and Hoblitt, R. P. (2002) "Constructing event trees for volcanic crises." *Bulletin of Volcanology*, 64, 1, 3–20.
- Newhall, C. G. and Punongbayan, R. S. (eds.) (1996) *Fire and Mud – Eruptions and Lahars of Mount Pinatubo, Philippines*, Philippine Institute of Volcanology and Seismology and University of Washington Press.
- Newhall, C. G. and Self, S. (1982) "The volcanic explosivity index (VEI) – an estimate of explosive magnitude for historical volcanism." *Journal of Geophysical Research*, 87, C2, 1231–8.
- Newhall, C. G., Bronto, S., Allowya, B., et al. (2000) "10,000 years of explosive eruptions of Merapi Volcano, Central Java: Archaeological and modern implications." *Journal of Volcanology and Geothermal Research*, 100, 9–50.
- NIOSH (1994) *Documentation for Immediately Dangerous to Life or Health Concentrations (IDLH)*. Center for Disease Control, Atlanta, Georgia. NTIS Publication No. PB-94-195047.
- Nixon, I. G. (1985) "The volcanic eruption of Thera and its effect on the Mycenaean and Minoan civilizations." *Journal of Archaeological Research*, 12, 9–24.
- Officer, C. B. and Drake, C. L. (1983) "The Cretaceous-Tertiary Transition." *Science*, 219, 1383–90.
- Ogden, D. E., Glatzmaier, G. A., and Wohletz, K. H. (2008) "Effects of vent overpressure on buoyant eruption columns: Implications for plume stability." *Earth and Planetary Science Letters*, 268, 283–92.
- Ohmoto, H. and Skinner, B. J. (eds.) (1983) "The Kuroko and related volcanogenic massive sulphide deposits." *Economic Geology*, Mongraph 5, 604p.
- Okubo, C. H. and Martel, S. J. (1998) "Pit crater formation on Kilauea volcano, Hawai'i." *Journal of Volcanology and Geothermal Research*, 86, 1–18.
- Okubo, P. G., Benz, H. M., and Chouet, B. A. (1997) "Imaging the crustal magma sources beneath Mauna Loa and Kilauea volcanoes, Hawai'i." *Geology*, 25, 10, 867–70.
- Okuno, M., Nakamura, T., and Kobayahi, T. (1998) "AMS ^{14}C dating of historic eruptions of the Kirishima, Sakura-jima, and Kaimon-dake volcanoes, southern Kyushu, Japan." In W. G. Mook and J. van der Plicht (eds.), *Proceedings of the 16th International ^{14}C Conference*, Radiocarbon, 40, pp. 825, 832.
- Ollier, C. D. (1969) *Volcanoes*, Boston, MIT Press.
- Omori, F. (1914) "The Sakura-jima eruption and earthquakes." *Bulletin of the Imperial Earthquake Investigation Committee (Japan)*, 8, 1–6, 1–34.
- Oppenheimer, C. M. M. (1991) "Lava flow cooling estimated from Landsat thematic mapper infrared data: The Loquimay, Chile eruption 1989." *Journal of Geophysical Research*, 96, 21856–78.
- Oswalt, J. S., Nichols, W., and O'Hara, J. F. O. (1996) "Meteorological observations of the 1991 Mount Pinatubo eruption." In C. G. Newhall, and R. S. Punongbayan (eds.) *Fire and Mud – Eruptions and Lahars of Mount Pinatubo, Philippines*. Quezon City, Philippine Institute of Volcanology and Seismology and University of Washington Press, pp. 625–36.
- Palister, J. S., Hoblitt, R. P., Meeker, G. P., et al. (1996) "Magma mixing at Mount Pinatubo – petrographic and chemical evidence from the 1991 deposits." In C. G. Newhall, and R. S. Punongbayan (eds.) *Fire and Mud – Eruptions and Lahars of Mount Pinatubo, Philippines*. Quezon City, Philippine Institute of Volcanology and Seismology and University of Washington Press, pp. 687–731.
- Parfitt, E. A. (2004) "A discussion of the mechanics of explosive volcanic eruptions." *Journal of Volcanology and Geothermal Research*, 134, 77–107.
- Parfitt, E. A. and Wilson, L. (2008) *Fundamentals of Physical Volcanology*. Oxford, Blackwell.

- Park, C. F. and McDiarmid, R. A. (1964) *Ore Deposits*. New York, W. H. Freeman, 475p.
- Paulick, H. and Franz, G. (1997) "The color of pumice: A case study on a trachytic fall deposit, Meidob volcanic field, Sudan." *Bulletin of Volcanology*, 59, 171–85.
- Peale, S. J., Cassen, P., and Reynolds, R. T. (1979) "Melting of Io by Tidal Dissipation." *Science*, 203, 892–4.
- Perfit, M. R., Cann, J. R., Fornari, J., et al. (2003) "Interaction of sea water and lava during submarine eruptions at mid-ocean ridges." *Nature*, 426, 62–5.
- Perret, F. A. (1924) *The Vesuvius Eruption of 1906*. Washington, DC, Carnegie Institution.
- Perret, F. A. (1935) *The Eruption of Mt. Pelée, 1929–1932*. Washington, DC, Carnegie Institution.
- Peterson, D. W. (1996) "Mitigation measures and preparedness plans for volcanic emergencies." In R. Scarpa and R. I. Tilling (eds.), *Monitoring and Mitigation of Volcanic Hazards*. Berlin, Springer, pp. 701–18.
- Peterson, D. W. and Tilling, R. I. (1980) "Transition of basaltic lava from pāhoehoe to `a`ā, Kilauea Volcano, Hawai`i – field observations and key factors." *Journal of Volcanology and Geothermal Research*, 7, 271–93.
- Pierson, T. C. (1995) "Flow characteristics of large, eruption-triggered debris flows at snow-clad volcanoes: Constraints for debris-flow models." *Journal of Volcanology and Geothermal Research*, 66, 283–94.
- Pierson, T. C. (2005) "Hyperconcentrated flow: Transitional process between water flow and debris flow." In J. Matthias and H. Oldrich (eds.), *Debris-flow Hazards and Related Phenomena*. Berlin, Springer-Praxis, pp. 159–202.
- Pierson, T. C., Daag, A. S., Delos, P. J., et al. (1996) "Flow and deposition of posteruption hot lahars on the east side of Mount Pinatubo, July–October 1991." In C. G. Newhall, and R. S. Punongbayan (eds.) *Fire and Mud – Eruptions and Lahars of Mount Pinatubo, Philippines*. Quezon City, Philippine Institute of Volcanology and Seismology and University of Washington Press, pp. 921–50.
- Pierson, T. C., Janda, R. J., Thouret, J.-C., et al. (1990) "Perturbation and melting of snow and ice by the 13 November, 1985 eruption of Nevado del Ruiz, Colombia and consequent mobilization, flow, and deposition of lahars." *Journal of Volcanology and Geothermal Research*, 41, 17–66.
- Pierson, T. C., Janda, R. J., Umbal, J. V., et al. (1992) "Immediate and long-term hazards from lahars and excess sedimentation in rivers draining Mt. Pinatubo, Phillipines." US Geological Survey Water Resource Investigations Report 92-4039, pp. 1–35.
- Pinkerton, H., James, M., and Jones, A. (2002) "Surface temperature measurements of active lava flows on Kilauea volcano, Hawai`i." *Journal of Volcanology and Geothermal Research*, 112, 159–76.
- Pioli, L. and Rosi, M. (2005) "Rheomorphic structures in high-grade ignimbrite: The Nuraxi Tuff, Sulcis volcanic district (SW Sardinia, Italy)." *Journal of Volcanology and Geothermal Research*, 142, 11–28.
- Platt, U. and Stutz, J. (2008) *Differential Optical Absorption Spectroscopy: Principles and Applications*. New York, Springer.
- Pollard, D. D. and Aydin, A. (1988) "Progress in understanding jointing over the past century." *Geological Society of America Bulletin*, 100, 1184–204.
- Ponomareva, V. V., Pezner, M. M., and Melekestsev, I. V. (1998) "Large debris avalanches and associated eruptions in the Holocene eruptive history of Shiveluch Volcano, Kamchatka, Russia." *Bulletin of Volcanology*, 59, 490–505.
- Porco, C. C., Helfenstein, P., Thomas, P. C., et al. (2006) "Cassini observes the active south pole of Enceladus." *Science*, 311, 1393–401.
- Porter, S. C. (1987) "Pleistocene subglacial eruptions on Mauna Kea." *Volcanism in Hawai`i, The 1980 Eruptions of Mount St. Helens*. US Geological Survey Professional Paper 1350, pp. 587–98.

- Powell, J. W. (1896) *The Physiography of the United States*, New York, National Geographic Society/American Book Company.
- Powers, H. A. and Wilcox, R. E. (1964) "Volcanic ash from Mt. Mazama (Crater Lake) and from Glacier Peak." *Science*, 144, 3624, 1334–6.
- Prueher, L. M. and Rea, D. K. (2001) "Tephrochronology of the Kamchatka-Kurile and Aleutian arcs: Evidence for volcanic episodicity." *Journal of Volcanology and Geothermal Research*, 106, 67–84.
- Pyle, D. M. (1989) "The thickness, volume, and grain size of tephra fall deposits." *Bulletin Volcanologique*, 51, 1–15.
- Pyle, D. M. (1995) "Mass and energy budgets of explosive volcanic eruptions." *Geophysical Research Letters*, 22, 5, 563–6.
- Pyle, D. M. and Elliott, J. R. (2006) "Quantitative morphology, recent evolution, and future activity of the Kameni Islands volcano, Santorini, Greece." *Geosphere*, 2, 5, 253–68.
- Quick, J. E., Sinigoi, S., and Denlinger, R. (1992) "Large scale evolution of the underplated igneous complex of the Ivrea-Verbano Zone." US Geological Survey Circular 1089, 14–15.
- Rampino, M. R. and Ambrose, S. H. (2000) "Volcanic winter in the Garden of Eden: The Toba super-eruption and the late Pleistocene human population crash." In F. W. McCoy and G. Heiken (eds.), *Volcanic Hazards and Disasters in Human Antiquity*, Geological Society of America Special Paper, 345, 71–82.
- Rampino, M. R. and Self, S. (1984) "The atmospheric effects of El Chichón." *Scientific American*, 250, 1, 48–57.
- Rampino, M. R. and Self, S. (1993) "Climate-volcanism feedback and the Toba eruption of ~74,000 years ago." *Quaternary Research*, 269–80.
- Rampino, M. R., and Strother, R. B. (1988) "Flood basalt volcanism during the past 250 million years." *Science*, 241, 663–8.
- Rapp, G. R. and Hill, C. L. (2006) *Geoarchaeology: The Earth Science Approach to Archaeological Investigations*, New Haven, Yale University Press.
- Ratte, J. C. and Steven, T. A. (1967) "Ash flows and related volcanic rocks associated with the Creede caldera, San Juan Mountains, Colorado." US Geological Survey Professional Paper 524-H, 58p.
- Rea, D. K. and Vallier, T. L. (1983) "Two Cretaceous volcanic episodes in the western Pacific Ocean." *Geological Society of America Bulletin*, 94, 1430–7.
- Reiche, P. (1937) "The Toreva-Block: A Distinctive Landslide Type." *Journal of Geology*, 45, 538–48.
- Reid, J. B., Jr., Murray, D. P., Hermes, O. D., et al. (1993) "Fractional crystallization in granites in the Sierra Nevada: How important is it?" *Geology*, 21, 587–90.
- Reihle, J. R., Miller, T. F., and Bailey, R. A. (1995) "Cooling, degassing, and compaction of rhyolitic lava flows: A computational model." *Bulletin of Volcanology*, 57, 319–36.
- Richards, A. F. (1959) "Geology of Islas Revillagigedo, Mexico, 1: Birth and development of Volcan Barcena, Isla San Benedicto (1)." *Bulletin Volcanologique*, 73–123.
- Ritmann, A. (1958) "Cenni sulle collate di ignimbrati." *Atti della Accademia Gioenia di Scienze Naturali in Catania*, 4, 524–33.
- Ritmann, A. (1962) *Volcanoes and Their Activity*. New York, John Wiley and Sons.
- River, E. P. and Harris, D. V. (1999) *Geology of U.S. Parklands*, New York, Wiley.
- Robin, C., Eissen, J. P., and Monzier, M. (1993) "Giant tuff cone and 12-mile wide associated caldera at Ambrym Volcano (Vanuatu, New Hebrides)." *Journal of Volcanology and Geothermal Research*, 225–38.
- Robock, A. and Oppenheimer, C. (2003) *Volcanism and the Earth's Atmosphere*. Washington, DC: American Geophysical Union.

- Roche, S. L., Davis T. L., Benson, R. D., et al. (2001) "Dynamic reservoir characterization: Application of time-lapse (4-D), multicomponent seismic to a CO₂ EOR project, Vacuum Field, New Mexico." Tulsa, American Association of Petroleum Geologists.
- Rogers, N. and Hawkesworth, C. (2000) "Composition of magmas." In H. Sigurdsson (ed.), *Encyclopedia of Volcanoes*. New York, Academic Press, pp. 115–31.
- Roggensack, K., Hervig, R. L., McKnight, S. B., et al. (1997) "Explosive basaltic volcanism from Cerro Negro Volcano: Influence of volatiles in eruptive style." *Science*, 277, 1639–42.
- Rohrer, R. (1965) *Base surges and Cloud Formation – Project Pre-Schooner*. Berkeley, Lawrence Livermore Laboratory, University of California, p. 10.
- Romagnoli, C., Kokelaar, P., Rossi, P. L., et al. (1993) "The submarine extension of Sciara del Fuoco feature (Stromboli Is.): Morphologic characterization." *Acta Volcanologica*, 3, 91–8.
- Rose, W. I., Newhall, C. G., Bornhorst, T. J., et al. (1987) "Quaternary silicic pyroclastic deposits of Aтитlan Caldera, Guatemala." *Journal of Volcanology and Geothermal Research*, 33, 57–80.
- Rosenbaum, J. G. and Waitt, R. B., Jr. (1981) "Summary of eyewitness accounts of the May 18 eruption." *Volcanism in Hawai`i*. US Geological Survey Professional Paper 1350, pp. 53–68.
- Rosenmuller, J. C. and Tillesius, W. G. (1799) *Beschreibung merkwu'diger Hoken, ein Beitrag zur physikalischen Beschreibung der Erde*. Leipzig, Breitkopf und Hartel, 294p.
- Ross, C. S. and Smith, R. L. (1961) *Ash-flow Tuffs: Their Origin, Geologic Relations, and Identification*. Washington, DC, US Geological Survey.
- Rowe, C., Aster, R., Kyle, P. R., et al. (2000) "Seismic and acoustic observations at Mount Erebus Volcano, Ross Island, Antarctica, 1994–1998." *Journal of Volcanology and Geothermal Research*, 20, 105–28.
- Rowland, S. K. and Munro, D. C. (1992) "The caldera of Volcan Fernandina: A remote sensing study of its structure and recent activity." *Bulletin Volcanologique*, 55, 97–109.
- Rowland, S. K., Smith, G., and Mouginiis-Mark, P. J. (1993) "Preliminary ERS-1 observations of Alaskan and Aleutian volcanoes." *Remote Sensing of Environment*, 48, 358–69.
- Rowley, P., Kuntz, M., and Macleod, N. (1981) "Pyroclastic flow deposits." *The 1980 Eruptions of Mount St. Helens*, US Geological Survey Professional Paper 1250, 489–512.
- Russell, I. C. (1902) *Geology and Water Resources of the Snake River Plains of Idaho*. Washington, DC, US Geological Survey.
- Russell, J. M., III, Luo, M., Cicerone, R. J., et al. (1996) "Satellite confirmation of the dominance of chlorofluorocarbons on the global stratospheric budget." *Nature*, 379, 526.
- Rutherford, M. J. (2008) "Magma ascent rates," *Reviews in Mineralogy and Geochemistry*, 69, 241–71.
- Ryan, M. P. (1987a) "Neutral buoyancy and the mechanical evolution of magmatic systems." In B. O. Mysen (ed.) *Magmatic Processes – Physicochemical Principles*. The Geochemical Society, Special Publication 1.
- Ryan, M. P. (1987b) "Elasticity and contractancy of Hawaiian olivine tholeiite and its role in the stability and structural evolution of subcaldera magma reservoirs and rift systems." *Volcanism in Hawai`i*. US Geological Survey Professional Paper 1350, pp. 1395–447.
- Ryan, M. P. (1988) "The mechanics and three-dimensional internal structure of active magmatic systems – Kilauea volcano, Hawai`i." *Journal of Geophysical Research*, 93, B5, 4213–48.
- Ryan, M. P. and Sammis, C. G. (1978) "Cyclic fracture mechanisms in cooling basalt." *Geological Society of America Bulletin*, 89, 1295–1308.
- Ryan, M. P., Koyanagi, R. Y., and Fiske, R. S. (1981) "Modeling the three-dimensional structure of magma transport systems: Application to Kilauea Volcano, Hawai`i." *Journal of Geophysical Research*, 86, 7111–29.

- Rymer, H. and Williams-Jones, G. (2000) "Volcanic eruption prediction: Magma chamber physics from gravity and deformation measurements." *Geophysical Research Letters*, 27, 16, 2389–92.
- Sable, J. E., Houghton, B. F., Wilson, C. J. N., et al. (2006) "Complex proximal sedimentation from Plinian plumes: The example of Tarawera 1886." *Bulletin of Volcanology*, 9, 89–103.
- Sahagian, D. (1985) "Bubble migration and coalescence during the solidification of basaltic lava flows." *Journal of Geology*, 93, 205–11.
- Sanford, A. R., Olsen, K. H., and Jashka, L. H. (1979) *Seismicity of the Rio Grande Rift: Tectonics and Magmatism*. Washington, DC, American Geophysical Union, pp. 145–68.
- Sarna-Wojcicki, C., Champion, D. E., and Davis, J. O. (1983) "Holocene volcanism in the conterminous United States and the role of silicic volcanic ash layers in correlation of latest-Pleistocene and Holocene deposits." In H. E. Wright (ed.), *Late-Quaternary Environments of the United States*. Minneapolis, University of Minnesota Press, pp. 52–77.
- Saunders, S. J. (2001) "The shallow plumbing system of Rabaul caldera: A partially intruded ring fault?" *Bulletin of Volcanology*, 63, 6, 406–20.
- Scailliet, B., Pichavant, M., and Cioni, R. (2008) "Upward migration of Vesuvius Magma Chamber over the past 20,000 Years." *Nature*, 455, 216–20.
- Scandone, R. (1990) "Chaotic collapse of calderas." *Journal of Volcanology and Geothermal Research*, 42, 282–302.
- Scandone, R., Arganese, G., and Galdi, F. (1993) "The evaluation of volcanic risk in the Vesuvius area." *Journal of Volcanology and Geothermal Research*, 58, 5–25.
- Scarpa, R. and Tilling, R. I. (eds.) (1996) *Monitoring and Mitigation of Volcano Hazards*. Heidelberg, Springer-Verlag.
- Scarth, A. (2009) *Vesuvius: A Biography*. Princeton University Press, 352p.
- Scharrer, K., Spieler, O., Meyer, Ch., et al. (2008) "Imprints of sub-glacial volcanic activity on a glacier surface – SAR study of Katla volcano, Iceland." *Bulletin of Volcanology*, 70, 4, 495–506.
- Schenk, P., Hargitai, H., Wilson, R., et al. (2001) "The mountains of Io: Global and geological perspectives from Voyager and Galileo." *Journal of Geophysical Research*, 106, 201–33.
- Schirnick, C., van der Boggaard, D., and Schmincke, H.-U. (1999) "Cone sheet formation and intrusive growth of an oceanic island – The Miocene Tejada complex on Gran Canaria (Canary Islands)." *Geology*, 27, 207–10.
- Schmidt, R. (1981) "Descriptive nomenclature and classification of pyroclastic deposits and fragments: Recommendations of the IUGS Subcommittee on the Systematics of Igneous Rocks." *Geology*, 9, 1, 41–3.
- Schmincke, H.-U. (1967) "Fused tuff and peperites in south-central Washington." *Geological Society of America Bulletin*, 78, 319–30.
- Schmincke, H.-U., Fisher, R. V., and Waters, A. C. (1973) "Antidune and chute and pool structures in the base surge deposits of the Laacher See area, Germany." *Sedimentology*, 20, 4, 553–74.
- Scholl, D. W., Kirby, S. H., and Platt, J. P. (1996) *Subduction: Top to Bottom*. American Geophysical Union Monograph Series, 96, 384 p.
- Schumacher, R. and Schmincke, H.-U. (1995) "Models for the origin of accretionary lapilli." *Bulletin of Volcanology*, 56, 626–39.
- Scott, W. E., Hoblitt, R. P., et al. (1996) "Pyroclastic flows of the June 15, 1991, climactic eruption of Mount Pinatubo." In C. G. Newhall and R. S. Punongbayan, (eds.) *Fire and Mud – Eruptions and Lahars of Mount Pinatubo, Philippines*. Quezon City, Philippine Institute of Volcanology and Seismology and University of Washington Press, pp. 545–70.
- Scrope, G. P. (1862) *Volcanoes: The Character of their Phenomena, their Share in the Structure and Composition of the Surface of the Globe, and their Relation to its Internal Forces with a Descriptive*

- Catalogue of All Known Volcanoes and Volcanic Formations*. London, Longman, Green, Longmans, and Roberts.
- Scrope, G. P. (1872) *Volcanoes: The Character of their Phenomena, their Share in the Structure and Composition of the Surface of the Globe, and their Relation to its Internal Forces with a Descriptive Catalogue of All Known Volcanoes and Volcanic Formations*. 2nd edn. London, Longmans, Green, Reader and Dyer.
- Segerstrom, K. (1950) *Erosion Studies at Parícutín, State of Michoacán, Mexico*. Washington DC, US Geological Survey.
- Self, S. (1992) "Krakatau revisited: The course of events and interpretation of the 1883 eruption." *Geojournal*, 28, 109–21.
- Self, S. (2006) "The effects and consequences of very large explosive volcanic eruptions." *Philosophical Transactions of the Royal Society*, 364, 2073–97.
- Self, S. and Sparks, R. S. J. (1978) "Characteristics of widespread pyroclastic deposits formed by the interaction of silicic magma and water." *Bulletin Volcanologique*, 41, 196–212.
- Shaw, H. P. (1972) "Viscosities of magmatic silicate liquids: An empirical method of prediction." *American Journal of Science*, 272, 9, 870–93.
- Sheets, P. D. (1979) "Environmental and cultural effects of the Illopango eruption in Central America." In P. D. Sheets and D. K. Grayson (eds.), *Volcanic Activity and Human Ecology*, New York, Academic Press, pp. 525–64.
- Sheets, P. D. (2002) *Before the Volcano Erupted – The Ancient Cerén Village in Central America*. Austin, University of Texas Press.
- Sheets, P. D. and Grayson, D. K. (1979) *Volcanic Activity and Human Ecology*. New York, Academic Press.
- Sheridan, M. F. and Wang, Y. (2005) "Cooling and welding history of the Bishop Tuff in Adobe Canyon and Chidago Canyon, California." *Journal of Volcanology and Geothermal Research*, 142, 119–44.
- Sherrod, D. R., Scott, W. E., and Stauffer, P. H. (eds.) (2008) *A Volcano Rekindled; The Renewed Eruption of Mount St. Helens, 2004–2006*. US Geological Survey Professional Paper 1750, 856p.
- Sheth, H. C. (2007) "Large Igneous Provinces (LIPs): Definition, recommended terminology, and a hierarchical classification." *Earth-Science Reviews*, 85, 3–4, 117–24.
- Shimozuru, D. (1968) "Discussion on the energy partition of volcanic eruption." *Bulletin of Volcanology*, 30, 383–94.
- Sigurdsson, H. (1999) *Melting the Earth: The History of Ideas on Volcanic Eruptions*, Oxford, Oxford University Press.
- Simkin, T. (1972) "Origin of some flat-topped volcanoes and guyots." *Geological Society of America Memoir*, 132, 183–93.
- Simkin, T. (1984) "Geology of Galapagos Islands." In R. Perry (ed.), *Galapagos*. Oxford, Pergamon Press, 14–41.
- Simkin, T. and Fiske, R. S. (1983) *Krakatau, 1883: The Volcanic Eruption and its Effects*. Washington, Smithsonian Inst. Press.
- Simkin, T. and Howard, K. A. (1970) "Caldera collapse in the Galápagos Islands, 1968." *Science*, 169, 429–37.
- Simkin, T. and Siebert, L. (1984) "Explosive eruptions in space and time – durations, intervals, and a comparison of the world's active volcanic belts." In N. R. C. Geophysics Study Committee. *Explosive Volcanism: Inception, Evolution, and Hazards*. Washington, DC, National Academy Press, pp. 110–21.
- Simkin, T. and Siebert, L. (1994) *Volcanoes of the World*, 2nd edn. Tucson, Geoscience Press in association with the Smithsonian Institution Global Volcanism Program.

- Simkin, T., Siebert, L., and Blong, R. (2001) "Volcano fatalities: Lessons from the historical record." *Science*, 291, 5502, 255.
- Simkin, T., Siebert, L., McClelland, L., et al. (1981) *Volcanoes of the World: A Regional Directory, Gazetteer, and Chronology of Volcanism During the Last 10,000 Years*. Stroudsburg, Hutchinson Ross Publishing, 240p.
- Simkin, T., Tilling, R. I., Under, J. D., et al. (2006) "This dynamic planet; World map of volcanoes, earthquakes, impact craters, and plate tectonics." I Map 2800, US Geological Survey Geologic Investigations Series.
- Singh, S. C., Crawford, W. C., Carton, C., et al. (2006) "Discovery of a magma chamber and faults beneath a Mid-Atlantic Ridge hydrothermal field." *Nature*, 442, 1029–32.
- Smellie, J. L. (2002) "The 1969 subglacial eruption on Deception Island (Antarctica): events and processes during an eruption beneath a thin glacier and implications for volcanic hazards." In J. L. Smellie and M. G. Chapman (eds.), *Volcano–Ice Interaction on Earth and Mars*. London, Geological Society of London. Special Publications, p. 431.
- Smith, A. L. and Roobal, M. J. (1982) "Andesitic pyroclastic flows." In R. S. Thorpe (ed.), *Orogenic Andesites*. New York, Wiley, pp. 415–33.
- Smith, D. R. and Leeman, W. P. (1987) "Petrogenesis of St. Helen's Dacitic Magmas." *Journal of Geophysical Research*, 92, 10,313–34.
- Smith, G. A. and Fritz, W. J. (1989) "Volcanic influences on terrestrial sedimentation." *Geology*, 17, 375–6.
- Smith, R. L. (1960) "Ash flows." *GSA Bulletin*, 71, 6, 795–841.
- Smith, R. L. (1979) "Ash-flow magmatism." In C. E. Chapin and W. E. Elston (eds.), *Ash-flow Tuffs*. Geological Society of America Special Paper, 180, 5–27.
- Smith, R. L., Friedman, I. I., and Long, W. D. (1958) "Welded tuffs, Expt. 1." *American Geophysical Union Transactions*, 39, 352–3.
- Soloman, S. C., Smrekar, S. E., Duane, L., et al. (1992) "Venus tectonics: An overview of Magellan observations." *Journal of Geophysical Research*, 97, 13, 199–256 .
- Sorey, M. L., Evans, W. C., Kennedy, B. M., et al. (1998) "Carbon dioxide and helium emissions from a reservoir of magmatic gas beneath Mammoth Mountain, California." *Journal of Geophysical Research*, 103, 15,303–23.
- Soriano, C., Zafrilla, S., Marti, J., et al. (2002) "Welding and rehomorphism of phonolitic fallout deposits from Las Canadas caldera, Tenerife, Canary Islands." *Geological Society of America Bulletin*, 114, 883–95.
- Sottili, G., Palladino, D. M., and Zanon, V. (2004) "Plinian activity during the early eruptive history of the Sabatini Volcanic District, Central Italy." *Journal of Volcanology and Geothermal Research*, 135, 361–79.
- Soule, S. A., Fornari D. J., Perfit, M. R., et al. (2007) "New insights into mid-ocean ridge volcanic processes from the 2005–2006 eruption of the East Pacific Rise, 9°46'N–9°56'N." *Geology*, 35, 12, 1079–82.
- Souther, J. G. (1990) "Volcano tectonics of Canada." In C. A. Wood and J. Kienle (eds.), *Volcanoes of North America: United States and Canada*. Cambridge, Cambridge University Press, pp. 111–45.
- Sparks, R. S. J. (1978) "The dynamics of bubble formation and growth in magmas: A review and analysis." *Journal of Volcanology and Geothermal Research*, 3, 1–37.
- Sparks, R. S. J. (1986) "The dimensions and dynamics of volcanic eruption columns." *Bulletin Volcanologique*, 48, 3–15.
- Sparks, R. S. J. (1988) "Petrology and geochemistry of the Loch Ba ring-dyke, Mull (N.W. Scotland): An example of the extreme differentiation of tholeiitic melts." *Contributions to Petrology and Mineralogy*, 100, 446–61.

- Sparks, R. S. J. and Walker, G. P. L. (1973) "The ground surge deposit: A third type of pyroclastic rock." *Nature*, 241, 62–4.
- Sparks, R. S. J. and Wilson, L. (1976) "A model for the formation of ignimbrite by gravitational collapse." *Journal of the Geological Society of London*, 132, 441–51.
- Sparks, R. S. J. and Wright, J. V. (1979) "Welded air-fall tuffs." In C. E. Chapin and W. E. Elston (eds.), *Ash-flow Tuffs*. Geological Society of America Special Paper 180, pp. 155–66.
- Sparks, R. S. J., Bursik, M. I., Carey, S. N., et al. (1997) *Volcanic Plumes*. New York, John Wiley and Sons.
- Sparks, R. S. J., Moore, J., and Rice, C. J. (1986) "The initial giant umbrella cloud of the May 18th, 1980 explosive eruption of Mount St. Helens." *Journal of Volcanology and Geothermal Research*, 28, 257–74.
- Sparks, R. S. J., Self, S., Grattan, J. P., et al. (2005) "Super-eruptions: Global effects and future threats." Geological Society of London, 28.
- Spence, R. J. S., Pomonis, A., Naxter, P. J. et al., (1997) "Building damage caused by the Mount Pinatubo eruption of June 15." In C. G. Newhall, and R. S. Punongbayan (eds.), *Fire and Mud – Eruptions and Lahars of Mount Pinatubo, Philippines*. Quezon City, Philippine Institute of Volcanology and Seismology and University of Washington Press, pp. 1055–61.
- Spencer, J. R., Pearl, J. C., Segura, M., et al. (2006) "Cassini encounters Enecladus: Background and discovery of a south polar hot spot." *Science*, 311, 1401–5.
- Spudis, P. D. (2000) "Volcanism on the Moon." In H. Sigurdsson (ed.), *Encyclopedia of Volcanoes*. San Diego, Academic Press, pp. 697–708.
- Stearns, H. T. (1925) "The explosive phase of Kilauea volcano, Hawai'i, in 1924." *Bulletin Volcanologique*, 12, 5, 193–208.
- Stelling, P., Gardner, J. E. and Beget, J. (2005) "Eruptive history of Fisher Caldera, Alaska, USA." *Journal of Volcanology and Geothermal Research*, 139, 3–4, 163–83.
- Stephens, C., Chouet, B. A., Page, R. A., et al. (1994) "Seismological aspects of the 1989–1990 eruptions at Redoubt Volcano, Alaska: The SSAM perspective." *Journal of Volcanology and Geothermal Research*, 62, 153–82.
- Steven, T. A. and Lipman, P. W. (1976) "Calderas of the San Juan volcanic field, southwestern Colorado." US Geological Survey Professional Paper, 958, 35.
- Stevenson, D. S. and Blake, S. (1998) "Modelling the dynamics and thermodynamics of volcanic degassing." *Bulletin Volcanologique*, 60, 307–17.
- Stofan, E. R., Sharpton, V. L., Schubert, G., et al. (1992) "Global distribution and characteristics of coronae and related features on Venus: Implications for origin and relation to mantle processes." *Journal of Geophysical Research*, 97, 13,347–78.
- Stoiber, R. E. and Rose, W. I., Jr (1970) "Geochemistry of Central American volcanic gas condensates." *Geological Society of America Bulletin*, 81, 2891–12.
- Stormer, J. C. J. and Carmichael, I. S. E. (1970) "The Kudo-Weill Plagioclase Geothermometer and Porphyritic Acid Glasses." *Contributions to Mineralogy and Petrology*, 28, 306–9.
- Strom, R. G., Schaber, G. G., and Dawson, D. D. (1994) "The global resurfacing of Venus." *Journal of Geophysical Research*, 99, 10,899–926.
- Strothers, R. B. (1984) "The Great Tambora eruption of 1815 and its aftermath." *Science*, 224, 1191–8.
- Sumner, J. M. (1998) "Formation of clastogenic lava flows during fissure eruption and scoria cone collapse: The 1986 eruption of Izu-Oshima Volcano, eastern Japan." *Bulletin Volcanologique*, 60, 195–212.
- Sutton, A. J., Elias, T., Gerlach, T. M., et al. (2001) "Implications for eruptive processes as indicated by sulfur dioxide emissions from Kilauea Volcano, Hawai'i, 1979–1997." *Journal of Volcanology and Geothermal Research*, 108, 1–4, 283–302.

- Suzuki, T. (1977) "Volcano types and their global population percentages (in Japanese with English abstract)." *Bulletin of the Volcanological Society of Japan*, 2nd series, 27–40.
- Swanson, D. A. (1973) "Pahoehoe flows from the 1969–1971 Mauna Ulu eruption of Kilauea volcano, Hawai'i." *Geology Society America Bulletin*, 84, 615–26.
- Swanson, D. A. and Holland, R. T. (1990) "Regularities in growth of the Mount St. Helens dacite domem 1980–1986." In J. H. Fink (ed.), *Lava Flows and Domes*, New York, Springer Publishing, 3–24.
- Swanson, D. A., Casadevall, T. J., Dzurisin, D., et al. (1982) "Forecasts and predictions of eruptive activity at Mt. St. Helens, USA." *Journal of Geodynamics*, 3, 397–423.
- Swanson, D. A., Wright, T. L., and Helz, R. T. (1975) "Linear vent systems and estimated rates of magma production and eruption for the Yakima Basalt on the Columbia Plateau." *American Journal of Science*, 275, 877–905.
- Swanson, D. A., Wright, T. L., and Hooper, P. R. (1979) "Revisions in stratigraphic nomenclature of the Columbia River Basalt Group." Washington, DC, US Geological Survey Bulletin 1457-G, 59.
- Symonds, G. J. (1888) *The Eruption of Krakatoa and Subsequent Phenomena*. London, Royal Society.
- Symonds, R. B., Rose, W., Bluth, G. J. S., et al. (1994) "Volcanic gas studies; methods, results and applications." *Reviews in Mineralogy and Geochemistry*, 30, 1–66.
- Takada, A. (1988) "Subvolcanic Structure of the Central Dike Swarm Associated with the Ring Complexes in the Shitara district, Central Japan." *Bulletin of Volcanology*, 50, 106–18.
- Taylor, B. (2006) "The single largest oceanic plateau: Ontong Java-Manahiki-Hikurangi." *Earth and Planetary Science Letters*, 241, 372–80.
- Taylor, G. A. (1958) "The 1951 eruption of Mt. Lamington, Papua." *Australia, Bureau of Mineral Resources Geology and Geophysics. Bulletin*, 38, 1–117.
- Tazieff, H. (1970) "The Afar Triangle." *Scientific American*, 222, 2, 32–40.
- Tazieff, H. (1977) "An exceptional eruption; Mt. Niragongo, Jan. 10th, 1977." *Bulletin of Volcanology*, 40, 4, 189–200.
- Teague, A. J., Seward, T. M., and Harrison, D. (2008) "Mantle sources for Oldoinyo Lengai carbonates: Evidence from helium isotopes in fumarole gases." *Journal of Volcanology and Geothermal Research*, 175, 366–90.
- Tepley, F. J., III, Davidson, J. R., Tilling, R. I., et al. (2000) "Magma mixing, recharge, and eruption histories recorded in plagioclase phenocrysts from El Chichón volcano, Mexico." *Journal of Petrology*, 41, 1397–411.
- Texter, C., Graf, H.-F., Timmreck, C., et al. (2004) "Emissions from volcanoes." In C. Granier, P. Artaxo and C. E. Reeves (eds.), "Emissions of Atmospheric Trace Compounds," *Advances in Global Change Research*, 18, 269–303.
- Thomas, R. M. E. and Sparks, R. S. J. (1992) "Cooling of tephra during fallout from eruption columns." *Bulletin Volcanologique*, 54, 542–53.
- Thorarinsson, S. (1954) "The eruption of Hekla, 1947–1948, II.3, The tephra-fall from Hekla on March 29th 1947." *Societas Scientiarum Islandica*, Reykjavik, 68p.
- Thorarinsson, S. (1967) "The Surtsey eruption and related scientific work." *Polar Record*, 13, 86, 571–8.
- Thorarinsson, S. and Sigvaldsson, G. E. (1962) "The eruption in Askja, 1961: A preliminary report." *American Journal of Science*, 260, 641–51.
- Thordarson, T. (2000) "Physical volcanology of Surtsey Island: A preliminary report." *Surtsey Research*, 11, 109–26.
- Thordarson, T. and Self, S. (1993) "The Laki (Skaftár Fires) and Grímsvötn eruptions in 1783–1785." *Bulletin of Volcanology*, 55, 233–63.

- Thordarson, T. and Self, S. (1998) "The Roza Member, Columbia River Basalt Group: A gigantic pahoehoe lava flow field formed by endogenous processes?" *Journal of Geophysical Research*, 103, 27,411–45.
- Thordarson, T., Miller, D. J., Larsen, G., et al. (2001) "New estimates of sulfur degassing and atmospheric mass-loading by the 934 AD Eldgja eruption, Iceland." *Journal of Volcanology and Geothermal Research*, 108, 33–54.
- Thordarson, T., Self, S., Larsen, G., et al. (2009) *Studies in Volcanology: The Legacy of George Walker*. IAVCEI Publications, International Union of Geodesy and Geophysics, 416p.
- Thornber, C. R. (2003) "Magma reservoir processes revealed by geochemistry of the on-going Pu`u `Ō`ō-Kūpaianaha eruption." In C. Helicker, D. A. Swanson and T. J. Takahashi (eds.) *The Pu`u `Ō`ō-Kūpaianaha Eruption of Kīlauea Volcano, Hawai`i: The First Twenty Years*, Washington, DC, US Geological Survey, 1676, 121–36.
- Thouret, J.-G. and Chester, D. K. (2005) *Volcanic Landforms, Processes and Hazards*. International Association of Geomorphology (IAG) Working Group on Volcanic Geomorphology, *Zeitschrift für Geomorphologie*, Supplementbände vol. 140, 231p.
- Tibaldi, A. (2001) "Multiple sector collapses of Stromboli Volcano, Italy: How they work." *Bulletin Volcanologique*, 63, 112–25.
- Tilling, R. I. (2005) "Volcano hazards." In J. Martí and G. Ernst (eds.), *Volcanoes and the Environment*. Cambridge, Cambridge University Press, pp. 56–89.
- Tilling, R. I., Christiansen, R. L., Duffield, W. A., et al. (1987) "The 1972–1974 Mauna Ulu eruption, Kilauea Volcano: An example of quasi-steady-state magma transfer." In R. W. Decker, T. L. Wright and P. H. Stauffer (eds), *Volcanism in Hawai`i*. US Geological Survey Professional Paper 1350, 1, 405–69.
- Tilling, R. I., Topinka, L., and Swanson, D. (1990) *Eruptions of Mount St. Helens; Past, Present, and Future*. US Geological Survey General Interest Publication, 56p.
- Tolan, T. L., Reidel, S. P., Beeson, M. H., et al. (1989) "Revisions to the estimates of the areal extent and volume of the Columbia River Basalt Group." In S. P. Reidel and P. R. Hooper (eds.), *Volcanism and Tectonism in the Columbia River Flood-Basalt Province*, Geological Society of America Special Paper, 239, pp. 1–20.
- Tomkeieff, S. (1940) "The basalt flows of the Giant's Causeway district of Northern Ireland." *Bulletin Volcanologique*, 6, 89–143.
- Tootell, B. (1985) *All Four Engines Have Failed: The True and Triumphant Story of Flight BA009 and the Jakarta Incident*. London, Andre Deutsch Press.
- Trial, A. F. and Spera, F. J. (1990) "Mechanisms for the generation of compositional heterogeneities in magma chambers." *Geological Society of America Bulletin*, 353–67.
- Trusdell, F. A. and Lockwood, J. P. (2009) "Geologic Map of the Northeast Flank of Mauna Loa Volcano, Island of Hawai`i, Hawai`i." *Scientific Investigations Map 2932-A*, Washington, DC, US Geological Survey.
- Tsuya, H. (1955) "Geological and petrological studies of volcano Fuji. 5. On the 1707 eruption of volcano Fuji." *Bulletin of the Earthquake Research Institute of Japan*, 33, 341–83.
- Tsuya, H. and Morimoto, R. (1963) "Types of volcanic eruptions in Japan." *Bulletin Volcanologique*, 26, 209–22.
- Turner, J. S. (1986) "Turbulent entrainment: The development of the entrainment assumption and its application to geophysical flows." *Journal of Fluid Mechanics*, 173, 431–71.
- Turner, M. B., Cronin, S. J., Bebbington, M. S., et al. (2008) "Developing probabilistic eruption forecasts for dormant volcanoes: A case study from Mt Taranaki, New Zealand." *Bulletin of Volcanology*, 70, 4, 507–15.

- Ugolini, F. C., and Zasoski, R. J. (1979) "Soils derived from tephra." in D. Sheets, and D. K. Grayson (eds.), *Volcanism and Human Habitation*, New York, Academic Press, 83–124.
- Ui, T. (1983) "Volcanic dry avalanche deposits: Identification and comparison with nonvolcanic debris stream deposits." *Journal of Volcanology and Geothermal Research*, 18, 1, 135–50.
- Ulrich, G. E. (1987) "SP Mountain cinder cone and lava flow, northern Arizona." In S. S. Beus (ed.), *Centennial Field Guide*, vol. 2, Rocky Mountain Section of Geological Society of America Annual Meeting, Flagstaff, Arizona.
- Ulrich, K. and Sindern, S. (1998) "Nd and Sr isotope signatures of fenites from Oldoinyo Lengai, Tanzania, and the genetic relationships between nephelinites, phonolites, and carbonatites." *Journal of Petrology*, 39, 1997–2004.
- Urbanski, N.-A., Hort, M. and Schmincke, H.-U. (2003) "Changing eruption dynamics during the Plinian phase of the Minoan eruption, Santorini, Greece (3500 yr BP): Insight from stratigraphic variation of fall deposit and pumice texture." *Geophysical Research Abstracts*, Nice, France.
- Valentine, G. A. (1987) "Stratified flow in pyroclastic surges." *Bulletin of Volcanology*, 49, 616–30.
- Valentine, G. A. (1998) "Eruption column physics." In A. Freundt and M. Rosi (eds.), *From Tephra to Magma: Modelling Physical Processes of Explosive Volcanic Eruptions*. North Holland, Elsevier, 91–138.
- Valentine, G. A. and Fisher, R. V. (1986) "Origin of layer 1 deposits in ignimbrites." *Geology*, 14, 146–8.
- Valentine, G. A., Wohletz, K. H., and Kieffer, S. W. (1992) "Effects of topography on facies and compositional zonation in caldera-related ignimbrites." *Geological Society of America Bulletin*, 104, 154–65.
- Vallance, J. W., Siebert, L., Rose, W. I., Jr, et al. (1995) "Edifice collapse and related hazards in Guatemala." *Journal of Volcanology and Geothermal Research*, 66, 1–4, 337–55.
- Van der Pluijm, B. and Marshak, S. (2003) *Earth Structure: An Introduction to Structural Geology and Tectonics*. New York, W. W. Norton, 672 p.
- van Wyk de Vries, B., Self, S., Francis, P. W., et al. (2001) "A gravitational spreading origin for the Socompa debris avalanche." *Journal of Volcanology and Geothermal Research*, 105, 225–47.
- Veeder, G. J., Matson, D. L., Johnston, T. V., et al. (1994) "Io's heat flow from infrared radiometry: 1983–1993." *Journal of Geophysical Research, Planets*, 99, 17,095–162.
- Verbeek, R. D. M. (1885) *Krakatau*. Batavia, Dutch East Indies, Landsdrukkerij. [Republished in 1886 as *Krakatau*. Batavia, Dutch East Indies, Imprimerie de l'Etat.]
- Verhoogen, J. (1980) *Energetics of the Earth*. Washington, DC, National Academy of Sciences.
- Verplank, E. P. and Duncan, R. A. (1987) "Temporal variations in plate convergence and eruption rates in the western cascades." *Tectonics*, 6, 197–209.
- Vicenzi, E. P., McBirney, A. R., White, W. M., et al. (1990) "The geology and geochemistry of Isla Marchena, Galapagos Archipelago: An ocean island adjacent to a mid-ocean ridge." *Journal of Volcanology and Geothermal Research*, 40, 291–315.
- Viljoen, M. J. (1999) "The nature and origin of the Merensky Reef of the western Bushveld Complex based on geological facies and geological data." *South African Journal of Geology*, 102, 3, 221–39.
- Violette, S., de Marsily, G., Carbonnel, J. P., et al. (2001) "Can rainfall trigger volcanic eruptions? A mechanical stress model of an active volcano: 'Piton de la Fournaise', Reunion Island." *Terra Nova*, 13, 1, 18–24.
- Vitaliano, D. B. (1973) *Legends of the Earth*. Bloomington, Indiana University Press.
- Vitousek, P. M., Aplet, G. H., Raich, J. W., Lockwood, J. P. (1995) "Biological perspectives on Mauna Loa volcano: A model system for ecological research. *American Geophysical Union Geophysical Monograph* 92: 117–26.
- Vogfjörd, K. S., Jakobsdóttir, S. S., Gudmundsson, G. B., et al. (2005) "Forecasting and monitoring a subglacial eruption in Iceland." *American Geophysical Union – EOS*, 86, 245–8.

- Wada, K. and Aomine, S. (1973) "Soil development on volcanic material during the Quaternary." *Soil Science*, 116, 170–7.
- Wadge, G. (1982) "Steady-state volcanism: Evidence from eruption histories of polygenetic volcanoes." *Journal of Volcanology and Geothermal Research*, 87, 4035–49.
- Walker, G. P. L. (1967) "Thickness and viscosity of Etnean lavas." *Nature*, 213, 484–5.
- Walker, G. P. L. (1973) "Explosive volcanic eruptions: A new classification scheme." *Geologische Rundschau*, 62, 431–46.
- Walker, G. P. L. (1980) "The Taupo Pumice: Product of the most powerful known (Ultraplinian) eruption?" *Journal of Volcanology and Geothermal Research*, 8, 1, 69–94.
- Walker, G. P. L. (1983) "Ignimbrite types and ignimbrite problems." *Journal of Volcanology and Geothermal Research*, 17, 65–8.
- Walker, G. P. L. (1989) "Gravitational (density) controls on volcanism, magma chambers, and intrusions." *Australian Journal of Earth Sciences*, 36, 149–65.
- Walker, G. P. L. (2009) "The endogenous growth of pāhoehoe lava lobes and morphology of lava-rise edges." In T. Thordarson, S. Self, G. Larsen, S. K. Rowland and A. Hoskuldsson. London, Geological Society of London, 17–32.
- Walker, G. P. L. and Croasdale, R. (1972) "Characteristics of some basaltic pyroclastics." *Bulletin of Volcanology*, 35, 303–17.
- Walker, G. P. L., Wilson, C. J. N., and Froggart, P. C. (1980) "Fines-depleted ignimbrite in New Zealand: The product of a turbulent pyroclastic flow." *Geology*, 8, 245–9.
- Walter, T. R. and Troll, V. R. (2001) "Formation of caldera periphery faults: An experimental study." *Bulletin of Volcanology*, 63, 2–3, 191–203.
- Wark, D. A. and Watson, E. B. (2006) "TitaniumQ: a titanium-in-quartz geothermometer." *Contributions to Mineralogy and Petrology*, 152, 743–54.
- Wark, D. A., Hildreth, W., Spear, F. S., et al. (2007) "Pre-eruption recharge of the Bishop magma system." *Geology*, 35, 235–8.
- Watanabe, K. (1986) "Size composition of the Tosu orange pumice flow deposit from the Aso caldera." *Bulletin of the Volcanological Society of Japan*, 31, 299.
- Watson, E. B., Wark, D. A., and Thomas, J. B. (2006) "Crystallization thermometers for zircon and rutile." *Contributions to Mineralogy and Petrology*, 151, 413–33.
- Webb, P. K. and Weaver, S. D. (1975) "Trachyte shield volcanoes: A new volcanic form from south Turkana, Kenya." *Bulletin Volcanologique*, 39, 294–312.
- Wellman, P. (1989) "Upper mantle, crust, and geophysical volcanology of Eastern Australia." In R. W. Johnson (ed.), *Intraplate Volcanism in Eastern Australia and New Zealand*. Cambridge, Cambridge University Press, 29–37.
- Westervelt, W. D. (1963) *Hawaiian Legends of Volcanoes*. Rutland, Vermont, Charles E. Tuttle.
- Westgate, J. A. and Gorton, M. P. (1981) "Correlation techniques in tephra studies." In S. Self and R. S. J. Sparks (eds.), *Tephra Studies*. Dordrecht, Reidel, pp. 73–93.
- White, J. C. and Urbanczyk, K. M. (2001) "Origin of a silica-oversaturated quartz trachyte-rhyolite suite through combined crystal melting and fractional crystallization: The Leyva Canyon volcano, Trans-Pecos Magmatic Province, Texas." *Journal of Volcanology and Geothermal Research*, 111, 155–82.
- White, J. D. L. (1996) "Impure coolants and interaction dynamics of phreatomagmatic eruptions." *Journal of Volcanology and Geothermal Research*, 71, 155–70.
- White, J. D. L., Smellie, J. L., and Clague, D. A. (eds.) (2003) *Explosive Subaqueous Volcanism*. Washington, DC, American Geophysical Union.
- Wicks, C. W., Thatcher, W., Dzurisin, D., et al. (2006) "Uplift, thermal unrest and magma intrusion at Yellowstone caldera." *Nature*, 440, 72–5.

- Wiebe, R. A., Frey, H., and Hawkins, D. P. (2001) "Pillow mounds in the Vinalhaven intrusion, Maine." *Journal of Volcanology and Geothermal Research*, 107, 171–84.
- Wiesnet, D. R. and D'Aguanno, J. (1982) "Thermal imagery of Mount Erebus from the NOAA-6 satellite." *Antarctic Journal of the United States*, 17, 32–4.
- Wignall, P. (2005) "The link between large igneous province eruptions and mass extinctions." *Elements*, 1, 5, 293–7.
- Wilcox, R. E. (1965) *Volcanic-ash Chronology, in Quaternary of the United States*. Princeton, Princeton University Press, pp. 807–16.
- Wilhelms, D. E. (1993) *To a Rocky Moon: A Geologist's View of Lunar Exploration*, Tuscon, University of Arizona Press.
- Wilhelms, D. E., McCauley, J. F., and Trask, N. J. (1987) *The Geologic History of the Moon*. US Geological Survey Professional Paper 1348, Washington DC, USGS.
- Williams, H. (1941) *Calderas and their Origin*. Berkeley, University of California Press.
- Williams, H. (1942) *The Geology of Crater Lake National Park, Oregon, With a Reconnaissance of The Cascade Range South to Mount Shasta*. Carnegie Institute of Washington Publication, 540, 162p.
- Williams, H. and McBirney, A. R. (1979) *Volcanology*. San Francisco, Freeman Cooper.
- Williams, R. S., Jr and Friedman J. D. (1970) "Satellite observation of effusive volcanism." *Journal of the British Interplanetary Society*, 23, 441–50.
- Williams, R. S. and Moore, J. G. (1983) "Man against volcano: The eruption on Heimaey, Vestmannaeyjar, Iceland." Available at: <http://pubs.usgs.gov/gip/heimaey/>
- Williams-Jones, G. and Rymer, H. (2002) "Detecting volcanic eruption pre-cursors: A new method using gravity and deformation measurements." *Journal of Volcanology and Geothermal Research*, 113, 379–89.
- Wilshire, H. and Kirby, S. H. (1989) "Dikes, joints, and faults in the upper mantle." *Tectonophysics*, 23–31.
- Wilshire, H. G., Nielson, J. E. and Hazlett, R. W. (2008) *The American West at Risk: Science, Myths, and Politics of Land Abuse and Recovery*. Oxford, Oxford University Press.
- Wilson, C. J. N. (1985) "The Taupo eruption, New Zealand, 2; The Taupo ignimbrite." *Philosophical Transactions of the Royal Society of London*, A314, 229–310.
- Wilson, C. J. N. (1993) "Eruption columns." In J. McPhie (ed.) *Explosive Volcanism: Processes and Products, Commission on Explosive Volcanism Short Course*. 4.1–4.10.
- Wilson, C. J. N. (2001) "The 26.5 ka Oruanui eruption, New Zealand: An introduction and overview." *Journal of Volcanology and Geothermal Research*, 112, 133–74.
- Wilson, C. J. N. and Hildreth, W. (1997) "Hybrid fall deposit in the Bishop Tuff, California: A novel pyroclastic depositional mechanism." *Geology*, 26, 7–10.
- Wilson, C. J. N. and Hildreth, W. (2003) "Assembling an ignimbrite: Mechanical and thermal building blocks in the Bishop Tuff, California." *Journal of Geology*, 111, 635–70.
- Wilson, C. J. N., Blake, S., Charlier, B. L. A., et al. (2006) "The 26.5 ka Oruanui Eruption, Taupo Volcano, New Zealand: Development, characteristics, and evacuation of a large rhyolitic magma body." *Journal of Petrology*, 47, 35–69.
- Wilson, C. J. N., Houghton, B. F., McWilliams, M. O., et al. (1995) "Volcanic and structural evolution of Taupo Volcanic Zone, New Zealand: A review." *Journal of Volcanology and Geothermal Research*, 68, 1–28.
- Wilson, J. T. (1963) "A possible origin of the Hawaiian Islands." *Canadian Journal of Physics*, 41, 863–70.
- Wohletz, K. (1985) *Volcanic Ash*. Berkeley, University of California Press, 246p .

- Wohletz, K. H. (1998) "Pyroclastic surges and compressible two-phase flow." In A. Freundt and M. Rosi, (eds.), *From Magma to Tephra: Modelling Physical Processes of Explosive Volcanic Eruptions*. North Holland, Elsevier, pp. 247–312.
- Wohletz, K. H. (2003) "Water/magma interaction: Physical considerations for the deep submarine environment." In J. D. L. White, J. L. Smellie and D. A. Clague (eds), *Geophysical Monograph 140*, Washington, DC, American Geophysical Union, pp. 25–49.
- Wohletz, K. H. and Heiken, G. (1992) *Volcanology and Geothermal Energy*. Berkeley, University of California Press.
- Wohletz, K. H. and McQueen, R. G. (1984) "Experimental studies of hydromagmatic volcanism in explosive volcanism: Inception, evolution, and hazards." *Studies in Geophysics*, 158–69.
- Wohletz, K. H. and Sheridan, M. F. (1979) "A model of pyroclastic surge." Geological Society America, Special Paper, 180, 177–93.
- Wohletz, K. H., McGetchin, T. R., Sandford, M. T., II, et al. (1984) "Hydrodynamic aspects of caldera-forming eruptions: Numerical models." *Journal of Geophysical Research*, 89, 8269–85.
- WoldeGabriel, G., Heiken, G., White, T. D., et al. (2000) "Volcanism, tectonism, sedimentation, and the paleo anthropological record in the Ethiopian Rift System." In W. Floyd and G. H. McCoy (eds.), *Volcanic Hazards and Disasters in Human History*, Washington, DC, Geological Society of America, pp. 82–99.
- Wolf, T. (1878) "Geognostische Mittheilungen aus Ecuador Part 5, Der Cotopaxi und seine letzte Eruption am 26. Juni 1877." In G. Leonhard and H. B. Geinitz (eds.), *Neues Jahrbuch für Mineralogie, Geologie und Palaeontologie*. Stuttgart, E. Schweizerbart'sche Verlagsbuchhandlung, pp. 113–67.
- Wolfe, E. W. and Hoblitt, R. P. (1996) "Overview of the eruptions." In C. G. Newhall, and R. S. Punongbayan (eds.), *Fire and Mud – Eruptions and Lahars of Mount Pinatubo, Philippines*. Quezon City, Philippine Institute of Volcanology and Seismology and University of Washington Press, pp. 3–20.
- Woo, G. (2008) "Probabilistic criteria for volcano evacuation decisions." *Natural Hazards*, 45, 87–97.
- Wood, C. (2009) *World Heritage Volcanoes: Global Review of Volcanic World Heritage Prospects: Present Situation, Future Prospects, and Management Requirements*. International Union for the Conservation of Nature World Heritage Studies No 8, 62p.
- Wood, C. A. (1980) "Morphometric evolution of cinder cones." *Journal of Volcanology and Geothermal Research*, 7, 387–413.
- Woods, A. W. (1988) "A fluid dynamics and thermodynamics of eruption columns." *Bulletin of Volcanology*, 50, 169–93.
- Woods, A. W. (1995) "The dynamics of explosive volcanic eruptions." *Reviews of Geophysics*, 33, 495–530.
- Wooley, A. R. and Church, A. A. (2005) "Known occurrences of carbonatites." *Lithos*, 85, 1–14.
- Wooster, R. J. and Rothery, D. A. (1997) "Thermal monitoring of Lascar volcano, northern Chile, using infrared data at high temporal resolution: A 1992 to 1995 time-series using the along-track scanning radiometer." *Buletin Volcanologique*, 58, 566–79.
- Workman, W. B. (1979) "The significance of volcanism in the prehistory of subarctic northwest North America." In P. D. Sheets and D. K. Grayson (eds.), *Volcanic Activity and Human Ecology*, New York, Academic Press, pp. 339–71.
- Wright, J. V. (1981) "The Rio Caliente ignimbrite: Analysis of a compound intraplinian ignimbrite from a major late Quaternary Mexican eruption." *Bulletin Volcanologique*, 44, 189–212.
- Wright, J. V. and Walker, G. P. L. (1977) "The ignimbrite source problem: Significance of a co-ignimbrite lag-fall deposit." *Geology*, 5, 729–32.

- Wright, T. L., Mangan, M., and Swanson, D. A. (1989) "Chemical data for flows and feeder dikes of the Yakima Basalt Subgroup, Columbia River Basalt Group, Washington, Oregon, and Idaho, and their bearing on a petrogenic model." *US Geological Survey Bulletin* 1821, 71p.
- Wyllie, P. J. and Huang, W. L. (1976) "High CO₂ solubilities in mantle magmas." *Geology*, 4, 21–44.
- Yamagishi, H. (1985) "Growth of pillow lobes: Evidence from pillow lavas of Hokkaido, Japan and North Island, New Zealand." *Geology*, 13, 499–502.
- Yamashita, S. (1999) "Experimental study of the effect of temperature on water solubility on natural rhyolite melt to 100 MPa." *Journal of Petrology*, 40, 1497–507.
- Yokoyama, I. (1981) "A geophysical interpretation of the Krakatau eruption." *Journal of Volcanology and Geothermal Research*, 9, 359–78.
- Young, D. (2003) *Mind over Magma: The Story of Igneous Petrology*. Princeton University Press, 704p.
- Yürür, M. T. and Chorowicz, J. (1998) "Recent volcanism, tectonics, and plate tectonics near the junction of the African, Arabian, and Anatolian plates in the eastern Mediterranean." *Journal of Volcanology and Geothermal Research*, 85, 1–15.
- Zimanowski, B., Wohletz, K., Dellino, P., et al. (2003) "The volcanic ash problem." *Journal of Volcanology and Geothermal Research*, 12, 1–2, 1–5.
- Zimbelman, J. R. (2000) "Volcanism on Mars." In H. Sigurdsson (ed.), *Encyclopedia of Volcanoes*, San Diego, Academic Press, pp. 771–83.
- Zimbelman, J. R. and Gregg, K. P. (2000) *Environmental Effects of Volcanic Eruptions*, Berlin: Springer Verlag.
- Zimbelman, J. R. and Gregg, T. K. P. (eds.) (2008) *Environmental Effects on Volcanic Eruptions: From Deep Oceans to Deep Space*, Dordrecht, Kluwer Academic/Plenum.
- Zlotnicki, J., Ruegg, J. C., Bacheley, P., et al. (1990) "Eruptive mechanism on Piton de la Fournaise volcano associated with the December 4, 1983, and January 18, 1984 eruptions from ground deformation monitoring and photogrammetric surveys." *Journal of Volcanology and Geothermal Research*, 40, 197–217.

Index

Page numbers given in *italics* refer to figures and figure captions, those in **bold** to boxes and tables. Standard US abbreviations for states have been used, e.g. CA for California.

- `a`a flows, 25, 136, 138, *166, 167, 278*, 326, 440
 - charcoal beneath, *171*
 - different names for, 136
 - extraterrestrial, 385
 - joints, *161*
 - and pāhoehoe, 135–8, *137, 152, 164–5*
 - surface structures, *162–5, 167*
 - vesicles, 156, *160*
 - see also* lava flows
- Absaroka Range, North America, 422
- accretionary lava balls, 151–2, *153*
- aeolian differentiation, 182
- aerosols, 401–3
- Afar hot spot, northeast Africa, 63, **268**
- Afar region, Ethiopia, 52
- African Plate, 62
- agglomerate, 180, 182
- Alaskan peninsula, 59, 318, 327
 - volcanic output, **59**
 - see also individual volcanoes*
- Alba Patera, Mars, 385
- alchemy, 30
- Aleutian Trench, 61
- Aleutian volcanic arc, Alaska, 59, 60, 327, *332*
- alkalic basalts, 74, 76, 99
- Alpine–Tethys collision zone, 53–4
- Alps, Europe, 99
- Ambrym, Vanuatu, 276, 540
- Amirani volcano, Io, 389
- Armero, Colombia, destruction of, 349, *349, 356–7, 413–14*
- amygdules, 160
- Anatahan Island, N. Marianas, 297
- Andean Southern Volcanic Zone, South America, 58, **59**
- Anderson, E. M., 331–335
- Anderson, Tempest, 35, **141**
- andesites, 24, 73, 74–5, 94, **94**, *168, 278, 301, 325*
- andosols, 407: *see also* soil fertility
- Aniakchak Tuff, Alaska, 242, 249, 540
 - caldera, 454
- Anjer, Indonesia, 420–1
- Antarctica, 53, 371–2
- antithetic faulting, *330, 331*
- Appalachian Mountains, USA, 46
- Apua Point, Hawai`i, *143*
- arc magmatism, episodicity, 59–60
 - see also* volcanic arcs
- arc–trench gap, 50
- Arizona, USA, 213
- Asama volcano, Japan, 38, 540
- Asayama Physics Research Laboratory, Japan, 38
- ascent rate, magma, 94–6, 95
- ascent rate, Plinian columns, 228–9
- ash *see* volcanic ash
- ash cones, 296–8, 298
 - see also* tuff cones
- ash-flow tuffs, 207, *337*: *see also*
 - pyroclastic density currents
- ash plumes, 225, 246–9, *248, 250*

- Askja, Iceland, 540
 1870 eruption, 122, 261
- Aso caldera, Japan, 184, 331, 540
- aspect ratios, 249
- asphalt volcanoes, 24
- atmosphere
 Earth, 397–8, 402–3
 composition of, 85, 397
 oxygen, 167
 ozone, 84
 other planets, 381, 383–4, 385, 387–8
see also carbon dioxide
- Augustine volcano, Alaska, 107, 540
- Australian volcanoes, 61–2, 278–9:
see also individual volcanoes
- autobreccias, 162, 214
- avalanches, volcanic, 342–7
 debris, 344, 345, 346–7, 418
 deposits, 342, 344
 and rainfall, 347, 351
 speeds, 345
 triggers, 342, 346–7
see also lahars; landslides
- aviation, risks, 8, 417, 453
- Azores, 200, 364
- Bachelor Mountain, CO, 211–12
- Bandai volcano, 190
 volcanic history, 190
- Bandelier Tuff, NM, 213, 215, 246
- Barcena volcano, Mexico, 540
 1952–3 eruption, 251, 253
- basalt, 72–4, 73, 75, 475
 alkalic, 62, 74, 76, 96, 99, 280
 flood *see* Large Igneous Provinces (LIPs)
 lava, 188: *see also* lava flows
 magma, 71, 72–3, 213
 tholeiitic, 52, 73, 280, 382
 viscosity, 94, **94**
- base surge, 251–2
- batholiths, 25, 54, 100, 336
- Battleship Rock, NM, 211
- bauxite, 181
- Bequerel, Henri, 67
- Bezymianny volcano, Kamchatka, 303,
 540
 1956 eruption, 37, 256
- Bible, the
 interpretations, 20–1
 as source of legend, 28–9, 31
- Big Pine volcanic field, CA, 312
- Bikini Atoll, Pacific Ocean, 251
- Billy Mitchell volcano, Solomon
 Islands, 124
- Bingham bodies, 243
- biogeochemical cycles, 398–9, 400
- biovolcanology, 397–8
- Bishop, Rev. Sereno, 404–5
- Bishop's ring phenomena, 405
- Bishop Tuff, CA, 90, 182, 210–12, 327
 Owens Gorge ignimbrite, 211, 212
 Sherwin Grade ignimbrite, 215
- Bismarck Sea, Papua New Guinea, 330
- blast pits, 168, 190: *see also* directed
 blast eruptions
- block lavas, 166
- block and ash flows, *see* pyroclastic
 flows
- Bolshoye Tol'batchik volcano,
 Kamchatka, 177
- bombs, volcanic, 176–8, 177, 292, 293
 breadcrust, 176, 177
 "cow-pie", 177
 spindle, 177
see also ejecta, volcanic
- bomb sags, 177, 178, 178
- Boulding, Kenneth, 398
- Bowen, Norman L. (1887–1956),
 69–71, 73
- Bowen's Reaction Series, 69–70, 169
- breadcrust bombs, 176, 177
- breccias, 179, 246: *see also* autobreccias
- Brigham, William T. **141**
- bromine, *see* halogen gases
- Brothers volcano, New Zealand, 476,
 540
- Buch, Christian Leopold von
 (1774–1853), 31, 321
- Buffon, Comte de (1707–88), 67, 68
- Bushveld Complex, South Africa,
 471–2
- calcite (CaCO₃), 77, 101
- calderas, 27, 55, 57, 58, 208, 321–9
 classification, 322
 collapse, **118**, 185, 323–4, 327, 335
 definition, 321
 drainage, 322–4
 explosive, 322, 324–9
 formation mechanisms, 335–6
 lakes, 353: *see also* crater lakes
 moat, 332
 nested, 328
 and plutonism, 336
 resurgent, 331–4, 334
 silicic, 75, 260, 261, 322, 325, 326,
 336, 337, 369
 submarine, 369: *see also* submarine
 volcanism
 types, 335
see also subcaldera intrusions;
individual calderas
- Cameroon "killer lakes", 442
- Cameroon Line, West Africa, 62, 62
- Campi Flegrei volcano, Italy, 475–6,
 540
- Canary Islands, 214, 285
- Capelinhos volcano, Azores,
 1957–8 eruption, 200, 540
- carbonatites, 76–7
- carbon cycle, 399–401
 volcanic input, 399, 400
- carbon dioxide (CO₂), 77–8, **80**, 81–2,
 202, 398, 399–401
 absorption by seawater, 399
 as driver for eruptions, 173, 370
 and forest soils, 81–2
 as hazard, 62, 418, 421–4, 424, 442
 human production, 85
 maars, 321
 magmatic, 424
 mofettes *see* mofettes
 monitoring, 441
 solubility, 83
 and subduction, 81
 on Triton, 391–2
 on Venus, 381
 from volcanic arcs and hot spots, 81
see also volcanic gases
- carbon isotopes, 170
- carbon monoxide (CO), **80**, 82

- Caribbean Basin, 33, 48, **268**
- Caribbean rim eruptions *see individual Caribbean volcanoes*
- Carnegie Institution, Washington DC, 36, 69
- Cascade Range, North America, 54–6, 55, 57, 58–9, 325
- ash deposits, 181
 - composition, 55
 - eruptions, 55
 - productivity, 59, **59**
 - lahars, 352–3
 - location, 55
 - magma reservoirs, 98
 - shields, 273, 278
 - spacing, 55–6
 - see also individual volcanoes*
- Casita volcano, Nicaragua, 346–7, 352, 540
- Cassini spacecraft, 388, 391, 392
- Catania, Italy, 438–9
- Catania Institute of Volcanology, 37
- Central American volcano arc, 56
- volcanic output, **59**
- Central Kamchatka Depression, 58, 58
- Chaîne des Puys, France, 53, 99
- Chaitén volcano, Chile, 416, 540
- Chaos Jumbles, CA, 304
- charcoal, 170, 171, 171
- Charon, moon of Pluto, 391
- Chicxulub meteor impact, 406
- Chief Joseph Dike Swarm, OR, 135
- chlorine *see* halogen gases
- Chocoyos Ash, Guatemala, 213; *see also* Los Chocoyos, Guatemala
- Cibanjuran River, Indonesia, 8, 8, 358
- Cikunir River, Indonesia, 8, 11, 13
- cinder cones, 27, 63, 99, 134, 290–6, 291, 292, 298
- craters, 290–2, 326
 - erosion, 312, 312
 - formation, 293
 - profile, 312
 - vents, 294
 - see also* ash cones; littoral cones; tuff cones
- Clark Air Force Base, Philippines, 107, 434, 435
- classification, eruption types, 113–23
- classification, magma and volcanic rocks, 72–3, 73
- climate change, 259, 403–4, 405, 418, 426, 444
- climatic influence of volcanoes, 398–405
- Cloos, Hans, 102
- coal, 31, 85
- Coan, Rev. Titus, 32, 138–40, **141**
- co-ignimbrites, 193, 195, 196, 209, 246–9
- ash plumes, 225, 246–7, 248
 - clouds, 225
 - see also* ignimbrites
- Colombia Geological Survey, 458
- Columbia River Plain, USA, 50, 163, 181, 267, **268**, 268–9, 405–6
- see also* Yellowstone National Park
- Columbia River Basalt Province, WA, 135, 136, 157, 213, 267
- columnar jointing, 101, 103, 160–2, 162
- composite volcanoes, 5, 6–16, 21, 22, 51, 97, 116, 173, 283–90
- erosion, 309, 309–10, 341
 - eruptive histories, 283, 289
 - hazards, 416
 - height, 286
 - structure, 284, 286–7
 - vents, 288
- cones, volcanic, 290–300: *see also* cinder cones; tuff cones
- cone sheets, 100, 101, 330, 331
- continental arcs, 51: *see also* volcanic arcs
- continental drift theory, 47, 47: *see also* plate tectonics
- convection, 68, 70
- coronet explosions, 304
- COSPEC monitoring, 453
- Cotopaxi, Ecuador, 357, 432, 540
- 1877 eruption, 242
- crater lakes, 201, 203, 321, 325, 353–4, 426
- eruptions, 353–4, 424–5
 - lahars, 353
 - see also* calderas; *individual crater lakes*
- Crater Lake, OR, 321, 325, 540
- caldera, 75, 325, 325–6, 326, 334
- Crater Lake National Park, OR, 57, 166, 215
- Wizard Island, 326, 326
- Craters of the Moon National Monument, ID, 270
- cryptodomes, 300
- cryptovolcanism, 362, 391
- crystalline structure of rock, 68–70, 69, 76
- crystallization
- vapor-phase, 214–15
 - at Kilauea Iki, 132
- Czech Republic, 99
- dacites, 75, **471**, 475
- dams, 436–7, 437
- Dana, James D. (1813–95), 32, 32, 138, 140, **141**
- Daly, Reginald A., 36, 149
- Deccan Traps, India, 405, 406
- Deccan Volcanic Province, India, **268**, 270
- Deception Island, Antarctica, 372, 540
- Decker, Robert, 123, 289, 443
- Devil's Postpile National Monument, CA, 162
- Devil's Tower volcanic neck, WY, 100, 101
- Diamond Head (Leahi), Hawai'i, 296
- diatremes, 53, 101–2
- Dieng Plateau, Indonesia, 422, 424, 540
- dikes *see* lava dikes
- dimethylsulfide (DMS), 401–2
- and phytoplankton, 401, 402
- directed-blast eruptions, 199, **219**, 236–7, 252, 255–8, 346
- case history, Mount St Helens, 256–8, 258
- domes, *see* volcanic domes
- Dunedin shield, New Zealand, 279–80
- Dutton, Clarence Edward, **141**
- Dvorak, John, 9–10

- Earth
 age of, 67
 atmosphere *see under* atmosphere
 crustal structure, 48, 48, 50, 384
 asthenosphere, 48, 50
 lithosphere, 48, 50, 53, 55, 273
 mantle, 71: *see also* mantle plumes;
 xenoliths
 tectonic plates, 49, 60, 63: *see also*
 continental drift theory;
 melting of rock, plate
 tectonics
 compared with other planets, 383–5
 core–mantle boundary, 61, 68
 formation and early history, 66–7,
 68–9, 384, 397
 cooling of interior, calculations for,
 67
 magnetic field, 46
 mantle–crust boundary, 94–5, 96
 moon *see* Moon, the
 “spaceship”, 398, 401
 sources of heat, 66–8, 66, 67, 67–8
 geothermal *see* geothermal energy
see also radiogenic decay
 stratosphere, 402
 tides *see* tides
 earthquakes, 38, 95–6, 342, 418, 455,
 456, 467, 467
 and landslides, 343
 precursor to volcanic eruptions, 8,
 13, 19, 20, 33, 55, 198, 256,
 305–6, 330, 342, 458
 and sector collapse, 342, 418
 shock waves, 92, 95
 teleseisms, 38
 trigger to lahars, 346, 347, 350–1:
see also lahars
 and tsunami, 418, 419
 types, 38
 volcanic *see* volcanic earthquakes
see also seismic monitoring
 East African Rift Zone, 52, 63, 77,
 407–8, 423
 history, 407–8
 East Pacific Rise, 52, 363, 364, 365
 economic volcanology, 465–77
 energy *see* geothermal energy
 mineral ores *see* ore deposits
 effusive eruptions, 128–71
 flood-basalt, 135–6, 161–2, 162,
 213, 267
see also under Large Igneous
 Provinces
 Hawaiian-type, 128–32, 130, 186,
 235
 Strombolian-type, 133–4, 176, 202,
 235, 277, 280, 296, 370
 Egmont volcano, New Zealand *see*
 Mt Taranaki
 Eifel volcanic field, Germany, 99, 208
 ejecta, volcanic, 174–219
 accidental, 200
 ash *see* volcanic ash
 ballistic, 175–9
 buoyancy, 224, 228, 228, 229:
see also eruption columns
 classification, 174–5
 and eruption magnitude, 224
 sorting, 187–8, 245
 hydroexplosive, 273
 shape and size, 174–5, 175
 tephra, definition of, 174
 vesicular, 184, 188
see also pyroclastic deposits; vulcanian
 deposits
 Elbrus, Russia, 54, 540
 El Chichón volcano, Mexico, 252–3,
 286, 415, 415, 540
 1982 eruption, 252, 253, 405
 Eldgjá–Laki ice age eruption, 375
 Eldgjá volcano, Iceland, 540
 934 eruption, 135, 402–3
 Electronic Distance Measurement
 (EDM), 450
 at Galunggung, 13, 15
 instruments, 9–11, 13, 15, 16, 16,
 450
 at Kilauea, 16
 Elephant Back, Yellowstone, WY, 168
 El Misti volcano, Peru, 344, 540
 Enceladus, moon of Saturn, 379, 391
 endogenous domes, 300
 energy, thermal *see under* volcanic energy
 erosion, 54, 281, 309, 309–14, 311
 cinder cones, 312, 312, 313
 composite volcanoes, 309–10, 341
 extraterrestrial, 386
 glacial *see* glaciation
 lava flows, 312, 313
 shield volcanoes, 311–12
 Erta Ale, Ethiopia, 52, 80, 540
 eruptions *see* volcanic eruptions
 eruption columns, 178, 180, 188, 193,
 225, 233, 234–5, 398
 ascent rate, 228–9, 230
 axial displacement, 230
 buoyancy, 226–8, 228
 collapse, 198, 234–5, 234
 definition, 188
 extraterrestrial, 390
 magma, 185
 Plinian *see under* Plinian eruptions
 rate of ascent, 228
 temperature, 226, 228, 229, 257
 umbrella region, 193, 195, 227, 228,
 228, 229, 231
 water vapor content, 228, 234, 236
 eruption diagrams, 37, 118, 119
 eruption intensity, 231–2
 and magnitude, 232, 233
 eruption triggers, 105–8
 Ethiopian plateau, 270
 event trees, 430–1, 430
 explosive eruptions, 173–219, 223–61
 hydrovolcanic *see* hydrovolcanic
 eruptions
 measuring magnitude, 223, 224
 products, 173–219
 processes, 225–
 submarine, 367–70
 deep water, 369–70
 shallow, 367–9
 Super-eruptions *see* Super-eruptions
 volatiles, 173
 Plinian-type *see* Plinian eruptions
 Vulcanian *see* Vulcanian eruptions
see also pyroclastic deposits; volcanic
 ash; Volcanic Explosivity
 Index

- extraterrestrial volcanoes, vii, 377–92
 compared with Earth, 379, **379**
see also individual planets
- eyewitness accounts
 Cotopaxi 1877, 242
 Galunggung 1983, 6–16
 El Chichón 1982, 253
 Krakatau 1883, 421
 Kīlauea 1974, 19–21
 Mauna Loa 1975, 165
 Mount St Helens 1980, 256, 257
 Mt Lamington 1951, 242
 Mt Pelée 1929–32, 241–2
 Paricutín 1943, 295–6
 Ruiz 1985, 356–7
 Vesuvius 79 CE, 198
 Vulcano 1888, 191–2
- farra, 382
- Faujas de Saint-Fond, Barthelemy
 (1741–1819)
- Fedotov, S. A., 123
- feldspar, 169, 215
- Ferdinandea, Italy, 367–8, 368
- Fernandina volcano, Galápagos Islands,
 322, 540
 caldera, 454
- fiamme, 210–11
- Fish Canyon Tuff, CO, 259, 328–9
see also La Garita caldera, CO
- Fisher Caldera, Alaska, 327, 540
 pre-caldera volcanism, 328
 eighth century BCE eruption, 328
 resurgence, 333, 334
 volcanic field, 333
- fisheries, 407
- flood-basalt provinces *see under*
 Large Igneous Provinces
 (LIPs)
- flow head elutriation jets, 245–6
- fluid behavior, 354–5
 criticality, 355, 356, 357, 370
see also lahars; Newtonian fluids;
 non-Newtonian fluids;
 water (H₂O)
- fluorine *see* halogen gases
- foidite, 73
- forsterite (magnesian olivine), 69
- fossils, 31, 157, 159
- Fouqué, Ferdinand, 301–2
- Friedlander, Immanuel, 37
- Froude numbers (*Fr*), 355
- Fuego volcano, Guatemala, 107, 540
- Fukazawa Mine, Japan, 477
- fumaroles, 81, 82, 83, 84–5, 473
 long-lasting 84–5
 temporary, 85
see also mofettes
- Galápagos Islands, 322, 366, 367–8
 calderas, 280
 hot spot, 280
 lavas, 280
 tectonic structure, 280
 shields, 280–1, 280
 compared with Icelandic, 280–1
- Galileo Galilei, 386
- Galileo Orbiter spacecraft, 388, 389, 390
- Galunggung (Indonesia), 8, 10, 204,
 417, 540
 1982 eruption, 6–16, 178, 183, 183
 ash clouds, 8–9, 417
 eruption column, 194, 228
 geodetic survey stations, 8, 10
 lahars, 348, 358
 lightning activity, 10, 417
 refugees, 7, 8, 10, 12, 15, 434–4
 sector collapse, 346
 tephra fall, 351, 434–4, 436
- Gamalama volcano, Indonesia, 540
 1980 eruption, 107, 177–8, 177, 178
- Gangetic Plain, India, 63
- gases *see* volcanic gases
- geognosic theory of geology, 30–1
- Geological Society of America, 35, 347
- geophysical monitoring, 451–2: *see also*
 seismic monitoring; volcano
 monitoring
- geothermal energy, 317, 467–9, 468
 direct-use applications, 469–70
- geothermobarometry, 70, 89–90, **90**
- geysers, 473
- Geysers field, CA, 468
- Geze classification diagram, 119, 120
- glaciation, 162, 325, 352: *see also*
 erosion
- Glacier Peak volcano, WA, 182, 540
- glaciers, 68, 168, 254–5, 352, 371–7,
 378
 continental, 371–2
 Icelandic, 371, 374
- glaciovolcanism, 361, 371–4, 378
- glass *see* volcanic glass
- Glasshouse Mountains, Queensland,
 Australia, 62
- Glass Mountain, Medicine Lake, CA,
 169, 278, 327
- Glicken, Harry, ii, 241
- Goethe, Johann Wolfgang von
 (1749–1832), 31, 65
- Goma, Democratic Republic of Congo,
 138, 416
- Goosenest volcano, CA, 56, 278
- Gorelli volcano, Kamchatka, 374, 540
- Gorshkov, Georgii S. (1921–75), 37, 37
- GPS (Global Positioning Satellite), 450
- grabens, 52–3, 99, 383
- Graham Island, 367–8, 368
- gravitational fractional crystallization, 70
- Great Dividing Range, Australia, 61–2
 hot spot, 61–2
 shield volcanoes, 278
- Great Basin, USA, 267
- Great Rift Valley, E. Africa, 279
- Great Plains, USA, 182
- Greek legends, 29
- greenhouse gases, 399: *see also* carbon
 dioxide; methane
- Greenland, 99
- “grey” volcanoes, 5–16: *see also*
 composite volcanoes;
 explosive eruptions
- Grímsvötn volcano, Iceland, 540
 1996 eruption, 372
 2003–4 activity, 372–3, 373
- Guatemala, 347: *see also individual*
Guatemala volcanoes
- Guettard, Jean-Etienne (1715–86), 30
- Gulf of Aden, 63
- Guadeloupe, 457
- guyots, 46: *see also* seamounts

- Hakone, Japan, 289, 540
- Haleakala Crater, Hawai'i, 293, 540
- Halema'uma'u crater, Hawai'i, 18, 26, 78, 133
- halogen gases, 82–3
 reaction with water vapor, 82, 85
 deposition of chlorides, 85
- Hamilton, Sir William, 164
- Hangay region, central Mongolia, 63
- Harar plateau, Ethiopia, 270
- harmonic tremor, 447–8, **448**
- Harzburgite, 73
- Hasan Dagi, Turkey, 408, 540
- Hawai'i, 61
 curtains of fire, 21, 128–9
 lava flows, 155, 167, 363–4
 shield volcanoes, 271–5, 273, 275
 eruptions, 273, 274
 lava flows, 274
 pit craters, 319
 profiles, 274
 rift zones, 273
 volcanic history, 74, 127, 291
see also individual volcanoes
- Hawaiian–Emperor volcanic chain, 61, 62, 62
 radiometric dating, 61
- Hawaiian “hot spot”, 61, 63
- Hawaiian Islands *see* Hawai'i
- Hawaiian shield volcanoes *see under* Hawai'i
- Hawaiian Volcano Observatory (HVO), 9, 16, 17, 35, 38, 107, 446
- Heimaey Island, Iceland, 440, 441, 442
- Hekla volcano, Iceland, 99 286, 453, 540
 1947 eruption, 196
 1970 eruption, 121–2
- helium, 81, 84
- Henry's Law, 79–80
- Hephaestus, god of metal and armor, 29–30, 29, 30
- Hess, Harry H. (1906–69), 46, 46, 47–8, 50, 366
see also plate tectonics
- Himalayas, Asia, 63
- Holmes, Sir Arthur (1890–1965), 47, 68
- Home Reef volcano, Tona, 369, 369, 540
- “hot spots,” 61–3, 267–8
 Pacific Ocean, 61, 61
 seismic studies, 62
 Venus, 383
see also intraplate volcanoes, 540
- Hualali volcano, Hawai'i, 291
- Huaynaputina volcano, Peru, 1600
 eruption, 403–4
- Huila volcano, Colombia, 351
- humanistic geology, 35
- humanistic volcanology, viii, 22, 395, 480
- Hunga Ha'apai, Tonga, 201
- Hurricane Mitch, 1998, 347
- Hutton, James (1726–97), 31, 45, 432–3
- HVO (Hawaiian Volcano Observatory), 16, 446
- hyaloclastite, 269, 272, 273, 378
- hydrochloric acid (HCl), **80**, 82–3
- hydroelectricity, 468
- hydrofluoric acid (HF), **80**, 82–3
- hydrogen, **80**, 398
- hydrogen sulfide (H₂S), **80**, 83, 85, 202, 401
- hydrovolcanic eruptions, 25, 199–204, 201, **235**, 252, 273, 298
see also pyroclastic surges; water (H₂O)
- hypabyssal rocks, 25
- hyperconcentrated flows, 347–8, 358:
see also lahars
- ice ages, 182, 375, 399: *see also* glaciation
- Iceland, 52, 181, 271, 318
 eighteenth-century field studies, 138
 hot spot, 63
 flood-basalt eruptions, 135
 glaciers, 372, 375–6, 378
 shield volcanoes, 273, 275–6
 submarine volcanism, 201, 361
see also individual volcanoes
- Idaho, USA, 168
see also Yellowstone–Snake River Plain, ID
- igneous rocks, 24–5, 45, 52
 classification, 72–3, 73
 felsic, 73, 475
 plugs, 100
 plutonic, 72, 100
 volcanic, 72–3, 74
- ignimbrites, 205, 207, 208–9 208, 210, 246, 246, 254, 276
 aspect ratios, 249, 250, 251
 colour, 213
 mineralization, 214–16
 rheomorphic, 213–14
 welding, 210, 212, 213, 214
see also pyroclastic flows
- Iliamna volcano, Alaska, 310, 540
- Ilopango volcano, El Salvador, 407, 408, 411, 540
- Indian subcontinent, 63
 plate collision, 63
- Indonesia, 38
- Indonesian volcanic arc, 56
- inert gases, 84
- inflation pits, 151, 152
- intensity, eruption, 123, 224
- International Association of Volcanology and Chemistry of the Earth's Interior (IAVCEI), 37
- International Civil Aviation Organization (ICAO), 417
- International Union of Geological Sciences (IUGS), 73
- intraplate volcanoes, 51, 60–3, 62, 367
- Io, moon of Jupiter, **379**, 386–90, 390
 atmospheric conditions, 387–8
 eruption columns, 390
 lithosphere, 390
 plate tectonics, 390
 surface temperature, 388–9
 tides, 387
 volcanic activity, 388, 389
 volcanoes, 388–9
- island arcs, 46, 51, 369
see also volcanic arcs; volcanic islands
- Isle of Mull, 330, 331
- isopach mapping, 119–20, 230
- isopleth mapping, 224

- Italy, effect of Vesuvius eruption, 409–10
- Izu-Ogasawara Ridge, Pacific Ocean, 368
- Jaggard, Thomas, viii, 34–5, 35, 36, 45–6, 136, **141**, 302, 422, 445, 480
and Japan, 38
- Japan, 38
ore deposits, 475
volcanic output, **59**: *see also individual volcanoes*
- Java, Indonesia, 6–16, **268**
- Jemez caldera, NM, 333, 334
- Johnston, David, ii, 256–7
- jökulhlaups, 372, 373
- Joya de Cerén, El Salvador, 411
- Jupiter, vii, 386
moons, 386–7: *see also* Io, moon of Jupiter
- Kagoshima volcano-tectonic depression, 338, 338
- Kaiserstuhl volcano, Germany, 52
- Kamchatka, Russia, 56–7, 374
volcanic arcs, 24, 37, 56–9, 58, 58, 60
see also individual volcanoes
- Katmai volcano, Alaska, 540
1912 eruption, 328, 331, 407, 467
Valley of Ten Thousand Smokes, 243, 249, 328
- Keanakako`i, Hawai`i, 19–20
- Kelut volcano, Indonesia, 353, 442, 540
- Kelvin, Lord, 67
- Kidd mine, Canada, 476
- Kilauea, Hawai`i, viii, 16–22, 35, **80**, 109, 456, 540
Aloi Crater, 155
caldera, 97, 131
dike formation, 104
East Rift Zone, 17, 96, 116, 130, 143, 146, 295, 402
eruptions
1841, 32, 139
1924, 183
1955, 439
1959, 131
1960, 200, 439, 440
1969, 177, 186
1974, 6, 19–22, 21
1983, 116, 439
faulting, 275, 275,
Halema`uma`u lava lake, 18, 26, 133, 402
Kazamura Cave, 143, 144–5
Keanakako`i crater, 21
Koko`olau Crater, 20
Kupaianaha vent, 154
lava flows, 90, 149, 150, 273
magma ascent, 95–7, **97**
magma chamber, 96, **97**
Mauna Ulu vent *see* Mauna Ulu, Kilauea
Pu`u O`o vent, 116, 402
south flank, 275, 365
Southwest Rift Zone, 104, 163
volcanic history, 16, 28, 36, 107, 403
- Kilauea Iki crater, 131–2
lava lake, 131, 132, 161
- kipuka, 155, 156
- Klyuchevskoi volcano, Kamchatka, 376, 540
- Klyuchevskoi–Shiveluch volcano
complex, Kamchatka, 57, 58, **80**, 286, 287
- Koko Head tuff cone, Hawai`i, 204, 254
- Koolau volcano, Hawai`i, 274
- Koryaksky volcano, Kamchatka, 310, 540
- Kos volcano, Aegean sea, 185, 540
- Krafla volcano, Iceland, 99, 540
- Krafft, Maurice and Katia, ii, 241
- Krakatau (Krakatoa) volcano, Indonesia, 421, 540
1883 eruption, 59, 184, 259, 328, 404
caldera collapse, 421
death toll, 9
eruption column, 420, 193,
global effects, 36, 181, 404, 418
tsunami, 33, 420–1
VEI, **124**
- location, 8
see also Rakata volcano, Indonesia
- Kronotsky National Park, Kamchatka, 57
- Kronotsky volcano, Kamchatka, 23, 26, 286, 540
- Kuril volcanic arc, Russia/Japan, 60
- Kuwae volcano, Vanuatu, 1452
eruption, **124**
- Laacher See, Germany, 208, 209
13 000 BP eruption, 208, 209
maar, 321
- laccoliths, 105
- Lacroix classification system, 117–18, **118**, **121**, 125
- Lacroix, François-Antoine Alfred (1863–1948), 33–4, 34, 117, 119, 128, 302–3
- La Garita caldera, CO, 328–9, 335
and Fish Canyon Tuff *see* Fish Canyon Tuff, CO
Super-eruption, 259
- La Garroxta volcanic field, 99
- lahars, 8, 11–12, 284, 288, 289, 313, 341, 342, 347–58
causes, 311, **348**, 350–8
definition, 347
deposits, 285, 288, 349, 358
destructiveness, 347, 349, 356–8, 418, 436
dynamics, 354–6
as fluids, 354–7
hazard, 8, 11–12, 288, 435–7:
see also risk mitigation;
volcanic hazards
hyperconcentrated flows, 347, 348, 349, 355, 356, 357
triggers, 347
volume, 348
- Lake Atitlan caldera, Guatemala, 213
- Lake Monoun, Cameroon, 422
- Lake Nyos, Cameroon, 62, 62, 321, 422, 424, 425, 443, 444, 540
- Lake Taal, Philippines, 216, 252
- Lake Taupo, New Zealand, 208, 250, 261

- Laki volcano, Iceland, 200, 540
1783–4 eruption, 135, 372
see also Eldgjá–Laki ice age eruption
- landslides, 342–7, 343
avalanches *see* avalanches
block-glide, 342
rotational, 342
- La Pacana caldera, Chile, 335, 540
- La Palma island, Canaries, 321
- La Réunion Island *see* Réunion Island
- lapilli, 182–6
accretionary, 183, 183, 252
agglomerate, 182
breccia, 182
cinder, 182
pumice, 208, 244
- Large Igneous Provinces (LIPs), 135, 267–70, 471
classifications, 267
and extinction events, 405–6
eruptions, 268, 405
examples, **268**
flood-basalt, 268–70, 277–8
submarine, 268, 366–7
volumes, 366–7
- Las Canadas, Canary Islands, 214
- Láscar volcano, Chile, 246, 247, 540
- Lassen Peak, CA, 55, 304, 540
- Lassen Volcanic National Park, CA, 278
- La Soufrière-Guadeloupe volcano, Caribbean, 456–7, 460, 540
- La Soufrière-St Vincent volcano, Caribbean, 229, 235, 540
1902 eruption, 33
1979 eruption, 457
dome formation, 303
- lava, 16, 17, 21, 127–30
`a`a *see* `a`a flows
alkalic basalt, 62, 73
block, 166
channels, **154**
clastogenic, 129
cooling, 90, **91**, 138, 138, 162
flows *see* lava flows
komatiite, 66
pāhoehoe *see* pāhoehoe
pillow *see* pillow lavas
see also basalt; magma;
- lava dikes, 100–5, 103–4, 104, 128, 135
features, 103–5
pseudodikes, 104–5
ring, 100–1, 101
see also cone sheets
- lava diversion, 438–42
barriers, 439, 440, 441
- lava falls, 145
- lava flows, 25, 31, 55, 77, 90, 99, 127, 128, 274
`a`a *see* `a`a flows
basalt, 163, 166, 188
flood, 269
classification, 127, 128
cooling, 137, 138, 138, 144, 145
and viscosity, 93, 186: *see also* magma viscosity
destructiveness, 438: *see also under* volcanic risk
environmental conditions, 154–5
erosion, 312
extraterrestrial, 389, 390
joints, 160–2, 161
columnar, 160–2, 161, 162
and magnetic history of the Earth, 47
pāhoehoe *see* pāhoehoe
siliceous, 166, 168–9: *see also* volcanic glass
structures, 157–69
submarine, 363–5
- lava fountains, 17, 104, 116, 128–9, 130, 176
submarine, 370
- lava lakes, 17, 18, 18–19, 129, 130–4
- lava shields, 26, 270, 279, 382: *see also* shield volcanoes
- lava stalactites and stalagmites, 145, 146
- lava trees, 155, 156, 157, 158
fossilized, 157
see also tree molds
- lava tubes, tunnels, and pipes: *see* pyroducts
- LeClerc, Georges-Louis *see* Buffon, Comte de
- legends, of volcanoes, 27–30
- Lesser Antilles islands, 46
- Libby, Willard, 170
- littoral cones, 176, 298–300, 298
- Loch Ba, Isle of Mull, UK, 330
- Loihi volcano, Hawai'i, 271–2, 273, 540
caldera, 271, 272
- Loki patera, Io, 389
- Loma caldera, El Salvador, 411
- Long Island volcano, New Guinea, **124**
- Long Valley caldera, CA, 98, 105, 333, 334, 540
- Los Angeles basin, CA, 99
- Los Chocoyos, Guatemala, 232
- Low Velocity Zone (LVZ), 48
- Lua Poholo pit crater, Hawai'i, 319–20, 320
- Lyell, Charles, 32
- maars 25, 53, 99, 101, 178, 200, 297–8, 321
lakes, 62, 334, 424
see also volcanic craters
- Madagascar, **268**
- Macdonald, Gordon A., vii, viii, 35
Volcanoes, vii, 120, 162, 163–4, 166, 188, 207, 243, 438–9
- magma, 5, 16, 25–6, 51–2, 471
andesitic, 74–6, 79
ascent *see* magma ascent and emplacement
basaltic, 71, 72, 73–4, 75: *see also* basalt
and gravity, 68, 95
mixing, 71
nature of, 65–86
partial melting *see under* melting of rocks
physical properties, 89–109
silica-rich, 74–6, 78
subduction zone, 50–1
temperatures *see under* temperature
viscosity *see* magma viscosity
volatiles, 78–85, **80**, 128, 154, 156;
see also vesicles
- magma ascent and emplacement, 94–100

- equilibrium, 95
 oceanic volcanoes, 95
 rates, **95**, 96
 magma chambers, 25, 27, 28, 70, 92–3,
 95, 96–7, 99
 boiling, 237
 energy transfer, 468
 eruption triggers, 105–6
 extraterrestrial, 384
 overpressurization, 106
 post-caldera stage, 328
 roof weakening and collapse, 106,
 321, 337: *see also* calderas
 shallow, 236, 332–3
 sub-caldera, 321, 328, 337
 tidal stresses, 107
 submarine, 362–3
 magma reservoirs, 22, 25, 74, 81, 281
 equilibrium, 105–6
 formation of, 96–7, 99
 magma viscosity, 75, 91–4
 magnetic field of Earth, 46
 history of, 47
 magnetic reversals, 46–7
 magnitude, eruption, 123, 224
 Makapu‘u Point, Hawai‘i, 145
 Maly Semyatchik crater lake,
 Kamchatka, 426, 540
 Mamaku Tuff, New Zealand, 215
 Mammoth Mountain volcano, CA,
 81–2, 84, 422, 540
 Mammoth Lakes, CA, 469
 Manjang Kul, South Korea, 146
 mantle plumes, 61, 62, 71, 268, 383
 mantle xenoliths, 95: *see also* xenoliths
 marginal seas, 49, 51
 maria lunar fields, 380, 381
 marine trenches, 46, 50
 Markhinin, Yevgennii, 397–8
 Mars, vii, **379**, 385–6
 atmospheric conditions, 385
 compared to Earth and Venus, 385
 erosion, 386
 Hellas Basin, 385
 meteorite impact, 385
 paterae, 386–6
 plate tectonics, 385
 plumes, 385
 volcanic activity, 385, 386
 volcanoes, 385–6, 387
 water, 385
 Martinique, 289
 see also Mt Pelée, Martinique;
 St Pierre, Martinique
 Massif Central, France, 312, 312
 mass-wasting processes, 275
 Matteucci, R. V., 36
 Mauna Kea volcano, Hawai‘i, 167, 176,
 273, 291, 374, 376, 540
 Mauna Loa volcano, Hawai‘i, 26, 273,
 274, 323, 456, 540
 1843 eruption, viii, 28, 107, 138,
 139, 142–3
 1859 lava flow, 142, 143
 1868 eruption, 299
 1880–1 lava flow, 140
 1950, 467
 1984 eruption, 165
 lava flows, 94, 103, 152, 273, 274,
 291
 diversion, 441, 442
 Lua Poholo Crater, 319–20
 Mokuaweoweo summit caldera, 322,
 323, 324
 Northeast Rift Zone, 139–40
 Panaewa Flow, 274
 Pu‘u ka Pele cinder cone, 291
 Mauna Loa Observatory, Hawai‘i, 441
 Mauna Ulu, Kilauea, 17–22
 lava lake, 18, 130
 Maxwell bodies, 92
 Mayan civilization, central America, 408
 Mayon volcano, Philippines, 107, 287,
 288, 288, 540
 Mayor Island volcano, New Zealand,
 276–7, **277**, 540
 Mazama Tuff, OR, 215, 243, 289
 mazuku, 423–4, 424: *see also* mofettes
 McDermott Caldera, OR, 61
 Medicine Lake shield volcano, CA, 55,
 98, 169, 277, 540
 history, 277–8
 magma reservoir, 99
 map of, 278
 Mediterranean Sea, 53–4
 Meidob volcanic field, Sudan, 184
 melting of rock, 69, 142
 decompression, 71
 containing water, 71, 74, 159
 partial, 18, 70, 72, 73
 Merapi volcano, Java, 9, **80**, 237, 409,
 540
 1994 pyroclastic flows, 247
 Mercalli, Guiseppe (1850–1914), 191–2
 methane, 156–7, 391, 398
 meteorites, impact of, 79
 on the Moon, 79
 Mid-Atlantic Ridge, 49, 52, 63
 Mid-Ocean Ridge (MOR), 46, 47, 51,
 52, 63, 84, 362–6, 363
 mineralization, 475
 profiles, 363
 Mihara volcano, Japan, 451
 Mimatsu, Masao, 305
 Minakami, Takeshi (1910–83), 38,
 38, 447
 mineral ores, 76, 317, 319
 Minoan civilization, 408–9
 Miyakejima volcano, Japan, 323–4,
 324, 540
 mofettes, 82, 318, 422, 423, 424
 Mogi, K., 450–1
 Mohorovic (M-) discontinuity, 96, 337
 Mojave Desert, CA, 122, 125
 Momotombo volcano, Nicaragua, **80**,
 540
 Monte Somma, Italy, 288–9
 Montserrat, Lesser Antilles, 247, 285–6
 see also Soufrière Hills volcano,
 Montserrat
 Montserrat Volcano Observatory, 446
 Monument Dike Swarm, OR, 135
 Moon, the, **379**, 381
 impact of meteorites, 79, 380
 effect on tides, 107
 flood basalt plains, 380, 381
 volcanic activity, 379
 Mopah Range, CA, 99, 100, 122
 Mount St Helens, WA, 23, 55, 97, 106,
 229, 540

- May 1980 eruption, viii–viii, 37, 117, 181, 196, 256–8, 286
 blast, 199, 256–7, 290
 early signs, 256, 449, 461
 energetics, 467
 eruption column, 227, 229, 234, 257
 pyroclastic flows, 243, 245, 247
 sector collapse, 285, 341, 342, 346, 418
 dome formation, 301, 303, 304, 305, 306
 eruptive history, 289–90, 346
 plugs, 100
 Spirit Lake, 258, 377, 442
 Whaleback spine, 305, 306
- Mt Adams, WA, 55
 Mt Ararat, 29, 29, 54
 Mt Baker, WA, 55
 Mt Cameroon, West Africa, 62, 164
 Mt Edgecombe, Taupo Volcanic Zone, 261
 Mt Erebus, Antarctica, 372
 Mt Etna, Italy, 53, 80, 127, 134, 540
 1669 eruption, 438
 1971 eruption, 261
 lava diversion barriers, 439, 440
 Mt Fuji, Japan, 23, 26, 283, 285, 408, 540
 1707 eruption, 283
 Mt Gambier, S. Australia, 278
 Mt Garibaldi, BC, 55
 Mt Hood, OR, 55, 310
 Mt Jefferson, OR, 55
 Mt Lamington, New Guinea, 415
 1951 eruption, 242
 Mt Mazama, OR, 55, 289, 325, 325
 ash, 182
 eruption, 181
 pre-caldera stage, 327
 Mt McLoughlin, OR, 55, 346
 Mt Pelée, Martinique, 33, 34, 289, 540
 1902 eruption, 33, 36, 302–3, 419, 445
 1929–32 activity, 36, 241
 Mt Pinatubo, Philippines, 285–6, 540
 1991 eruption, viii, 107–8, 184, 225, 243, 260, 350, 351–2, 357, 404, 405, 431, 434, 444, 448
 Mt Rainier volcano, WA, 55, 182, 310, 346, 352–3, 353, 540
 Mt Shasta, CA, 23, 285, 310, 540
 avalanches, 346
 and Shastina, 286
 Mt Spurr, Alaska, 192, 454, 540
 Mt St Helens *see* Mount St Helens, WA
 Mt Taranaki, New Zealand, 283–5, 285
 mudflows *see* lahars
 mud volcanoes, 24, 84
 Mull, Isle of, 330–1
 Munch, Edvard, *The Scream* (1893), 404, 404
 Myōjin-Shō volcano, Japan, 368–9, 540
 caldera, 369
 Myvatn, Iceland, 200, 318
 Navajo legends, New Mexico, 28
 Neptune, 391: *see also* Triton, moon of Neptune
 Neptunists, 31
 neutral buoyancy, 78
 in eruption columns, 225, 226, 229
 in magma, 95, 96
 on Venus, 384
 Nevado Coropuna, Peru, 310
 Nevado del Ruiz volcano, Colombia *see* Ruiz volcano, Colombia
 Nevado del Toluca volcano, Mexico, 346, 540
 Newberry Shield Volcano, OR, 55, 98, 277, 540
 New Caledonia island, South Pacific, 474
 Newer Volcanics, S. Australia, 279
 Newtonian fluids, 92–3, 155, 255, 354–5
 New Zealand, 260
 volcanic activity, 53, 63, 259, 260–1, 279–80
see also individual volcanoes
 Newer Volcanics, Victoria, Australia, 60
 Nigorikawa caldera, Japan, 335
 nitrogen, 391–2, 398
 in soils, 407
 non-Newtonian fluids, 92–3, 243, 354
 Novarupta, Alaska, 124, 300, 540
 1912 eruption, 181, 184–5, 249
 nuclear testing, 251
 nuclear waste, 215
 nuées ardentes *see* pyroclastic flows
 Nuuanu slide, Koolau volcano, Hawai'i, 274, 275
 Nyamuragira volcano, Democratic Republic of Congo, 423, 540
 Nyiragongo volcano, Democratic Republic of Congo, 132, 423, 424, 540
 summit crater, 133
 1977 eruption, 157, 159
 2002 eruption, 138, 155, 156, 416, 416
 obduction, 95: *see also* subduction process
 Observatoire Volcanologique de la Montagne Pelée, Martinique, 23
 obsidian, 169, 276, 277, 278
 ocean floor, vii, 97
 subduction, 50–1: *see also* subduction process
 oceanic volcanoes, 97–8, 98, 362–7
see also island arcs; submarine volcanism; volcanic arcs; volcanic islands
 ogives, 168
 Okmok caldera, Alaska, 314, 331, 332, 353, 455, 540
 Olangapo, Philippines, 434
 Oldoinyo Lengai, East Africa, 77, 77, 78, 540
 Oligocene era, 329
 eruptions, 259
 rocks, 60
 olivine, 69, 69, 70, 73
 Olot Volcanic Field, Spain, 53
 Olympus Mons, Mars, 386, 388, 391
 Omori, Fusakichi (1868–1923), 38, 449, 451
 Ontake volcano, Japan, 342, 343, 351, 540

- Ontong Java plateau, 268, **268**, 366–7
 oral tradition, 28
 ore deposits, 317, 329, 370, 470–6
 definition, 470
 gold, 473, 475
 hydrothermal activity, 471, 472, 473
 fluid inclusions, 472
 and magmatic processes, 471
 nickel, 474
 non-metallic, 475–6
 porphyry copper, 473–4
 tungsten, 473
 volcanic associations, **471**
 ore mineralization, 470–1, 472
 sea-floor, 475
- Oregon, USA, volcanoes, 346
 see also individual volcanoes
 origin of life, 397–8
 Oruanui, New Zealand, 260–1, 540
 Oruanui Tuff, New Zealand, 260–1
 temperature, 260
 volcanic deposits, 122, 249, 260–1
 osmium, 62
 Osservatorio Vesuviano (Vesuvius
 Volcano Observatory), 35,
 36, 445
 ozone, atmospheric, 84
- Pacific oceanic crust, 61
 “hot spots”, 61, 61
 Pacific Plate, 60, 61
 Pacific Rim of Fire, 37, 46, 53, 54
 pāhoehoe, 18, 28, 93, 129, 130, 135–8,
 168
 charcoal beneath, 171
 different names for, 136
 fluidity, 154–5
 inflation and deflation, 149, 151
 and shield volcanoes, 275
 surface features, 147–51, 147, 148,
 149, 152–5
 submarine, 363
 toes, 149
 volatiles, 154–5
 see also lava flows
 pāhoehoe/`a`ā transition, 137, 138, 138
- Palouse Falls State Park, WA, 163
 Parícutín, Mexico, 296, 438, 540
 cinder cone, 293, 295–6
 volcano, 120, 134, 294
 Parker volcano, Philippines, **124**
 paterae volcanoes, 385, 389
 PDCs *see* pyroclastic density currents
 Pedragal lava flow, Mexico, 159
 Pele, Hawaiian goddess, 16, 28, 157
 Pele’s hair, 129
 Pele volcano, Io, 387–8, 390
 Perret, Frank A., 35, 36, 36, **141**,
 241–2, 445–6
 phenocrysts, 72, 73, 76, 182, 211
 quartz, 90
 PHILVOLCS (Philippine Institute of
 Volcanology and
 Seismology), 446
 phoenix plumes, 249
 phreatic eruptions, 25, 183, 190–1,
 199–200, 307, 318, 377, 458
 kinetic energy, 466
 Phreatomagmatic, 260
 Phreatoplinian, 200, 208
 volatiles, 318: *see also* volatile gases
 see also Plinian eruptions
 pillow lavas, 363–4, 364, 365, 370,
 374, 376
 pipe vesicles, 159, 160
 pit craters, 319, 320, 320
 Piton de la Fournaise, Réunion Island,
 106, 155, 281, 282, 540
 Domomieu Crater, 319
 Piton des Neiges, Réunion Island, 281–2
 plate boundaries, 48–9, 50, 54
 convergent, 49, 51, 51, 53–60, 75,
 76, 95, 336
 divergent, 49, 51–3, 63
 location of volcanoes, 51–2
 plate tectonics, 47–8, 49, 51, 278–9,
 385
 drivers for, **67**, 68
 extraterrestrial, 380–1, 385, 390
 see also plate boundaries
 Plato, 408–9
 Plinian eruptions, 175, 185, 192–3
 compared with Vulcanian, 189, 190
- columns, 193, 194, 195, 196,
 224–36
 dynamics, 224–6
 ejecta/deposits, 193, 195, 199, 205–6,
 209, 229, 232, 273, 285
 extraterrestrial, **378**, 385
 lightning, 397–8
 mass eruption rate, 228, 232–3, 232
 vent diameters, 232
 measuring magnitude, 224
 Pliny the Elder, Roman naturalist, 192
 Pliny the Younger, Roman patrician,
 198, 229, 419
 Ploskii Tol’batchik, Kamchatka, 57
 Pluto, 392: *see also* Charon, moon of
 Pluto
 plutonic rock, 72, 100
 Plutonists, 31
 plutons, 25, 54, 54, 99, 336
 Poisson analysis, 427–8, **429**
 Pomona Basalt, WA, 213
 Pompeii, Italy, 409, 410
 and 79 CE eruption of Vesuvius,
 197–8, 409
 Popocatepetl volcano, “traffic-light”
 scheme, 431, 432
 pozzolan, 475, 477
 prehistoric cultures, 27–8, 169: *see also*
 Mayan civilization
 probability, 427–31: *see also* event trees
 Pulido, Dionisio, 295–6
 pumice, 184–6, 193–4, 208, 210, 214,
 349, 369
 and ash, 185, 189–90, 193, 197, 245
 blocks, 247
 eruption columns, 232
 properties, 184
 rafts, 369
 silicic, 369
 vesicles, 185–6
 Pu`u Hou, Hawai`i, 129
 pyroclastic density currents (PDCs), 26,
 174, 175, 179, 185, 192,
 197–8, 204–5
 definition, 118, 235–6
 fabrics, 244
 and fluid mechanics, 254–5

- origins, 236–7
see also pyroclastic deposits; pyroclastic flows, pyroclastic surges
- pyroclastic deposits, 187–92, 196–218, 209, 218, **219**, 224, 260–1
- aggradation, 243
- erosion, 313
- imbrication, 243–44
- layering, 187–8, 187, 193
- submarine, 370
see also explosive eruptions; pumice; pyroclastic dunes; pyroclastic flows; pyroclastic surges; volcanic ash
- pyroclastic dunes, 216, 217, 218, 253
- pyroclastic flows, 13, 184, 195, 205–6, 213, **219**, 225, 246
- block-and-ash, 205–7, 296
- boilover, 237, 242–3
- cooling units, 211–12
- deposition mechanics, 213, 243–5, 246
- dynamics, 236–42
- and eruption intensity, 232, 328
- features, 246
- speed, 242
- pyroclastic surges, 205, 216, 218, **219**
- base surges, 251–2, 298
- comparison with pyroclastic flows, 237, 244–5, 252
- deposits, 216, 244:
- ground surges, 252, 254
- origin, 251–4
- sorting, 208, 209, 218, 255
- pyroducts, 138–47, 142, 143, 146
- definition, 140
- features, 146
- formation, 140–7, 142
- origin of term, 139–40, **141**
- and pāhoehoe flows, 147
- quartz, 69
- phenocrysts, 90
- Rabaul Volcano Observatory, 459
- Rabaul volcano, Papua New Guinea, 422, 540
- caldera, 99, 189, 312, 330, 330–1
- radar interferometry, 455, 456
- radiocarbon dating, 170–1
- radiogenic decay, **67**, 67–8, 84, 170:
see also radiocarbon dating
- radiogenic heat sources, 66, **67**, 67–8, **379**
- radiometry, 9, 380, 432;
- Rakata volcano, Indonesia, 421
- Rangitoto volcano, New Zealand, 279, 540
- Redoubt volcano, Alaska, 192, 417, 540
- Red Sea, 63
- “red” volcanoes, 5, 16–22, 116, 173
- hazards, 416
see also effusive eruptions
- remote sensing, 450–55
- Remotely Operated Vehicles (ROVs), vii, 365
- repose intervals, 108–9
- reticulite, 129, 186, 186; *see also* pumice
- Reynolds numbers, 255
- Réunion Island, 281–2
- calderas, 282
- hot spot, 282
- map, 281
- shield volcanism, 281–2
- rheomorphism, 213
- rheology *see* magma rheology
- rhyodacite, 325
- rhyolites, 73, 167–8, 211, 213, 214, 334, 475
- panellerite, 276
- plateaus, 207–8
- rift zones, 17, 26, 52–3, 97, 100, 272
- gravitational stress, 272
- and volcano growth, 323
see also individual rift zones
- ring complexes, 330
- ring dikes, 100–1, 101, 330, 331
- Rio Grande Rift, North America, 53
- risk assessment *see under* volcanic risk
- risk mitigation, 427, 431–42
- intervention, 433–4
- lakes, 442
- lava diversion, 438–42
- barriers, 438–40
- explosives, 442
- water cooling, 440, 441
- land-use planning, 432
- public education, 431–2, 455–6, 459
see also volcanic crisis management
- Rittman, Alfred (1893–1980), 37, 37, 118, 213
Vulkane und ihre Tätigkeit (1936), 37
- eruption diagrams, 118, 119
- rock cycle, 45
- Rota-1 volcano, 370, 371, 540
- Rotongaio Ash, New Zealand, 202
- Rotorua volcano, Taupo Volcanic Zone, 261, 540
- Royal Gardens, Hawai‘i, 167
- Ruapehu volcano, New Zealand, 98, 250, 345, 540
- 1953 lahar train disaster, 354, 354
- 1971 eruption, 201–2, 203
- crater lake, 201, 203, 354
- lahars, 425
- lahar deposits, 350, 354
- sector collapse, 345
- Ruiz volcano, Colombia, 310, 349, 540
- 1985 eruption, 349, 349, 356–7, 373–4, 431, 432, 458–9
- crisis management, 458, 461
- ice breccias, 375
- Russell, I. C., 269–70
- safety
- nuclear reactors, 202
- precautions, 155, 165,
- survival tips, **14**, **19**, **21**, **148**, **154**, **157**, **165**, **179**, **242**, **286**, **424**
- Sagan, Carl, 389
- Sakurajima volcano, Japan, 449, 540
- San Andreas Fault System, CA, 99
- sand waves *see* pyroclastic dunes
- San Francisco earthquake, 1906, 35
- San Francisco volcanic field, AZ, 134
- San Juan Mountains, CO, 211–12, 322, 329
- caldera cluster, 328, 329
- volcanic field, 335
- Santa Maria volcano, Guatemala, 1907
- eruption, **124**, **540**

- Santorini volcano, Greece, 213, 289, 540
 1645–25 BCE eruption, 408–9
 1866 eruption, 301–2
 dome formation, 304
 submerged caldera, 302
- Sarychev volcano, Kurile Islands, 225
- satellites, monitoring, 453–5
- Saturn, vii, 391: *see also* Enceladus,
 moon of Saturn
- S-C tectonites, 214, 214
- School of Volcanists, 30
- scoria, 182
- scoria cones *see* cinder cones
- Scrope, George Poulett (1797–1876),
 32, 32
- sea-floor spreading, 48; *see also* plate
 tectonics
- seamounts, 61, 366, 367
see also submarine volcanism; volcanic
 landforms
- sector collapses, 282, 285, 321, 342–7
 and earthquakes, 346
 hazards, 418
 preconditioning, 346
 scars, 346
 triggers, 346
- Sedgwick, Adam, 32
- sedimentary rocks, 45, 347
- seismic activity, 350–1, 447–8
see also earthquakes; seismic
 monitoring
- seismic monitoring, 8, 11, 17–18, 19,
 37, 161, 364, 365, 447–9,
 448
- seismic tomography, 98–9
- seismographs, 38
- Semain shield volcano, 270
- shatter rings, 142, 143
- shield volcanoes, 26, 26, 56, 101,
 270–83
 comparison with flood-basalt
 provinces, 270
 definition, 270–1
 erosion, 311–12
 extraterrestrial, 379, 382, 387
 formation, 272, 278
 Hawai'i *see under* Hawai'i
- Icelandic, 275–6
 intraplate, 278–80, 322
 schematic cross-section, 273
 summary, 282–3
 summit calderas, 274
 Turkana-type, 279
 in volcanic arcs, 276–8
see also individual volcanoes
- Shiprock volcanic neck, NM, 100, 102
- Shishaldin volcano, Alaska, 327, 540
- Shiveluch volcano, Kamchatka, 346, 540
 1964 avalanche, 346
see also Klyuchevskoi–Shiveluch
 volcano complex, Kamchatka
- Showa Shinzan volcano, Japan, 449
 domes, 305, 307, 307, 308
- Siberian Traps, Russia, 405
- Sierra Madre Occidental plateau,
 Mexico, 267
- Sierra Nevada range, North America,
 93, 100, 473
- silica (SiO₂), 24–5, 69, 74, 215
 tetrahedra, 69, 74
- siliceous glass *see under* volcanic glass
- silicon ions, 68–9, 69
 fluxing, 69
- silicon oxide *see* silica
- Silliman, Benjamin, 32
- sills, 105
- Skjaldbreiður volcano, Iceland, 275–6,
 278, 540
- Sobetsu River, Japan, 306, 307
- social impacts of volcanic activity,
 407–10
- Socompa volcano, Chile, 342–4, 540
- soil efflux, 81
- soil fertility, 406–8
 and volcanic ash, 406–7
- Solfatara Crater, Italy, 85
- solar radiation, 466
- Solar System, the, vii, 67, 73, 378–9,
 390
 Kuiper Belt, 391
 planet formation, 66–7
 volcanoes, 378–92
see also individual planets
- sonar imaging, vii, 46
- Soufrière Hills volcano, Montserrat, viii,
 106, 237, 240, 243, 248,
 303, 303, 540
 1995 eruption, 446
- Soufrière-St Vincent *see* La Soufrière-St
 Vincent volcano
- Sound Fixing and Ranging (SOFAR)
 channel, 369
- Snake River Plain, Yellowstone *see*
 Yellowstone–Snake River
 Plain, ID
- snowmelt, 352–3, 374
 as lahar trigger, 352
see also glaciovolcanism
- SP Mountain, Arizona, 294
- spatter cones, 129, 130, 151, 270,
 293, 295
- spatter ramparts, 128, 129
- spiracles, 159, 160
- Sredinny Range, Kamchatka, 58
- statistical analysis of risk, 427–9
 Poisson analysis, 427–8, 429
- steady state volcanic activity, 109
- Stefan's Law, 165–6
- St Pierre, Martinique, 1902 devastation,
 33, 34, 36, 419
see also Mt Pelée, Martinique
- stratovolcanoes *see* composite volcanoes
- Stromboli volcano, Italy, 54, 107, 117,
 134, 289, 540
 characteristic activity, 134: *see also*
under effusive eruptions
- sector collapse, 342
- subcaldera intrusions, 330–1
- subduction process, 47, 50–1, 50, 57
 subglacial volcanism *see*
 glaciovolcanism
- submarine volcanism, 51–2, 54, 200,
 201, 272, 361, 362–6, 398
see also marine trenches; subduction
 process; seamounts; volcanic
 islands
- submersible vehicles, vii, 19, 367, 370
- Sub-Plinian eruptions, 246, 276, 285
see also Plinian eruptions
- Sudbury intrusive complex, Canada, 474
- Sudradjat, Dr Adjat, 9

- sulfates, 401, 402: *see also* hydrogen sulfate
- sulfur (S₂), **80**, 82, 85, 401–6, 477
 anthropogenic sources, 85
 deposits, 477
 on Io, 388, 390
 metal bonding, 475
see also dimethylsulfide (DMS),
 hydrogen sulfate; hydrogen sulfide
- sulfur cycle, 401, 402
- sulfur dioxide (SO₂), 78, 83, 85, 104, 154, 381, 418
- sulfuric acid (H₂SO₄), 202
- Super-eruptions, 213, 258–61
 and climate change, 259, 418, 426
 definition, 258
 frequency, 259, 426
 popularization, 258
- Super-volcanoes, 223, 258
- Surtsey volcanic island, Arctic Ocean, 201, 276, 453, 540
- Surtseyan eruptions, 201–2, 367
- Survival tips for field volcanologists, **14**, **19**, **21**, **148**, **154**, **157**, **165**, **242**, **286**, **424**
- Swabia, Germany, 102
- Taal volcano, the Philippines, 540
 1965 eruption, 252, 253
- table mountains *see* tuya
- Tacitus, Roman historian, 198
- Tambora volcano, Indonesia, **124**, 181, 193, 259–60, 404, 467, 540
- Tarawera volcano, New Zealand, 261, 540
 1886 eruption, 198–9
- Tasikmalaya, Indonesia, 9, 344
- Taupo Volcanic Zone, New Zealand, 260, 261, 540
 186 CE eruption, 229, 242, 246, 260
 ash flows, 249, 250
 compared with Oruanui eruption, 260
- caldera, 99, 198, 250, 260
 geothermal field, 469
 ignimbrites, 246, 246, 249, 250, 260
- Tavurvur volcano, Papua New Guinea, 189, 331, 459
- Teide volcano, Canary Islands, 422, 540
- temperature
 of eruption columns, 226, 229
 increase at depth, 468
 of magma, 74, 75, 89–91, 93–4, 208, 212
 and viscosity, 94
 oxidation, 142
 Plinian flows, 208, 241
 pyroclastic flows, 241
 of Venus, 388–9
 and viscosity, 93–4, **94**
 welding, 208, 211, 212
- Tenerife, Canary Islands, 213, 285
- tephra *see* ejecta, volcanic terminology, 22–7
- Ternate Island, Indonesia, 107, 177
- Thera, Greece, 408–9
- thermal plumes, 61
- Three Sisters, OR, 55
- tholeiitic basalt *see under* basalt
- Thomson, William, Lord Kelvin, 67
- thorium-232, **67**
- Tibetan Plateau, Asia, 63
- tides, 107, 387
 as eruption triggers, 107
- Titan, moon of Saturn, **379**, 392
- Toba caldera, Sumatra, 326–7, 540
 Super-eruption, 125, 259, 408
- Tonga, South Pacific, 201
- Tonga–Kermadec island arc, 369
- toreva blocks, 344–5, 345
- trachyte, 279, 280
- trap rocks, 270, 271
- trees, 155–6, 158, 258, 436: *see also* lava trees
- Triton, moon of Neptune, **379**, 391–2
- Trolladyngja volcano, Iceland, 275
- tsunami, 418, 419
 causes, 419–20
 fatalities, 420
 volcanic, 419, 419–21
- tuff, 90, 101, 102, 102, 180, 204, 213
- tuff cones, 296–8, 297
see also ash cones
- Tumalo tuff, OR, 244
- tumuli *see under* pāhoehoe
- turbidity currents, 298
- tuya, 374, 378
- Tuya Butte, British Columbia, 378
- Twain, Mark, 18
- typhoons, 107–8, 351–2, 467
- Typhoon Yunya, 1991, 351–2
- Ubehebe crater, Death Valley, CA, 200, 216, 540
- Ukinrek maars, Alaska, 318, 318, 540
- Ultraplinian eruptions, 193
- umbrella clouds *see under* eruption columns
- Umnak Island, Alaska, 314, 332
- Undara volcano, Queensland, Australia, 144
- United Nations Disaster Relief Organization (UNDRO), 458
- Unzen volcano, Japan, 343, 437, 540
 1792 eruption, 342, 346, 418, 420
 cause of tsunami, 343, 420
 sector collapse, 343
 1984 landslide, 343
 1991 eruption, 241
 sabo dam, 437
- uranium 238, 67
- Uranus, vii
- Urey, Harold, 397
- US Geological Survey (USGS), 9, 446
- Usu volcano, Japan, 305, 540
 1943–4 eruption, 305–8
see also Showa Shinzan
- Valley of Ten Thousand Smokes (VTTS), Alaska, 243, 249, 328
- Vatnajökull glacier, Iceland, 372, 375
- VDAP *see* Volcano Disaster Assistance Program
- VEI *see* Volcanic Explosivity Index
- Veniaminoff volcano, Alaska, 454, 540
- Vening Meinesz, F. A., 46, 47, 48
- vents *see* volcanic vents
- Venus, **379**, 380–5
 atmospheric conditions, 381, 383–4
 coronae calderas, 382–3, 384

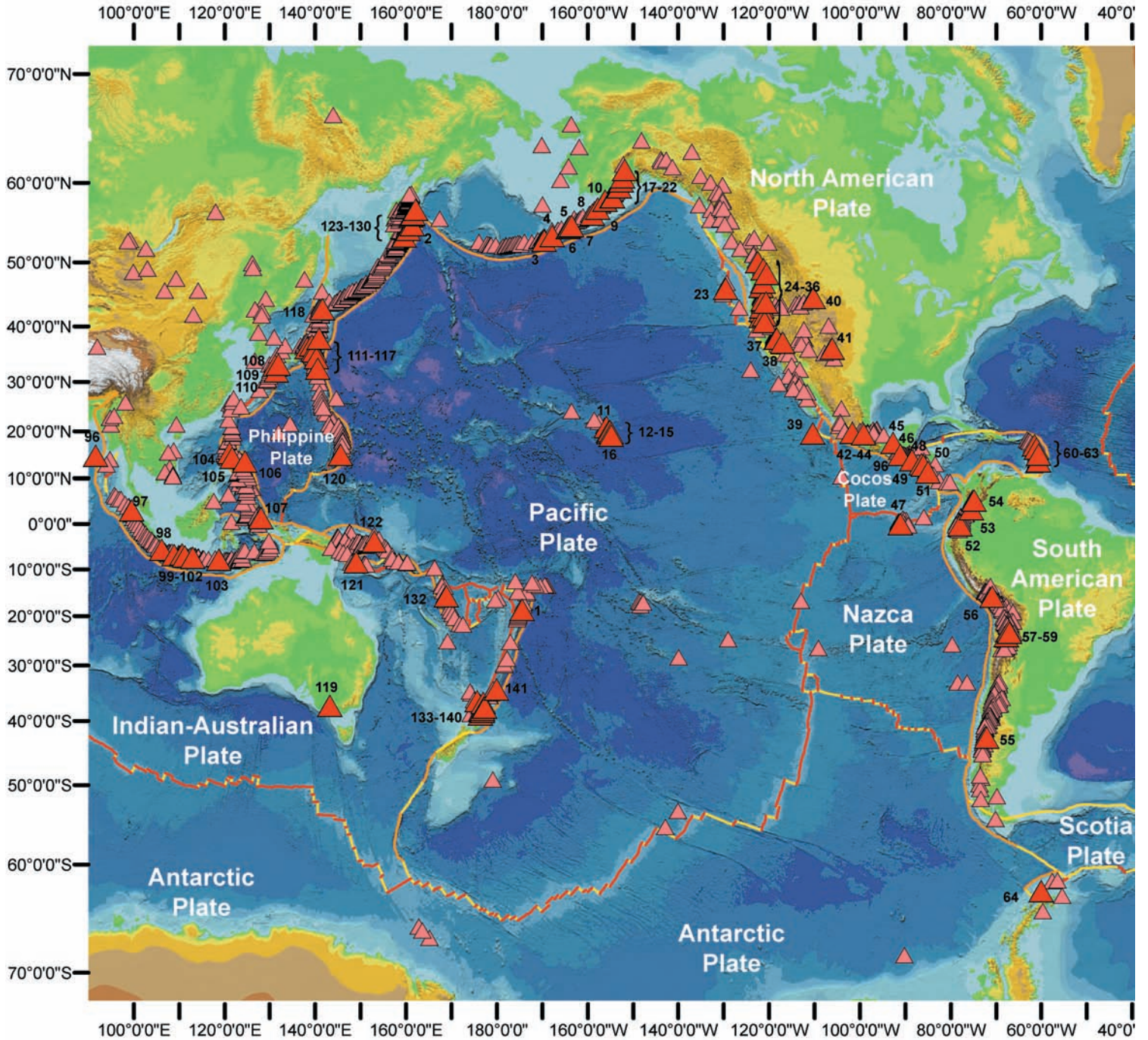
- canali, 382
 compared to Earth, 380
 farra, 382, 383
 grabens, 383
 hot spots, 383
 lithosphere, 382
 mantle plumes, 383, 385
 volcanic activity, 380–1, 382, 384
 Verbeek, Rogier, 421
 vesicles, 72, 93, 103, 133–4, 157–60, 299–300
 magma *see under* magma viscosity
 pipe, 159, 160
 in pumice, 184
 shapes, 160
 spiracle, 159, 160
 types, 160
 and welding, 210
 Vesuvius, Italy, 31, 32, 54, 97–8, 116, 218, 540
 79 CE eruption, 192, 193, 197–8, 197, 229, 235, 409–10, 41
 deposits, 195, 195, 197, 253
 1906–7 eruption, 33, 34, 36, 188, 439
 1944 eruption, 116, 342
 magma reservoir, 97
 ore deposits, 472–3
 Virunga volcanic belt, central Africa, 28
 viscosity, of magma *see* magma viscosity
 vitrophyre, 169
 VMS ores *see* Volcanic Massive Sulfide deposits
 Vogelsberg volcanic field, 42–3
 volatile gases, 26, 78–85, **80**, 128, 243
 as eruption triggers, 105, 106, 120–1
 see also halogen gases; organic gases; water (H₂O)
 volcanic arcs, 54–60
 and volcano-tectonic depressions, 336–7
 volcanic vigor, 59–60
 see also island arcs
 volcanic ash, 12, 102, 174–5, 180–2, 189, 197–8
 clouds, 122–3, 188: *see also* eruption columns
 cones, 204
 crystal, 180
 definitions, 25, 180
 deposits, 180–2
 erosion, 313
 elutriation, 245–6, 246, 254
 fallout, 179–82
 hazards, 9, 22, 418, 434: *see also* safety; volcanic hazards
 particle shapes, 121, 175
 and pumice, 185, 197
 plumes *see* ash plumes
 pyroclastic, 22, 25, 122, 174–5: *see also under* pyroclastic deposits
 agglomerate, 180
 brecchia, 103, 180, 272
 see also ejecta, volcanic; lahars; pyroclastic deposits; vulcanian deposits
 Volcanic Ash Advisory Centres (VAACs), 373, 417
 volcanic blocks, 178, 178
 volcanic bombs *see* bombs, volcanic
 volcanic centers, 27
 volcanic craters, 317–21
 collapse, 319–21
 formation, 317–20
 maars *see* maars
 multiple, 318
 nested, 318
 pit, 319, 320, 322–3
 resemblance to meteor impact craters, 319
 types, 318
 see also calderas; *individual craters*
 volcanic complexes, 289
 volcanic cones, 290–300: *see also* cinder cones; tuff cones
 volcanic crisis management, 455–61, 460–1
 volcanic domes, 26, 27, 238, 300–8
 collapse, 236–7, 301, 346
 cryptodomes, 237, 256, 308
 formation, 300–5, 321:
 growth, 350
 spines, 303, 304
 volcanic earthquakes, 447–8
 and eruptions *see under* earthquakes
 Minakami classification, 38, 447
 volcanic ejecta *see* ejecta, volcanic
 volcanic energy, 465–9
 geothermal power, 467–70: *see also* geothermal energy
 volcanic eruptions, 5, 32, 33, 115–25
 classifying, 115, 117–18
 and earthquakes, 8, 198, 306
 economic impact, 10
 effusive *see* effusive eruptions
 and electromagnetic fields, 451
 episodicity, 59–60, 289
 explosive *see* explosive eruptions
 and global cooling, 403–4, 405, 418
 hydrovolcanic *see* hydrovolcanic eruptions
 magmatic, 25, 353
 on other planets, vii, 127
 probabilities *see* statistical analysis of risk
 social impact, 408–11
 and soil fertility *see* soil fertility
 submarine, 366–70: *see also* submarine volcanism
 Super-eruptions *see* Super-eruptions
 triggers *see* eruption triggers
 Vulcanian *see* vulcanian eruptions
 volcanic explosions *see* explosive eruptions
 Volcanic Explosivity Index (VEI), **118**, 123–5, **124**, 258
 volcanic fields, 27, 468–9; *see also individual volcanic fields*
 volcanic fumes *see* volcanic gases
 volcanic gases, 18, 78–80, 403
 blast pits, 168
 compositions, **80**, 81–4, 402–3
 hazards, 418: *see also under* carbon dioxide
 magmatic, 424
 monitoring, 452
 role in eruptions, 78–9, 105, 106, 120–1
 solubility, 79
 and welding, 211

- volcanic glass
 crystallization, 215
 hyaloclastite, 269, 272, 273, 375
 obsidian, 169
- volcanic hazards, 6–7, 8, 10, 12, 22,
 190, 191, 197, 199, 200–1,
 253, 372, 413–25, 426–7
- volcanic islands, 200, 323
see also island arcs; *individual islands*
- volcanic lakes, 424–5
 degassing, 442
- Volcanic Massive Sulphide (VMS)
 deposits, 475, 475, 476
- Volcanic necks and plugs, 100–2, 300
- volcanic risk, 414, 425–31
 maps, 433
 mitigation, 431–45
see also volcanic crisis management;
 volcano monitoring
- volcanic rocks *see under* igneous rocks
- volcanic vents, 232, 288–9, 294, 300–1
see also under PDCs, Plinian
 eruptions
- volcanic vigor, 59–60, 289–90
 extraterrestrial, 383, 390
see also arc magmatism
- volcanism, submarine *see* submarine
 volcanism
- Volcano Disaster Assistance Program
 (VDAP), 446
- volcanoes
 active, dormant, and extinct, 414–16
 extraterrestrial *see* extraterrestrial
 volcanoes
 grey *see* composite volcanoes
 intraplate (hot spot) *see* intraplate
 volcanoes
 oceanic *see* oceanic volcanoes
 and plate boundaries, 51
 red *see* “red” volcanoes
 shapes of, 23–4, 23, 24, 26, 350–1
 submarine, 54, 98: *see also*
 seamounts; submarine
 volcanism
see also mud volcanoes; Pacific Rim of
 Fire; shield volcanoes;
individual volcanoes
- Volcanological Survey of Indonesia
 (VSI), 6, 8, 9
 Cikasah Observatory, 6, 15
- volcanologists, 3, 22, 32–8
 and the media, 459
 and risk, 426: *see also* safety; volcano
 monitoring
- volcanology, science of, vii, 479–80
 definition, 3
 history, 27–39, 45–50, 59–60, 479
 terminology, 5, 22–39, 115–16
see also humanistic volcanology
- volcano monitoring, 443–55
- volcano-tectonic depressions, 58,
 336–8
- Voyager spacecraft, 386, 387–8, 391,
 392
- Vulcan, *see* Haphaestus, god of metal
 and armor
- Vulcan volcano, Papua New Guinea,
 331
- vulcanian deposits, 189–90, 205–6
- Vulcanian eruptions, 188–92, **235**
- Vulcano volcano, Sicily, 30, 54, 190,
 540
 1888 eruption, 190, 191
- Wairakei geothermal area, New
 Zealand, 469, 470
- Walcott Tuff, ID, 211
- Walker, George Patrick Leonard
 (1926–2005), 38, 94,
 119–23, 188, 249
- Walker eruption classification system,
 119–21, 120
 fragmentation index, 120
 limitations, 122
- Washington, H. S., 304
- water (H₂O), 81, 269, 398
 behavior, 354–5
 bonding, 215
 cooling effect, 211
 cycle, 398–9
 geysers, 473
 ground, 81
 as eruption trigger, 120
 on other planets, 385, 391
- in rocks, 70–6, 159
 solubility, **80**
 vapor (steam), 78, 79, **79**, **80**, 81,
 181, 192–3, 228, 234, 370,
 377, 421
see also hydrovolcanic eruptions;
 glaciovolcanism; snowmelt;
 vesicles
- weathering *see* erosion
- Wegener, Alfred (1880–1930), 47
- welding, 207, 210–12, 212
 temperature, 211, 212
 in fallout deposits, 213, 254
 sequence, 214
- Werner, Abraham Gottlob
 (1749–1817), 30–1
- Westdahl volcano, Alaska, 327, 454,
 540
- West Maui volcano, Hawai`i, 272
- Whitney Seismological Laboratory,
 Hawai`i, 38
- Williams, Howell, 322
- Wilson, J. Tuzo, 61
- World Organization of Volcano
 Observatories (WOVO), 446
- World War II, 38, 46, 473
- xenoliths, 74, 472
 mantle, 95
- Yellowstone National Park, Wyoming
 caldera, 61, 62, 84, 98
 geysers, 473
 hot spot, 61, 63, **268**
 ignimbrites, 213
 lava flows, 168
 magma chamber, 98
- Yellowstone–Snake River Plain, ID, 61,
 267–8, 269–70, 276
- Yellowstone Plateau, USA, 208, 329,
 540
 caldera, 329, 334
 Plinian eruption, 329
- Yosemite National Park, CA, 327
- Yucca Mountains, NV, 215
- Zeitschrift für Vulkanologie*, 37
 zeolites, 215

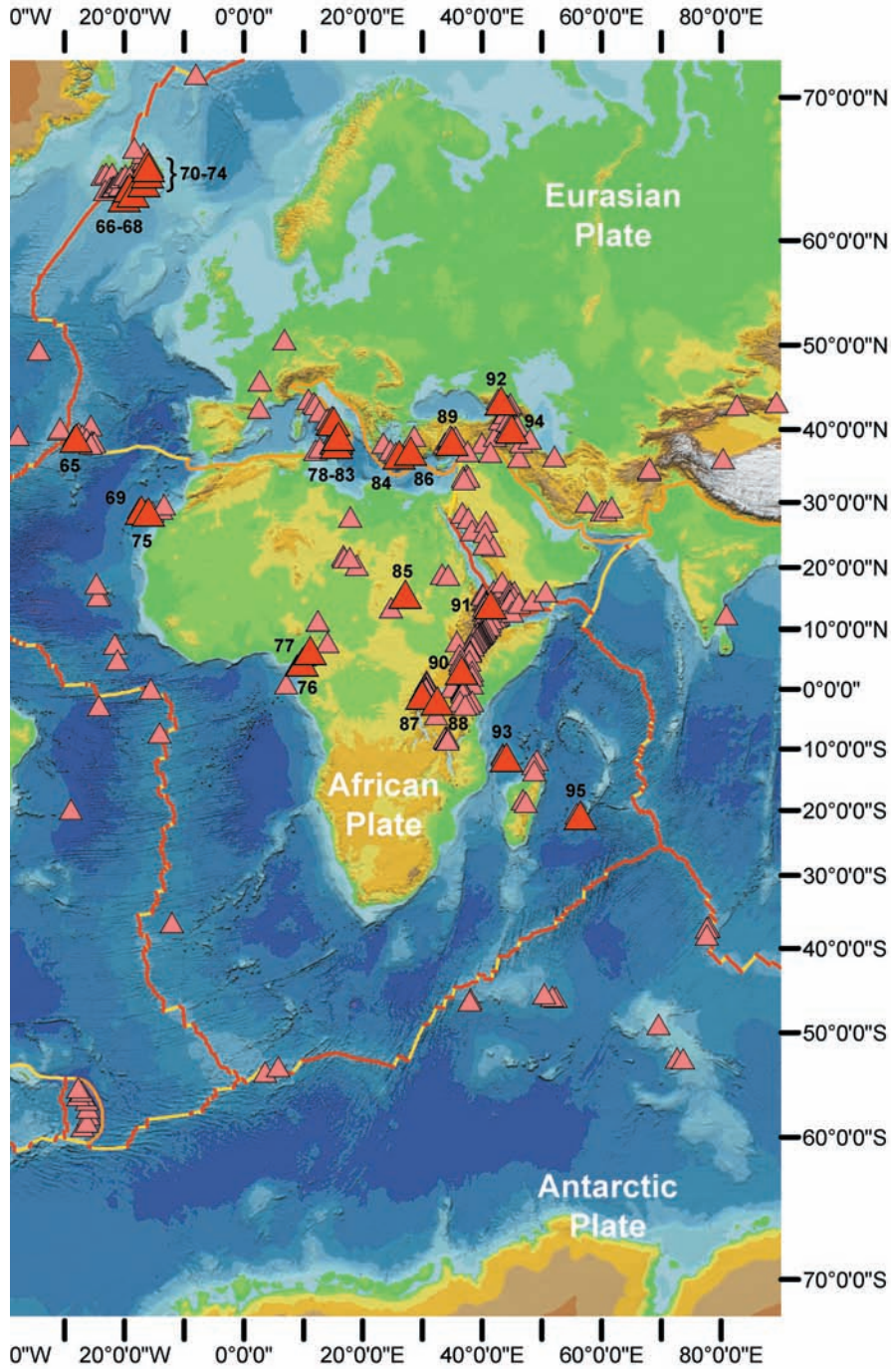
Map number	Name	Smithsonian number	Region	Latitude (dec.deg.)	Longitude (dec.deg.)	Type	Last known eruption (approx. for early dates)
1	Home Reef	0403-08=	SW Pacific	18.99S	174.78W	Submarine volcano	2006
2	Gorely	1007-07	Kamchatka	52.56N	172.51W	Composite volcano	1993
3	Cleveland	1101-24	Aleutians	52.83N	169.94W	Composite volcano	2009
4	Okmok	1101-29	Aleutians	53.43N	168.13W	Shield volcano/caldera	1997
5	Westdahl	1101-34	Aleutians	54.52N	164.65W	Composite volcano	1992
6	Fisher Caldera	1101-35	Aleutians	54.65N	164.43W	Caldera	1830
7	Shishaldin	1101-36	Aleutians	54.76N	163.97W	Composite volcano	2004
8	Veniaminoff	1102-07	Aleutians	56.17N	159.38W	Composite volcano	2006
9	Aniakchak	1102-09	Aleutians	56.88N	158.17W	Caldera	1931
10	Ukinrek maars	1102-131	Aleutians	57.83N	156.51W	Maar craters	1977
11	Haleakala	1302-06	Hawai'i	20.71N	156.25W	Shield volcano	1750 (?)
12	Hualalai	1302-04	Hawai'i	19.69N	155.87W	Shield volcano	1801
13	Mauna Loa	1302-02	Hawai'i	19.48N	155.61W	Shield volcano	1984
14	Mauna Kea	1302-03	Hawai'i	19.82N	155.47W	Shield volcano	2460 BCE ± 100 years
15	Kilauea	1302-01	Hawai'i	19.42N	155.29W	Shield volcano	2010 (continuing)
16	Loihi	1302-00	Hawai'i	18.92N	155.27W	Submarine volcano	1996?
17	Novarupta	1102-18	Alaska	58.27N	155.16W	Caldera	1912
18	Katmai	1102-17	Alaska	58.28N	154.96W	Composite volcano	1912
19	Augustine	1103-01	Alaska	59.36N	153.43W	Composite volcano	2006
20	Iliamna	1103-02	Alaska	60.03N	153.09W	Composite volcano	1876
21	Retoubt	1103-03	Alaska	60.48N	152.74W	Composite volcano	1990
22	Spurr	1103-04	Alaska	61.30N	152.25W	Composite volcano	1992
23	Axial	1301-021	E. Pacific	45.95N	130.00W	Submarine volcano	1998
24	Garibaldi	1200-20	Cascades	49.85N	123.00W	Composite volcano	8060 BCE ± 500 years
25	Mt. McLoughlin	9999-99	Cascades	42.40N	122.30W	Shield volcano	Pleistocene
26	Shasta	1203-01	Cascades	41.41N	122.19W	Composite volcano	1786
27	Mount St Helens	1201-05	Cascades	46.20N	122.18W	Composite volcano	2008
28	Crater Lake (Mt. Mazama)	1202-16	Cascades	42.93N	122.12W	Composite volcano	2290 BCE ± 300 years
29	Baker	1201-01=	Cascades	48.78N	121.81W	Composite volcano	1880
30	North Sister	1202-07	Cascades	44.17N	121.77W	Composite volcano	440 CE ± 150 years
31	Rainier	1201-03	Cascades	46.85N	121.76W	Composite volcano	1894
32	Medicine Lake	1203-02	Cascades	41.61N	121.55W	Composite volcano	870 CE ± 25 years
33	Lassen	1203-08	Cascades	40.49N	121.510	Composite volcano	1917
34	Newberry	1202-11-	Cascades	43.72N	121.23W	Shield volcano	690 CE ± 100 years
35	Glacier Peak	1201-02-	Cascades	48.11N	121.11W	Composite volcano	1700 ± 100 years
36	Mammoth Mountain	1203-15	California	37.63N	119.03W	Composite volcano	Holocene
37	Long Valley Caldera	120314A	California	37.70N	118.87W	Caldera	Pleistocene
38	Ubehebe Craters	1203-16	California	37.02N	117.45W	Cinder cones	4050 BCE (?)
39	Barcena	1401-02	E. Pacific	19.30N	110.82W	Cinder cones	1050 BCE (?)
40	Yellowstone	1205-01	Wyoming	44.43N	110.67W	Calderas	1050 BCE (?)
41	Valles	121002-D	New Mexico	35.86N	106.57W	Caldera	Pleistocene
42	Jorullo	1401-06-2	Mexico	19.48N	102.25W	cinder cones	1774
43	Parícutín	1401-06-1	Mexico	19.50N	102.20W	Cinder cone and flow	1952
44	Nevado del Toluca	1401-07	Mexico	19.11N	99.760	Composite volcano	1350 BCE (?)
45	El Chichón	1401-12	Mexico	17.36N	93.23W	Lava domes	1982
46	Santa Maria / Santiaguillo	1402-03	Guatemala	14.76N	91.55W	Composite volcano/dome	2010 (continuing)
47	Fernandina	1503-01	Galapagos	00.37S	91.55W	Shield volcano	2005
48	Ilopango	1403-06	El Salvador	13.67N	89.05W	Caldera	1880
49	Casita	1404-02=	Nicaragua	12.70N	87.00W	Composite volcano	Holocene
50	Momotombo	1404-09	Nicaragua	12.42N	86.54W	composite cone	1905
51	Orosí	1405-01=	Costa Rica	10.98N	85.47W	Composite volcano	Unknown
52	Cotopaxi	1502-05	Ecuador	00.68S	78.44W	Composite volcano	1940
53	Nevado del Huila	1501-05=	Colombia	02.93N	76.03W	Composite volcano	2009
54	Nevado del Ruiz	1501-02	Colombia	04.90N	75.32W	Composite volcano	1991
55	Chaitén	1508-041	Chile	43.00S	72.65W	Composite volcano	2009
56	El Misti	1504-01=	Peru	16.29S	71.41W	Composite volcano	1985
57	Socompa	1505-109	Chile	24.40S	68.25W	Composite volcano	5250 BC (?)
58	Láscar	1505-10=	Chile	23.37S	67.73W	Composite volcano	2007
59	La Pacana Caldera	None Available	Chile	23.74S	67.540	Calder	Pliocene
60	Soufriere Hills – Montserrat	1600-05	Caribbean	16.72N	62.18W	Composite volcano/dome	2010 (continuing)
61	Soufriere – Guadeloupe	1600-06	Caribbean	16.05N	61.67W	Composite volcano	1977
62	Soufriere – St. Vincent	1600-15	Caribbean	13.33N	61.18W	Composite volcano	1979
63	Pelée	1600-12	Caribbean	14.82N	61.17W	Composite volcano	1932
64	Deception Island	1900-03=	Antarctica	62.97S	60.65W	Caldera	1970
65	Capelinhos	1802-01	Azores	38.60N	28.73W	Littoral cone	1958
66	Surtsey	1702-01	Iceland	63.30N	20.62W	Littoral cone	1967
67	Hekla	1702-07	Iceland	63.98N	19.70W	Composite volcano	2000
68	Katla (Eldgjá)	1702-03=	Iceland	63.63N	19.05W	Subglacial volcano	1999
69	Cumbre Vieja	1803-01-	Canary Is.	28.57N	17.83W	Composite volcano	1971

70	Grimsvötn	1703-01=	Iceland	64.42N	17.33W	Caldera	2004
71	Laki	1703-01	Iceland	64.42N	17.33W	Fissure vents	2004
72	Krafla	1703-08=	Iceland	65.73N	16.78W	Caldera	1984
73	Askja	1703-06	Iceland	65.03N	16.75W	Composite volcano	1961
74	Skjaldbreiður (Fremnamur)	1703-07=	Iceland	65.43N	16.65W	Composite volcano	800 BCE ± 300 years
75	Teide	1803-03	Canary Is.	28.27N	16.64W	Composite volcano	1909
76	Mt. Cameroon	0204-01	Cameroon	04.20N	9.17E	Composite volcano	2000
77	Lake Nyos	0204-03	Cameroon	06.25N	10.50E	Composite volcano	Holocene
78	Campi Flegrei	0101-01	Italy	40.83N	14.14E	Caldera	1538
79	Vesuvius	0101-02	Italy	40.82N	14.43E	Composite volcano	1944
80	Lipari	0101-042	Italy	38.48N	14.95E	Composite volcano	ca. 1000 CE
81	Vulcano	0101-05	Italy	38.40N	14.96E	Composite volcano	1890
82	Etna	0101-06	Italy	37.73N	15.00E	Composite volcano	2009
83	Stromboli	0101-04	Italy	38.79N	15.21E	Composite volcano	2010 (continuing)
84	Santorini	0102-04	Greece	36.40N	25.40E	Shield volcano	1950
85	Meidob	0205-05=	Sudan	15.31N	26.47E	Cinder cones	2950 BCE ± 500 years
86	Kos	010206=A	Greece	36.85N	27.25E	Caldera	Pleistocene
87	Nyamuragira	0203-02=	Dem. Rep. of Congo	01.41S	29.20E	Shield volcano	2010
88	Nyiragongo	0203-03	Dem. Rep. of Congo	01.52S	29.25E	Composite volcano	2010 (continuing)
89	Hasan Dagi	0103-002	Turkey	38.13N	34.17E	Composite volcano	7550 BCE ± 50 years
90	Oldoinyo Lengai	0202-12	Tanzania	2.76N	35.91E	Composite volcano	2009
91	Erta Ale	0201-08	Ethiopia	13.60N	40.67E	Shield volcano	2010 (continuing)
92	Eibrus	0104-01-	Caucasus	43.33N	42.45E	Composite volcano	50 CE ± 50 years
93	Karhala	0303-01=	Comoros Is.	11.75S	43.38E	Shield volcano	2007
94	Ararat	0103-04	Turkey	39.70N	44.30E	Composite volcano	1840
95	Piton de la Fournaise	0303-02	Reunion	21.23S	55.71E	Shield volcano	2010
96	Fuego	1402-09=	Guatemala	14.47N	90.88E	Composite volcano	2010 (continuing)
97	Toba	0601-09	Indonesia	02.58N	98.83E	Caldera	Pleistocene
98	Krakatau	0602-00	Indonesia	06.10S	105.42E	Caldera	2009
99	Galunggung	0603-14	Indonesia	07.25S	108.06E	Composite volcano	1983
100	Dieng	0603-20=	Indonesia	07.20S	109.92E	Composite volcano / phreatic	2009
101	Merapi	0603-25	Indonesia	07.54S	110.44E	Composite volcano	2007
102	Kelut	0603-28	Indonesia	07.93S	112.31E	Composite volcano	2008
103	Tambora	0604-04	Indonesia	08.25S	118.00E	Composite volcano	1967 ?
104	Pinatubo	0703-083	Philippines	15.13N	120.35E	Composite volcano	1993
105	Taal	0703-07	Philippines	14.00N	120.99E	Composite volcano	1977
106	Mayon	0703-03	Philippines	13.26N	123.69E	Composite volcano	2006
107	Gamalama	0608-06=	Indonesia	00.80N	127.33E	Composite volcano	2003
108	Unzen	0802-10	Japan	32.76N	130.29E	Dome complex	1996
109	Sakurajima	0802-08	Japan	31.59N	130.66E	Composite volcano	2010 (continuing)
110	Aso	0802-11=	Japan	32.88N	131.11E	Caldera	2006
111	Ontake	0803-04=	Japan	35.89N	137.48E	Composite volcano	1980
112	Asama	0803-11	Japan	36.40N	138.53E	Composite volcano	2004
113	Fuji	0803-03	Japan	35.36N	138.73E	Composite volcano	1708
114	Hakone	0803-02=	Japan	35.25N	139.02E	Complex volcano	1170 CE ± 100 years
115	Miyakejima	0804-04=	Japan	34.08N	139.53E	Composite volcano	2008
116	Myōjin-Shō	0804-061	Japan	32.10N	139.85E	Submarine volcano	1953
117	Bandai-san	0803-16	Japan	37.60N	140.08E	Composite volcano	1888
118	Usu	0805-03	Japan	42.54N	140.84E	Composite volcano	2001
119	Gambier	0509-01-	Australia	37.77S	142.50E	Shield volcanoes	2900 BCE ± 150 years
120	Rota-1	0804-211	Marianas	14.60N	144.78E	Submarine volcano	2010 (continuing)
121	Lamington	0503-01	Papua New Guinea	08.95S	148.15E	Composite volcano	1956
122	Rabaul	0502-14	Papua New Guinea	04.27S	152.20E	Caldera	2010 (continuing)
123	Koryaksky	1000-09=	Kamchatka	53.32N	158.69E	Composite volcano	2009
124	Avachinsky	1000-10=	Kamchatka	53.26N	158.83E	Composite volcano	2001
125	Maly Semyachik	1000-14=	Kamchatka	54.13N	159.67E	Composite volcano	1952
126	Toibachik	1000-24	Kamchatka	55.83N	160.33E	Shield volcano	1976
127	Kronotsky	1000-20=	Kamchatka	54.75N	160.53E	Composite volcano	1923
128	Bezmianny	1000-25	Kamchatka	55.98N	160.59E	Composite volcano	2010 (continuing)
129	Kliuchevskoi	1000-26	Kamchatka	56.06N	160.64E	Composite volcano	2010
130	Shiveluch	1000-27	Kamchatka	56.65N	161.36E	Composite volcano	2010 (continuing)
131	Erebus (plots off map)	1900-02	Antarctica	77.53S	167.17E	Composite volcano	2010 (continuing)
132	Ambrym	0507-04	Vanuatu	16.25S	168.12E	Shield volcano	2010 (continuing)
133	Rangitoto	0401-02=	New Zealand	36.90S	174.87E	Shield volcano	1350 CE (?)
134	Ruapehu	0401-10	New Zealand	39.28S	175.57E	Composite volcano	2006
135	Taupo	0401-07=	New Zealand	38.82S	176.00E	Caldera	260 CE (?)
136	Oruanui	0401-061	New Zealand	38.42S	176.08E	Calderas	180 CE (?)
137	Mayor Island	0401-021	New Zealand	37.28S	176.25E	Shield volcano	5060 BCE ± 200 years
138	Rotorua	0401042A	New Zealand	38.08S	176.27E	Caldera	Pleistocene
139	Okataina	0401-05=	New Zealand	38.12S	176.50E	Volcanic center	1981
140	Tarawera	0401-05	New Zealand	38.12S	176.5E	Fissure system	1873
141	Brothers	0401-15	Kermadec	34.87S	179.08E	Submarine caldera	Holocene

Prominent World Volcanoes



See pp. 538 and 539 for list of volcano names and details



Map modified by Jacob G. Smith (University of Hawai'i at Hilo) after "This Dynamic Planet", 2006, Simkin, Tom, Tilling, R.I., Vogt, P.R., Kirby, S.H., Kimberly, Paul, Stewart, D.B.